Investigation of biomarkers of hepatic and renal toxicity in the Han Wistar rat

Inês Maria de Barros Pereira

Thesis submitted in accordance with the requirements of UCL School of Pharmacy for the degree of Doctor of Philosophy

February 2014

UCL SCHOOL OF PHARMACY

29-39 Brunswick Square

London WC1N 1AX

DECLARATION

This thesis describes the research conducted in University College London School of Pharmacy between February 2010 and February 2014 under the supervision of Dr. Michael Munday. I, Inês Maria de Barros Pereira, confirm that the work presented in this thesis is my own. Where information has been derived from other sources, I confirm that this has been indicated in the thesis. I also certify that I have written all the text herein and have clearly indicated by suitable citation any part of this dissertation that has already appeared in publication.

Signature:_____ **Date:**_____

Abstract

The aim of this project was to identify urinary markers of hepatic and renal toxicity in the male Hanover-Wistar rat; acute and chronic injury models were developed by administration of CCl_4. Nephrotoxicity was induced by administration of HCBD.

In an acute dose study, CCl_4-induced nephrotoxicity occurred above 2.0 mL/kg CCl_4. To avoid kidney injury, 2.0 mL/kg CCl_4 was chosen as the optimal dose. ^{1}H NMR revealed many changes to the urinary metabolome following CCl_4-induced liver injury including an increase in the resonances of taurine, creatine and formate and a decrease in hippurate and creatinine.

Protein and gene expression markers were investigated in a HCBD-model of nephrotoxicity. Urinary α-GST, KIM-1 and albumin were the most sensitive biomarkers of proximal tubular injury. These markers could be used to detect unwanted kidney injury in future CCl_4 hepatic studies.

In a time course study, maximal liver injury from CCl_4 was reached 24-48 hours post-dosing. Urinary metabolites followed the same trend and levels increased during the first 18-24 hours post-dosing. After 24 hours, there was a tendency for metabolites to return to control levels.

A chronic model of CCl_4-induced liver fibrosis was developed by dosing animals 3 times a week for 6 weeks to investigate the potential for reversibility and changes in urinary metabolites. After 6 weeks of CCl_4-administration there was development of fibrous structures in the liver parenchyma followed by slight regeneration during the recovery period. Urinary metabolites that best reflected the development of fibrosis were creatinine, citrate and succinate. Taurine and hippurate may be useful for showing regenerative changes.

In this project, we developed a good rat model of fibrosis which showed potential to reverse. ^{1}H NMR analysis allowed characterisation of urinary metabolite changes in acute and chronic studies. Some of these metabolites have potential to be urinary markers for hepatic fibrosis.

Acknowledgments

I would like to thank my supervisors Dr Mike Munday, Dr Mire Zloh, Dr John Turton and Dr Rosemary Smyth for giving me the opportunity to do the PhD. I have learned immensely from you. I admire your dedication, your enthusiasm and all the amazing work you put into this project. Thank for your constant help and advice.

I also thank Fundacao para a Ciencia e Tecnologia for the funding which allowed me to pursue the PhD.

I want to thank our collaborators at GlaxoSmithKline who were involved in the project and who contributed greatly to this thesis, Malcolm York, Aubrey Swain, Fiona McClure, Ian Harman and Marcello Tontodonati.

To my friends with whom I shared these last 4 years! Thank you for keeping my spirits up. You made this experience a whole lot more enjoyable! I do hope you know how important you are. I want to see much more of you now that the thesis is over!

To my mum, dad and sister, there is nothing I can say but to thank you for believing in me. I am sorry for the texts and the emails that never got a reply because I was writing. I love you and I miss you every day! I am so proud to have you.

To Dave, thank you for your constant support and for making me stay focused when I couldn't do it anymore. You kept me sane and looked after me! You were a great part of this journey. Most of all I want to thank you for putting up with me for the last months, it can't have been easy!

Table of contents

List of tables

List of figures

List of abbreviations

α-GST	α-glutathione S-transferase
α-SMA	α-smooth muscle actin
°C	degree Celsius
µg	microgram
µl	microlitre
µm	micrometre
µM	micromole
A2M	α2-macroglobulin
ACTA2	α-smooth muscle 2
AGP	α-1-acid glycoprotein
AKI	acute kidney injury
ALP	alkaline phosphatase
ALT	alanine aminotransferase
ANIT	α-naphthyl isothiocyanate
ANOVA	analysis of variance
ANXA7	annexin A7
AST	aspartate aminotransferase
ATP	adenosine triphosphate
AUROC	area under the receiver operating characteristic curves
BCG	bromocresol green
BHT	butylated hydroxytoluene
BUN	blood urea nitrogen
BW	body weight
c.p.	collection period

CAD	chromotrope-aniline-blue
cm	centimetre
COMET	The Consortium on Metabonomic Toxicology
CRYAB	crystalline, αB
Ct	cycle threshold
CV	cross-validation
CYP1A1	cytochrome P-4501A1
CYP2C	cytochrome P-4502C
DNA	deoxyribonucleic acid
ECM	extracellular matrix
EMA	European Medicines Agency
EPHX1	epoxide hydrolase (microsomal) 1
FDA	US Food and Drug administration
g	gram
G6PDH	glucose-6-phosphate dehydrogenase
G6PDX	Glucose-6-phosphate dehydrogenase
GaIN	D-(+)-galactosamine hydrochloride
GCLC	glutamate-cysteine ligase, catalytic subunit
GFAP	glial fibrillary acid protein
GFR	glomerular filtration rate
GI	gastrointestinal tract
GLDH	glutamate dehydrogenase
GSR	glutathione reductase
GST	glutathione S-transferase
GSTM4	glutathione S-transferase isoform mu 3
GSTYb1	glutathione S-transferase Yb1

h	hour
H&E	haematoxylin and eosin
HA	hyaluronic acid
HCBD	hexacloro-1:3-diene
HCC	hepatocellular carcinoma
HMOX1	heme oxygenase (decycling) 1
HSC	hepatic stellate cells
Hz	Hertz
i.p.	intraperitoneal
IDL	intermediate-density lipoproteins
IGF1	insulin-like growth factor-1
IMS	industrial methylated spirit
J	coupling constant
K.I.E	killed in extremis
kb	kilobase
kDa	kiloDalton
kg	kilogram
KNG1	kininogen 1
L	Litre
LC-MS	liquid-chromatography mass spectrometry
LDH	lactate dehydrogenase
LDL	low-density lipoproteins
M	mole
m	quantum number
MALB	Microalbumin
MCP1	monocyte chemoattractant factor 1

MCP-NAG	*m*-cresolsulfonphthaleinyl N-acetyl-β-D-glucosaminidase
MDH	malate dehydrogenase
mL	millilitre
mm	millimetre
mM	millimole
MMP	matrix metalloproteinases
mRNA	messenger ribonucleic acid
MVA	multivariate data analysis
NADH	nicotinamide adenine dinucleotide
NADPH	nicotinamide adenine dinucleotide phosphate
NAG	N-acetyl-β-D-glucosaminidase
ng	nanogram
nm	nanometre
NMR	nuclear magnetic resonance
OPLS	orthogonal partial least square
OPLS-DA	OPLS-discriminant analysis
PAI-1	plasminogen activator inhibitor-1
PBC	primary biliary cirrhosis
PC	principal components
PCA	principal component analysis
PCR	polymerase chain reaction
PDGF	β-platelet-derived growth factor
PEG	polyethylene glycol
PLS	partial least square
ppm	parts per million
PR	pattern recognition

RNA	ribonucleic acid
ROS	reactive oxygen species
rpm	revolutions per minute
SD	standard deviation
TGF-β1	transforming growth factor-β1
TIMP	tissue inhibitors of metalloproteinases
TIMP-1	tissue inhibitor of metalloproteinase 1
TNF-α	tumour necrosis factor-α
TSP	3-(trimethylsilyl) propionate
TXRND1	thioredoxin reductase 1
U	enzyme unit
UGT1A6	UDP glucuronosyltransferase 1A6
US	ultrasonography
UV	unit variance
VIP	variable importance plot
VLDL	very low-density lipoproteins

CHAPTER ONE

Introduction

Chapter 1

1.1 The liver

1.1.1 Anatomy of the liver

The liver is one of the largest organs in the body and is located in the right upper quadrant of the abdominal cavity just beneath the diaphragm and held in place by several ligaments (Ramadori et al., 2008; Wu et al., 2013).

The liver is the most metabolically active organ in the body and normally is a dark red colour due to the large quantity of blood it contains.

The rat liver consists of four lobes of different size: left, middle, right and caudate; each representing approximately 30, 40, 21 and 7 % of the total liver mass respectively (Kogure et al., 1999) (Figure 1.1). The middle lobe is divided into right and left portions, by one of the ligaments; the right liver lobe is located on the right side of the vena cava and is divided into 2 portions, the right superior and the right inferior lobe. The caudate lobe is located on the left side of the vena cava, and is divided into the superior caudate lobe and inferior caudate lobe (Madrahimov et al., 2006). The paracaval tissue is composed of the bases of the right superior, right inferior and caudate lobes covering the intrahepatic vena cava and makes up between 2.5 to 3 % of the liver (Madrahimov et al., 2006).

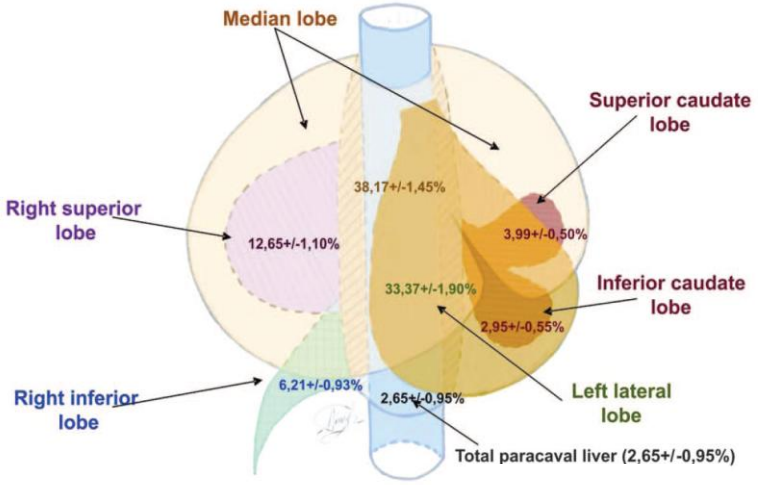

Figure 1.1 Weight distribution of rat liver lobes (Madrahimov et al., 2006).

The vascular system of the rat liver includes the hepatic arterial system and the hepatic portal venous system. The hepatic artery delivers arterial blood and is responsible for 25 % of the blood supply to the liver. The hepatic portal vein is responsible for the remaining 75 % of the blood supply and delivers deoxygenated blood which is rich in nutrients from the spleen, stomach, small and large intestine, gallbladder and pancreas (Eipel et al., 2010). The portal venous system is composed of conducting systems that ensure blood is delivered to the farthest corner of the liver, and multiple branching and branches of different lengths to ensure the even blood supply to the liver parenchyma. The portal venous system also has distributing systems which are responsible for the exchanges between blood and the hepatocytes (Saxena et al., 1999). The portal vein enters the liver at the hilus before dividing into a capillary network, known as liver sinusoids which supply the different lobes of the liver (Kogure et al., 1999). Blood is drained from the liver via the hepatic vein, and joins the inferior vena cava (Kogure et al., 1999).

1.1.2 Histology

Hepatocytes, or parenchymal liver cells, make up approximately 80 % of the liver volume (Blouin et al., 1977). They are polyhedral in shape and have a diameter of 25 to 30 µm in length and between 20 to 25 µm in width (Motta, 1984). Each hepatocyte contains a large nucleus occupying 5-10 % of the cell volume with the cytoplasm constituting approximately 50 % of the volume. The hepatocytes are joined together to form rows of cells, approximately 1 cell thick, that branch out from the central vein. The liver sinusoids line each side of a row of hepatocytes. Blood flowing in the sinusoids empties into the central vein (Figure 1.2).

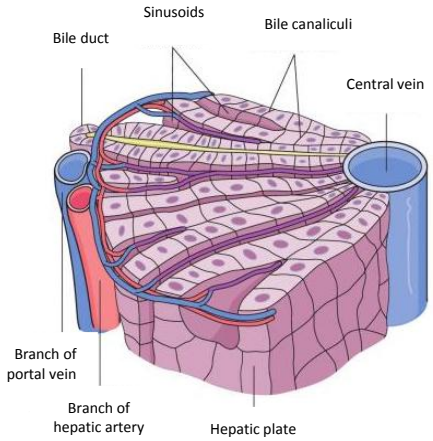

Figure 1.2 Organisation of the liver. A central vein is presented in the centre of the lobule with radially arranged plates of hepatocytes. Branches of the portal vein and hepatic artery are located in the periphery of the lobule (Haschek et al., 2010).

Three major concepts have been suggested to the structure of the functional units of the liver: the classical lobular organisation, the portal lobule of Mall and the liver acinus of Rappaport (Figure 1.3).

In the classical lobular organisation, each of the 4 liver lobes is divided into many hexagonal lobules. A central vein is located at the centre of each lobule; and portal tracts, each containing a branch of the portal vein, hepatic arteriole and a bile duct are located at each corner of the lobule. Each lobule has 3 regions: centrilobular, which is closest to the central vein, midzonal and periportal (Bhunchet and Wake, 1998). Mall's proposal describes the liver as a hexagonal unit with the portal tract as its axis. The functional unit of the liver according to Rappaport (1958) is divided into 3 zones and is known as the hepatic acinus. Zone 1 is closest to the portal tracts, whereas zone 3 is closest to the central vein.

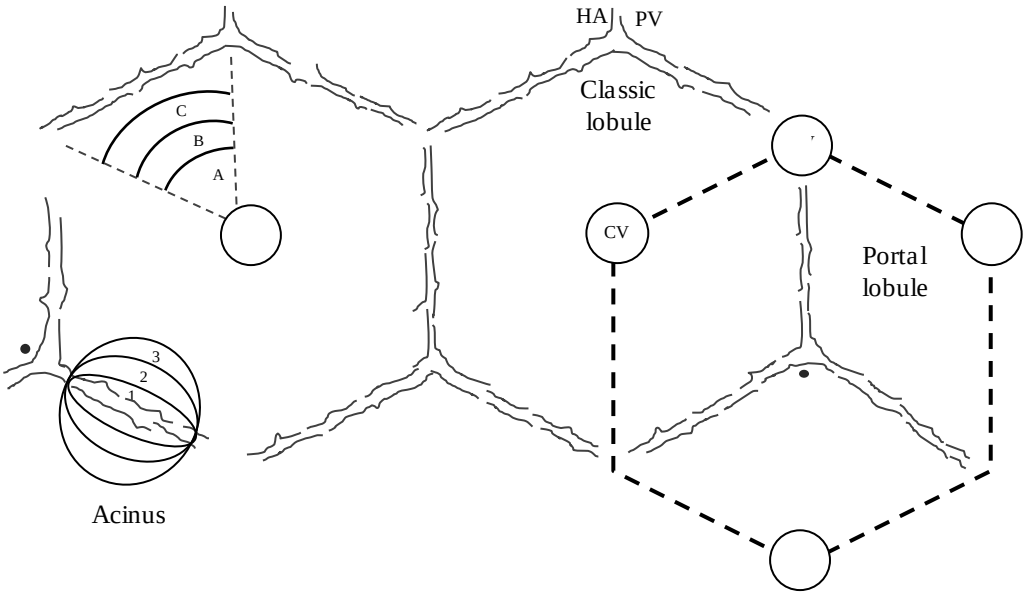

Figure 1.3 Representation of the classical liver lobule, portal lobule and liver acinus. PV: portal vein, HA: hepatic arteriole; CV: central vein. Zone 1 of the liver acinus is the closest to the portal vein and zone 3 is closest to the central vein, with its axis composed of the portal tract. A, B and C represent the centrilobular, midzonal and periportal zones of the classical liver lobule with the central vein at its axis (adapted from McQueen, 2010).

Each of the zones in the liver acinus has different blood pressure, oxygen and nutrient supply, metabolism and enzymatic activity. Blood flows unidirectionally from zone 1 to 3. Therefore, zone 1 is exposed to the most oxygenated blood and has the highest level of nutrients whereas, zone 3 is closest to the central vein and therefore is the least oxygenated zone (Saxena et al., 1999). Centrilobular hepatocytes have a greater number

and bigger mitochondria which may potentially reflect the high metabolic activity of these cells (Blouin et al., 1977).

The hepatic sinusoids are lined by endothelial cells which have fenestrated membranes and lack a basement membrane. Between the endothelium layer and the hepatocytes is a space known as the space of Disse. The space of Disse is normally between 0.2 and 0.5 µm wide and contains components of the extracellular matrix. The presence of pores along the endothelial membrane facilitates the exchange of substances between the lumen of the sinusoids, the space of Disse and the hepatocytes. Kupffer cells and Ito cells are the 2 other major cells found in the sinusoidal space. Kupffer cells comprise approximately 15 % of all liver cells (Wisse, 1974; Naito et al., 2004). These cells are phagocytic and are the macrophages of the liver (Naito et al., 2004). It has also been shown that Kupffer cells are most frequently found in the periportal region (Sleyster and Knook, 1982). The Kupffer cells located in the periportal region are different from those found in the centrilobular area in terms of enzyme activity, receptors and subcellular structures. In the periportal region, Kupffer cells are larger, have greater phagocytic activity and generate less superoxide anions (Mochida et al., 1989). Ito cells, also known as fat-storing cells or stellate cells, account for 8 % of total cells in the liver (Hautekeete and Geerts, 1997; Unanue, 2007; Winau et al., 2007). In the presence of cellular damage Ito cells differentiate into myofibroblast-like cells with high proliferative capacity and produce extracellular matrix proteins such as collagens (I, III, IV, V and VI), and extracellular matrix degrading metalloproteinases and the corresponding inhibitors (Mallat et al., 1995; Hautekeete and Geerts, 1997).

1.1.3 Functions

The liver has many functions and is involved in: secretory; metabolic; detoxification; storage; excretory and synthesis processes.

The liver is responsible for the production of bile. Bile is composed of bile salts, phospholipids and organic anions; bile salts are synthesised from cholesterol. Bile is synthesised in the hepatocytes and secreted into the bile canaliculi. From here the bile travels to the gall bladder where it is concentrated. Bile salts and bile are released from the gall bladder into the duodenum where they promote digestion and, in particular, the absorption of fat through the process of micellar emulsification (Alrefai and Gill, 2007). Bile salts have a hydrophobic layer and a hydrophilic layer. Therefore, micelles are

water soluble due to their hydrophilic shell, but can carry hydrophobic substances in their lipid core. These micelles can diffuse through the water to the enterocytes where its components are absorbed.

The liver has a key role in the metabolism of carbohydrates by the processes of: glycogenesis, glycogenolysis and gluconeogenesis. In glycogenesis, glycogen is synthesised in the liver from glucose when glucose is present in high amounts. Glycogen is then stored in the liver. When the glucose levels in the blood are low the liver acts as a source of glucose by breaking down the glycogen reserves to release glucose, a process known as glucogenolysis. The process of gluconeogenesis describes the synthesis of glucose from non-carbohydrate sources including amino acids (Nordlie et al., 1999).

The liver is also responsible for the synthesis and degradation of lipids. The liver synthesises very low-density lipoproteins (VLDL) from fatty acids. VLDLs are converted into intermediate-density lipoproteins (IDL) and low-density lipoproteins (LDL) (Adiels et al., 2008). VLDLs have a high concentration of triglycerides, whereas LDLs are the primary carrier of cholesterol in the blood. Degradation of lipids occurs via the action of lipoprotein lipase which is responsible for hydrolysing triglycerides, cholesterol and phospholipids into fatty acids (Zambon et al., 2003). β-oxidation is the process by which fatty acids are oxidised to generate energy and occurs in the mitochondria (Rao and Reddy, 2001).

The majority of proteins are synthesised and degraded in the liver. The liver is also the main site for the production of most plasma proteins, including albumin, α- and β-globulins; clotting factors such as fibrinogen, factors V, VII, IX and X; enzymes and cholesterol; and of non-essential amino acids (Turton and Hooson, 2005).

The liver is the primary organ involved in the metabolism of xenobiotics via Phase I and II reactions. Phase I reactions involve hydrolysis, reduction and oxidation reactions and the major enzyme involved is the microoxygenase system cytochrome P-450. The product of Phase I reactions is often a highly reactive free radical species. Phase II reactions include glucuronidation, glutathione conjugation and acetylation (Turton and Hooson, 2005).

1.2 Liver injury

The liver is very susceptible to injury following exposure to toxicants. One of the main reasons is that most xenobiotics enter the body via the gastrointestinal (GI) tract and are transported via the hepatic portal vein to the liver, thus exposing the liver to high concentrations of the chemical (Sturgill and Lambert, 1997). Additionally, the liver has a very high concentration of xenobiotic-metabolising enzymes such as cytochrome P-450s which metabolise many toxicants to a more water-soluble form allowing them to be more readily excreted from the body (Davidson, 2000). However, some toxic compounds form highly reactive metabolites, such as free radicals, upon metabolism by cytochrome P-450. These reactive metabolites can induce injury to the local hepatic area. Consequently, hepatic injury is commonly localised to the centrilobular region, since this region has the highest concentration of cytochrome P-450 enzymes (Lindros, 1997; Sweeney, 1981).

1.2.1 Fatty liver

Fatty liver disease covers both fatty liver without inflammation (hepatic steatosis) and fatty liver that is associated with inflammation (steatohepatitis). Hepatic steatosis is reversible but it may develop into steatohepatitis, cirrhosis and liver cancer if exposure to the stimuli continues (Reddy and Rao, 2006). Hepatic steatosis is characterised by the excessive accumulation of triglycerides in the hepatocytes, usually more than 5-10 % by weight (Kelishadi et al., 2013). The accumulation of triglycerides may result from increased fatty acid synthesis via *de novo* lipogenesis, decreased β-oxidation of fatty acids and decreased secretion of cholesterol esters and triglycerides from the liver as VLDL. VLDLs are usually secreted from the liver and taken up by peripheral tissues such as the heart, skeletal muscle and adipose tissue (Minehira et al., 2008). A decreased ability to produce and secrete VLDL may be the result of decreased production of apolipoproteins by the liver (Elias et al., 1999; Maugeais et al., 2000). Apolipoproteins are carrier proteins that combine with lipids to form lipoprotein particles (Cryer et al., 1986). The liver is the major site for apolipoprotein synthesis; therefore, conditions in which liver function is affected, including cirrhosis, may be accompanied by decreased levels of apolipoproteins (Lombardi and Ugazio, 1965; Ciccarese et al., 1998). In animals this can occur following the exposure of rats to compounds such as CCl_4 (Boll et al., 2001). Accumulation of triglycerides may also

occur as a result of excessive dietary intake (Donnelly et al., 2005, Kallwitz et al., 2008).

Hepatic steatosis may be described as microvesicular when there is accumulation of small intracytoplasmic fat droplets, and macrovesicular if the fat droplets are large (Reddy and Rao, 2006).

1.2.2 Cell death/necrosis

Cell death can occur by one of two mechanisms: apoptosis or necrosis. During the process of apoptosis, the cells often shrink and become more dense, the chromatin condenses and the nucleus fragments (Elmore, 2007). Apoptotic cells usually lack inflammatory cell infiltrates. The reason for this is that apoptotic cells do not release their cellular contents and, therefore, there is insufficient release of chemoattractants from individual cells to produce a large scale inflammatory response (Majno and Joris, 1995).

Necrosis is characterised histologically by changes to the nucleus such as karyolysis (complete dissolution of the chromatin due to the increased activity of DNAase); pyknosis (irreversible condensation of chromatin in the nucleus of a cell) and karyorhexis (nuclear fragmentation) (Arredondo et al., 2005; Stoica and Faden, 2010). These changes are accompanied by cellular swelling, swollen mitochondria, distended endoplasmic reticulum and the formation of cytoplasmic vacuoles. Cytoplasmic eosinophilia occurs due to the dissociation of ribosomes from the endoplasmic reticulum, as well as a disruption of the membranes of cellular organelles and the denaturation of proteins (Majno and Joris, 1995; Itoh et al., 2002; Elmore, 2007; Kroemer et al., 2009). The loss of cellular membrane integrity, due to necrosis, leads to the release of cytoplasmic contents including enzymes. The release of cellular contents produces an inflammatory response and this can lead to more severe injury occurring as a result of the influx of inflammatory cells, secretion of cytokines and production oxygen species (Majno and Joris, 1995; Darzynkiewicz et al., 1997; Elmore, 2007).

Hepatocyte necrosis can occur after exposure to a hepatotoxicant agent. This is due to the particularly high concentration of cytochrome P-450 that can be found in the centrilobular region (Lindros, 1997; Sweeney, 1981). Centrilobular necrosis commonly occurs in rats exposed to compounds that undergo cytochrome P-450 bioactivation such as CCl_4 (Slater, 1978; Smyth et al., 2007; Smyth et al., 2008; Smyth et al., 2009a),

acetaminophen (Waters et al., 2001; James et al., 2003) and thioacetamide (Diaz-Gil et al., 1987; Caballero et al., 2001).

Midzonal necrosis is the least common type of hepatocellular injury and generally involves 2 or 3 cells in the middle of the lobule (Mackie et al., 2009). Midzonal necrosis has been described following phytol administration to mice (Mackie et al., 2009).

In periportal necrosis, the necrotic hepatocytes are confined to the areas close to the portal tracts. This region is exposed first to blood containing toxicants and arriving at the liver via the portal vein. This type of injury often happens with compounds that do not require bioactivation, for example allyl alcohol (Belinsky et al., 1984).

In the liver, necrosis can be focal, involving the death of a small number of cells in the central, midzonal or periportal regions, or massive, involving the death of a large number of cells, spanning to different lobules. In the case of focal necrosis there is potential for regeneration and repair since dead cells may be replaced by adjacent hepatocytes.

Massive necrosis may occur when the liver is exposed to high concentrations of a toxicant agent, or a toxic compound is delivered directly to the vascular system, in particular to the portal vein. However, the liver has a great regenerating capacity, and therefore, even the death of a large number of hepatocytes may not be critical (Michalopoulos, 2007; Michalopoulos, 2011).

1.2.3 Fibrosis

Hepatic fibrosis is characterised by an excessive accumulation of extracellular matrix (ECM) proteins, in particular collagens, and occurs as a result of chronic injury to the liver (Clouthier et al., 1997). Fibrosis is a wound healing process that begins with inflammation and cellular necrosis which may undergo regeneration and repair. However, repeated injury may lead to increased synthesis of ECM proteins accompanied by decreased degradation. This imbalance between ECM production and degradation leads to deposition of excess collagens and scarring of the tissue (Parsons et al., 2004). The main causes of liver fibrosis in humans include hepatitis C, alcohol abuse and non-alcoholic steatohepatitis (Bataller and Brenner, 2005).

ECM proteins including α-smooth muscle actin (α-SMA), vimentin, desmin and glial fibrillary acid protein (GFAP) perform numerous functions in the liver (Lin et al.,

1998). These proteins have architectural and mechanical roles; are involved in providing tensile strength and resilience; modulate diffusion and vascular flow and participate in the process of regulating cell movement (Wells, 2008).

The production of ECM is under the control of hepatic stellate cells (HSCs), also known as lipocytes, perisinusoidal or Ito cells. These are vitamin-A storing cells located in the perisinusoidal space of Disse (Jiao et al., 2009). Following hepatic insult the HSCs become activated and change to a myofibroblast-like cell with a corresponding reduction in the amount of vitamin-A stored within the cell (Figure 1.4) (Fallowfield, 2011). HSC activation occurs in two sequential steps: initiation and perpetuation. The first step refers to the early events which occur after exposure to the hepatotoxicant and include the induction of β-platelet-derived growth factor (PDGF) and transforming growth factor-β1 (TGF-β1) receptors. The induction of these receptors makes the cells more responsive to cytokines. The perpetuating phase (second phase) comprises the response of the activated stellate cell to a variety of signals such as cytokines and growth factors (Friedman, 2008). The myofibroblast-like cells then proliferate and produce components of the ECM, including α-SMA, GFAP, vimentin and desmin as well as fibrillar collagen (collagen type-I and type-III) (Carpino et al., 2005; Friedman, 2008; Krizhanovsky et al., 2008).

α-SMA is an isoform of actin and a specific marker for activated HSCs displaying a myofibroblastic phenotype (Skalli et al., 1986). GFAP is an intermediate filament that has been shown to be present in the HSC in a normal rat liver and reported to be increased in response to acute hepatic injury but decreased in chronic injury (Niki et al., 1996). The initial upregulation seen in the early stages of hepatic damage suggested that GFAP could be related to the process of HSC activation (Carotti et al., 2008).

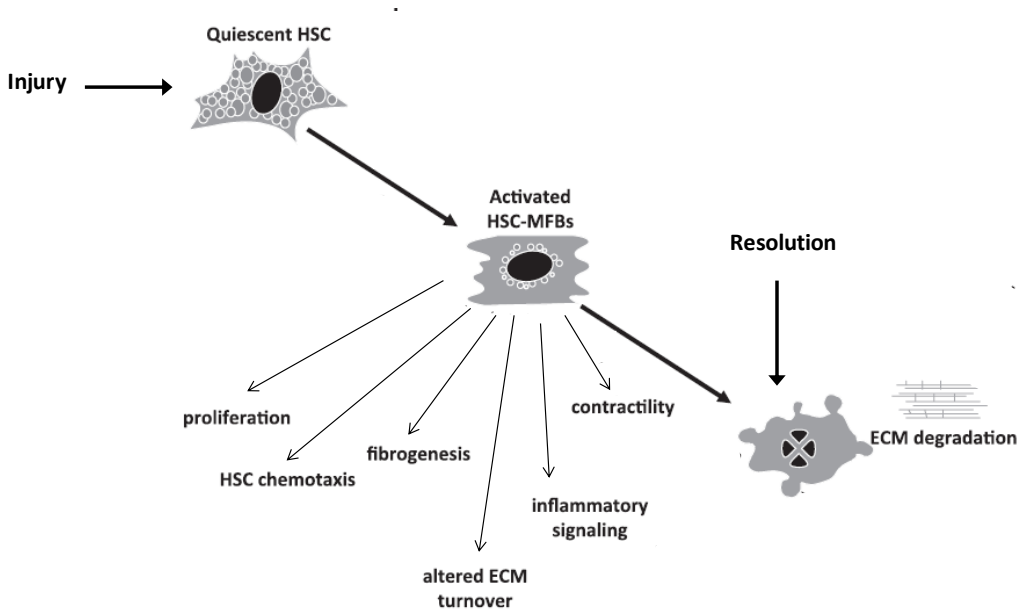

Figure 1.4 Activation of hepatic stellate cells and resolution (modified from Fallowfield, 2011). Following injury, hepatic stellate cells (HSCs) undergo activation, whereby they change from vitamin-A storage cells into myofibroblast (MFB). The major phenotypic changes include proliferation, contractility, fibrogenesis, matrix degradation, chemotaxis and cytokine release.

Activated HSCs also produce matrix metalloproteinases (MMPs), which degrade the ECM proteins (Nagase et al., 2006). MMPs are part of a family of zinc dependent endoproteinases capable of degrading fibrillar collagen such as collagens I, II, III, V and XI (Curran and Murray, 2000). According to their preferred substrates, MMPs can be divided into collagenases (MMP-1), gelatinases (MMP-2 and MMP-9), stromelysins (MMP-3, MMP-10 and MMP-11), matrilysins (MMP-7 and MMP-26) and membrane-type MMPs (MMP-14, MMP-15, MMP-16) (Nagase et al., 2006).

MMPs are synthesised as proenzymes and the structure includes a catalytic domain and an autoinhibitory pro-domain. Activation of MMPs requires the removal of the pro-domain by proteases such as plasmin (Visse and Nagase, 2003; Page-McCaw et al., 2007). Plasmin is generated from plasminogen by plasminogen activators (Lee et al., 1996).

It has also been shown that HSCs are capable of synthesising plasminogen activator inhibitor-1 (PAI-1) which in turn inhibits plasmin synthesis (Leyland et al., 1996). This suggests that decreased synthesis of plasmin by activated HSCs may have a role in the progression of the fibrotic process by inhibiting the activation of MMPs and hence the

degradation of excessive ECM proteins (Leyland et al., 1996). TGF-β is secreted by Kupffer cells and HSCs and contributes to the pathogenesis of fibrosis by stimulating the expression of fibronectin, collagens, and matrix proteoglycans (components of the ECM), and also via the induction of MMP inhibitors and PAI-1 (Branton and Kopp, 1999). It has been previously reported that TGF-β can be inhibited by α2-macroglobulin (A2M) by binding to activated TGF-β (Tiggelman et al., 1997). A2M is secreted by hepatocytes and is an acute phase protein and a proteinase inhibitor (Kawser et al., 1998). Tiggelman et al., (1997) suggested an antifibrogenic effect for A2M due to their ability to bind and inactivate TGF-β, and therefore, inhibit the TGF-β-induced collagen synthesis.

The activity of MMPs is regulated by tissue inhibitors of metalloproteinases (TIMPs) which bind to MMPs and block their proteolytic activity (Brew et al., 2000; Han, 2006). TIMPs expression is induced by TGF-β (Knittel et al., 2000). The decrease in the catalytic activity of MMPs is an important regulator in the progression of fibrosis. Increased TIMP-1 expression by HSCs has been reported in rats following repeated administration of CCl_4 (Iredale et al., 1996; Herbst et al., 1997).

Accumulation of ECM can disrupt the normal liver architecture and compromise liver function. An increase in fibrillar collagen in the space of Disse may result in the defenestration of the hepatic sinusoidal epithelium, a process known as sinusoidal capillarisation (Hahn et al., 1980; Siegmund et al., 2005). In the fibrotic liver this sinusoidal epithelium becomes rich in collagen and fibronectin and the loss of the pores blocks the bidirectional exchange of substances between the sinusoidal lumen and the adjacent hepatocytes (Hahn et al., 1980; Friedman, 1993). This leads to an increase in the intrahepatic vascular resistance and may result in the development of portal hypertension which is characterised by an increase in pressure in the portal vein (Rockey, 1997).

Fibrosis was previously considered to be an irreversible condition. However, evidence now indicates that even advanced stages of fibrosis may be reversible and that increased collagenolytic activity is one of the major factors contributing to the recovery (Benyon and Iredale, 2000). Survival factors such as insulin-like growth factor-1 (IGF-1) and tumour necrosis factor-α (TNF-α) regulate the activity of HSCs. Loss of these survival factors makes activated HSCs more susceptible to apoptosis. Activated HSCs have been reported to be more susceptible to apoptotic signals (Li and Friedman, 1999). Thus,

during resolution of fibrosis there is an increase in the number of cells undergoing apoptosis. Consequently, the decrease in the number of HSC will result in decreased levels of TIMP and therefore, the activity of MMPs increases. Iredale and colleagues (1998) have shown that spontaneous liver recovery is accompanied by loss of α-SMA positive HSCs indicating a loss of activated HSCs. It has been proposed that this is due to apoptosis as opposed to a regression of phenotype from the activated to a quiescent HSC (Iredale et al., 1998).

Currently, there remains great debate regarding the mechanism for the reversibility of fibrosis and the origin of the myofibroblast-like cells is not yet completely understood (Ramachandran and Iredale, 2012; Sohrabpour et al., 2012; Czaja, 2014; Machado and Diehl, 2014). The latest antifibrotic therapy strategies have focused on increasing the rate of HSC apoptosis, or in targeting myofibroblasts (Liu et al., 2013), whereas Rosenbloom et al., (2013) suggested the selective inhibition of the TGF-β pathway as a possible therapy.

1.2.4 Cirrhosis

Cirrhosis is defined as the "histological development of regenerative nodules surrounded by fibrous bands in response to chronic liver injury" (Schuppan and Afdhal, 2008). Liver cirrhosis is the end result of fibrosis. In the Western world, cirrhosis is frequently associated with alcoholic liver disease and hepatitis C, whereas hepatitis B is an important cause in Africa (Schuppan and Afdhal, 2008).

Cirrhosis is characterised by extensive fibrous scarring of the liver tissue leading to loss of hepatic architecture and distortion of the hepatic vasculature. This compromises the exchanges between hepatic sinusoids and hepatocytes (Vollmar et al., 1997; Kamath et al., 2000). Histological examination of cirrhotic livers is characterised by the presence of vascularised fibrotic septa that surround hepatocytes creating islands devoid of a central vein (Schuppan and Afdhal, 2008). Human patients with cirrhosis often suffer from arterial vasodilatation, increased cardiac output, hyponatremia (serum sodium level of less than 135 mEq/L in humans) and hepatorenal syndrome (Lee, 2009). Hepatorenal syndrome describes the compromise of renal function occurring as a consequence of cirrhosis. In a cirrhotic liver, portal hypertension often arises and is characterised by an increase in pressure in the portal vein. This event is followed by the release of vasodilators, for example nitric oxide, which can escape from the splanchnic

circulation into the systemic circulation causing vasodilatation, this in turn will be counteracted by stimulation of the vasoconstrictor systems as well as retention of salt and water in an attempt to maintain the blood pressure. It is this constant vasoconstriction that can lead to renal failure (Ginès et al., 2003; Betrosian et al., 2007). Ascites is one of the most common complications of cirrhosis and is described as the accumulation of fluid in the peritoneal cavity. Ascites occurs as a consequence of portal hypertension. It results from a leakage of lymph fluid from the blood vessel of the GI tract into the peritoneal cavity. Eventually, sodium and water also move from the capillaries into the peritoneal space resulting in the development of ascites (Kashani et al., 2008).

Splenomegaly is also frequently observed in patients with portal hypertension. This enlargement of the spleen is a consequence of the increase in the portal vascular resistance which compromises the blood flow through the splenic vein (Gusberg et al., 1994).

Anatomically, cirrhosis can be classified as either micronodular or macronodular. In micronodular cirrhosis the nodules are smaller than 3 mm and it is often observed in Wilson's disease and primary biliary cirrhosis (PBC). PBC is characterised by the accumulation of lymphocytes and plasma cells close to the intrahepatic bile ducts leading to the inflammation of the bile ducts, loss of ducts and eventual impairment of the bile flow. This damages the liver cells leading to the scarring of the tissue and eventually cirrhosis (Selmi et al., 2011). The nodules in micronodular cirrhosis are of the same order of size as the original lobule and the lesions are regularly distributed throughout the liver. In macronodular cirrhosis, nodules are enlarged to 3 mm or larger in size and are encircled by collagen bands (Scheuer, 1970). Macronodular cirrhosis is often seen in patients with viral hepatitis and in animal models of drug-induced injury (Yu et al., 2010a).

In rodents, cirrhosis can occur following repeated, low dose, CCl_4 administration (Proctor and Chatamra, 1983; Ariosto et al., 1989; Lee et al., 2005; Jaramillo-Juarez et al., 2008).

Traditionally, cirrhosis is classified as an irreversible condition, however, it has been suggested that cirrhosis may potentially reverse (Benyon and Iredale, 2000; Friedman, 2003; Pinzani et al., 2011). It has been recently proposed that reversibility of cirrhosis in humans may occur but it is a very slow process that may take years and that not all

patients have this ability. However, at a certain point cirrhosis of the liver is considered to be irreversible (Sohrabpour et al., 2012). In humans, it has been shown that absence of alcohol for at least 6 months was associated with regression of cirrhosis in 8 % of the patients in a retrospective study (Serpaggi et al., 2006). Signs of cirrhosis regression have also been described in rat models of CCl_4-induced cirrhosis (Di Vinicius et al., 2005).

1.2.5 Liver cancer

Hepatocellular carcinoma (HCC) is the sixth most common cancer and one of the top 3 causes of cancer-related deaths in the world (Parkin et al., 2005; Forner et al., 2012). The pathogenic process includes the development of regenerative nodules leading to invasive HCC (Schuppan and Afdhal, 2008). Risk factors for HCC include cirrhosis, viral hepatitis B and C and aflatoxin exposure. The mechanism by which viral hepatitis increases the risk of hepatocellular carcinoma is not completely understood but is thought to be dependent upon oxidative stress-induced DNA damage (Mendy and Walton, 2009). The formation of reactive oxygen species (ROS) may result from both endogenous and exogenous stimuli. Xenobiotics such as 2-butoxyethanol and CCl_4 undergo cytochrome P-450 metabolism to form free radicals (Sasaki, 2006). Additionally, it has been shown that Kupffer cells and macrophages have the ability to generate ROS in the hepatocytes (Friedman, 2003). It is thought that nicotinamide adenine dinucleotide phosphate (NADPH) oxidase in the Kupffer cells catalyses the reduction of O_2 to $O_2^{\cdot -}$ (Cubero and Nieto, 2012). Oxidative stress results from the imbalance between the generation of ROS and the antioxidant mechanisms (Suzuki et al., 2013). It is thought that these reactive oxygen species have an effect on the normal proliferation of hepatocytes leading to tumour development (El-Serag and Rudolph, 2007).

1.3 Detection of hepatic injury

This project is concerned with the identification of biomarkers of hepatotoxicity. A biomarker was described by Atkinson et al., (2001) as “a characteristic that is objectively measured and evaluated as an indicator of normal biological processes, pathogenic processes, or pharmacologic responses to a therapeutic intervention”.

Currently, biomarkers are used to determine the severity of a disease and its prognosis. However, biomarkers are also used in preclinical and clinical studies to evaluate new

candidate drugs with regards to safety and effectiveness and have great use in toxicology studies (Lewin and Weiner, 2004).

An ideal biomarker should indicate the early stages of a disease or injury, be organ specific and have a strong correlation with well defined histomorphologic changes. A biomarker is more ideal if it can be detected by tests which are simple to perform, reliable, inexpensive and high-throughput. Non-invasive collection of samples is also preferential to invasive methods such as blood collection (Ozer et al., 2008).

1.3.1 Serum enzymes

Traditionally, liver injury has been assessed by the measurement of serum enzymes such as alanine aminotransferase (ALT), aspartate aminotransferase (AST) and glutamate dehydrogenase (GLDH). These enzymes are called hepatic leakage enzymes since they are released from the hepatocytes when there is loss of cellular membrane integrity (Solter, 2005; Schmidt and Schmidt, 1988; Gores et al., 1990; Van Hoof et al., 1997). This may occur as a result of cell necrosis or inflammation (Bridges et al., 1983). The standard unit used to quantify the amount of enzyme is called the international unit of enzyme activity (U), which measures the amount of enzyme needed to convert 1 µmol of substrate into product in 1 minute. Enzyme concentration is expressed as U/L, that is, enzyme activity divided by volume.

ALT is a cytosolic enzyme which is mainly located in the liver, but low levels of the enzyme are also found in skeletal muscle and heart tissues. The highest concentration of this enzyme has been reported to be found in the periportal hepatocytes with lower concentrations in the centrilobular region (Rappaport, 1958). AST is found in both the cytosol and mitochondria and is present in high concentrations in a number of tissues including the heart, brain, skeletal muscle and liver (Wroblewski, 1959). Therefore, injury to any of these tissues may result in significant serum AST elevations. Therefore, ALT is more specific to hepatic injury than AST (Ramaiah, 2007).

Additionally, ALT has a longer half-life than AST (approximately 50 hours for ALT and 16 hours for AST) (Krishnamurthy et al., 2009).

The ratio of AST to ALT is often used to provide information about the causes of liver disease. Serum AST is generally increased by greater amounts compared to ALT in chronic liver damage, whereas, acute liver injury results in increased levels of ALT

compared to AST (Williams and Hoofnagle, 1988). The AST/ALT ratio tends to be greater than 2 in patients with alcoholic liver disease and less than 1 in patients with chronic hepatitis (Williams and Hoofnagle, 1988). A study has shown that mitochondrial AST is not released into the blood circulation until most of the cytosolic enzyme has leaked out. This suggests that mitochondrial enzymes only leak from hepatocytes when a greater degree of injury has occurred than that which results in leakage of the cytosolic enzymes (Kamiike et al., 1989).

GLDH is located both in the cytosol and mitochondrial matrix (O'Brien et al., 2002) with the highest concentration found in the liver. However, GLDH can also be found in the kidneys, lungs, brain and skeletal muscle (Mihara et al., 1982, Schmidt and Schmidt, 1988, Lee et al., 1999). Within the liver, GLDH levels are greatest in the centrilobular region and therefore, injury to this area will produce a significant increase in plasma GLDH concentration (O'Brien et al., 2002). GLDH is thought to be a good biomarker for acute liver injury since its levels increase significantly after hepatocellular damage and it has high tissue specificity (O'Brien et al., 2002; Ramaiah, 2007).

Alkaline phosphatase (ALP) is mainly located within the biliary canaliculi and epithelial cells comprising the bile ducts (Kaplan and Righetti, 1970). ALP can also be found in the bone and kidneys (Yusa et al., 2000). Increases in the plasma levels of this enzyme are considered a marker of hepatobiliary effects and cholestasis (Swain et al., 1993; Ramaiah, 2007).

The current standard for assessing liver injury relies on the measurement of ALT and AST. The problem with these enzymes is that the levels do not change considerably from control values, until a great degree of injury has been induced. Also, neither of these enzymes are uniquely specific to the liver; therefore, increased blood levels do not necessarily mean hepatocyte injury. This has led to a major increase in the investigation for new biomarkers that perform better and can easily translate from preclinical to clinical studies (Schmidt and Schmidt, 1988; Gores et al., 1990; Van Hoof et al., 1997; Giffen et al., 2002).

1.3.2 Markers of fibrosis

Serum biomarkers for liver fibrosis can be differentiated into 2 categories: indirect and direct markers. Indirect markers may be released into the blood as a result of inflammation (ALT and AST) (Giffen et al., 2002) and also include molecules that are

synthesised or excreted by the liver, for example albumin, clotting factors and bilirubin. Additionally, markers of biochemical pathways that may be disrupted as a consequence of impairment to liver function, including for example the development of insulin resistance, can be considered indirect markers (Adams, 2011; Castera, 2011). Direct markers of fibrosis include degradation products of extracellular matrix (for example MMPs, TIMPs, hyaluronic acid (HA)).

1.3.2.1 Indirect markers

Albumin is the most abundant plasma protein and is synthesised in the liver. Consequently, a reduction in plasma albumin levels often occurs when there is impaired liver function, such as fibrosis and cirrhosis (Carey and Carey, 2010). Decreases in the serum concentration of albumin have been previously reported in models of CCl_4-induced hepatic fibrosis/cirrhosis (Gou et al., 2013).

Most of the clotting factors, including factors I, II, V, VII, IX and X, are synthesised in the liver by parenchymal cells, therefore, disruption of hepatocellular function will be reflected in coagulation abnormalities (Mammen, 1992). In cirrhosis, the liver function is compromised and consequently there is decreased production of clotting factors which results in increased prothrombin time (Kujovich, 2005; Amarapurkar and Amarapurkar, 2011).

Increased bilirubin is also frequently observed in end stage cirrhosis (Grigorescu et al., 2007; Carey and Carey, 2010). Bilirubin results from the breakdown of haemoglobin in the liver and may be classified as direct or indirect bilirubin. Direct or conjugated bilirubin is the form that has been removed from the blood by the liver and absorbed by the hepatocytes, whereas indirect or unconjugated bilirubin may increase in cases of anaemia or diseases where there is increased breakdown of red blood cells.

Indirect markers of fibrosis also include glucose, which is often increased in the serum as a consequence of insulin resistance. Impaired insulin sensitivity and subsequent impaired glucose tolerance are often present in chronic liver disease including cirrhosis (Petrides et al., 1998; Hickman and Macdonald, 2007).

Monocyte chemoattractant factor 1 (MCP1) is thought to be a marker of liver fibrosis and the expression of MCP1 has been widely studied in several pathological conditions including pulmonary fibrosis, kidney disease and atherosclerosis (Yu et al., 1993;

Grandaliano et al., 1996). However, the role of MCP1 in the liver has not been fully studied. Marra and colleagues (1993) demonstrated that MCP1 is one of the most important chemotactic factors secreted by HSCs. Data collected from both *in vitro* and *in vivo* studies suggests a role for HSC in the expression of MCP both in chronic and acute liver injury (Maher and McGuire, 1990; Czaja et al., 1994; Marra et al., 1998). In a experimental model of CCl_4-induced liver damage in mice MCP1 levels were found to be increased in the serum (Karlmark et al., 2009).

A2M is a plasma globulin secreted by hepatocytes and functions as an inhibitor of the coagulation and fibrinolytic systems (Kawser et al., 1998). A2M has been shown to bind and inactivate proteases from the metalloproteinase class including collagenases (Barrett and Starkey, 1973). Therefore, the increase in A2M expression is thought to play a role in mediating the decrease in MMP activity as fibrosis progresses (Truden and Boros, 1988; Kawser et al., 1998).

α-1-acid glycoprotein (AGP) is one of the major acute phase proteins. It is mainly secreted by hepatocytes and has been shown to increase following hepatic injury (Fournier et al., 2000). Sugihara and co-workers proposed a mechanism for the increase in AGP plasma levels involving necrosis of the parenchymal cells and infiltration of inflammatory cells leading to the secretion of cytokines which would in turn trigger the production of acute-phase proteins like AGP (Sugihara et al., 1992). Goldberg et al., (1983) have also previously reported increases in plasma AGP levels in rat models of CCl_4-induced hepatic necrosis. Similarly, upregulation of AGP expression has been documented in cirrhotic livers (Mirpuri et al., 2002).

1.3.2.2 Direct markers

As described in Section 1.3.2, liver fibrosis can be detected by measurement of direct markers for the fibrotic process. ECM degradation is mediated by MMPs which in turn are regulated by TIMPs (Brew et al., 2000). In hepatic fibrosis there is a significant accumulation of ECM that results from both increased synthesis and decreased degradation. This leads to a wound healing process characterised by progression of the scarring of the tissue instead of resolution (Benyon and Arthur, 2001).

TIMPs are important regulators of MMPs, including interstitial collagenase and gelatinase A and B (Murphy et al., 1991; Iredale et al., 1996). TIMPs act by inhibiting the proteolytic activity of the MMPs (Brew et al., 2000).

Both MMPs and TIMPs are regulated by growth factors such as TGF-β resulting in downregulation of MMP expression and upregulation of TIMP expression (McAnulty et al., 1991; Hall et al., 2003).

The major sources for TIMP-1 production in liver fibrosis are activated HSCs and Kupffer cells (Herbst et al., 1997; Wang et al., 2011). Therefore, serum levels of TIMP-1 are thought to be good indicators of liver fibrosis (Roderfeld et al., 2006). TIMPs are known to increase in expression as fibrosis progresses which will result in greater inhibition of MMPs. Therefore, decreased levels of MMPs and increased TIMP levels in the serum are strongly associated with fibrotic progression and will be apparent with increased injury. Previous studies investigating interstitial collagenase activity during CCl_4-induced liver fibrosis have shown a decrease in activity as the disease progresses (Montfort and Perez-Tamayo, 1978) and an increase in TIMP-1 expression by HSCs (Iredale et al., 1996; Herbst et al., 1997).

Hyaluronic acid (HA) is classified as a direct marker of liver fibrosis. It is a component of the extracellular matrix and is synthesised by hyaluronic acid synthases located in HSCs (Rostami and Parsian, 2013). HA is a high molecular weight polymer ($>1x10^6$ Da) (Maharjan et al., 2011), and can be found in the extracellular, pericellular and intracellular spaces (Rostami and Parsian, 2013). The main function of HA is to regulate water flow in the extracellular matrix; water flow is important for maintaining the structural organisation of the tissue (George et al., 2004). The liver is responsible for both the synthesis and removal of HA by sinusoidal endothelial cells which have the ability to uptake and metabolise HA (Deaciuc et al., 1993). During liver injury, HA breaks down into smaller fragments (Maharjan et al., 2011). In fibrosis, dysfunctional sinusoidal endothelial cells are responsible for increased serum levels of HA as the ability to eliminate HA is compromised. Accumulation of HA in the sinusoidal endothelial cells plays a major role in the formation of the basement membrane responsible for the capillarisation of sinusoids (George et al., 2004). CD44 is the major receptor for HA in sinusoidal endothelial cells and regulates the degradation of HA. Decreased levels of this receptor have been reported in models of cirrhosis (George et al., 2004). Additionally, activation of HSCs and proliferation during fibrogenesis may also contribute to an increased expression of HA which can leak into the blood. Consequently, increased serum levels of HA can be used to measure the progression of liver fibrosis (Deaciuc et al., 1993; Saegusa et al., 2002; Rossi et al., 2007).

1.3.3 Serum marker panels

Since no one serum marker is reliable enough to be used individually for the detection of fibrosis, several different serum markers have been selected for the creation of algorithms which can be used to evaluate fibrosis. These biomarker panels may include direct and indirect serum markers of fibrosis. The diagnostic value of these panels is assessed by calculating the area under the receiver operating characteristic curves (AUROC), which represents the probability that a particular test will be able to correctly classify 2 patients, one with a normal liver biopsy and one with a liver biopsy considered abnormal (Bedossa and Carrat, 2009). These scores have been able to substantially increase diagnostic accuracy.

Currently, there are several different serum panels for differentiating control from fibrotic livers. These include the FibroTest, which measures A2M, haptoglobin, γ-glutamyltransferase, apolipoprotein A1 and bilirubin; and the Fibrometer which comprises platelet count, prothrombin index, AST, A2M, HA, urea and age (Rossi et al., 2003; Friedrich-Rust et al., 2010).

1.3.4 Imaging techniques

Deposition of ECM is responsible for causing changes to the liver microstructure and architecture that can be detected using imaging techniques. Some of these techniques include ultrasonography (US) and transient ultrasound elastography.

1.3.4.1 Ultrasonography

Ultrasonography (US) is one of the imaging techniques used for non-invasive estimation of the degree of fibrosis. US uses high-frequency sound waves to create an image of the internal organs. Sound waves that are reflected to the transducer are converted into an image (Nishiura et al., 2005).

Hepatic US is inexpensive and is considered to be a reliable tool in detecting hepatocellular carcinoma (Nishiura et al., 2005). US allows the characterisation of several parameters that are useful in assessing the degree of chronic liver injury, including the nodularity of the tissue, degree of homogeneity of the liver parenchyma, size of the lymph nodes around the hepatic artery, size of the spleen and presence of ascites (Outwater, 2010).

Echogenicity refers to the variety of characteristics that define the appearance of tissues. Normally, the hepatic parenchyma is homogeneous with medium level echogenecity and equal or slightly more echogenic than the kidneys. Its echogenic texture is interrupted by the portal and hepatic veins; whereas a fibrotic/cirrhotic liver is characterised by heterogeneous patchy or diffuse echogenecity and this is related to the development of fatty liver and scar tissue (Tchelepi et al., 2002).

1.3.4.2 Transient ultrasound elastography (FibroScan)

This imaging technique measures the stiffness of the liver parenchyma by using a combination of ultrasound and low frequency elastic waves. The fibrotic liver is harder than a normal liver due to the deposition of collagen fibres which alter the architecture of the liver and increase the rigidity of the parenchyma. The FibroScan is composed of a probe that generates an elastic shear wave that propagates within the liver. Measurements are made to determine the speed of the shear wave and this correlates directly with tissue stiffness, the harder the tissue the faster this waves propagates. Measurements can take less than 5 minutes to collect (Baranova et al., 2011). However, this technique is considered unreliable in humans if the patient is obese or has ascites. Additionally, it cannot detect the early stages of the disease.

1.3.5 Liver biopsy

Currently, liver biopsy is still regarded as the gold standard for the diagnosis and assessment of hepatic fibrosis (Bataller and Brenner, 2005; Rossi et al., 2007; Martinez et al., 2011). It is a highly invasive procedure where, by using a needle, a tissue sample is surgically removed for histological examination. Therefore, liver biopsy cannot be used as a routine clinical method for assessing liver disease, and due to the reduced sample size may provide erroneous results (Bedossa et al., 2003; Standish et al., 2006; Carey and Carey, 2010).

Therefore, a combination of routine biochemical tests, and abdominal US examination remain the most frequently used methods for the diagnosis of hepatic injury (Schuppan and Afdhal, 2008). More recently, the problems inherent to liver biopsy have fuelled the need for alternative methods of assessing liver injury, particularly in regards to their ability to detect early stages of disease (Castera, 2011).

It is the need for more specific and more sensitive biomarkers, which can be measured by non-invasive means, preferably in urine samples, that was the main driving force behind this project.

1.4 Carbon tetrachloride

CCl_4 is one of the most commonly used hepatotoxicants (de Zwart et al., 1998; Hiyoshi et al., 2009). CCl_4 is metabolised in the liver by cytochrome P-450 to produce reactive free radicals which can initiate lipid peroxidation (Recknagel and Ghoshal, 1966; Recknagel, 1967; Brattin et al., 1985).

CCl_4 is metabolised in the liver smooth endoplasmic reticulum by cytochrome P-450, mainly the cytochrome P-450 2E1 isoform. The product of this metabolism is the trichloromethyl free radical ($CCl_3^{\bullet}$) which can undergo both anaerobic and aerobic reactions (Brattin et al., 1985). The half-life of the trichloromethyl free radical is approximately 100 μs, therefore, toxic effects caused by the radical tend to be close to the site of production (Slater, 1966). The concentration of cytochrome P-450 is greatest in the centrilobular region making this area most susceptible to injury (Recknagel et al., 1989). Early studies proposed that the mechanism responsible for the formation of the free radical was the homolytic cleavage of CCl_4 (Brattin et al., 1985). However, this reaction is thermodynamically unfavourable and requires 68 kcal/mol for the homolytic cleavage of the C-Cl bond. Therefore, it is considered that the mechanism involved in CCl_4 metabolism consists of a one-electron reduction of CCl_4 by the NADPH-cytochrome P450 system which transfers one electron from NADPH to CCl_4. This process results in the formation of an anion radical that will produce $CCl_3^{\bullet}$ and a chlorine ion (Cl^-) (Figure 1.5) (Brattin et al., 1985).

In the absence of oxygen, $CCl_3^{\bullet}$ may diffuse into the phospholipid bilayer of the endoplasmic reticulum (Rao and Recknagel, 1969; Trudell et al., 1982) where it may abstract a hydrogen atom from a methylene group on polyunsaturated fatty acids to form chloroform ($CHCl_3$) (Trudell et al., 1982). Under these conditions, the $CCl_3^{\bullet}$ free radical can also bind to lipids, proteins and DNA (Figure 1.5).

Under aerobic conditions, the $CCl_3^{\bullet}$ can react with oxygen to form a trichloromethylperoxyl free radical ($Cl_3COO^{\bullet}$) (Figure 1.5). This radical has been proven to be a stronger electrophilic agent and more reactive than $CCl_3^{\bullet}$ and can abstract a hydrogen atom from polyunsaturated fatty acids in the membrane to generate further

free radicals (Recknagel et al., 1989; Weber et al., 2003). This leads to a claim of free radicals and the initiation of a cascade of events called lipid peroxidation (Recknagel, 1967; Brattin et al., 1985). This chain reaction terminates with the production of lipid breakdown products, including lipid alcohols, aldehydes or malondialdehyde (Recknagel, 1967; Bagchi et al., 1993; Fanelli and Castro, 1993). Ultimately, the chain of events results in the destruction of membrane structure and loss of organelle integrity. The products of lipid peroxidation have much longer half-lives than the trichloromethyl free radical or the trichloromethylperoxyl free radical and therefore they can migrate and induce more widespread injury (Slater et al., 1985). It has been proposed that the trichloromethylperoxyl free radical is responsible for most of the CCl_4-induced toxic effects since the $CCl_3^{\bullet}$ radical is less reactive. In fact, the covalent binding of $CCl_3^{\bullet}$ to proteins occurs in the absence of oxygen, but the destruction of other enzymes of the endoplasmic reticulum requires oxygen to be present.

Instead of initiating lipid peroxidation the trichloromethylperoxyl free radical may react further to produce trichloromethanol, which in turn can lead to the generation of phosgene and a chlorine radical (Figure 1.5). Phosgene was once thought to play an important role in CCl_4-induced hepatotoxicity. However, *in vitro* studies using cysteine, a known phosgene scavenger, have shown that eliminating phosgene does not reduce the toxic effects of CCl_4 (Waller and Recknagel, 1982). In addition, phosgene undergoes a high rate of spontaneous hydrolysis which means large concentrations would be required to produce the toxic effect of CCl_4. The amount of phosgene produced from CCl_4 metabolism is much lower than the necessary concentration (Brattin et al., 1985).

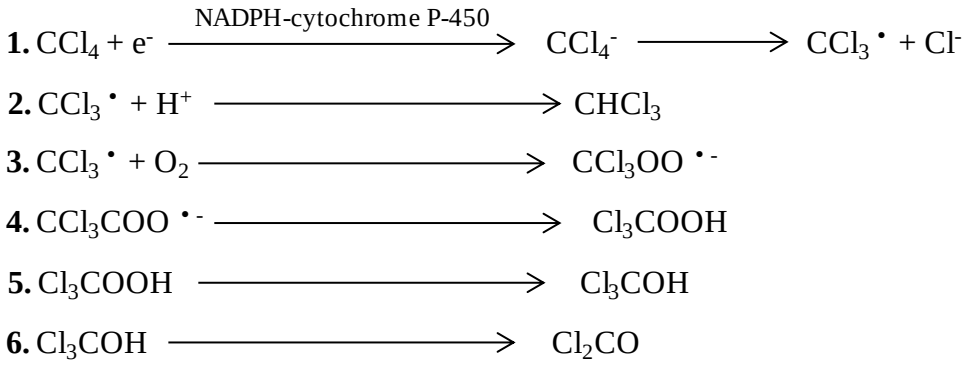

Figure 1.5 Biotransformation of carbon tetrachloride. 1. One-electro reduction catalysed by $NADPH^-$ cytochrome P-450 system and production of trichloromethyl free radical ($CCl_3^{\bullet}$) and chlorine ion (Cl^-); 2. trichloromethyl free radical abstract a hydrogen to produce chloroform ($CHCl_3$); 3. trichloromethyl free radical reacts with oxygen to generate trichloromethylperoxyl free radical ($CCl_3COO^{\bullet}$); 4./5. trichloromethylperoxyl free radical further reacts to produce trichloromethanol (Cl_3COH); 6. trichloromethanol reacts to produce phosgene (Cl_2CO).

Lipid peroxidation occurs rapidly following CCl_4 administration (Recknagel, 1983). It is known that CCl_4-induced lipid peroxidation can be detected within 5 minutes of dosing (Recknagel, 1967; Rao and Recknagel, 1968). One of the main processes affected by lipid peroxidation is the capacity of the endoplasmic reticulum to sequester Ca^{2+} ion. This would result in the release of Ca^{2+} from the endoplasmic reticulum into the cytosol with pathological consequences (Recknagel, 1983; Pencil et al., 1984). The level of cytosolic free Ca^{2+} is reported to participate in the regulation of several processes, such as intracellular traffic of VLDLs and secretion of triglycerides by the liver cells. Disruption of this process will result in the accumulation of triglycerides and consequently, in the development of a fatty liver (Recknagel, 1983). Moreover, it has been shown that decreased amounts of calcium sequestered in the endoplasmic reticulum have an inhibitory effect on protein synthesis (Mandl et al., 1982; Kimball and Jefferson, 1992). This leads to a decrease in the synthetic function of the liver.

One of the mechanisms that appears to confer some protection against CCl_4-induced toxicity is the administration of a small dose of CCl_4 prior to the administration of a much larger dose 24 hours later (Ugazio et al., 1972). Ugazio et al., (1972) demonstrated maximal protection from the second larger dose at 24 hours after a smaller first dose. This mechanism has been referred to as "suicidal inactivation" (Manno et al., 1992). Hepatocytes were protected for 3 days before susceptibility to CCl_4-induced toxicity returned (Ugazio et al., 1972). This self protection is related to a depression of cytochrome P-450 enzyme activity by the first dose of CCl_4 prior to the administration of a larger dose level.

1.5 The kidney

The kidney is composed of two regions: the outer cortex and the inner medulla. The main functional unit of the kidney is the nephron; each nephron consists of a glomerulus surrounded by the Bowman's space, a proximal tubule, and a distal tubule. The proximal tubule plays an important part in maintaining homeostasis via the reabsorption of water, sodium and chloride ions, and also by a number of absorptive and secretory mechanisms (Zhang, 1999).

The kidneys are responsible for the regulation of body fluid osmolarity and volume, electrolyte and acid-base balance and for maintaining blood pressure. Additionally, they are also involved in excretory and secretory processes and are the main site of

elimination of metabolic products and toxins as well as the production and secretion of hormones such as erythropoietin (Lote, 2012).

1.5.1 Urine formation

Urine formation occurs in 3 sequential steps: glomerular filtration, tubular reabsorption and tubular secretion.

The filtration step occurs in the glomerulus and involves the ultrafiltration of plasma in the glomerulus. Blood is supplied to the kidney by the renal artery, before entering and leaving the nephron via the afferent and efferent arteriole. As blood flows through the glomerulus it is filtered into the Bowman's capsule. The glomerulus is a semi-permeable membrane which has a fenestrated endothelium, a glomerular basement membrane and a podocyte layer. This semi-permeable membrane is freely permeable to water and small molecules but is impermeable to larger molecules and blood particles. The hydrostatic pressure within the glomerular capillaries forces the protein-free plasma out of the capillaries and into the Bowman's capsule (Khurana, 2009).

There are however, two forces that oppose the hydrostatic pressure: the plasma osmotic pressure which results from the difference in protein concentration across the glomerular membrane; and the Bowman's capsule hydrostatic pressure which is the pressure exerted by the fluid in the initial part of the tubule. Therefore, the net filtration pressure is the result of the balance between the hydrostatic pressure within the glomerular capillaries, that favours filtration; the plasma osmotic pressure and the Bowman's capsule hydrostatic pressure, that oppose filtration (Williams and Schafer, 1987).

Tubular reabsorption of substances such as potassium, sodium and bicarbonates, consists of the passage from the tubular lumen into the blood capillaries and involves active and passive transport mechanisms. Cells in the proximal convoluted tubules actively reabsorb nutrients, ions and proteins from the tubular fluid. In man, virtually all proteins are reabsorbed back into the blood. However, if the concentration of the proteins being filtered increases significantly, some of these proteins may appear in the urine. The reabsorption of sodium into the cytosol of the epithelial cells, and further into the interstitium and subsequently into the blood creates an osmotic gradient leading to water reabsorption from the tubules. The final result is a highly concentrated fluid. In the ascending limb of the loop of Henle, Na^+ and Cl^- are actively pumped out of the

tubular fluid by Na^+-K^+ ATPase pump. In the distal tubule and collecting duct, Na^+, Cl^- and Ca^{2+} are reabsorbed along with water whereas K^+ and H^+ are secreted (Ashalatha and Deepa, 2011).

The final step in urine formation consists of the movement of substances out of the capillaries and into the distal and collecting tubules (Sands and Layton, 2009)

Once urine has been formed in the kidneys it travels through the ureters to the urinary bladder. Peristaltic contractions of the ureteral wall force the movement of urine into the bladder (Sherwood, 2013).

The human urinary protein content is very different from that of rat urine. Indeed, it appears that the humans only excrete approximately 1 % of the protein concentration found in urine samples from male rats (Olson et al., 1990).

1.6 Kidney injury

The kidneys are one of the main target organs for drug-induced toxicity for several reasons. Firstly, the kidneys have a high blood flow. Therefore, drugs which are present in the systemic circulation will be delivered to the kidneys in particularly high amounts. Secondly, most toxicants will be excreted via the urine and often these xenobiotics become concentrated in the nephron as a result of water reabsorption. Progressive concentration of xenobiotics in the nephron may cause them to precipitate thus inducing acute kidney injury (AKI) secondary to tubular obstruction. Renal transport and metabolism of toxicants also greatly contribute to increased susceptibility of the kidney to drug-induced injury (Werner et al., 1995; Pfaller and Gstraunthaler, 1998).

1.6.1 Biomarkers of kidney injury

Biomarkers of renal injury can be used to: identify the primary location of the injury; determine the duration of kidney failure; distinguish between different types of AKI and different aetiologies; define the course of disease and monitor the response to interventions (Devarajan, 2007).

1.6.1.1 Serum markers

Traditionally, clinical evaluation of renal function relied on the measurement of blood urea nitrogen (BUN) and serum creatinine as markers of a reduction in the glomerular

filtration rate (GFR). Both urea and creatinine are freely filtered in the glomerulus. Creatinine undergoes tubular secretion, whereas, urea is not secreted but instead is reabsorbed by the renal tubules (Schrier, 2008). A decrease in renal blood flow or compromised kidney function, as a result of kidney injury, can reduce the glomerular filtration rate, and consequently result in increased serum creatinine and urea.

Serum creatinine levels can also reflect several non-renal factors including body weight, age, gender, race, muscle metabolism and protein intake (Doi et al., 2009). Additionally, creatinine is not a very sensitive biomarker for kidney function in AKI, since levels do not reflect injury until approximately 50 % of the renal function is lost (Burke et al., 1984; Jacobs et al., 2004).

AKI is characterised by a rapid decrease in renal function with a reduced ability to excrete toxins, concentrate the urine and maintain fluid balance.

1.6.1.2 Urinary markers

Urine is the preferred biofluid for biomarker detection and measurement since it can be obtained by non-invasive methods, causes minimal stress to the patient or animal, allows repeated sampling and can be obtained in large quantities.

In man, the presence of a large protein concentration in the urine is often a sign of renal dysfunction since proteins are not normally filtered from the glomerulus into the Bowman's space. Additionally, almost 100 % of the protein that is filtered is reabsorbed in the proximal tubules. Increased urinary protein may occur when there is an excess of protein in the filtrate which exceeds the tubular reabsorptive capacity; a compromise of the glomerular permeability, thus allowing increased filtration of plasma proteins; or when there is an overflow of low-molecular weight proteins in the blood that are freely filtered by the glomerulus (overflow proteinuria) (for example. haemoglobinuria occurring in states of intravascular haemolysis, or myoglobinuria which occurs when there is severe muscle injury).

In the last decade many studies have contributed to the development of useful panels of kidney injury biomarkers, including α-glutathione S-transferase (α-GST), glutathione S-transferase Yb1 (GST Yb1), lipocalin-2 and osteopontin (Wang et al., 2008). More recently, in response to data arising from the search for biomarkers of renal injury in toxicology studies, the Food and Drug Administration (FDA) and the European

Medicines Agency (EMA) have allowed the inclusion of 7 urinary biomarkers in investigational or regulatory rat studies. These include KIM-1, albumin, total protein, β-2 microglobulin, cystatin-C, clusterin and trefoil factor-3. These biomarkers can be used to evaluate kidney damage during animal studies as part of the drug-review process. Their inclusion is not compulsory but if measured they should be reported to the FDA. The ultimate goal is to be able to translate these biomarkers to human tests for detecting drug-induced kidney injury in people as early as possible, thus allowing healthcare professionals to closely monitor patients and therapeutics.

Glutathione-S-transferases (GSTs) are cytosolic enzymes which are present in the proximal and distal tubules. GSTs are involved in the detoxification process of many compounds including electrophilic substrates, by decreasing their reactivity with cellular macromolecules (Armstrong, 1997; Lock and Reed, 1998; van Lieshout et al., 1998). α-GST is thought to make up as much as 2 % of the total protein present in the cytosol of tubular epithelial cells and following damage to the cellular membranes the enzyme is released into the tubular lumen (Bruning et al., 1999). GSTs can also be found in the liver, testes, lungs and brain (Eaton and Bammler, 1999). Urinary α-GST levels appear to correlate well with histopathological evidence of degeneration and reflect the role of the enzyme as a marker of increased cellular membrane permeability and cellular damage (Maguire et al., 2013). GST Yb1 can be mainly found in the epithelial cells of the distal renal tubules (Rozell et al., 1993; Otieno et al., 1997). Both α-GST and GST Yb1 are considered to be good biomarkers of kidney injury and are often used in toxicological studies. Increased urinary levels of these enzymes have been previously reported in models of HCBD-induced proximal tubular injury (Swain et al., 2012; Maguire et al., 2013).

Lipocalin-2 is a 25-kDa glycoprotein classified as an extracellular transport protein with a high affinity for hydrophobic proteins such as fatty acids and cholesterol (Kjeldsen et al., 1994; Borkham-Kamphorst et al., 2011). It is present in many tissues including liver, kidneys, lungs, adipocytes and macrophages (Liu and Nilsen-Hamilton, 1995). Lipocalin-2 is highly expressed and released by the liver in response to inflammation (Liu and Nilsen-Hamilton, 1995; Flo et al., 2004). A study by Borkham-Kamphorst et al., (2011) showed increased lipocalin-2 expression in CCl_4 injured hepatocytes compared to control animals in both acute and chronic liver injury models and it was hypothesised that damaged hepatocytes were the main source of lipocalin-2 production (Borkham-Kamphorst et al., 2013). However, there is evidence that lipocalin-2 is

excreted into the urine in the event of renal toxicity (Paragas et al., 2011). Therefore, urinary lipocalin-2 levels are often measured as a marker for ischemic renal injury (Mishra et al., 2003, Mori et al., 2005) despite the lack of specificity (Liu and Nilsen-Hamilton, 1995).

Osteopontin is a glycoprotein with a molecular weight of approximately 44 kDa. It is expressed in different tissues such as the kidney, lung and liver (Xie et al., 2001b). Osteopontin is secreted by the kidneys into the urine by epithelial cells, including the loop of Henle and distal convoluted tubule (Kleinman et al., 1995). It is thought to act as an inhibitor of calcium oxalate formation, thus having a role in preventing mineral precipitation and renal stone formation, since these are comprised of calcium oxalate (Asplin et al., 1998; Xie et al., 2001b). Osteopontin is normally found in cells in the distal tubules (Verhulst et al., 2002) and osteopontin mRNA expression has been shown to be upregulated in rodent models of kidney injury (Verstrepen et al., 2001). However, the is also evidence suggesting the association between increased urinary levels of osteopontin and histopathological signs of regeneration of the proximal tubular cells (Persy et al., 1999; Xie et al., 2001a; Swain et al., 2012). Xie et al., (2001a) hypothesised that the mechanism for osteopontin-mediated regeneration could be attributed to its ability to bind to CD44, which would block the binding of HA to CD44. HA has been shown to inhibit tubular cell proliferation and to have an inhibitory effect on cell growth and cell differentiation. By binding to CD44, osteopontin would block the inhibition of HA (Xie et al., 2001a).

KIM-1 is a transmembrane protein and expression has been shown to increase in the proximal tubule of the post-ischemic rat kidney (Han et al., 2002; Ichimura et al., 2008; Zhou et al., 2008; Swain et al., 2012). KIM-1 is expressed on the apical membrane of proximal tubular cells followed by cleavage of the ectodomain (90 kDa) which is then released in the urine (Pennemans et al., 2011). The ectodomain of this protein is shed from the outside of the cell and is considered to be a marker of both kidney degeneration and repair (Swain et al., 2011; Swain et al., 2012; Maguire et al., 2013). It is found in the proximal epithelial cells of the S3 segment and is thought to be involved in the phagocytosis of apoptotic cells in the renal tubular lumen (Ichimura et al., 2008; Ichimura et al., 2012).

Clusterin is a protein expressed on the proximal tubular cells and has been shown to protect cells from stress, transport lipids and promote cell aggregation. Clusterin is also

present in the testes, liver, stomach and brain; in the kidneys it has been suggested to have anti-apoptotic functions (Rosenberg and Silkensen, 1995; Dieterle et al., 2010; Garcia-Martinez et al., 2012). Clusterin has a molecular weight of 76-80 kDa and under normal conditions the concentration found in the urine is very low. Consequently, the appearance of increased clusterin in the urine is accompanied by renal damage (Dieterle et al., 2010). Increased urinary levels of clusterin have been reported following ischemic and reperfusion injury to the kidney, as well as toxicant-induced renal injury (Witzgall et al., 1994).

β-2 microglobulin is a polypeptide chain with a molecular weight of 12 kDa. Normally, only a very small fraction of the β-2 microglobulin that is filtered by the glomerulus is excreted in the urine (0.3 %) (Dieterle et al., 2010). The majority of β-2 microglobulin is reabsorbed and degraded in the proximal tubules (Miyata et al., 1998). However, when tubular function is compromised, for example in AKI, the reabsorption of β-2 microglobulin is impaired and therefore increased levels are present in the urine (Vaidya et al., 2008). Consequently, urinary β-2 microglobulin is measured as a marker for proximal tubular dysfunction (Miyata et al., 1998).

Cystatin-C is a low molecular weight protein (13 kDa) that is filtered from the blood in the glomerulus (Vaidya et al., 2008). Similar to β-2 microglobulin, cystatin-C is freely filtered in the glomerulus and almost completely reabsorbed before being metabolised in the proximal tubules (Herget-Rosenthal et al., 2007; Dieterle et al., 2010). Consequently, impairment in the reabsorption of cystatin-C in the proximal tubules will result in the appearance of increased urinary levels of cystatin-C (Conti et al., 2006; Herget-Rosenthal et al., 2007).

Trefoil factor-3 is a protein secreted by mucus-producing cells and by epithelial cells of several tissues including the kidney (Yu et al., 2010b). In humans, trefoil factor-3 is predominantly found in the cells of the proximal and distal tubules and in the collecting duct (Rinnert et al., 2010). Trefoil factor-3 has been shown to be involved in the formation of mucous barriers and has antiapoptotic effects. Yu and co-workers (2010b) reported a decrease in urinary trefoil factor-3 levels following the administration of cisplatin (a known nephrotoxicant) to rats. It has been proposed that this decrease in urinary levels of trefoil factor-3 is mediated by a gene regulatory response to tubular toxicity, however, the mechanism for this observation has yet to be fully described (Yu et al., 2010b).

Albumin is filtered from the blood and is almost completely reabsorbed by the proximal tubule (Lazzara and Deen, 2007); therefore, injury to the proximal tubules may result in albuminuria. Albumin is considered to be a marker for both proximal tubular function and glomerular integrity (Swain et al., 2011). Recent studies, investigating the potential for albumin as a urinary marker of AKI, have shown that it outperforms both serum creatinine and urea in terms of sensitivity (Yu et al., 2010b; Bolisetty and Agarwal, 2011).

In this project we are investigating urinary biomarkers of CCl_4-induced liver toxicity. Therefore, it is of the utmost importance to guarantee that there will be no nephrotoxicity. These urinary markers of nephrotoxicity will be analysed to determine sensitivity to low levels of kidney injury and consequently used to detect any potential nephrotoxicity in our CCl_4 liver models.

1.7 Hexachlorobutadiene

Hexachlorobutadiene (HCBD) is a halogenated solvent formed as a by-product of trichloroethylene and perchloroethylene (Ishmael and Lock, 1986).

HCBD is known to have a toxic effect on the kidneys (Lock and Ishmael, 1981; Ishmael and Lock, 1986; Birner et al., 1995; Birner et al., 1998). It causes damage selectively to the *pars recta* of the proximal tubule in the rat. This segment is especially sensitive due to the concentration of cysteine β-lyase, which is involved in the mechanism for HCBD-induced toxicity, than can be found here (Berndt and Mehendale, 1979; Lock and Ishmael, 1979).

In the liver, HCBD undergoes conjugation with glutathione to give S-(pentachlorobutadienyl)-glutathione (Nash et al., 1984). The toxic conjugate S-(pentachlorobutadienyl)-glutathione is then translocated to the kidneys to be converted to S-(pentachlorobutadienyl)-L-cysteine (Birner et al., 1995). Alternatively, S-(pentachlorobutadienyl)-glutathione may be converted by intestinal γ-glutamyl transpeptidases and dipeptidases to S-(pentachlorobutadienyl)-L-cysteine, which is reabsorbed from the gut and translocated to the kidneys (Dekant et al., 1988; Birner et al., 1995; Birner et al., 1998). In the kidneys, S-(pentachlorobutadienyl)-L-cysteine is N-acetylated producing N-acetyl-S-(pentachlorobutadienyl)-L-cysteine which is either excreted via the urine (Dekant et al., 1986) or cleaved by cysteine conjugate β-lyase to give pyruvate, ammonia and a reactive thiol (Nash et al., 1984; Dekant et al., 1986;

Ishmael and Lock, 1986; Dekant et al., 1988). This reactive thiol group may covalently bind to macromolecules, such as lipids and proteins, initiating a sequence of events which leads to an increase in the levels of cytosolic free Ca^{2+} and, consequently, necrosis (Chen et al., 1992; Townsend et al., 2003). It has also been suggested that the reactive thiol can bind to mitochondrial DNA and nuclear DNA and this can lead to the mechanism of HCBD-induced carcinogenesis (Schrenk and Dekant, 1989). Renal mitochondrial DNA is thought to be a target as a result of the high concentration of β-lyase present in the mitochondrial membrane (Schrenk and Dekant, 1989).

The histopathological lesion characteristic of HCBD-induced nephrotoxicity has been extensively described in the literature (Lock and Ishmael, 1979; Lock and Ishmael, 1981; Ishmael et al., 1982; Lock et al., 1985; Ishmael and Lock, 1986; Birner et al., 1995; Birner et al., 1998; Swain et al., 2011; Swain et al., 2012; Maguire et al., 2013). The nephrotoxic changes consist of degeneration and necrosis of the S3 segment of the proximal tubule. However, the glomeruli, loops of Henle, distal tubules and collecting tubules are often unaffected. The earliest pathological HCBD-induced changes occur 8 hours post-administration and include aggregation of the smooth endoplasmic reticulum; mitochondrial swelling; cytoplasmic vacuoles, resulting from lysosomal degranulation, and cellular necrosis. By 16 to 24 hours post-dosing, there is more extensive tubular necrosis, particularly to the S3 segment (Ishmael et al., 1982). The presence of luminal granular casts has also been described in the distal segments of the nephron following HCBD administration (Ishmael et al., 1982). Casts consist of particles and debris from cellular breakdown as a consequence of necrosis of the proximal tubule segments (Hard, 2008).

The accumulation of α-2μ globulin, which is a protein synthesised in the liver of the male rats (Roy et al., 1966; Pahler et al., 1997; Hard, 2008; Swain et al., 2011) is the primary cause for the observation of presence of hyaline droplets (Hard, 2008). Approximately half of the α-2μ globulin synthesised in the liver is excreted in the urine and the rest is reabsorbed in the proximal tubules (Swenberg, 1993). The reabsorbed protein is retained in vesicles known as hyaline droplets. The vesicles fuse with lysosomes and the protein is degraded. Hyaline bodies appear as small eosinophilic bodies following H&E staining. Hyaline droplets can be present in different sizes and are most often seen in proximal convoluted tubules. Accumulation of hyaline droplets is the first step in α-2μ globulin nephropathy (Cristofori et al., 2013). The occurrence of hyaline bodies may also be associated with xenobiotic administration, including HCBD.

It has been reported that HCBD can bind to α-2μ globulin, thus inhibiting its degradation in the lysosomes. This leads to accumulation of α-2μ globulin in the cells and may cause degeneration and cell necrosis (Lehman-McKeeman et al., 1990).

1.8 Metabolomics and metabonomics

Global metabolic profiling refers to the study of low molecular weight molecules, up to approximately 1000 Da, including amino acids, sugars, bile acids as well as intermediaries of biochemical pathways including the tricarboxylic acid cycle (Clarke and Haselden, 2008). Metabolic profiling studies are concerned with the investigation of metabolite changes that reflect the dynamic multiparametric response of living organisms to genetic modification, physiological and pathophysiological stimuli (Holmes et al., 2001; Clarke and Haselden, 2008; Wu et al., 2011).

When describing the study of metabolites, metabonomics and metabolomics are two terms which are often used interchangeably in the literature. The term metabolome refers to the measurement of a complete set of metabolites within a cell under a particular set of conditions (Oliver et al., 1998). The metabolome changes depending on the physiological or pathophysiological state of the cell, tissue or organism (Oliver et al., 1998). Several types of metabolomes exist including the endogenous metabolome, the microbial metabolome and the xenometabolome, which includes metabolites that are a result of the metabolism of drugs and dietary compounds (Holmes et al., 2007; Monteiro et al., 2013).

The study of the metabolome has gained importance in toxicological studies where the main objective is to investigate changes in metabolites following the administration of drugs (Aardema and MacGregor, 2002; Cockerell et al., 2002). Drug-induced toxicity may alter metabolic pathways, leading to changes in metabolite levels which may be detected in biological samples. Many of these metabolites may pass into the circulation and are present in the urine. Therefore, serum and urinary metabolites have the potential to provide a "snapshot" of the recent events happening in a biological pathway (Clarke and Haselden, 2008). The metabolome is the final downstream product of gene transcription and is closest to the phenotype of the biological system studied compared to the transcriptome or the proteome; it reflects changes to the metabolic pathways that are occurring in the cells at a particular time. Therefore, in the present studies, a ^{1}H nuclear magnetic resonance (NMR) metabolomics-based investigation of changes to

urinary metabolites with drug-induced toxicity was preferred over a proteomics/genomics approach.

Metabolomics-based studies have been successfully applied to the investigation of models of nephrotoxicity (Robertson et al., 2000; Wei et al., 2008; Hanna et al., 2013) and hepatotoxicity (Beckwith-Hall et al., 1998; Holmes et al., 2000; Nicholls et al., 2001). Studies have focused on the identification of metabolite biomarkers for liver injury in animal studies using ^{1}H NMR spectrometry following the administration of hepatotoxicants, such as CCl_4, hydrazine and thioacetamide (model hepatotoxicant agents) in both acute and chronic models (Beckwith-Hall et al., 1998; Robertson et al., 2000; Nicholls et al., 2001; Wu et al., 2005). In the urine of rats treated with a single dose of CCl_4 the metabolite taurine was identified as a marker of hepatotoxicity (Waterfield et al., 1991; Waterfield et al., 1993; Waterfield et al., 1998). Repeated administration of CCl_4 resulted in increased urinary excretion of citrate as detected by gas chromatography coupled to mass spectrometry (Gou et al., 2013). An acute dose study with hydrazine revealed decreased urinary excretion of hippurate, citrate and succinate in the male Hanover-Wistar rat (Nicholls et al., 2001). A chronic study using thioacetamide as the hepatotoxicant agent reported increases in lactate, acetate and alanine in hepatic extracts from thioacetamide-treated rats (Constantinou et al., 2007).

The general metabolomics/metabonomics approach includes several steps; the first being sample generation/collection and preparation. Data collection follows and this is done by either mass spectrometry or NMR methods. Data collected by these methods requires processing prior to statistical analysis. For data obtained by NMR, data processing consists of peak alignment, data normalisation, signal extraction, baseline correction and integration. Multivariate statistical analysis is carried out using the processed data by pattern recognition methods such as principal component analysis (PCA). Variables displaying treatment-related effects are highlighted and potential biomarkers identified. Metabolite biomarkers require biological interpretation to confirm the relevance of the finding and prior to clinical application all biomarkers need to be validated in multiple studies (Figure 1.6) (Monteiro et al., 2013).

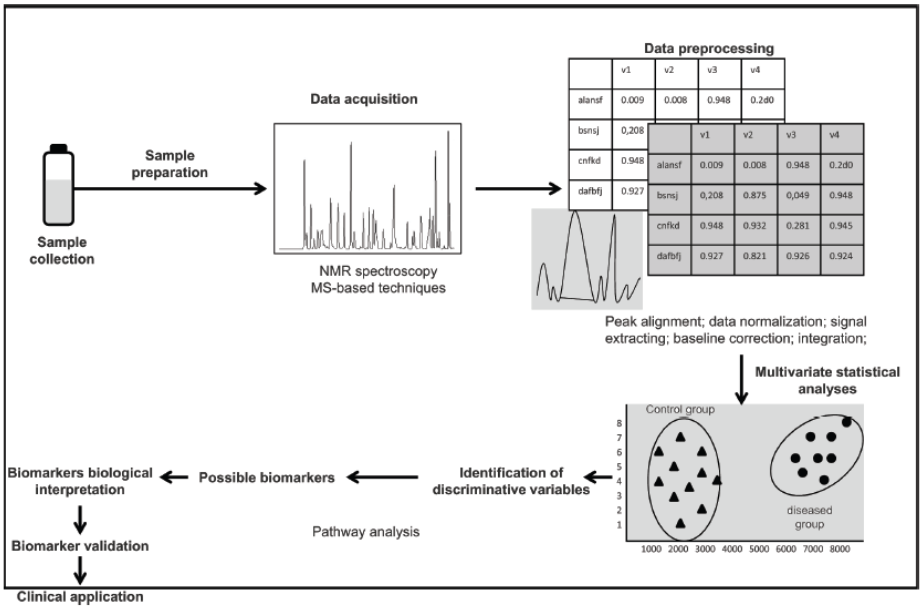

Figure 1.6 NMR metabolomics based-metabolite investigation of metabolites workflow (Monteiro et al., 2013).

The Consortium on Metabonomic Toxicology (COMET) was formed between 5 pharmaceutical companies and Imperial College, London, with the main objective to create a ^{1}H NMR-derived database of biofluids to be used in the assessment of drug candidates (Lindon et al., 2003; Lindon et al., 2005; Nicholson et al., 2007). The COMET project collected data from a large number of studies in which different toxicants were administered to rodents and ^{1}H NMR analysis of urine and serum samples was carried out. The NMR data was used to create a database that could be used for future reference in toxicological studies (Lindon et al., 2003). The information can be used to create a profile of metabolite changes according to the toxic compound administered. The ultimate goal is to provide a correlation between the ^{1}H NMR data, clinical chemistry and histopathological outcomes to predict metabolite biomarkers for toxicology (Nicholson et al., 2007). The COMET project was able to create a database comprising approximately 35,000 NMR spectra for the prediction of toxicity which has been transferred to the sponsoring companies (Lindon et al., 2005).

1.8.1 Application of technologies to biomarker identification

NMR has been widely used in metabolomic studies. Other techniques include MS, liquid-chromatography mass spectrometry (LC-MS), and less commonly Raman and infrared spectroscopy. However, due to the great volume of data that can be generated

by metabolomic/metabonomic studies, chemometric analysis is essential for data interpretation and for the development of statistical pattern recognition (PR) models that will allow identification of biomarkers.

In the present studies ^{1}H NMR was the technique chosen to carry out the identification of biomarkers. In comparison to MS, NMR can provide detailed structural information, can be used to quantitatively analyse mixtures containing known compounds and allows for a fast analysis time. However, this technique lacks sensitivity and unknown peaks in NMR spectra require identification by MS. MS on the other hand is characterised by a high degree of sensitivity and coupled with liquid chromatography (LC-MS) can be used to separate and identify complex samples. Quantitative analysis using MS analysis is also more difficult to perform and more expensive than using NMR (Banoub and Limbach, 2010).

1.8.1.1 Nuclear magnetic resonance (NMR) spectrometry

NMR-based metabolite profiling presents several advantages over other techniques since it is a non-destructive technique that requires minimal sample preparation (Holmes et al., 2000; Beckonert et al., 2007; Beger et al., 2010). It is a highly reproducible method with the potential to analyse liquids including urine and serum, as well as solid tissue samples (Wang et al., 2010a; Monteiro et al., 2013). However, the main disadvantage associated with this technology is the low sensitivity. NMR has a limit of detection of 10 μM (Pan and Raftery, 2007) which means that metabolites present in low concentrations may be missed. In spite of this, NMR has the capacity to detect hundreds of metabolites and each spectrum includes thousands of signals, many of which overlap. The intensity of each peak is proportional to the concentration of that metabolite in the sample (Bollard et al., 2005).

The NMR technique is based on the magnetic properties of atomic nuclei. Electrons, protons and neutrons spin on an axis. In the absence of a magnetic field these nuclei are randomly oriented, but when exposed to an external magnetic field (H_0) they can absorb energy that will cause a transition from a low to a high energy state (Brown et al., 2012).

The overall spin of the nuclei depends on the number of protons and neutrons. If the number of both of these particles is even the nuclei does not spin. When the sum of the protons and neutrons adds up to an odd number this nuclei will have a half-integer spin

(e.g. ½). If the number of protons and neutrons are both odd numbers than the nucleus has integer spin (1, 2…). The overall spin is called the nuclear spin quantum number (I) (Shmaefsky, 2006).

A proton has an atomic number of 1 and therefore this nucleus has a spin. The number of energy levels is determined using the spin quantum number according to the rule: 2I+1. Therefore, a nucleus with spin 1/2 will have 2 possible orientations. When no external field is present these 2 orientations are of equal energy; however, when a magnetic field is applied the energy levels split and each level is given a magnetic quantum number (m) (-1/2, +1/2). The energy difference between the 2 states is proportional to the strength of the external magnetic field applied (Hayes, 2007).

When an external magnetic field is present the nuclei will align themselves either with the magnetic field or against the magnetic field. When the proton is aligned with the field it is at a lower energy state, known as the α-spin state. A proton aligned against the external magnetic field occurs at a higher energy state known as the β-spin state. The α-spin state is lower in energy; therefore, there will be more α-spins than β-spins (Figure 1.7) (Balci, 2005).

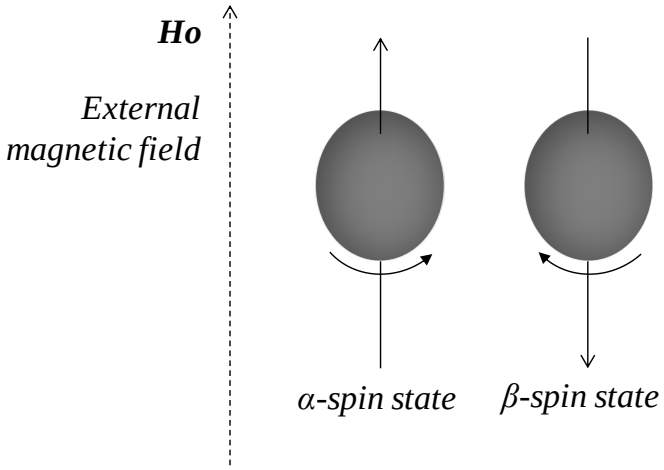

Figure 1.7 Schematic representation of the α and β-spin states (lower and higher energy levels, respectively).

The application of a radiofrequency pulse results in the nuclei absorbing energy and inverts the spins from a lower energy orientation to a higher energy orientation (i.e. the less stable alignment), thus changing them from the aligned state to the opposed to the magnetic field state. When this happens the nucleus is said to be "in resonance" and the energy required for this change in states is called resonance frequency. Consequently,

when the radiofrequency is switched off the nucleus undergoes relaxation to its original lower energy orientation producing a NMR signal in the form of spectra composed of a pattern of resonance peaks which are unique to each molecule. The NMR spectrum is a plot of the intensity of NMR signals versus the magnetic field in reference to an internal reference, such as 3-(trimethylsilyl) propionate (TSP). The position of each peak within a molecule in the spectrum depends on the chemical environment of the nuclei. The area under each peak is proportional to the concentration of that molecule in the sample (Goldsmith et al., 2010).

However, in a given molecule the electrons circulate and in doing so they generate a magnetic field that opposes the externally applied field. When this happens the magnetic field at the nucleus is weaker than the external field, thus, the nucleus is said to be shielded. The effective magnetic field at the shielded proton results from the difference between the external magnetic field applied by the NMR spectrometer and the local magnetic field due to the movement of electrons around the nuclei. The greater the electron density surrounding the nucleus the greater the local magnetic field. This will result in a weaker effective magnetic field at the proton and subsequently a stronger external field will be required to achieve resonance at a given frequency. The result of this is a shift of signals to the right in the NMR spectrum (upfield) (Vollhardt and Schore, 2003).

Protons that are in the presence of electronegative groups in a molecule are said to be deshielded. Protons will have higher chemical shift values and the NMR signals will move to the left of the spectrum (downfield). The chemical shift can be defined as the difference in parts per million (ppm) between the resonance frequency of the proton being studied, and that of the internal standard. The electrons in TSP (internal standard) are very well shielded resulting in a high-field absorption defined as 0 ppm. Most NMR absorptions are therefore downfield of TSP, to the left of the TSP peak. The NMR instrument measures the difference in magnetic field between the frequency at which the protons in the sample absorb and that at which TSP absorbs (Vollhardt and Schore, 2003).

If all the protons in a molecule had the same magnetic environment, i.e., they had the same degree of shielding they would be chemically equivalent protons. Therefore, all the protons would appear at the same chemical shift in an NMR spectrum. This occurs in symmetrical compounds such as benzene. Consequently, the number of different

chemical shifts in a spectrum is an indication of the number of different types of protons present (Balci, 2005). The position of the absorptions (chemical shifts) in the NMR spectrum and therefore the amount of shielding and deshielding provides information regarding the structure of the molecule.

The intensity of the signal (integration) is proportional to the number of protons that make that signal (Walker et al., 2011).

NMR signals normally appear as a pattern of split triangles labelled as doublets (2 peaks), triplets (3 peaks) and quartets (4 peaks) described as signal splitting. Information obtained from the splitting of the signals helps to describe the influence of nearby protons on a proton spin (Fox and Whitesell, 2004). The process by which the spinning of the nucleus of one proton influences another proton in an adjacent carbon is called spin-spin coupling. The distance between each peak is called coupling constant (*J*) and is expressed in Hertz (Hz). The proximity of "n" equivalent protons on a neighbouring carbon atom causes the signals to be split into "N+1" rule.

In this project we will use NMR to examine the possibility of identifying urinary biomarkers of hepatic fibrosis. The ^{1}H NMR spectrum of urine samples results from the superimposition of the spectra of all the metabolites in the sample that contain resonating atomic nucleus (Wang et al., 2010a).

1.8.2 Chemometrics

Chemometrics has been defined as the "application of mathematical and statistical methods to chemistry" (Wold, 1995; Beger et al., 2010). The use of chemometrics facilitates the interpretation of complex data sets generated by NMR and MS. Mathematical and statistical models are applied to the data to extract the most relevant trends. When used in combination with NMR, chemometrics has the ability to facilitate the identification and discrimination of the variables that change due to disease and physiological or pathological status.

Prior to chemometric analysis, it is necessary to perform a pre-processing step known as "bucketing" or "binning". After exclusion of the water peaks, NMR spectra are reduced to regions 0.04 ppm wide from δ 10.0 to 0.2 producing 250 integral regions per spectrum. The area under the peaks in each integral region is calculated giving an integrated value for that region. This operation results in the production of a bucket table (X matrix) where the rows represent individual samples and the columns

(comprising 250 variables or buckets/bins) represent integrated peak areas. This table can then be imported into a chemometrics software to carry out the analysis (Wiklund, 2008).

One of the areas of chemometrics that has grown more rapidly is pattern recognition (PR) analysis which includes unsupervised (e.g. principal component analysis (PCA)) and supervised models (orthogonal partial least square (OPLS)).

PCA is a form of multivariate data analysis (MVA) which is used when several measurements are made on each individual. Measurements refer to variables (integration areas in NMR spectrum/buckets) and individuals refer to observations (analytical samples). The main objective is to compare the variables to understand the relationships between them and identify variables that are related, i.e., those which co-vary together. Covariance describes the influence that one variable has on other variables. MVA is commonly used in metabolomics studies since very large data sets are generated and MVA can be applied to establish the relationship between the many variables (Everitt and Hothorn, 2011).

PCA is the oldest projection method and it consists of a mathematical manipulation of the data to reduce a great number of variables to a much smaller number, known as principal components (PCs). PCA, therefore, allows separation of samples according to the similarities and differences between them. It provides an overview of the data and facilitates the visualisation of groups of observations, trends and outliers (Eriksson et al., 2006). PCA is concerned with extracting the systematic variation in a data matrix X. This matrix (X) is composed of rows (N), also called observations (e.g. samples), and columns (K) which are called variables (integral regions/peak intensities) (Figure 1.8).

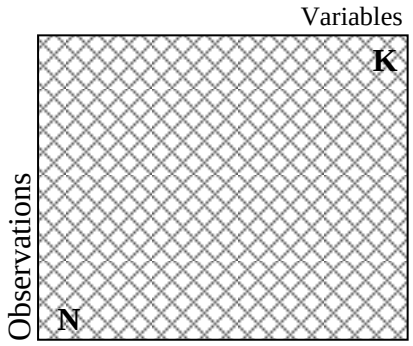

Figure 1.8 Data matrix X in a PCA model. Rows (observations) are shown as N and can be analytical samples. Columns (variables) are shown as K and may be of spectral origin (NMR integral regions) (Eriksson et al., 2006).

The first steps towards generating a PCA model include the pre-processing of the data. Pre-processing includes scaling and mean-centering of the data. The scaling of the data is important since variables can have different intensities between different samples. Thus, variables with large variances in intensity may influence the data set and are more likely to dominate the PCA model, therefore making it difficult to identify chemical shift regions with lower variances. Therefore, scaling is applied to the data prior to analysis to ensure the data is normally distributed.

There are several ways to scale the data, including unit variance (UV) or Pareto scaling. In UV scaling the standard deviation is calculated for each variable and each variable is then divided by its standard deviation so that the variance of scaled variables is 1. UV scaling gives the same weight to all the variables. Pareto scaling is normally preferred in metabolomics studies since variables tend to show large variance in intensities between different samples. This is used when variables with large variances dominate the PCA/OPLS model and overwhelm medium features. This method of scaling has the potential to give more relevance to medium features without inflating the baseline noise. In Pareto scaling, each variable is divided by the square root of its standard deviation (Wiklund, 2008).

Following Pareto scaling of the data mean-centering is performed. This consists of calculating the average value of each variable and then subtracting this value from all the individual data to improve the interpretability of the model.

The second step in generating a PCA model is to create a K-dimensional space (Figure 1.9). A K-dimensional space may include thousands of variables (e.g. the information collected from a bucket table). Each variable (integral region) represents one co-ordinate axis and the integrated area for each observation is plotted on the co-ordinate axis. Each observation is known as a scores point and represents a sample spectrum (observation). This K-dimensional space has as many dimensions as the number of variables in the X matrix. Each observation of the X-matrix (analytical sample) is placed in the variable space (Wiklund, 2008).

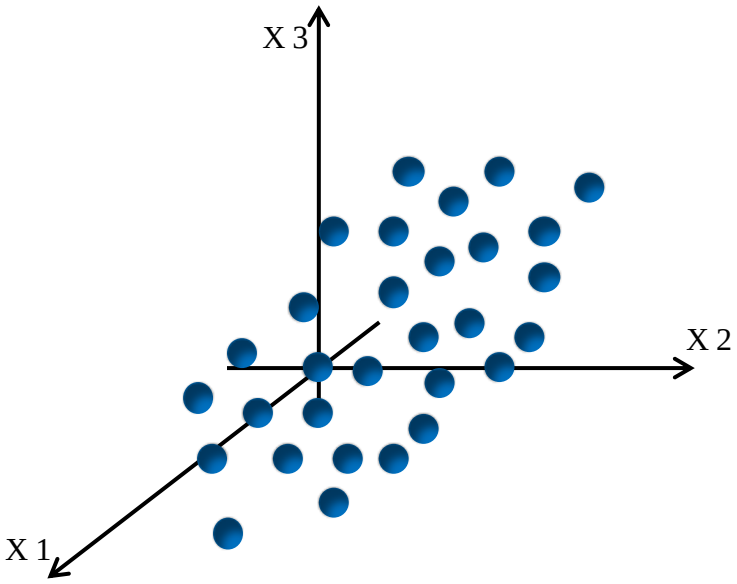

Figure 1.9 Representation of the K-dimensional space. The observations (rows in the X matrix) are placed in the K-dimensional space where each variable (columns in the X matrix/buckets) represents one co-ordinate axis. The K-dimensional space has as many dimensions as there are variables (Wiklund, 2008).

When observations are placed in the K-dimensional space they form a cluster in the space and the data set is then represented as principal components (PCs). The first PC is a line in the K-dimensional space that goes through the average point and best describes the shape of the cluster and shows the maximum variation between the points. Each observation is projected onto this line in order to get a co-ordinate value along the PC-line. This is known as a score. The second PC (PC2) also goes through the average point and is orthogonal to the first PC (PC1). PC2 describes the second largest variation in the data. When the PC2 is computed it is possible to define a plane with PC1. Each observation can then be projected onto this low-dimensional plane. The co-ordinate values of the observations on this plane are called scores and this is called a score plot (Figure 1.10) (Wiklund, 2008).

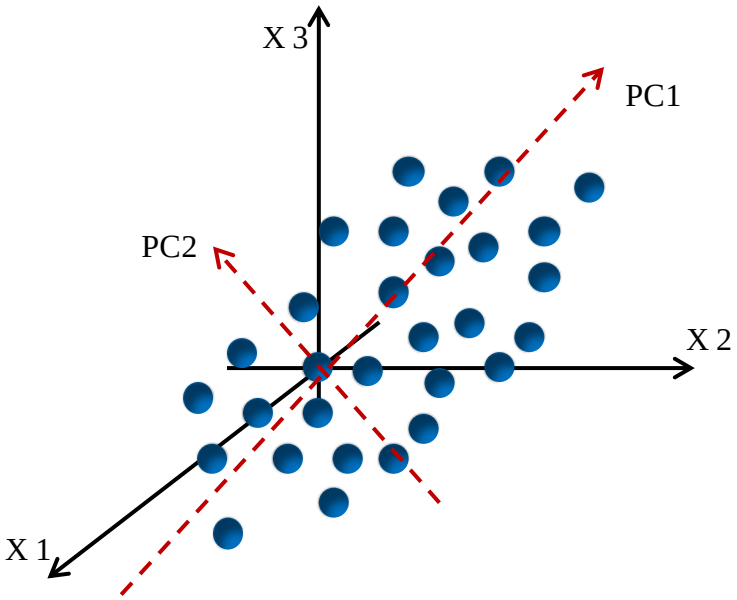

Figure 1.10 Representation of PC1 and PC2. PC1 is the line going through the average point that best describes the shape of the points in the K-dimensional space and represents the maximum variance in the data. PC2 also goes through the average point, is orthogonal to PC1 and explains the second largest source of variation in the data (Wiklund, 2008).

Each consequent PC (PC3, PC4 etc) contributes towards explaining the total variance between the observations not described by the previous PC, with PC1 describing the greatest source of variability. All PCs generated from a PCA model can be interpreted together to gain as much information regarding the relationship between different observations. The ideal situation would be to have a very small number of PCs describing as much information as possible in the model so that the rest of the variance can be attributed to noise (Robertson, 2005).

The information obtained in a PCA model can be presented in two types of PCA plots: a scores plot where each point in the plot represents one single NMR spectrum (observation), and a loadings in which points represents one variable (chemical shift region/integral region) (Figure 1.11) (Bollard et al., 2005, Beger et al., 2010). Samples that cluster together in the scores plot have similar spectra and, therefore, are considered to be biochemically similar.

The scores plot allows the observation of patterns, clusters and outliers between samples/observations. The loadings plot provides the information about the spectral regions which are associated with the observed sample clustering in the scores plot. Thus, the loadings plot is used as the basis for metabolite interpretation and

identification. The loadings plot represents how the original variables (integral regions) contribute to the direction of PC1. For each PC of the PCA model a new set of loadings will be required to explain the direction of that individual PC in relation to the original variables.

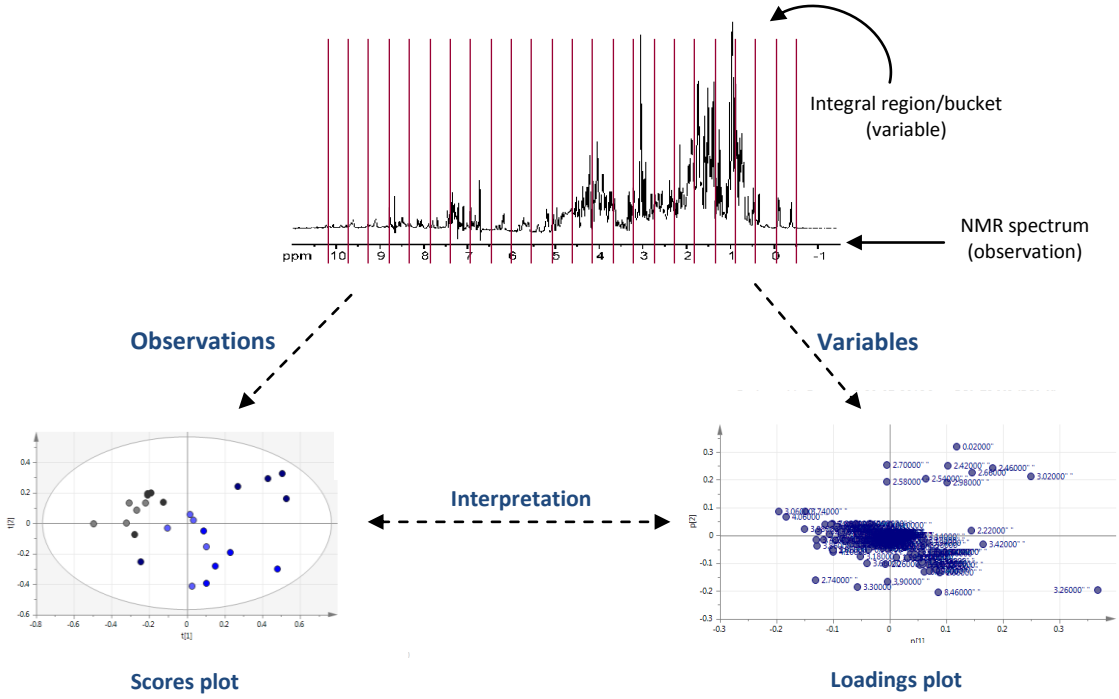

Figure 1.11 Schematic representation of the PCA process. Each NMR spectrum (observation) is reduced to 250 regions (variables) which are manipulated to produce the scores plot and the loadings plot.

If a variable has a very small loading it should not be used for interpretation, because that variable is badly accounted for by the PC. If a variable has a positive loading, it means that all samples with positive scores on the scores plot have higher than average values for that variable. All samples with negative scores have lower than average values for that variable. The higher the positive score of a sample, the larger its values for variables with positive loading. If a variable has a negative loading it means that all samples with positive scores have lower than average values for that variable and all samples with negative scores have higher than average values for that variable. The more negative the score of a sample, the smaller its values for variables with positive loading. Variables that are negatively, or inversely correlated, are positioned on opposite sides of the scores plot origin in diagonally opposed quadrants. Consequently, it is the combined interpretation of both the scores and loading plots that will allow

acquisition of the most detailed information concerning the samples being analysed (Eriksson et al., 2006).

The quality of a PCA model can be evaluated by the goodness of fit (R^2X) and the goodness of prediction (Q^2X). R^2X refers to the fraction of the variation of the X variables that is explained by the model whereas Q^2X is related to the fraction of the variation of the X variables that is predicted by the model. Therefore, high R^2X and Q^2X are desirable. Q^2X is calculated by cross-validation and is used to find the optimal model, and identify the ideal number of components to describe the PCA model. By default, data are divided into 7 groups and a PCA model is created for the data excluding 1 of the groups. The model that is created is then used to predict the data that was excluded from the model. This process is repeated 7 times. The predictive data are then compared with the original data. When a new component enhances the predictive power compared to a previous model this new component is kept. This operation is performed by the software (Jackson, 1991).

OPLS (orthogonal partial least squares) is a supervised prediction and regression method that finds the information in the X matrix data that is related to known information, called the Y variable. Regression is a measurement of how values vary together whereas prediction tells us how well the known information is predicted. OPLS models are an extension of partial least square (PLS) (Wiklund, 2008).

In OPLS, Y variables contain information about the observations. They can be measured or known information such as continuous variables (e.g. time), or discrete variables (male/female, or control/treated). When the Y variable is a discrete variable, the OPLS model is known as OPLS-discriminant analysis (OPLS-DA). OPLS-DA models use the same algorithm as OPLS and are of particular interest in classification studies and biomarker identification to distinguish variables which are due to gender or treatment groups (Wiklund, 2008).

Pre-processing of the data prior to generating an OPLS/OPLS-DA model is carried out and includes scaling and mean-centering, as described previously for PCA models.

Similar to PCA, OPLS-DA is a projection method and interpretation of plots is easiest if only 2 classes are used. The main advantage of OPLS-DA models is the ability to facilitate interpretation of data by separating the predictive variation, or the correlated variation between X and Y (e.g. effect of toxin concentration), and the orthogonal

variation, which describes the uncorrelated variation between X and Y (e.g. age of animals). The use of OPLS-DA models is, therefore, very useful in toxicology studies investigating the effect of treating animals with a particular toxicant, but when the age or gender of the animals used is also a contributor to the X matrix. Consequently, OPLS-DA often reveals sample clustering that was not evident in PCA models of the same data. In this project, OPLS-DA was used to compare control and CCl_4-treated samples at different dose levels or time points.

In OPLS-DA scores plots, the information that is correlated between X and Y will be shown along the discriminating component t[1] (e.g. control and treated samples), and interpretation of this information in the loadings plot will be carried out by analysis of the loadings p_1. The orthogonal information (e.g. as a result of gender or intra-group variation), will be visualised along the orthogonal vector t[0] in the scores plot, and p_0 in the loadings plot. This makes it easier to see clustering which is due only to treatment with the toxicant.

In OPLS and OPLS-DA models the goodness of fit (R^2) is divided into predictive and orthogonal. R^2X (cum) refers to the predictive and orthogonal variation in the X matrix that is explained by the model. R^2X shows how much variation in the X matrix (made up of rows/observations and columns/chemical shifts) is related to the Y variable (e.g. different treatment dose levels). R^2Y (cum) represents the total sum of variation in Y that is explained by the model (i.e. how good is the separation between the Y variables). Q^2 (cum) is the goodness of prediction that is calculated by cross validation and represents the variation that is not related to our Y variable. Therefore, the higher the R^2Y and Q^2 the better the model and the separation between samples (Wiklund, 2008).

Interpretation of the loadings plot in OPLS-DA models is compromised if there are more than 2 classes. OPLS-DA models allow the visualisation of the data in an S-plot which is useful for potential biomarker identification. The S-plot represents an alternative way of visualising the information shown in a loadings plot. The S-plot models the data so that if the X matrix (observations and variables) has a variation in peak intensities, the plot will take the shape of an "S". The p_1 axis in this plot describes the magnitude of each variable in X, whereas the $p(corr)_1$ axis describes the reliability of each variable in X. Potential biomarkers will have high magnitude and high reliability values and will therefore be located in the extremes of the S-plot. The S-plot gives a list of chemical shifts that are statistically significant.

After creating a list of the most relevant metabolites in sample separation the next step is metabolite identification. Chemical shift regions that are different in the S-plot or loadings plot are then examined in the 1D ^{1}H NMR spectra to obtain the exact chemical shifts of peaks in this region. These are then compared to relevant spectra in published literature for identification.

^{1}H NMR is a technique that has been extensively applied to biomarker studies. The fact that is non-destructive, requires minimal samples preparation and is highly reproducible have contributed greatly to its vast application in metabolomic studies in humans investigating inflammatory bowel disease (Dawiskiba et al., 2014), acetaminophen-induced hepatotoxicity (Kim et al., 2013) and pulmonary disease (Wang et al., 2013). In this project, ^{1}H NMR spectrometry will be used for the identification of urinary biomarkers in a rat model of CCl_4-induced acute and chronic injury.

1.9 Aim of this project

The aim of the current studies is to identify novel urinary biomarkers of CCl_4-induced acute and chronic hepatic injury in the male Hanover-Wistar rat. Urine was chosen for biomarker identification since it can be easily collected in relatively large volumes and without any associated pain, distress and discomfort to the animal. The identification of non-invasive markers of liver damage that could be used in the preclinical toxicology assessment and clinical safety testing of drugs would provide relevant information to the process of drug development and could be extremely useful in monitoring target organ toxicity in clinical trials.

In the present investigations acute and chronic animal models of liver toxicity will be developed using CCl_4 as the hepatotoxicant. Initially, a single administration of CCl_4 at a range of concentrations will be used to determine the optimal dose level for our acute hepatic injury model. CCl_4 exerts its toxic effects mainly in the liver; however, injury has also been detected in other organs, including the kidneys. Therefore, our primary goal will be to identify the dose level of CCl_4 that is below the threshold for nephrotoxicity. To reliably determine the presence of renal damage we will investigate the sensitivity of a panel of kidney injury biomarkers recently approved by the FDA to use in toxicology studies. These will be used in our hepatic injury model to confirm the absence of a CCl_4-induced toxic effect in the kidneys. Confirmation of absence of renal damage will be made by means of histopathological examination of kidney samples collected at autopsy.

With the preliminary information collected from the dose response study regarding the most sensitive urinary markers of renal damage we will then focus on the development of a model of CCl_4-induced liver fibrosis in the male rat.

Identification of biomarkers in the urine samples collected from animals with hepatic injury in this project will be carried out using a metabonomics approach. ^{1}H NMR combined with PCA and OPLS/OPLS-DA will be used for the identification of potential biomarkers. These biomarkers will be further assessed for sensitivity. A time course study will help to determine how sensitive any urinary biomarker is to early signs of injury and subsequent recovery following acute hepatotoxicity. A good biomarker for hepatic fibrosis will be present at the early stages and should regress

during a recovery period if the fibrotic lesion recovers. We will investigate this in a rat hepatic fibrosis model measuring urinary biomarkers.

CHAPTER TWO

Materials and Methods

Chapter 2

2.1 List of materials

Rats were supplied by Harlan Laboratories Inc., Bicester, Oxfordshire, UK. The metabolism cages were manufactured by Techniplast, Kettering, Northants, UK. The animal diet came from SDS Ltd., Wiltham, Essex, UK.

Euthatal (pentobarbital sodium) came from Merial, Harlow, Essex, UK. Qiagen, Crawley, West Sussex, UK, supplied the RNALater tubes. Bouin's fixative, 10.5 % (v/v) phosphate buffered formalin fixative and industrial methylated spirit (IMS) were supplied by Sigma-Aldrich Co. Ltd, Gillingham, Dorset, UK.

Carbon tetrachloride was purchased from Fluka Chemicals, Gillingham, Dorset, UK. Hexachloro-1:3-butadiene was purchased from Sigma-Aldrich Chemie GmbH, Steinheim, Germany. The corn oil used in animal experiments was purchased from Mazola Corn Oil, Mazola Edible Foods, Liverpool, UK.

SST^{TM} microtainer tubes came from Becton Dickinson and Co., Plymouth, Devon, UK.

Trimethylsilyl propionate (TSP) and D_2O were purchased from Cambridge Isotopes Laboratories, Inc., Maryland, USA.

Sodium phosphate monobasic (NaH_2PO_4) and dibasic (Na_2HPO_4) for the preparation of NMR buffers were purchased from Sigma-Aldrich Co. Ltd, Gillingham, Dorset, UK.

2.2 Animals and animal husbandry

Male Hanover-Wistar rats, weighing approximately 180 to 200 g (approximately 7 weeks of age), were used throughout except for studies in Chapter 4 when both younger and older animals were used. Rats were caged in groups of 5 when not in individual metabolism cages. Animals were allowed to acclimatise for a minimum of 3 days prior to each experiment. When in communal cages rats had access to diet and water *ad libitum* (Rat and Mouse No. 1, SDS, Witham, Essex, UK) and were bedded on wood shavings. A temperature of 19-22ºC was maintained with relative humidity of 45-65% and a light:dark cycle of 12:12 hours (lights on at 7 am). Animals were weighed on the day of delivery, before administration of the toxicant and at appropriate times post-

dosing. Animals were observed daily for signs of ill health throughout the study. All animal procedures were conducted according to local Ethical Committee guidelines and approval for Home Office Project and Personal Licenses and followed the UK Home Office (1989) "Code of Practice for the Housing and Care of Animals used in Scientific Procedures". For urine collection animals were placed individually in metabolism cages with water but no diet. Urine was collected over ice.

2.3 Carbon tetrachloride administration

CCl_4 was dissolved in corn oil and administered by gavage. Control animals (vehicle-treated) were also dosed by gavage with an equivalent volume of corn oil. Dosage volumes were adjusted according to the body weight of individual animals so that the maximum volume they received did not exceed 1.5 mL per rat.

2.4 Hexacloro-1:3-diene administration

HCBD was dissolved in corn oil and administered by intraperitoneal (i.p.) injection. Control animals were dosed in the same way with an equivalent volume of corn oil. For all animals a constant dosing volume of approximately 0.3 mL was administered.

2.5 Ultrasonographic examination

Animals were scanned using a Vivid 7i system (GE Medical Systems, Norway) equipped with a 10-14 MHz linear transducer (M12L). The system uses specific built-in software for rodent imaging, thus allowing an optimised ultrasonography examination for small anatomical parts. Images obtained for each animal were stored on the system as a loop or still frame image for off-line analysis.

Animals were anaesthetised with isoflurane (3-4% isoflurane in 100% oxygen) in an anaesthesia chamber before undergoing ultrasonographic examination. Body temperature was maintained by the use of a thermal blanket. Animals were shaved in the abdominal region and US coupling gel was applied. Appropriate levels of anaesthesia were used throughout to minimise discomfort and to facilitate good acquisition of images.

Images of the right or left kidney were recorded for comparison of echographic texture to that of the liver. Imaging acquisition was obtained by moving the scanhead from the

xyphoid region to the right or left in order to maximise both the sagittal and transverse liver planes and the vascular anatomy and cranial poles of the kidney.

2.6 Post mortem

Animals were killed by i.p. injection of pentobarbital sodium and exsanguinated from the abdominal aorta. At all autopsies blood was taken into SST^{TM} microtainer tubes for the separation of serum. After 30 minutes at room temperature serum tubes were centrifuged at 5000 rpm for 5 minutes. Serum was store at -80 ºC for future analysis.

Both clinical and internal observations of the animals were made and recorded during the autopsies. The liver and the kidneys were removed and weighed. A section 2-3 mm wide and 20-30 mm long was cut from the left lobe of the liver, sliced into 5/6 pieces, placed in RNALater tubes and stored at 4 ºC until later gene expression analysis at GlaxoSmithKline, Ware. A section was also cut from the right kidney, placed in RNALater tubes and stored at 4 ºC until analysis at GlaxoSmithKline. The remainder of the liver and kidney were placed in 10.5 % (v/v) phosphate buffered formalin fixative for later histopathological examination.

For dose ranging experiments, other tissues including the spleen, right and left adrenals, thymus and heart were removed at autopsy. Organs were weighed and placed in 10.5 % (v/v) phosphate buffered formalin fixative. The pancreas, lungs (inflation fixed with formalin), thyroid and head were removed and placed in 10.5 % (v/v) phosphate buffered formalin fixative.

In the sexual maturity study, the right and left testes were removed, weighed and placed in Bouin's fixative. After 24 hours, the Bouin's fixative was removed from the testes and replaced with IMS. The epididymides were also collected at autopsy, placed in Bouins's solution for 24 hours followed by replacement of the Bouin's with IMS.

Organs weights were expressed as grams per kilogram body weight (relative weight).

2.7 Serum and urine clinical chemistry

All serum and urine biochemistry was carried out at GlaxoSmithKline.

Urine and serum samples were assayed on the Siemens Advia 1650 Clinical Chemistry System (Siemens Healthcare, Frimley, Surrey, UK) using commercially available

reagent kits. Testosterone was measured using a commercially available kit from R&D Systems (R&D Systems Europe Ltd, Abindgon, UK).

2.7.1 Serum clinical chemistry

2.7.1.1 ALT assay

The enzyme ALT transfers one amino group from L-alanine to 2-oxoglutarate forming pyruvate and glutamate (Bergmeyer et al., 1986a). Pyruvate then enters a second reaction with nicotinamide adenine dinucleotide (NADH), catalysed by lactate dehydrogenase (LDH), producing lactate and NAD^+. Absorbance is measured at 340 nm and the decrease due to NADH consumption is directly proportional to the ALT activity in the sample.

$$\text{L-Alanine} + \text{2-Oxoglutarate} \xleftrightarrow{\text{ALT}} \text{L-Glutamate} + \text{Pyruvate}$$

$$\text{Pyruvate} + \text{NADH} + H^+ \xrightarrow{\text{LDH}} \text{D-Lactate} + NAD^+$$

2.7.1.2 AST assay

In this reaction AST catalyses the reversible transamination of L-aspartate and 2-oxoglutarate to oxalacetate and L-glutamate (Bergmeyer et al., 1986b). Oxalacetate then reacts with NADH and is then further reduced to malate in the presence of malate dehydrogenase (MDH). AST activity is determined by measuring the rate of oxidation of NADH at 340 nm.

$$\text{L-Aspartate} + \text{2-Oxoglutarate} \xleftrightarrow{\text{AST}} \text{L-Glutamate} + \text{Oxalacetate}$$

$$\text{Oxalacetate} + \text{NADH} + H^+ \xrightarrow{\text{MDH}} \text{D-Malate} + NAD^+$$

2.7.1.3 ALP assay

The enzyme ALP hydrolyses p-nitrophenylphosphate to form p-nitrophenol which is a yellow chromogen. The increase in absorbance at 415 nm due to the production of p-nitrophenol is proportional to the ALP activity (Rec Gscc (DGKC) (1972)).

$$\text{p-Nitrophenylphosphate} + H_2O \xrightarrow{\text{ALP}} \text{Phosphate} + \text{p-Nitrophenol}$$

2.7.1.4 GLDH assay

Measurement of GLDH occurs according to the reaction below and was measured using the kinetic DGKC method (Rec Gscc (DGKC) (1972)). Ammonia and 2-oxoglutarate are converted to glutamate in a reaction catalysed by GLDH. Simultaneously, one mole of NADH is oxidised. The absorbance is read at 340 nm and the decrease in absorbance per minute is proportional to the GLDH activity.

$$\text{2-Oxoglutarate} + \text{NADH} + NH_4^+ \xrightarrow{\text{GLDH}} \text{Glutamate} + NAD^+ + H_2O$$

2.7.1.5 Glucose assay

In this reaction glucose receives a phosphate group from adenosine triphosphate (ATP) in a reaction catalysed by hexokinase (Wright et al., 1971). The resulting product, glucose-6-phosphate, is then oxidised in the presence of NAD^+. This reaction is catalysed by the enzyme glucose-6-phosphate dehydrogenase (G6PDH). At the same time NAD^+ is reduced to NADH. The increase in absorbance at 340 nm due to the NADH formation is directly proportional to the glucose concentration.

$$\text{Glucose} + \text{ATP} \xrightarrow{\text{Hexokinase}} \text{Glucose-6-phosphate} + \text{ADP}$$

$$\text{Glucose-6-phosphate} + NAD^+ \xrightarrow{\text{G6PDH}} \text{6-Phosphogluconate} + \text{NADH}$$

2.7.1.6 Urea assay

The enzyme urease catalyses the hydrolysis of urea to carbamate and ammonia (Talke and Schubert, 1965). Carbamate then spontaneously decomposes to yield ammonia and carbonic acid. The ammonia then reacts with 2-oxoglutarate and NADH in a reaction catalysed by GLDH with the production of NAD^+. The decrease in absorbance at 340 nm due to the decrease in NADH is proportional to the urea levels.

$$\text{Urea} + 2\,H_2O \xrightarrow{\text{Urease}} 2\,NH_4^+ + 2\,HCO_3^-$$

$$\text{2-Oxoglutarate} + \text{NADH} + NH_4^+ \xrightarrow{\text{GLDH}} \text{Glutamate} + NAD^+ + H_2O$$

2.7.1.7 Creatinine assay

This is a multi-step reaction; the first step consists of the conversion of creatinine to creatine by the enzyme creatinine amidohydrolase (Moss et al., 1975). Creatine is then converted to urea and sarcosine. Further reactions result in the production of a coloured chromogen and the change in absorbance is read at 545 nm.

$$\text{Creatinine} + H_2O \xrightarrow{\text{Creatinine amidohydrolase}} \text{Creatine}$$

$$\text{Creatine} + H_2O \xrightarrow{\text{Creatine amidinohydrolase}} \text{Sarcosine} + \text{Urea}$$

$$\text{Sarcosine} + H_2O + O_2 \xrightarrow{\text{Sarcosine oxidase}} \text{Glycine} + \text{Formaldehyde} + H_2O_2$$

$$2\,H_2O_2 + \text{4-Aminoantipyridine} + \text{ESPMT} \xrightarrow{\text{Peroxidase}} \text{Quinoneimine dye} + 4\,H_2O$$

(ESPMT: N-ethyl-N-sulfopropryl-m-toluidine)

2.7.1.8 Total protein assay

Total protein measurement based on the Biuret assay (Lubran, 1978). This assay is based on the fact that peptides bonds have the ability to form a purple complex with copper salts in alkaline solution. Absorbance is read at 540 nm.

2.7.1.9 Albumin assay

Serum albumin was measured using the bromocresol green (BCG) method (Doumas et al., 1971). BCG forms a coloured complex with albumin and the intensity of the colour, measured at 620 nm is directly proportional do the albumin concentration in the sample.

2.7.1.10 Acetoacetate and β-Hydroxybutyrate assay

The acetoacetate assay is based on the automated method of Galan et al., (2001). The 2 assays are based on endpoint reactions catalysed by β-hydroxybutyrate dehydrogenase. The generation or consumption of NADH is measured by changes in absorbance at 340 nm.

$$\beta\text{-Hydroxybutyrate} + NAD^- \xleftrightarrow{\beta\text{-Hydroxybutyrate dehydrogenase}} \text{Acetoacetate} + NADH^- + H^+$$

2.7.2 Urinary clinical chemistry

Urinary glucose and creatinine measurements were performed using the methods described in Sections 2.7.1.5 and 2.7.1.7, respectively.

2.7.2.1 Total protein

Urinary protein concentration was measured based on the pyrogallol red procedure, which is based on the change in absorbance that occurs when pyrogallol red-molybdate complex binds to basic amino acids of proteins (Watanabe et al., 1986). Absorbance is read at 600 nm and the increase is proportional to protein concentration.

$$\text{Protein} + \text{Pyrogallol Red-Molybdenum Complex} \longrightarrow \text{Protein Pyrogallol-Red Molybdenum Complex}$$

2.7.2.2 N-acetyl-β-D-glucosaminidase assay

The detection of N-acetyl-β-D-glucosaminidase (NAG) is based on the method by Noto et al., (1983). This is a colourimetric assay using sodium *m*-cresolsulfonphthaleinyl N-acetyl-β-D-glucosaminidase (MCP-NAG). NAG hydrolyses MCP-NAG to MCP and NAG. MCP shows maximum absorption at 580 nm.

2.7.2.3 Testosterone assay

Testosterone was measured in urine samples using a competitive enzyme immunoassay. A monoclonal antibody specific for testosterone binds to the goat anti-mouse antibody coated onto the microplate. The plate is washed to remove excess monoclonal antibody

and the testosterone present in the sample competes with a fixed amount of horseradish peroxidase-labelled testosterone for sites on the monoclonal antibody. This step is followed by another wash to remove excess conjugate and unbound sample after which a substrate solution is added to the wells to determine the bound enzyme activity. Absorbance is read at 450 nm and the intensity of the colour is inversely proportional to the concentration of testosterone in the sample.

2.7.2.4 Microalbumin detection assay

Microalbumin was measured on the Advia 1650 by Polyethylene glycol (PEG)-enhanced immunoturbidimetric assay (Harmoinen et al., 1987).

2.7.3 Meso Scale Discovery Immunoassays

Where stated urine and serum samples were assayed for kidney biomarkers using two multiplexed test kits - the Rat Kidney Injury Panel 1 (albumin, KIM-1, lipocalin-2, osteopontin) and the Argutus Acute Kidney Injury Panel (α-GST, GST Yb1, RPA1), and one single-plex test kit - the Clusterin Test Kit. Levels of TIMP-1, MCP1, A2M and AGP were also measured in the samples using two different multiplexed kits. Responses were evaluated on the Sector® Imager 6000 (Meso Scale Discovery; MSD, Gaithersburg, MD, USA).

All assays were two-antibody type assays, except for albumin which was a single antibody in a competitive assay. In the two-antibody type assays the sample is premixed with a solution containing the corresponding detection antibodies conjugated with SULFO-TAG™ labels. The mixture is then incubated with a plate pre-coated with the capture antibodies. If the analytes are present in the sample they will be captured by the immobilised antibodies and will attract the detection antibodies completing the sandwich. Inside the instrument a voltage is applied to the plate electrodes causing the labels bound to the electrode surface to emit light and the intensity is measured by the instrument to give a quantitative measure of the analytes in the sample.

In the competitive assay used to measure albumin, free albumin in the samples (unconjugated) competes with the SULFO-TAG™ labelled albumin for binding sites on the immobilised antibodies. The signal strength is therefore inversely proportional to the levels of free albumin in the sample.

2.8 Histopathological examination

Histopathology examination was carried out at GlaxoSmithKline.

Organs were removed at autopsy and taken into 10.5 % (v/v) phosphate buffered formalin fixative or Bouin's fixative (testes and epididymides). Tissues were fixed overnight before being dehydrated using increasing concentrations of IMS. In the last dehydrating step 100 % IMS was used to ensure that no water was present prior to the next step which is a clearing step. The dehydrating agent was removed with a substance that is miscible with the embedding medium (paraffin) and the dehydrating agent (alcohol). The most commonly used clearing agent is xylene. Samples were then infiltrated with the embedding agent (molten paraffin) at 60 ºC for 2 to 4 days and the tissue wax allowed to cool in an ice tray for microtomy. Sections of approximately 3 µm thickness were cut and floated onto a water bath containing warm distilled water and picked up onto a glass slide. Prior to staining slides were dried in an incubator.

Slides were then stained with haematoxylin and eosin (H&E) or chromotrope-aniline-blue (CAD).

2.9 Gene expression measurement

Gene expression measurement was carried out at GlaxoSmithKline.

2.9.1 RNA isolation and conversion to complementary DNA

Liver or kidney tissue previously stored in RNAlater (4 °C) was homogenised using a Tissue Lyser homogeniser (Retsch GmbH, Haan, Germany) and RNA/DNA extracted using the RNeasy Mini Kit (Qiagen). Samples were then treated for the removal of genomic DNA using DNase I enzyme (Ambion, Huntingdon, UK). Quantitation was performed using the RiboGreen RNA Quantitation Kit (Invitrogen, Paisley, UK) and RNA was converted to cDNA template using the High Capacity cDNA Reverse Transcription Kit protocol (Applied Biosystems, Warrington, UK).

2.9.2 Real-time polymerase chain reaction analysis of gene expression

Quantitative real-time polymerase chain reaction (PCR) was performed using the 7900 HT Sequence Detection System (Applied Biosystems) and TaqMan^{R} Universal PCR Master Mix (Roche, New Jersey, USA) using between 2 and 5 ng cDNA per assay.

Specific TaqManR Gene Expression Assay number Rn00597703 m1 (Applied Biosystems) was used to quantify KIM-1 mRNA. Other mRNA levels were assayed using custom low density arrays (Applied Biosystems). Cycle threshold (Ct) values were converted to copy number using the equation: copy number=10 exp[(39 − Ct)/3.4].

2.10 1D ^{1}H Nuclear Magnetic Resonance (NMR) spectroscopy

Urine samples for ^{1}H NMR spectroscopy were prepared by the addition of 200 μL buffer solution (0.2 M Na_2HPO_4/0.2 M NaH_2PO_4, pH 7.4) to 400 μL of urine. The mixture was allowed to stand at room temperature for 10 minutes followed by centrifugation at 13,000 rpm for 10 minutes. 500 μL aliquots were placed in 5 mm NMR tubes to which 50 μL of a standard solution of TSP in D_2O was added (final concentration = 1 mM). The D_2O and TSP provide both a chemical shift reference (δ 0.0) and a deuterium lock signal for the NMR spectrometer.

One-dimensional ^{1}H NMR spectra of urine were measured at 500.00 MHz on a Bruker DRX-500 spectrometer using a standard pre-saturation pulse sequence for water suppression with irradiation at the water frequency during the relaxation delay of 3 s and the pulse sequence mixing time of 100 ms. Following 4 dummy scans, spectra were acquired using 64 scans into 64K points using a spectral width of 10,080 Hz, an acquisition time of 4.68 s, and a total pulse recycle time of 7.68 s. The free induction decays (FIDs) were multiplied by an exponential weighting function corresponding to a line broadening of 0.3 Hz prior to FT.

All ^{1}H NMR spectra were phase and baseline corrected using TopSpin (Bruker Analytik, Rheinstetten, Germany) and data reduced using AMIX (Bruker Analytik, Rheinstetten, Germany) to regions 0.04 ppm wide from δ 10.0 to 0.2 producing 250 chemical shifts (variables), an operation known as binning or bucketing. The bucket size was chosen to allow for small changes in chemical shift due to variations in pH within the samples. The region between δ 6.1-4.5 in the urine spectra was set to zero integral value for the purposes of pattern recognition analysis to remove the variability in presaturation of the water resonance and cross-relaxation effects on the urea signal.

The second step in data processing is a row operation known as normalisation. For each region of the spectra (bucket) (minus the water region), the area under the curve was calculated and expressed as an integral value. All regions of the spectra were normalised

to the sum of the integrals to reduce any significant differences in concentration between individual urine samples as described by Craig et al., (2006). The data were then imported into Microsoft Excel and converted into a bucket table. Each bucket table was then imported into SIMCA 13 (Simca v. 13, MKS Umetrics AB, Sweden). The pre-processed data was compiled to create a bucket table where the rows represent individual samples and the columns (comprising 250 variables/buckets) represent integrated and normalised peak areas.

Finally, a step is carried out to reduce the noise in the data. This is a column operation that acts on each spectral intensity across all samples, a process known as scaling. Mean-centering scaling was carried out in which the column mean is subtracted from each value in the column, so that each column has a mean of zero. This was followed by Pareto scaling where each variable is divided by the square root of its standard deviation.

2.11 Pattern recognition analysis of ^{1}H NMR spectral data of urine and serum

PCA, OPLS and OPLS-DA were performed using SIMCA 13 (Simca v. 13, MKS Umetrics AB, Sweden).

PCA is an unsupervised method which is used to identify similarities and differences between samples from controls and treated animals. It reduces the dimensionality of a data set by creating a new set of variables, known as Principal Components (PCs). PCs are uncorrelated, with the first component (PC1) explaining the largest variance in the data and the subsequent PCs describing progressively smaller proportions of the total variance (Wu et al., 2005; Rousseau et al., 2008). PCA was performed to determine the presence of patterns and outliers among samples which appeared distinct from other samples. Outliers are shown outside the Hotelling's T^2 elipse which defines the 95 % confidence interval. In the present studies, outlier samples that fell outside the Hotelling's T2 plot were individually analysed and excluded from further analysis when necessary.

The PCA scores plots were used to identify the presence of inherent clustering patterns between groups of samples and the corresponding loadings plot to identify the regions in the spectra that most contributed to the separation of groups of samples on the scores plot (Constantinou et al., 2007).

OPLS is a regression model used to describe the relationship between a descriptor matrix X, and a response matrix Y containing quantitative values. When OPLS is applied to qualitative data, such as discriminant analysis it is known as OPLS-DA. A variable importance plot (VIP) was also used to identify putative markers of CCl_4-induced toxicity. This type of plot describes which X variables characterise the X matrix well and which variables correlate with Y. The VIP values summarise the overall contribution of each X-variable to the OPLS model. Variables with small VIP scores, usually less than 0.5, are less important and can therefore be excluded from the model.

Variables identified from the VIP plot as contributing to sample separation were then matched to chemical shifts in the ^{1}H NMR spectra. Identification was carried out by visual comparison of peaks in the ^{1}H NMR collected from this project with peaks in spectra from previously published literature (Nicholls et al., 2001).

The quality of the PCA, OPLS and OPLS-DA models was calculated by determining the predictive ability of the models (Q^2) and the correlation coefficient (R^2) which is a measurement of how well the model fits the data. The predictive ability (Q^2) was evaluated by performing a cross-validation (CV). Q^2 values greater than 0.5 are generally considered good. The greater the value for R^2 the better the fit.

2.12 Statistical analysis

Urine data were corrected for volume and are reported as 'per collection period' (c.p.). Urine, and serum clinical chemistry data were log transformed before analysis. Data are presented as means (SD) for groups of animals.

Group means and SD were compared by one-way analysis of variance (ANOVA) followed by a post-hoc Dunnet's test, or by the means of a Student's t-test using the software package SPSS (IBM SPSS statistics 19, Portsmouth, Hampshire, PO6 3AU). Significance was set at $^{*}P<0.05$, $^{**}P<0.01$ and $^{***}P<0.001$.

For ^{1}H NMR statistical analysis of integral regions, a Student's t-test was performed.

CHAPTER THREE

Dose response study for the identification of a dose level to induce hepatotoxicity but not injury to other organs following CCl_4 administration

Chapter 3

3.1 Introduction

In the present studies carbon tetrachloride (CCl_4) was chosen as the hepatotoxicant agent since it is one of the most commonly used compounds for the investigation of liver toxicity (Brattin et al., 1985). CCl_4 is metabolised in the liver by cytochrome P-450 2E1 to produce reactive free radicals. Since the concentration of CYP450 is greatest in the centrilobular region of the liver this area is most susceptible to injury (Lindros, 1997; Sweeney, 1981). However, CCl_4 is highly lipophilic and therefore can be readily distributed throughout the body resulting in injury to other organs such as the kidneys, the lungs and the brain (Lundh, 1964; Striker et al., 1968; Chen et al., 1977; Boyd et al., 1980; Tjalve and Lofberg, 1983; Paakko et al., 1996).

The primary aim of this project was to identify biomarkers of hepatic toxicity; therefore, the first objective was to create a model of hepatotoxicity in the male Hanover-Wistar rat. Firstly, it was necessary to establish the optimal dose level of CCl_4 capable of causing maximal hepatotoxicity without inducing injury to other tissues. Therefore, a dose response experiment was conducted to investigate the effect of a single CCl_4 administration in potential target organs. There is limited data available on CCl_4-induced injury to other organs. Consequently, in this experiment a wide range of animal tissues were histologically evaluated including the kidneys, pancreas, spleen, adrenals, thymus, thyroid, heart with lungs inflated, head and testes. Histological examination would confirm the presence or absence of CCl_4-induced injury in the organs.

Previous studies have showed the potential for CCl_4-induced kidney damage in the rat in both single (Ozturk et al., 2003; Makni et al., 2012) and repeat dose studies (Deb and Chakravarty, 1962; Ogeturk et al., 2005). It has been previously demonstrated that the renal cytochrome P-450 concentration is lower than the concentration in the liver (Renaud et al., 2011). Therefore, the kidney has a reduced capacity for CCl_4 metabolism compared to the liver and consequently, nephrotoxicity requires the administration of higher dose levels of CCl_4. CCl_4-induced nephrotoxicity may affect the kidney structure resulting in the compromise of glomerular filtration or reabsorption processes. This could lead to an increase in the urinary protein and metabolite concentration as a result of altered kidney function. We are interested in identifying urinary biomarkers of hepatic toxicity; therefore, injury to the kidney could affect our sample collection and

biomarker identification. In this situation, it would be difficult to determine if biomarkers identified in our study were present as a result of hepatic toxicity, nephrotoxicity or both. Consequently, in this study, great importance was attached to finding a dose level that induced hepatotoxicity but not nephrotoxicity.

Serum samples obtained from animals in the study were analysed for serum enzymes. Levels of hepatic leakage enzymes such as ALT, AST and GLDH, are described as markers of hepatic injury and could thus help to confirm injury (Schmidt and Schmidt, 1988; Gores et al., 1990; Van Hoof et al., 1997; Giffen et al., 2002)

However, since the main focus of the present investigation was the identification of biomarkers of hepatotoxicity, which can be collected non-invasively, urine was chosen as the preferred biofluid for analysis. One of the main advantages of using urine as the sample for biomarker identification is the fact that it can be easily collected in relatively large volumes and without any associated pain, distress and discomfort to the animal or patient, if in a clinical setting (Hewitt et al., 2004; Wu et al., 2010; Boekelheide and Schuppe-Koistinen, 2012). Urine proteomic and metabolomic methods have been extensively used in the identification of urinary biomarkers for a wide range of disease types including heart disease (Schwedhelm et al., 2004; de Zeeuw et al., 2006; Larsson, 2013), lung disease (Bode et al., 2000; Cannas et al., 2010; Niu et al., 2012), cancer (Yamaguchi et al., 2005; Sanchez-Carbayo et al., 2000; Slupsky et al., 2010) and kidney disease (Jorres et al., 1994; Kamijo et al., 2004; Dieterle et al., 2010). Previous metabolomic studies have identified taurine as a biomarker for liver toxicity (Waterfield et al., 1991; Waterfield et al., 1993).

Therefore, the objective of the present study was to develop a good model of acute hepatotoxicity without inducing toxicity to other organs. Upon development of the model, urine samples were analysed for the identification of biomarkers of liver injury.

3.2 Animal experimental design

Sixty male Hanover-Wistar rats (mean body weight 199.7 ± 28.6 g) were divided into 10 groups of 6 animals each and dosed by gavage with CCl_4 at 0 (controls), 0.4, 0.8, 1.2, 1.6, 2.0, 2.4, 2.8, 3.2 and 3.6 mL/kg. Control animals were dosed with equivalent volumes of corn oil by gavage. After dosing, animals were returned to their communal cages for 6 hours during which water and diet were available *ad libitum*. At 6 hours post-dosing, animals were placed individually in metabolism cages for the collection of 18 hour urine samples (6-24 hours post-dosing). During this period, animals had no access to diet. Urine samples were collected over ice and stored at -80 ºC for future analysis. All animals were weighed before dosing, before being placed in metabolism cages and at 24 hours post-dosing, just prior to autopsy.

At autopsy (24 hours after dosing) blood was taken for the preparation of serum which was stored at -80 ºC until analysis. The liver, kidneys, spleen, pancreas, adrenals, thymus, thyroid, testes, heart with lungs inflated and head were removed and placed in fixative as described in Section 2.8.

3.3 Results

3.3.1 Observations during the study

Throughout the study, animals were observed for signs of ill-health and clinical observations were recorded during the post-mortem procedure. The behaviour of the animals was observed to guarantee their welfare and as a first indicator of pain and distress. During the period in the metabolism cages, animals treated with CCl_4 at 3.2 mL/kg and above appeared to be slightly subdued in comparison to the control animals. One animal treated with 3.6 mL/kg CCl_4 had a hunched posture. At autopsy, i.e., 24 hours post-dosing, livers from CCl_4-treated animals appeared paler in colour when compared to the control livers and the change in colour was more pronounced as the CCl_4 dose level increased.

3.3.2 Body weights

Table 3.1 shows the change in body weight (for both control and CCl_4-treated animals) during the 18 hour period while rats were in the metabolism cages. The mean change in body weight for CCl_4-treated animals was compared to the change in body weight for controls. Although all animals lost weight over the 18 hour period the decrease in body weight for animals in the 1.2 mL/kg dose level group was the greatest (-19.83 g). Animals dosed at 2.8 mL/kg lost the least weight, -9.03 g ($^{**}P<0.01$). However, there appears to be no clear CCl_4 dose-related effect on body weight of the animals.

Table 3.1 Body weight change for male Hanover-Wistar rats treated with increasing doses of CCl_4 during an 18 hour period in metabolism cages. Animals were dosed with vehicle (control, 0 mL/kg) or CCl_4 by gavage and placed individually in metabolism cages for the collection of 18 hour urine samples as described in Section 3.2. Animals had access to water but not diet while in the metabolism cages. Weight changes are shown as mean and SD of 6 animals per group. Changes in weight that are statistically different to the changes for control animals by one-way ANOVA test are shown: $^{**}P<0.01$.

Dose level of CCl_4 (mL/kg)	Mean (SD) change in body weight (g)
0	-16.12 (2.09)
0.4	-19.25 (1.95)
0.8	-15.13 (2.89)
1.2	-19.83 (2.16)
1.6	-16.33 (1.84)
2.0	-17.15 (2.32)
2.4	-9.23** (3.01)
2.8	-9.03** (3.77)
3.2	-12.22 (4.52)
3.6	-16.17 (2.58)

3.3.3 Liver weights

Figure 3.1 A shows the mean relative liver weights at each CCl_4 dose level. The liver weights for CCl_4-treated animals were significantly increased over controls ($^{**}P<0.01$) at 0.8 mL/kg and above, and there was a dose-related increase. At the highest dose level (3.6 mL/kg), relative liver weights were approximately 2-fold greater than control animals ($^{***}P<0.001$).

3.3.4 Kidney weights

The mean relative kidney weights for rats treated with CCl_4 were similar to control at the lower dose levels (0.4, 0.8, 1.2, 1.6 and 2.0 mL/kg CCl_4) (Figure 3.1 B). However, at 2.4 mL/kg the relative kidney weights (4.23 g/kg BW) were significantly greater than controls (3.64 mg/kg BW) ($^{*}P<0.05$), and at the highest dose level (3.6 mL/kg) there was a 1.23-fold increase over control weights ($^{**}P<0.01$). However, there was no significant difference in kidney weights at 2.8 and 3.2 mL/kg CCl_4 when compared to controls.

3.3.5 Weights of other organs

At post-mortem, the spleen, thymus, heart, adrenals and testes were removed and the relative weights calculated (Table 3.2). There were no CCl_4-treatment related effects on the relative weights of the spleen, thymus and heart in this study. The mean relative adrenal weight was significantly decreased at 2.0 mL/kg compared to control animals (0.18 and 0.24 g/kg BW respectively; $^{*}P<0.05$) but similar to control at all other dose levels. The relative mean weight of the testes was decreased by 19 % in the 2.8 mL/kg group ($^{**}P<0.01$) and by 16 % in the 3.6 mL/kg group ($^{*}P<0.05$) when compared to control animals, however, in general, there was no CCl_4 dose-related trend.

A

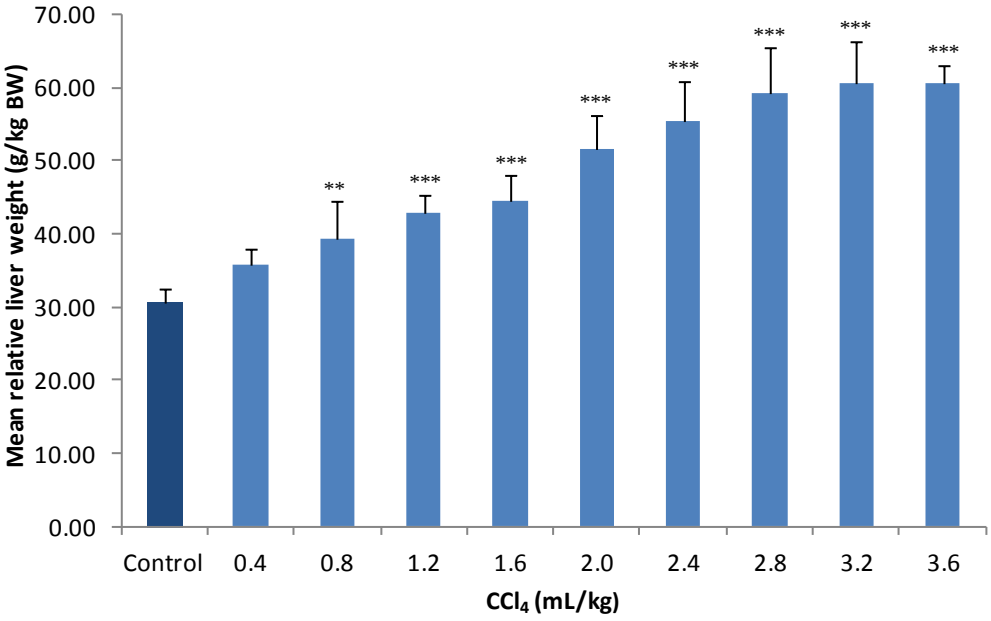

B

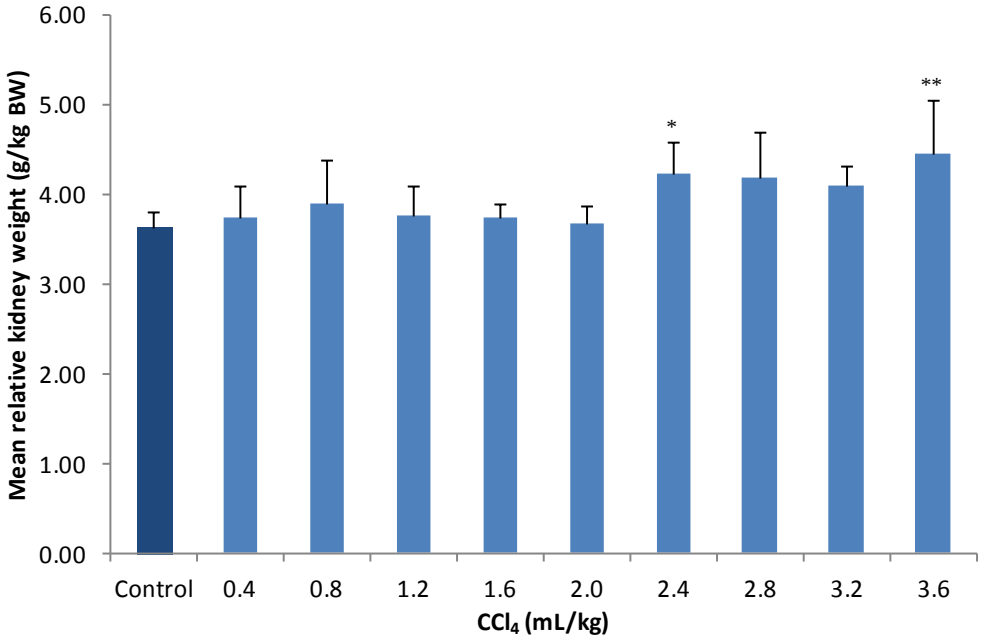

Figure 3.1 Relative liver (A) and kidney (B) weights from male Hanover-Wistar rats treated with increasing doses of CCl_4. Animals were dosed with vehicle (control, 0 mL/kg) or CCl_4 by gavage. At 24 hours post-dosing animals were killed, livers and kidneys were removed and weighed as described in Section 3.2. The kidney weight was expressed as a mean of the left and right kidneys. Results are shown as mean organ weight per kg body weight (BW) with SD indicated by vertical bars of 6 animals per group. Relative organ weights that differ significantly from controls by one-way ANOVA test are shown: $^{*}P<0.05$; $^{**}P<0.01$; $^{***}P<0.001$.

Table 3.2 Relative organ weights from male Hanover-Wistar rats treated with increasing doses of CCl_4. Animals were dosed with vehicle (control, 0 mL/kg) or CCl_4 by gavage. At 24 hours post-dosing animals were killed, organs were removed and weighed as described in Section 3.2. The testes and adrenals weight was expressed as a mean of the left and right organs. Results are shown as mean organ weight per kg body weight (BW) and SD of 6 animals per group. Relative organ weights that differ significantly from controls by one-way ANOVA test are shown: $^{*}P<0.05$; $^{**}P<0.01$.

Dose level of CCl_4 (mL/kg)	Relative organ weight (g/kg BW) (SD)				
	Spleen	**Thymus**	**Heart**	**Adrenals**	**Testes**
0	2.54 (0.36)	2.82 (0.31)	3.41 (0.19)	0.24 (0.04)	7.08 (0.68)
0.4	2.31 (0.30)	2.25 (0.21)	3.69 (0.45)	0.42 (0.04)	6.62 (0.25)
0.8	2.67 (0.24)	2.53 (0.22)	3.75 (0.47)	0.23 (0.02)	7.27 (0.84)
1.2	2.75 (0.42)	2.64 (0.65)	3.61 (0.43)	0.22 (0.03)	6.88 (0.46)
1.6	2.47 (0.33)	2.60 (0.54)	3.32 (0.24)	0.25 (0.04)	6.81 (0.65)
2.0	2.27 (0.24)	2.30 (0.59)	3.54 (0.36)	0.18^{*} (0.03)	6.33 (0.32)
2.4	2.80 (0.79)	3.05 (0.42)	3.86 (0.50)	0.22 (0.05)	6.27 (0.49)
2.8	2.64 (0.61)	3.11 (0.22)	3.67 (0.15)	0.23 (0.04)	5.74^{**} (0.39)
3.2	2.72 (0.65)	2.84 (0.83)	3.69 (0.19)	0.24 (0.02)	6.98 (0.89)
3.6	2.55 (0.41)	2.78 (0.45)	3.43 (0.22)	0.23 (0.04)	5.98^{*} (0.37)

3.3.6 Serum clinical chemistry

Clinical biochemical parameters including ALT, AST, GLDH, ALP, TIMP-1, MCP1, A2M, AGP, lipocalin-2, urea, creatinine, albumin, glucose and total protein were measured in the serum from control (vehicle-treated animals) and animals dosed with CCl_4 at 0.4, 0.8, 1.2, 1.6, 2.0, 2.4, 2.8, 3.2 and 3.6 mL/kg (Figure 3.2, Table 3.3).

Levels of ALT, AST and GLDH were measured to determine liver injury. There was an increase in ALT levels with increasing dose of CCl_4 indicating a dose response relationship. At the lowest dose level serum ALT levels were 2.5-fold greater than control (89.67 and 35.83 U/L, respectively), however, this increase was not significantly different from control. At 0.8 mL/kg CCl_4 and above, ALT levels were significantly increased in comparison to controls. At the highest dose level (3.6 mL/kg) the mean ALT value was 4640.17 U/L representing a 130-fold increase over controls. AST levels also showed a dose-related trend and were 1.4-fold greater than control values at the lowest dose level (0.4 mL/kg). However, the increased AST levels for animals dosed with CCl_4 at 0.4, 0.8, 1.2 and 1.6 mL/kg were not statistically significant but were significant at 2.0 mL/kg CCl_4 and above. At 2.0 mL/kg and 3.6 mL/kg CCl_4 serum AST levels were 9.25-fold and 47-fold greater than control, respectively ($^{***}P<0.001$) (Figure 3.2).

Serum GLDH also increased with increasing dose level of CCl_4 and levels were statistically greater than controls at all dose levels except at 0.4 mL/kg CCl_4. At the highest dose level (3.6 mL/kg) there was a 136-fold increase in GLDH levels in treated animals compared to the values for control animals ($^{***}P<0.001$) (Figure 3.2).

ALP levels were significantly increased in all CCl_4-treated groups and also demonstrated a general dose-related trend. The highest ALP measurement was 1142.17 U/L for animals treated with 3.6 mL/kg CCl_4 ($^{***}P<0.001$); this represented a 3.2-fold increase (Table 3.3).

Serum TIMP-1 levels were elevated over control in all CCl_4-treated groups (Table 3.3). The increase was statistically significant at 1.2 mL/kg CCl_4 ($^{**}P<0.01$) and above with values of 24.67 μg/L in animals treated at 1.2 mL/kg CCl_4, whereas control animals had an average TIMP-1 level of 7.00 μg/L. At 3.6 mL/kg CCl_4 there was a 25-fold increase over control TIMP-1 levels (7.00 and 177.83 μg/L for control and CCl_4-treated group, respectively).

MCP1 levels in serum were similar to control for animals treated with CCl_4 at 0.4 mL/kg, however, mean values were increased 2-fold in the 0.8 mL/kg group and at 1.6 mL/kg CCl_4 and above the increase was statistically significant. A2M levels were similar to controls in all treated groups except at 2.4 mL/kg where there was a 2-fold significant increase over control ($^{*}P<0.05$). Mean serum AGP was increased in all CCl_4-treated animals but only statistically greater than control at 2.0 mL/kg and above. Values of lipocalin-2 were similar to control in the lower dose level groups (0.4, 0.8, 1.2 and 1.6 mL/kg). At dose levels above 1.6 mL/kg lipocalin-2 levels rose with increasing CCl_4 dose, however, the values were only significant at 2.8 mL/kg and above ($^{**}P<0.01$) (Table 3.3).

To evaluate the possibility of kidney injury, which could affect the urinary proteome and metabolome, kidney function was assessed by measuring the serum levels of urea and creatinine (Table 3.3). Mean urea levels were higher than control in the serum from all CCl_4-treated animals; at the lowest dose level (0.4 mL/kg) values were almost 2-fold greater than that of controls (6.62 compared to 13.12 mmol/L, respectively). Serum creatinine levels for CCl_4-treated animals were not significantly different from control except for animals in the 3.6 mL/kg group (highest dose level). At this dose level creatinine was 3-fold increased over control (73.00 μmol/L for CCl_4-treated and 25.17

µmol/L for controls, respectively; **P<0.01). Serum albumin and glucose were similar to control in all CCl_4-treated animals. At 2.4 mL/kg serum total protein levels were significantly lower in CCl_4-treated animals compared to control. However, at all other CCl_4 dose levels there was no significant difference in protein levels between control and CCl_4-treated animals.

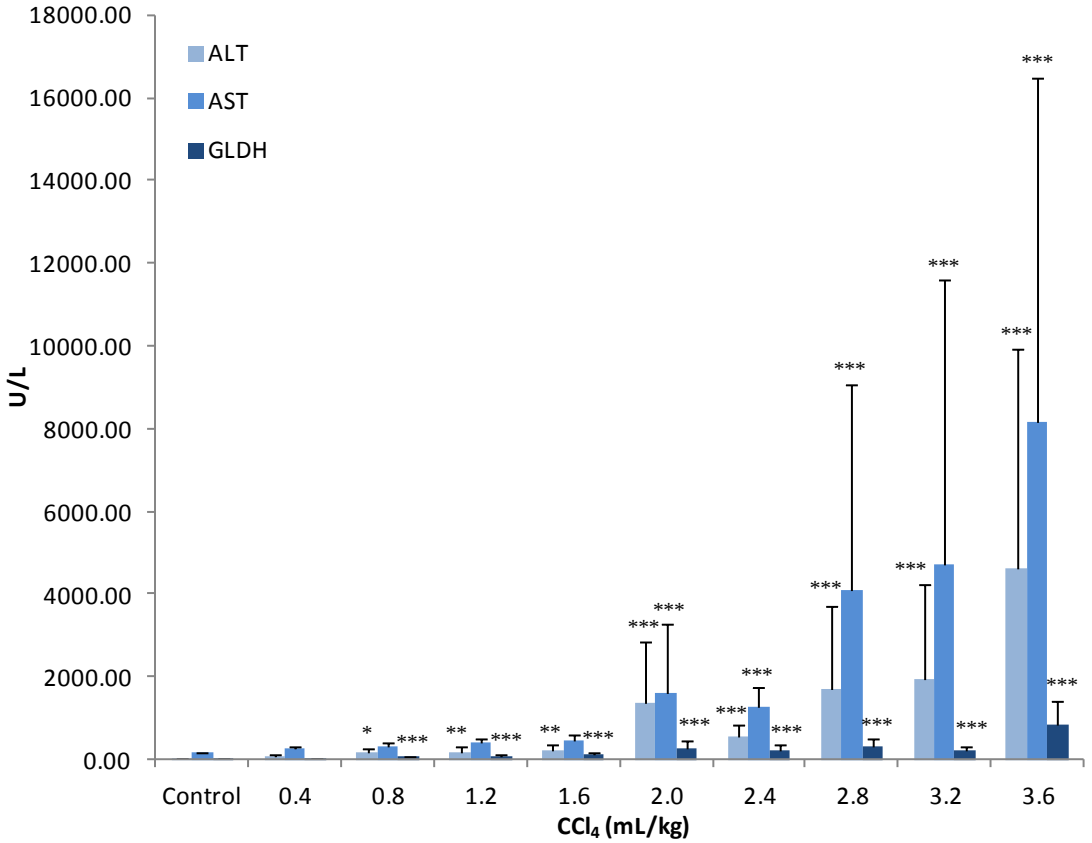

Figure 3.2 Serum ALT, AST and GLDH levels for male Hanover-Wistar rats treated with increasing doses of CCl_4. Animals were dosed with vehicle (control, 0 mL/kg) or CCl_4 by gavage. At 24 hours post-dosing, serum was collected as described in Section 3.2 and enzymes were assayed as described in Section 2.7. Values are the means with SD indicated by vertical bars of 6 animals per group. Values that differ significantly from controls by one-way ANOVA test are shown: *P<0.05; **P<0.01; ***P<0.001.

Table 3.3 Serum clinical chemistry parameters for male Hanover-Wistar rats treated with increasing doses of CCl_4. Animals were dosed with vehicle (control, 0 mL/kg) or CCl_4 by gavage. At 24 hours post-dosing, serum was collected as described in Section 3.2 and enzymes were assayed as described in Section 2.7. Values are the means and SD of 6 animals per group. Values that differ significantly from controls by one-way ANOVA test are shown: $^{*}P<0.05$; $^{**}P<0.01$; $^{***}P<0.001$.

Serum parameters	CCl_4 dose level (mL/kg)									
	0	**0.4**	**0.8**	**1.2**	**1.6**	**2.0**	**2.4**	**2.8**	**3.2**	**3.6**
ALP	356.00	521.83*	544.83**	642.17***	609.50**	759.67***	822.50***	1144.50***	884.17***	1142.17***
(U/L)	(45.17)	(107.76)	(94.71)	(169.41)	(96.42)	(122.07)	(218.99)	(270.71)	(133.30)	(195.28)
TIMP-1	7.00	8.33	15.83	24.67**	23.50**	45.00***	39.83***	82.33***	70.33***	177.83***
(µg/L)	(1.10)	(1.86)	(5.74)	(9.63)	(5.79)	(38.16)	(21.45)	(50.43)	(19.77)	(189.76)
MCP1	8.33	7.67	14.67	23.83	28.83**	65.17***	54.67***	138.00***	117.50***	206.67***
(µg/L)	(0.82)	(1.75)	(5.92)	(15.65)	(5.19)	(69.16)	(37.65)	(105.46)	(110.95)	(123.67)
A2M	45.00	30.33	42.67	40.33	35.00	29.17	86.83*	55.50	59.50	44.17
(mg/L)	(11.83)	(9.87)	(13.87)	(9.69)	(10.06)	(6.05)	(43.60)	(17.52)	(24.52)	(10.83)
AGP	45.00	63.83	66.33	76.00	82.50	138.00**	130.33*	106.50*	155.17**	128.83*
(mg/L)	(11.42)	(9.02)	(14.77)	(36.33)	(25.91)	(86.84)	(112.33)	(39.35)	(114.08)	(89.30)
Lipocalin-2	75.17	77.17	81.50	93.00	90.33	437.50	612.17	854.67**	2054.50**	1099.50***
(µg/L)	(13.12)	(14.13)	(25.24)	(25.51)	(5.72)	(704.85)	(857.02)	(748.44)	(4185.14)	(748.17)
Urea	6.62	13.12***	10.33***	10.57***	10.43***	10.82***	8.68*	9.07***	9.90***	13.03***
(mmol/L)	(0.67)	(0.72)	(1.72)	(1.02)	(1.29)	(1.31)	(1.03)	(0.64)	(1.32)	(4.65)
Creatinine	25.17	32.67	24.17	26.67	33.33	32.83	24.50	33.67	29.33	73.00**
(µmol/L)	(0.75)	(4.23)	(1.60)	(1.21)	(11.57)	(11.23)	(3.78)	(16.46)	(12.21)	(55.02)
Albumin	35.33	36.50	35.67	35.67	34.83	34.67	34.50	33.67	34.50	35.50
(g/L)	(0.82)	(1.05)	(1.03)	(0.82)	(1.72)	(1.03)	(0.84)	(2.16)	(1.22)	(1.87)
Glucose	5.60	6.15	5.74	5.50	5.97	5.81	5.28	4.29	5.41	4.34
(mmol/L)	(1.17)	(0.40)	(0.53)	(0.62)	(0.57)	(0.65)	(0.36)	(1.35)	(0.48)	(2.22)
Total protein	53.83	56.00	54.50	53.83	52.67	52.33	50.00**	49.00	50.33	53.67
(g/L)	(1.17)	(1.41)	(1.05)	(1.47)	(2.80)	(1.63)	(2.68)	(4.29)	(2.66)	(2.50)

ALP: alkaline phosphatase; TIMP-1: tissue inhibitor of matrix metalloproteinase; MCP 1: monocyte chemoattractant factor 1; A2M: alpha-2 macroglobulin; AGP: alpha-1 acid glycoprotein.

3.3.7 Urine clinical chemistry

Urine clinical chemistry was carried out to further assess the possibility of kidney injury.

Table 3.4 shows that creatinine levels were similar to control in all CCl_4-treated groups apart from at 2.8 mL/kg and 3.2 mL/kg CCl_4 when a statistically significant decrease was observed ($^{**}P<0.01$ and $^{*}P<0.05$, respectively).

Urinary total protein concentration was significantly lower than control in all CCl_4-treated rats apart from at the lowest dose (0.4 mL/kg) when levels were similar to control. However, there was no evidence of a dose-related trend. Urinary albumin levels were not affected by CCl_4 administration in a dose-related manner; however, at the highest dose level (3.6 mL/kg) urinary albumin was significantly increased by 4.6-fold over control ($^{*}P<0.05$). Urinary glucose levels were increased in all CCl_4-treated animals with the greatest increase occurring in animals in the 2.0 mL/kg CCl_4 group. Animals in this group had mean glucose levels of 6.17 µmol/c.p. in comparison to 3.00 µmol/c.p. for the controls ($^{***}P<0.001$).

Table 3.4 Urinary clinical chemistry parameters for male Hanover-Wistar rats treated with increasing doses of CCl_4. Animals were dosed with vehicle (control, 0 mL/kg) or CCl_4 by gavage and urine collected for 18 hours post-dosing as described in Section 3.2. Clinical parameters were assayed as described in Section 2.7. Values are the means and SD of 6 animals per group and are expressed as c.p. (collection period, 18 hours). Values that differ significantly from controls by one-way ANOVA test are shown: $^{*}P<0.05$; $^{**}P<0.01$; $^{***}P<0.001$.

Urinary parameters	**CCl_4 dose level (mL/kg)**									
	0	**0.4**	**0.8**	**1.2**	**1.6**	**2.0**	**2.4**	**2.8**	**3.2**	**3.6**
Creatinine	34.17	43.83	31.50	35.00	34.83	40.50	26.67	22.17**	23.67*	27.67
(µmol/c.p.)	(9.04)	(4.17)	(2.26)	(2.45)	(2.56)	(8.02)	(10.03)	(2.48)	(4.13)	(4.23)
Total protein	6.13	6.02	2.25***	1.95***	2.23***	2.42**	1.45***	1.32***	1.47***	3.90*
(mg/c.p.)	(1.83)	(1.47)	(0.27)	(0.58)	(0.60)	(0.66)	(0.62)	(0.24)	(0.68)	(3.18)
Albumin	149.98	216.37	146.42	125.99	130.83	225.64	199.49	154.26	204.26	688.33*
(ng/c.p.)	(70.37)	(56.12)	(89.83)	(43.14)	(10.78)	(107.93)	(67.43)	(75.37)	(152.58)	(660.78)
Glucose	3.00	5.00**	4.17	4.50*	4.33	6.17***	5.17**	4.00	4.50*	5.67***
(µmol/c.p.)	(0.63)	(0.89)	(0.98)	(0.55)	(1.03)	(1.72)	(1.94)	(0.89)	(0.84)	(1.51)
Volume	10.48	11.77	19.90	28.73**	20.05	18.13	12.97	15.28	9.70	11.87
(mL)	(4.90)	(5.74)	(7.07)	(8.43)	(10.14)	(15.07)	(5.65)	(9.41)	(3.79)	(4.11)

3.3.8 Histopathology

Animals were autopsied as described in Section 3.2. Tissue samples were collected and placed in fixative for histopathological examination.

In this study, kidneys, liver and nasal cavity were examined in all animals, except for those in the 2.4 or 3.2 mL/kg CCl_4-treated groups. These groups were eliminated as a result of the large number of tissue samples generated and the time taken to process the samples. In addition, adrenals, heart, lungs, pancreas, spleen, testes, thyroid and thymus were only examined from control animals and animals dosed at 2.0, 2.8 and 3.6 mL/kg CCl_4 as the probability of finding CCl_4-treatment-related injuries increases with increasing dose level.

For each of the histopathological changes described below, Table 3.5 to Table 3.8 show the number of animals in each dose group exhibiting the pathological change.

Hepatocellular changes associated with CCl_4 treatment were apparent at all CCl_4 dose levels (Table 3.5, Figure 3.3). Centrilobular hepatocellular vacuolation was either marked or very marked and a proportion of centrilobular hepatocytes showed ballooning of the cytoplasm in all treated animals (Figure 3.3). Hepatocyte necrosis was recorded in animals administered CCl_4 at 0.8 mL/kg and above, the extent of which became more marked with increasing dose level. There was also a focal mixed inflammatory cell infiltrate present in all CCl_4-treated animals.

In the kidneys, pathological findings considered to be related to CCl_4 treatment were observed in a small number of the animals at dose levels of 2.8 mL/kg and above. These changes included granular casts in collecting ducts, dilatation of distal and/or collecting tubules, and minimal proximal tubular necrosis (Table 3.6, Figure 3.4).

Sections of the nasal cavity were prepared to include the ethmoid turbinates (Table 3.7). Turbinate bone refers to the thin and curved bone structures that project from the walls of the nasal cavity into the respiratory passage in vertebrates. The ethmoid turbinates extend from the ethmoid bone. Degeneration of the olfactory epithelium, characterised by necrosis and vacuolation, was present at all CCl_4 dose levels. The severity and extent of nasal cavity injury varied between animals in a group and there was no clear dose response relationship, except for the findings of ulceration of the olfactory epithelium which only occurred in some animals administered CCl_4 at 2.0 mL/kg and above. Additional histology sections of the nasal cavity were examined to evaluate the extent

of the lesion and in the 3.6 mL/kg CCl_4 group 2 animals showed evidence of respiratory epithelial ulceration.

Histological examination revealed that there was no evidence of CCl_4-related toxicity in any of the other organs examined (spleen, pancreas, adrenals, thymus, thyroid, heart and lungs) apart from the testes where the presence of multinucleate spermatid giant cells was found in 1 animal in the 3.6 mL/kg CCl_4 group (Table 3.8). Atrophy of the seminiferous tubules was seen in 1 control animal.

In summary there were CCl_4-treatment-related findings in the liver and nasal cavity at all CCl_4 dose levels and in the kidneys at dose levels of 2.8 mL/kg CCl_4 and above.

Table 3.5 Histopathological findings in the liver of male Hanover-Wistar rats treated with increasing doses of CCl_4. Animals were dosed with vehicle (control, 0 mL/kg) or CCl_4 by gavage and autopsied at 24 hours post-dosing as described in Section 3.2. Six animals per group were examined. Each column represents the number of animals in that dose group showing the pathological changes described in the rows.

	CCl_4 dose level (mL/kg)							
	0	**0.4**	**0.8**	**1.2**	**1.6**	**2.0**	**2.8**	**3.6**
No abnormality detected	**6**	**0**	**0**	**0**	**0**	**0**	**0**	**0**
Centrilobular vacuolation								
Marked	0	6	6	5	0	0	1	0
Very marked	0	0	0	1	6	6	5	6
Centrilobular cytoplasmic ballooning								
Minimal	0	5	0	0	0	0	0	0
Mild	0	1	2	1	0	1	1	5
Moderate	0	0	2	4	4	1	4	1
Marked	0	0	2	1	2	4	0	0
Very marked	0	0	0	0	0	0	1	0
Focal and mixed inflammatory cell infiltrate								
Mild	0	6	4	2	1	0	0	0
Moderate	0	0	2	4	5	5	6	6
Marked	0	0	0	0	0	1	0	0
Centrilobular hepatocyte necrosis								
Minimal	0	0	2	2	0	0	0	0
Mild	0	0	0	1	1	0	0	0
Moderate	0	0	0	1	5	4	0	0
Marked	0	0	0	0	0	2	6	2
Very marked	0	0	0	0	0	0	0	4

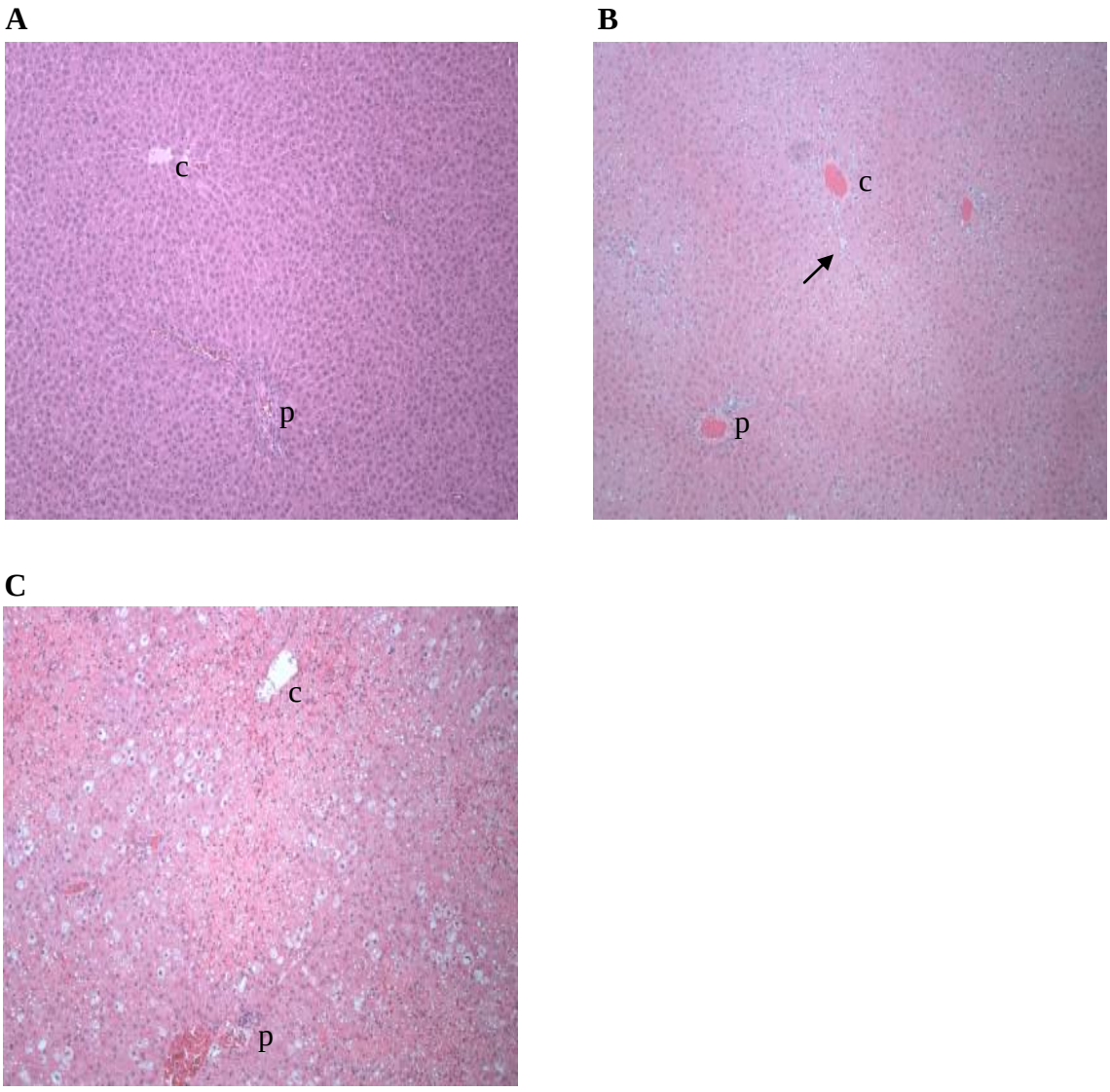

Figure 3.3 Histology of liver sections from male Hanover-Wistar rats treated with different doses of CCl_4. Original magnification of all images, x 100; H&E Animals were dosed with vehicle (control, 0 mL/kg) or CCl_4 at 0.4 and 3.6 mL/kg by gavage. At autopsy, liver samples were collected and processed for histopathological examination as described in Section 2.8. (A) control rat: central vein (c) and portal vein (p); (B) 0.4 mL/kg CCl_4-treated rat: vacuolation of centrilobular hepatocytes (arrow) (central vein (c) and portal vein (p)); (C) 3.6 mL/kg CCl_4-treated rat: necrosis of centrilobular hepatocytes and widespread vacuolation (central vein (c) and portal vein (p)).

Table 3.6 Histopathological findings in the kidneys of male Hanover-Wistar rats treated with increasing doses of CCl_4. Animals were dosed with vehicle (control, 0 mL/kg) or CCl_4 by gavage and autopsied at 24 hours post-dosing as described in Section 3.2. Six animals per group were examined. Each column represents the number of animals in that dose group showing the pathological changes described in the rows.

	CCl_4 dose level (mL/kg)							
	0	**0.4**	**0.8**	**1.2**	**1.6**	**2.0**	**2.8**	**3.6**
No abnormality detected	**0**	**4**	**5**	**5**	**5**	**0**	**0**	**0**
Proximal tubule vacuolation								
Minimal	4	0	0	0	0	4	2	0
Mild	0	0	0	0	0	0	4	4
Focal tubular basophilia								
Minimal	1	0	0	0	0	1	2	0
Granular casts in papillary collecting ducts								
Mild	0	0	0	0	0	0	0	2
Granular casts in collecting tubules								
Minimal	0	0	0	0	0	0	1	1
Mild	0	0	0	0	0	0	0	1
Distal and collecting tubule dilatation								
Mild	0	0	0	0	0	0	0	2
Hyaline droplets in proximal tubule								
Minimal	5	2	1	1	1	5	0	2
Proximal tubule necrosis								
Minimal	0	0	0	0	0	0	0	2

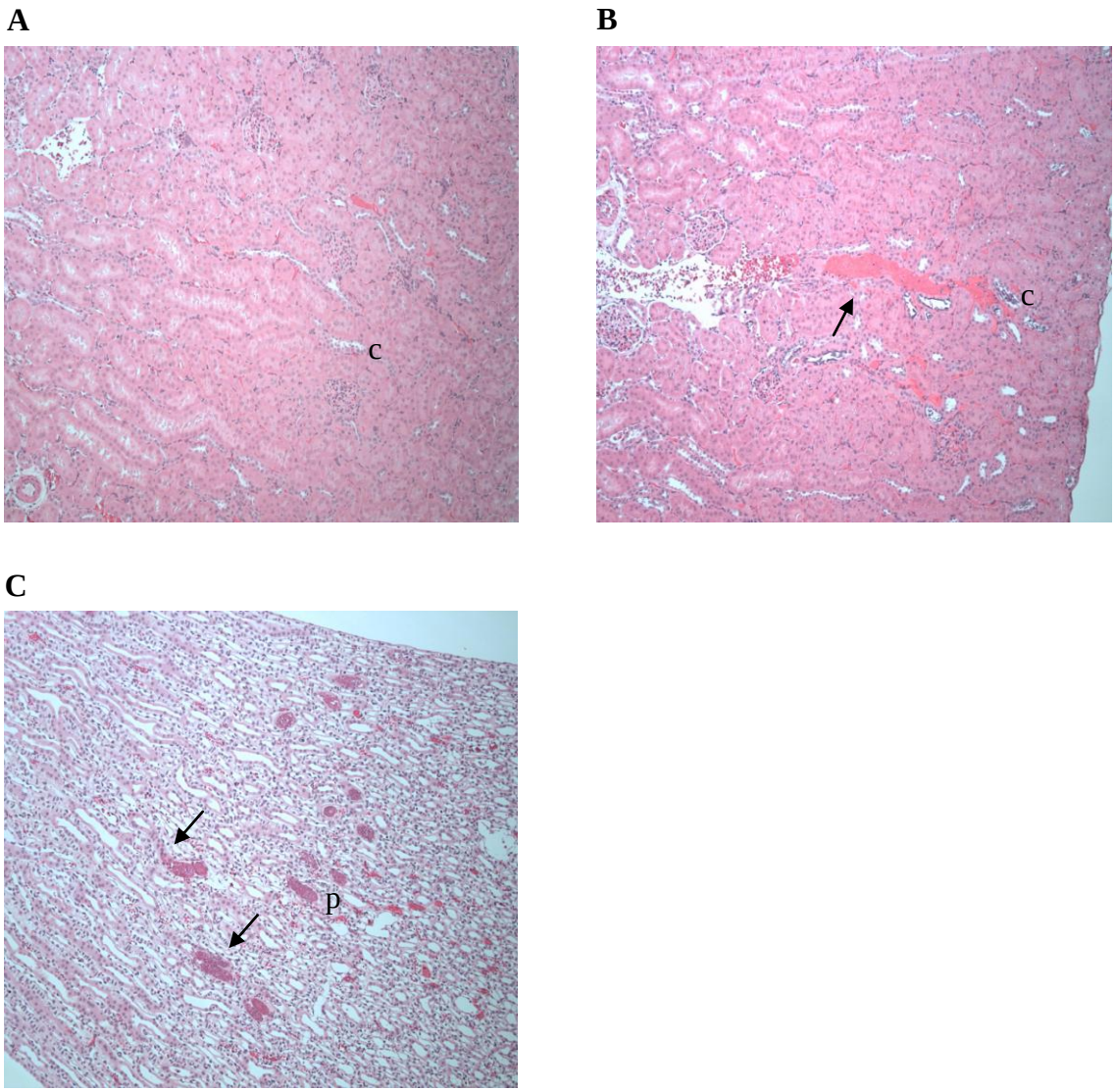

Figure 3.4 Histology of the kidney cortex from male Hanover-Wistar rats treated with different doses of CCl_4. Original magnification of all images, x 100; H&E. Animals were dosed with vehicle (control, 0 mL/kg) or CCl_4 at 3.6 mL/kg by gavage. At autopsy, kidney samples were collected and processed for histopathological examination as described in Section 2.8. (A) control rat: collecting tubule (c); (B) 3.6 mL/kg CCl_4-treated rat: casts in a collecting tubule (c) (arrow); (C) 3.6 mL/kg CCl_4-treated rat: casts in collecting duct (p) (arrows).

Table 3.7 Histopathological findings in the nasal cavity of male Hanover-Wistar rats treated with increasing doses of CCl_4. Animals were dosed with vehicle (control, 0 mL/kg) or CCl_4 by gavage and autopsied at 24 hours post-dosing as described in Section 3.2. Six animals per group were examined. Each column represents the number of animals in that dose group showing the pathological changes described in the rows.

	CCl_4 dose level (mL/kg)							
	0	**0.4**	**0.8**	**1.2**	**1.6**	**2.0**	**2.8**	**3.6**
No abnormality detected	**6**	**0**	**0**	**0**	**0**	**0**	**0**	**1**
Olfactory epithelium vacuolation								
Minimal	0	0	0	0	1	0	0	0
Mild	0	5	2	1	4	1	2	2
Moderate	0	1	4	5	1	3	3	1
Olfactory epithelium degeneration								
Minimal	0	0	1	0	4	1	0	1
Mild	0	2	2	3	0	2	4	0
Moderate	0	3	1	3	0	3	1	2
Marked	0	0	0	0	0	0	0	2
Olfactory epithelium ulceration	0	0	0	0	0	2	3	3
Respiratory epithelium ulceration	0	0	0	0	0	0	0	2

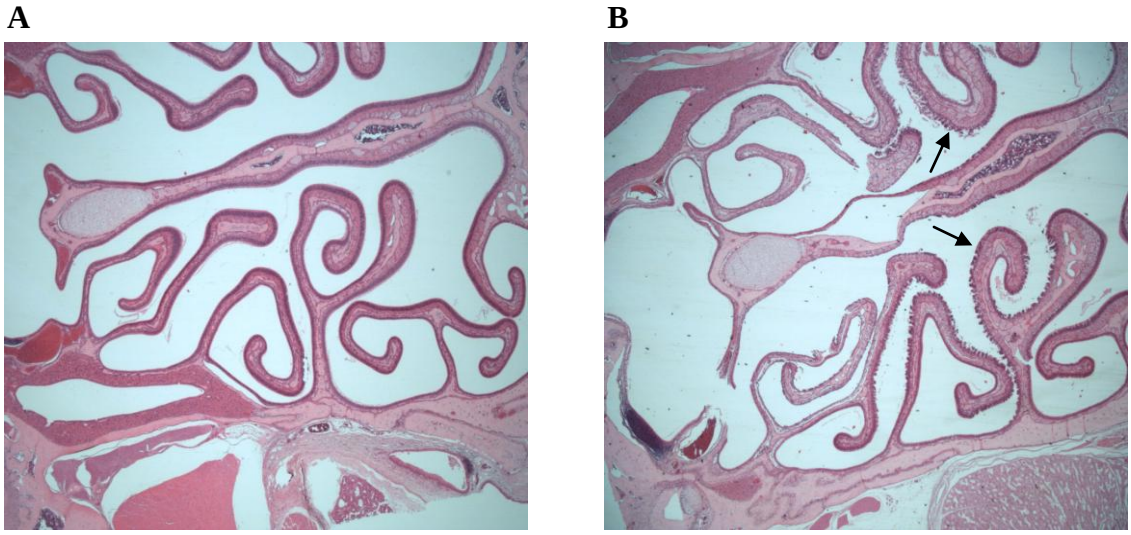

Figure 3.5 Histology of the nasal cavity from male Hanover-Wistar rats treated with different doses of CCl_4. Original magnification of all images, x 20; H&E. Animals were dosed with vehicle (control, 0 mL/kg) or CCl_4 at 3.6 mL/kg by gavage. At autopsy, samples were collected and processed for histopathological examination as described in Section 2.8. (A) control rat; (B) 3.6 mL/kg CCl_4-treated rat: degeneration of the olfactory epithelium and extensive necrosis (arrows).

Table 3.8 Histopathological findings in the testes of male Hanover-Wistar rats treated with increasing doses of CCl_4. Animals were dosed with vehicle (control, 0 mL/kg) or CCl_4 by gavage and autopsied at 24 hours post-dosing as described in Section 3.2. Six animals per group were examined. Each column represents the number of animals in that dose group showing the pathological changes described in the rows.

	CCl_4 dose level (mL/kg)			
	0	**2.0**	**2.8**	**3.6**
No abnormality detected	**5**	**6**	**6**	**5**
Focal unilateral atrophy of the seminiferous tubules				
Minimal	1	0	0	0
Multinucleate spermatid giant cells				
Minimal	0	0	0	1

3.3.9 1D ^{1}H NMR spectrometry

Urine samples were collected from rats between 6 and 24 hours post-dosing with a single dose of CCl_4 at 0, 0.4, 0.8, 1.2, 1.6, 2.0, 2.4, 2.8, 3.2 and 3.6 mL/kg. Urine samples were prepared by the addition of D_2O and analysed by 1D ^{1}H NMR to assess changes in the urinary metabolite profile.

Resonances in the urine 1D ^{1}H NMR spectra were observed and identified as described in Section 2.11.

Visual inspection of characteristic 1D ^{1}H NMR spectra of urine samples revealed similarities between the metabolite profiles of CCl_4-treated animals and control rats. However, some differences (e.g. change in peak intensity/concentration) in the profiles were evident particularly when urine from 3.6 mL/kg CCl_4-treated animals (highest dose group) was compared to controls. Peaks displaying changes due to CCl_4-induced injury included taurine (δ 3.14, δ 3.30), succinate (δ 2.30), creatine (δ 2.94, δ 3.78), creatinine (δ 3.02), 2-oxoglutarate (δ 2.34, δ 2.90), hippurate (δ 3.86, δ 7.54, δ 7.58, δ 7.74), fumarate (δ 6.54) and citrate (δ 2.42, δ 2.62).

Before analysis, spectra were pre-processed and multivariate data analysis was carried out using mean-centered data and Pareto-scaling as described in Section 2.11. PCA, an unsupervised pattern recognition method was used to analyse the spectra from the 6 animals at each dose level. PCA is a pattern recognition technique that allows separation of samples into clusters according to the similarities between them. Results can be visualized into two types of plots, the scores plot where each point represents an individual sample, and allows the observation of patterns, clusters and outliers; and the

loadings plot, where each point represents a variable, i.e., a spectral signal. The loadings plot provides the basis for metabolite differences interpretation and identification. The PCA scores plot was obtained from the 1D ^{1}H NMR analysis of the urine samples as described in Section 2.11. There was no evidence of distinct clustering patterns between control and CCl_4-treated samples at the different dose levels and many of the data points displayed overlap (Figure 3.6). Outlier samples that fell outside the Hotelling's T2 plot were individually analysed and excluded from further analysis when necessary as described in Section 2.11.

The lack of distinct clustering patterns between the control and CCl_4-treated samples may have been due to the type of data analysis (PCA) carried out. Therefore, to further investigate the possibility of metabolomic differences between vehicle-treated (control) and CCl_4-treated samples, a supervised pattern recognition method (OPLS) was used. OPLS is a prediction and regression method that finds the information in the X data (which can be 1D ^{1}H NMR spectral data) that is related to known information, the Y data (which can be class information, treatments, time or dose).

Figure 3.7 A shows the OPLS scores plot of urine samples treated at 0, 0.4, 0.8, 1.2, 1.6, 2.0, 2.4, 2.8, 3.2 and 3.6 mL/kg CCl_4. There was an increased degree of sample separation compared to the PCA model (Figure 3.6), and it appeared there was a dose-related trend. As the CCl_4 dose level increased there was a shift towards the right hand side of the plot. Consequently, urine samples from control and CCl_4 treated groups at 0.4, 0.8, 1.2 and 1.6 mL/kg were mainly located on the left half of the plot, whereas urine samples from higher CCl_4 dose levels (2.0 mL/kg CCl_4 and above) clustered on the right half of the scores plot.

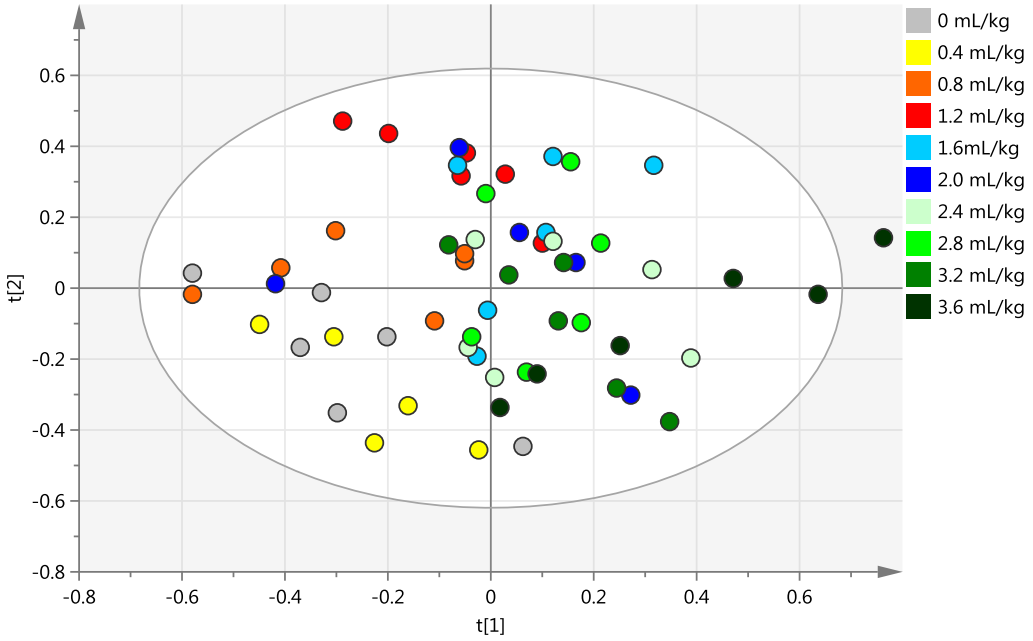

Figure 3.6 PCA scores plot from a PCA model derived from 1D ^{1}H NMR spectral data of urine samples from male Hanover-Wistar rats treated with increasing doses of CCl_4. Rats were treated with vehicle (control, 0 mL/kg) or CCl_4 by gavage and urine collected for 18 hours as described in Section 3.2. Each spot in the scores plot represents one urine sample. R^2X (cum) = 0.508, Q^2 (cum) = 0.251.

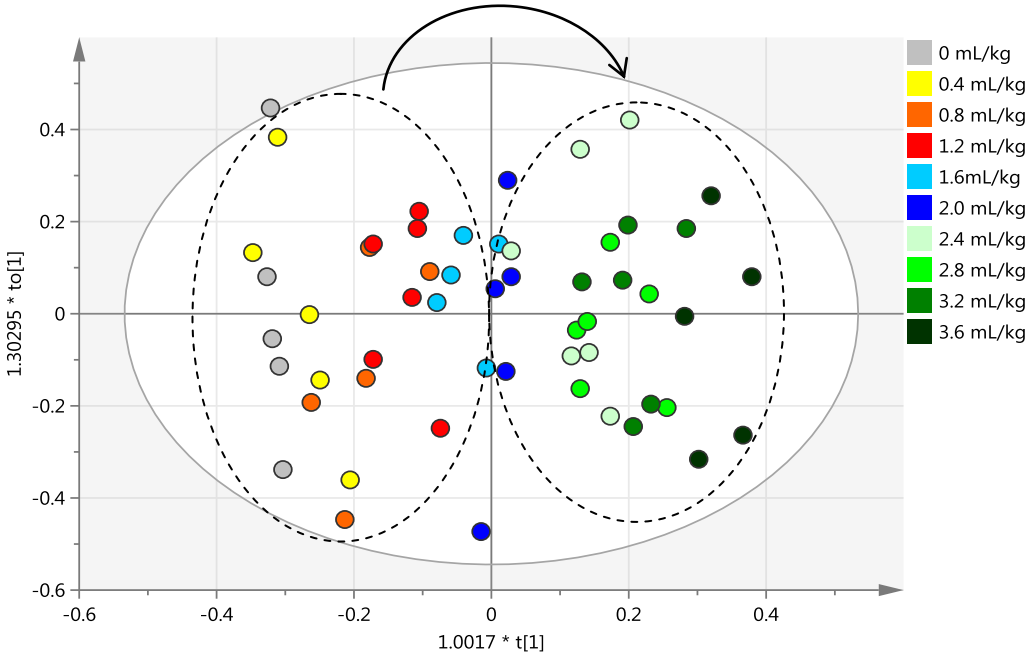

Figure 3.7 OPLS scores plot from an OPLS model derived from 1D ^{1}H NMR spectral data of urine samples from male Hanover-Wistar rats treated with increasing doses of CCl_4. Rats were treated with vehicle (control, 0 mL/kg) or CCl_4 by gavage and urine collected for 18 hours as described in Section 3.2. Each spot in the scores plot represents one urine sample. R^2X (cum) = 0.615, Q^2 (cum) = 0.855. Arrows represent direction of movement.

A second OPLS model was constructed after exclusion of urine samples from animals treated with CCl_4 at dose levels above 2.0 mL/kg (Figure 3.8). At these higher dose levels, histopathological examination confirmed CCl_4-induced kidney injury (see discussion in Section 3.4). Therefore, metabolite changes in the urine from animals dosed with CCl_4 above 2.0 mL/kg may reflect nephrotoxicity as well as hepatotoxicity. Since the aim of these studies was to identify biomarkers of hepatotoxicity, the elimination of these samples from the analysis ensures that changes in metabolite levels are solely due to liver injury.

Figure 3.8 shows the scores plot and the corresponding loadings plot for the OPLS model. The scores plot shows the presence of 6 different clusters corresponding to each of the treatment groups (controls, 0.4, 0.8 1.2, 1.6 and 2.0 mL/kg). A clear dose-dependent separation along the first component (t[1]) is present; arrows in the scores plot represent the shift along PC1. By removing CCl_4-treatment groups where urinary renal toxicity-specific metabolites may have been present we were able to eliminate confounding factors that were unrelated to the effect studied and therefore enhance the correlation between the X matrix and the Y variable of the OPLS model.

The loadings plot (Figure 3.8 B) reveals the chemical shifts which contribute to sample separation in the scores plot. The position of each NMR variable on the loadings plot is related to the direction of its contribution to the separation of samples on the scores plot. Therefore, spectral regions corresponding to the chemical shifts located on the right hand side of the loadings plot were increased in urine samples from CCl_4-treated rats at the higher dose levels.

To further investigate the differences between control and treated samples an OPLS-DA model was used (Figure 3.9). When the Y variable in an OPLS model is a discrete variable (for example, male or female, control and treated or different dose levels, like in the present study), the model becomes an OPLS-DA model. OPLS-DA models are mostly useful in sample discrimination, that is, in the identification and classification of potential biomarker candidates and in the separation of multiple treatments (Rezzi et al., 2007). In the OPLS-DA model, control samples were treated as class 1 and CCl_4-treated urine samples were treated as class 2. Consequently, the data was modelled so that information contributing to sample separation was forced onto the first component (t[1]), whereas orthogonal information relating to intra group variability was modelled in the successive components.

A

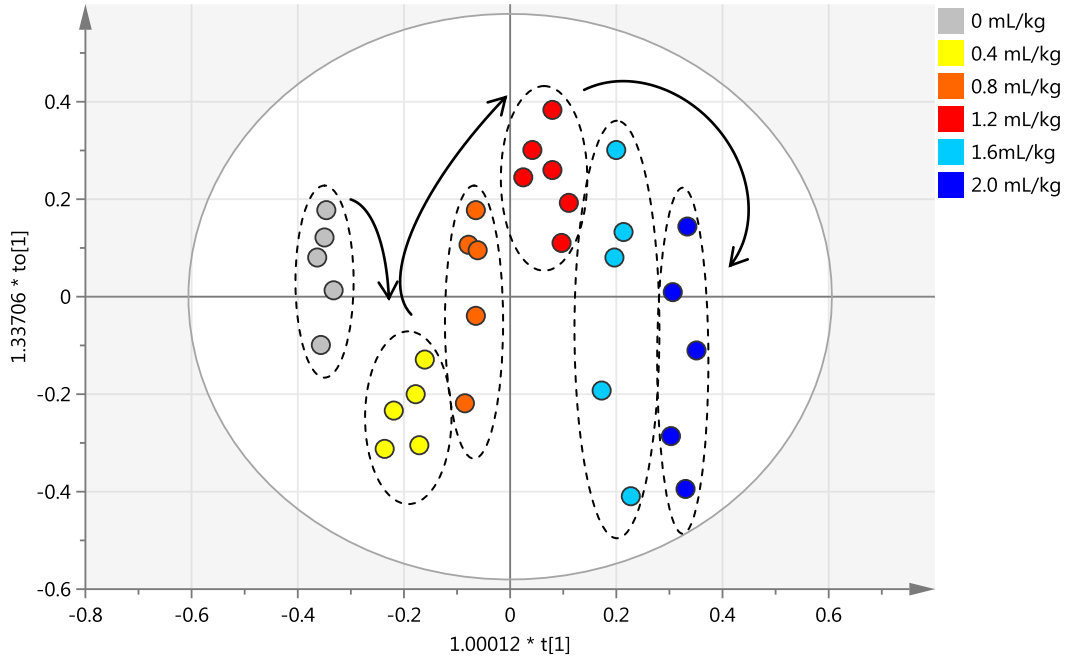

B

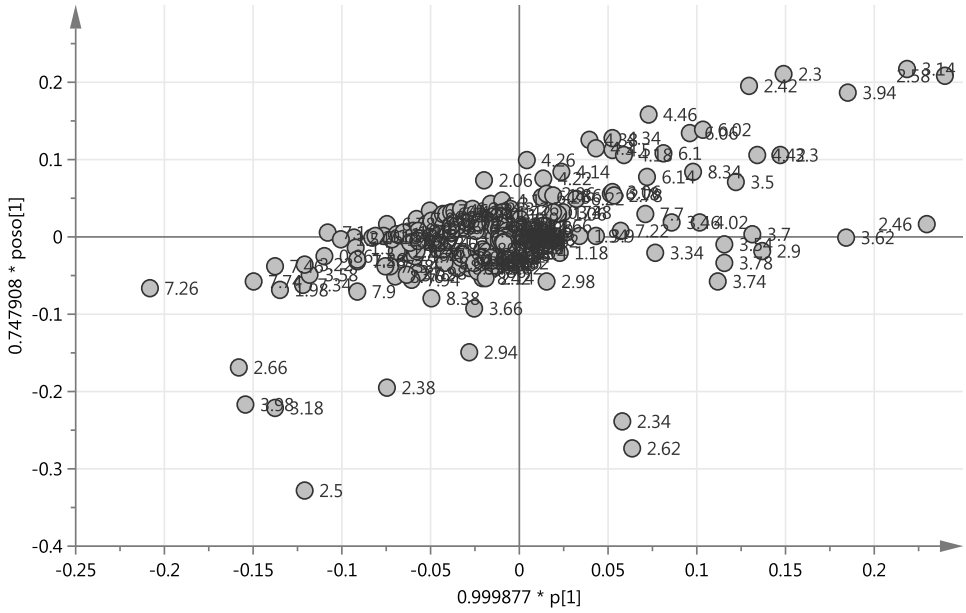

Figure 3.8 OPLS scores plot (A) and loadings plot (B) from an OPLS model derived from 1D ^{1}H NMR spectral data of urine samples from male Hanover-Wistar rats treated with increasing doses of CCl_4. Rats were treated with vehicle (control, 0 mL/kg) or CCl_4 by gavage and urine collected for 18 hours as described in Section 3.2. Each spot in the scores plot represents one urine sample and each spot in the loadings plot represents a 1D ^{1}H NMR variable labelled as chemical shift in ppm. R^2X (cum) = 0.790, Q^2 (cum) = 0.864. Arrows represent direction of movement.

Interpretation of an OPLS-DA loadings plot is difficult to achieve with more than 2 classes due to the presence of multiple sample clusters which all have the ability to influence the loadings plot simultaneously. Therefore, individual OPLS-DA models for control and treated samples at 0.4, 0.8, 1.2 and 1.6 mL/kg CCl_4 were performed and are shown in Figure 3.9. These plots revealed a very good degree of separation between control and treated samples along the discriminating component t[1]. In all plots, control samples clustered on the left hand side of the scores plot and CCl_4-treated samples clustered on the right hand side.

In this study, the maximum CCl_4 dose level which induced hepatotoxicity without causing kidney injury was 2.0 mL/kg as confirmed by histopathological examination which reported the absence of a CCl_4-induced nephrotoxic effect at this dose level. Therefore, this dose level was chosen as the optimal CCl_4 concentration for the further investigation of potential biomarkers of hepatotoxicity.

The OPLS-DA scores plot, corresponding loadings plot, S-plot and VIP plot for control samples and samples treated at 2.0 mL/kg CCl_4 are shown in Figure 3.10. The S-plot is used to visualise the OPLS-DA loadings plot and helps to extract potential biomarkers. An ideal biomarker should have a high magnitude and high reliability; therefore, variables which are responsible for most of the clustering separation will be located at the extremes of the S-plot. The upper right quadrant of the S-plot shows the chemical shifts that are increased in CCl_4-treated samples, whereas chemical shifts located in the lower left quadrant of the S-plot are increased in control samples (Figure 3.10 C).

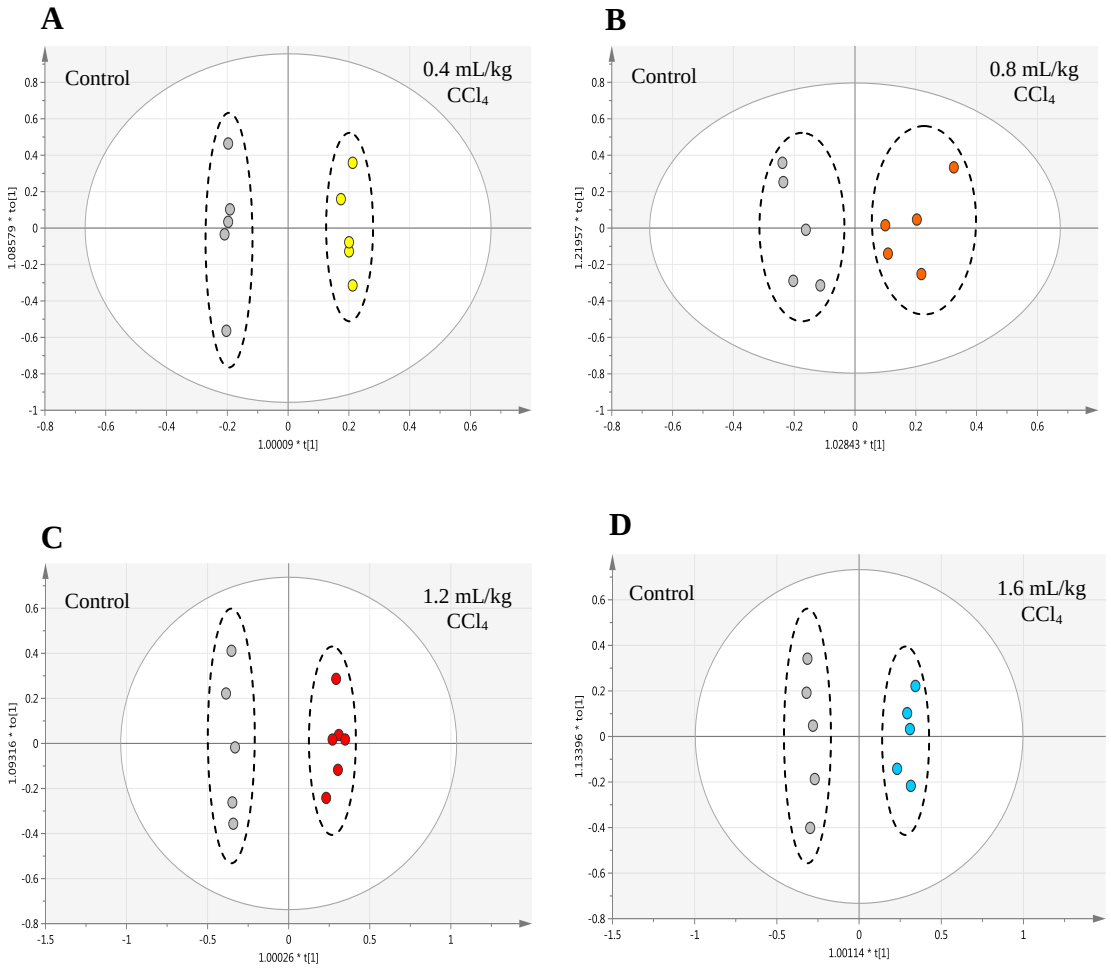

Figure 3.9 Scores plots from OPLS-DA models derived from 1D ^{1}H NMR spectral data of urine samples from male Hanover-Wistar rats treated with increasing doses of CCl_4. Rats were treated with vehicle (control, 0 mL/kg) or CCl_4 by gavage and urine collected for 18 hours as described in Section 3.2. Each spot in the scores plot represents one urine sample. (A) control and 0.4 mL/kg CCl_4-treated animals; (B) control and 0.8 mL/kg CCl_4-treated animals; (C) control and 1.2 mL/kg CCl_4-treated animals and (D) control and 1.6 mL/kg CCl_4-treated animals. Grey spots = control samples; coloured spots = CCl_4-treated samples.

A

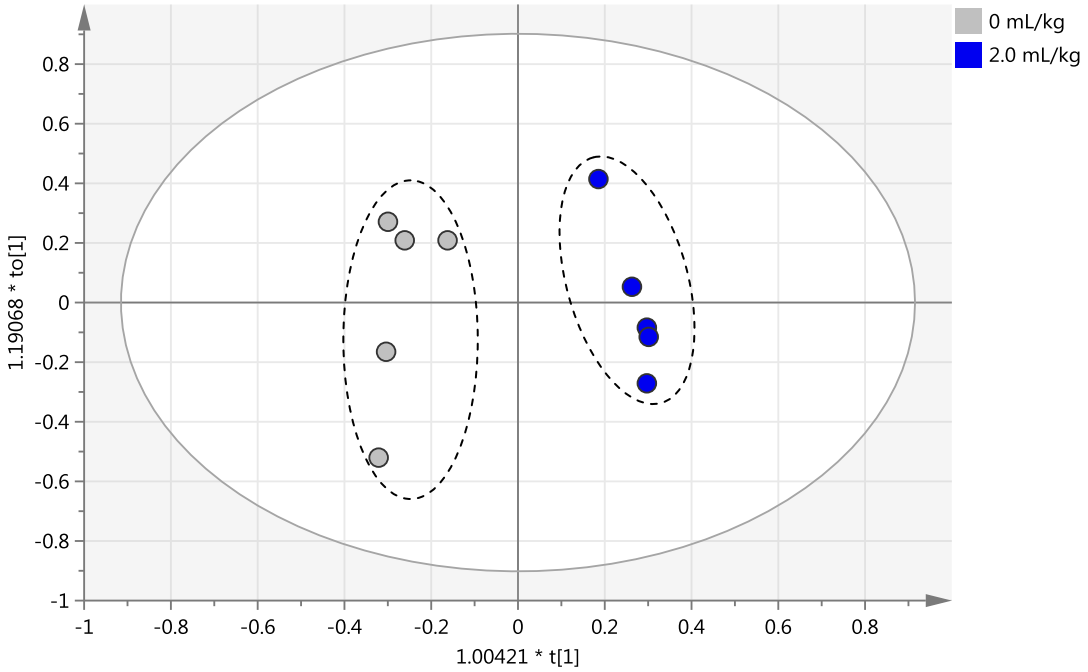

B

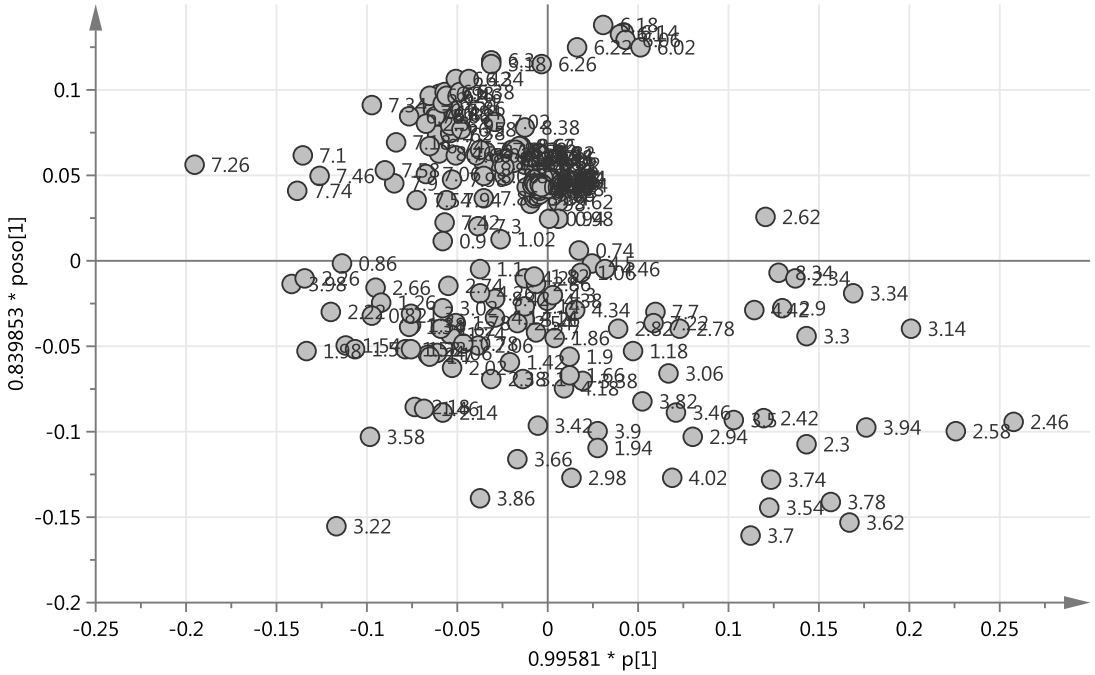

C

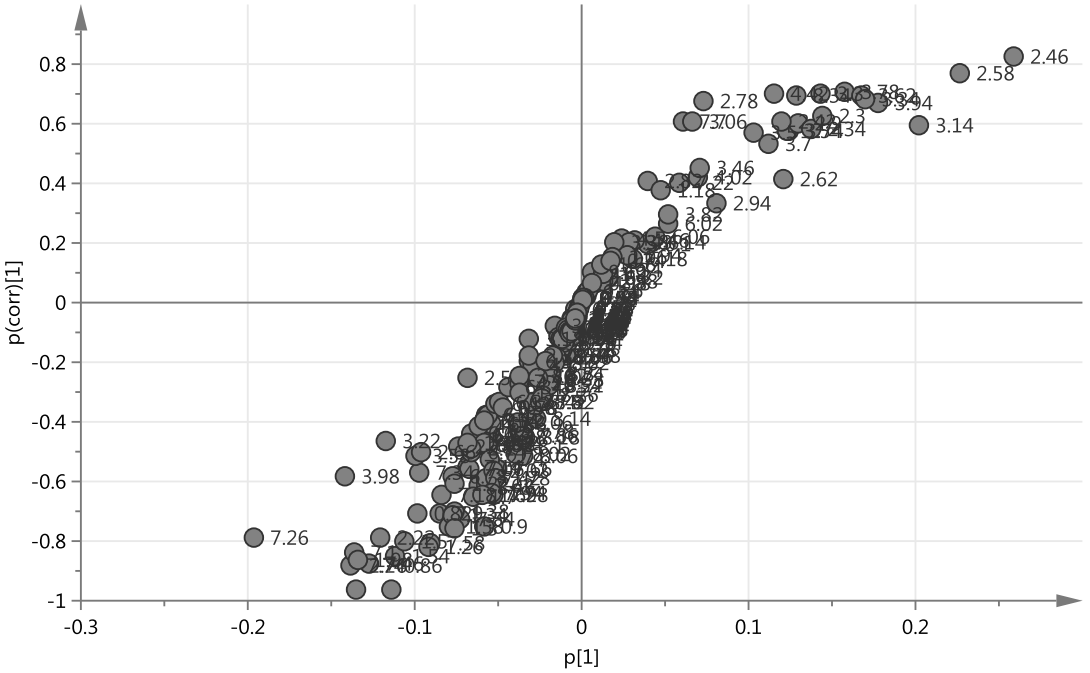

D

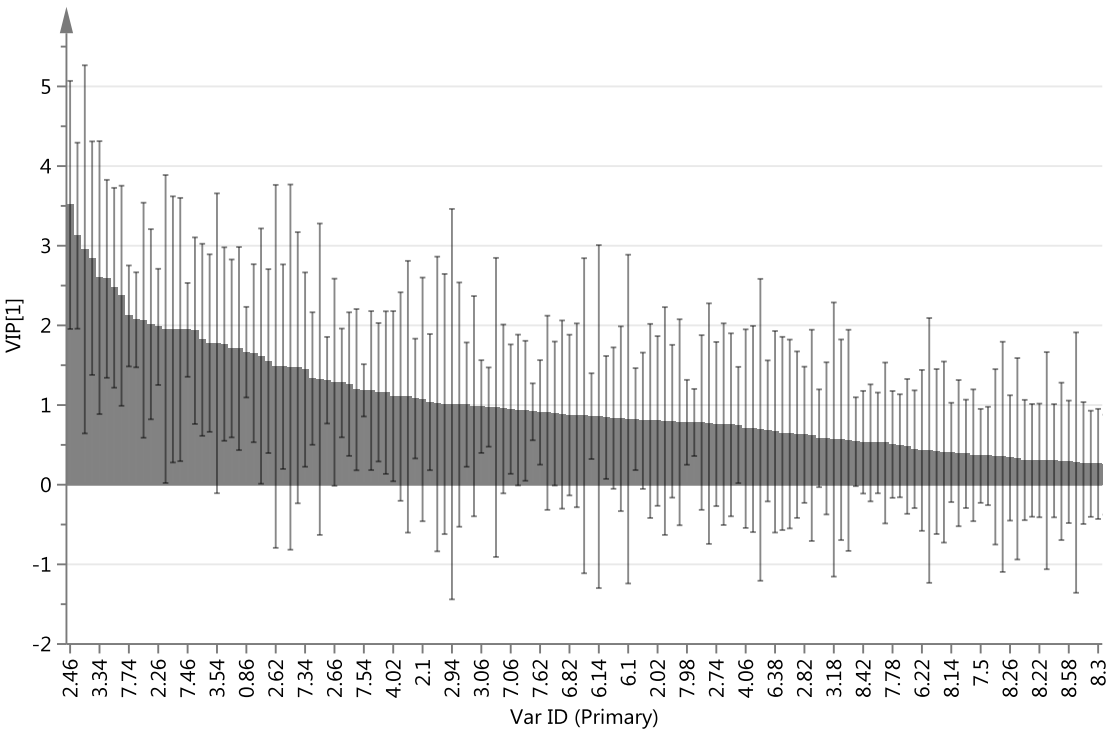

Figure 3.10 Scores plot (A), loadings plot (B), S-plot (C) and VIP-plot (D) from an OPLS-DA model derived from 1D ^{1}H NMR spectral data of urine samples from male Hanover-Wistar rats treated with vehicle (control) or CCl_4 at 2.0 mL/kg. Rats were dosed by gavage and urine collected for 18 hours as described in Section 3.2. Each spot in the scores plot represents one urine sample and each spot in the loadings plot, S-plot and VIP-plot represents a 1D ^{1}H NMR variable labelled as chemical shift in ppm. R^2X (cum) = 0.680, Q^2 = 0.695.

Variables of interest were chosen based on the variable importance in the projection plot (VIP) values (VIP≥1), having a high p[1] value and p(corr)[1] value (Figure 3.10 D). Each of these variables represents a chemical shift region (bin). Therefore, the NMR spectra were visually inspected at each of the regions identified. Peaks in these regions were evaluated for chemical shift value and multiplicity and this data was compared with data in previously published literature (Nicholls et al., 2001). Several other chemical shifts were also identified as major contributors to class separation but could not be assigned to metabolites. Subsequently, a list of some of the metabolites showing changes between control and 2.0 mL/kg CCl_4-treated samples was constructed (Table 3.9). A Student's t-test was carried out to determine the statistical significance of the difference in the integral values for the chemical shift regions.

The most relevant changes in the 1D ^{1}H NMR urinary metabolomic profile of male Hanover-Wistar following the administration of 2.0 mL/kg CCl_4 include an increase in the resonances of taurine, formate, creatine, 2-oxoglutarate, citrate, glucose and succinate, and a decrease in the resonances of hippurate, fumarate and creatinine. These changes in resonance relate to increases and decreases in the urinary concentration of these metabolites.

Table 3.9 OPLS-DA detected 1D ^{1}H NMR chemical shifts responsible for the separation of 1D ^{1}H NMR derived spectra in the urine of male Hanover-Wistar rats treated with vehicle (control) or CCl_4 at 2.0 mL/kg. Rats were dosed by gavage and urine collected for 18 hours as described in Section 3.2. Chemical shifts were statistically compared by means of a Students' t-test. Values that differ significantly from controls are shown: $^{*}P<0.05$; $^{**}P<0.01$; $^{***}P<0.001$.

Chemical shift (δ), multiplicity	Endogenous metabolites	Change in urinary metabolite concentration (increase (+); decrease (-))
8.34-8.38 (s)	Formate	+*
7.74-7.78 (d)	Hippurate	-***
7.58-7.62 (t)	Hippurate	-**
7.54-7.58 (t)	Hippurate	-**
7.46-7.50	Unidentified	-***
7.26-7.30	Unidentified	-*
7.10-7.14	Unidentified	-**
6.54-6.58 (s)	Fumarate	-
4.42-4.46	Unidentified	+*
3.98-4.02	Unidentified	-
3.94-3.98	Unidentified	+*
3.86-3.90 (d)	Hippurate	-
3.78-3.82 (s)	Creatine	+*
3.74-3.78 (m)	Glucose	+
3.70-3.74	Unidentified	+
3.62-3.66 (m)	Glucose	+*
3.54-3.58 (m)	Glucose	+
3.50-3.54	Unidentified	+
3.34-3.38 (m)	Glucose	+*
3.30-3.34 (t)	Taurine	+*
3.22-3.26 (s)	TMAO	-
3.14-3.18 (t)	Taurine	+
3.02-3.06 (s)	Creatinine	-
2.94-2.98 (s)	Creatine	+
2.90-2.94 (t)	2-oxoglutarate	+
2.62-2.66 (d)	Citrate	+
2.58-3.62	Unidentified	+*
2.46-2.50	Unidentified	+*
2.42-2.46 (d)	Citrate	+
2.34-2.38 (t)	2-oxoglutarate	+
2.30-2.34 (s)	Succinate	+
2.22-2.26	Unidentified	-**
1.98-2.02	Unidentified	-**
1.54-1.58	Unidentified	-**

S, singlet; d, doublet; t, triplet; m, multiplet. TMAO=Trimethylamine N-oxide.

3.4 Discussion

One of the primary objectives of this acute dose response study was to define a dose level of CCl_4 that would induce injury to the liver of the male Hanover-Wistar rat, but not to the kidney. CCl_4 was the toxic compound chosen for these studies since it is a widely used model compound for hepatotoxicity (Brattin et al., 1985). It is known to induce apoptosis and centrilobular necrosis acutely, followed by hepatic fibrosis when administered repetitively (Rees et al., 1961; Bruckner et al., 1986; Lindros et al., 1990).

In the present study male Hanover-Wistar rats of approximately 7 weeks of age were administered CCl_4 at dose levels from 0.4 to 3.6 mL/kg by gavage. At autopsy (24 hours post-dosing), organs were removed from all animals and weighed. In toxicology studies a change in relative organ weight has long been accepted as a potential initial indicator of organ toxicity (Peters and Boyd, 1966; Michael et al., 2007). In the present study, relative liver weights were significantly increased in all CCl_4-treated animals at 0.8 mL/kg and above and a dose-related trend was apparent (Figure 3.1 A). At the highest dose level relative liver weights were almost double control weights (60.65 g/kg BW and 30.55 g/kg BW for CCl_4-treated and control animals respectively). These results strongly suggest that injury to the liver had occurred. A previous study by Smyth and co-workers (2008) also reported increases in relative liver weights compared to control rats following the administration of a single dose of CCl_4 at a range of concentrations between 0.4 and 2.0 mL/kg.

Serum ALT, AST and GLDH were measured in this study and found to be increased over controls at all dose levels (Figure 3.2). The first significant changes were apparent at 0.8 mL/kg CCl_4. GLDH showed the greatest fold increase over control (9.56-fold), whereas the fold increase for ALT and AST was 4.44-fold and 1.81-fold at this dose level, respectively. It would appear that as the CCl_4 dose level increased so did the levels of these hepatic enzymes in the serum. At the highest dose level (3.6 mL/kg) ALT, AST and GLDH were 130-fold, 48-fold and 136-fold increased over controls ($^{***}P<0.001$) (Figure 3.2). ALT, AST and GLDH are often called hepatic leakage enzymes as they can leak out of the cytoplasm into the circulation when hepatocytes are damaged and membrane permeability is affected (Schmidt and Schmidt, 1988, Gores et al., 1990, Van Hoof et al., 1997).

A previous study evaluating the effect of administering 350 mg/kg CCl_4 intraperitoneally to male Sprague-Dawley rats on serum enzyme levels reported ALT and GLDH to have the greatest predictive value for hepatic necrosis (Carakostas et al., 1986). The authors used a statistical method to determine if enzymes could be used to distinguish histopathologically different liver lesions. GLDH, which is a mitochondrial enzyme, was found to have the greatest predictive value for the presence of necrosis in any hepatic location. However, this also meant that GLDH was not very specific in differentiating the origin of liver damage (Carakostas et al., 1986). There was, however, no correlation between the degree of injury as detected by histopathological examination and the levels of the increased serum enzymes. Campo et al. (2001) measured serum ALT in male Sprague-Dawley rats 48 hours after a single i.p. injection of 1.0 mL/kg CCl_4. Mean values were significantly increased over basal levels collected immediately after treatment. Ichi et al. (2007) also demonstrated a significant increase in AST activity in the serum of rats 12 hours after a single administration of 4 mL/kg CCl_4 by gavage. In the same study, ALT levels were significantly increased over controls as early as 6 hours post-dosing. A study in female Wistar rats dosed orally with 1.5 mL/kg CCl_4 and autopsied at 0, 3, 6, 12, 48 and 72 hours after treatment revealed AST, ALT and GLDH levels peaked between 12 and 48 hours post-dosing (Teschke et al., 1983; Teschke et al., 1984).

ALP is a non specific protein phosphatase and is mostly found in the bile canalicular membrane in hepatocytes (Alvaro et al., 2000; Chida and Taguchi, 2011). Increased serum levels of ALP are associated with obstructive liver disease and the increase in ALP serum level is a result of an inability of the liver to excrete excess ALP produced in other tissues such as bone and intestines (Talageri et al., 1951; Kaplan and Righetti, 1970). In the present study, levels of ALP were statistically greater than control at 0.4 mL/kg CCl_4 ($^{*}P<0.05$) and there appeared to be a dose-related trend (Table 3.3). In animals treated with 3.6 mL/kg CCl_4 serum levels of the enzyme were over 3-times greater than control ($^{***}P<0.001$). A study by Janakat and co-workers (2002) also reported increased serum ALP levels in male Wistar albino rats following the administration of a single i.p. dose of CCl_4 at 2.0 mL/kg.

TIMP-1 is involved in the regulation of MMPs, by inhibiting the proteolytic activity of these enzymes (Brew et al., 2000) which are responsible for the degradation of ECM (Murphy et al., 1991). Disruption of this equilibrium may result in conditions such as fibrosis where an uncontrolled turnover of matrix protein is present (Wight and Potter-

Perigo, 2011; Siebuhr et al., 2012). The major sources for TIMP-1 production in liver fibrosis are activated HSC and Kupffer cells (Herbst et al., 1997; Wang et al., 2011). Therefore, TIMP-1 has been suggested to be a serum marker of liver fibrosis (Roderfeld et al., 2006). However, TIMP-1 was measured in the present acute dose study and levels were found to be increased in all CCl_4-treated animals (Figure 3.2). At 0.8 mL/kg the mean value was 2-fold greater than control animals, and at 1.2 mL/kg and above the increase over control was statistically significant. At the highest dose level TIMP-1 was 25-fold greater ($^{**}P<0.01$). Herbst and colleagues (1997) investigated TIMP RNA expression in an acute rat model of CCl_4 toxicity. Female Sprague-Dawley rats were treated i.p. with CCl_4 at 1.25 mL/kg and autopsied at 0.5, 1, 3, 6, 12, 24, 48, or 72 hours after dosing. As early as 1 hour after a single dose of CCl_4, TIMP RNA expression was shown to be activated in HSCs in the rat liver. Another study has demonstrated that increased expression of TIMP mRNA is present in CCl_4-induced hepatic fibrosis (Iredale et al., 1996).

In this current study serum MCP1 levels were significantly increased over controls (Table 3.3) at 1.6 mL/kg and above and at the highest dose level (3.6 mL/kg) there was a 25-fold increase ($^{***}P<0.001$). Marra and colleagues (1993) described MCP1 as one of the most important chemotactic factors secreted by HSCs, which are responsible for ECM accumulation during chronic liver injury/disease (Marra et al., 1993). Data previously collected from both *in vitro* and *in vivo* studies suggests that HSCs are involved in the expression of MCP during both chronic and acute hepatic injury (Maher and McGuire, 1990; Czaja et al., 1994; Marra et al., 1998). In one study, MCP1 gene expression was induced 2 hours after CCl_4 administration suggesting an important early role for MCP1 in the recruitment and activation of macrophages and monocytes following toxic insult to the liver (Czaja et al., 1994).

AGP is a positive acute phase serum protein that is produced by the liver and secreted into the circulation in response to inflammation and infection (Fournier et al., 2000). Levels of AGP were greater in all CCl_4-treated animals than in controls. However, the increases were only statistically significant at 2.0 mL/kg CCl_4 and above. Increased AGP plasma levels have been reported following CCl_4 administration and it appears that this increase may be related to the formation of reactive oxygen species but an exact mechanism for this has not yet been proposed. Goldberg et al., (1983) also reported increases in AGP plasma levels in Wistar rats following administration of 2.0 mL/kg CCl_4.

Lipocalin-2 is a 25-kDa glycoprotein (Kjeldsen et al., 1994). It has been found to be present in several tissues, such as the liver, kidneys, lungs, adipocytes and macrophages (Liu and Nilsen-Hamilton, 1995). Values of serum lipocalin-2 in this study were similar to control in the lower dose level groups. However, at 2.8 mL/kg CCl_4 and above lipocalin-2 was significantly increased in treated animals compared to controls (Table 3.3). Lipocalin-2 is highly expressed and released by the liver in response to inflammation (Liu and Nilsen-Hamilton, 1995; Flo et al., 2004). Borkham-Kamphorst et al. (2013) investigated the change in lipocalin-2 levels in a mouse model. In this study, mice were injected with a single dose of 0.8 mL/kg CCl_4 intraperitoneally and autopsied at 48 hours post-dosing. This study by Borkham-Kamphorst demonstrated an increase in hepatic and serum lipocalin-2 levels following CCl_4 administration and also evidence of a good degree of correlation between serum lipocalin-2 and serum AST and ALT levels. However, it has also been shown that in the event of renal toxicity lipocalin-2 is secreted by the thick ascending limb of the loop of Henle, distal tubule and convoluted tubule and excreted into the urine (Paragas et al., 2011). This suggests that lipocalin-2 is a potential biomarker of acute kidney injury which could predict the progression to chronic kidney disease (Bolignano et al., 2009).

In the current study hepatic injury was confirmed by histopathological examination revealing hepatocellular changes associated with CCl_4 administration at all dose levels. These changes consisted of vacuolation of centrilobular hepatocytes as well as the presence of hepatocyte necrosis. As the dose level increased the degree of injury increased; at 0.8 mL/kg only minimal centrilobular hepatocyte necrosis was present whereas at the highest dose level all animals had marked or very marked degeneration and necrosis (Figure 3.5, Figure 3.3). The centrilobular region is the area most susceptible to CCl_4 due to the high concentration of cytochrome P-450 here, however, it has been reported that CCl_4 does not affect all lobes of the liver equally. Matsubara and colleagues (1983) reported that CCl_4-induced toxicity was greatest predominantly in the median lobe of the liver since this lobe has the highest concentration of cytochrome P-450. The CCl_4-induced microscopical changes reported in the present study compare to previous studies by Giffen et al., (2002) and Zira and colleagues (2013) who described hepatocellular degeneration and necrosis following the administration of CCl_4 at 0.8 mL/kg and 1 mL/kg to rats, respectively.

At autopsy kidneys were removed and weighed; kidney weights were similar for control and CCl_4-treated animals except for animals treated with CCl_4 at 2.4 mL/kg ($^{*}P<0.05$)

and 3.6 mL/kg ($^{**}P<0.01$) (Figure 3.1 B). At these dose levels kidney weights were significantly greater than controls which may suggest the presence of kidney injury in these groups, but not in lower dose level groups. After a single administration of 3.6 mL/kg CCl_4 kidney weights were 22 % increased over control relative weights. Another study has also reported an increase in kidney weights in male Wistar rats dosed at 3 mL/kg CCl_4 of approximately 57 % (Khan et al., 2010). Smyth and colleagues (2008) reported significant increases in kidney weights in female Hanover-Wistar rats following a single administration of CCl_4 at 1.2, 1.6 and 2.0 mL/kg (Smyth et al., 2008). At the highest dose level the relative kidney weights were heaviest and were 34 % increased over controls.

In the present dose response study, analysis of serum urea and creatinine revealed that mean urea was greater in CCl_4-treated animals than in controls at all dose levels but there was no dose-related trend (Table 3.3). Creatinine levels were similar to controls in all CCl_4-treated groups apart from at the highest dose level where there was a 2.9-fold increase ($^{***}P<0.001$). Increased urea and creatinine levels are suggestive of possible renal injury. Both urea and creatinine are freely filtered in the glomerulus. However, whereas creatinine undergoes tubular secretion, urea is not secreted but instead is reabsorbed by the renal tubules (Schrier, 2008). Decreased renal blood flow or compromised kidney function can cause a decrease in the glomerular filtration rate, and this will in turn result in increased serum creatinine and urea levels. Similar changes were previously reported in female Hanover-Wistar rats following a single administration of CCl_4 at 1.2 mL/kg. At this dose level, histopathological examination of kidneys indicated kidney damage (Smyth et al., 2008).

In the present study, urinary creatinine levels were significantly decreased over control at 2.8 and 3.2 mL/kg CCl_4 ($^{**}P<0.01$ and $^{*}P<0.05$, respectively) (Table 3.4). Decreased urinary creatinine levels are indicative of compromised kidney function and are often accompanied by increased serum creatinine. When the filtering capacity of the kidneys is affected, creatinine clearance is reduced; consequently, urinary creatinine levels are also decreased. In the present study, a statistically significant decrease in urinary creatinine was recorded at 2.8 and 3.2 mL/kg CCl_4, and increased serum creatinine levels were also recorded at these dose levels even though the increase was not enough for statistical significance. This adds further evidence of CCl_4-induced nephrotoxicity following the administration of 2.8 and 3.2 mL/kg CCl_4 in this study. Total protein levels in the urine were significantly decreased in CCl_4-treated animals at 0.8 mL/kg

and above compared to control rats (Table 3.4). Urinary albumin and glucose, however, were significantly increased over control at the highest dose level (3.6 mL/kg CCl_4), but there was no evidence of a dose related effect (Table 3.4). Albumin is filtered from the blood in the kidneys and is almost completely reabsorbed in the proximal tubule (Lazzara and Deen, 2007). Albuminuria is therefore a consequence of damage to the proximal tubules. Glucose is not normally found in urine and is almost completely reabsorbed in the proximal tubule (Bishop et al., 1978). Therefore, the presence of glucose in the urine suggests a reduced tubular function (Wolf et al., 2009; Swain et al., 2011).

Data collected from urinary biomarkers provided an answer on a dose level at which CCl_4-induced kidney toxicity was avoided. Changes to urinary creatinine, albumin and glucose levels suggested the presence of CCl_4-induced renal damage at the highest dose levels. In the next Chapter we will assess the sensitivity of more specific and recently approved biomarkers for nephrotoxicity. However, in the present chapter, nephrotoxicity was confirmed by histopathological examination of tissue samples.

Histopathological analysis of the kidneys revealed CCl_4-related findings in a small proportion of the animals administered CCl_4 at dose levels of 2.8 mL/kg and above (Table 3.6, Figure 3.4). These changes included granular casts in collecting ducts, dilatation of distal and/or collecting tubules, and minimal proximal tubular necrosis (Figure 3.4). In a study by Adams et al (1952) pathological effects in the kidneys were observed following exposure of Wistar rats by inhalation of 50 ppm CCl_4. These changes included cloudy swelling of the tubular epithelium (Adams et al., 1952). Our results in the present study also compare with the study by Smyth et al., (2008) who described proximal tubular swelling and degeneration following administration of CCl_4 at 1.2, 1.6 and 2.0 mL/kg to female Hanover-Wistar rats.

Histopathological examination of kidneys removed at autopsy was able to identify and confirm the threshold for CCl_4-induced kidney toxicity in the male Hanover-Wistar rat. At concentrations equal to or greater than 2.8 mL/kg CCl_4 there was microscopic evidence of renal damage. However, due to the great number of tissue samples generated in the study, kidneys from animals treated at 2.4 mL/kg were not assessed histopathologically for confirmation of nephrotoxicity. Therefore, we defined our optimal CCl_4 dose level for inducing hepatotoxicity and not kidney toxicity as being 2.0

mL/kg, as at this concentration, there was no histopathological report of CCl_4-induced renal damage.

In the present study other organs including the adrenals, heart, lungs, pancreas, spleen, thymus, thyroid, testes and nasal cavity were evaluated for signs of CCl_4-induced toxicity. A statistically significant decrease in the mean relative weight of the testes was recorded for animals treated with CCl_4 at 2.8 mL/kg (20 % decrease; $^{**}P<0.01$) and at 3.6 mL/kg (16 % decrease; $^{*}P<0.05$) (Table 3.2). However, histopathology revealed no abnormal findings in the testes in this study, apart from 1 rat at 3.6 mL/kg CCl_4 with the presence of multinucleate spermatid giant cells. Manjrekar et al. (2008) previously described a decrease in the testes weight in albino Wistar rats following the administration of 0.5 mL/kg CCl_4 by i.p. injection for 7 days. Histopathological examination of the testes showed tubular disorganisation and a reduced number of mature spermatozoa (Manjrekar et al., 2008). In another study, CCl_4-induced changes in the spermatogenic cycle and degeneration in seminiferous tubules were described in the Hanover-Wistar rat treated with 0.25 mL/kg CCl_4 intragastrically once a week for a period of 10 weeks (Horn et al., 2006). These reported findings in the testes were in a repeat dose study, whereas in the present study a single dose of CCl_4 was administered.

In the current study, CCl_4-induced organ toxicity was present in the nasal cavity at all dose levels; the degree of severity increased with increasing dose of CCl_4 (Table 3.7, Figure 3.5). The effects were confined to the olfactory epithelium in all treated animals except for 2 animals at 3.6 mL/kg CCl_4 in which signs of respiratory epithelial ulceration were also present. CCl_4 undergoes cytochrome P-450 2E1 metabolism and there are considerable levels of this CYP isoform in the nasal cavity (Boyd et al., 1980). However, in the present study, there was no evidence of dose-related effect. We hypothesise that the observed effect could be the result of gastroesophageal reflux during dosing, which has been shown to happen with the administration of oily preparations. Most studies investigating CCl_4-induced injury to the respiratory tract are inhalation studies, and limited information is available regarding respiratory tract effects of oral administration of CCl_4. Therefore, we consider this to be an interesting finding that could be further investigated.

The main objective of this project was to identify urinary biomarkers of hepatic injury, therefore, urine samples collected during this dose response study were analysed by 1D ^{1}H NMR and pattern recognition methods for identification of spectral regions which

related to metabolite resonances, and ultimately, metabolite concentrations, that varied between control and CCl_4-treated samples.

A PCA model of the spectra obtained for all urine samples was constructed to identify outliers and clustering trends. Samples were widely spread across the scores plot with no evident clustering patterns and no CCl_4-induced metabolite changes were apparent (Figure 3.6).

The same data was used to create an OPLS model (Figure 3.7) which revealed a better degree of sample separation along the first component compared to the PCA model (Figure 3.6). OPLS is a supervised pattern recognition method whereby, by introducing a new variable, we provide the model with a greater deal of information. OPLS models have the ability to separate the predictive variation, which is the correlated variation between the NMR spectral data and the CCl_4 dose levels; from the orthogonal variation, which is the uncorrelated variation between the spectral data and the treatment concentration used. This property increases the potential for sample clustering compared to an unsupervised method, such as PCA.

In the OPLS scores plot (Figure 3.8) it was clear that samples from animals treated with 0.4, 0.8, 1.2 and 1.6 mL/kg CCl_4 were clustered closer to the control group (left half of the scores plot), whereas samples from groups treated at 2.0, 2.4, 2.8, 3.2 and 3.6 mL/kg occupied the right half of the scores plot. This correlates well with the histopathological changes observed in the liver since, in general, mild and moderate changes were observed at 0.4 and 0.8 mL/kg, whereas a greater percentage of animals at the highest dose level groups showed marked/very marked changes (Table 3.5, Figure 3.3). In this study, histopathology analysis revealed kidney injury at 2.8 mL/kg CCl_4 and above. However, samples from animals treated at 2.4 mL/kg were not histopathologically examined to confirm the absence of CCl_4-induced kidney toxicity. Therefore, this dose level was excluded from the metabolomics-based investigation of urinary metabolites, and 2.0 mL/kg was determined to be the optimal CCl_4 dose level where no nephrotoxicity was present in this study. This project was concerned with the identification of biomarkers of hepatotoxicity, therefore, in order to avoid identifying urinary metabolites which may be increased following nephrotoxicity, samples from animals treated with CCl_4 at 2.4 mL/kg and above were removed from the analysis. Exclusion of these samples from the OPLS model (Figure 3.8 A) allowed much better cluster separation as potential confounding factors, such as urinary metabolites resulting

from CCl_4-induced nephrotoxicity were eliminated. Also, by reducing the number of sample groups, we were able to increase the scores plot area available for positioning of sample points.

The corresponding loadings plot (Figure 3.8 B) provides information on the spectral regions that are responsible for sample clustering along the first component t[1], which means that chemical shifts located on the right hand side of the loadings plot were related to samples located on the right hand side of the scores plot, and spectral regions located on the left hand side of the loadings plot were related to samples also located on the left hand side of the scores plot. However, as observed in the scores plot shown in Figure 3.8 A, the CCl_4-treated groups were distributed along the whole extension of the first component, both on the left and right hand side of the scores plot, therefore compromising the interpretation of the loadings plot which did not allow differentiation of urinary metabolites between the different CCl_4 treated groups.

For improved cluster separation and metabolite identification, OPLS-DA models were used. It was decided from the histopathology data that 2.0 mL/kg CCl_4 was the optimal dose level for inducing CCl_4 hepatotoxicity without nephrotoxicity, therefore, an OPLS-DA model of control and urine samples from rats treated at 2.0 mL/kg was constructed (Figure 3.10). The corresponding loadings plot and S-plot were used to determine the most relevant spectral regions and potential biomarkers were then identified (Table 3.9).

Urinary levels of creatine and taurine were found to be increased in CCl_4-treated animals. Increased urinary excretion of both creatine and taurine has been previously reported following hydrazine administration to rodents (Beckwith-Hall et al., 1998; Holmes et al., 2000; Nicholls et al., 2001). Urinary levels of taurine have also been found to be raised after CCl_4 administration (Waterfield et al., 1991; Waterfield et al., 1993). Taurine has been described as a specific urinary marker for hepatotoxicity (Waterfield et al., 1998) since it is mainly synthesised in the liver and it is thought that injury to the liver may result in leakage from the hepatocytes (Waterfield et al., 1993). Another possible reason for increased urinary taurine levels may be due to changes to the pool of cysteine, the precursor amino acid for taurine. CCl_4-induced hepatotoxicity may cause an inhibition of protein synthesis which can result in increased levels of cysteine and consequently elevated synthesis of taurine (Timbrell et al., 1995). Taurine may also be consumed in the diet and is extensively reabsorbed in the kidneys (Jacobsen and Smith, 1968; Chesney, 1985). Consequently, nephrotoxicity could affect

the excretion of taurine in the urine. However, in this study we excluded urine samples from animals treated at higher dose levels of CCl_4, therefore, the increase in the urinary levels of taurine is thought to be a result of CCl_4-induced hepatotoxicity. Creatine is synthesised and metabolised in the liver (Waters et al., 2005) which suggests that the increase in creatine levels is likely to be a result of leakage from damaged hepatocytes (Waterfield et al., 1993). Alternatively, increased creatine may be due to increased cysteine synthesis since creatine is a by-product of cysteine synthesis (Clayton et al., 2003; Clayton et al., 2004).

A decrease in the resonances of hippurate at δ 7.74, 7.58, 7.54 and 3.86 was observed in animals treated with CCl_4 in this study. Hippurate is formed when benzoate is metabolised by benzoyl-CoA synthetase to benzoyl-CoA, a process that requires ATP (Gatley and Sherratt, 1977). ATP depletion typically occurs during hepatic necrosis and therefore, may ultimately result in a decrease in the production of hippurate (Kim et al., 2008b). Beckwith et al., (1998) described similar results in the urine of Sprague-Dawley rats following the administration of model hepatotoxins such as α-naphthyl isothiocyanate (ANIT), D-(+)-galactosamine hydrochloride (GaIN) and butylated hydroxytoluene (BHT) to Sprague-Dawley rats.

Another finding from the present study was an increase in the resonances of metabolite peaks belonging to TCA cycle intermediates including citrate, 2-oxoglutarate and succinate and a decrease in the resonances of fumarate. Other groups have reported a decrease in the urinary levels of TCA cycle intermediates following administration of hepatotoxicants agents (Holmes et al., 2000; Nicholls et al., 2001). Studies have shown that when liver function is compromised acetyl-CoA is prevented from entering the TCA cycle, leading to a decrease in the levels of citrate, fumarate, succinate and 2-oxoglutarate (Lu et al., 2010).

At 2.0 mL/kg CCl_4, ^{1}H NMR creatinine resonances in this study appeared to be decreased in the urine of treated rats compared to control animals, but this decrease was not statistically significant. These results correlate with the urine chemistry measurements as shown in Table 3.4 which did not reveal a statistically significant difference at this CCl_4 dose level. Nicholls et al. (2001) described a decrease in urinary creatinine levels following administration of hydrazine to male Hanover-Wistar rats. However, the authors did not report evidence of a hydrazine-induced effect in the kidneys. Creatinine is freely filtered in the glomerulus, therefore, a decreased level of

urinary creatinine has been described as a marker of impaired kidney function (Wu et al., 2005). At the optimal dose level for CCl_4-induced hepatotoxicity in the present study (2.0 mL/kg), no histopathological evidence of kidney toxicity was recorded and this is in agreement with the ^{1}H NMR data which did not reveal significant changes in urinary creatinine following the administration of 2.0 mL/kg CCl_4.

In this study, urinary TMAO levels were found to be decreased in the urine of rats treated with CCl_4. Similar findings were reported by Nicholls et al. (2001) in an acute model of hydrazine-induced toxicity in the rat. TMAO results from the oxidation of trimethylamine, which in turn is derived from the metabolism of the nutrient choline. Choline is an essential nutrient and the liver is the main organ responsible for choline metabolism (Corbin and Zeisel, 2012). In cirrhotic livers, the conversion of methionine to S-adenosylmethionine (catalysed by S-adenosylmethionine synthetase), a precursor of choline, may be impaired, due to a deficiency in S-adenosylmethionine synthetase and therefore may act as the limiting step in choline metabolism (Duce et al., 1988; Lieber, 2002) which in turn would affect the production of TMAO. We suggest that the same pathway might be responsible for decreased urinary TMAO levels following a single administration of CCl_4.

Other chemical shift resonances changed in this study in response to CCl_4-induced hepatic injury but the metabolites involved have yet to be identified.

While interpreting the data resulting from the NMR analysis it is important to consider that in this preliminary NMR study, the pH of the urine samples was not adjusted, therefore the chemical shifts described for metabolites will vary slightly according to the pH of individual samples. Unlike other biofluids, such as plasma, which are under a tight homeostatic control, urine samples have different protein concentration, pH and ionic strength (Beckwith-Hall et al., 1998; Holmes et al., 2000; Bollard et al., 2005). Such differences are likely to affect the chemical shift of metabolites in the ^{1}H NMR spectra due to changes in the equilibrium between acids and bases and in solute-solute interactions (Lauridsen et al., 2007; Schreier et al., 2013). In most studies the pH of urine samples is kept within a very tight interval by the addition of buffers such as sodium phosphate buffers (Holmes et al., 2000; Nicholls et al., 2001). Under normal physiological conditions the rat urine pH usually varies between 7.3 and 8.5 (Krinkle, 2000). In the present study we carried out the analysis without adjusting the pH, which should be taken into account for future studies. However, since we are interested in

comparing control and CCl_4-treated animals, we assume that differences in peaks intensities will not be affected and therefore, this should not have an impact in identifying differences in metabolites excretion in the urine.

In the present study a rat model of acute hepatotoxicity was developed. The results revealed that hepatic injury occurs at 0.4 mL/kg CCl_4 and above, whereas kidney injury was present at 2.8 mL/kg and above. Since histological examination was not carried out for kidneys at 2.4 mL/kg CCl_4, it was decided in order to confidently stay below the threshold of nephrotoxicity the maximum dose level of CCl_4 in future studies would be 2.0 mL/kg. 1D ^{1}H NMR analysis of urine samples collected during the study allowed the identification of possible urinary biomarkers of hepatotoxicity in the male Hanover-Wistar rat following a single administration of CCl_4. Some of the metabolites revealed in this study have yet to be identified. One of the most important characteristic of an ideal biomarker is that it should be sensitive to early changes in the liver and remain in the biofluid long enough to be detected. This will be examined closely in a time course study (Chapter 6) to investigate the pattern of change in metabolite levels as injury occurs and during the recovery/regeneration of liver period. Further, it would be interesting to determine if the same metabolite changes are present following chronic hepatic injury (Chapter 7).

CHAPTER FOUR

Evaluation of biomarkers of nephrotoxicity

Chapter 4

4.1 Introduction

In this project CCl_4 was used as the model toxicant to induce hepatotoxicity. CCl_4 has also been shown to induce kidney damage at high dose levels via the production of free radicals following metabolism by cytochrome P-450 (Abraham et al., 1999). The high levels of cytochrome P-450 that can be found in the kidneys, particularly in the cells of the *pars recta* of the proximal and distal tubule, make these areas particularly vulnerable to damage (Cummings et al., 1999). Therefore, the kidneys are often listed as secondary organs of CCl_4-induced toxicity (Deb and Chakravarty, 1962; Ogeturk et al., 2005; Makni et al., 2012).

Additionally, the kidney is the primary organ involved in the clearance of endogenous waste products and in the excretion of chemicals from the body, making it particularly susceptible to injury by many toxicants (Perazella, 2009; Bonventre et al., 2010).

It is vital in our urinary biomarker studies that we are able to reliably detect even low degrees of nephrotoxicity in our CCl_4-liver model. Therefore, in this Chapter, the commonly used and recently approved nephrotoxicity biomarkers will be evaluated for sensitivity.

HCBD was used as a model compound to induce nephrotoxicity in this Chapter. HCBD is known to cause degeneration/necrosis specifically to the *pars recta* of the renal proximal tubule in the rat (Lock and Ishmael, 1979; Ishmael et al., 1982; Hook et al., 1983; Cristofori et al., 2007).

The mechanism by which HCBD induces injury involves hepatic conjugation with glutathione in a reaction catalysed by glutathione-S-transferase (GST). This reaction results in the formation of metabolites, such as S-(pentachlorobutadienyl)-glutathione which are then further transformed to S-(pentachlorobutadienyl)-L-cysteine (Nash et al., 1984). The latter is transported to the kidneys where it accumulates and where it undergoes further reactions leading to the production of a reactive thiol by renal cysteine conjugate β-lyase. This highly reactive thiol intermediate may bind to DNA, proteins and macromolecules and is thought to be the responsible agent for the nephrotoxic effect of HCBD (Birner et al., 1995; Birner et al., 1998). Although cysteine β-lyase is mainly found in the proximal tubule, particularly in the S3 segment, it is also

present in the liver, where it can therefore, induce injury via the formation of the reactive thiol (Tateishi et al., 1978). Hence the importance given in the present study to measuring markers of liver injury, to guarantee there is no hepatotoxicity following HCBD administration.

Traditional markers to detect nephrotoxicity include serum creatinine and urea. Creatinine (113 kDa) is a product of muscle creatine metabolism. Serum creatinine is freely filtered by the glomerulus and undergoes tubular secretion. Urea (60 kDa) is the primary metabolite derived from dietary protein catabolism. Serum urea is also freely filtered by the glomerulus; however, it is reabsorbed by the renal tubules. It is estimated that approximately 40 % of the urea filtered in the glomerulus is reabsorbed in the proximal tubule. Therefore, the amount of urea excreted in the urine should not exceed 60 % of the filtered urea (Popovtzer et al., 1971).

The measurement of urinary creatinine is used in the calculation of creatinine clearance which in turn is used to estimate the glomerular filtration rate. A decrease in the glomerular filtration rate, that is, the rate at which blood flows through the kidneys, will result in increased levels of serum creatinine and urea (Schrier, 2008). Serum creatinine and urea values often remain within the normal range until greater than 50 % of the renal function is affected. Therefore, urea and creatinine have been shown to lack sensitivity to kidney injury, and significant changes usually only occur when there is more severe kidney injury (Dharnidharka et al., 2002; Dieterle et al., 2010).

Recently, the Food and Drug Administration (FDA) and the European Medicines Agency (EMA), approved the voluntary introduction of a panel of biomarkers for drug-induced renal toxicity in nonclinical and clinical drug development studies in response to the lack of reliable biomarkers (FDA, 2008). These include KIM-1, albumin, clusterin, trefoil factor-3 (as biomarkers of drug-induced acute kidney tubular alterations) and total protein, β-2 microglobulin and cystatin-C (biomarkers of acute drug-induced glomerular alterations/injury and impairment of renal tubular reabsorption) (FDA, 2008).

Limited data exists on the sensitivity of these biomarkers; a good kidney biomarker will be sensitive to early changes to the kidney pathology and remain in the biofluid long enough to be detected.

In this Chapter, two studies were carried out to extensively characterise traditional and novel serum, urinary and gene expression markers of nephrotoxicity following HCBD-induced nephrotoxicity and to correlate these with changes in renal histopathology to determine the sensitivity to severity of injury. The first study was a dose response study, in which a single dose of HCBD was administered to Hanover-Wistar rats at a range of dose levels from 5 to 90 mg/kg to investigate the sensitivity of the biomarkers. The second study was a time course study, in which animals received a single dose of HCBD (at a dose level as determined by the dose-response study) and biomarker measurements were carried out at various time points up to 28 days post-dosing. This experiment evaluated the biomarker levels as injury was induced and as recovery occurred.

In summary, the main goal of the dose response and time course study described in this Chapter was to characterise a panel of renal biomarkers. The information collected would be used in our future CCl_4 liver injury studies to rule out potential CCl_4-induced kidney injury by evaluating the most reliable panel of nephrotoxicity biomarkers.

4.2 Animal experimental design

4.2.1 Dose response study

Sixty male Hanover-Wistar rats (mean body weight 224.0 ± 5.58 g) were divided into eight groups (n=6) and dosed intraperitoneally with HCBD at 0 (controls), 5, 10, 15, 20, 25, 30, 35, 45 and 90 mg/kg in a total volume not exceeding 0.3 mL per animal. The vehicle for HCBD was corn oil and control animals were dosed intraperitoneally with equivalent volumes of corn oil. After dosing, animals were immediately placed in metabolism cages for the collection of 24 hour urine samples. During this period animals had access to water but not diet. Urine samples were collected over ice and stored at -80 ºC for further analysis. All animals were weighed before dosing, before being placed in metabolism cages and at 24 hours post-dosing, just prior to autopsy.

At autopsy (24 hours after dosing) blood was taken for the preparation of serum which was stored at -80 ºC until future analysis. The liver and the kidneys were removed and weighed. For gene expression analysis a section was cut from the left lobe of the liver and from the left kidney, placed in RNALater tubes and stored at 4 ºC until analysis. The remainder of the left kidney and liver, plus the right kidney were placed in fixative as described in Section 2.8.

4.2.2 Time course study

One hundred and twenty male Hanover-Wistar rats (mean body weight 215.3 ± 5.14 g) were divided into ten groups (n=12). At time 10:00 hr on day 1 of the study, six animals in each group were dosed with corn oil (controls) (rats 1-6) (60 animals in total) and six animals in each group were dosed with HCBD at 45 mg/kg (rats 7-12) (60 animals in total) by i.p. injection. For all animals, a constant dosing volume of approximately 0.3 mL was administered and animals were weighed prior to dosing. After dosing, all rats were returned to their communal cages where they had access to diet and water *ad libitum*.

At 16:00 hr on the day of dosing (i.e., 6 hours post-dosing), 6 controls and 6 treated animals (group 1) were weighed and placed in metabolism cages for the collection of 18 hour urine samples during which period animals had access to water but not diet. At 10:00 hr the following day (24 hours post-dosing) this group of animals were removed from the metabolism cages and autopsied (day 1 post-dosing). At 16:00 hr on day 1

post-dosing, a second group of animals (group 2) were weighed and placed in metabolism cages for 18 hour urine collection. These animals were autopsied at 10:00 hr the following day (day 2 post-dosing). This process was repeated for the remaining groups of animals to collect data at days 3, 4, 5, 6, 7, 10, 14 and 28 post-dosing.

All urine samples were collected over ice and stored at -80 ºC for future analysis. At each autopsy blood was taken for the preparation of serum and stored at -80 ºC until analysis. The liver and the kidneys were removed and weighed. For gene expression analysis a section was cut from the right kidney, placed in RNALater tubes and stored at 4 ºC until analysis. The remainder of the right kidney and liver, plus the left kidney were placed in fixative as described in Section 2.8.

4.3 Results for the dose response study

4.3.1 Observations during the study

No abnormal observations were noted during the dosing period in this study. During the autopsy some of the livers and kidneys from animals treated at 90 mg/kg were paler in colour when compared to control organs. No other abnormal observations were recorded.

4.3.2 Body weight data

Table 4.1 shows the change in body weight (for both control and HCBD-treated animals) during the 24 hour period while the rats were in the metabolism cages. All animals lost weight during the metaboling period. However, there did not appear to be a dose-related effect on body weight loss. Animals in the 10 mg/kg HCBD group lost the most weight (25.15 g compared to 18.10 g in the control group; $^{**}P<0.01$).

Table 4.1 Body weight change for male Hanover-Wistar rats treated with increasing doses of HCBD during a 24 hour period in metabolism cages. Animals were dosed with vehicle (control, 0 mg/kg) or HCBD by intraperitoneal injection and placed individually in metabolism cages for the collection of 24 hour urine samples as described in Section 4.2.1. Animals had access to water but not diet while in the metabolism cages. Weight changes are shown as mean and SD of 6 animals per group. Changes in body weight that are statistically different to the change for control animals by one-way ANOVA test are shown: $^{*}P<0.05$; $^{**}P<0.01$.

Dose level of HCBD (mg/kg)	Mean (SD) change in body weight (g)
0	-18.10 (8.74)
5	-18.35 (2.45)
10	-25.15** (1.08)
15	-22.00 (2.02)
20	-22.73 (1.37)
25	-24.63* (1.55)
30	-20.38 (2.30)
35	-21.53 (2.85)
45	-25.03** (2.32)
90	-20.53 (2.65)

4.3.3 Liver weights

Livers from animals treated at the highest HCBD dose level (90 mg/kg) were significantly increased over controls (40.72 g/kg BW and 35.38 g/kg BW, for HCBD-treated animals and control rats respectively; $^{**}P<0.01$). At all other HCBD dose levels liver weights were similar to controls (Figure 4.1 A).

4.3.4 Kidney weights

The mean relative kidney weights for rats treated with HCBD at 5, 10 and 15 mg/kg were similar to controls (Figure 4.1 B) whereas at 20 mg/kg HCBD, relative kidney weights were approximately 10 % lower than controls ($^{*}P<0.05$). However, at 90 mg/kg, relative kidney weights were 1.2-fold greater than controls (5.06 g/kg BW and 4.23 g/kg BW respectively; $^{***}P<0.001$). There was no clear dose response relationship.

A

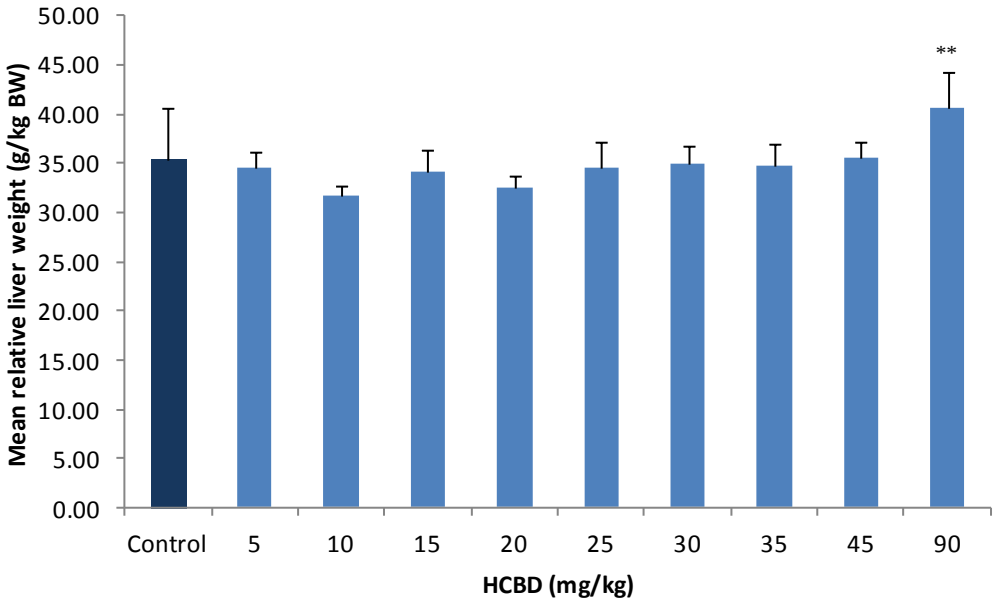

B

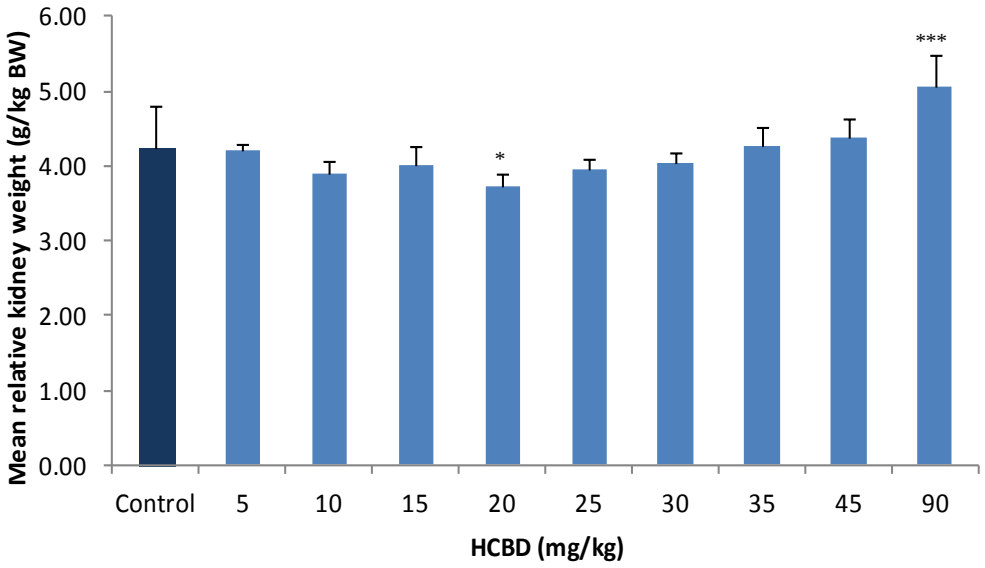

Figure 4.1 Relative liver (A) and kidney (B) weights from male Hanover-Wistar rats treated with increasing doses of HCBD. Animals were dosed with vehicle (control, 0 mg/kg) or HCBD by intraperitoneal injection. At 24 hours post-dosing animals were killed, livers and kidneys were removed and weighed. The kidney weight was expressed as a mean of the left and right kidneys. Results are shown as mean organ weight per kg body weight (BW) with SD indicated by vertical bars of 6 animals per group. Relative organ weights that differ significantly by one-way ANOVA test from control values are shown: $^{*}P<0.05$; $^{**}P<0.01$; $^{***}P<0.001$.

4.3.5 Serum clinical chemistry

Serum levels of ALT, AST and GLDH were measured in samples from rats treated with HCBD at 0 (controls), 5, 10, 15, 20, 25, 30, 35, 45 and 90 mg/kg. These are traditionally used as serum parameters of liver injury and were measured to guarantee that no hepatotoxicity was present as the liver may be a secondary site for HCBD-induced damage.

ALT and GLDH were significantly increased over controls at the highest dose level (90 mg/kg); ALT was 1.85-fold increased ($^{**}P<0.01$), whereas GLDH was 4.08-fold increased ($^{***}P<0.001$) above controls (Figure 4.2).

Mean levels for ALP did not show evidence of a treatment-related effect except in the serum from animals treated at the highest HCBD dose level (90 mg/kg); enzyme activity was approximately twice as great as the activity measured in the serum from vehicle-treated (control) animals (425.50 and 831.17 U/L for control and HCBD-treated animals respectively; $^{***}P<0.001$) (Table 4.2).

Measurement of other serum clinical chemistry parameters, such as urea, creatinine, glucose, albumin and total protein was performed to evaluate kidney function. Serum urea levels were significantly decreased at 5, 20 and 25 mg/kg HCBD ($^{*}P<0.05$, $^{**}P<0.01$ and $^{*}P<0.05$, respectively) but at 90 mg/kg they were 3-fold greater than controls (21.58 and 8.08 mmol/L respectively; $^{***}P<0.001$) (Table 4.2). Creatinine levels were similar to controls at most HCBD dose levels but at 45 and 90 mg/kg HCBD, levels were significantly increased (1.8-fold and 5.7-fold respectively). Glucose levels in the serum did not follow a clear HCBD dose-related trend but were significantly decreased at 10, 20, 35 and 90 mg/kg HCBD (Table 4.2). Albumin and total protein mean values were similar to controls at all dose levels (Table 4.2).

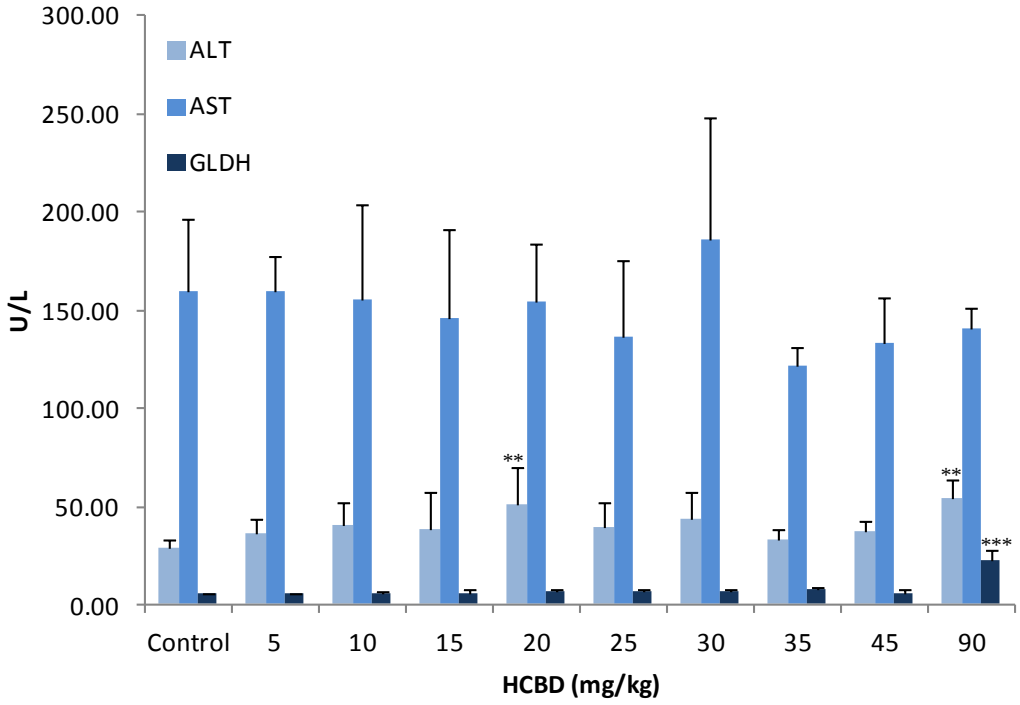

Figure 4.2 Serum ALT, AST and GLDH levels for male Hanover-Wistar rats treated with increasing doses of HCBD. Animals were dosed with vehicle (control, 0 mg/kg) or HCBD by intraperitoneal injection. At 24 hours post-dosing, serum was collected as described in section 4.2.1 and enzymes were assayed as described in Section 2.7. Values are the means with SD indicated by vertical bars of 6 animals per group. Values that differ significantly from controls by one-way ANOVA test are shown: $^{**}P<0.01$; $^{***}P<0.001$

Table 4.2 Serum clinical chemistry parameters for male Hanover-Wistar rats treated with increasing doses of HCBD. Animals were treated with vehicle (control, 0 mg/kg) or HCBD by intraperitoneal injection. At 24 hours post-dosing, serum was collected as described in Section 4.2.1 and serum biomarkers were assayed as described in Section 2.7. Values are the means and SD of 6 animals per group. Values that differ significantly from controls by one-way ANOVA test are shown: $^{*}P<0.05$; $^{**}P<0.01$; $^{***}P<0.001$.

Serum parameters	**HCBD dose level (mg/kg)**									
	0	**5**	**10**	**15**	**20**	**25**	**30**	**35**	**45**	**90**
ALP (U/L)	425.50 (111.67)	397.50 (61.80)	426.00 (74.45)	358.50 (80.52)	374.50 (45.28)	343.00 (36.44)	424.00 (48.97)	446.17 (114.03)	469.83 (115.81)	831.17*** (169.22)
Urea (mmol/L)	8.08 (1.71)	6.33* (0.50)	7.63 (0.61)	6.82 (1.18)	5.82** (0.53)	5.88* (0.85)	8.60 (1.81)	6.78 (1.47)	9.57 (2.06)	21.58*** (3.83)
Creatinine (µmol/L)	23.33 (3.14)	22.00 (0.89)	26.50 (1.87)	23.17 (2.32)	25.83 (1.60)	25.67 (2.66)	26.33 (4.50)	29.67 (7.63)	42.00** (19.83)	133.50*** (38.81)
Glucose (mmol/L)	5.84 (0.59)	4.91 (0.92)	2.95*** (0.38)	6.06 (1.40)	3.90** (0.77)	4.41 (0.74)	6.40 (1.03)	3.24*** (0.37)	4.56 (1.12)	4.41* (1.21)
Albumin (g/L)	32.67 (67 (0.82)	32.83 (0.75)	33.33 (0.82)	33.33 (0.82)	32.67 (0.52)	32.50 (1.38)	32.83 (0.75)	32.83 (1.17)	33.17 (0.75)	31.67 (1.75)
Total protein (g/L)	53.00 (1.67)	53.17 (1.17)	55.33 (1.37)	54.33 (1.21)	54.33 (1.21)	53.67 (1.97)	53.33 (1.51)	54.17 (1.72)	54.00 (1.10)	50.50 (3.56)

APL: alkaline phosphatase.

4.3.6 Urinary biomarkers of kidney injury

Mean urinary levels of α-GST and GST Yb1 for HCBD-treated animals were increased over controls at all dose levels. However, the differences were only statistically significant at 20 mg/kg and above for α-GST and at 10 mg/kg and above for GST Yb1. There was a general dose-related trend for both. At 90 mg/kg HCBD, α-GST excretion was 649-fold greater in HCBD-treated animals compared to controls, whereas the increase for GST Yb1 corresponded to a 7-fold increase over controls (Table 4.3).

There were no significant changes in the levels of urinary osteopontin following HCBD-treatment. Lipocalin-2 levels were significantly decreased at 30 mg/kg HCBD ($^{*}P<0.05$), but no other significant differences were present (Table 4.3).

Urinary β-HBA was increased at all dose levels but only significantly at 10 mg/kg HCBD and above; there appeared to be a dose-dependent increase. Levels were 3.3-fold greater than controls in the 10 mg/kg group, whereas at 90 mg/kg the fold increase was approximately 31-fold ($^{***}P<0.001$) (Table 4.3). Acetoacetate levels in urine showed no evidence of an HCBD treatment-related change at the lower dose levels. However, at 35 mg/kg HCBD and above, there was a significant increase in acetoacetate levels. In the highest dose group (90 mg/kg) the mean acetoacetate value was 55.47 µmol/c.p. in comparison to 0.10 µmol/c.p. for controls which corresponded to a 554.7-fold increase ($^{***}P<0.001$) (Table 4.3).

Urinary creatinine was significantly increased over controls at most HCBD dose levels (10, 15, 20, 25, 30 and 35 mg/kg HCBD). Levels appeared to increase with increasing HCBD dose level to a maximum at 20 mg/kg, after which there was a gradual decrease in urinary creatinine levels. At 90 mg/kg HCBD, urinary creatinine was decreased to approximately 70 % of the control values (27.12 µmol/c.p. and 39.88 µmol/c.p., for HCBD-treated and control animals, respectively; $^{***}P<0.001$) (Table 4.3). Urinary excretion of glucose was similar to controls at all dose levels up to and including 30 mg/kg HCBD. At 35 mg/kg HCBD there was a 2.7-fold increase in urinary glucose but this was not statistically significant. In animals treated with 45 mg/kg and 90 mg/kg HCBD mean glucose levels in the urine were approximately 19- and 103-fold greater than controls, respectively ($^{***}P<0.001$) (Table 4.3).

Urinary levels of clusterin were only significantly different from controls at 90 mg/kg HCBD (highest dose level). At this dose level, the mean clusterin level in the urine of

HCBD-treated animals was 462.78 ng/c.p., whereas in control animals the level was 61.91 ng/c.p., thus representing an 8-fold increase ($^{***}P<0.001$). KIM-1 values were similar to control in the urine from animals treated with HCBD at 5, 10 and 15 mg/kg but were significantly increased at 20 mg/kg and higher (Table 4.3). However, the KIM-1 concentration at the highest HCBD dose does not fit a dose related trend.

Total protein was increased in the urine of HCBD-treated animals at 15 mg/kg and above to a maximum of approximately 5-fold at the highest HCBD dose (Table 4.3).

Albumin was significantly greater than controls at 20 mg/kg HCBD and above (Table 4.3). At the highest HCBD dose level the mean albumin concentration in the urine was 17.45 mg/c.p., representing a 134-fold increase over control ($^{***}P<0.001$).

Table 4.3 Urinary biomarkers in male Hanover-Wistar rats treated with increasing doses of HCBD. Rats were treated with vehicle (control, 0 mg/kg) or HCBD by intraperitoneal injection and urine was collected for 24 hours as described in section 4.2.1. Biomarkers were assayed as described in Section 2.7. Values are the means and SD of 6 animals per dose level group and are expressed as c.p. (collection period, 24 hours). Values that differ significantly by one-way ANOVA test from controls are shown: $^{*}P<0.05$; $^{**}P<0.01$; $^{***}P<0.001$.

Urinary parameters	HCBD dose level (mg/kg)									
	0	**5**	**10**	**15**	**20**	**25**	**30**	**35**	**45**	**90**
α-GST	537.59	765.59	2182.13	5391.33	17961.58**	25684.65**	38617.67***	86390.53*	142453.80***	348893.83***
(ng/c.p.)	(228.62)	(245.21)	(1108.45)	(2927.94)	(8854.04)	(20354.78)	(16212.37)	(85383.66)	(122150.47)	(78878.72)
GST Yb1	82.48	90.67	171.67*	292.56***	287.28***	319.53***	244.67***	454.74***	388.52***	572.55***
(ng/c.p.)	(51.48)	(25.90)	(48.86)	(92.18)	(31.30)	(106.42)	(102.99)	(336.09)	(146.91)	(224.68)
Osteopontin	33.75	44.32	40.54	37.33	39.37	38.54	39.58	50.88	53.69	54.12
(ng/c.p.)	(24.25)	(23.00)	(19.19)	(14.70)	(20.48)	(11.91)	(11.91)	(16.53)	(23.04)	(37.13)
Lipocalin-2	8028.38	5859.20	7780.25	4660.00	4424.25	5560.83	3792.97*	7159.17	5890.45	7505.00
(ng/c.p.)	(2731.95)	(2428.48)	(6013.78)	(2204.25)	(1113.63)	(3643.41)	(978.24)	(3260.80)	(1610.70)	(2679.98)
β-HBA	5.17	9.34	17.07**	46.18***	50.66***	47.35***	54.85***	73.70***	106.51***	161.29***
(µmol/c.p.)	(1.72)	(3.14)	(7.63)	(11.14)	(14.16)	(11.60)	(9.15)	(41.24)	(71.52)	(81.37)
Acetoacetate	0.10	0.09	0.19	0.41	0.04	0.15	0.54	13.56**	38.71***	55.47***
(µmol/c.p.)	(0.17)	(0.14)	(030)	(0.55)	(0.10)	(0.29)	(1.01)	(17.16)	(38.45)	(50.62)
Creatinine	39.88	41.38	49.78**	53.34***	58.10***	54.55***	47.84*	47.31*	38.53	27.12***
(µmol/c.p.)	(5.95)	(2.94)	(2.47)	(4.12)	(3.73)	(4.64)	(5.21)	(4.77)	(1.41)	(4.16)
Glucose	4.80	6.09	5.73	6.71	5.41	5.99	4.94	13.02	90.77***	496.25***
(µmol/c.p.)	(0.77)	(1.25)	(0.90)	(1.82)	(1.02)	(0.57)	(0.91)	(14.16)	(98.62)	(235.37)
Clusterin	61.91	58.50	63.05	80.80	48.92	49.28	42.90	80.57	150.74	462.78***
(ng/c.p.)	(27.28)	(12.53)	(29.75)	(45.49)	(16.52)	(12.91)	(16.02)	(64.10)	(121.23)	(161.84)
KIM-1	8.57	9.49	12.78	15.55	22.60**	27.89**	34.43***	35.23***	57.69***	37.17***
(ng/c.p.)	(1.90)	(1.49)	(1.22)	(3.23)	(6.87)	(12.91)	(19.18)	(24.93)	(41.75)	(20.19)
Total protein	6.52	8.79	8.37	11.65*	11.01*	13.62**	10.39	13.95**	18.22***	33.49**
(mg/c.p.)	(2.62)	(1.89)	(1.87)	(4.41)	(2.39)	(1.98)	(3.02)	(5.03)	(1.01)	(9.86)
Albumin	0.13	0.20	0.17	0.28	0.56*	1.01**	1.26**	3.63***	7.12***	17.45***
(mg /c.p.)	(0.02)	(0.08)	(0.06)	(0.09)	(0.20)	(0.63)	(0.76)	(2.30)	(6.53)	(5.22)

α-GST: α-glutathione-S-transferase; GST Yb1: glutathione-S-transferase Yb1; KIM-1: kidney injury molecule-1, β-HBA: β-hydroxybutyrate.

4.3.7 Liver gene expression

The liver is responsible for the primary metabolism of HCBD. Therefore, gene expression analysis of the liver was performed to track the interplay of changes between the liver and the kidney, based on the metabolism and potential toxic effects of HCBD.

Liver gene expression data was only collected from animals at 0, 5, 10, 15, 20, 30, 45 and 90 mg/kg due to the large number of samples generated during the study (Table 4.4). Genes were separated according to functional category: xenobiotic metabolism, oxidative stress, inflammation and regeneration/repair.

Significant upregulation of most of the genes involved in xenobiotic metabolism was noted in the livers of animals treated with HCBD. Epoxide hydrolase (microsomal) 1 (EPHX1), UDP glucuronosyltransferase 1A6 (UGT1A6), glutathione S-transferase isoform mu 3 (GSTM4), cytochrome P-4502C (CYP2C) and glutathione S-transferase Yc2 subunit (alpha 3) GSTA3 were upregulated at all HCBD dose levels, whereas cytochrome P-4501A1 (CYP1A1) was downregulated in HCBD-treated animals, although this downregulation was only significant at 45 and 90 mg/kg HCBD.

There was also significant upregulation in the expression of markers of oxidative stress. Glutamate-cysteine ligase, catalytic subunit (GCLC), glutathione reductase (GSR) and thioredoxin reductase 1 (TXRND1), were increased at all HCBD dose levels and showed evidence of a dose-related response (Table 4.4).

Inflammatory markers such as kininogen 1 (KNG1) and tissue inhibitor of metalloproteinase 1 (TIMP-1), were downregulated in the livers of animals treated with HCBD (Table 4.4). TIMP-1 was significantly downregulated at 45 mg/kg HCBD ($^{*}P<0.05$). Lipocalin-2 appeared to be upregulated at 10 mg/kg and 30 mg/kg HCBD but this was not statistically significant. However, at 15, 20, 45 and 90 mg/kg HCBD, lipocalin-2 expression in the liver was downregulated.

At the highest HCBD-dose level there was significant upregulation of annexin A7 (ANXA7) and crystalline, αB (CRYAB) which are genes involved in regeneration and repair. Other genes in this category including COL1A1, GPNMB and also ANXA7 at lower HCBD dose levels (5, 10, 15, 120 mg/kg) were downregulated compared to control animals (Table 4.4).

Table 4.4 Liver gene expression in male Hanover-Wistar rats treated with increasing doses of HCBD. Rats were treated with vehicle (control, 0 mg/kg) or HCBD by intraperitoneal injection. At autopsy, 24 hours post-dosing, liver expression was measured as described in Section 2.9. Results are represented as copy number [x10^3/2 ng cDNA]. Values are the means and SD of 6 animals per dose level group. Values that differ significantly by one-way ANOVA test from controls are shown: *P<0.05; **P<0.01; ***P<0.001.

		HCBD dose level (mg/kg)							
Functional category/gene name	**symbol**	**0**	**5**	**10**	**15**	**20**	**30**	**45**	**90**
Xenobiotic metabolism									
Epoxide hydrolase 1 (microsomal)	EPHX1	298 (92)	534** (115)	978*** (251)	1576*** (323)	1749*** (633)	1771*** (506)	2832*** (1796)	7399*** (2718)
UDP glucuronosyltransferase 1A6	UGT1A6	29 (5)	60*** (15)	102*** (43)	158*** (29)	163*** (25)	242*** (58)	217*** (129)	570*** (177)
Glutathione S-transferase isoform mu 3	GSTM4	658 (74)	923*** (114)	1340*** (234)	1975*** (395)	1892*** (392)	2466*** (586)	2543*** (1055)	5469*** (756)
Cytochrome P450 2C	CYP2C	549 (124)	1029* (369)	903** (222)	1398*** (334)	1166** (429)	1309*** (498)	996** (364)	974** (323)
Glutathione S-transferase Yc2 subunit (alpha 3)	GSTA3	13 (7)	37** (10)	52** (34)	75*** (21)	84*** (41)	154*** (63)	208*** (99)	486*** (122)
Cytochrome P450 1A1	CYP1A1	9 (10)	8 (7)	4 (4)	3 (2)	6 (8)	6 (2)	2* (1)	2* (3)
ATP-binding cassette, subfamily C member3	ABCC3	4 (1)	4 (1)	5 (3)	5 (4)	3 (1)	10* (7)	26** (16)	134*** (45)
NAD (P)H dehydrogenase, quinone 1	NQO1	28 (19)	47 (22)	47 (24)	68* (22)	107*** (29)	110** (61)	101* (77)	196*** (86)
Oxidative stress									
Glutamate-cysteine ligase, catalytic subunit	GCLC	56 (12)	75* (11)	106** (30)	140*** (31)	118** (41)	156*** (61)	183*** (59)	247*** (105)
Glutathione reductase	GSR	100 (19)	129* (19)	169*** (31)	195*** (27)	205*** (34)	237*** (33)	287*** (130)	497*** (94)
Thioredoxin reductase 1	TXNRD1	108 (18)	153** (19)	190*** (36)	206*** (25)	216*** (20)	291*** (35)	305*** (122)	691*** (187)
Glucose-6-phosphate dehydrogenase	G6PDX	17 (4)	13 (4)	13* (3)	10*** (1)	12** (1)	11** (2)	10** (2)	27 (13)
Heme oxygenase (decycling) 1	HMOX1	93 (16)	117 (36)	100 (29)	73 (27)	96 (43)	417** (344)	158 (120)	320** (182)
Inflammation									
Chemokine (C-C motif) ligand 2	CCL2	0.6 (0.7)	0.8 (0.5)	1.0 (0.7)	1.2 (1.1)	0.7 (0.3)	1.1 (0.6)	0.5 (0.3)	0.8 (0.7)
Interleukin-1beta	IL1B	6.4 (5.7)	7.4 (3.0)	4.9 (3.2)	3.0 (1.0)	4.3 (0.7)	4.4 (1.5)	2.6 (0.5)	3.7 (1.1)
Kininogen 1	KNG1	12887 (4615)	10285 (5194)	9800 (3977)	5715** (1519)	10620 (5291)	12551 (7313)	6376** (1538)	9324 (996)
Tissue inhibitor of metalloproteinase 1	TIMP1	19 (10)	18 (11)	18 (9)	16 (8)	11 (5)	14 (6)	10* (3)	12 (3)
Lipocalin-2	LCN2	310 (237)	105 (129)	1128 (2577)	15*** (7)	73* (115)	653 (946)	115* (187)	32** (18)
Regeneration/repair									
Annexin A7	ANXA7	23 (3)	18* (3)	21 (6)	18* (3)	21 (3)	23 (4)	24 (7)	39*** (6)
Crystallin, alpha B	CRYAB	2.6 (0.5)	2.8 (0.6)	2.9 (0.2)	2.7 (0.5)	2.8 (0.6)	2.7 (0.4)	3.0 (0.4)	3.8** (0.3)
Collagen, type 1, alpha 1	COL1A1	21 (2)	21 (2)	20 (4)	13*** (3)	13** (4)	14** (4)	17 (5)	19 (3)
Glycoprotein (transmembrane) nmb	GPNMB	21 (10)	19 (7)	19 (9)	11** (2)	14 (4)	11* (4)	10** (1)	11* (4)
Matrix metallopeptidase 12	MMP12	0.1 (0.1)	0.1 (0.1)	0.1 (0.0)	0.1 (0.1)	0.1 (0.1)	0.1 (0.1)	0.1 (0.1)	0.1 (0.1)

4.3.8 Kidney gene expression

Table 4.5 shows the mean values for gene expression in the kidney of the male Hanover-Wistar rats treated with vehicle (controls) or HCBD at 5, 10, 15, 20, 30, 45 and 90 mg/kg HCBD and autopsied 24 hours post-dosing.

Twenty four hours after HCBD administration, there was significant upregulation of some of the genes involved in xenobiotic metabolism in all treated animals, e.g. EPHX1, UGT1A6, GSTA3, ABCC3 and NQO1 (Table 4.5). ABCC3, EPHX1 and NQO1 mRNA increased in a dose-related manner and at the highest dose level (90 mg/kg HCBD) mRNA levels had increased 7-, 24- and 28-fold respectively ($^{***}P<0.001$). Levels of CYP2C mRNA were downregulated at all HCBD dose levels compared to controls. This downregulation was statistically significant at 10, 15, 30, 45 and 90 mg/kg HCBD. CYP1A1 expression was significantly downregulated at 90 mg/kg ($^{***}P<0.001$) (Table 4.5).

In the oxidative stress category, all genes, except for GCLC were significantly upregulated in the kidneys at all HCBD dose levels. Glucose-6-phosphate dehydrogenase (G6PDX) and heme oxygenase (decycling) 1 (HMOX1) showed a dose-related response (Table 4.5). GCLC was significantly downregulated in comparison to control animals at 30 mg/kg and above.

All inflammatory genes were significantly upregulated in the kidneys from animals treated with HCBD at the highest dose level (90 mg/kg) ($^{***}P<0.001$) (Table 4.5). However, lipocalin-2 was also significantly downregulated at 5 and 15 mg/kg HCBD ($^{*}P<0.05$) (Table 4.5).

In the category of regeneration/repair, KIM-1 was the most sensitive marker with changes in expression at the lowest dose level (5 mg/kg HCBD) and was upregulated at all dose levels in a dose-related manner. CRYAB was upregulated at 10 mg/kg and above, except at 90 mg/kg when it was significantly downregulated. ANXA7 mRNA levels were increased at 20 mg/kg HCBD and above, whereas GPNMB only showed statistical changes at the highest dose levels (45 and 90 mg/kg HCBD). Matrix metallopeptidase 12 (MMP12) was significantly upregulated at 20 mg/kg and 90 mg/kg and COL1A1 was downregulated at 15, 20 and 30 mg/kg.

Table 4.5 Kidney gene expression in male Hanover-Wistar rats treated with increasing doses of HCBD. Rats were treated with vehicle (control, 0 mg/kg) or HCBD by intraperitoneal injection. At autopsy, 24 hours post-dosing, kidney expression was measured as described in Section 2.9. Results are represented as copy number [x10^3/2 ng cDNA]. Values are the means and SD of 6 animals per dose level group, except at 20 mg/kg HCBD when n=5. Values that differ significantly by one-way ANOVA test from controls are shown: *P<0.05; **P<0.01; ***P<0.001.

		HCBD dose level (mg/kg)							
Functional category/gene name	**symbol**	**0**	**5**	**10**	**15**	**20**	**30**	**45**	**90**
Xenobiotic metabolism									
Epoxide hydrolase 1 (microsomal)	EPHX1	495 (96)	1466*** (348)	3009*** (988)	3815*** (685)	6250*** (1011)	6043*** (1459)	5423*** (1629)	11665*** (2596)
UDP glucuronosyltransferase 1A6	UGT1A6	188 (40)	632*** (91)	801*** (136)	858*** (45)	1047*** (150)	918*** (73)	721*** (83)	720*** (147)
Glutathione S-transferase isoform mu 3	GSTM4	44 (12)	58 (11)	60* (11)	64** (8)	78** (7)	75* (25)	84** (22)	197*** (72)
Cytochrome P450 2C	CYP2C	60 (36)	35 (25)	18* (12)	17** (6)	30 (27)	22* (15)	7** (7)	0*** (0)
Glutathione S-transferase Yc2 subunit (alpha 3)	GSTA3	30 (6)	83*** (17)	123*** (26)	147*** (26)	174*** (32)	196*** (25)	156*** (25)	171*** (40)
Cytochrome P450 1A1	CYP1A1	55.3 (22.4)	80.1 (50.8)	77.3 (43.8)	84.7 (28.9)	52.1 (36.5)	78.3 (48.7)	23.4 (24.7)	0.2*** (0.1)
ATP-binding cassette, subfamily C member3	ABCC3	13 (2)	19** (4)	28*** (5)	31*** (4)	44*** (5)	47*** (6)	44*** (14)	82*** (12)
NAD (P)H dehydrogenase, quinone 1	NQO1	5 (1)	32*** (13)	46*** (12)	60*** (15)	108*** (35)	105*** (44)	111*** (57)	140*** (28)
Oxidative stress									
Glutamate-cysteine ligase, catalytic subunit	GCLC	3027 (361)	3184 (265)	3107 (222)	3012 (224)	3169 (187)	2396* (495)	1923*** (584)	742*** (154)
Glutathione reductase	GSR	476 (83)	657** (64)	746*** (72)	770*** (83)	854*** (91)	827*** (62)	735*** (103)	944*** (89)
Thioredoxin reductase 1	TXNRD1	235 (62)	364** (42)	541*** (111)	670*** (311)	750*** (69)	845*** (68)	767*** (268)	1331*** (197)
Glucose-6-phosphate dehydrogenase	G6PDX	67 (9)	109*** (21)	151*** (26)	180*** (23)	261*** (34)	262*** (14)	248*** (89)	458*** (55)
Heme oxygenase (decycling) 1	HMOX1	20 (5)	46*** (6)	110*** (54)	176*** (45)	272*** (95)	498*** (181)	709*** (473)	679*** (224)
Inflammation									
Chemokine (C-C motif) ligand 2	CCL2	1.7 (1.0)	1.4 (0.7)	1.4 (1.4)	0.9 (0.4)	2.4 (1.9)	2.4 (1.2)	2.4 (1.7)	12.3*** (2.2)
Interleukin-1beta	IL1B	2.7 (0.9)	2.9 (0.9)	2.7 (1.6)	2.4 (0.4)	4.1* (0.8)	2.8 (0.5)	4.8 (2.8)	9.9*** (1.8)
Kininogen 1	KNG1	14 (7)	10 (3)	11 (3)	11 (1)	17 (4)	22* (4)	43 (32)	194*** (39)
Tissue inhibitor of metalloproteinase 1	TIMP1	28 (31)	15 (8)	21 (13)	12 (4)	18 (7)	18 (5)	43 (27)	322*** (224)
Lipocalin-2	LCN2	28 (10)	18* (3)	24 (8)	18* (2)	25 (7)	35 (18)	109 (76)	1036*** (637)
Regeneration/repair									
Kidney injury molecule-1	KIM-1	0.2 (0.0)	0.4* (0.2)	1.5*** (0.6)	2.5*** (0.6)	11.9*** (7.1)	28.2*** (14.2)	52.4*** (40.4)	84.6*** (25.9)
Annexin A7	ANXA7	60 (9)	59 (3)	69 (4)	68 (9)	90** (14)	98*** (10)	95* (31)	174*** (22)
Crystallin, alpha B	CRYAB	635 (93)	775 (109)	970** (208)	1108*** (183)	1208** (322)	1062** (256)	1023* (301)	373*** (104)
Collagen, type 1, alpha 1	COL1A1	159 (37)	185 (44)	158 (78)	116** (32)	141* (13)	108** (16)	226 (77)	327 (130)
Glycoprotein (transmembrane) nmb	GPNMB	2.2 (0.9)	1.9 (0.9)	1.7 (0.5)	1.6 (0.4)	2.1 (0.5)	2.3 (0.6)	6.3* (3.7)	22.5*** (8.2)
Matrix metallopeptidase 12	MMP12	0.3 (0.1)	0.2 (0.1)	0.3 (0.1)	0.3 (0.1)	0.5* (0.2)	0.4 (0.2)	0.6 (0.3)	2.1*** (1.2)

4.3.9 Histopathology

Due to the large number of tissue samples generated during this study livers and kidneys from rats treated at 25 and 35 mg/kg HCBD were not histologically examined.

Table 4.6 shows the number of animals in each dose level group showing pathological changes to the kidney.

Histological examination of the kidneys did not reveal HCBD-induced degenerative changes at 5 mg/kg (Figure 4.3 C). At 10 mg/kg HCBD (Figure 4.3 E), however, there was minimal degeneration which consisted of individual degenerate cells, and at 15 mg/kg and above there appeared to be a dose-related increase in the severity of the degenerative changes. In animals dosed at 20 mg/kg HCBD there were clusters of two to four degenerate cells with pyknotic nuclei (Figure 4.3 G), and at the highest dose level (90 mg/kg) there was hypereosinophilia and loss of cellular and nuclear detail in marked numbers of proximal tubular epithelial cells (Figure 4.3 I). All tubules in the S3 segment were affected.

At 5 mg/kg HCBD there was an increase in the number of hyaline droplets in the convoluted tubules proximal to the S3 segment and also an increase in the number of animals where hyaline droplets were reported compared to the control group (Figure 4.3 D). Hyaline droplets result from the accumulation of α-2μ globulin, are most often seen in the proximal convoluted tubules and may occur as a result of HCBD administration (Cristofori et al., 2013). At 10 mg/kg HCBD there was evidence of small hyaline droplets affecting multiple tubules (Figure 4.3 F) and at 20 and 90 mg/kg HCBD there were high numbers of hyaline droplets in the majority of the tubules (Figure 4.3 H and J respectively). At higher HCBD dose levels there appeared to be a dose-related increase in the severity of hyaline droplet formation (Figure 4.3 B, D, F, H and J).

There were no HCBD treatment-related morphological changes findings in the liver at any dose level (data not shown).

Table 4.6 Histopathological findings in the kidneys of male Hanover-Wistar rats treated with increasing doses of HCBD. Animals were dosed with vehicle (control, 0 mg/kg) or HCBD by intraperitoneal injection and autopsied at 24 hours post-dosing as described in Section 4.2.1. Six animals per group were examined. Each column represents the number of animals in that dose group showing the pathological changes described in the rows.

	HCBD dose level (mg/kg)							
	0	**5**	**10**	**15**	**20**	**30**	**45**	**90**
No abnormality detected	**6**	**6**	**1**	**0**	**0**	**0**	**0**	**0**
Degeneration								
Minimal	0	0	5	4	1	0	0	0
Mild	0	0	0	2	3	1	2	0
Moderate	0	0	0	0	2	5	1	0
Marked	0	0	0	0	0	0	3	1
Very marked	0	0	0	0	0	0	0	5
No abnormality detected	**4**	**0**	**0**	**0**	**0**	**0**	**0**	**0**
Hyaline droplets								
Minimal	2	2	0	0	0	0	0	0
Mild	0	4	6	5	4	4	3	3
Moderate	0	0	0	1	2	2	3	3

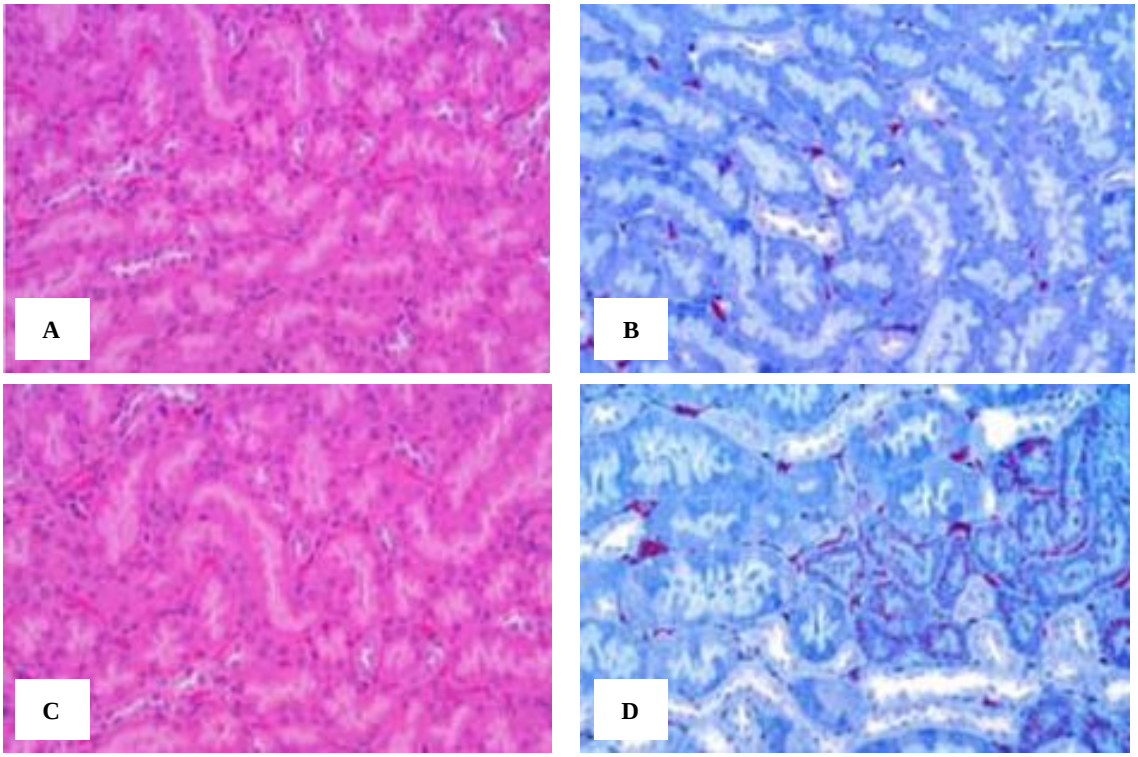

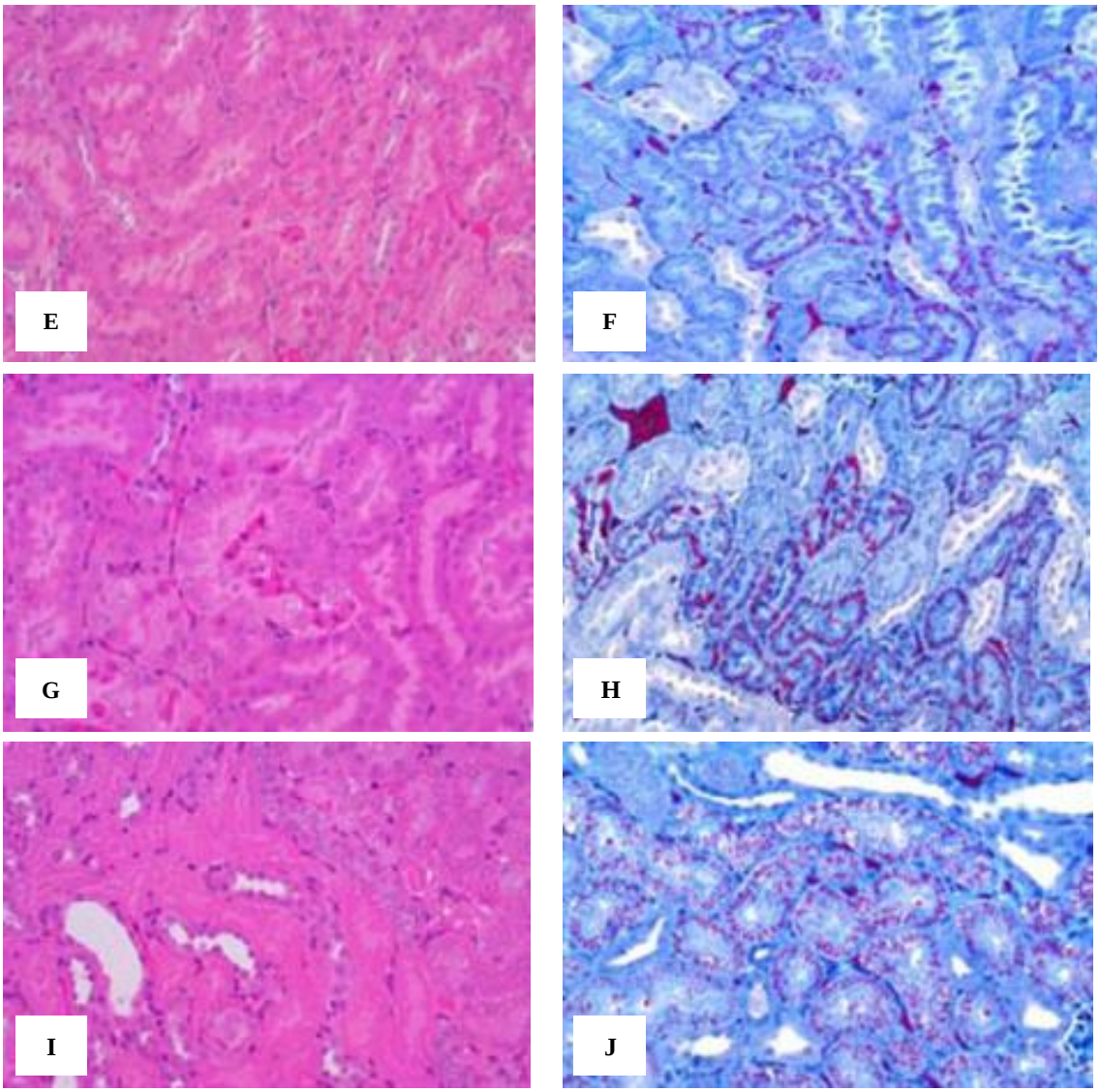

Figure 4.3 Histology of renal medulla sections from male Hanover-Wistar treated with increasing doses of HCBD. Original magnification of all images, x 200. At autopsy, 24 hours post-dosing, kidney samples were collected and processed for histopathological examination as described in Section 2.8. Sections A, C, E, G and I, were subjected to H&E staining; sections B, D, F, H and J, were subjected to chromotrope-aniline-blue staining (CAD) (hyaline droplets). Each panel shows a representative section from one of six animals per dose. Rats were treated with HCBD at doses of 0 mg/kg (control; sections A, B), 5 mg/kg (sections C, D: absence of histopathological changes (C); accumulation of low number of hyaline droplets (D)), 10 mg/kg (sections E, F: occasional degenerate cell (E); small scattered hyaline droplets (F)), 20 mg/kg (sections G, H: clusters of 2 to 4 degenerate cells (G); high number of variable size hyaline droplets (H)) and 90 mg/kg (I, J: loss of cellular and nuclear detail (I); high number of hyaline droplets (J)).

4.4 Results for the time course study

In this experiment sixty animals were administered with a single dose of HCBD at 45 mg/kg and sixty animals were dosed with vehicle (controls). Six HCBD-treated rats and six control animals were autopsied at days 1, 2, 3, 4, 5, 6, 7, 10 and 28 after dosing. This dose level was chosen based on the results from the dose response study, since this dose level produced consistent histopathological evidence of proximal tubular degeneration.

4.4.1 Observations during the study

During the post-dosing period observations were recorded at each autopsy time point. After 1, 2, 3, 4 and 5 days of receiving a single dose of HCBD, the kidneys from HCBD-treated rats appeared enlarged and paler in colour when compared to control rats at the same time point. No other abnormalities were recorded.

4.4.2 Nonresponders

During the course of this study, 6 rats out of the 60 treated with HCBD, were considered to have been mis-dosed since they did not show any HCBD-related effects. One animal per group at days 2, 3, 5 and 7 post-dosing and 2 animals on day 6 post-dosing were considered to be mis-dosed. Histopathology examination of these animals revealed no evidence of proximal tubular injury and thus data from these rats was not included in the results section.

4.4.3 Body weights

Table 4.7 shows the change in body weight (for both control and HCBD-treated animals) while the animals were in the metabolism cages for 18 hour urine collection prior to autopsy at each time point. Animals lost weight while in the metabolism cages. There was no clear evidence of a HCBD-treatment related effect on body weight loss at any of the time points studied.

Table 4.7 Body weight change for male Hanover-Wistar rats treated with a single dose of vehicle (control) or HCBD at 45 mg/kg during an 18 hour period in metabolism cages. Animals were dosed by intraperitoneal injection and placed individually in metabolism cages for the collection of 18 hour urine samples as described in Section 4.2.2. Animals had access to water but not diet while in the metabolism cages. Values are means and SD of at least 4 animals at each time point (as described in Section 4.4.2) and indicate change in body weight. Values that are different from corresponding controls at the respective time point by Students' t-test are shown: $^{*}P<0.05$.

	Mean (SD) change in body weight (g)	
Time (days after dosing)	**0 mg/kg HCBD**	**45 mg/kg HCBD**
1	-14.65 (1.26)	-17.12* (2.12)
2	-15.77 (1.75)	-14.72 (1.63)
3	-18.20 (2.75)	-21.42 (2.38)
4	-18.15 (1.75)	-15.75 (2.80)
5	-18.22 (2.03)	-15.20* (2.47)
6	-18.75 (2.81)	-17.97 (3.71)
7	-19.10 (2.43)	-20.42 (2.27)
10	-22.70 (2.51)	-20.30 (2.59)
14	-18.27 (0.90)	-18.72 (3.82)
28	-17.85 (2.05)	-20.13 (1.78)

4.4.4 Liver weights

Relative liver weights were calculated as preliminary indicators of potential HCBD-induced hepatotoxicity. Relative liver weights for HCBD-treated rats were significantly increased over the respective controls on days 1, 2, 3 and 4 post-dosing (Figure 4.4 A). After this time point there were no significant differences between control and HCBD-treated liver weights.

4.4.5 Kidney weight

Relative kidney weights for vehicle-treated (controls) and HCBD-treated animals are shown in Figure 4.4 B. Kidney weights were significantly increased over controls at days 1, 2, 3, 4 and 5 after dosing. At day 4 following a single dose of HCBD, kidneys from HCBD-treated animals were 40 % increased over controls ($^{***}P<0.001$). From day 6 onwards there was no difference between control and kidneys from HCBD-treated animals.

A

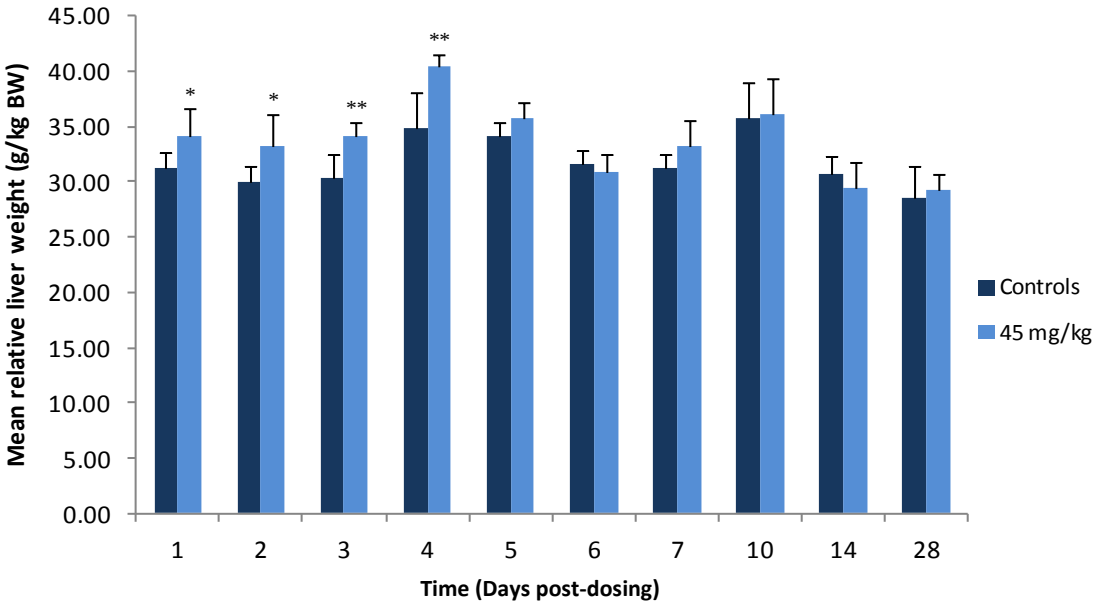

B

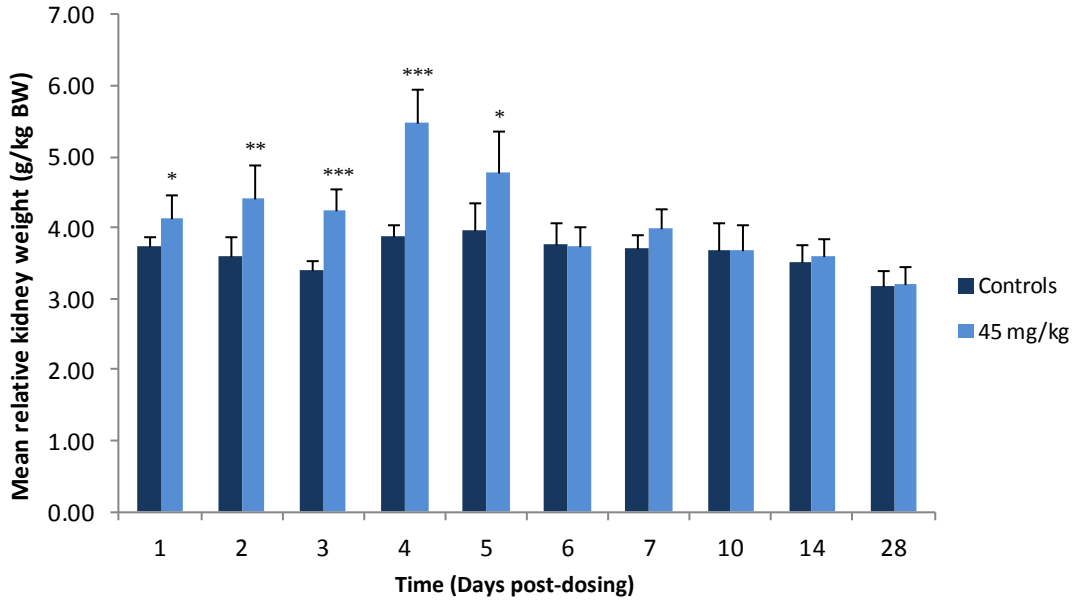

Figure 4.4 Relative liver (A) and kidney (B) weights from male Hanover-Wistar rats treated with a single dose of vehicle (control) or HCBD at 45 mg/kg and sampled at various time points post-dosing. Animals were dosed on day 0 and autopsied at several time points following treatment. At autopsy animals were killed, livers and kidneys were removed and weighed. The kidney weight was expressed as a mean of the left and right kidneys. Results are shown as mean body weight per kg body weight (BW) with SD indicated by vertical bars of at least 4 animals at each time point (as described in Section 4.4.2). Values that differ significantly from corresponding controls at the respective time points by Students' t-test are shown: $^{*}P<0.05$; $^{**}P<0.01$; $^{***}P<0.001$.

4.4.6 Serum clinical chemistry

Serum ALT, AST, GLDH and ALP were measured in control (vehicle-treated animals) and HCBD-treated rats at day 1 to 28 post-dosing. Levels of these enzymes revealed no clear HCBD-treatment related effects with time (Figure 4.5). Mean ALT values were decreased by 30 % compared to the respective controls at day 4 post-dosing but not at any other time points. Serum GLDH was significantly increased over controls on days 2 and 3 post-dosing. No other differences were noted.

Serum levels of urea, albumin, glucose and total protein were measured in this study but there were no significant changes between control and HCBD-treated animals at any time point (Table 4.8).

Creatinine levels in the serum, however, were approximately 2-fold increased over concurrent controls on days 1 and 2 post-dosing. At all later time points there was no difference between creatinine levels in control and HCBD-treated rats (Table 4.8).

A

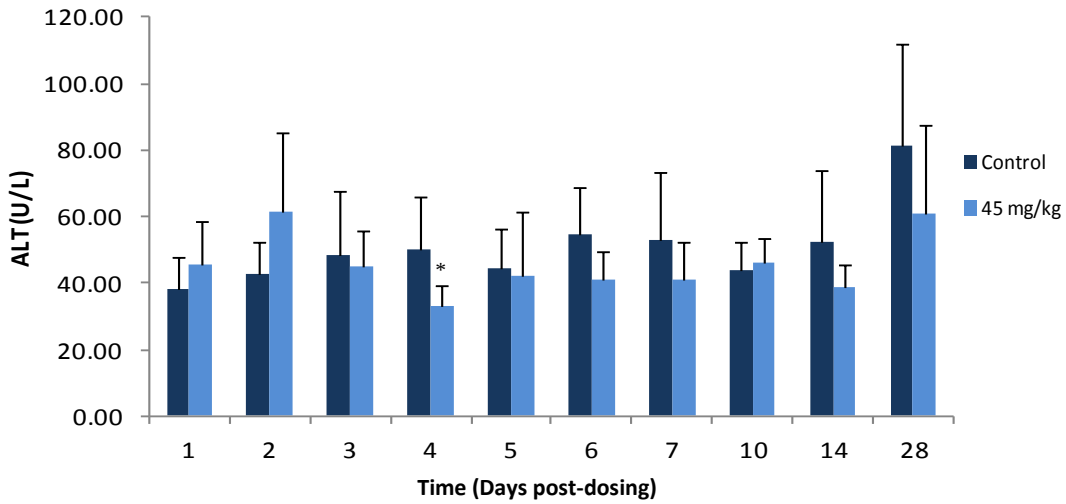

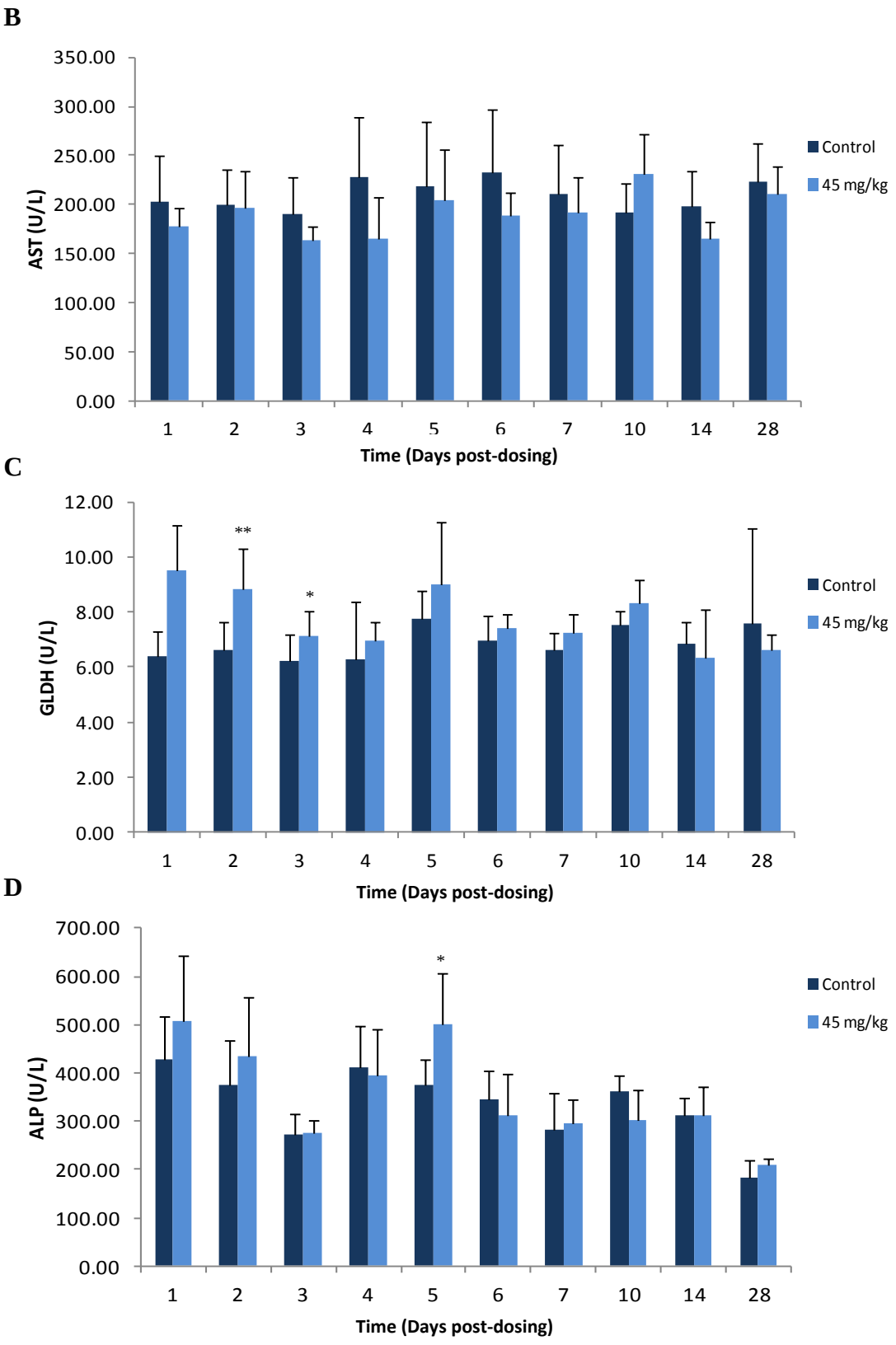

Figure 4.5 Serum ALT (A), AST (B), GLDH (C) and ALP (D) levels for male Hanover-Wistar rats treated with a single dose of vehicle (control) or HCBD at 45 mg/kg and sampled at various time points post-dosing. Animals were dosed on day 0 and autopsied at several time points following treatment. At autopsy serum was collected according to section 4.2.2 and enzymes were assayed as described in Section 2.7. Values are means with SD indicated by vertical bars of at least 4 animals at each time point (as described in Section 4.4.2). Values that differ significantly from corresponding controls at the respective time points by Students's t-test are shown: $^{*}P<0.05$; $^{**}P<0.01$.

Table 4.8 Serum clinical chemistry parameters levels for male Hanover-Wistar rats treated with a single dose of vehicle (control) or HCBD at 45 mg/kg and sampled at various time points post-dosing. Animals were dosed on day 0 and autopsied at several time points following treatment. At autopsy serum was collected according to section 4.2.2 and enzymes were assayed as described in Section 2.7. Values are means and SD of at least 4 animals at each time point (as described in Section 4.4.2). Values that differ significantly from corresponding controls at the respective time points by Students's t-test are shown: $^{*}P<0.05$. C: control, T: treated.

Serum parameters		Time (days post-dosing)									
		1	**2**	**3**	**4**	**5**	**6**	**7**	**10**	**14**	**28**
Urea (mmol/L)	C	7.80 (0.75)	7.17 (0.74)	9.72 (0.85)	8.02 (0.62)	7.67 (0.90)	7.55 (1.12)	6.47 (0.70)	10.62 (1.53)	6.53 (1.14)	7.68 (1.36)
	T	9.27 (2.37)	10.12 (3.61)	10.88 (1.68)	8.22 (1.71)	6.88 (0.60)	7.40 (0.83)	7.26 (1.01)	10.12 (1.02)	7.82 (1.06)	7.90 (1.16)
Albumin (g/L)	C	34.00 (1.67)	33.00 (1.67)	33.17 (1.17)	33.17 (0.75)	34.00 (1.26)	33.00 (1.10)	33.83 (1.47)	32.50 (0.55)	32.33 (1.51)	34.67 (1.75)
	T	33.33 (0.82)	33.60 (1.14)	32.60 (1.95)	33.17 (0.98)	34.60 (0.89)	33.25 (2.36)	32.60 (1.52)	32.67 (1.21)	33.50 (1.64)	34.67 (1.75)
Glucose (mmol/L)	C	3.77 (1.00)	4.76 (0.79)	7.27 (2.49)	8.36 (0.72)	4.84 (1.37)	4.11 (1.46)	4.30 (1.09)	7.40 (0.42)	4.19 (0.84)	6.65 (1.23)
	T	2.85 (0.77)	4.12 (0.96)	7.27 (0.93)	8.61 (0.45)	5.13 (0.70)	3.90 (1.19)	5.56 (1.44)	7.44 (0.31)	3.86 (1.26)	6.20 (1.10)
Total protein (g/L)	C	55.50 (2.51)	54.17 (1.72)	56.17 (1.94)	53.67 (1.03)	55.00 (2.28)	52.83 (2.23)	54.33 (2.16)	53.17 (0.98)	52.83 (2.04)	55.50 (3.62)
	T	53.67 (1.63)	54.00 (2.00)	53.20 (2.95)	53.17 (1.60)	55.20 (1.92)	54.00 (3.83)	53.60 (0.89)	54.17 (1.94)	54.33 (2.58)	57.50 (4.14)
Creatinine (µmol/L)	C	25.00 (1.79)	26.00 (1.90)	29.17 (2.48)	22.17 (1.33)	23.33 (2.42)	22.00 (3.41)	23.00 (2.00)	24.67 (1.21)	24.33 (2.58)	29.33 (2.73)
	T	48.67* (22.92)	50.60* (26.81)	34.60 (13.61)	23.83 (4.26)	23.40 (1.67)	25.00 (1.41)	25.20 (1.79)	25.00 (1.41)	25.00 (6.39)	31.83 (2.79)

4.4.7 Urinary biomarkers of kidney injury

Levels of the same urinary biomarkers that were measured in the dose response study in this Chapter (Section 4.3) were measured to assess the sensitivity of the markers at various time points after the induction of acute kidney injury.

Urinary α-GST and GST Yb1 both peaked at 24 hours (day 1) following a single dose of HCBD at 45 mg/kg (an approximate 357- and 17-fold increase was measured for α-GST and GST Yb1 respectively; $^{***}P<0.001$). From day 2 post-dosing, levels of both enzymes gradually declined with time, but were still significantly elevated over controls at day 4 post-dosing. However, at day 5 post-dosing, α-GST levels in HCBD-treated animals were significantly lower than the concurrent controls ($^{*}P<0.05$), whereas GST Yb1 was similar to control (Table 4.9).

Urinary osteopontin was significantly increased over controls at days 2 to 5 post-dosing and also at day 7 (Table 4.9).

Lipocalin-2 was significantly decreased in HCBD-treated animals compared to controls on day 3 post-dosing ($^{*}P<0.05$), however, the mean control value was much greater at this time point than the control lipocalin-2 values at the other time points. This was due to 2 animals in the group having elevated serum levels of lipocalin-2 (when compared to the lowest value in the group, these 2 animals showed an approximate 2.5-fold increase). At other time points in the study, there appeared to be no evidence of an HCBD-related effect on lipocalin-2 (Table 4.9).

Urinary creatinine levels showed no evidence of an HCBD-treatment related effect apart from a significant decrease in the treated animals at day 6 (43.00 and 38.25 µmol/c.p. for control animals and HCBD-treated rats respectively) ($^{*}P<0.05$) (Table 4.9). Urinary glucose was significantly increased in HCBD-treated animals at the first time point (day 1) and up to day 4 post-dosing (inclusively) (Table 4.9).

Clusterin was significantly increased over controls at days 1, 4, 5 and 7 after HCBD-treatment; there were also increases at days 2 and 3 but these were not statistically significant (Table 4.10). The greatest fold increase was measured on day 4 post-dosing (6.5-fold increase over concurrent controls; $^{***}P<0.001$). Levels for KIM-1 were significantly increased in HCBD-treated rats from day 1 to 7 post-dosing. KIM-1 levels

in urine peaked on day 4, at which time point an approximate 84-fold increase was reported over concurrent controls (5.42 and 454.01 ng/c.p.) (***P<0.001) (Table 4.10).

Urinary total protein was significantly increased in HCBD-treated animals at the first time point (day 1) and up day 4 post-dosing (inclusively). Total protein levels peaked on day 1 (24 hours post-dosing) (***P<0.001).

Albumin was 156-fold increased over concurrent controls on day 1 post-dosing, and remained significantly increased at days 2, 3, 4 and 5 post-dosing. However, 7 days after HCBD-treatment, mean albumin levels were decreased when compared to the respective controls (*P<0.05) (Table 4.10). At all other time points urinary albumin for HCBD-treated animals was similar to controls.

Table 4.9 Urinary levels of α-GST, GST Yb1, osteopontin, lipocalin-2, creatinine and glucose for male Hanover-Wistar rats treated with a single dose of vehicle (control) or HCBD at 45 mg/ kg and sampled at various time points post-dosing. Animals were dosed on day 0 and autopsied at several time points following treatment. Urine was collected for 18 hours prior to autopsy at each time point and analysed as described in Section 4.2.2. Values are means and SD of at least 4 animals at each time point (as described in Section 4.4.2) and are expressed as c.p. (collection period, 18 hours). Values that differ significantly from corresponding controls at the respective time points by Students's t-test are shown: *P<0.05; **P<0.01; ***P<0.001. C: control, T: treated.

Urinary parameters		Time (days)									
		1	2	3	4	5	6	7	10	14	28
α-GST (ng/c.p.)	C	504.81 (381.55)	347.91 (166.50)	836.71 (279.54)	459.88 (153.93)	619.37 (280.95)	622.97 (456.92)	926.04 (290.47)	456.93 (149.47)	782.62 (313.00)	1677.10 (743.08)
	T	180179.28*** (125447.39)	31051.80*** (19835.69)	5552.50*** (2325.36)	1202.20*** (265.63)	301.00* (106.14)	516.43 (209.97)	615.12 (233.18)	565.94 (1335.61)	835.77 (180.34)	1604.55 (524.74)
GST Yb1 (ng/c.p.)	C	38.91 (19.61)	34.44 (25.46)	79.03 (40.13)	38.52 (9.45)	43.38 (31.79)	39.21 (18.05)	105.96 (50.27)	46.09 (17.41)	78.91 (37.11)	155.93 (36.23)
	T	640.83*** (271.43)	345.25*** (176.50)	359.33*** (103.25)	111.67** (39.32)	45.48 (17.58)	44.54 (24.99)	63.19 (23.44)	81.35* (3.64)	72.82 (17.31)	179.24 (61.64)
Osteopontin (ng/c.p.)	C	21.60 (10.58)	17.56 (9.45)	23.87 (6.31)	14.02 (4.23)	21.56 (9.87)	14.58 (5.06)	40.19 (11.85)	37.88 (12.30)	39.27 (11.07)	28.02 (6.81)
	T	32.61 (17.10)	63.79** (45.56)	90.86*** (49.25)	92.33*** (16.66)	58.26** (18.33)	24.08 (11.00)	67.56* (17.43)	41.04 (12.28)	29.02 (11.80)	38.95* (7.23)
Lipocalin-2 (ng/c.p.)	C	3394.52 (1461.95)	4558.70 (1797.72)	8024.93 (3348.34)	6426.62 (3456.35)	3871.45 (901.47)	2689.30 (329.85)	4529.62 (657.45)	3793.58 (1255.27)	2829.77 (966.21)	3255.00 (602.18)
	T	5492.22 (3696.26)	3421.98 (1574.78)	4263.62* (346.09)	5568.55 (1047.33)	3354.32 (503.13)	2209.35 (516.90)	4230.86 (638.72)	4012.78 (1317.64)	2105.25 (382.96)	2681.78 (637.14)
Creatinine (µmol/c.p.)	C	36.17 (3.92)	32.17 (7.36)	48.33 (2.73)	35.83 (1.72)	30.67 (5.28)	43.00 (2.97)	45.50 (1.52)	46.00 (9.17)	49.83 (11.53)	69.83 (13.70)
	T	32.17 (2.23)	32.00 (9.00)	53.00 (4.12)	37.33 (3.27)	29.80 (2.05)	38.25* (2.99)	44.20 (5.40)	47.67 (4.23)	47.00 (5.37)	69.67 (2.66)
Glucose (µmol/c.p.)	C	3.50 (0.55)	3.33 (1.03)	3.67 (0.52)	4.33 (1.03)	3.33 (0.82)	4.83 (0.75)	4.00 (0.63)	6.33 (1.75)	4.67 (1.37)	5.00 (1.10)
	T	105.67* (151.79)	170.40** (144.94)	57.40* (56.81)	22.00*** (18.42)	8.20 (10.52)	4.00 (0.82)	3.60 (0.55)	7.17 (1.83)	3.67 (0.52)	5.67 (1.03)

α-GST: α-glutathione-S-transferase; GST Yb1: glutathione-S-transferase Yb1.

Table 4.10 Urinary levels clusterin, KIM-1, total protein and albumin for male Hanover-Wistar rats treated with a single dose of vehicle (control) or HCBD at 45 mg/ kg and sampled at various time points post-dosing. Animals were dosed on day 0 and autopsied at several time points following treatment. Urine was collected for 18 hours prior to autopsy at each time point and analysed as described in Section 4.2.2. Values are means and SD of at least 4 animals at each time point (as described in Section 4.4.2) and are expressed as c.p. (collection period, 18 hours). Values that differ significantly from corresponding controls at the respective time points by Students's t-test are shown: *P<0.05; **P<0.01; ***P<0.001. C: control, T: treated.

Urinary parameters		Time (days)									
		1	**2**	**3**	**4**	**5**	**6**	**7**	**10**	**14**	**28**
Clusterin (ng/c.p.)	C	82.96 (29.43)	141.48 (55.51)	125.29 (19.43)	104.98 (22.32)	90.28 (12.30)	190.84 (123.07)	82.64 (34.16)	110.13 (26.91)	83.62 (45.39)	85.66 (22.51)
	T	329.02* (372.02)	299.52 (212.95)	290.20 (182.21)	682.93*** (242.13)	346.26** (175.45)	198.38 (93.74)	200.73** (50.34)	133.98 (17.11)	96.17 (45.07)	92.45 (29.03)
KIM-1 (ng/c.p.)	C	4.56 (1.02)	3.73 (0.46)	4.80 (0.78)	5.42 (0.91)	4.81 (1.17)	5.21 (1.28)	7.28 (0.53)	9.72 (1.99)	6.57 (1.64)	6.35 (0.97)
	T	32.02*** (15.40)	360.53*** (144.26)	233.07*** (125.15)	454.01*** (148.65)	124.37*** (100.54)	13.76** (4.66)	14.81*** (1.29)	10.25 (1.18)	6.81 (2.08)	7.10 (1.74)
Total protein (mg/c.p.)	C	4.17 (0.54)	4.83 (2.85)	5.88 (1.48)	5.23 (1.54)	5.23 (1.01)	9.30 (1.33)	7.12 (1.99)	5.03 (1.58)	7.08 (2.22)	9.10 (3.45)
	T	18.12*** (8.79)	12.10** (3.08)	11.40*** (1.83)	9.45** (1.28)	5.76 (1.71)	6.75** (0.97)	5.88 (2.09)	5.23 (1.33)	5.92 (1.06)	7.93 (1.04)
Albumin (mg /c.p.)	C	0.07 (0.08)	0.07 (0.03)	0.08 (0.02)	0.15 (0.10)	0.07 (0.03)	0.10 (0.03)	0.13 (0.05)	0.79 (0.64)	0.12 (0.04)	0.16 (0.06)
	T	10.94*** (6.51)	9.45*** (5.61)	1.25* (0.92)	3.09*** (2.46)	0.76* (0.82)	0.07 (0.01)	0.08* (0.04)	0.53 (0.54)	0.16 (0.04)	0.14 (0.04)

KIM-1: kidney injury molecule-1.

4.4.8 Gene expression

In the dose response study in this Chapter most of the changes in gene expression markers for the liver corresponded to genes involved in xenobiotic metabolism and oxidative stress. This reflects the metabolism of HCBD in the liver with the production of a toxic metabolite in the kidneys and did not indicate a toxic response. Therefore, in the present study, it was not considered necessary to carry out gene expression analysis of the liver.

Table 4.11 shows the gene expression data in the kidneys of the male Hanover-Wistar rats treated with vehicle (controls) or a single dose of 45 mg/kg HCBD and autopsied at day 1 to 28 post-dosing. Three HCBD-treated animals and 3 concurrent control animals were randomly selected at each time point.

Twenty four hours after HCBD administration (day 1), there was significant upregulation of all the genes involved in xenobiotic metabolism, except CYP1A1 and CYP2C which were downregulated. NQO1 was upregulated 26-fold compared to controls at the same time point ($^{***}P<0.001$). EPHX1 mRNA was approximately 15-fold greater than concurrent controls ($^{***}P<0.001$) (Table 4.11). ABCC3, GSTM4, GSTA3 and UGT1A6 were also significantly upregulated over controls at day 1 post-dosing but fold increases recorded were smaller (4.1-fold for ABCC, 3.3- for GSTM4 and 5-fold for both GSTA3 and UGT1A6 respectively; $^{**}P<0.01$). All of these genes remained upregulated at days 2 and 3 and most had returned to normal expression levels by day 4 post-dosing.

The expression of CYP1A1 appeared to be downregulated at all time points but the only statistically significant differences were noted on days 5 and 7 post-dosing. CYP2C expression remained downregulated until day 10 post-dosing but this was not statistically significant on day 6.

In the category of oxidative stress, G6PDX, GSR, HMOX1 and TXNRD1 mRNA levels were significantly increased over concurrent controls from day 1 to day 3 post-dosing. GCLC was the only gene in this category to be downregulated when compared to control animals; however, this downregulation was not statistically significant (Table 4.11).

The inflammatory gene LCN2 was upregulated as early as day 2 after dosing ($^{**}P<0.01$) and remained significantly upregulated up to and including day 5 post-dosing. Expression levels of LCN2 were also significantly upregulated on day 7 and 14 post-dosing. Also in this category, TIMP1 was upregulated on day 1 and 2 post-dosing and also on days 4 and 5 post-dosing.

In the functional category of regeneration and repair ANXA7, COL1A1, CRYAB, KIM-1 and MMP12 were all significantly upregulated on day 1 post-dosing. The fold increase in mRNA expression at 24 hours following a single dose of 45 mg/kg HCBD was greatest for KIM-1 (242-fold increase, $^{***}P<0.001$) and expression of this gene remained upregulated until day 5 after dosing, and on day 7 and day 10 post-dosing. ANXA7 was upregulated between days 1 and 4 post-dosing; expression of this gene was highest on day 2 post-dosing ($^{***}P<0.001$).

Table 4.11 Kidney gene expression in male Hanover-Wistar rats treated with a single dose of vehicle (control) or HCBD 45 mg/ kg and sampled at various time points post-dosing. Animals were dosed on day 0 and autopsied at several time points following treatment. At autopsy, kidney expression was measured as described in Section 2.9. Results are represented as copy number [x10^3/5 ng cDNA]. Values are the means and SD of 3 animals per dose level group. Values that differ significantly from corresponding controls at the respective time points by Students' t-test are shown: *P<0.05; **P<0.01; ***P<0.001. Control values are only shown for day 1 post-dosing.

			Days post-dosing									
Functional category/gene name	**symbol**	**Control (Day 1)**	**1**	**2**	**3**	**4**	**5**	**6**	**7**	**10**	**14**	**28**
Xenobiotic metabolism												
Cytochrome P450 1A1	CYP1A1	111.8 (37.5)	34.5 (34.8)	13.7 (16.5)	15.8 (25.2)	3.2 (2.8)	2.7* (4.3)	19.9 (6.5)	6.7* (4.4)	55.3 (26.9)	24.4 (31.4)	56.1 (36.3)
Cytochrome P450 2C	CYP2C	56.9 (20.5)	8.6* (9.4)	1.1** (1.0)	6.5** (5.3)	3.7** (5.2)	0.6* (1.0)	22.6 (1.0)	11.8* (18.1)	25.3* (14.0)	77.3 (31.7)	237.4 (26.0)
NAD (P)H dehydrogenase, quinone 1	NQO1	10.6 (3.0)	263.1*** (51.2)	115.4*** (39.2)	74.3*** (6.5)	15.4 (3.0)	24.9* (2.3)	21.5 (8.8)	14.0 (2.5)	9.1 (0.3)	11.7* (0.8)	9.7 (1.8)
ATP-binding cassette, subfamily C member3	ABCC3	18.5 (4.8)	75.9** (21.3)	48.0** (7.2)	32.3* (2.8)	22.0 (3.7)	24.1 (2.4)	21.9 (1.2)	24.1** (2.1)	24.1 (2.2)	27.0 (0.9)	22.4 (4.1)
Glutathione S-transferase isoform mu 3	GSTM4	52.9 (1.7)	174.0** (41.6)	150.3** (31.1)	175.3** (20.8)	80.4 (19.8)	79.4 (24.6)	70.7 (12.6)	61.2 (11.8)	131.9 (38.6)	70.8 (3.5)	62.5 (17.6)
Glutathione S-transferase Yc2 subunit (alpha 3)	GSTA3	67.6 (22.3)	334.4** (80.3)	300.4** (90.2)	202.2** (57.6)	72.9 (14.5)	94.7* (10.5)	92.0 (12.2)	50.8 (12.4)	44.7 (2.6)	58.0 (13.8)	59.3 (7.2)
UDP glucuronosyltransferase 1A6	UGT1A6	241.3 (74.3)	1241.2** (55.4)	971.3*** (167.9)	560.0** (102.4)	322.3* (15.1)	325.5 (71.6)	322.3 (104.5)	273.2 (66.3)	143.1** (13.3)	263.3* (17.2)	254.5* (28.6)
Epoxide hydrolase 1 (microsomal)	EPHX1	635.6 (113.0)	9486.9*** (1805.4)	4397.5*** (1326.1)	2094.8** (618.7)	701.3 (60.8)	693.7 (115.1)	709.4 (97.6)	620.8 (36.8)	561.1 (72.1)	796.7 (131.9)	697.1 (81.3)
Oxidative stress												
Glucose-6-phosphate dehydrogenase	G6PDX	79.2 (9.9)	379.7*** (52.7)	307.9** (67.9)	193.1** (3.2)	123.1 (9.9)	110.4 (32.7)	105.0* (4.3)	102.0 (20.2)	90.4 (12.7)	116.5 (9.0)	114.2 (13.3)
Glutathione reductase	GSR	551.3 (67.7)	1134.8** (114.2)	934.7*** (53.0)	810.3** (22.0)	566.6 (49.7)	584.7 (127.8)	684.7 (117.8)	631.6 (49.3)	684.0 (97.7)	712.0 (79.4)	593.4 (122.7)
Heme oxygenase (decycling) 1	HMOX1	12.8 (2.4)	614.2*** (230.1)	194.9*** (55.6)	58.8** (15.4)	33.2* (7.5)	32.9 (11.5)	15.6 (0.5)	21.7 (7.5)	16.4 (2.2)	18.9 (2.9)	16.1 (2.2)
Thioredoxin reductase 1	TXNRD1	293.9 (26.4)	125.0*** (242.4)	729.3** (112.2)	586.4*** (32.0)	330.4 (17.4)	322.6 (29.2)	371.0 (27.9)	318.0 (36.7)	301.0 (24.2)	373.6 (48.0)	363.2 (36.8)
Glutamate-cysteine ligase, catalytic subunit	GCLC	4372.3 (1050.1)	2642.2 (837.4)	2350.6 (996.6)	2323.7 (1313.9)	1607.9** (636.8)	1235.6 (584.3)**	2820.7 (342.4)	2968.8** (436.2)	4754.8 (1426.3)	6049.5 (1761.1)	6436.0 (410.9)
Inflammation												
Lipocalin-2	LCN2	22.1 (4.6)	186.6 (218.2)	139.2** (47.2)	183.0* (137.7)	226.0** (74.2)	293.7* (256.0)	45.9 (1.3)	58.0* (15.8)	42.5 (5.5)	37.3* (4.6)	31.7 (11.1)
Chemokine (C-C motif) ligand 2	CCL2	4.5 (1.3)	17.4 (13.7)	11.9 (5.1)	14.7 (7.0)	16.4 (4.7)	12.8 (11.4)	4.7 (0.1)	5.9 (2.1)	9.5 (2.6)	10.3 (8.5)	7.6 (0.6)
Kininogen 1	KNG1	19.7 (5.8)	106.4 (98.4)	87.4* (40.3)	46.6 (26.3)	43.0 (28.9)	54.0 (51.0)	15.6 (1.2)	15.9 (7.1)	15.2 (3.7)	13.9 (3.5)	14.7 (1.5)
Tissue inhibitor of metalloproteinase 1	TIMP1	11.7 (3.0)	84.7* (62.8)	62.3* (18.7)	75.0 (48.0)	81.8* (26.4)	57.7* (30.7)	32.2 (21.7)	29.6 (16.9)	32.4 (5.5)	22.2 (5.4)	18.6 (4.9)
Regeneration/repair												
Annexin A7	ANXA7	78.1 (15.5)	158.4* (44.3)	186.9*** (10.5)	163.0* (27.8)	131.0** (11.5)	121.6 (24.7)	99.4 (15.6)	104.6 (16.2)	104.4 (9.4)	109.9 (5.9)	99.4 (7.8)
Collagen, type 1, alpha 1	COL1A1	133.6 (28.5)	221.7* (32.2)	213.5 (61.7)	339.9 (122.0)	737.7 (502.7)	578.5** (110.8)	262.8 (104.0)	322.8 (148.5)	265.8 (94.9)	291.5 (78.0)	120.1 (30.1)
Crystallin, alpha B	CRYAB	1060.1 (82.3)	1567.4* (234.8)	1282.9 (152.4)	647.3 (295.5)	507.4** (109.5)	461.9* (175.1)	727.0 (63.4)	625.9* (126.6)	831.8 (71.9)	968.6 (262.2)	1009.9 (37.7)
Kidney injury molecule-1	KIM-1	0.2 (0.0)	48.3*** (33.6)	65.2*** (11.5)	79.8*** (43.3)	59.1*** (24.7)	33.2*** (26.0)	3.9 (0.5)	3.0*** (0.4)	1.4* (0.8)	0.8 (0.6)	0.6 (0.5)
Matrix metallopeptidase 12	MMP12	0.2 (0.0)	1.6** (0.7)	1.6 (0.2)	1.0* (0.4)	1.2 (0.6)	0.7 (0.3)	0.2 (0.1)	0.4 (0.1)	1.6 (0.6)	0.9 (0.2)	1.0 (0.8)
Glycoprotein (transmembrane) nmb	GPNMB	2.3 (1.0)	13.8 (8.1)	15.1** (3.1)	17.8 (9.9)	22.8** (5.1)	24.8* (12.0)	7.5 (2.7)	10.6*** (0.9)	6.6 (1.8)	5.5 (0.2)	3.3 (0.4)

4.4.9 Histopathology

Histological examination of the kidneys following a single administration of 45 mg/kg HCBD revealed evidence of degeneration and regeneration in the S3 segment of the proximal renal tubules

Table 4.12 shows the number of animals at each time point that demonstrated histopathological changes to the kidneys. There were signs of degeneration from day 1 to day 3 post-dosing (Table 4.12, Figure 4.6 B, C and D). On day 1 post-dosing there was evidence of tubular degeneration and hypereosinophilia, which was also observed on day 2. On day 3, there were focal areas of degeneration (labelled with (*) in Figure 4.6 B, C and D). However, the severity of degeneration changed with time; no animals on day 1 displayed evidence of marked degeneration, whereas on day 2, 3 out of the 5 animals examined had marked degeneration and 1 out of 5 on day 3 showed marked degeneration. After day 3, no animals were found to have histopathological evidence of degeneration.

Regeneration of the S3 segment of the proximal tubule was first observed on day 2 post-dosing (5 out of 5 animals at that time point) but was only moderate or marked. Regeneration is labelled with (†) in Figure 4.6 C and D. At days 4 and 5 post-dosing all animals showed very marked signs of regeneration suggesting that regeneration peaked at these time points. Figure 4.6 C shows mitotic figures evidenced with arrows and eosinophilic proteinaceous debris in the tubule lamina **(+).** By day 10 most animals were only showing minimal or mild signs of regeneration and tubules had a morphologic appearance almost similar to control.

Kidneys from control animals and livers from all animals did not reveal any evidence of HCBD-treatment related effect at any of the time points in this study.

Table 4.12 Histopathological findings in the kidneys of male Hanover-Wistar rats treated with a single dose of vehicle (control) or HCBD at 45 mg/kg and sampled at various time points post-dosing. Animals were dosed on day 0 and autopsied at several time points following treatment. Each column represents the number of animals in that dose group showing the pathological changes described in the rows. A minimum of at least 4 animals was examined at each time point (as described in Section 4.4.2).

	Time (days post-dosing)									
	1	**2**	**3**	**4**	**5**	**6**	**7**	**10**	**14**	**28**
No degenerative abnormality detected										
	0	**0**	**0**	**6**	**5**	**4**	**5**	**6**	**6**	**6**
Minimal	2	0	0	0	0	0	0	0	0	0
Mild	2	0	2	0	0	0	0	0	0	0
Moderate	2	2	2	0	0	0	0	0	0	0
Marked	0	3	1	0	0	0	0	0	0	0
Very marked	0	0	0	0	0	0	0	0	0	0
No regenerative abnormality detected										
	6	**0**	**0**	**0**	**0**	**0**	**0**	**1**	**2**	**4**
Minimal	0	0	2	0	0	0	0	5	1	2
Mild	0	0	0	0	0	0	0	0	3	0
Moderate	0	1	0	0	0	1	1	0	0	0
Marked	0	4	3	0	0	2	0	0	0	0
Very marked	0	0	0	6	5	1	4	0	0	0

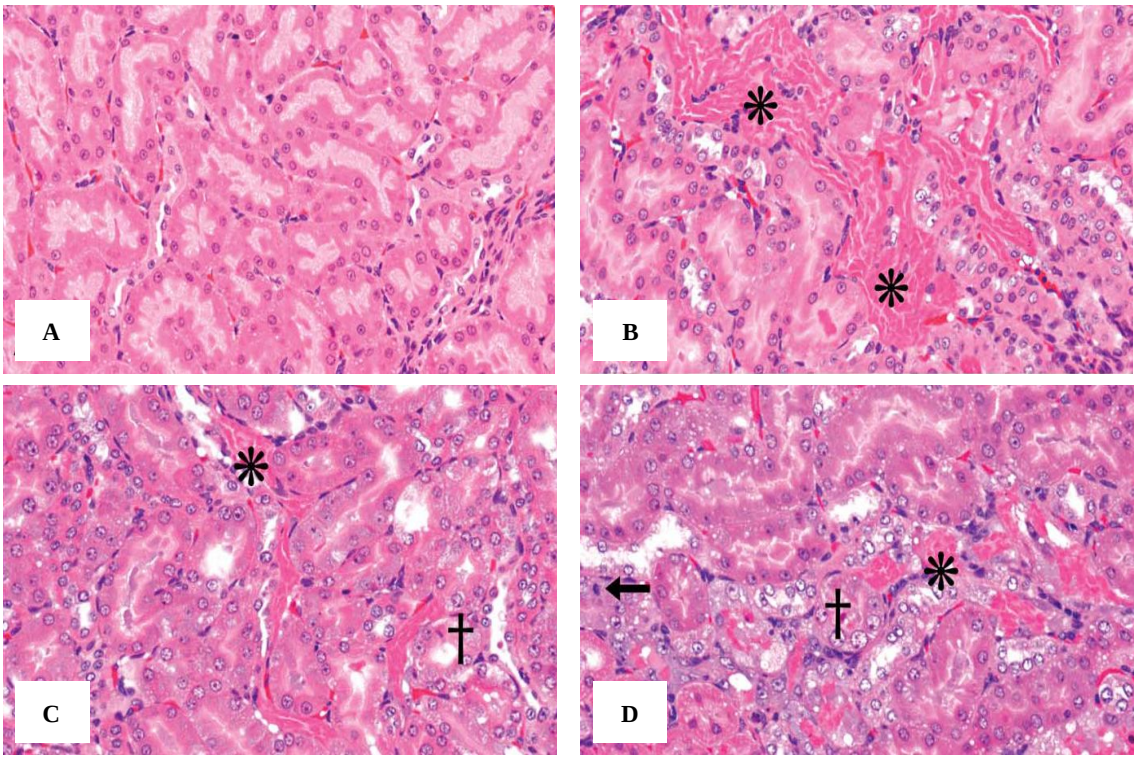

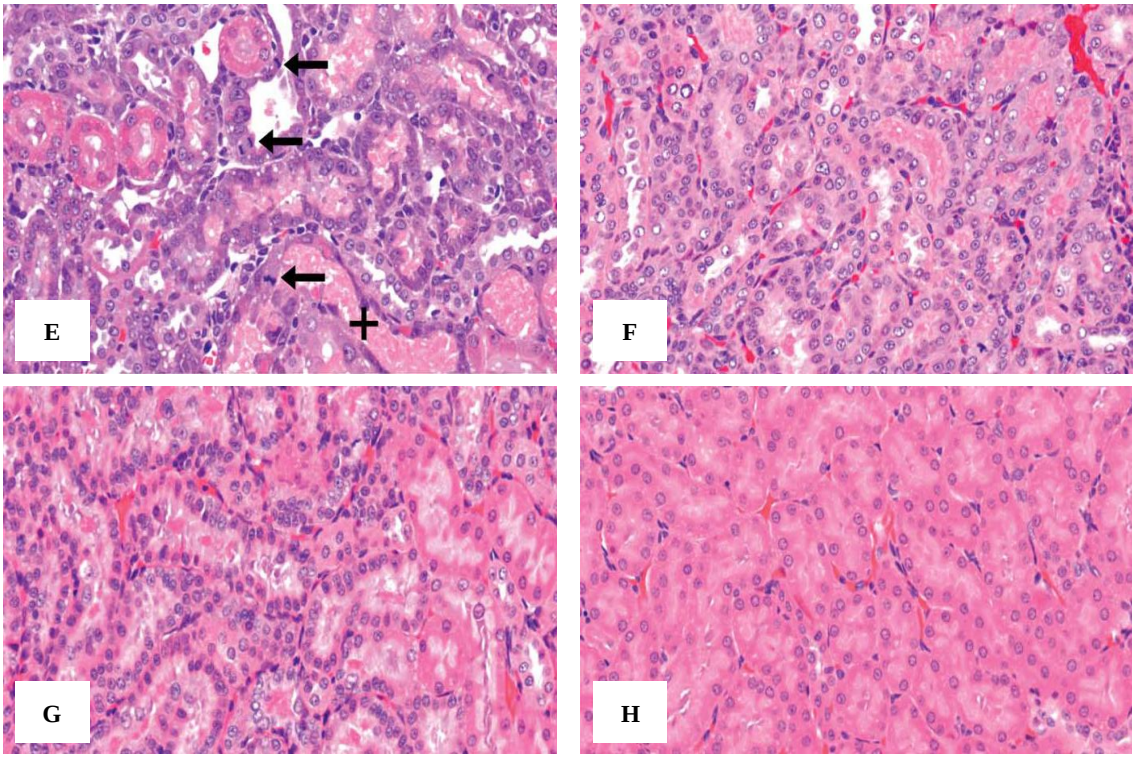

Figure 4.6 Histology of renal cortex sections from male Hanover-Wistar rats treated with a single dose of vehicle (control) or HCBD at 45 mg/kg and sampled at various time points. Original magnification of all images, x 200; H&E. Animals were dosed on day 0 and autopsied at several time points following treatment. Rats were dosed by intraperitoneal injection and autopsied at various time points post-dosing. At autopsy kidney samples were collected and processed for histopathological examination as described in Section 2.8. (A) control rat at day 1; (B) HCBD-treated day 1: tubular degeneration and hypereosinophilia (*); (C) HCBD-treated day 2: degeneration (*) and areas of regeneration (†); (D) HCBD-treated day 3: focal areas of degeneration (*); (E) HCBD-treated day 4: marked regeneration with the majority of tubules displaying increased basophilia, increased nuclear and cellular size, mitotic figures (arrows) and eosinophilic proteinaceous debris in the tubule lamina (+); (F) HCBD-treated day 5: continued regeneration; (G) HCBD-treated day 6: less evidence of regeneration; (H) HCBD-treated day 10: normal appearance of renal medulla.

4.5 Discussion

The first objective of the dose response study presented in this Chapter was to define a dose level of HCBD that induced nephrotoxicity in the male Hanover-Wistar rat and use this in a second experiment, a time course study, to evaluate the sensitivity of a range of urinary biomarkers for kidney injury.

In the dose response study animals were dosed with HCBD at dose levels ranging from 5 to 90 mg/kg.

HCBD undergoes primary metabolism in the liver to form a glutathione conjugate prior to secondary metabolism in the kidney. The kidneys are the main target organ for HCBD-induced toxicity, however, it has been reported that the liver also has the enzyme cysteine β-lyase, and therefore, is capable of producing the toxic compound responsible for HCBD-induced toxicity (Tateishi et al., 1978; Stevens, 1985a; Stevens, 1985b). Therefore, in the present studies, great importance was given to guarantee that the liver did not show evidence of an HCBD-induced toxic effect.

In this dose response study, relative liver weights, as recorded at autopsy, were significantly increased over controls at the highest HCBD dose level, but were similar to controls at all other dose levels (Figure 4.1 A). In a previous study by Lock et al., (1981) male rats administered with a single i.p. injection of 300 mg/kg HCBD had heavier livers than control animals and this was associated with an increase in the liver water content. Similar results were reported in another study by Lock and co-workers (1985) when male Alderley Park mice were administered with HCBD at 100 and 200 mg/kg. Liver weights were increased at 24 hours post-dosing which was accompanied by an increase in the liver water content. Histological evaluation of the liver revealed cytoplasmic vacuolation of the periportal hepatocytes.

Serum ALT, AST and GLDH activity were measured as indicators of hepatic injury, however, the only changes were an increase in ALT and GLDH at the highest dose level (90 mg/kg HCBD) (Figure 4.2). In the study by Lock and colleagues (1985), a significant increase in ALT activity was reported at 4 and 8 hours following administration of 50 mg/kg HCBD to mice but by 16 hours post-dosing levels had returned to normal. These were also the time points when the first ultrastructural changes were reported in the liver which consisted of disorganisation and swelling of

the rough endoplasmic reticulum particularly in the centrilobular hepatocytes (4 hours post-dosing). At 8 hours post-dosing there was evidence of mitochondrial swelling in periportal hepatocytes whereas at 16 hours after HCBD administration there was mitochondrial swelling and proliferation of smooth endoplasmic reticulum in periportal hepatocytes. However, in the present study, no evidence was found of an HCBD-induced toxic effect in the liver at any of the dose levels used.

Gene expression data analysis of the liver (Table 4.4) revealed significant upregulation of all genes involved in xenobiotic metabolism at the lowest dose level (5 mg/kg), except for ABCC3, CYP1A1 and NQO1. EPHX1, GSTM4 and GSTA3 mRNA levels were significantly increased following the administration of HCBD (1.8-, 1.4- and 2.8-fold respectively). NQO1 mRNA was 2.1-fold upregulated over controls but this change was not statistically significant. Epoxides react with nucleophilic molecules such as DNA, RNA and proteins and the enzyme epoxide hydrolase (EPHX1) converts the epoxide into a more excretable molecule (Archer, 1997). NQO1 is induced by oxidative stress and combats oxidative stress by catalysing the conversion of quinone to hydroquinone suppressing the formation of the reactive hemiquinone (Nioi and Hayes, 2004). GSTs are enzymes involved in the first step of the metabolism of HCBD, which involves the conjugation of reduced glutathione to organic molecules during the detoxification process which occurs in the liver (Mannervik et al., 1985). Therefore, the increase in gene expression reflects the increased xenobiotic metabolising activity of the liver in the presence of HCBD.

In the category of oxidative stress, the first genes to show evidence of statistically significant upregulation were GLCL, GSR and TXRND1 with an average 1.3-fold increase in mRNA levels over control values (Table 4.4). HMOX1 upregulation did not occur at the lower dose levels but expression was maximal at 30 mg/kg HCBD. At this dose level HMOX1 mRNA was found to be upregulated to approximately 4.5-fold.

Inflammatory and regeneration/repair gene expression changes in the liver did not show evidence of a dose-related effect. Thus, gene expression changes in the liver reflect the primary metabolism of HCBD prior to the production of a toxic metabolite in the kidney (Table 4.4).

Histopathological examination of the liver sections from this study confirmed the absence of morphologic changes consistent with HCBD-administration at any dose level.

In the current dose response study the relative kidney weights were approximately 1.2-fold increased over control animals at the highest HCBD dose level (Figure 4.1 B). Lock and colleagues (1981) also reported a significant increase in the relative kidney weight at 24 hours following the administration of a single dose of 300 mg/kg HCBD. Lock et al., (1981) suggested the increased weight was associated with an increase in tissue water content. In another study, 28 and 63 day old male and female rats were administered with a single dose of HCBD at 25, 50 and 100 mg/kg and the relative kidney weights were shown to be significantly increased over controls (Kuo and Hook, 1983). In our study we did not see an increase in kidney weights below 90 mg/kg.

Routine clinical chemistry revealed significant increases in serum creatinine and urea levels following the administration of HCBD at 45 and 90 mg/kg ($^{**}P<0.01$ and $^{***}P<0.001$, respectively) (Table 4.2); this suggests the presence of kidney injury at these dose levels. In another study, Lock and Ishmael (1979) administered HCBD at 100, 200 and 300 mg/kg to male Alderley Park albino rats and found a statistically significant increase in the serum urea concentration. Significant increases in urea and serum creatinine were also reported following a single administration of HCBD at 100 mg/kg to male Wistar rats (Chiusolo et al., 2010). Sedeghnia et al., (2013) described an increase in the mean urea and creatinine serum levels at 24 hours following the administration of 100 mg/kg HCBD to female Wistar rats. The results from our study suggest that serum creatinine and urea may not be very sensitive in response to kidney injury, since they were similar to control levels at the lowest dose levels, and did not appear to correlate with the histopathology data which showed evidence of degeneration following administration of 10 mg/kg HCBD and above.

Urinary levels of the cytosolic enzymes α-GST and GST Yb1 were significantly raised over control animals at 20 and 10 mg/kg HCBD, respectively (Table 4.3). There also appeared to be a dose-dependent relationship, with a 33.4- and a 2.08-fold increase for α-GST (at 20 mg/kg) and GST Yb1 (at 10 mg/kg) over controls, respectively (Table 4.3). Pinches et al. (2012) measured urinary biomarker levels following a single dose of 0.1, 1 or 2.5 mg/kg cisplatin to male and female Hanover-Wistar rats. They found that α-GST and GST Yb1 did not appear to be more sensitive than traditional markers such

as serum urea and creatinine. The results also indicated that increases in α-GST may be influenced by the sex of the animals (Pinches et al., 2012).

The increase in urinary α-GST and GST Yb1 following renal injury is due to cellular damage resulting in the enzymes being released from tubular epithelial cells and into the tubular lumen (Harrison et al., 1989). α-GST is located in the epithelial cells of the proximal renal tubules, whereas GST Yb1 can be predominantly found in the epithelial cells of the distal renal tubules (Rozell et al., 1993; Otieno et al., 1997). However, in this study, histological examination revealed HCBD-induced injury mainly to the S3 segment of the proximal tubule (Figure 4.3). Additionally, it is thought that there was some degree of cross-reactivity in the GST Yb1 assay with α-GST due to a lack of antibody specificity, particularly at dose levels up to 15 mg/kg HCBD. α-GST is known to cross-react with the MSD GST Yb1 assay by 7.22 % (Argutus, 2010). Therefore, increases in the urinary excretion of GST Yb1 should be interpreted with caution.

No evidence of a dose-related effect was recorded for the urinary levels of osteopontin suggesting this to be a less sensitive biomarker. Lipocalin-2 excretion in the urine was not increased in HCBD-treated animals at any HCBD dose levels (at 30 mg/kg HCBD there was a significant decrease) (Table 4.3). In a previous study by Swain et al., (2011), with female rats dosed with HCBD at 0, 90 and 135 mg/kg, urinary lipocalin-2 was found to be significantly increased over controls at both HCBD dose levels. However, these dose levels were greater than the HCBD concentrations administered in our current dose response study and this may account for the differences in urinary levels of lipocalin-2. The usefulness and specificity of lipocalin-2 as a urinary marker for renal damage may be compromised by the fact that this protein is released by the liver in response to inflammation (Liu and Nilsen-Hamilton, 1995) and has been previously shown to be increased following CCl_4-induced liver toxicity (Smyth et al., 2009b; Borkham-Kamphorst et al., 2013).

Urinary β-HBA levels were significantly increased over controls at 10 mg/kg HCBD (3.3-fold) and remained elevated at all other HCBD dose levels, peaking at 90 mg/kg HCBD (31-fold increase, $^{***}P<0.001$) (Table 4.3). β-HBA is a ketone body which is produced in the liver, mainly from fatty acid metabolism. Increased levels of β-HBA have been previously reported in the urine of rats following administration of 100 mg/kg HCBD (Berndt and Mehendale, 1979; Davis et al., 1980). Gartland et al, (1989) investigated the effect on β-HBA urinary levels following the administration of 3

nephrotoxicant agents, including HCBD. The increase in β-HBA levels was only observed after HCBD administration. In the present study, acetoacetate urinary levels were significantly increased over controls at 35 mg/kg HCBD and there appeared to be a dose-related increase (Table 4.3); acetoacetate is also a ketone body. Increased urinary levels of ketone bodies generally indicate a state of diabetic ketoacidosis.

HCBD has also been previously shown to cause lactic aciduria. This may occur as a consequence of damage to the proximal tubules which may result in decreased reabsorption of lactic acid in this segment of the kidneys (Hohmann et al., 1974; Gartland et al., 1989). A study by Xu et al., (2008) revealed that administration of cisplatin and gentamicin also resulted in an increase in urinary levels of β-HBA and acetoacetate. The authors suggest that the lactic aciduria and ketonuria observed may be a consequence of a reduction in the number of functional tubule transporters in kidney cells rather than a perturbation of the metabolic pathway. We, therefore, hypothesise that the mechanism for ketonuria observed in this study, may be due to a HCBD-induced reduction in the number of membrane transporters in the proximal tubule.

Creatinine was the most sensitive of the traditional urinary markers of kidney injury. Urinary creatinine was significantly decreased compared to control rats at the highest HCBD dose level (90 mg/kg) (Table 4.3; $^{***}P<0.001$). In acute kidney injury, the glomerular filtration rate will be reduced, resulting in a decrease in the creatinine clearance and consequently, in reduced urinary creatinine levels (Mitch and Walser, 1978). Decreased urinary creatinine has been previously reported following the administration of 10 mg/kg cisplatin to rodents (Bulacio and Torres, 2013).

Urinary glucose levels were only significantly increased over control at 40 mg/kg HCBD (approximate 20-fold increase; $^{***}P<0.001$). Glucose is not normally found in urine so the presence of glucose suggests a reduced tubular function (Wolf et al., 2009; Swain et al., 2011). In a previous study investigating the effect of HCBD in female rats, urinary glucose was found to be significantly increased over control levels at 90 (218-fold increase) and 135 mg/kg (210-fold increase) (Swain et al., 2011). Berndt et al., (1979) also reported increased urinary glucose levels following the administration of 100 mg/kg HCBD to male Sprague-Dawley rats.

Urinary clusterin was only significantly increased over controls at the highest dose level (90 mg/kg HCBD), whereas KIM-1 urinary levels were significantly increased over

controls at dose levels of 20 mg/kg HCBD (2.6- fold increase; $^{**}P<0.01$) and above ($^{***}P<0.001$) (Table 4.3). Increased urinary levels of clusterin and KIM-1 were also reported by Swain and colleagues following HCBD-induced acute nephrotoxicity (Swain et al., 2011). Clusterin had a molecular weight of 76-80 kDa and has been described as having anti-apoptotic functions, however, the exact mechanism is still unknown (Rosenberg and Silkensen, 1995). Appearance of clusterin in the urine has been shown to be accompanied by renal damage (Dieterle et al., 2010).

KIM-1 is predominantly found in proximal epithelial cells of the S3 segment and is considered to be involved in the phagocytosis of apoptotic cells in the renal tubular lumen (Ichimura et al., 2008). Increased urinary KIM-1 has been reported following exposure to several nephrotoxicants, including folic acid and cisplatin (Ichimura et al., 2004; Vaidya et al., 2006). In a study by Vaidya et al. (2010) KIM-1 was shown to be increased in the urine as early as 3 hours after renal injury was induced suggesting it to be a sensitive marker.

The first significant change in mean total protein levels in the urine was detected at 15 mg/kg HCBD when an approximate 2-fold increase over controls was observed ($^{*}P<0.05$). Proteinuria is often used as a marker of nephropathy as kidney injury may lead to renal failure resulting in increased protein levels in the urine (Shihabi et al., 1991). Increased urinary total protein was previously reported following HCBD administration to rats (Berndt and Mehendale, 1979; Swain et al., 2011).

Urinary albumin was 4.3-fold increased over controls at 20 mg/kg HCBD ($^{*}P<0.05$) (Table 4.3). Urinary albumin is considered to be a marker of both proximal tubular function and glomerular integrity (Swain et al., 2011). Albumin that is filtered from the blood is almost completely reabsorbed by the proximal tubule (Lazzara and Deen, 2007). Therefore, injury to the proximal tubules may result in albuminuria. Increased urinary albumin levels were reported by Swain and colleagues (2011) in a model of HCBD-induced renal damage.

The results of the present dose response study suggest the most sensitive urinary biomarker of HCBD-induced injury to be β-HBA and GST Yb1 (significantly increased at 10 mg/kg HCBD), followed by α-GST (significantly increased at 20 mg/kg HCBD). At 10 mg/kg HCBD, GST Yb1 was 2-fold increased over control whereas the increase for α-GST was 4-fold. However, due to a great standard deviation in the groups the

increase in α-GST urinary levels was not enough to show statistical significance. Additionally, the results from GST Yb1 may be due to a cross reaction with α-GST as discussed previously, and therefore should be interpreted with caution. The changes in β-HBA levels are thought to be a HCBD-specific nephrotoxic effect and therefore may not be useful for evaluating any potential CCl_4-induced nephrotoxicity in our future studies.

Gene expression analysis was carried out on the kidney samples in this study (Table 4.5). Changes to genes involved in xenobiotic metabolism and oxidative stress were seen at the lowest dose level. NQO1 mRNA expression showed the greatest fold change at 5 mg/kg HCBD which corresponded to a 6.4-fold increased compared to controls. NQO1 is an enzyme that is induced by oxidative stress and has been shown to be upregulated following the induction of renal toxicity (Nioi and Hayes, 2004, Zhu et al., 2008). In a previously reported dose response study, NQO1 was also found to be significantly upregulated in the kidney following the administration of 90 and 135 mg/kg HCBD to female Hanover-Wistar rats (Swain et al., 2011). The upregulation in NQO1 levels appears to be related to the mechanism of action for HCBD which involves the production of reactive oxygen species following activation by β-lyase (Scatena et al., 2007). GSTA3 and GSTM4 were significantly upregulated at 5 and 10 mg/kg HCBD. In a previous study by Swain et al., (2011) in female rats, both GSTM4 and GSTA3 mRNA levels were significantly upregulated following the administration of 90 mg/kg HCBD (3.7 and 2.5-fold respectively).

In the oxidative stress functional category, the greatest change in gene expression in the kidney was noted for HMOX1. The first significant change was present at 5 mg/kg HCBD and there was evidence of a clear dose-related increase in mRNA levels. HMOX1 is located in the proximal and distal tubules of the rat kidney (da Silva et al., 2001) and is involved in protecting the kidneys against oxidative stress. HMOXI also acts to degrade the heme derived from haemoglobin and cytochrome molecules resulting in the production of bilirubin which has antioxidant properties via the scavenging of reactive oxygen species (Abraham and Kappas, 2005). Previous studies have shown that the metabolite formed by cysteine β-lyase in the kidneys has the ability to interact with components of the inner mitochondrial membrane causing uncoupling of oxidative phosphorylation (Wallin et al., 1987). This leads to the generation of

reactive oxygen species which will be responsible for the increase in oxidative stress (Wallace, 1999).

Changes in the expression of genes involved in the inflammation process were only present at the highest dose level (90 mg/kg HCBD) suggesting a lack of inflammatory response following HCBD administration.

In this study, the most sensitive gene for HCBD-induced kidney injury was KIM-1; the expression of KIM-1 was significantly upregulated at 5 mg/kg HCBD ($^{*}P<0.05$) and there was evidence of a dose-dependent increase. The greatest fold increase was also seen for KIM-1 expression and corresponded to a 423-fold increase over controls at the highest dose level (90 mg/kg HCBD). A previous study in male rats treated with different nephrotoxicant agents: chromate (S1-S2 segment specific), cephaloridine (S2 segment specific) and HCBD (S3 segment specific), revealed significant upregulation of KIM-1 expression in toxin-treated rats (Chiusolo et al., 2010).

Histopathological examination of the kidneys revealed the presence of HCBD treatment-related findings in the treated animals consistent with injury to the S3 segment of the nephron (Table 4.6). Evidence of degeneration was present at 10 mg/kg HCBD; this was also the first dose level at which the urinary biomarkers measured were significantly increased over control (Table 4.3). At 10 mg/kg there was minimal degeneration of individual cells followed by increased severity of degenerative changes with increasing HCBD dose level. Degenerating cells showed an irregular outline, condensed cytoplasm with swollen mitochondria; the nuclear outline was also irregular and in some cells the nucleus was pyknotic. These observations are in agreement with the findings described in the literature for HCBD-induced tubular degeneration (Ishmael et al., 1982). This dose-related response was also apparent in the urinary biomarkers, for e.g., α-GST and β-HBA. Histopathologically, there was an increase in the number of hyaline droplets present in the convoluted tubules proximal to the S3 segment at 5 mg/kg HCBD, and both the number of droplets and the number of animals affected appeared to increase with increasing dose level of HCBD. Therefore, hyaline droplet accumulation was detected at a lower dose level than the first signs of degeneration and also changes to the urinary biomarkers (10 mg/kg HCBD). However, KIM-1 gene expression was upregulated at 5 mg/kg. Hyaline droplet accumulation has been reported by several authors following HCBD administration (Bouthillier et al., 1991; Pahler et al., 1997; Cristofori et al., 2013).

Hyaline droplets are frequently observed in the proximal renal tubules of male rats (Swenberg, 1993). The development of these hyaline droplets is related to the presence of α-2μ globulin which is synthesised in the liver of the male rat, secreted into the plasma and filtered by the glomerulus and is subject to androgenic control (Roy et al., 1966; Pahler et al., 1997; Hard, 2008; Swain et al., 2011). Approximately 50 % of the α-2μ globulin that is present in the glomerular filtrate is reabsorbed in the proximal tubule and the remaining α-2μ globulin is excreted in the urine (Swenberg, 1993). This reabsorption occurs by endocytosis followed by hydrolytic digestion inside lysosomes (Swenberg, 1993). Accumulation of hyaline droplets is the first step in α-2μ globulin nephropathy (Cristofori et al., 2013). The lesion begins with individual cell necrosis and the formation of granular casts and may progress to renal tumour (Swenberg, 1993; Cristofori et al., 2013). HCBD has been shown to bind to α-2μ globulin, therefore, inhibiting its degradation in the lysosomes, which then leads to degeneration and cell necrosis (Lehman-McKeeman et al., 1990).

In the current dose response study, we wished to evaluate a panel of urinary and gene expression biomarkers with regards to sensitivity. The purpose of this study was to identify the most sensitive kidney biomarkers. At higher dose levels, CCl_4 is known to induce nephrotoxicity and the effect on the kidney after chronic dosing is not well documented, thus we wished to determine the most ideal and sensitive kidney biomarkers to use in our future studies so that we can rule out CCl_4-induced nephrotoxicity. The results of the dose response study suggest that the most sensitive urinary biomarkers are α-GST and albumin (significantly increased at 20 mg/kg and displaying the greatest fold changes), followed by KIM-1. KIM-1 gene expression was upregulated at the lowest dose level suggesting this to be the most sensitive marker from invasive sample collection.

In this Chapter, we chose 45 mg/kg as the dose level to use for our time course study since in the dose response study histopathological proximal tubular degeneration was present in animals treated with HCBD at this dose level. Histopathological examination of the livers revealed no changes consistent with HCBD-induced hepatotoxicity at any of the dose levels used in the dose response study. However, relative liver weights were significantly increased after administration of HCBD at 90 mg/kg (Figure 4.1 A) and serum ALT and GLDH were also significantly increased over control at the highest dose level (Figure 4.2).

In the time course study, 6 out of 60 animals, did not appear to respond to HCBD treatment and there was no evidence of injury to the proximal tubules, therefore, data from these animals was excluded from analysis. Mis-dosing of animals via the i.p. route has been previously documented and may account for a 11 to 20 % failure rate (Lewis et al., 1966).

At autopsy, liver weights from HCBD-treated animals were significantly increased over controls from day 1 to day 4 post-dosing (Figure 4.4 A). Lock et al. (1982) reported a significant increase in the relative liver weight of HCBD-treated animals at 300 mg/kg within 24 hours of dosing, which was associated with an increase in the liver water content. However, Kuo and Hook (1983) described no change to liver weight following the administration of 25, 50 and 100 mg/kg HCBD.

GLDH was the only serum enzyme to be significantly increased over controls (days 2 and 3) (Figure 4.5 C) and histopathological examination of the liver revealed no structural changes. These results suggest the absence of a HCBD-induced injury to the liver.

The same urinary biomarkers that were measured in the dose response study were evaluated in this time course study to record changes with time as renal proximal tubule injury is induced and recovery occurs (Table 4.9, Table 4.10). α-GST and GST Yb1 appeared to be sensitive urinary markers (356.9- and 16.5-fold increased over controls respectively); peaking on day 1 post-dosing and remaining significantly elevated over concurrent controls up to day 4 post-dosing (Table 4.9). In another study by Gautier et al., (2010), urinary excretion of α-GST was increased in animals dosed at 3 mg/kg cisplatin on days 3 and 5 after dosing and correlated well with the histopathology data showing moderate or marked necrosis of the S3 segment. They also found α-GST to be increased over controls to a greater extent and at earlier time points than the other urinary markers tested (serum creatinine, urea, NAG and total protein). Kharasch et al. (1997) also described α-GST as the most sensitive urinary marker of proximal tubular cell necrosis. In the present study, there was a good degree of correlation between urinary α-GST and the histopathology evidence of HCBD-induced nephrotoxicity. Maximum levels of α-GST were present on day 1 post-dosing representing degeneration of the tubules.

Urinary osteopontin was significantly raised over control levels at days 2, 3, 4, 5 and 7 post-dosing (Table 4.9). The fold increase was greatest on day 4 (7-fold) which suggests that osteopontin is a marker of epithelial regeneration since on day 4 post-dosing all animals showed very marked evidence of regeneration. However, the fold changes in this study revealed osteopontin to be less sensitive than KIM-1 as a marker of regeneration. In fact, urinary KIM-1 peaked at day 4 post-dosing at which time point it was 84-fold increased over control (Table 4.9). Also, in the previous dose response study, no changes were recorded for urinary osteopontin at 24 hours post-dosing. This fact adds further evidence that osteopontin is likely to be a marker of regeneration rather than degeneration.

In a study carried out by Pinches et al., (2012) male and female rats were administered a single dose of cisplatin and increased urinary osteopontin was observed on day 5 post-dosing. Osteopontin is expressed in the healthy kidney; reports regarding its localisation are contradictory with some authors reporting that it is normally present at the apical surface of cells in the distal nephron (Verhulst et al., 2002) and others reporting osteopontin to be present in the proximal tubules (Mark et al., 1988). Osteopontin has been shown to be expressed by macrophages. It is involved in cellular functions such as cell adhesion, migration and regulation of inflammatory responses of macrophages, by promoting their migration and retention at sites of acute and chronic inflammation (Lund et al., 2009). However, in the present study histopathological examination revealed injury predominantly to the S3 segment of the proximal tubules and therefore, we suggest that the increase in urinary osteopontin is likely to be mainly due to release from proximal tubular cells. The association of osteopontin with regeneration of tubular cells has been previously described by Xie et al. (2001a) following the administration of gentamicin. The mechanism is not yet fully described but it appears that osteopontin has the ability to interact with CD44 which is a widely distributed cell receptor and is thought to interact with hyaluronic acid. By interacting with CD44, osteopontin blocks the binding site for hyaluronic acid and therefore blocks its inhibition of cell growth and differentiation (Xie et al., 2001a). Persy and colleagues (1999) also reported an association between osteopontin staining in the proximal tubules and evidence of morphologic regeneration. During the period of tubular injury the authors observed loss of brush border of tubular cells. During regeneration, however, the tubular basement membrane became lined with a flat epithelium and there was restoration of the brush border by tubular cells (Persy et al., 1999).

Lipocalin-2 excretion in the urine was not significantly increased following treatment with HCBD at 45 mg/kg at any time point (Table 4.9). However, analysis of the gene expression data, revealed LCN-2 mRNA in the kidney to be significantly upregulated on days 2 to 5, 7 and 14 post-dosing (Table 4.11). In the dose response study in this Chapter there was no evidence of an effect on the urinary lipocalin-2 levels with HCBD administration. However, others have reported significant increases to urinary lipocalin-2 in response to kidney injury. Swain et al., (2011) reported increases to urinary lipocalin-2, 24 hours after a single dose of 120 mg/kg HCBD to female rats, whereas in a study in mice (Mishra et al., 2004) urinary levels of lipocalin-2 increased with time following the administration of 20 mg/kg and were maximal at 48 hours post-dosing.

In the dose response study described in this Chapter, urinary creatinine was significantly increased over control at 10 mg/kg HCBD and then at dose levels above 20 mg/kg HCBD urinary creatinine appeared to decrease with increasing dose level (Table 4.3). In this time course study there was no effect on urinary creatinine levels suggesting this to be an insensitive unreliable marker of nephrotoxicity.

Glucose levels in the urine were significantly increased over controls at day 1 and remained elevated until day 4 (Table 4.9). On day 1 post-dosing the fold increase over concurrent controls was approximately 30, but maximal levels were reached on day 2 post-dosing (170.40 µmol/c.p. compared to 3.33 µmol/c.p. for control animals, which corresponded to a 51.2-fold increase). Pinches et al., (2012) also reported significant increases in urinary glucose following the administration of cisplatin and found good correlation between increased levels of glucose in the urine and the degree of proximal tubular necrosis. However, in the dose response study, there was no evidence of an HCBD effect on glucose levels in the urine at dose levels below 45 mg/kg (Table 4.3). Therefore, it could be suggested that the increase in urinary glucose may be the result of loss of functional capacity of the kidneys, as a result of more severe injury.

Urinary clusterin levels were highest on day 4 and 5 post-dosing. At these time points mean levels were 6.5- and 3.8-fold increased over concurrent controls (Table 4.10). Another research group has reported increases in urinary clusterin in Hanover-Wistar rats at days 3 and 5 following cisplatin-induced nephrotoxicity (Gautier et al., 2010). The temporal pattern for clusterin may therefore reflect its antiapoptotic properties (Rosenberg and Silkensen, 1995). It has been suggested that clusterin may be induced to promote cell interactions since one of the first steps in the apoptotic pathway is loss of

cell contacts (Rosenberg and Silkensen, 1995). Hidaka et al. (2002) reported that clusterin reaches maximum concentration 2 days after an ischemic insult. The S3 segment is the portion of the nephron most susceptible to ischemia, and the authors of this study suggested that the majority of the clusterin detected in the urine comes from the cellular debris in the S3 segment of the proximal tubule. Dieterle et al., (2010) have also described a good degree of correlation between urinary clusterin levels and proximal tubular injury. In the present study, we also consider the source of clusterin to be the proximal renal tubular epithelium.

KIM-1 urinary excretion was significantly increased on day 1 post-dosing, with a 7-fold increase over controls ($^{***}P<0.001$) and mean levels remained significantly elevated up to day 7 post-dosing (Table 4.10). However, the greatest fold increase was noted on day 4 post-dosing (83.8-fold; $^{***}P<0.001$), which was the time point when histopathology examination revealed very marked evidence of regeneration in 6 out of 6 HCBD-treated animals. Swain et al., (2011) dosed female rats with 120 mg/kg HCBD and sampled at various time points. Urinary KIM-1 was significantly increased over controls on day 1 post-dosing (7-fold increase) but the greatest fold change was seen on day 4 following HCBD treatment when a 33-fold increase was recorded. In a study by Vaidya et al., (2010) urinary KIM-1 levels were increased as early as 3 hours in a model of kidney tubular damage. These studies suggest KIM-1 to be a sensitive urinary marker to both tubular degeneration and the regeneration/recovery period.

Mean albumin levels in the urine were significantly increased over controls at day 1 (156-fold) and remained elevated until day 5, respectively (Table 4.10). This suggests albumin is a sensitive and specific marker for detection of early stages of renal injury and this correlated well with the histopathology showing injury at these time points.

Gene expression analysis revealed upregulation of several genes involved in the metabolism of xenobiotics and oxidative stress, particularly on day 1 post-dosing (Table 4.11). These include the increased expression of NQO1 (detoxification gene). NQO1 is a gene that encodes a cytosolic flavoenzyme which plays a role in the mechanism of defence by preventing the production of reactive oxygen species (Ross, 2004; Vasiliou et al., 2006). The expression of the NQO1 is increased by oxidative stress (Nioi and Hayes, 2004) and it has been detected at high concentrations in the rat liver (Sharkis and Swenson, 1989). NQO1 protects the kidneys from both oxidative and inflammatory stress (Bolati et al., 2013). The mechanism for HCBD-induced injury involves the

formation of reactive thiols after activation by the enzyme β-lyase, thus causing oxidative stress (Scatena et al., 2007). In experiment 1 (dose response study) levels of NQO1 were upregulated at an HCBD dose level of 5 mg/kg and NQO1 has been previously reported to be upregulated following 1,2-dithiole-3-thione-induced renal injury (Zhu et al., 2008). NQO1 appears to be a sensitive marker for early signs of kidney injury. EPHX1 expression was maximal on day 1 post-dosing in the current time course study (14-fold upregulated when compared to concurrent controls). This result compares to the previous dose response study, where a 10-fold upregulation was noted over control animals. Epoxide hydrolases are predominantly found in the liver, kidney and testes. Epoxides can be formed by action of cytochrome P-450 and have the ability to bind to macromolecules such as DNA, RNA and proteins and are thought to be responsible to the carcinogenic properties of many compounds. Epoxide hydrolases act by converting the epoxides into more excretable forms (Archer, 1997).

Cytochrome P450 2C was downregulated from day 1 to day 5 post-dosing; this gene was also downregulated in experiment 1. Zordoki et al., (2011) found the expression of cytochrome P-450 2C to be decreased in the male rat kidney following the induction of injury by doxorubicin. Doxorubicin is known to cause nephrotoxicity by increasing capillary permeability and glomerular atrophy (Zordoky et al., 2011).

HMOX1 was increased in expression by 48-fold on day 1 and was significantly increased until day 4 post-dosing. HMOX1 is involved in protecting the kidneys against oxidative stress by the production of bilirubin which has anti-inflammatory properties (Abraham and Kappas, 2005). HMOX1 has been previously reported to be upregulated following the induction of kidney injury (Nath, 2006; Takahashi et al., 2004). In a study by Rokushima et al. (2008) cephaloridine was administered to male rats to induce kidney injury. This group found HMOX1 to be upregulated at 24 hours following treatment and the authors suggested HMOX1 as a potential nephrotoxicity biomarker. In the dose response study described earlier in this Chapter, HMOX1 expression was upregulated at a dose level of 5 mg/kg HCBD and above, but this upregulation was only statistically significant at 30 and 90 mg/kg HCBD. Other genes in this category for which mRNA expression was upregulated include GSR and TXNRD1. Overall, these changes reflect the mechanism for HCBD-induced injury.

Lipocalin-2 mRNA levels (functional category of inflammation) were upregulated from day 2 to 5, and on day 7 and 14 post-dosing. However, no correlation was apparent with urinary biomarker levels.

In the category of regeneration and repair, upregulation of gene transcription was seen for all genes, except GPNMB, as early as day 1 post-dosing. This preceded the first pathological sign of regeneration which were only noted on day 2 post-dosing and were maximal at day 4. KIM-1 mRNA expression was increased from day 1 to 5 and on day 7 and 10, and was maximal on day 3 post-dosing. This correlated with the urinary changes recorded for KIM-1 for which peak levels were seen at day 4, but remained significantly increased up to and including day 7 post-dosing. It appeared that the upregulation seen in mRNA levels occurred before the highest urinary concentration was recorded.

In the HCBD studies in this Chapter, we were able to characterise a wide panel of serum and urinary markers for injury to the proximal tubule of the kidneys. The changes in biomarker levels were correlated with histopathological evidence of kidney toxicity. In our CCl_4-induced hepatic injury studies we are aware that CCl_4 also causes nephrotoxicity at higher dose levels. Therefore, we need to be able to detect even very low degrees of kidney injury if we are to have confidence that any urinary metabolite markers we identify are a result of hepatic injury and not of both liver and kidney toxicity. The combined interpretation of the data collected from both the dose response and time course study has revealed α-GST and albumin to be the most sensitive urinary biomarkers followed by KIM-1. However, histological evidence of hyaline droplet formation was seen even before changes to urinary markers were reported, at a dose level of 5 mg/kg HCBD. At this dose level gene expression data was more sensitive than any of the urinary markers, however, this data is collected after autopsy and therefore they are not non-invasive markers.

With regards to temporal changes following acute injury it was shown that α-GST, albumin, KIM-1, glucose, clusterin and osteopontin may be reliable markers for proximal tubular injury, degeneration and regeneration to normal function. In terms of gene expression data, NQO1 and HMOX1 showed upregulation in comparison to the concurrent controls and this was associated with proximal tubular injury whereas, KIM-1 and ANXA7 expression coincided with evidence of proximal tubular regeneration.

These markers will be of great use in our future CCl_4 studies and will be used in Chapters 5, 6 and 7.

CHAPTER FIVE

Studies to determine the change in urinary metabolites with increasing age of the male rat; the age at which sexual maturity is reached and comparison of metabolomic changes to the urine following CCl_4-induced hepatic injury in the pre- and post-sexually mature rat

Chapter 5

5.1 Introduction

In our previous liver studies in Chapter 3, we used animals approximately 7 weeks old and consequently developed our hepatic model in animals of this age. However, a number of physiological factors and conditions are known to have an effect on hepatocyte enzyme induction such as the hormonal status, gender, age, nutritional status and infection (Bollard et al., 2005; Maronpot et al., 2010). Age-related differences in susceptibility to drugs and toxicants have been proposed to be due to either toxicokinetic or toxicodynamic processes. This includes differences in absorption, distribution, biotransformation and excretion of xenobiotics, as well as differences in the sensitivity of the affected tissues (Klaassen, 1972; Klaassen, 1973; Birnbaum, 1991). For example, it has been previously reported that the rat liver has increased susceptibility to ethanol toxicity as the animals get older and also that the kidneys from old animals are more sensitive to ischemia than the kidneys from younger animals (Miura et al., 1987; Rikans et al., 1999). Therefore, the age of the animals used in our studies should be carefully considered if these factors are to be taken into account. CCl_4 is metabolised by cytochrome P-450 to the trichloromethyl free radical and if this step is affected by age the induction of hepatic injury will also be affected.

Previous investigative studies have focused on the hepatic expression and activity of cytochrome P-450 enzymes, which in turn is dependent on the development of sexual maturity. In this Chapter we focused on determining the age at which male Hanover-Wistar rats become sexually mature. This information was then used in a comparative study of the effects of a single dose of CCl_4 at 1.2 mL/kg, in 7 week old rats (pre-maturity) and in 13 week old rats (post-maturity).

As mentioned above, the hormonal status of the animal is thought to have an effect on enzyme induction (Marshall and McLean, 1969; Waxman et al., 1985). The animals we used in previous studies were 7 weeks old which is likely to be prior to sexual maturity of the rat. When the male rat becomes sexually mature and thus fully fertile, there will be a dramatic change to the hormone levels, in particular to testosterone levels (Ghanadian et al., 1975; Fujita et al., 1990; Chen et al., 1994). A change in sexual hormone levels is likely to result in changes to the urinary metabolome.

Consequently, in this Chapter we conducted a series of experiments investigating the development of sexual maturity in the male rat, and changes to the urine metabolite profile as the animal ages. Additionally, we determined if animals both pre- and post-sexual maturity have different urinary metabolite profiles following the induction of CCl_4-induced hepatic injury.

5.2 Animal experimental design

In this Chapter, 3 animal studies were carried out: a growth curve study investigating metabolite changes in the rat urine with age, a sexual maturity study, and a CCl_4 comparative study in young and older fertile animals.

5.2.1 Experiment 1: Growth curve study

Twenty male Hanover-Wistar rats (mean body weight 48.0 ± 3.46 g) at 22 days of age were divided into groups of 5 in communal cages with free access to water and diet *ad libitum*. Ten animals were kept in the communal cages throughout the whole study and weighed 3 times a week for a period of 10 weeks. The remaining 10 animals were weighed 3 times a week and metaboled for 24 hour urine collection every two weeks at 26, 40, 54, 68, 84 and 91 days of age with access to water but not diet.

5.2.2 Experiment 2: Sexual maturity study

Thirty six male Hanover-Wistar rats (mean body weight 53.93 ± 6.97 g) were housed in groups of 6 animals. Animals were weighed 3 times a week and autopsied at 24, 33, 52, 63, 77 and 90 days. At autopsy, testes and epididymides were removed and taken into Bouin's fixative and processed as described in Section 2.8.

5.2.3 Experiment 3: Studies comparing the urinary metabolome following CCl_4–induced hepatic toxicity in animals at 7 and 13 weeks of age

The toxicological effects of a single CCl_4 administration were investigated in the male Hanover-Wistar rat at 7 weeks (pre-sexual maturity) and 13 weeks (post-sexual maturity) of age.

For the 7 week old study, 20 male Hanover-Wistar rats (mean body weight 221.7 ± 12.1 g) were divided into 2 groups (n=10) and dosed with CCl_4 by gavage at 0 (controls) and 1.2 mL/kg. Control animals were dosed with equivalent volumes of corn oil. After dosing, animals were returned to their communal cages for 6 hours with access to water and food *ad libitum*. At 6 hours post-dosing they were placed in individual metabolism cages for the collection of 18 hour urine samples (6 to 24 hours post-dosing). While in the metabolism cages animals had access to water but not diet.

A second group of 20 animals at 13 weeks of age were dosed with CCl_4 at 0 (controls) and 1.2 mL/kg. Immediately after dosing, animals (mean body weight 358.6 ± 25.8 g) were placed in metabolism cages for the collection of 24 hour urine samples.

For both groups of animals urine samples were collected over ice and stored at -80 ºC for future analysis. All animals were weighed before dosing, before being placed in metabolism cages and at 24 hours post-dosing, just prior to autopsy.

At autopsy (24 hours after dosing) blood was taken for the preparation of serum which was stored at -80 ºC until analysis. The liver and kidneys were removed and placed in 10.5% (v/v) phosphate buffered formalin fixative and processed as described in Section 2.8.

5.3 Growth curve study

5.3.1 Body weights

Figure 5.1 shows the growth curve of male Hanover-Wistar rats between 3 and 13 weeks of age. Both groups of animals (those in communal cages and those metaboled at regular intervals) gained weight at a steady rate. Rats in the group which were metaboled every 2 weeks lost weight during the 24 hours in metabolism cages (arrows in Figure 5.1 indicate the time points). However, the animals regained this weight shortly after return to communal cages and the overall rate of weight gain was not affected. By the end of the 10 week period both groups of animals had similar body weights (368.68 g and 348.77 g for control and metaboled animals, respectively).

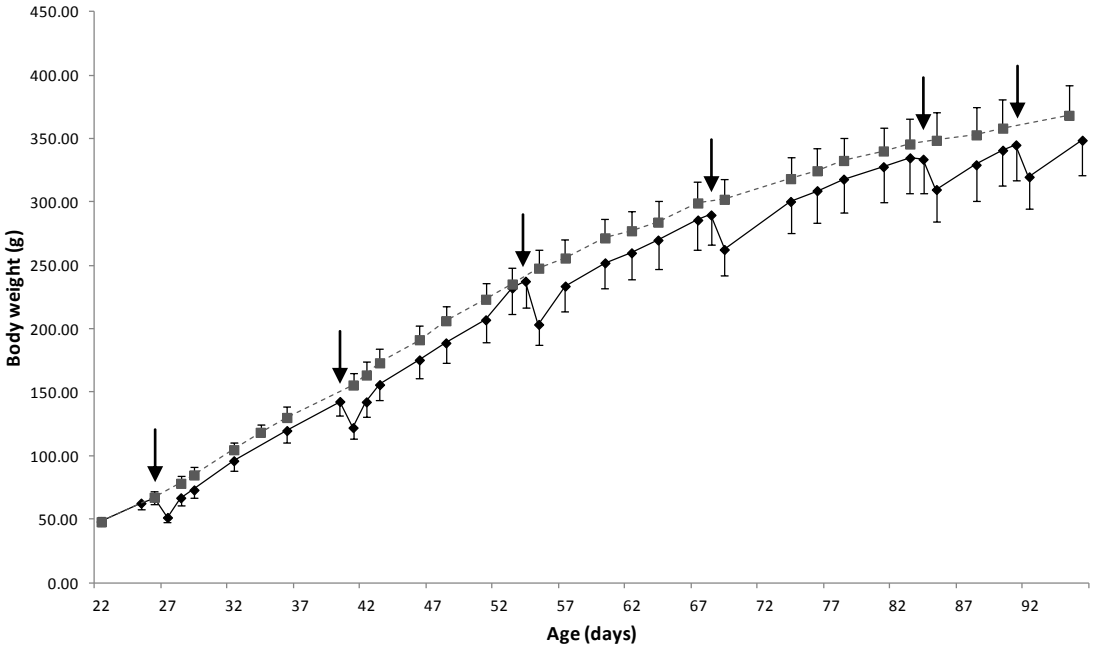

Figure 5.1 Increase in body weight from 3 to 13 weeks of age for Hanover-Wistar rats. Animals (◆) were placed in metabolism cages for 24 hours on 6 occasions (indicated by arrows) and at all other times housed in communal cages as described in Section 5.2.1. Animals represented by (■) were housed in communal cages for the whole study. Values are the means with SD indicated by vertical bars of 10 animals per group.

5.3.2 Urine output and water consumption for animals in metabolism cages

Mean urine output was recorded hourly during each 24 hour period in the metabolism cages (Table 5.1).

Great variation, as shown by the large standard deviations, was noted between the urine volume produced by individual animals and this was consistent throughout the study. The same was observed for water consumption during the same period. There was a tendency for water consumption and urine production to increase with age up until 68 and 84 days old.

Table 5.1 Urine output and water consumption in male Hanover-Wistar rats during a 24 hour period in metabolism cages at different ages. Animals were placed in metabolism cages for 24 hours on 6 occasions (26, 40, 54, 68, 84 and 91 days of age) and at all other times housed in communal cages as described in Section 5.2.1. Urine production and water consumption were measured every hour, starting at 12.00 h. Values are the means and SD of 10 animals per group.

Age (days)	Mean total urine volume (SD) over 24 h (mL)	Mean total water consumption (SD) over 24 h (mL)
26	4.45 (1.97)	8.72 (9.78)
40	12.45 (3.04)	10.55 (4.05)
54	17.06 (4.51)	14.16 (6.06)
68	20.65 (5.40)	12.25 (5.21)
84	19.61 (5.69)	15.34 (5.62)
91	18.96 (7.99)	13.11 (7.43)

5.3.3 Urine clinical chemistry

Urine samples collected during this study were analysed for levels of kidney biomarkers to determine control levels as the animals aged.

Levels of urinary α-GST were significantly increased between 26 and 40 days old ($^{***}P<0.001$), however, there was a very dramatic increase between 54 and 68 days of age (Figure 5.2 A). At 68 days of age the mean value was 910.50 ng/c.p. compared to 56.06 ng/c.p. for 54 day old rats, representing an approximate 16-fold increase ($^{***}P<0.001$). After 68 days, levels decreased slightly but α-GST at 91 days remained over 50-fold greater than urinary levels in 26 days old rats.

Mean urinary GST Yb1 followed the same trend as α-GST. GST Yb1 increased slightly with age in animals up to 54 days old; however, at 68 days old there was a dramatic increase followed by a plateau at 84 and 91 days old. Values for GST Yb1 were 16.41 and 82.24 ng/c.p. for animals at 54 and 68 days of age respectively (5-fold increase; $^{***}P<0.001$) (Figure 5.2 B).

Mean KIM-1 urinary values were significantly increased in 40 and 54 day old rats compared to the respective previous time points ($^{***}P<0.001$) (Table 5.2). The highest measurement was 13.79 ng/c.p. for animals at 54 days old. After day 54, urinary KIM-1 levels appeared to decrease slightly, however, this decrease was not statistically significant. Microalbumin (MALB) and osteopontin both appeared to follow the same trend as KIM-1 and both peaked at 54 days into the study and then showed a decrease with age.

RPA1 and clusterin increased as the animals aged. At 91 days the mean urinary RPA1 value was almost 6-fold greater than at 26 days of age (41.81 ng/c.p. and 7.63 ng/c.p. respectively), whereas clusterin was approximately 5-fold increased in the urine of rats at 91 days old compared to at 26 days old (Table 5.2).

Urinary NAG and lipocalin-2 increased with increasing age and reached maximum levels at 68 days old after which the levels stabilised (Table 5.2). At 68 days mean values were 206.30 mU/c.p. and 4503.31 ng/c.p. for NAG and lipocalin-2, respectively. Creatinine was also measured in the urine of rats during this study. Mean values increased steadily with age and at 91 days urinary creatinine was 8.6-fold greater than at 26 days. However, values were only statistically significant at 40, 54 and 68 days (Table 5.2).

Total protein concentration followed the same trend as α-GST and GST Yb1 (Table 5.2). Mean values increased slightly up to day 54, but a dramatic increase was seen at 68 days. At 84 and 91 days of age a slight decrease was observed. Glucose levels increased with age and peaked in the urine of 91 days old animals.

A

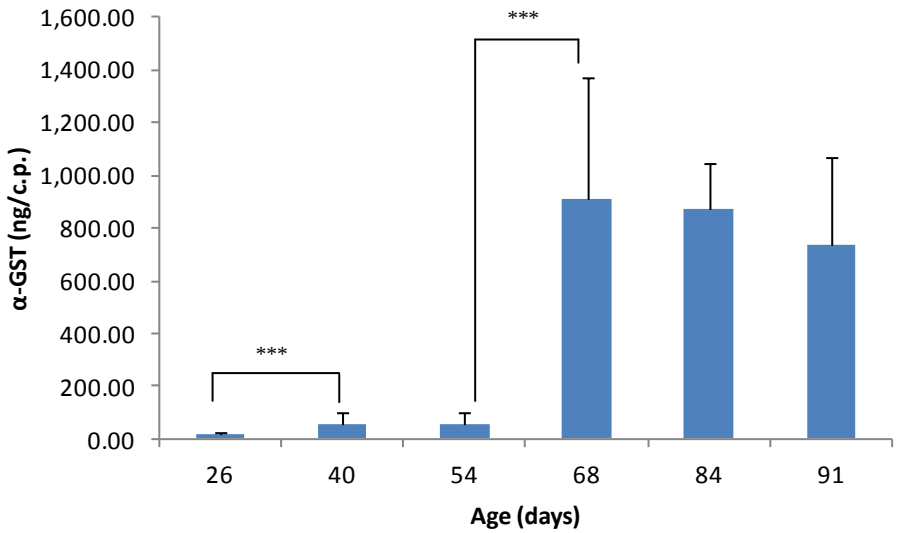

B

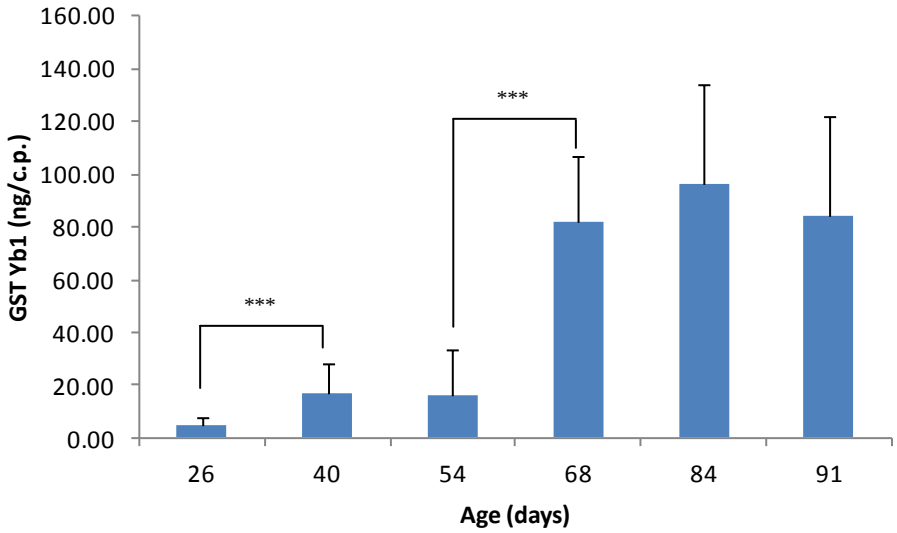

Figure 5.2 Urinary α-GST (A) and GST Yb1 (B) for male Hanover-Wistar rats at different ages. Animals were placed in metabolism cages for 24 hour urine collection on 6 occasions (26, 40, 54, 68, 84 and 91 days of age) and at all other times housed in communal cages as described in Section 5.2.1 Assays were carried out according to the methods described in Section 2.7. Values are means with SD indicated by vertical bars of 10 animals per group. Values that differ significantly from previous time point by Students' t-test are shown: $^{***}P<0.001$.

Table 5.2 Urinary clinical chemistry parameters for male Hanover-Wistar rats at different ages. Animals were placed in metabolism cages for 24 hour urine collection on 6 occasions (26, 40, 54, 68, 84 and 91 days of age) and at all other times housed in communal cages as described in Section 5.2.1. Assays were carried out according to the methods described in Section 2.7. Values are means and SD of 10 animals per group. Values that differ significantly from previous time by Students' t-test are shown: $^{*}P<0.05$; $^{***}P<0.001$.

Urinary parameters	Days of age					
	26	**40**	**54**	**68**	**84**	**91**
KIM-1 (ng/c.p.)	3.86 (1.90)	9.82*** (1.84)	13.79*** (3.05)	12.65 (3.10)	11.05 (2.59)	10.66 (2.76)
MALB (mg/c.p.)	0.09 (0.05)	0.25*** (0.11)	0.35*** (0.13)	0.26* (0.11)	0.23 (0.08)	0.22 (0.08)
Osteopontin (ng/c.p.)	21.62 (12.24)	54.95*** (15.33)	73.01*** (22.07)	53.21* (13.03)	41.48* (9.41)	42.37 (8.28)
RPA1 (ng/c.p.)	7.63 (4.29)	19.66*** (4.96)	26.25*** (7.46)	31.97* (10.75)	40.96** (12.36)	41.81 (12.08)
Clusterin (ng/c.p.)	24.13 (12.78)	63.19*** (17.84)	83.88** (24.91)	109.8* (41.52)	126.14 (59.79)	126.21 (53.19)
NAG (mU/c.p.)	46.70 (20.34)	123.30*** (23.26)	166.50*** (19.17)	206.30* (49.78)	205.10 (36.66)	205.00 (51.44)
Lipocalin-2 (ng/c.p.)	1184.93 (536.19)	3204.46*** (996.43)	4228.15** (1304.66)	4503.31 (1099.70)	4382.22 (1591.45)	4374.74 (2029.94)
Creatinine (µmol/c.p.)	10.60 (4.38)	27.20*** (3.36)	37.70*** (5.27)	78.60*** (16.11)	88.90 (14.81)	91.30 (18.82)
Total protein (mg/c.p.)	0.69 (0.33)	1.79*** (0.45)	2.46*** (0.62)	11.60*** (2.97)	11.14 (4.39)	10.43 (4.88)
Glucose (µmol/c.p.)	1.60 (0.84)	4.00*** (1.05)	5.60*** (1.26)	7.20* (1.99)	7.00 (1.15)	7.20 (1.87)

KIM-1: kidney injury molecule-1; MALB: microalbumin; RPA-1: renal papillary antigen-1; NAG: NAG: N-acetyl-D-glucosamine.

5.3.4 Testosterone levels in urine

Testosterone levels were measured in the urine of rats at 26, 40, 54, 68, 84 and 91 days of age (Figure 5.3). Testosterone is a measure of sexual maturity (Lee et al., 1975). Mean testosterone values at each time point are shown in Figure 5.3. Between days 26 and 54 there was a modest increase in testosterone values (1.89 to 5.93 ng/c.p. respectively) with a significant increase between days 26 and 40 ($^{***}P<0.001$). However, between days 54 and 68 there was an approximate 6-fold increase. Values were further increased between days 68 and 84 (a fold difference of 1.44-fold) to a mean urinary testosterone level of 49.95 ng/c.p. At 91 days old there was a slight non-significant decrease to 45.99 ng/c.p.

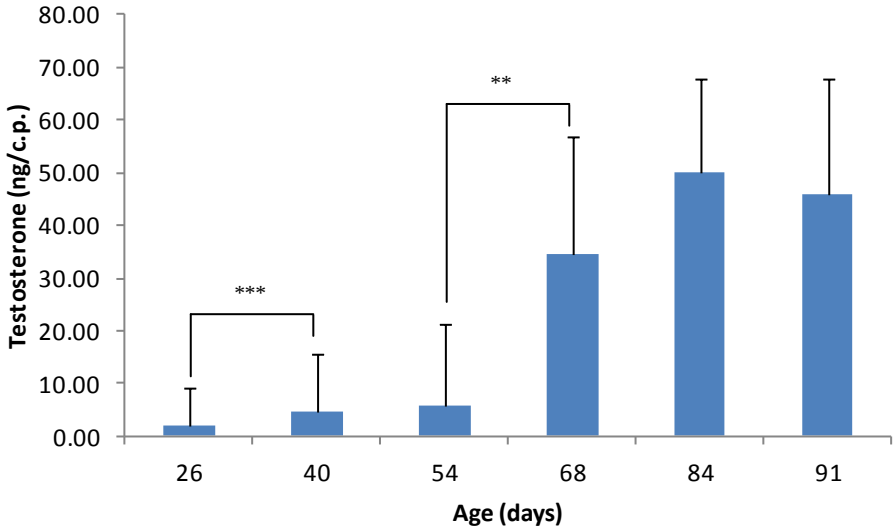

Figure 5.3 Urinary testosterone for male Hanover-Wistar rats at different ages. Animals were placed in metabolism cages for 24 hour urine collection on 6 occasions (26, 40, 54, 68, 84 and 91 days of age) and at all other times housed in communal cages as described in Section 5.2.1. Testosterone assay was carried out according to the methods described in Section 2.7. Values are means with SD indicated by vertical bars of 10 animals per group. Values that differ significantly from previous time point by Students' t-test are shown: $^{**}P<0.01$; $^{***}P<0.001$.

5.3.5 1D ^{1}H NMR spectrometry

Urine samples were collected from 10 male Hanover-Wistar rats at 26, 40, 54, 68, 84 and 91 days of age and prepared as described in Section 2.10 for metabolite analysis by 1D ^{1}H NMR.

A PCA scores plot for these samples is shown in Figure 5.4 A. Outliers in the scores PCA plot and outliers in individual OPLS-DA models (Figure 5.5) were excluded from analysis.

There was a great degree of overlap between samples from animals at 26, 40, 54, 68 and 91 days of age, all located on the left hand side of the plot. However, a separate sample cluster was visible on the right upper quadrant of the scores plot. These spots represented urine samples collected from 84 day old rats. This PCA analysis suggests the presence of age-related urinary metabolite differences in rats at 84 days old compared to the other time points.

The separation of samples from rats at 84 days old from those at other time points was further confirmed by OPLS analysis (Figure 5.4 B). The OPLS demonstrated an age-dependent shift of samples along the discriminating component t[1] to the right hand

side of the scores plot. All samples appeared to follow the shift with time apart from urine samples collected from animals at 84 days of age which occupied a different position on the scores plot.

A

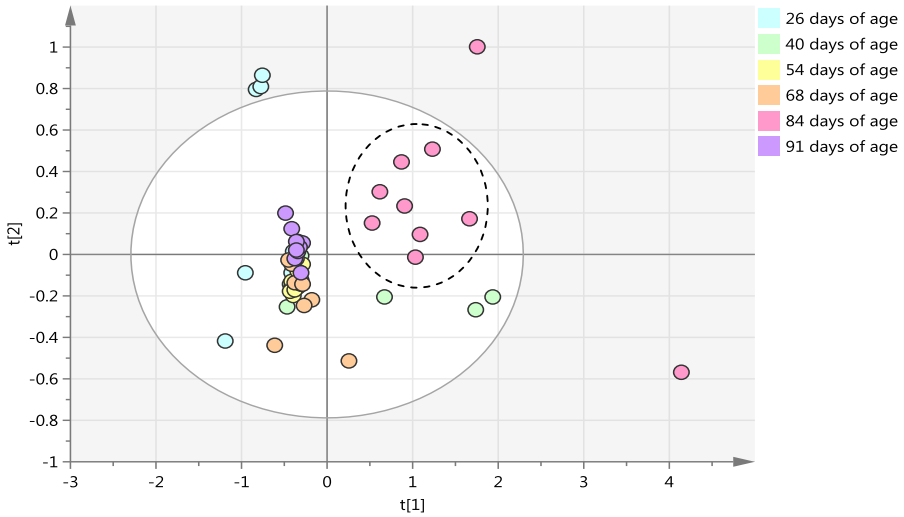

B

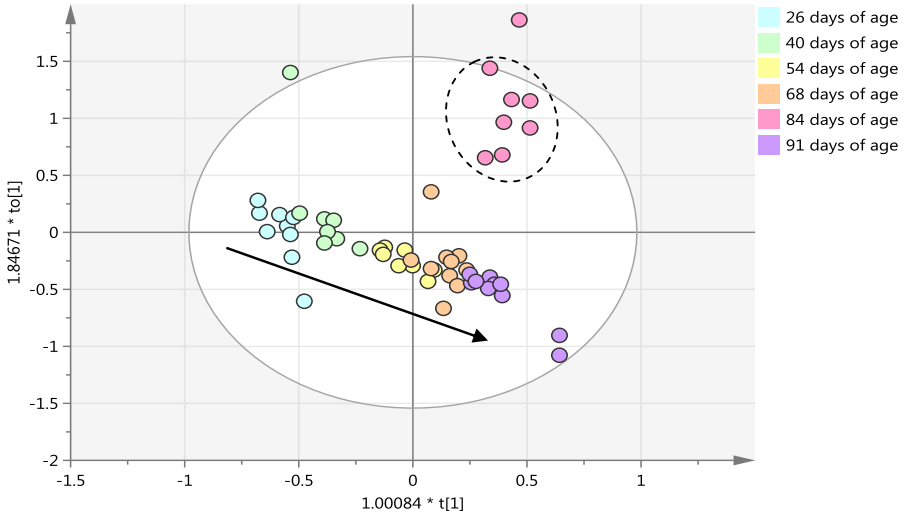

Figure 5.4 PCA scores plot (A) and OPLS scores plot (B) from models derived from 1D ^{1}H NMR spectral data of urine samples from male Hanover-Wistar rats at different ages. Animals were placed in metabolism cages for 24 hour urine collection on 6 occasions (26, 40, 54, 68, 84 and 91 days of age) as described in Section 5.2.1. Each spot in the score plot represents one urine sample. (A) R^2X (cum) = 0.961, Q^2 (cum) = 0.834; (B) R^2X (cum) = 0.821, Q^2 = 0.887. Arrow represents direction of movement. Circled spots correspond to urine samples collected from 84 days old rats.

To further investigate the differences between urine samples collected from animals at consecutive time points, individual OLPS-DA models were performed based on the urine 1D ^{1}H NMR spectra of animals at 26 and 40, 40 and 54, 54 and 68, 68 and 84, and 84 and 91 days old rats (Figure 5.5). In the OPLS-DA scores plot, separation across the discriminating component t[1] relates to changes in metabolite levels between groups due to increasing age of the animals, whereas separation along the orthogonal component relates to changes in metabolite levels within groups, i.e., that are not the result of age differences. Clear cluster separation was observed along the discriminating component t[1] between rats belonging to each 2 consecutive age groups showing a change in metabolites with age.

However, since Figure 5.4 B revealed that urine samples from rats at 84 days old were very different to those at the other time points, further investigation was required to attempt to identify some of the metabolites responsible for this difference. The OPLS-DA scores plots for samples at 68 and 84 days of age (Figure 5.5 D) and 84 and 91 days of age (Figure 5.5 E) show a good separation between samples. The corresponding loadings plots are shown in Figure 5.6 A and B. The chemical shifts that are labelled in the loadings plots were selected based on the combined interpretation of the S-plot and the VIP plot (data not shown) and thought to contribute the most to the separation of samples at 84 days from all other samples. Integrated regions corresponding to these chemical shifts were statistically analysed using a Student's t-test as described in Section 2.11. Chemical shifts and spectral regions were then identified by visual analysis of spectral data, and by comparison with chemical shifts and signal multiplicity described in previously published literature.

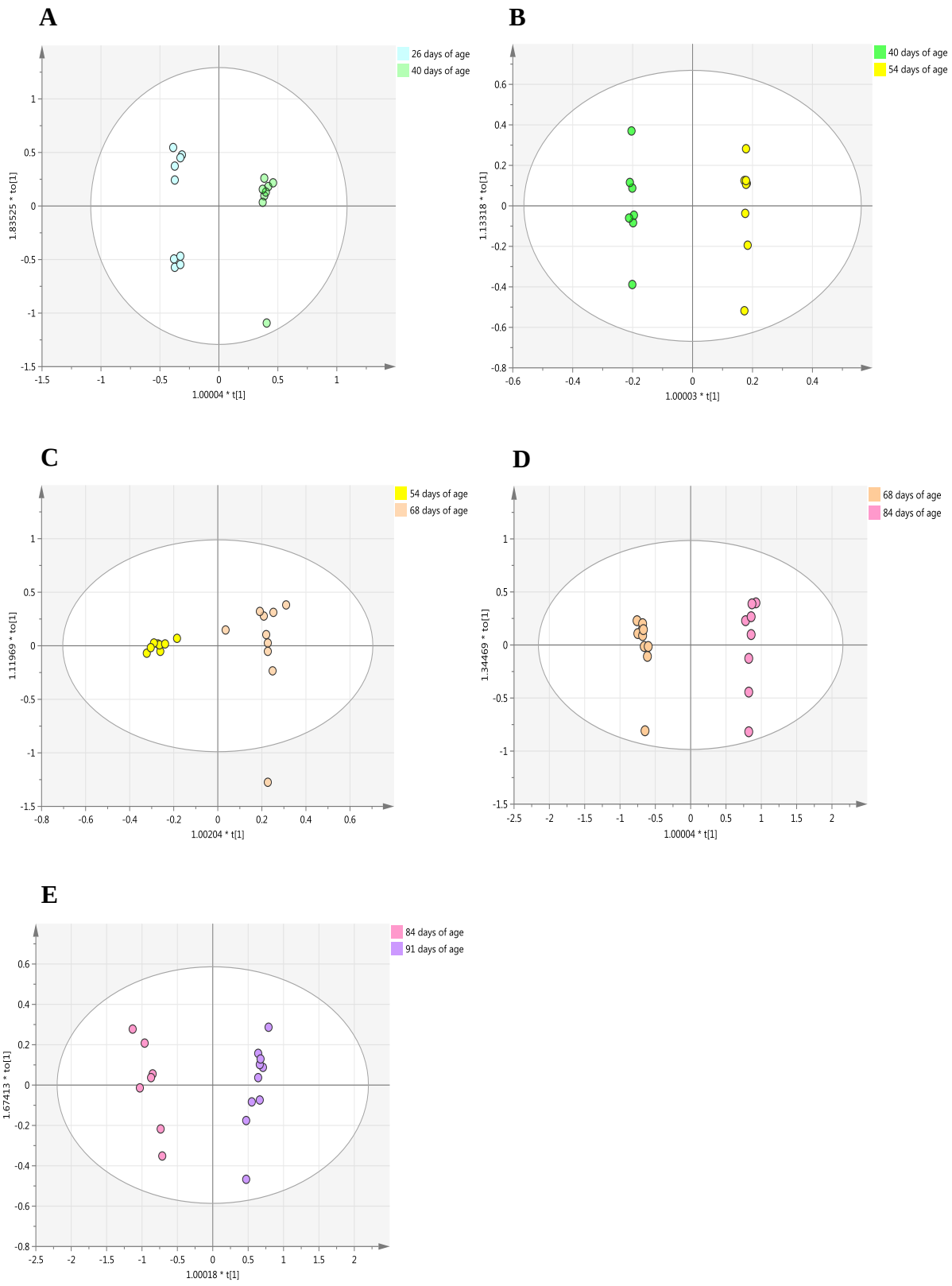

Figure 5.5 Scores plots from OPLS-DA models derived from 1D ^{1}H NMR spectral data of urine samples from male Hanover-Wistar rats at different ages. Animals were placed in metabolism cages for 24 hour urine collection on 6 occasions (26, 40, 54, 68, 84 and 91 days of age) as described in Section 5.2.1. (A) 26 and 40 days; (B) 40 and 54 days; (C) 54 and 68 days; (D) 68 and 84 days; (D) and 84 and 91 days. Each spot in the score plot represents one urine sample.

A

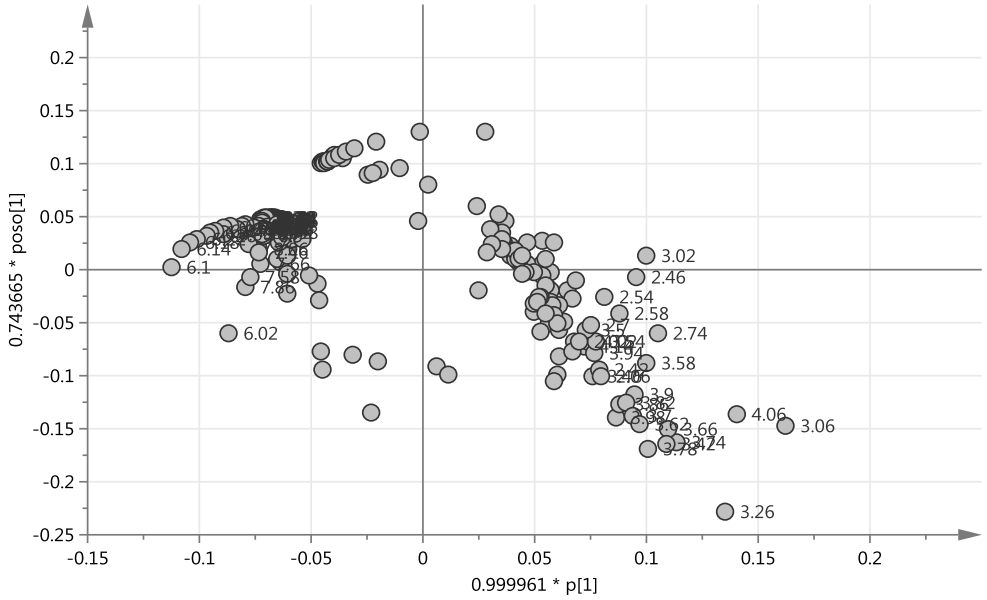

B

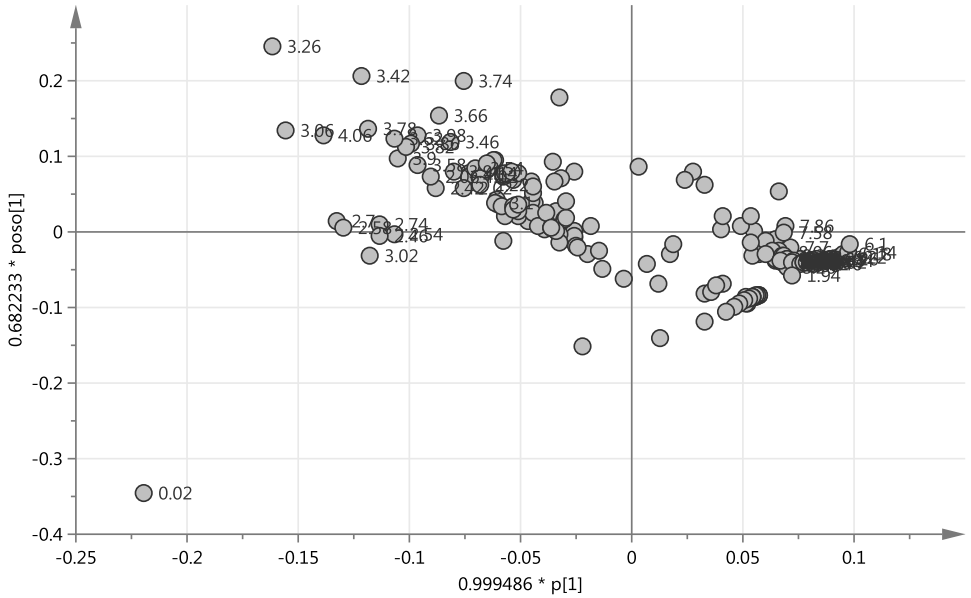

Figure 5.6 OPLS-DA loadings plots from OPLS-DA models derived from 1D ^{1}H NMR spectral data of urine samples from male Hanover-Wistar rats at different ages. Animals were placed in metabolism cages for 24 hour urine collection on 6 occasions (26, 40, 54, 68, 84 and 91 days of age) as described in Section 5.2.1. (A) 68 and 84 days (R^2X (cum) = 0.949, Q^2 = 0.958); (B) and 84 and 91 days (R^2X (cum) = 0.877, Q^2 = 0.858). Each spot in the loadings plot represents a NMR variable labelled as chemical shift in ppm**.**

Identification of the chemical shifts and statistical testing of integral values at all time points revealed the main metabolites showing changes with increasing age of the rat (Table 5.3). Rats at 40 days of age excreted significantly greater levels of creatinine, creatine, 2-oxoglutarate, citrate and succinate than at 26 days old. Rats at 54 days of age

excreted greater levels of creatinine and 2-oxoglutarate compared to 40 days old animals. However, spectral signals for citrate, succinate, creatine and taurine were decreased in the urines at this time point and the decrease for creatine was statistically significant. Animals at 68 days of age excreted significantly greater levels of creatinine and taurine compared to 54 days old rats. However, succinate, citrate, 2-oxoglutarate and creatine were decreased with respect to the previous time point.

From the analysis of the loadings plots for 68 and 84 and 84 and 91 days in Figure 5.6 A and B, it appeared that, at 84 days of age, most of the chemical shifts showed positive loadings for PC1, whereas most of the labelled chemical shifts identified in the loadings plot in Figure 5.6 B (84 and 91 days) showed negative loadings for PC1. This demonstrates that the integral intensities of most chemical shift regions were increased in the urine samples from 84 days old rats in comparison to younger animals (68 days old) and older animals (91 days old). At 84 days it would appear that most metabolites were present in the highest concentration in the rat urine.

Table 5.3 OPLS-DA detected 1D ^{1}H NMR chemical shifts responsible for the separation of 1D ^{1}H NMR derived spectra from the urine of male Hanover-Wistar rats at different ages. Animals were placed in metabolism cages for 24 hour urine collection on 6 occasions (26, 40, 54, 68, 84 and 91 days of age) as described in Section 5.2.1. Chemical shifts were statistically compared by means of a Students' t-test. Values that differ significantly from the previous time point are shown *P<0.05; **P<0.01; ***P<0.001.

		Change in metabolite concentration with age in days (increase (+); decrease (-))				
Chemical shift (δ), multiplicity	**Endogenous metabolites**	**40**	**54**	**68**	**84**	**91**
8.46-8.50 (s)	formate	-	+	-	-	+
7.70-7.74 (d)	hippurate	-	+	+	-	+
7.62-7.66 (t)	hippurate	+	+	+	-	+
7.54-7.58 (t)	hippurate	+	+	+	-	+
4.06-4.10 (s)	creatinine	+**	+	+**	+***	-***
3.98-4.02 (d)	hippurate	+	-	-	+	-
3.94-3.98 (s)	creatine	+*	-*	-	+**	-**
3.42-3.46 (t)	taurine	+	+	+***	+*	-**
3.26-3.30 (t)	taurine	-	-	+***	+*	-*
3.06-3.10 (s)	creatinine	+**	+	+**	+***	-***
2.98-3.02 (t)	2-oxoglutarate	+**	+	-	+**	-**
2.70-2.74 (d)	citrate	+**	-	-	+	-**
2.54-2.58 (d)	citrate	+	-	-	+*	-**
2.42-2.46 (t)	2-oxoglutarate	+**	+	-	+**	-**
2.38-2.42 (s)	succinate	+	-	-	+	-

S, singlet; d, doublet; t, triplet

5.4 Sexual maturity study

In order to investigate if the development of sexual maturity of the Hanover-Wistar was a contributor to the changes in urinary proteins and metabolites with age, a group of 36 animals was sampled every week between the age of 24 and 90 days for histological examination of relevant tissues.

5.4.1 Body weights

Rats were weighed 3 times a week for the duration of the study and the body weight growth curve followed a similar trend to that observed previously (Figure 5.1).

5.4.2 Testes weight

Figure 5.7 A shows the mean relative weight for the right and left testes for 6 animals at each autopsy. Mean relative weights increased up to 52 days ($^{***}P<0.001$ compared to weights at 33 days old). In 24 day old rats the relative weight for the testes was 3.76 g/kg whereas in 52 day old rats the testes weighed 5.52 g/kg, representing a 1.5-fold increase. After this time point there were no further increases in testes weight and there appeared to be a decrease in weight at 91 days. However, this is due to one animal having significantly lighter testes than the rest of the animals in the same group thus contributing to the large standard deviation.

5.4.3 Epididymides weight

At autopsy, epididymides were collected and relative weights were calculated and recorded. Epididymides weight was expressed as a mean of right and left epididymides. Relative weights increased up to day 77 when they were over 3 times heavier than at 24 days (6.26 and 1.27 g/kg BW, respectively). At 90 days of age relative weights were approximately 25 % less than at the previous time point (Figure 5.7 B). This was due to one animal that had lighter epididymides than the rest of the group.

A

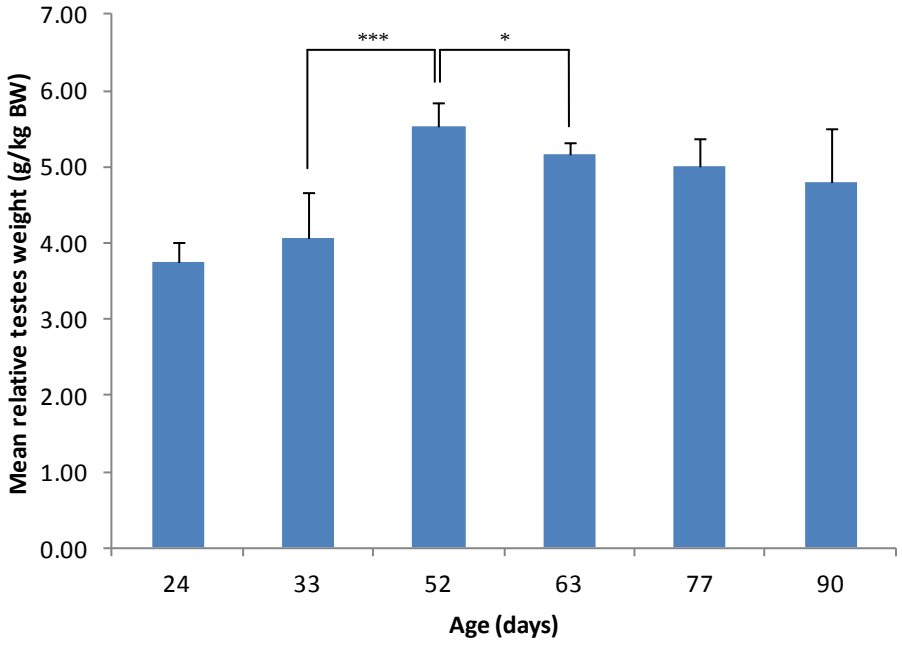

B

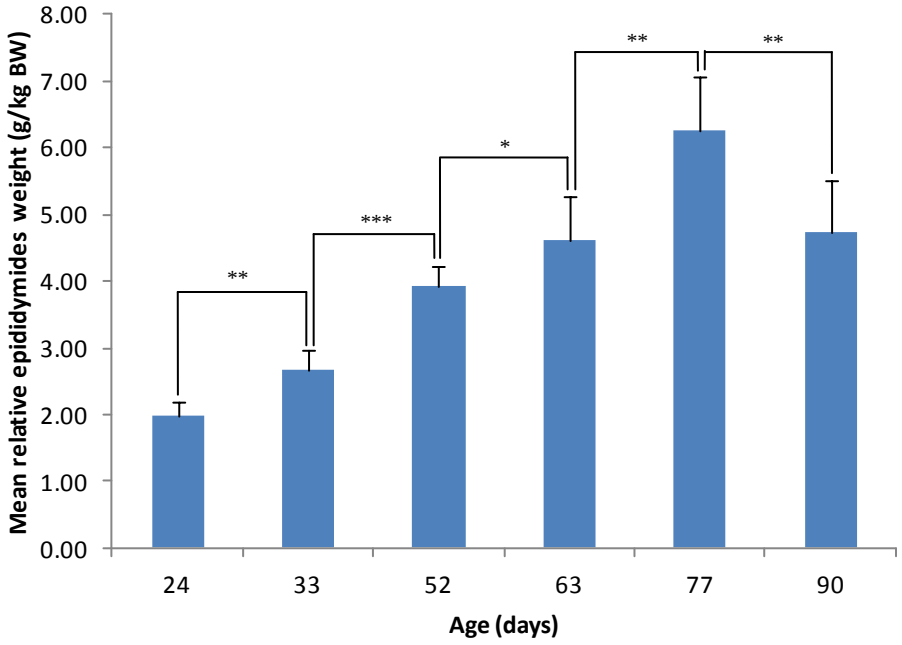

Figure 5.7 Relative testes (A) and epididymides (B) weights for male Hanover-Wistar rats at different ages. Animals were housed in communal cages and autopsied at the time points shown as described in Section 5.2.2. Values are means of relative organ weight expressed as g per kg body weight (BW) with SD indicated by vertical bars of 6 animals per group. Both the testes and the epididymides weights were expressed as a mean of both the right and left organs. Organ weights that differ significantly from previous time point by Students' t-test are shown: $^{*}P<0.05$, $^{**}P<0.01$, $^{***}P<0.001$.

5.4.4 Histopathology

Tissue samples collected at autopsy were further processed for histological examination (Figure 5.8).

At 52 days, the seminiferous epithelium demonstrated all of the normal stages of spermatogenesis, and the epididymides contained sperm. However, the sperm count was lower than that found in a fully mature animal. Therefore animals were considered to be sexually mature at 52 days old as they produced viable sperm, but were not considered to be fully fertile adults.

At 63 days of age, animals were considered to be fully fertile as the number of sperm present in the epididymides was much greater than at 52 days (Table 5.4). Samples taken on or after day 77 revealed full maturity of the testes and a normal complement of sperm in the epididymides. Apart from one animal, killed on day 90, with extensive bilateral atrophy of the testes and aspermia of the epididymides, no remarkable pathological changes were recorded in any of the samples.

A

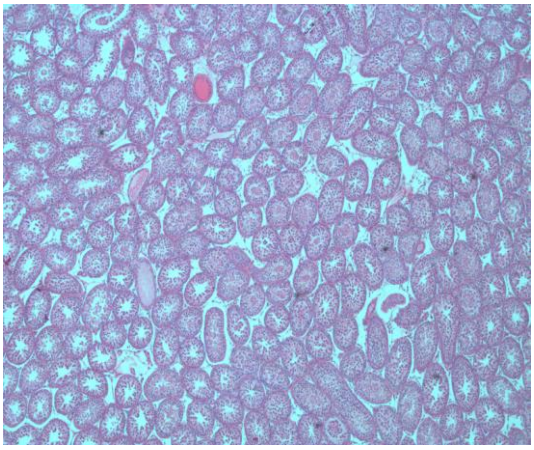

B

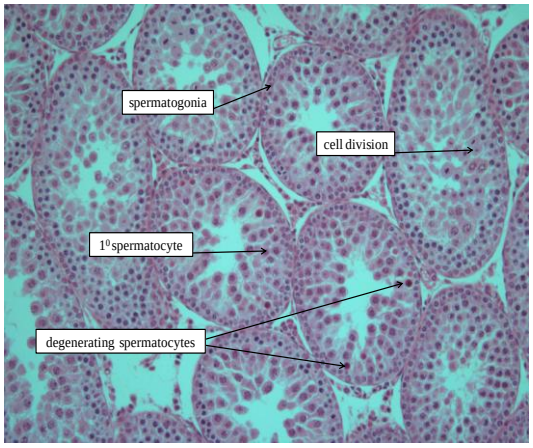

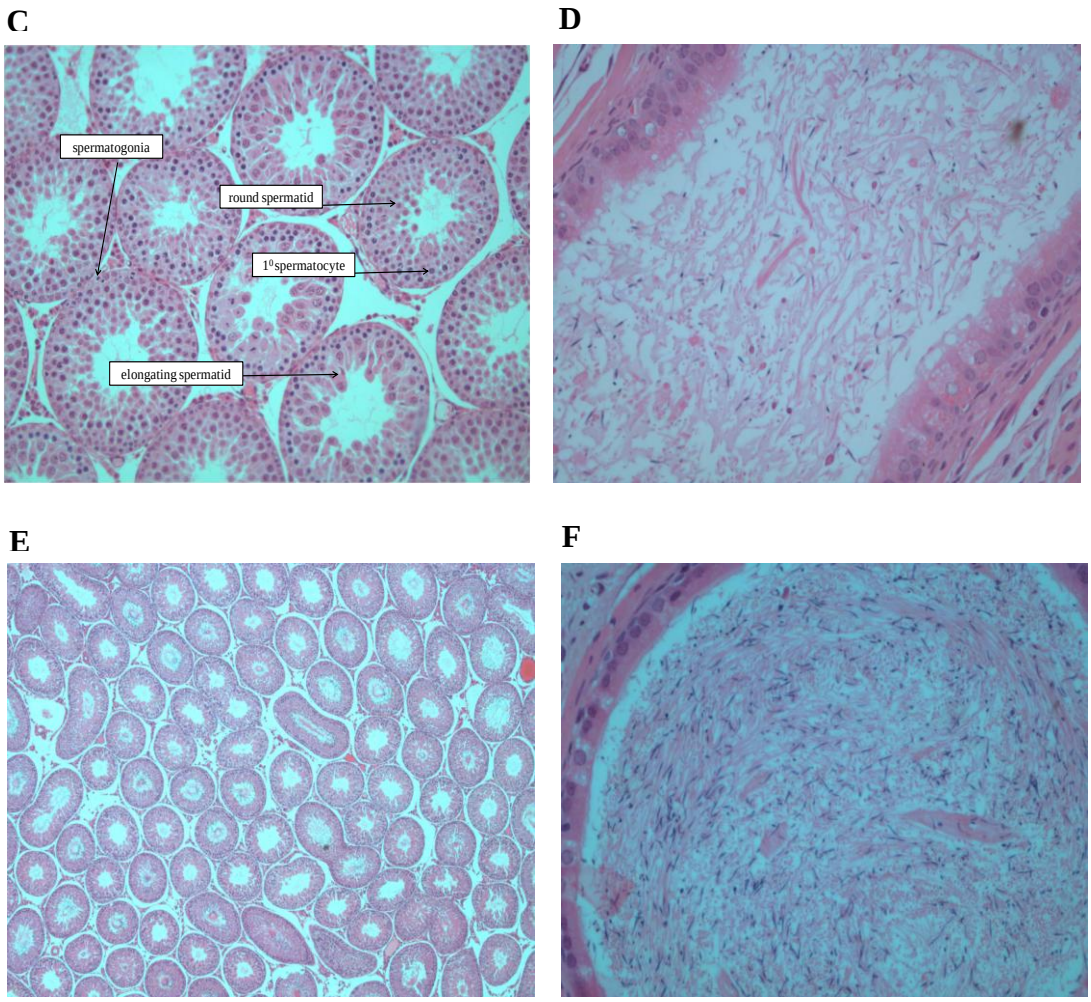

Figure 5.8 Histology of the seminiferous tubules in the testes and epididymides of male Hanover-Wistar rats at different ages. Original magnification A and E, x 100; B, C, D and F, x 200. H&E. Animals were housed in communal cages and autopsied at the time points described in Section 5.2.2. At autopsy, the seminiferous tubules and the testes were collected and processed for histopathological examination as described in Section 2.8. (A) 24 day old rat: seminiferous tubules appear very similar; (B) 24 day old rat: seminiferous tubules showing spermatogonia and spermatocytes; (C) 33 day old rat: seminiferous tubules showing the beginning of spermatid development; (D) 52 day old rat: seminiferous tubules showing spermatozoa but in low levels; (E) 63 day old rat: seminiferous tubules showing similar appearance to testes at day 52; (F) 63 day old rat: epididymides showing full complement of sperm.

Table 5.4 Elongating spermatids and presence of sperm in epididymides with increasing age of male Hanover-Wistar rat. Animals were housed in communal cages and autopsied at 24, 33, 52, 63, 77 and 90 days as described in Section 5.2.2. At autopsy, the seminiferous tubules and the testes were collected and processed for histopathological examination as described in Section 2.8.

Age (days)	Testes with elongating spermatids present	Epididymides (spermatozoa present in cauda)
24	No	No
33	A few	No (minimal cell debris present)
52	Yes	Yes (in low numbers)
63	Yes	Yes
77	Yes	Yes
90	Yes	Yes

5.5 Comparison of metabolomic changes to the urine following CCl_4-induced hepatic injury in the pre- and post-sexually mature rat

In experiment 1 in this Chapter, levels of urinary testosterone suggest that sexual maturity occurred between 54 and 68 days, since between these time points the greatest fold-increase was observed. Histopathological results from experiment 2 indicate that sexual maturity occurs between 52 and 63 days. Therefore, this study examines rats at 7 weeks (49 days) to represent immature rats, and animals at 13 weeks (91 days) to represent post-sexually mature rats.

5.5.1 Observations during the study

No abnormal observations were recorded during the study. However, at autopsy, livers from both 7 and 13 week old CCl_4-treated animals appeared paler in colour when compared to control livers.

5.5.2 Liver weights

Liver weights were significantly increased over controls in both groups of CCl_4-treated animals (7 week old and 13 week old) ($^{***}P<0.001$) (data not shown).

5.5.3 Kidney weights

Kidney weights were significantly decreased compared to control values in the animals dosed with 1.2 mL/kg CCl_4 at 7 weeks old (mean relative weights were 3.83 and 3.60 g/kg BW for control and 1.2 mL/kg CCl_4-treated animals respectively; $^{*}P<0.05$). However, no CCl_4-treatment related effect was evident in the relative kidney weight in older animals (13 week old) (data not shown).

5.5.4 Serum clinical chemistry

Figure 5.9 and Figure 5.10 show that serum ALT and AST were significantly increased in all rats following treatment with 1.2 mL/kg CCl_4. In younger animals (7 weeks) there was a 7.91- and a 3.25-fold increase over control levels for ALT ($^{***}P<0.001$) and AST ($^{**}P<0.01$), respectively (Figure 5.9). Whereas, in 13 week old rats, much greater fold increases were measured (Figure 5.10). Control mean values were 64.50 and 187.40 U/L whereas levels in the serum of treated animals were 2116.20 and 1792.50 U/L for

ALT and AST, respectively. This represented a 33-fold increase over controls for ALT ($^{*}P<0.05$) and an approximate 10-fold increase over control values for AST ($^{*}P<0.05$).

In 7 week old rats mean serum levels of GLDH were 22-fold increased in CCl_4-treated rats compared to vehicle-treated animals ($^{***}P<0.001$), whereas in older animals (13 weeks) the increase recorded for serum GLDH levels was 42-fold ($^{**}P<0.01$) (Figure 5.9, Figure 5.10).

ALP also increased after dosing with CCl_4 from 541.10 U/L to 719.30 U/L in 7 week old rats (1.33-fold increase; $^{*}P<0.05$), and from 207.70 U/L to 322.70 U/L in 13 week old rats (1.55-fold increase; $^{***}P<0.001$) (Table 5.5, Table 5.6).

For animals at 7 weeks of age all other parameters were similar for control and CCl_4-treated animals, except for urea which was significantly increased above controls following CCl_4 administration (1.53-fold increase; $^{***}P<0.001$). However, in older animals (13 weeks) serum albumin and creatinine were significantly increased following treatment with CCl_4, whereas glucose was statistically significantly decreased in the serum of CCl_4-treated rats (7.73 and 5.70 mmol/L for vehicle and CCl_4-treated animals, respectively; $^{***}P<0.001$). Serum urea was significantly raised above controls for CCl_4-treated animals in both age groups (1.70-fold increase; $^{***}P<0.001$) (Table 5.5, Table 5.6).

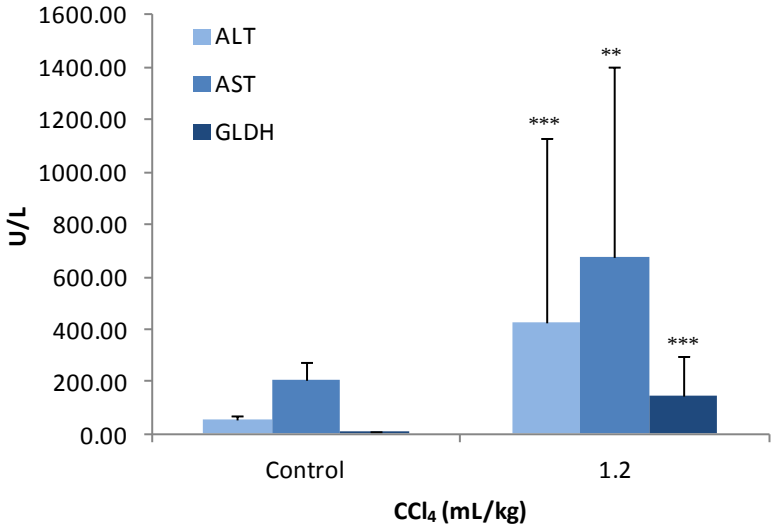

Figure 5.9 Serum ALT, AST and GLDH levels for 7 week old male Hanover-Wistar rats treated with vehicle (control) or CCl_4 at 1.2 mL/kg. Animals were dosed by gavage. At 24 hours post-dosing serum was collected as described in Section 5.2.3 and enzyme assays were carried out as described in Section 2.7. Values are the means with SD indicated by vertical bars of 10 animals per group. Values that differ significantly from controls by Students' t-test are shown: $^{**}P<0.01$; $^{***}P<0.001$.

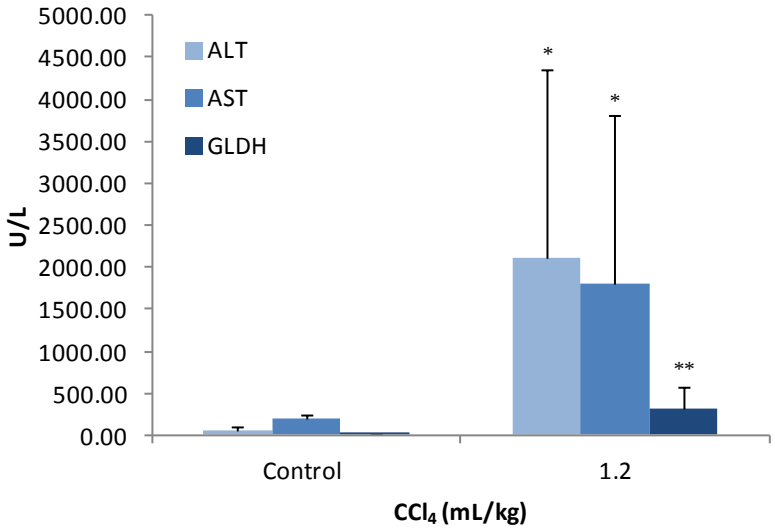

Figure 5.10 Serum ALT, AST and GLDH levels for 13 week old male Hanover-Wistar rats treated with vehicle (control) or CCl_4 at 1.2 mL/kg. Animals were dosed by gavage. At 24 hours post-dosing serum was collected as described in Section 5.2.3 and enzyme assays were carried out as described in Section 2.7. Values are the means with SD indicated by vertical bars of 10 animals per group. Values that differ significantly from controls by Students' t-test are shown: $^{*}P<0.05$; $^{**}P<0.01$.

Table 5.5 Serum clinical chemistry parameters for 7 week old rats treated with vehicle (control) or CCl_4 at 1.2 mL/kg. Animals were dosed by gavage. At 24 hours post-dosing serum was collected as described in Section 5.2.3 and enzyme assays were carried out as described in Section 2.7. Values are means and SD of 10 animals per group. Values that differ significantly from controls by Students' t-test are shown: $^{*}P<0.05$; $^{***}P<0.001$.

Serum parameters	CCl_4 dose level (mL/kg)	
	0	1.2
ALP (U/L)	541.10 (187.37)	719.30* (142.73)
Albumin (g/L)	35.89 (1.22)	36.74 (0.80)
Creatinine (µmol/L)	23.60 (2.46)	26.70 (3.56)
Glucose (mmol/L)	5.51 (1.31)	5.30 (0.69)
Urea (mmol/L)	6.14 (1.04)	9.37*** (0.92)
Total protein (g/L)	55.50 (1.51)	55.80 (1.40)

ALP: alkaline phosphatase.

Table 5.6 Serum clinical chemistry parameters for 13 week old rats treated with vehicle (control) or CCl_4 at 1.2 mL/kg. Animals were dosed by gavage. At 24 hours post-dosing serum was collected as described in Section 5.2.3 and enzyme assays were carried out as described in Section 2.7. Values are means and SD of 10 animals per group. Values that differ significantly from controls by Students' t-test are shown: $^{*}P<0.05$; $^{***}P<0.001$.

Serum parameters	CCl_4 dose level (mL/kg)	
	0	1.2
ALP (U/L)	207.70 (43.66)	322.70*** (50.65)
Albumin (g/L)	34.60 (0.52)	37.00*** (1.49)
Creatinine (µmol/L)	29.00 (2.73)	33.40* (5.62)
Glucose (mmol/L)	7.73 (0.78)	5.70*** (0.37)
Urea (mmol/L)	5.69 (0.66)	9.66*** (0.79)
Total protein (g/L)	56.30 (1.70)	58.50 (2.88)

ALP: alkaline phosphatase.

5.5.5 Urine clinical chemistry

Total protein in the urine was significantly decreased in comparison to control animals in CCl_4-treated animals at both 7 and 13 weeks of age (Table 5.7, Table 5.8).

Urinary levels for NAG, creatinine and glucose did not show evidence of a CCl_4-treatment related effect in either 7 or 13 weeks old animals (Table 5.7, Table 5.8).

Table 5.7 Urinary clinical chemistry parameters for 7 week old rats treated with vehicle (control) or CCl_4 at 1.2 mL/kg. Animals were dosed by gavage and urine collected for 18 hours post-dosing as described in Section 5.2.3. Clinical parameters were assayed as described in Section 2.7. Values are means and SD of 10 animals per group. Values that differ significantly from controls by Students' t-test are shown: $^{***}P<0.001$. c.p. = collection period (18 hours).

Urinary parameters	CCl_4 dose level (mL/kg)	
	0	1.2
Total protein (mg/c.p.)	4.91 (0.99)	1.93*** (0.33)
NAG (mU/c.p.)	172.00 (22.86)	144.70 (29.65)
Creatinine (µmol/c.p.)	37.50 (4.17)	37.50 (3.24)
Glucose (µmol/c.p.)	4.10 (0.57)	4.70 (0.67)
Volume (mL)	19.40 (8.26)	29.10 (15.91)

NAG: N-acetyl-D-glucosamine.

Table 5.8 Urinary clinical chemistry parameters for 13 week old rats treated with vehicle (control) or CCl_4 at 1.2 mL/kg. Animals were dosed by gavage and urine collected for 24 hours post-dosing as described in Section 5.2.3. Clinical parameters were assayed as described in Section 2.7. Values are means and SD of 10 animals per group. Values that differ significantly from controls by Students' t-test are shown: $^{*}P<0.01$; $^{***}P<0.001$. c.p. = collection period (24 hours).

Urinary parameters	CCl_4 dose level (mL/kg)	
	0	1.2
Total protein (mg/c.p.)	10.29 (2.16)	3.78*** (1.53)
NAG (mU/c.p.)	168.60 (29.99)	143.60 (27.02)
Creatinine (µmol/c.p.)	74.30 (4.76)	66.90 (13.15)
Glucose (µmol/c.p.)	5.70 (0.67)	6.30 (1.43)
Volume (mL)	17.19 (7.92)	29.99* (16.39)

NAG: N-acetyl-D-glucosamine.

5.5.6 Histopathology

At autopsy livers and kidneys were removed for all animals for histopathological examination (Figure 5.11).

For all CCl_4-treated animals (7 and 13 week old) hepatic injury was present and characterised by centrilobular hepatocellular vacuolation with ballooning of the cytoplasm and hepatocyte necrosis. There was also a focal mixed inflammatory infiltrate present. Vacuolated cells were seen in midzonal to periportal regions (Figure 5.11).

In the kidneys, CCl_4 treatment-related findings were present in 2 animals at 13 weeks of age and consisted of proximal epithelial vacuolation. For all other CCl_4-treated animals there was no evidence of CCl_4-induced kidney injury.

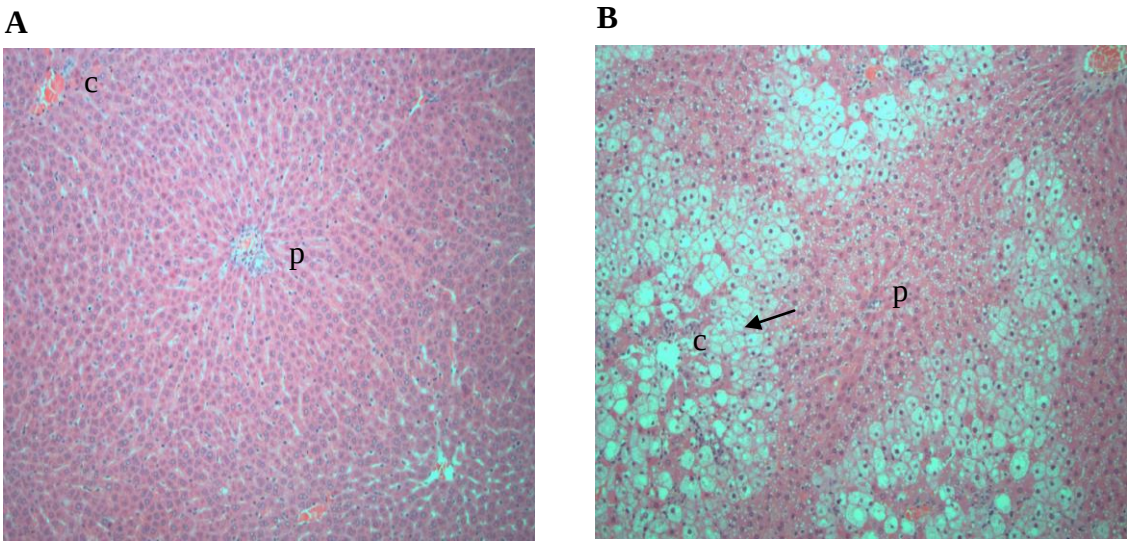

Figure 5.11 Histology of liver sections from 7 week old male Hanover-Wistar rats treated with vehicle (control) or CCl_4 at 1.2 mL/kg and autopsied 24 hours post-dosing. Original magnification, x 100; H&E. Rats were dosed by gavage. At autopsy, liver samples were collected and processed for histopathology as described in Section 2.8. (A) control rat: central vein (c) and a portal vein (p); (B) CCl_4-treated rat at 1.2 mL/kg: central vein (c) with some degenerate hepatocytes; others showing vacuolation (arrow indicates area of vacuolation).

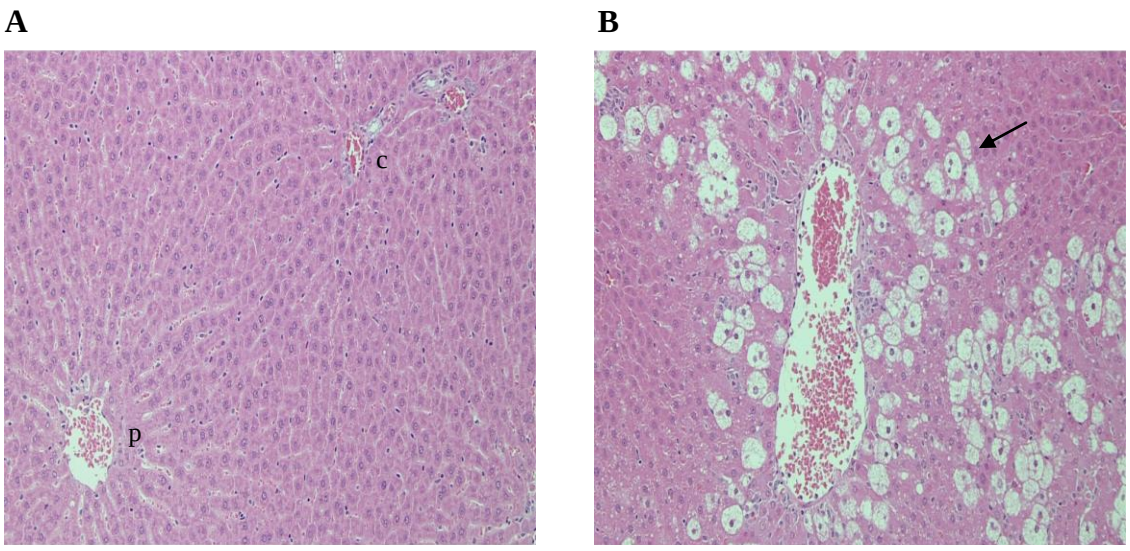

Figure 5.12 Histology of liver sections from 13 week old male Hanover-Wistar rats treated with vehicle (control) or CCl_4 at 1.2 mL/kg and autopsied 24 hours post-dosing. Original magnification, x 100; H&E. Rats were dosed by gavage. At autopsy, liver samples were collected and processed for histopathology as described in Section 2.8. (A) control rat: central vein (c) and a portal vein (p); (B) CCl_4-treated rat at 1.2 mL/kg: centrilobular vacuolation, necrosis (arrow indicates area of vacuolation).

5.5.7 1D ^{1}H NMR spectrometry

To investigate the urinary metabolite changes following CCl_4-induced hepatic injury in 7 and 13 week old male Hanover-Wistar rats, urine samples from this study were analysed by 1D ^{1}H NMR spectrometry.

Firstly, urine samples from control and CCl_4-treated animals at 7 weeks of age were compared by OPLS-DA. The scores plot for the OPLS-DA model is shown in Figure 5.13 A. Control samples were clustered on the left hand side of the score plot whereas samples from animals treated at 1.2 mL/kg were located on the right half of the plot and there was perfect separation along the discriminating component t[1]. As in the previous metabolomic studies there was great intragroup variation (displayed in the orthogonal component). The corresponding S-plot is shown in Figure 5.13 B.

Variables that may discriminate between control and CCl_4-treated samples are located on the extremes of the S-shaped curve, i.e., on the upper right quadrant or lower left quadrant of the plot. Chemical shifts labeled in the S-plot in Figure 5.13 B were selected based on the VIP plots for the corresponding models (data not shown).

A

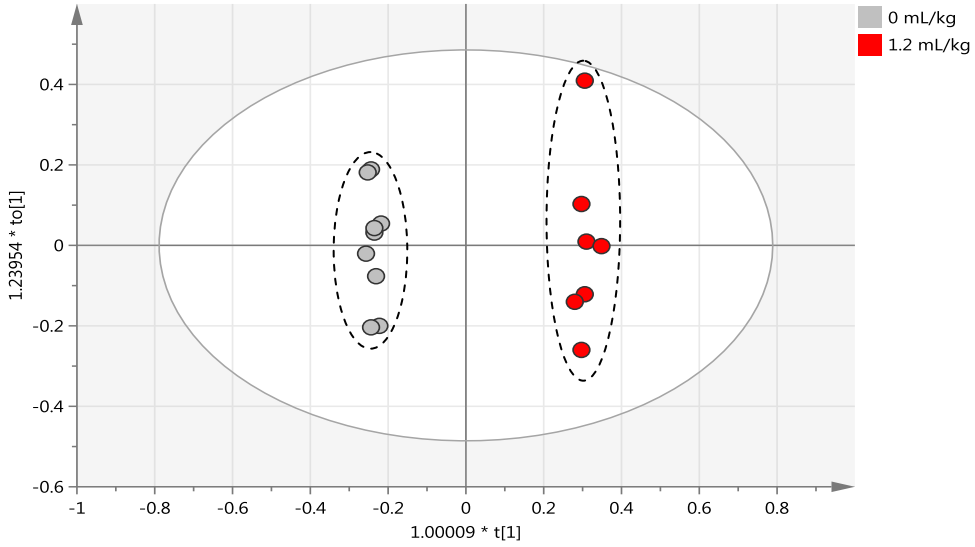

B

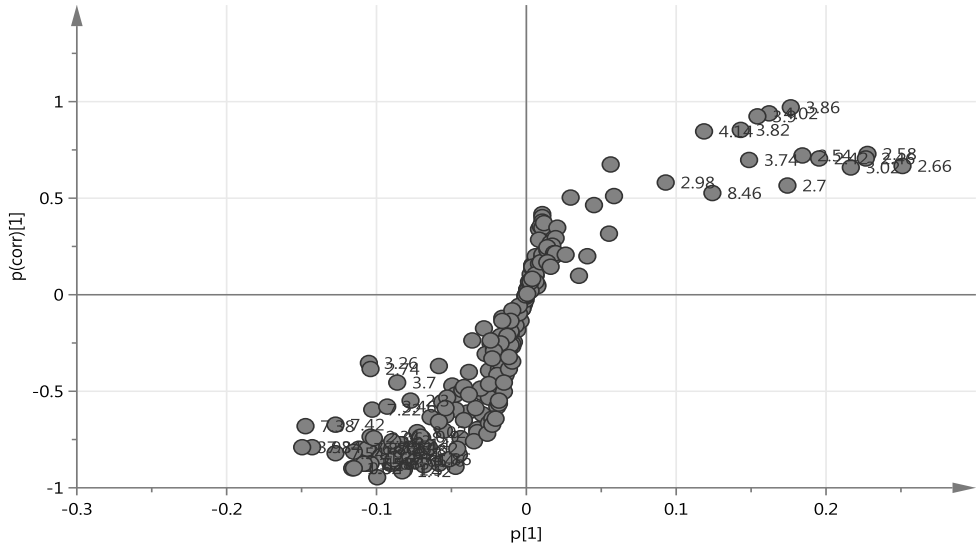

Figure 5.13 Scores plot (A) and S-plot (B) from an OPLS-DA model derived from 1D ^{1}H NMR spectral data of urine samples from 7 week old male Hanover-Wistar rats treated with vehicle (control) or CCl_4 at 1.2 mL/kg. Rats were dosed by gavage and urine collected for 18 hours as described in Section 5.2.3. Each spot in the scores plot represents one urine sample. Each spot in the S-plot represents a NMR variable labelled as chemical shift in ppm. R^2X (cum) = 0.757, Q^2 = 0.956).

Chemical shifts were identified according to previously published data and Table 5.9 shows the changes to urinary metabolite concentration following the administration of a single dose of 1.2 mL/kg CCl_4 to 7 week old rats. Integral regions were compared using a Student's t-test for statistical significant differences between control and 7 week old animals treated at 1.2 mL/kg CCl_4. Decreases were found in the resonances of

hippurate, taurine and creatinine whereas increases were noted for formate, 2-oxoglutarate, citrate, creatine and succinate.

Table 5.9 OPLS-DA detected 1D ^{1}H NMR chemical shifts responsible for the separation of 1D ^{1}H NMR derived spectra from the urine of 7 week old male Hanover-Wistar rats treated with vehicle (control) or CCl_4 at 1.2 mL/kg. Rats were dosed by gavage and urine collected for 18 hours as described in Section 5.2.3. Chemical shifts were compared by means of a Students' t-test. Values that differ significantly from controls are shown: $^{*}P<0.05$; $^{**}P<0.01$; $^{***}P<0.001$.

Chemical shift (δ), multiplicity	Endogenous metabolites	Change in urinary metabolite concentration (increase (+); decrease (-))
8.46-8.50 (s)	formate	+*
7.70-7.74 (d)	hippurate	-***
7.62-7.66 (t)	hippurate	-***
7.54-7.58 (t)	hippurate	-***
4.06-4.10 (s)	creatinine	-
3.98-4.02 (d)	hippurate	-***
3.94-3.98 (s)	creatine	+
3.42-3.46 (t)	taurine	-
3.26-3.30 (t)	taurine	-
3.06-3.10 (s)	creatinine	-
2.98-3.02 (t)	2-oxoglutarate	+
2.70-2.74 (d)	citrate	+
2.54-2.58 (d)	citrate	+**
2.42-2.46 (t)	2-oxoglutarate	+
2.38-2.42 (s)	succinate	+

S, singlet; d, doublet; t, triplet.

Urine samples from 13 week old Hanover-Wistar rats treated with CCl_4 at 0 and 1.2 mL/kg were analysed by 1D ^{1}H NMR. Due to technical reasons spectra could only be obtained for 5 control and 5 CCl_4-treated samples. The corresponding OPLS-DA scores plot and S-plot are shown in Figure 5.14. As with the 7 week old animals, urine samples from 13 week old rats displayed great cluster separation between control and CCl_4-treated samples.

Chemical shifts identified from the S-plot that were considered to be mainly responsible for cluster separation were labelled and a Students' t-test was carried out to statistically compared these chemical shifts in CCl_4-treated urine samples to control. Table 5.10 shows the major metabolites changes following CCl_4-induced hepatic injury to 13 week old male Hanover-Wistar rats. These changes include an increase in the resonances of

formate, taurine, creatine, 2-oxoglutarate and citrate, and a decrease in the resonances of hippurate, creatinine and succinate.

A

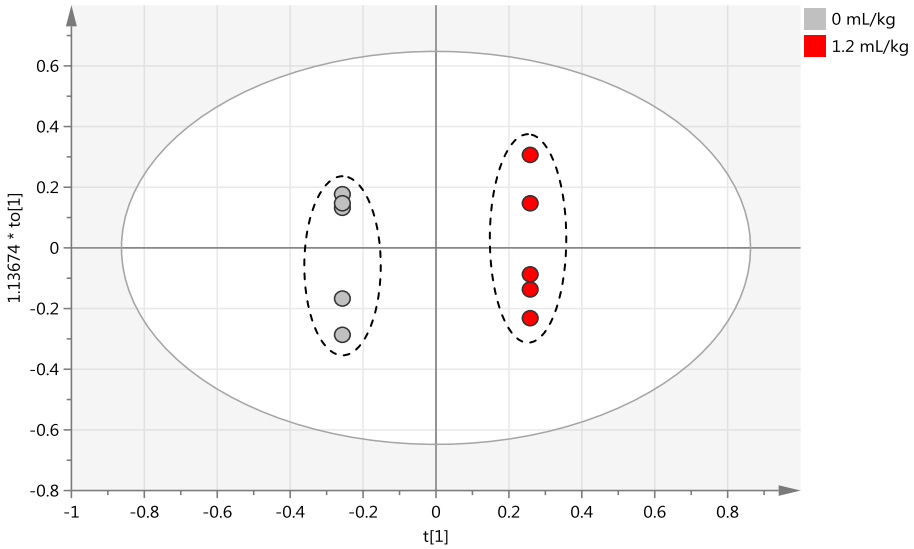

B

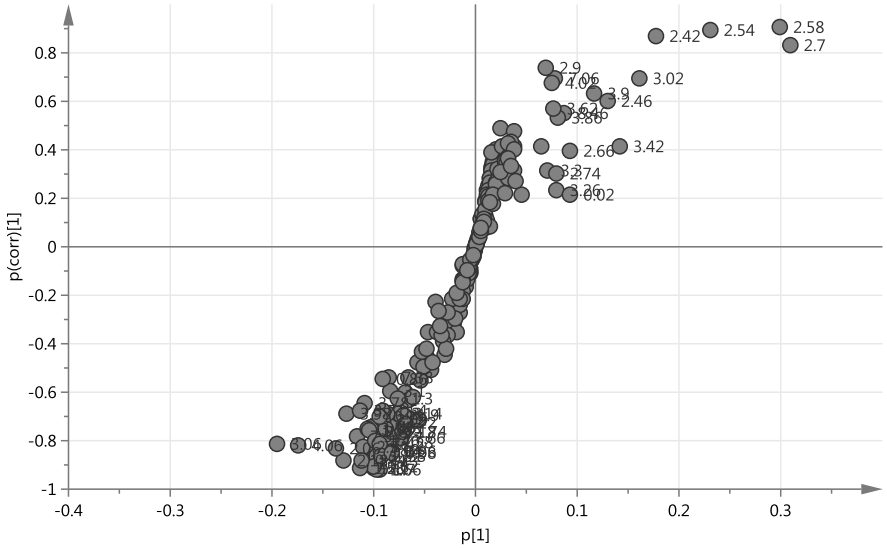

Figure 5.14 Scores plot (A) and S-plot (B) from an OPLS-DA model derived from 1D ^{1}H NMR spectral data of urine samples from 13 week old male Hanover-Wistar rats treated with vehicle (control) or CCl_4 at 1.2 mL/kg. Rats were dosed by gavage and urine collected for 24 hours as described in Section 5.2.3. Each spot in the scores plot represents one urine sample. Each spot in the S-plot represents a NMR variable labelled as chemical shift in ppm. R^2X (cum) = 0.946, Q^2 = 0.995.

Table 5.10 OPLS-DA detected 1D ^{1}H NMR chemical shifts responsible for the separation of 1D ^{1}H NMR derived spectra from the urine of 13 week old male Hanover-Wistar rats treated with vehicle (control) or CCl_4 at 1.2 mL/kg. Rats were dosed by gavage and urine collected for 24 hours as described in Section 5.2.3. Chemical shifts were compared by means of a Students' t-test. Values that differ significantly from controls are shown: $^{*}P<0.05$; $^{**}P<0.01$.

Chemical shift (δ), multiplicity	Endogenous metabolites	Change in urinary metabolite concentration (increase (+); decrease (-))
8.46-8.50 (s)	formate	+
7.70-7.74 (d)	hippurate	-*
7.62-7.66 (t)	hippurate	-*
7.54-7.58 (t)	hippurate	-**
4.06-4.10 (s)	creatinine	-**
3.98-4.02 (d)	hippurate	-*
3.94-3.98 (s)	creatine	+
3.42-3.46 (t)	taurine	+
3.26-3.30 (t)	taurine	+
3.06-3.10 (s)	creatinine	-**
2.98-3.02 (t)	2-oxoglutarate	+*
2.70-2.74 (d)	citrate	+**
2.54-2.58 (d)	citrate	+**
2.42-2.46 (t)	2-oxoglutarate	+**
2.38-2.42 (s)	succinate	-

S, singlet; d, doublet; t, triplet.

The main objective of this experiment was to compare the effect on urinary metabolites of administering 1.2 mL/kg CCl_4 to male Hanover-Wistar rats at different ages (7 and 13 weeks old). A PCA model was constructed for the urine samples from control and CCl_4-treated animals at both time points (7 and 13 weeks old) (Figure 5.15). It will be important to rule out changes to urinary metabolites due to the different ages of the rats. However, in Figure 5.15, the 2 groups of control samples were mostly located on the same quadrant of the scores plot suggesting the absence of significant differences between them. This is in agreement with the scores plot in Figure 5.4 A from the growth curve in which samples from both time points appeared to be overlapped.

To compare changes to urinary metabolites at the 2 different ages (7 and 13 weeks) following the induction of hepatic injury a OPLS-DA model was performed for the urine 1D ^{1}H NMR spectral data collected from animals dosed with 1.2 mL/kg CCl_4 at 7 and at 13 weeks (Figure 5.16). The scores plot for this model is shown in Figure 5.16 A. Separation according to age occurred along the discriminating component t[1], with 2

clear sample clusters; one for urine from 7 week old animals, and the other from 13 week old rats.

The corresponding S-plot is shown in Figure 5.16 B. The upper right quadrant shows the chemical shifts that were increased in older animals after the administration of CCl_4 at 1.2 mL/kg; and in the lower left quadrant integral regions that were increased in younger animals (7 weeks) following CCl_4 treatment.

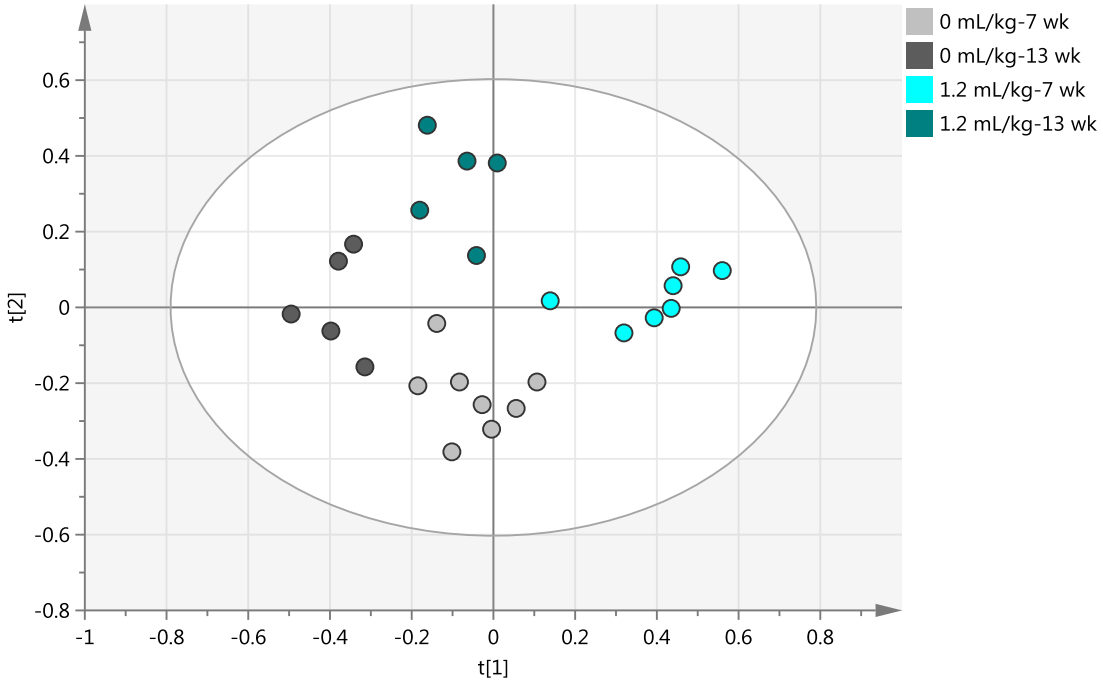

Figure 5.15 PCA scores plot from a PCA model derived from 1D ^{1}H NMR spectral data of urine samples from 7 week old and 13 week old male Hanover-Wistar rats treated with vehicle (control) or CCl_4 at 1.2 mL/kg. Rats were dosed by gavage and urine collected for 18 and 24 hours for 7 and 13 week old rats respectively, as described in Section 5.2.3. Each spot in the scores plot represents one urine sample. R^2X (cum) = 0.815, Q^2 = 0.327.

A

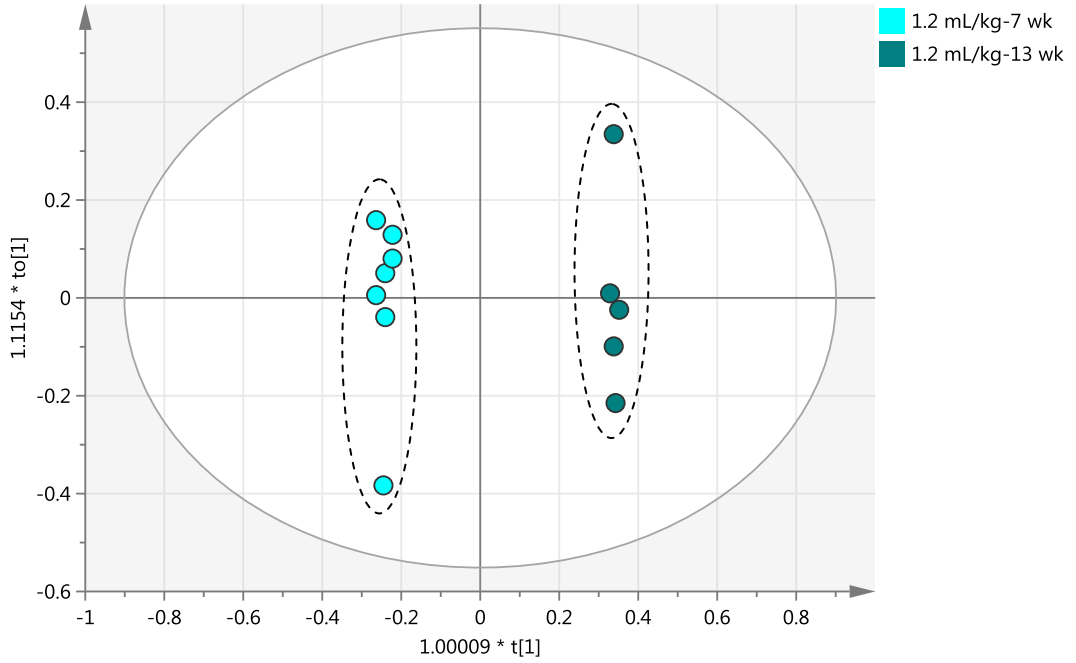

B

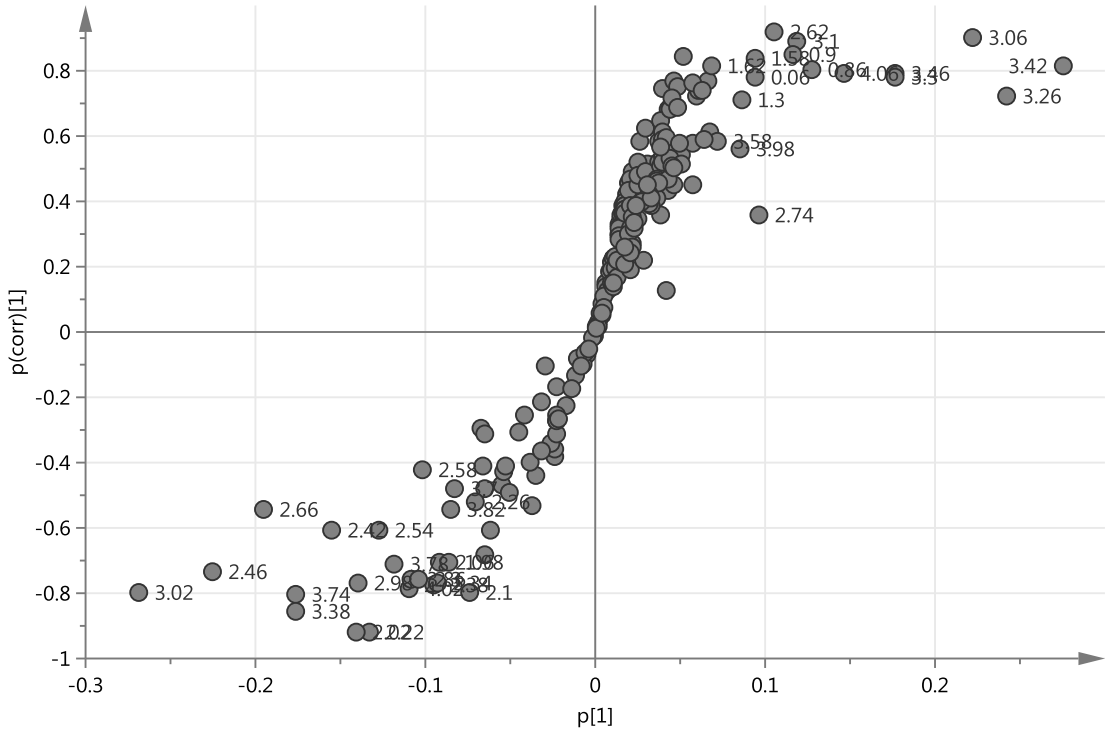

Figure 5.16 Scores plot (A) and S-plot (B) from an OPLS-DA model derived from 1D ^{1}H NMR spectral data of urine samples from 7 week old and 13 week old male Hanover-Wistar rats treated with CCl_4 at 1.2 mL/kg. Rats were dosed by gavage and urine collected for 18 and 24 hours for 7 and 13 week old rats respectively, as described in Section 5.2.3. Each spot in the scores plot represents one urine sample. Each spot in the loadings plot represents a NMR variable labelled as chemical shift in ppm. R^2X (cum) = 0.677, Q^2 = 0.958.

The chemical shifts labelled on the S-plot were identified and statistical analysis was carried out with integral values to determine significant differences between the 7 week and 13 week old animals (as described in Section 2.11). At 13 weeks of age, CCl_4-treated animals had greater urinary levels of creatinine, hippurate, creatine, taurine and creatinine, and lower levels of citrate, 2-oxoglutarate and succinate, when compared to rats at 7 weeks old following administration of CCl_4 at the same dose level.

Table 5.11 OPLS-DA detected 1D ^{1}H NMR chemical shifts responsible for the separation of 1D ^{1}H NMR derived spectra from the urine of 7 and 13 week old male Hanover-Wistar rats treated with CCl_4 at 1.2 mL/kg. Rats were dosed by gavage and urine samples collected for 18 and 24 hours for 7 and 13 week old rats respectively, as described in Section 5.2.3. Chemical shifts were compared by means of a Students' t-test. Values that differ significantly from 7week old rats are shown: $^{*}P<0.05$; $^{**}P<0.01$; $^{***}P<0.001$.

Chemical shift (δ), multiplicity	Endogenous metabolites	Change in metabolites concentration in 13 week old rats when compared to 7 week old rats (increase (+); decrease (-))
4.06-4.10 (s)	creatinine	+**
3.98-4.02 (d)	hippurate	+
3.94-3.98 (s)	creatine	+
3.42-3.46 (t)	taurine	+**
3.26-3.30 (t)	taurine	+**
3.06-3.10 (s)	creatinine	+***
2.98-3.02 (t)	2-oxoglutarate	-**
2.70-2.74 (d)	citrate	-
2.54-2.58 (d)	citrate	-*
2.42-2.46 (t)	2-oxoglutarate	-*
2.38-2.42 (s)	succinate	-**

S, singlet; d, doublet; t, triplet.

5.6 Discussion

In the dose response study described in Chapter 3 we determined the optimal dose level of CCl_4 that would induce hepatotoxicity but not cause injury to other tissues. In Chapter 3, male rats of approximately 7 weeks of age were used. However, we did not know if animals at this age were sexually mature or fully fertile, or even if this change is an important factor in a CCl_4-induced hepatotoxicity model. Therefore, in the present Chapter we wished to monitor changes in urinary metabolite levels with age and determine the age at which the animals became sexually mature. With this information, we then wished to conduct a comparative study of metabolites in the urine following CCl_4 administration in pre- and post-sexually mature rats.

Experiment 1 was a growth curve study to characterise changes to the urinary metabolite profile as the animals became older and to define baseline levels for some of the most commonly measured protein biomarkers at the different ages.

Some animals in the study (n=10) were placed individually in metabolism cages for 24 hour urine collection every 2 weeks. While in the metabolism cages a significant drop in body weight was observed (Figure 5.1). However, by the end of the study the animals that had been metaboled on 6 separate occasions were of a similar weight to the group of animals that had not been metaboled. This data suggests that the process of metaboling animals for 24 hours during which rats have no access to diet, has no impact on the overall growth rate of the animals (Figure 5.1).

Urine samples collected during the study at days 26, 40, 54, 68, 84 and 91 were analysed for urinary biomarkers such as α-GST, GST Yb1, clusterin, KIM-1, RPA1, MALB, NAG, osteopontin, lipocalin-2, creatinine, glucose and total protein to establish baseline levels for each of the markers as the animals aged (Figure 5.2, Table 5.2).

Urinary levels of α-GST, GST Yb1 and total protein showed a moderate increase from 26 to 40 and from 40 to 54 days old, followed by a dramatic increase at 68 days old (Figure 5.2, Table 5.2). Mean KIM-1, MALB and osteopontin levels in urine increased with age during the first 3 time points and peaked at day 54, after which there was a slight decrease in levels. Urinary levels of RPA1 and clusterin increased up to day 84, after which a plateau was reached. Urinary levels of NAG, lipocalin-2 and glucose

increased from day 26 and were at its highest in 68 days old rats, whereas urinary creatinine levels increased consistently with age and were highest at 91 days.

Age-related differences in urinary protein levels in the rat have been extensively studied in the literature (Sellers et al., 1950; Neuhaus and Flory, 1978; Owen and Heywood, 1986; Williams et al., 2005). Sellers and colleagues (1950) investigated differences in urinary protein levels between male, female and castrated rats of the Slonaker-Addis strain. The authors demonstrated that after castration the level of urinary protein decreased considerably in the males whereas the same did not happen in female animals. However, an increase in urinary protein concentration was apparent for both male and female rats following the administration of testosterone propionate to castrated animals. Therefore, it was suggested that the action site of testosterone is the kidney and not the accessory sex glands. The exact mechanism for this interaction is not clear and previous authors have demonstrated that testosterone has an effect in the epithelium of the proximal and distal tubules, mainly by the induction of hypertrophy (Korenchevsky and Ross, 1940). However, it was not clear from the study by Korenchevsky et al., (1940) if this effect is enough to affect the glomerular permeability to urine, or to decrease the ability of the tubule to reabsorb protein that may be present in the glomerular filtrate. Therefore, it is possible that in our study the increased α-GST, GST Yb1 and total protein levels in 68 days old rats may be due to increased testosterone levels. Subsequently, in the present study, testosterone levels were also measured in the urine of rats at 26, 40, 54, 68, 77 and 91 days of age (experiment 2) and it became apparent that urinary testosterone followed the same pattern of change as α-GST, GST Yb1 and total protein (Figure 5.2, Figure 5.3, Table 5.2).There was a moderate increase up to 54 days of age followed by a sharp rise in mean levels at 68 days.

Fujita and colleagues (1990) studied the correlation of cytochrome P-450 enzyme activity and plasma testosterone levels. In their study, male rats were sacrificed at 3, 6, 12, 25, 28 and 30 months of age. The authors reported a decrease in plasma testosterone levels with age which was accompanied by changes in the activity of the drug metabolising enzymes. However, the time points in our current study were different and consequently only the last collection point of our study overlaps with the first collection time point in Fujita's (1990) study (3 months). In the present study urinary testosterone levels reached peak levels at 84 days, and there was a slight decrease at 91 days (3 months).

In the present study, the correlation of urinary protein levels and testosterone adds further evidence to the proposed relationship between testosterone levels and proteinuria. The observed increase in urinary testosterone levels may be due to the rat reaching sexual maturity at these time points.

Urine samples collected during this study from the same animals at different time points were analysed by 1D ^{1}H NMR and statistical methods for the detection of age-related changes in metabolite concentration. The PCA and OPLS scores plots demonstrated evidence of some cluster separation between samples collected from 84 days old rats and the urine samples at all other time points (Figure 5.4). The OPLS model showed perfect separation of samples along the discriminating component t[1] except for those samples from 84 day old rats which appeared in an entirely different quadrant on the scores plot. This suggested there was a change in metabolites with increasing age but with additional different changes occurring at 84 days old (Figure 5.4 B).

There was some degree of variability in most of the chemical shifts but there was a general trend of increased levels of many metabolites at 84 days followed by a decrease at 91 days. Metabolites which followed this pattern included creatinine, creatine, taurine, 2-oxoglutarate, citrate and succinate (Table 5.3).

In this study, regions containing the 2 triplets for taurine had opposite loadings at 40 and 54 days old, therefore the effect of increasing age was difficult to determine. However, at day 68 there was a highly significant increase ($^{***}P<0.001$) followed by a decrease at 91 days old when compared to day 84, but levels remained increased compared to 84 days. Williams et al., (2005) investigated the effect of age on the profile of endogenous metabolites in the male Alderley-Park rat. They found that urinary taurine levels varied significantly throughout the study increasing at 4 and 6 weeks of age, then dropping at week 8 followed by a sharp increase at week 10 and a decrease at week 14. The significant increases observed in urinary taurine levels in the present study at day 68 (approximately week 10), compares with the data described by Williams et al., (2005), for which the greatest fold increase was also recorded at week 10.

A study by Bell at al., (1991) reported increases in urinary levels of creatinine and taurine in the ageing rat. The authors suggested that the increase in creatinine levels reflects the growth of the animals, particularly the growing muscles of bigger and heavier rats, and the age-related increase in glomerular filtration rate. Creatinine is

spontaneously produced when the phosphate bond in creatine phosphate is hydrolysed for the release of energy in the muscle (Ropero-Miller et al., 2000; Waters et al., 2005). Therefore, creatinine levels in the body are affected by muscle mass. Changes in taurine levels in this study appeared to follow the temporal pattern of creatinine. However, it has also been shown that urinary taurine is dependent not only on the age of the animals but also on their nutritional status and consequently their diet (Connor et al., 2004). More recently, a study was conducted investigating the effect of taurine on male reproduction in Wistar rats of different ages (Yang et al., 2010b). The authors reported a decrease in the biosynthesis of taurine in the testis in the ageing rat. In the male reproductive system, taurine has been reported to be present in Leydig cells, vascular endothelial cells, interstitial cells of testis and epithelial cells of the efferent ducts (Yang et al., 2010c). Yang et al (2010c) reported that taurine has a positive effect in reproduction by stimulating testosterone secretion in Leydig cells, therefore suggesting a role for taurine in testicular function.

The changes to urinary levels described in the present study for citrate and hippurate mirror the results reported by Williams et al., (2005). In the study by Williams et al., (2005), there was evidence of an age-dependent decrease in urinary levels of citrate and in our study, a similar decrease was present. Succinate excretion appeared to follow the same changes in urine as citrate. Bell et al., (1991) proposed that the variability in urinary levels of some TCA cycle intermediates may be the result of changes to the acid-base balance in the kidneys. The excretion of TCA cycle intermediates via the urine depends on the rate at which they are reabsorbed into the tubular cells, which in turn depends on the pH of the kidney. Therefore, an imbalance in any of these factors will be reflected in the urinary metabolites (Nicholson et al., 1985; Bell et al., 1991).

In the present study levels of the metabolite hippurate demonstrated an age-related increase up to 68 days of age; at 84 days the levels were decreased when compared to those at 68 days, but greater at 91 days than 84 days. In the study by Williams and colleagues (2005) hippurate levels were relatively low at weeks 4 and 6 but increased dramatically at 8 weeks of age (56 days) after which there was evidence of an age-dependent decrease up to 14 weeks followed by a slight increase after this time point. In our study we also found a similar trend although the time points were slightly different. Williams et al (2005) suggested that the changes in hippurate levels at the earlier time point may be due to changes in the gut microflora of the young rat (4 weeks of age) as

the animals mature and adapt to the diet. Hippurate results from the conjugation of benzoate with glycine. Benzoate in turn, is produced by the microbial degradation of aromatic compounds in the intestine (Williams et al., 2010). Therefore, the maturation of the gut microflora is likely to be responsible for the age-related changes seen in younger animals.

Overall, the growth curve study revealed that between the age of 68 and 84 days of age, there were major changes to the serum and urine clinical chemistry, as well as in the urinary metabolite profile of the male Hanover-Wistar rat. Since the urinary testosterone levels followed the same general trend these changes are likely to be due to sexual maturation of the rat. Consequently, a sexual maturity study was carried out to determine the exact age at which the male Hanover-Wistar rat used in our studies reaches sexual maturity.

In a study by Robb and colleagues (1978) it was shown in Wistar rats that the absolute testicular weight increased rapidly up to 75 days of age, and then continued to increase although at a slower rate. The authors suggested that sexual maturity was reached between the age of 75 and 100 days based on sperm production rates and epididymal sperm numbers. A more recent study by Campion et al. (2013) reported that in the Hanover-Wistar rat the absolute testis weight increased consistently until day 70 after which it remained essentially unchanged. The authors considered the male Hanover-Wistar rat to reach sexual maturity at 70 days of age (10 weeks).

In this study relative weights for the testes peaked at day 52 and after this time point slightly decreased (Figure 5.7 A). The relative weight of the epididymides also increased with age and peaked in 77 days old rats. Histological examination of the testes and epididymides were carried out. For classification purposes in this study, sexual maturity was considered to be the stage at which mature sperm were produced and stored in the caudal epididymides. Consequently, at day 63 (9 weeks), animals were considered to be both sexually mature and fully fertile. This is in agreement with the growth curve study data in which levels of urinary testosterone were found to be significantly increased at day 68. We therefore, defined the age at which the male Hanover-Wistar reaches sexually maturity as 63 days old.

Since there was a fluctuation in urinary biomarker levels in control animals as sexual maturity occurs, it was considered of interest to determine biomarker levels in our CCl_4-

induced hepatic model in pre- and post-sexually mature animals. For this comparative study we chose animals at 7 weeks (49 days) and 13 weeks (91 days). The 7 week old animals should reflect low testosterone levels according to Figure 5.2 and those at 91 days fall just after the peak in urinary testosterone. Hepatic injury was induced in both groups of animals as determined by serum enzyme measurements and histopathology of the liver. There were great differences in the fold increase over control values for some serum parameters in the 2 groups of animals. For example, ALT levels in the serum of animals treated with 1.2 mL/kg CCl_4 were 7.91- and 33-fold increased above controls, in 7 and 13 week old rats respectively. The fold increase for AST was 3.25 and 10 for younger and older animals, respectively (Figure 5.9, Figure 5.10).

In 7 week old rats serum urea revealed a statistical significant difference and values were 1.52-fold greater in the CCl_4-treated group compared to control animals ($^{***}P<0.001$) (Table 5.5). In 13 week old rats, serum levels of albumin, urea and creatinine were all significantly increased over controls (1.7- and 1.2-fold, for urea and creatinine respectively) (Table 5.6). These results suggest a difference in the effect CCl_4 has on serum biochemistry as the animals reach sexual maturity. It would appear that the older animals (13 week old) have a greater degree of injury as shown by the larger fold increases in serum ALT and AST; however, this was not evident in the histopathology reports.

In this experiment urine samples were collected for 18 hours for 7 week old rats, and for 24 hours for 13 week old rats. However, urinary chemistry is expressed per collection period, and therefore, it is corrected for the urine volume produced. Even though collection periods were different for rats at different ages, they were the same for vehicle-treated and CCl_4-treated animals at the same age, therefore allowing comparison of urinary levels.

The main purpose of this study was to compare the effect of CCl_4-induced hepatotoxicity on the urinary metabolite profile at the 2 different ages (pre- and post-sexually maturity).

OPLS-DA models were constructed to investigate changes to urinary metabolites at the 2 different ages. When compared to control samples, treated samples from animals at 7 weeks of age had increased levels of formate, 2-oxoglutarate, citrate, creatine and succinate and decreased concentrations of hippurate, creatinine and taurine (Table 5.9).

The integral regions including the 2 triplet peaks for taurine were decreased compared to control samples, but did not show evidence of a statistically significant difference. These results generally compare to those described in the dose response study in Chapter 3 where similar changes were present with the exception of taurine which was significantly increased.

In the 13 week old rats, there was an increase in the resonances corresponding to the metabolites formate, taurine, creatine, 2-oxoglutarate and citrate, and a decrease in the levels of metabolites hippurate, creatinine and succinate following CCl_4-induced hepatic injury (Table 5.10).

Therefore, similar changes (either increase/decrease in level) were observed for most of the identified metabolites when the treated samples are compared to controls at their respective time points. However, since 7 week old animals, as shown by the previous study, have lower testosterone levels than 13 week old animals it is possible that there may be a greater degree of change for some metabolites at the 2 different rat ages (Bassil et al., 2009).

The PCA scores plot revealed no significant differences between both groups of control samples as they clustered on the same principal component (Figure 5.15). This analysis was necessary in order to prove that any difference to metabolite levels in the treated animals were mainly due to CCl_4 administration and not to increasing age.

An OPLS-DA model to identify differences between 7 week old and 13 week old rats treated with CCl_4 at 1.2 mL/kg (Figure 5.16) showed very clear clustering separation between the 2 groups. Further statistical analysis of the integral regions revealed that, following the administration of the same dose level of CCl_4 (1.2 mL/kg), older animals (13 weeks) appeared to excrete greater levels of creatinine, hippurate, creatine and taurine, whereas a decrease was noted in the urinary excretion of 2-oxoglutarate, citrate and succinate compared to 7 week old rats (Table 5.10). Therefore, this suggests that the higher testosterone levels in older rat (13 weeks) have an influence in the response to CCl_4-induced hepatic injury as reflected in changes to the urinary metabolome.

Previous studies have investigated the influence of age on the toxicological response to several model compounds for hepatic injury, and, in particular, changes to the metabolising enzymes (cytochrome P-450) with age. However, the results are often

contradictory and while some authors report a decrease in cytochrome P-450 levels with age (Rikans and Notley, 1982; Rikans, 1989), other authors suggest the absence of an age-related effect both in rats (Schmucker and Wang, 1981) and in humans (Hunt et al., 1990).

Carbon tetrachloride is metabolised by cytochrome P-450 2E1 forming the free radicals responsible for the initiation of damage. Consequently a change in CYP2E1 levels or activity with age would change the rate of metabolism of CCl_4. Wauthier et al., (2004) reported an increase in CYP2E1 activity between 3 to 8 months of age, followed by a decrease at 18 months. However, those time points are much later than in the current experiment. In another study in Long Evans rats, it was shown that hepatic CYP2E1 content decreased with age from 3 to 6 weeks and then remained constant up to 12 week old animals (Thomas et al., 1987). Najakima et al., (1987) also reported a decrease in CYP2E1 levels between 3 week old (21 days) rats and 18 week old (126 days) rats. These studies demonstrating a decrease in CYP activity have all been carried out in male rats. A similar change is not thought to occur in female rats, thus leading to the proposal of the existence of 2 forms of cytochrome P-450: a male P-450 and a female P-450 (Kamataki et al., 1983). It has also been suggested that it is the decrease in testosterone levels that leads to a decrease in the enzyme activity for the male form of cytochrome P-450. This in turn, will lead to the feminization of the male rats with regards to the cytochrome P-450 composition (Kamataki et al., 1985).

Overall, the series of investigations in this Chapter has allowed the characterisation of the sexual maturation process of the male Hanover-Wistar. An extensive ^{1}H NMR-based metabolomics investigation was carried out to determine levels of urinary metabolites with increasing age up to and just beyond sexual maturity in the male Hanover-Wistar rat.

The outcome of the present studies is that we can now confirm that the male Hanover-Wistar rat reaches sexual maturity at 63 days old. This is characterised by a significant increase in urinary testosterone levels which is thought to decrease again with age after sexual maturity is reached. Previous reports describing a possible link between testosterone and CYP activity should be considered when designing our experiments with CCl_4. Consequently, we now know that at 7 weeks old (the age of the animals used in our previous CCl_4 studies in Chapter 3), urinary testosterone levels have not yet reached the peak that they do at 9 weeks of age. Therefore, testosterone levels are

unlikely to affect our CCl_4-induced hepatic model. Hence, we will continue to use 7 week old animals for our future CCl_4 studies in Chapters 6 and 7. In Chapter 7 we will present results of a chronic dose study and we should keep in mind that there may be a change in urinary metabolites in this study as the animal ages.

CHAPTER SIX

CCl_4 time course study

Chapter 6

6.1 Introduction

In Chapter 3 we developed an acute model of hepatic injury using CCl_4 and we are confident that at dose levels of 2.0 mL/kg and below CCl_4-induced kidney injury is avoided. In Chapter 4, we determined the most sensitive biomarkers for nephrotoxicity and these will be evaluated in this Chapter to ensure CCl_4-induced nephrotoxicity does not occur. We also identified many changes to the urinary metabolome following the induction of hepatic injury as described in Chapters 3 and 5. In the current Chapter we wish to evaluate the sensitivity of these urinary metabolite markers as injury is induced and regeneration occurs. We did this by conducting a time course study.

In our Chapter 3 studies, animals were placed in metabolism cages at 6 hours post-dosing and urine samples collected for 18 hours. This means our animals had access to diet immediately after dosing. Therefore, it would be interesting to analyse the urinary metabolites identified in Chapter 3 during the period between 0 and 6 hours following CCl_4 administration. To incorporate this question into the current time course study it was decided that we should collect urine samples every 6 hours for the first 24 hours and at regular time intervals post 24 hours. Therefore, in the present study, animals were placed in metabolism cages for only 6 hours at a time during the first 24 hours and for 12 hours at later time points. In the present study animals were fasted for shorter periods of time. We should be aware, therefore, that this may affect the urinary metabolite profile in this study.

CCl_4 is known to induce a toxic response within 5 minutes of administration (Recknagel, 1967; Rao and Recknagel, 1968), and maximal injury has been reported to occur at 24-36 hours (Rao et al., 1996). Peak levels of serum enzymes ALT and AST have been reported at 36 hours post-CCl_4 administration to rats (Giffen et al., 2003; Zira et al., 2013). Rao et al., (1997) also reported maximal centrilobular necrosis at 24 to 48 hours post-dosing. Therefore, we would hope to see maximum change in the urinary metabolites at approximately 24 hours post-dosing. The liver has great regenerative ability and studies have shown complete restoration of normal liver architecture within 3 to 6 days following a single dose of 1.0 mL/kg CCl_4 (Zira et al., 2013). Urine samples in this study were collected for up to 10 days following CCl_4 administration to

demonstrate further changes to the urinary metabolome as the liver undergoes regeneration.

Thus, the primary purpose of the current Chapter was to determine if the urinary metabolites described in Chapter 3 were sensitive indicators of hepatic injury. A good biomarker will indicate early changes following a toxic insult, will be sensitive to the level of injury induced, and remain in the biofluid long enough to be detected. In addition, a return to control values would demonstrate a good response to recovery from the injury.

Urine samples collected in this study were analysed by 1D ^{1}H NMR and pattern recognition methods such as PCA to determine the response of the previously identified metabolites with time following a single dose of CCl_4 to the Hanover-Wistar rat.

6.2 Animal experimental design

Eighty male Hanover-Wistar rats (mean body weight 215.3 ± 5.14 g) were divided into 8 groups of 10 animals each (groups were labelled A to H). At time 0 hours, 5 animals in each group were dosed by gavage with corn oil (controls) (rats 1-5) and 5 animals were dosed with 2.0 mL/kg CCl_4 (rats 6-10). Immediately after dosing (0 hours), animals in group A were placed in metabolism cages for 6 hour urine collection prior to autopsy at 6 hours post-dosing. At 6-12 hours post-dosing, group B were housed in metabolism cages prior to autopsy at 12 hours. This process of urine collection for 6 hour time slots continued up to 24 hours post-dosing according to the schedule shown in Table 6.1. At all time points after 24 hours post-dosing urine was collected for 12 hours. To keep the numbers of animals used in this study to a minimum, some groups were bled from the tail-vein upon removal from the metabolism cages instead of from the abdominal aorta at autopsy.

The first 24 hours were thought to be the most crucial and therefore, these animals were killed in order to obtain tissue samples for histopathological examination.

At autopsy, blood was taken for the preparation of serum which was stored at -80 ºC until analysis. The liver and kidneys were removed and placed in fixative as described in Section 2.8.

Table 6.1 Schedule showing the time points at which animals were placed in metabolism cages for urine collection prior to collection of a blood sample. Animals were placed in metabolism cages for either 6 or 12 hour urine sample collections. At the end of the metabolism cage session a blood sample was obtained from the animal either from the tail vein (TVB) or by killing the animal and sampling from the abdominal aorta at autopsy (Terminal) (n=10).

Time point post-dosing	Animal group	Type of sample collected
0-6 hours	A	Terminal
6-12 hours	B	Terminal
12-18 hours	C	Terminal
18-24 hours	D	Terminal
24-36 hours	E	TVB
36-48 hours	F	Terminal
48-60 hours	G	TVB
60-72 hours	E	Terminal
72-84 hours	H	TVB
84-96 hours	G	Terminal
Day 6	H	TVB
Day 10	H	Terminal

6.3 Results

6.3.1 Body weights

The mean change in body weight for CCl_4-treated animals was compared to the change in body weight for the concurrent control animals (Table 6.2). At 6-12, 12-18 and 60-72 hours post-dosing, CCl_4-treated animals lost significantly less weight than the control rats ($^{*}P<0.05$). However, CCl_4-treated animals at 24-36 hour post-dosing lost more weight than the corresponding control group (11.36 and 14.96 g, for control and CCl_4-treated rats respectively; $^{*}P<0.05$).

Table 6.2 Body weight change for male Hanover-Wistar rats treated with vehicle (control) or CCl_4 at 2.0 mL/kg and sampled at various time points post-dosing. Animals were dosed by gavage and placed individually in metabolism cages for the collection of urine samples at the time points shown according to the schedule in Table 6.1. Animals had access to water but not diet while in the metabolism cages. Weight changes are shown as mean and SD of 5 animals per group. Changes in weight that are statistically different to the changes for control animals by Students' t-test are shown: $^{*}P<0.05$.

	Change in mean (SD) body weight (g)	
Time post-dosing	**0 mL/kg CCl_4**	**2.0 mL/kg CCl_4**
0-6 hours	-8.92 (1.69)	-9.76 (1.72)
6-12 hours	-10.18 (2.83)	-6.50* (2.07)
12-18 hours	-12.20 (1.92)	-8.66* (2.44)
18-24 hours	-10.94 (1.67)	-13.12 (1.33)
24-36 hours	-11.36 (1.15)	-14.96* (2.24)
36-48 hours	-15.52 (2.87)	-13.12 (6.72)
48-60 hours	-13.76 (0.68)	-11.26 (4.03)
60-72 hours	-15.04 (1.28)	-11.84* (2.08)
72-84 hours	-13.32 (0.79)	-12.72 (0.83)
84-96 hours	-15.00 (2.58)	-13.72 (1.09)
Day 6	-16.50 (1.51)	-16.50 (2.08)
Day 10	-13.76 (1.14)	-14.40 (2.22)

6.3.2 Liver weights

Relative liver weights for CCl_4-treated rats were significantly increased over the respective controls up to 96 hours (day 4) post-dosing (Figure 6.1 A). At 24 hours post-dosing, there was a 1.4-fold increase over concurrent controls ($^{***}P<0.001$) which was the maximum fold difference observed. By day 10 post-dosing, liver weights from CCl_4-treated animals were similar to controls.

6.3.3 Kidney weights

The mean relative kidney weights for rats treated with CCl_4 were similar to control at all time points, except for 18 hours post-dosing when they were significantly decreased (5.74 and 5.39 g/kg BW, respectively; $^{*}P<0.05$) (Figure 6.1 B).

A

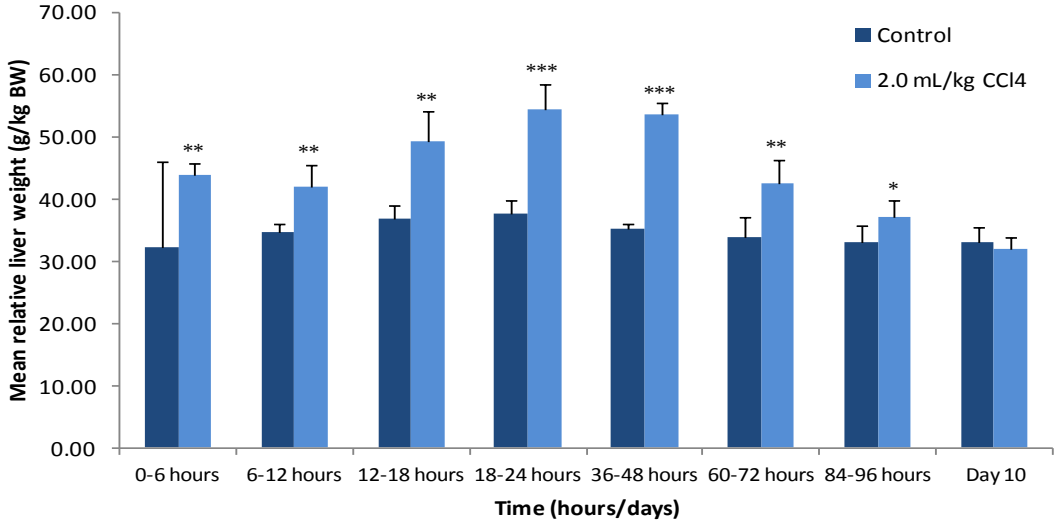

B

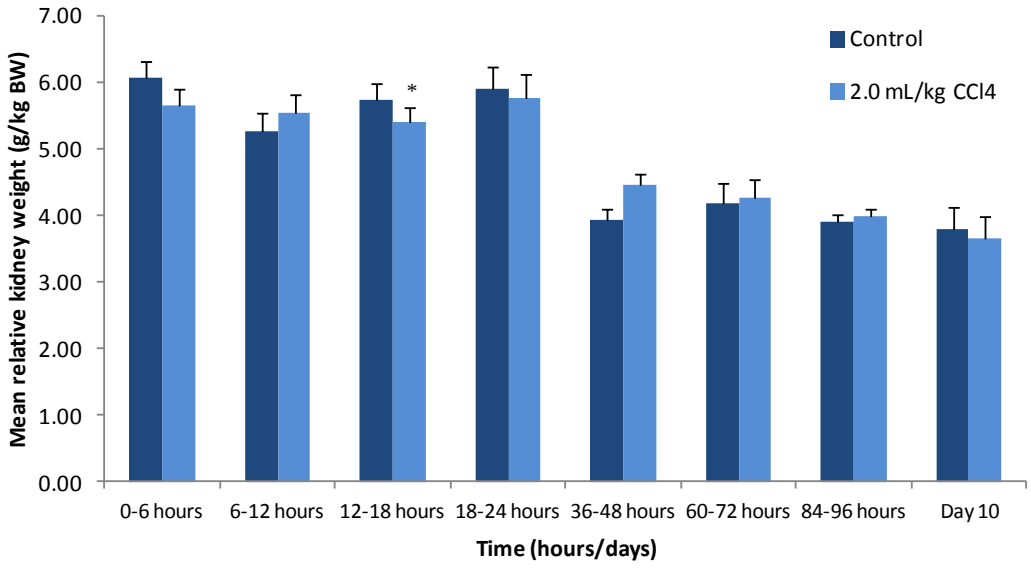

Figure 6.1 Relative liver (A) and kidney (B) weights from male Hanover-Wistar rats treated with vehicle (control) or CCl_4 at 2.0 mL/kg and sampled at various time points post-dosing. Animals were dosed by gavage. At the time points shown, animals were killed, livers and kidneys were removed and weighed as described in Section 6.2. The kidney weight was expressed as the mean of the left and right kidneys. Results are shown as mean organ weight per kg body weight (BW) with SD indicated by vertical bars of 5 animals per group. Relative organ weights that differ significantly from controls at the respective time point by Students' t-test are shown: $^{*}P<0.05$; $^{**}P<0.01$; $^{***}P<0.001$.

6.3.4 Serum clinical chemistry

Clinical chemistry parameters including ALT, AST, GLDH, ALP, TIMP-1, MCP1, A2M, AGP, lipocalin-2, urea, creatinine, albumin, glucose and total protein were measured in the serum from vehicle-treated (control) and CCl_4-treated animals in this study.

Serum ALT was significantly raised over concurrent controls at 12 hours post-dosing, reaching a peak between 12-24 hours. At 18 hours post-dosing there was a 72-fold increase in ALT levels ($^{*}P<0.05$) (Figure 6.2 A), and serum ALT remained significantly increased over control until 48 hours post-dosing. By day 4 (96 hours post-dosing), control and CCl_4-treated ALT levels were similar.

AST was statistically increased at the first time point (6 hours post-dosing) (10-fold; $^{*}P<0.05$) (Figure 6.2 B). Levels of AST increased steadily up to 24 hours post-dosing when a maximum serum level was reached (4944.00 U/L for CCl_4-treated animals and 101.80 U/L for control rats; $^{*}P<0.05$). After 48 hours, the AST values began to fall and were back to control levels.

Mean GLDH was significantly increased at 6 hours post-dosing (10-fold increase; $^{***}P<0.001$). Levels of GLDH peaked at 48 hours when there was a 243-fold increase over concurrent controls; however this was not statistically significant. After 48 hours there appeared to be a decrease in GLDH levels with time back to control levels at day 10 (Figure 6.2 C).

Serum ALP was significantly increased over controls in CCl_4-treated animals at 12 hours post-dosing reaching peak levels at 18 hours (938.20 U/L compared to a control mean value of 440.20 U/L, $^{*}P<0.05$) (Table 6.3, Table 6.4). After 18 hours, ALP levels began to fall and were similar to controls by day 10 post-dosing.

At 24 to 36 hours post-dosing serum ALP, AST, GLDH and ALP levels for CCl_4-treated animals are the means of 4 rats, since there was not enough serum sample from 1 animal to measure the levels of these enzymes.

TIMP-1 serum levels were significantly increased above controls at all time points between 6 and 60 hours post-dosing. Peak values of TIMP-1 were reached at 48 hours

post-dosing, when an approximate 14-fold increase over controls was observed. TIMP-1 levels returned to control values by day 6 post-dosing (Table 6.3, Table 6.4).

Serum A2M mean values were significantly greater than controls at 12, 24, 72 and 84 hours and at days 6 and 10 post-dosing (Table 6.3, Table 6.4). The greatest fold-increase was observed at 84 hours post-dosing (33.40 and 79.20 mg/L for controls and CCl_4-treated animals respectively; $^{*}P<0.05$).

MCP1 serum levels were almost 2-fold greater than concurrent controls at 6 hours post-dosing and levels remained significantly elevated up to 36 hours. The greatest fold increase was recorded at 24 hours post-dosing, when an approximate 29-fold increase was seen (7.40 and 211.80 µmol/L, respectively; $^{**}P<0.01$) (Table 6.3, Table 6.4). MCP1 levels were similar to controls at 72 hours post-dosing.

Mean AGP levels were significantly greater than control values between 18 and 96 hours post-dosing. Serum AGP increased up to 48 hours post-dosing reaching a peak of approximate 10-fold increase over control (65.40 and 614.00 mg/L; $^{**}P<0.01$). By day 10, AGP levels had returned to control values (Table 6.3, Table 6.4).

Serum lipocalin-2 was increased over controls from 6 hours post-dosing, however, values were only significantly different from control at 12, 24, 48, 60 and 72 hours post-dosing. Levels peaked at 48 hours with a 27-fold increase over controls (37.80 and 1021.25 µg/L, respectively $^{*}P<0.05$). By day 6, lipocalin-2 was similar in control and CCl_4-treated animals.

Levels of TIMP-1, MCP and lipocalin-2 at 24 to 36 hours, are the means of 3 control and 3 CCl_4-treated animals, whereas levels of A2M and AGP are the means of 4 control and 3 CCl_4-treated animals as there was not enough sample from the missing animals in each group to carry out the serum assays. Similarly, at 36 to 48 hours the values for serum TIMP-1, A2M, MCP, AGP and lipocalin-2 are the means of 4 CCl_4-treated animals.

To assess the possibility of kidney injury, mean urea, creatinine, albumin, glucose and total protein were also measured in the serum of all animals in this study (Table 6.3, Table 6.4). At 24 to 36 hours post-dosing values for urea, creatinine, albumin, glucose and total protein are the means of 4 CCl_4-treated animals.

Urea levels were significantly raised over concurrent controls as early as 6 hours post-dosing (1.44-fold increase). Levels reached a maximum at 48 hours and after this time point serum levels were similar in control and CCl_4-treated animals. Serum creatinine was significantly increased in CCl_4-treated animals at 18, 24, 36, 48 and 60 hours post-dosing (Table 6.3, Table 6.4). The greatest fold difference was observed at 48 hours post-dosing (1.6-fold increase) ($^{**}P<0.01$).

Serum albumin was significantly increased in CCl_4-treated animals at 12 hours post-dosing but no other differences were apparent (Table 6.3, Table 6.4).

Glucose levels, however, were significantly decreased in the serum of CCl_4-treated animals between 6 and 24 hours post-dosing. At 36 hours, glucose was increased in the serum from CCl_4-treated animals, before showing a decrease at 48 and 60 hours post-dosing. By 84 hours post-dosing serum glucose levels in CCl_4-treated animals were similar to control.

Total protein levels in the urine were significantly increased over concurrent controls at 12 hours post-dosing (1.03-fold increase, $^{*}P<0.05$), but at the following time point (12-18 hours post-dosing) levels were significantly decreased compared to controls at the same time point ($^{*}P<0.05$).

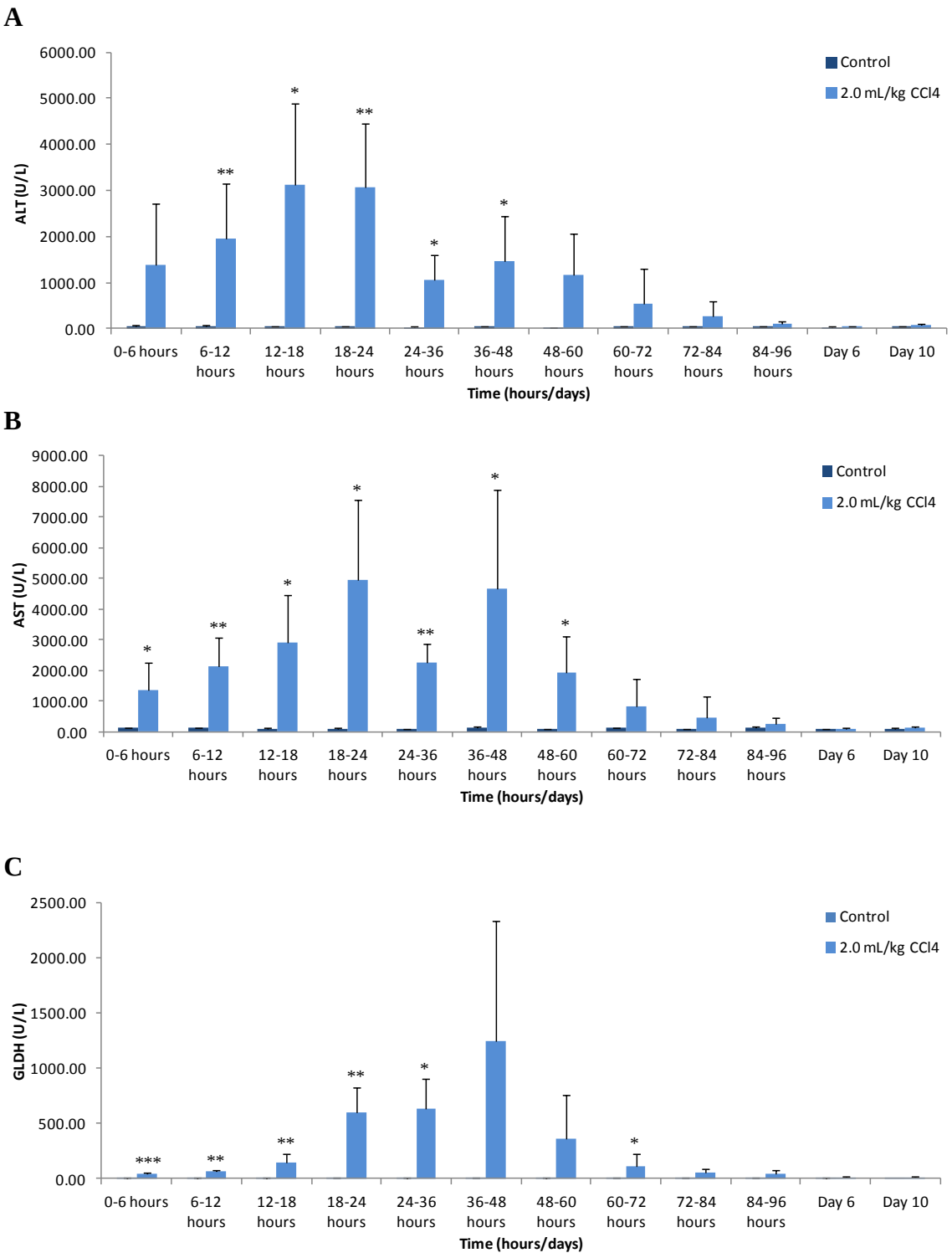

Figure 6.2 Serum ALT, AST and GLDH levels for male Hanover-Wistar rats treated with vehicle (control) or CCl_4 at 2.0 mL/kg and sampled at various time points post-dosing. Animals were dosed by gavage and sampled at the time points shown according to the schedule in Table 6.1. Serum was collected as described in Section 6.2 and enzymes were assayed as described in Section 2.7. Values are means with SD indicated by vertical bars of 5 animals per group, except at 24 to 36 hours post-dosing where n=4. Values that differ significantly from controls by Students' t-test are shown: $^{*}P<0.05$; $^{**}P<0.01$; $^{***}P<0.001$.

Table 6.3 Serum clinical chemistry for male Hanover-Wistar rats treated with vehicle (control) or CCl_4 at 2.0 mL/kg and sampled at various time points between 6 and 48 hours post-dosing. Animals were dosed by gavage and sampled at the time points shown according to the schedule in Table 6.1. Serum was collected as described in Section 6.2 and enzymes were assayed as described in Section 2.7. Values are the means and SD of 5 animals per group except at 24 to 36 hours post-dosing where TIMP-1, MCP and lipocalin-2 values are the means of 3 control and 3 CCl_4-treated animals, and A2M and AGP values are the means of 4 controls and 3 CCl_4-treated animals. At 36 to 48 hours post-dosing, TIMP-1, A2M, MCP, AGP and lipocalin-2 are the means of 4 CCl_4-treated animals. Values that differ significantly from controls by Students' t-test are shown: $^{*}P<0.05$; $^{**}P<0.01$; $^{***}P<0.001$. C: control; T: CCl_4-treated rats.

Time (hours)		Serum parameters										
		ALP (U/L)	**TIMP-1 (µg/L)**	**A2M (mg/L)**	**MCP1 (µg/L)**	**AGP (mg/L)**	**Lipocalin-2 (µg/L)**	**Urea (mmol/L)**	**Creatinine (µmol/L)**	**Albumin (g/L)**	**Glucose (mmol/L)**	**Total protein (g/L)**
0-6 hours	C	590.00 (217.19)	5.60 (1.34)	34.60 (8.08)	11.20 (1.48)	61.80 (7.22)	34.00 (5.05)	6.44 (1.00)	21.60 (1.14)	34.80 (1.30)	9.46 (0.63)	56.20 (3.11)
	T	783.80 (244.92)	18.00* (7.00)	34.80 (8.20)	23.40* (8.93)	83.40 (19.78)	77.00 (53.63)	9.28** (1.12)	23.00 (2.55)	35.20 (1.10)	7.28** (0.97)	55.40 (1.67)
6-12 hours	C	405.80 (110.03)	6.00 (2.00)	18.60 (2.51)	9.00 (1.22)	61.00 (14.09)	38.00 (7.14)	6.68 (0.74)	25.00 (2.00)	33.40 (0.89)	8.48 (0.30)	54.20 (0.84)
	T	560.80* (78.66)	20.80*** (3.96)	26.20* (5.54)	28.00* (9.95)	70.60 (13.72)	102.60* (58.82)	8.44** (0.60)	25.20 (2.59)	34.80* (0.84)	7.02** (0.51)	55.60* (0.55)
12-18 hours	C	440.40 (106.00)	5.60 (1.67)	21.60 (7.96)	8.00 (1.22)	80.40 (21.10)	34.40 (4.61)	6.06 (0.72)	22.80 (2.59)	33.40 (0.89)	10.29 (0.70)	54.20 (1.30)
	T	938.20* (340.23)	33.75* (12.39)	30.00 (9.92)	51.00* (23.47)	108.40 (50.56)	269.00 (383.47)	8.32** (0.80)	32.40* (5.90)	34.20 (0.84)	6.81*** (0.70)	52.20* (0.84)
18-24 hours	C	456.60 (10.67)	6.00 (1.22)	24.40 (6.80)	7.40 (1.14)	66.60 (12.30)	30.00 (2.92)	6.00 (0.87)	21.20 (1.64)	33.20 (0.84)	9.39 (1.09)	52.40 (1.14)
	T	839.80* (215.27)	85.40*** (27.92)	35.60* (6.88)	211.80** (83.45)	365.20** (114.62)	867.20* (455.53)	9.52*** (0.81)	37.40** (5.90)	34.60 (1.34)	6.69** (0.54)	54.80 (2.59)
24-36 hours	C	385.60 (110.92)	7.33 (1.15)	32.00 (8.52)	8.67 (1.53)	49.50 (6.61)	47.33 (10.60)	4.12 (0.54)	20.80 (0.45)	34.20 (1.48)	6.76 (1.21)	53.80 (1.92)
	T	686.50* (204.45)	75.33* (19.86)	53.00 (14.93)	157.33** (24.79)	457.67** (116.07)	432.33 (261.78)	7.15** (1.28)	28.75* (3.59)	35.50 (1.73)	8.50* (0.38)	55.50 (3.42)
36-48 hours	C	403.40 (139.70)	7.20 (1.64)	41.40 (12.54)	8.00 (0.71)	65.40 (16.56)	37.80 (4.60)	7.62 (0.59)	23.60 (1.67)	32.40 (2.07)	7.89 (0.88)	50.60 (3.78)
	T	756.00* (288.38)	100.50* (41.97)	82.75 (38.06)	94.75 (70.23)	614.00** (127.57)	1021.25* (560.15)	11.14* (2.80)	37.60** (8.79)	33.20 (3.03)	5.85** (0.70)	52.80 (4.87)

ALP: alkaline phosphatase; TMIP-1: tissue inhibitor of matrix metalloproteinase; A2M: alpha-2 macroglobulin; MCP 1: monocyte chemoattractant factor 1; AGP: alpha-1 acid glycoprotein.

Table 6.4 Serum clinical chemistry for male Hanover-Wistar rats treated with vehicle (control) or CCl_4 at 2.0 mL/kg and sampled at various time points between 48 hours and day 10 post-dosing. Animals were dosed by gavage and sampled at the time points shown according to the schedule in Table 6.1. Serum was collected as described in Section 6.2 and enzymes were assayed as described in Section 2.7. Values are the means and SD of 5 animals per group except at 24 to 36 hours post-dosing where values are the means of 4 CCl_4-treated animals. Values that differ significantly from controls by Students' t-test are shown: $^{*}P<0.05$; $^{**}P<0.01$; $^{***}P<0.001$. C: control; T: CCl_4-treated rats.

Time (hours/days)		Serum parameters										
		ALP (U/L)	TIMP-1 (µg/L)	A2M (mg/L)	MCP1 (µg/L)	AGP (mg/L)	Lipocalin-2 (µg/L)	Urea (mmol/L)	Creatinine (µmol/L)	Albumin (g/L)	Glucose (mmol/L)	Total protein (g/L)
48-60 hours	C	327.00 (43.10)	6.40 (1.95)	41.20 (14.31)	8.60 (1.14)	60.20 (10.94)	40.20 (3.27)	5.52 (0.77)	21.40 (1.14)	34.60 (1.52)	7.64 (0.47)	54.40 (2.19)
	T	669.00 (314.66)	54.00** (19.13)	77.80 (71.75)	38.60 (32.76)	404.00** (119.42)	400.80* (273.02)	6.66 (2.16)	27.20** (2.77)	34.40 (2.30)	5.52** (0.72)	53.60 (1.67)
60-72 hours	C	393.20 (103.74)	6.00 (1.58)	30.60 (11.26)	7.00 (1.58)	45.20 (7.19)	42.20 (6.46)	7.44 (0.62)	23.40 (2.41)	34.20 (1.30)	8.19 (1.02)	53.80 (1.64)
	T	616.60 (258.83)	27.00 (20.43)	55.20* (18.06)	9.80 (4.21)	274.80** (97.68)	211.80* (114.94)	7.74 (1.32)	25.60 (3.05)	35.40 (1.14)	6.83 (1.08)	55.60 (1.67)
72-84 hours	C	427.60 (104.18)	6.40 (1.52)	33.40 (8.96)	8.20 (1.48)	54.60 (4.16)	46.40 (2.30)	6.00 (0.64)	20.80 (1.64)	36.00 (1.58)	7.39 (1.40)	56.80 (2.59)
	T	623.80 (297.58)	15.40 (8.73)	79.20* (36.96)	9.00 (3.46)	249.80* (138.59)	237.80 (211.85)	5.64 (1.44)	23.40 (2.61)	34.40 (2.07)	7.90 (0.82)	55.00 (3.74)
84-96 hours	C	325.60 (32.78)	5.80 (1.64)	32.60 (16.52)	7.60 (0.89)	73.00 (23.48)	44.00 (2.74)	7.46 (0.39)	24.20 (1.48)	34.40 (1.14)	7.06 (1.04)	55.00 (1.41)
	T	400.20 (88.86)	9.60* (2.97)	61.40 (46.60)	7.40 (1.34)	151.80* (49.09)	90.20 (67.63)	6.34 (1.10)	23.00 (1.41)	34.40 (1.14)	7.04 (0.39)	54.80 (1.92)
Day 6	C	391.40 (85.98)	6.60 (1.82)	27.20 (5.72)	9.00 (0.71)	61.80 (11.54)	44.60 (6.50)	7.76 (1.10)	22.20 (4.76)	33.20 (1.30)	8.74 (0.54)	53.60 (2.61)
	T	432.20 (85.83)	7.40 (1.34)	47.20* (12.76)	7.80 (3.70)	89.80 (27.22)	41.60 (6.58)	7.02 (1.39)	21.60 (2.30)	34.60 (2.51)	8.41 (1.81)	54.80 (3.27)
Day 10	C	369.00 (75.92)	5.40 (1.34)	20.00 (5.29)	8.40 (0.89)	54.20 (9.15)	39.40 (3.44)	7.94 (0.99)	23.60 (2.41)	34.80 (1.10)	8.94 (0.26)	56.00 (2.83)
	T	387.80 (59.74)	6.20 (0.84)	27.60* (4.28)	8.00 (1.58)	61.20 (9.15)	34.60 (4.34)	8.80 (0.75)	21.80 (1.30)	35.00 (1.41)	9.33 (0.90)	55.20 (1.64)

ALP: alkaline phosphatase; TMIP-1: tissue inhibitor of matrix metalloproteinase; A2M: alpha-2 macroglobulin; MCP 1: monocyte chemoattractant factor 1; AGP: alpha-1 acid glycoprotein.

6.3.5 Urine clinical chemistry

Urine samples generated in this study were analysed for markers of kidney toxicity (Table 6.5, Table 6.6) as measured in Chapter 4.

Levels of urinary α-GST in CCl_4-treated animals did not show evidence of a statistically significant difference compared to controls during the first 24 hours post-dosing but at 36 hours there was a significant decrease (Table 6.5). At 48 hours after the CCl_4 administration, mean urinary α-GST was approximately 12-fold increased over controls, but this was not statistically significant. Urinary GST Yb1 was significantly increased at 12 hours post-dosing and then showed a non-significant increase in levels at 48 hours (Table 6.5, Table 6.6).

KIM-1 was significantly increased at 12 hours and at 84 hours post-dosing but was similar to control at all other time points (Table 6.5, Table 6.6). Clusterin levels in the urine were significantly increased in CCl_4-treated animals compared to control at 36 and 48 hours post-dosing. Levels of clusterin were then lower than controls at 84 hours post-dosing and at day 6 of the study (Table 6.5, Table 6.6).

Osteopontin showed no evidence of a CCl_4-administration related effect at the earlier time points but urinary levels were significantly increased at 36 hours post-dosing. At 48 to 60 hours post-dosing mean urinary values in CCl_4-treated animals were approximately 5 times greater than control values (58.00 and 12.00 ng/c.p. for CCl_4-treated and control animals respectively; $^{*}P<0.05$). Urinary lipocalin-2 was increased over controls in CCl_4-treated animals as early as 12 hours post-dosing (2.4-fold) and by 48 hours post-dosing the fold increase was 107 for CCl_4-treated animals compared to concurrent controls (2242.00 and 241574.00 ng/c.p. for control and treated animals respectively; $^{**}P<0.01$) (Table 6.5, Table 6.6). Lipocalin-2 levels were similar to controls by day 6 of the study.

Urinary creatinine was significantly decreased by 1.8-fold when compared to controls at 6 hours post-dosing ($^{*}P<0.05$). At 72 hours post-dosing mean creatinine levels were also significantly decreased in CCl_4-treated animals ($^{**}P<0.01$) but at all other time points creatinine levels were similar to controls (Table 6.5, Table 6.6).

Urinary total protein concentration was lower in CCl_4-treated animals than in control at all time points except at 48 hours post-dosing when a 3-fold increase was observed

(Table 6.5, Table 6.6). However, this increase was not statistically significant due to the large standard deviation within the group.

Albumin was significantly increased in CCl_4-treated animals when compared to controls at intermittent time points (12, 48 and 60 hours post-dosing). Urinary excretion of albumin was greatest at 48 hours post-dosing (1246.20 ng/c.p. over 44.00 ng/c.p. for CCl_4-treated and control rats respectively; $^{*}P<0.05$). However, at 84 hours, and at day 6, urinary albumin levels were significantly decreased compared to controls ($^{**}P<0.01$ and $^{*}P<0.05$, respectively) (Table 6.5, Table 6.6).

Urinary glucose did not show evidence of a CCl_4 treatment-related effect whereas urine volume was significantly increased over controls in CCl_4-treated animals at 24 and 48 hours post-dosing ($^{*}P<0.05$).

Table 6.5 Urinary clinical chemistry for male Hanover-Wistar rats treated with vehicle (control) or CCl_4 at 2.0 mL/kg and sampled at various time points between 6 and 48 hours post-dosing. Animals were dosed by gavage and sampled at the time points shown according to the schedule in Table 6.1. Urine was collected as described in Section 6.2 and clinical parameters were assayed as described in Section 2.7. Values are the means and SD of 5 animals per group. Values that differ significantly from controls by Students' t-test are shown: $^{*}P<0.05$; $^{**}P<0.01$; $^{***}P<0.001$. C: control; T: CCl_4-treated rats. c.p. = collection period, 6 hours (6-24 hours) and 12 hours (24 hours-day 10).

Time (hours/days)		Urinary parameters										
		α-GST (ng/c.p.)	GST Yb1 (ng/c.p.)	Clusterin (ng/c.p.)	KIM-1 (ng/c.p.)	Osteopontin (ng/c.p.)	Lipocalin-2 (ng/c.p.)	Creatinine (µmol/c.p.)	Total protein (mg/c.p.)	Albumin (mg/c.p.)	Glucose (µmol/c.p.)	Volume (mL)
0-6 hours	C	72.00 (90.11)	10.00 (0.00)	10.20 (6.02)	4.40 (1.14)	28.00 (29.50)	1086.00 (359.35)	16.40 (4.04)	2.64 (0.69)	55.00 (25.90)	2.60 (0.89)	7.40 (4.28)
	T	42.00 (21.68)	8.00 (4.47)	9.60 (5.90)	2.60 (1.82)	10.00 (7.07)	394.00** (157.00)	9.00* (2.83)	0.90** (0.32)	27.60 (19.31)	1.60 (0.55)	6.80 (3.56)
6-12 hours	C	22.00 (10.95)	8.00 (8.37)	13.80 (7.89)	3.60 (1.52)	36.67 (15.28)	636.00 (111.94)	14.80 (4.66)	2.30 (0.90)	25.00 (9.75)	1.80 (0.84)	8.20 (6.02)
	T	112.00 (98.08)	38.00* (14.83)	5.40 (1.67)	6.20* (1.30)	24.00 (5.48)	1544.00*** (398.79)	20.40 (4.51)	1.32* (0.46)	145.40* (125.89)	3.20 (1.64)	5.40 (1.67)
12-18 hours	C	50.00 (35.36)	10.00 (0.00)	20.80 (8.07)	2.00 (1.22)	24.00 (18.17)	620.00 (374.63)	12.80 (2.49)	2.40 (0.74)	47.20 (38.43)	2.20 (0.45)	8.80 (2.59)
	T	98.00 (84.08)	18.00 (8.37)	14.40 (6.35)	3.60 (1.95)	44.00 (20.74)	2118.00 (1300.68)	16.80 (4.76)	0.78** (0.31)	51.60 (21.82)	3.00 (1.22)	14.40 (6.35)
18-24 hours	C	86.00 (66.18)	10.00 (7.07)	14.80 (12.91)	3.80 (1.48)	40.00 (30.00)	916.00 (487.83)	14.40 (3.91)	2.98 (2.08)	36.06 (34.98)	2.40 (0.89)	7.46 (3.27)
	T	60.00 (28.28)	26.00 (18.17)	49.60 (41.13)	4.20 (2.28)	40.00 (20.00)	10052.00** (6747.47)	17.60 (2.61)	1.04* (0.33)	82.60 (82.30)	2.60 (0.55)	24.00* (14.98)
24-36 hours	C	514.00 (257.45)	26.00 (15.17)	10.40 (3.85)	6.80 (0.84)	8.00 (4.47)	1314.00 (382.79)	27.80 (4.32)	2.46 (0.80)	50.00 (12.81)	3.20 (0.45)	7.60 (1.67)
	T	82.00* (105.69)	18.00 (8.37)	22.00* (9.59)	6.20 (2.59)	30.00* (7.07)	14098.00** (13245.64)	21.40 (5.41)	1.14** (0.29)	70.80 (44.53)	2.60 (0.55)	10.80 (3.03)
36-48 hours	C	262.00 (353.37)	170.00 (318.98)	21.40 (8.35)	5.40 (1.52)	18.00 (8.37)	2242.00 (592.22)	20.60 (4.39)	2.26 (0.62)	44.00 (32.89)	2.80 (1.10)	13.00 (6.00)
	T	3106.00 (4290.29)	1332.00 (1739.82)	75.80* (64.41)	4.40 (2.30)	54.00* (31.30)	241574.00** (223697.62)	20.60 (1.52)	6.90 (6.97)	1246.20* (1337.29)	1.80 (0.45)	25.80* (6.26)

α-GST: glutathione S-transferase; GST Yb1: glutathione S-transferase Yb1; KIM-1: kidney injury molecule-1.

Table 6.6 Urinary clinical chemistry for male Hanover-Wistar rats treated with vehicle (control) or CCl_4 at 2.0 mL/kg and sampled at various time points between 48 hours and day 10 post-dosing. Animals were dosed by gavage and sampled at the time points shown according to the schedule in Table 6.1. Urine was collected as described in Section 6.2 and clinical parameters were assayed as described in Section 2.7. Values are the means and SD of 5 animals per group. Values that differ significantly from controls by Students' t-test are shown: $^{*}P<005$; $^{**}P<0.01$; $^{***}P<0.001$. C: control; T: CCl_4-treated rats. c.p. = collection period, 12 hours (24 hours-day 10).

Time (hours/days)		Urinary parameters										
		α-GST (ng/c.p.)	**GST Yb1 (ng/c.p.)**	**Clusterin (ng/c.p.)**	**KIM-1 (ng/c.p.)**	**Osteopontin (ng/c.p.)**	**Lipocalin-2 (ng/c.p.)**	**Creatinine (µmol/c.p.)**	**Total protein (mg/c.p.)**	**Albumin (mg/c.p.)**	**Glucose (µmol/c.p.)**	**Volume (mL)**
48-60 hours	C	462.00 (423.52)	68.00 (87.01)	14.80 (8.44)	6.80 (3.70)	12.00 (8.37)	1584.00 (732.69)	26.00 (12.02)	3.02 (1.55)	93.20 (31.92)	3.40 (1.67)	8.80 (4.15)
	T	56.00* (33.62)	40.00 (15.81)	13.80 (7.36)	9.60 (2.79)	58.00* (33.47)	133698.00*** (150960.30)	27.80 (5.81)	1.70 (0.23)	144.40* (82.43)	2.40 (0.55)	11.60 (5.77)
60-72 hours	C	138.00 (180.47)	28.00 (13.04)	45.20 (14.25)	6.20 (1.48)	34.00 (11.40)	2026.00 (1136.06)	24.40 (3.91)	2.02 (0.41)	46.00 (23.24)	2.80 (0.45)	17.20 (4.15)
	T	134.00 (104.31)	22.00 (10.95)	40.40 (10.24)	5.60 (1.52)	26.00 (8.94)	11462.00** (10174.38)	15.60** (3.76)	0.88** (0.25)	31.20 (22.52)	1.40** (0.55)	17.20 (5.93)
72-84 hours	C	126.00 (59.41)	14.00 (8.94)	18.80 (7.43)	6.00 (1.87)	26.00 (8.94)	1786.00 (441.28)	22.40 (4.83)	3.76 (1.48)	74.80 (27.11)	3.20 (1.30)	9.20 (2.28)
	T	50.00* (23.45)	28.00 (29.50)	16.00* (15.68)	9.00* (1.22)	44.00 (18.17)	46002.00* (59102.75)	27.20 (2.77)	1.30** (0.24)	24.60** (6.99)	2.20 (0.84)	9.40 (1.34)
84-96 hours	C	76.00 (40.37)	26.00 (13.42)	37.40 (6.47)	5.60 (0.89)	34.00 (5.48)	1476.00 (441.17)	22.40 (5.68)	2.28 (0.83)	34.80 (23.39)	2.40 (0.89)	16.00 (6.44)
	T	194.00* (70.92)	88.00 (124.78)	42.20 (39.58)	8.00 (6.16)	18.00** (4.47)	6476.00** (5561.73)	21.20 (2.28)	0.98** (0.13)	26.40 (19.57)	2.40 (0.55)	10.60 (3.58)
Day 6	C	44.00 (15.17)	22.00 (4.47)	49.20 (11.63)	7.40 (1.67)	40.00 (10.00)	2170.00 (617.74)	30.40 (7.23)	3.98 (1.06)	86.00 (45.25)	4.40 (1.52)	17.20 (4.38)
	T	66.00 (61.07)	116.00* (138.31)	29.60* (7.80)	6.20 (1.48)	32.00 (21.68)	2036.00 (469.61)	23.80 (4.87)	1.42** (0.53)	24.80* (10.73)	2.80* (0.84)	14.00 (4.90)
Day 10	C	44.00 (15.17)	24.00 (8.94)	18.20 (12.58)	3.20 (1.10)	8.00 (4.47)	594.00 (244.81)	17.20 (5.54)	2.64 (0.54)	36.20 (17.78)	0.40 (0.89)	12.20 (3.35)
	T	66.00 (61.07)	14.00 (5.48)	10.20 (8.11)	3.40 (3.21)	4.00 (5.48)	620.00 (687.86)	13.40 (10.04)	1.42 (1.06)	18.00 (15.18)	0.40 (0.55)	9.60 (2.41)

α-GST: glutathione S-transferase; GST Yb1: glutathione S-transferase Yb1; KIM-1: kidney injury molecule-1.

6.3.6 Histopathology

In this study, liver and kidney samples were analysed from 3 randomly chosen CCl_4-treated animals and 1 control animal at each time point due to the large number of samples generated (Figure 6.3).

At the first time point (6 hours post-dosing) there was vacuolation of hepatocytes, mainly in the midzonal area. By 12 hours post-dosing, the eosinophilic staining had increased in intensity, which indicates early cellular degeneration. At 18 hours post-dosing there was clear evidence of degeneration or necrosis of these centrilobular cells. The degeneration and necrosis had become more widespread by 24 hours post-dosing and there was also evidence of early inflammatory cell infiltration in the centrilobular zone. By 48 hours, there was a marked increase in centrilobular mixed inflammatory cells infiltration and mitotic midzonal hepatocytes were also evident.

At 72 hours a very small number of necrotic hepatocytes were still present and there was less centrilobular inflammatory cell infiltrate. However, an increase in the number of fibroblasts was apparent. By day 10 post-dosing the architecture of the liver had returned to near-normal.

In the kidneys of some CCl_4-treated animals, changes were similar across all time points and consisted of minimal or trace vacuolation of proximal tubular epithelium.

A

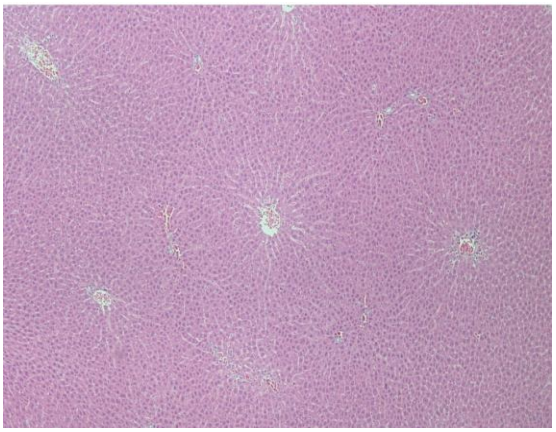

B

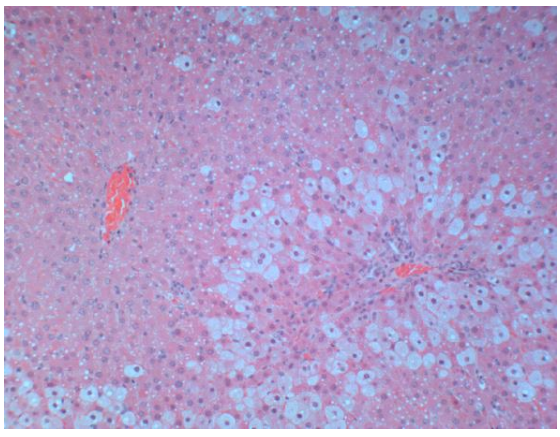

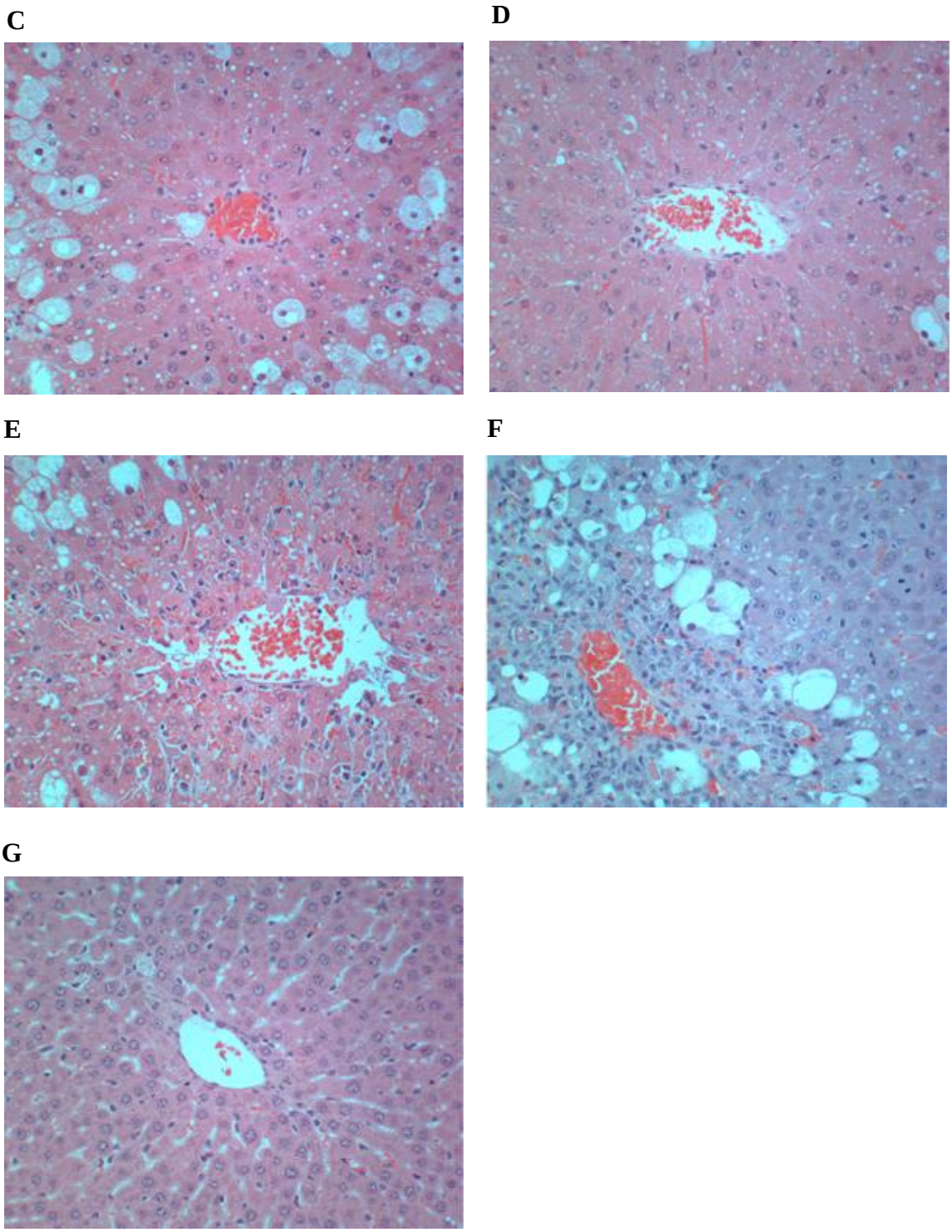

Figure 6.3 Histology of liver sections from male Hanover-Wistar rats treated with vehicle (control) or CCl_4 at 2.0 mL/kg and sampled at various time points post-dosing. H&E staining. Rats were treated with vehicle or CCl_4 and autopsied at 6, 12, 18, 24, 48 hours and at day 10 post-dosing. At autopsy, liver samples were collected and processed for histopathological examination as described in Section 2.8. (A) control liver: central (c) and portal vein (p) (original magnification, x 40); (B) CCl_4-treated rat at 6 hours post-dosing: midzonal vacuolation (original magnification, x 200); (C) CCl_4-treated rat at 12 hours post-dosing: degenerative changes in centrilobular hepatocytes (original magnification, x 200); (D) CCl_4-treated rat at 18 hours post-dosing: degeneration and necrosis of centrilobular hepatocytes (original magnification, x 200); (E) CCl_4-treated rat at 24 hours post-dosing: extensive degeneration and necrosis of centrilobular hepatocytes (original magnification, x 200); (F) CCl_4-treated rat at 48 hours post-dosing: necrosis of centrilobular hepatocytes with cellular infiltration and midzonal mitotic hepatocytes (original magnification, x 200); (G) CCl_4-treated rat at day 10 post-dosing: near normal architecture (original magnification, x 200).

6.3.7 1D ^{1}H NMR spectrometry

In this study we wished to investigate the pattern of urinary metabolites as hepatic injury occurs and with subsequent recovery from the injury over a period of 10 days post-dosing.

Due to technical problems with the NMR instrument urine samples collected between 24 and 48 hours post-dosing were not analysed by 1D ^{1}H NMR. All other samples were analysed for the construction of a temporal map of urinary metabolite changes. A PCA scores plot of all these samples did not allow visualisation of a pattern of change since the high number of samples did not allow good separation on the scores plot (data not shown).

A PCA model for all urine samples from CCl_4-treated animals in this study revealed the presence of outliers located outside the Hotelling's T2 ellipse. Of these outliers, 3 were above the 99 % T2 critical value in the Hotelling's T2 range plot (1 sample at 12-18 hours, 1 sample at 48-60 hours, and 1 sample at day 10 post-dosing). The spectra for these data points were visually inspected and it was considered that spectra acquisition was compromised either due to poor water suppression or problems with the NMR instrument. The remaining samples were not excluded from the model. The PCA scores plot for this model is shown in Figure 6.4.

The great number of samples included in this PCA model did not allow the identification of a trajectory pattern since many points overlapped and did not cluster well. Therefore, a new PCA model was constructed using only the average spectrum for each group of control and CCl_4-treated samples in the study (Figure 6.5).

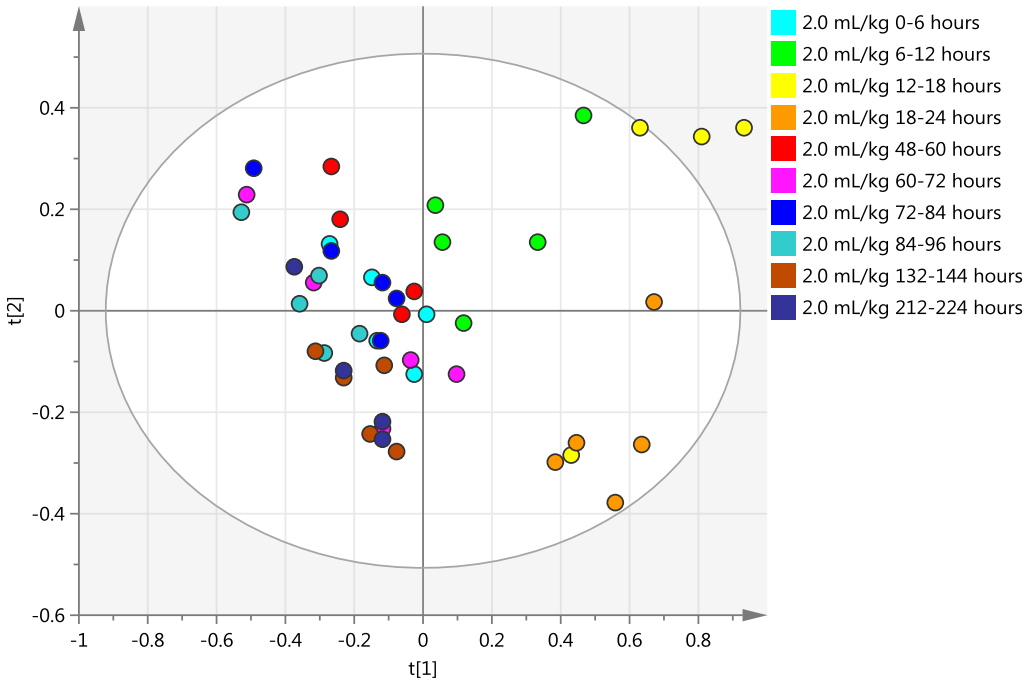

Figure 6.4 PCA scores plot from a PCA model derived from 1D ^{1}H NMR spectral data of urine samples from male Hanover-Wistar rats treated with CCl_4 at 2.0 mL/kg and sampled at various time points post-dosing. Rats were dosed by gavage and sampled at the time points shown and urine collected as described in Section 6.2. Each spot in the scores plot represents one urine sample. R^2X (cum) = 0.683, Q^2 (cum) = 0.476.

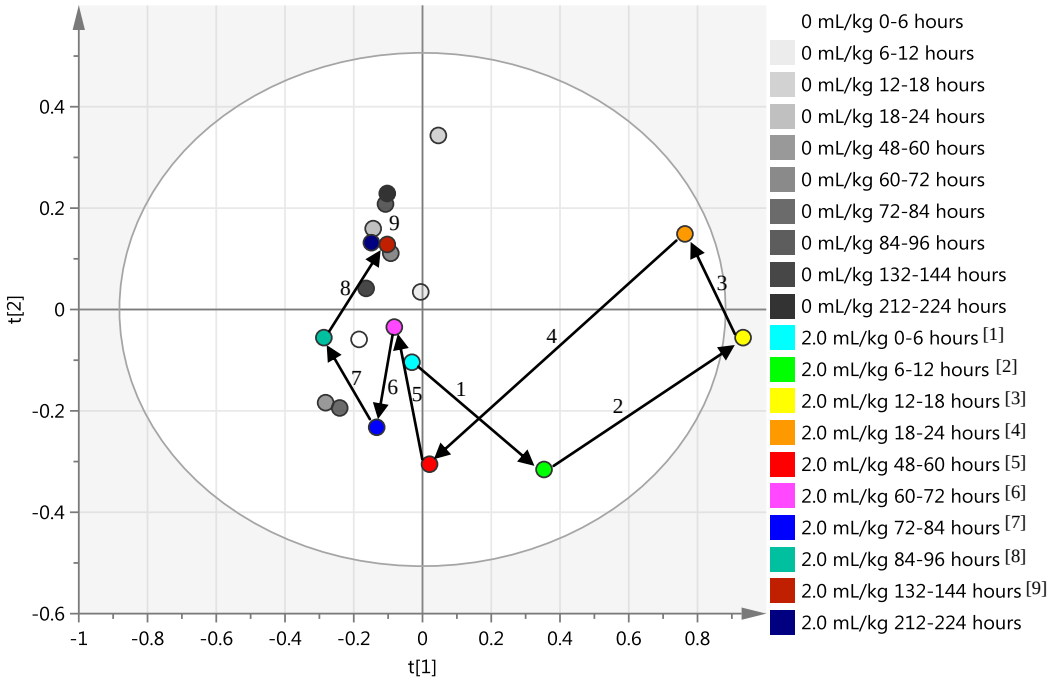

Figure 6.5 PCA trajectory plot from a PCA model derived from 1D ^{1}H NMR spectral data of urine samples from male Hanover-Wistar rats treated with vehicle (control) or CCl_4 at 2.0 mL/kg and sampled at various time points post-dosing. Rats were dosed by gavage and sampled at the time points shown and urine collected as described in Section 6.2. Points in the trajectory plot represent the spectra created from the average of integral regions for each group of samples. R^2X (cum) = 0.695, Q^2 (cum) = 0.445. Arrows represent direction of movement.

The trajectory plot shown in Figure 6.5 demonstrated the change in location on the PCA scores plot with time which corresponded to a change in metabolites with time. The numbers (1-9) labelled on the scores plot represent the order of sample collection with time. Inspection of this PCA plot revealed that the average urine sample collected between 0 to 6 hours post-dosing positioned closely to the control samples, shown in grey colour and located on the left hand-side of the scores plot. Urine samples collected between 6 and 24 hours following a single dose of CCl_4 had shifted towards the right side of the scores plot, away from controls and the 0 to 6 hours time point. However, at the 48 to 60 hours post-dosing time point it was observed that sample points had moved back towards the left side of the plot closer to control samples, indicating a possible return to an almost control-like urinary metabolite composition. At later time points, samples from CCl_4-treated animals were located in the same quadrant as the respective controls and no separation was clearly visible.

The 2 different trends in this PCA model of acute liver injury were in opposite directions and correspond to the injury occurring in the first 24 hours followed by a period of hepatic regeneration, during which the liver tissue recovers from the injury and restores its normal appearance.

To identify the specific changes to urinary metabolites which were responsible for sample clustering and trajectory trends, individual OPLS-DA models were constructed. For the first plot CCl_4-treated samples at 6 hours post-dosing were compared to controls and thereafter CCl_4-treated samples from consecutive time points were compared (Figure 6.6). The discriminating component on the scores plots t[1] showed the variance between the samples, whereas t[0] corresponded to intragroup variation. Individual OPLS-DA scores plot revealed evidence of very good degrees of separation between CCl_4-treated samples at the different time points.

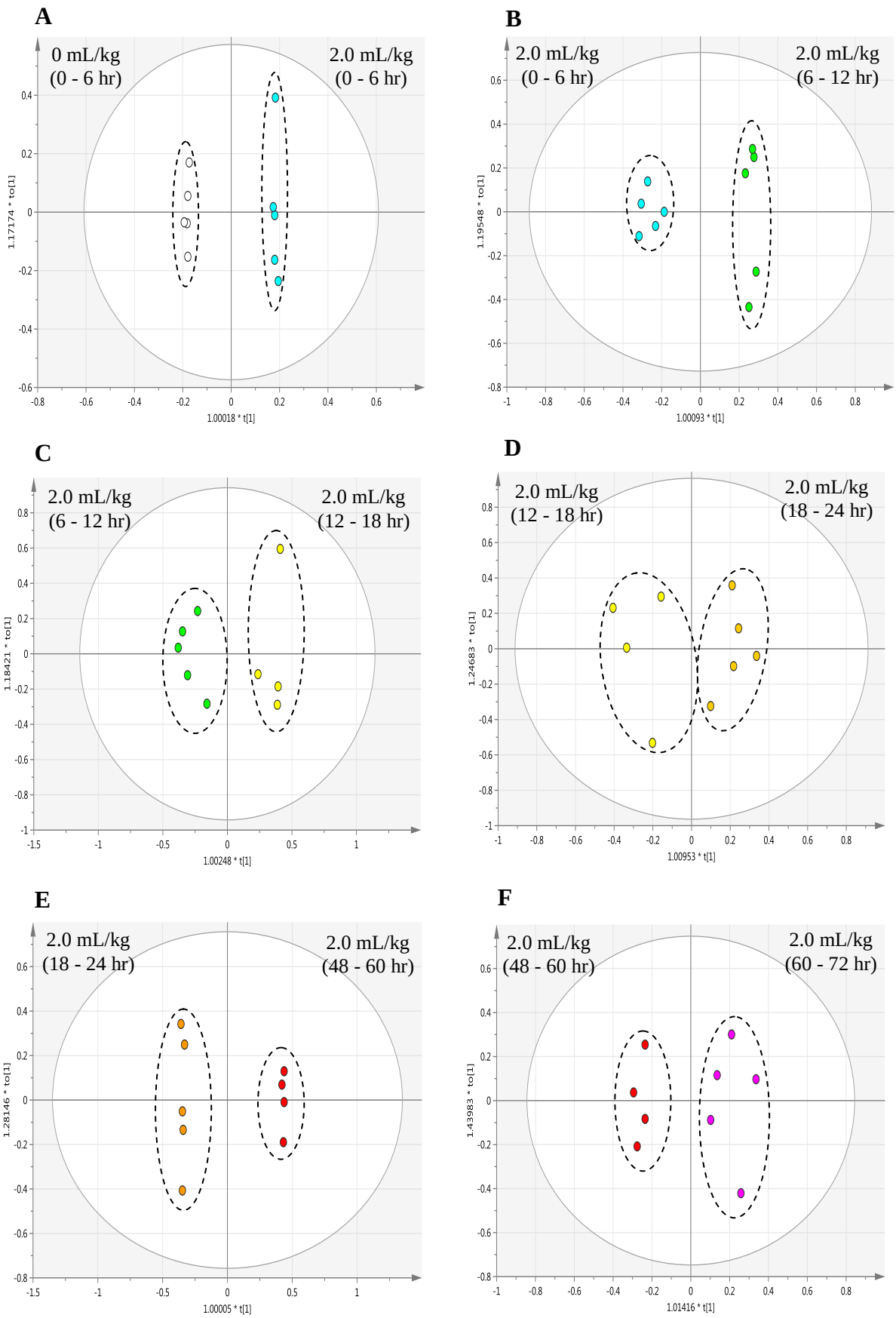
A
0 mL/kg
(0 - 6 hr)
2.0 mL/kg
(0 - 6 hr)
1.17174 * to[1]
1.00018 * t[1]
B
2.0 mL/kg
(0 - 6 hr)
2.0 mL/kg
(6 - 12 hr)
1.19548 * to[1]
1.00093 * t[1]
C
2.0 mL/kg
(6 - 12 hr)
2.0 mL/kg
(12 - 18 hr)
1.18421 * to[1]
1.00248 * t[1]
D
2.0 mL/kg
(12 - 18 hr)
2.0 mL/kg
(18 - 24 hr)
1.24683 * to[1]
1.00953 * t[1]
E
2.0 mL/kg
(18 - 24 hr)
2.0 mL/kg
(48 - 60 hr)
1.28146 * to[1]
1.00005 * t[1]
F
2.0 mL/kg
(48 - 60 hr)
2.0 mL/kg
(60 - 72 hr)
1.43983 * to[1]
1.01416 * t[1]

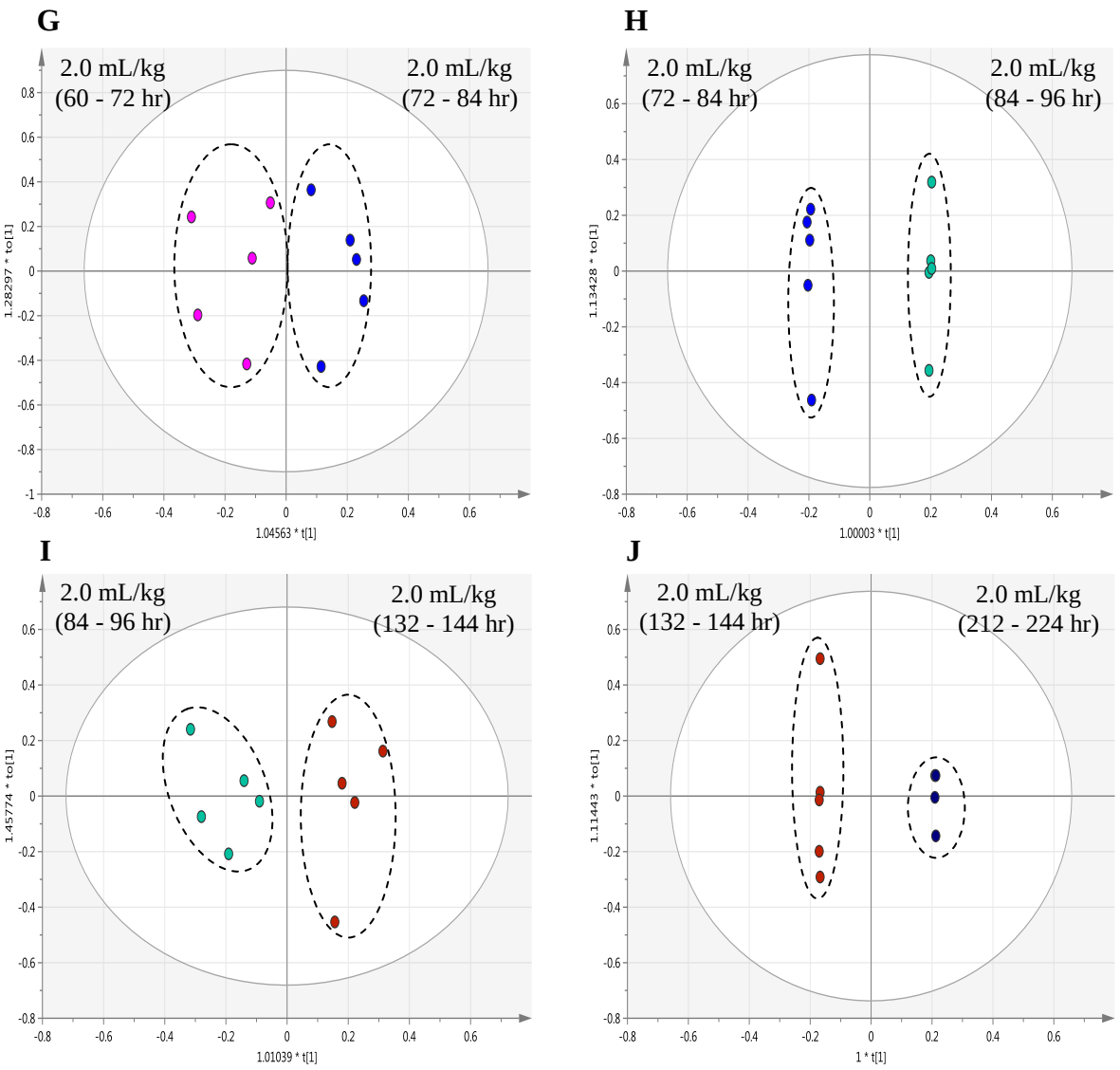

Figure 6.6 Scores plots from OPLS-DA models derived from 1D ^{1}H NMR spectral data of urine samples from male Hanover-Wistar rats treated with vehicle (control) or CCl_4 at 2.0 mL/kg and sampled at various time points post-dosing. Rats were treated dosed by gavage and urine collected as described in Section 6.2. (A) Control and CCl_4-treated animals at 0 to 6 hours post-dosing; (B) CCl_4-treated animals at 0 to 6 hours and 6 to 12 hours post-dosing; (C) CCl_4-treated animals at 6 to 12 hours and 12 to 18 hours post-dosing; (D) CCl_4-treated animals at 12 to 18 hours and 18 to 24 hours post-dosing; (E) CCl_4-treated animals at 18 to 24 hours and 48 to 60 hours post-dosing; (F) CCl_4-treated animals at 48 to 60 hours and 60 to 72 hours post-dosing; (G) CCl_4-treated animals at 60 to 72 hours and 72 to 84 hours post-dosing; (H) CCl_4-treated animals at 72 to 84 hours and 84 to 96 hours post-dosing; (I) CCl_4-treated animals at 84 to 96 hours and 132 to 144 hours post-dosing and (J) CCl_4-treated animals at 132 to 144 hours and 212 to 224 hours post-dosing.

Potential biomarkers were selected based on the S-plots and VIP plots (data not shown) and were statistically compared using a Students's t-test. The changes in metabolites with time following a single dose of CCl_4 are summarized in Table 6.7. However, we also wished to characterise changes in the urine of CCl_4-treated animals compared to controls at 24 hours and at day 10 post-dosing respectively (Figure 6.7, Table 6.8).

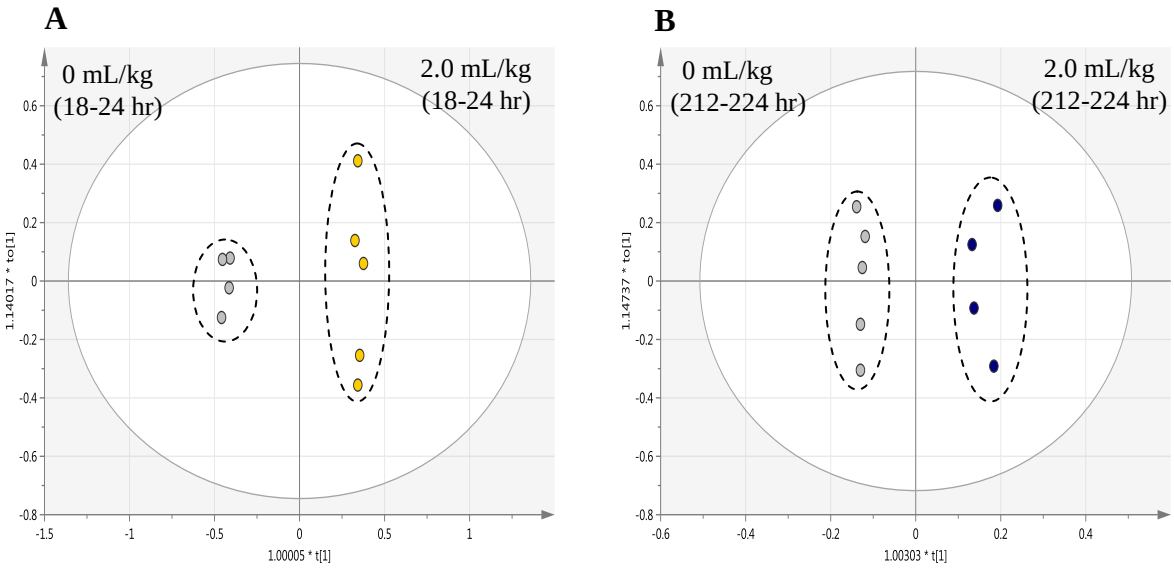

Figure 6.7 Scores plots from OPLS-DA models derived from 1D ^{1}H NMR spectral data of urine samples from male Hanover-Wistar rats treated with vehicle (control) or CCl_4 at 2.0 mL/kg and sampled at 24 hours and 224 hours (day 10) post-dosing. Rats were dosed by gavage and urine collected as described in Section 6.2. (A) Control and CCl_4-treated animals at 18 to 24 hours post-dosing; (B) Control and CCl_4-treated animals at 212 to 224 hours (day 10) post-dosing.

Formate was increased in CCl_4-treated samples at 6 hours when compared to control (Table 6.7). This level decreased at 12 hours compared to CCl_4-treated animals at the previous time point. There was an increase in urinary formate in CCl_4-treated animals at 18 and 24 hours post-dosing. At 24 hours post-dosing urinary formate was increased in CCl_4-treated animals compared to controls at the same time point (Table 6.8). After this time point there appeared to be a decreasing trend in urinary formate excretion and by day 10, formate levels in the urine of CCl_4-treated animals were decreased compared to concurrent control rats (Table 6.8).

Taurine was decreased at the first time point (6 hours) when compared to control, however, CCl_4-treated samples at 12 and 18 hours had increased amounts of taurine

compared to treated samples at 6 and 12 hours respectively (Table 6.7). From 18 hours post-dosing, taurine levels decreased with time in the CCl_4-treated samples, but were still increased over concurrent controls in CCl_4-treated animals at 24 hours post-dosing (Table 6.8). From 48 hours to day 10 post-dosing urinary taurine levels decreased consistently compared to previous time points and there appeared to be a return to control levels at day 10 (Table 6.8). Creatinine levels showed an increasing trend during the first 24 hours and at this time point they were significantly increased in CCl_4-treated rats over vehicle-treated animals (Table 6.7). By day 10 post-dosing, urinary creatinine levels were decreased in CCl_4-treated rats compared to concurrent controls (Table 6.8).

Urinary 2-oxoglutarate appeared to decrease in CCl_4-treated animals during the first 18 hours post-dosing up to 24 hours post-dosing at which time levels were significantly decreased compared to the concurrent controls (Table 6.7, Table 6.8). At the later time points levels increased indicating a possible correlation with regeneration of the liver but by day 10 levels had still not reached control values (Table 6.8). Citrate followed a similar pattern of change with time post-dosing; at 24 hours levels were significantly decreased compared to control rats, after which they appeared to increase with time and by day 10 they were increased over control animals (Table 6.7, Table 6.8). Hippurate levels in the urine were decreased at the earlier time points and at 24 hours they were significantly decreased compared to concurrent controls. Levels increased at the later recovery time points from 60 hours post-dosing; again indicating a correlation with injury and regeneration in this model (Table 6.7, Table 6.8).

Metabolites that appeared to show an increasing trend during the first 18 hours following CCl_4-administration include formate, creatinine, creatine, taurine and succinate whereas hippurate, 2-oxoglutarate and citrate demonstrated a decrease in urinary excretion during the first 24 hours of treatment. After this time point there appeared to be a general decrease in the levels of creatine and taurine excretion in the rat urine, and an increase in the resonances corresponding to the metabolites 2-oxoglutarate and citrate.

Table 6.7 OPLS-DA detected 1D ^{1}H NMR chemical shift regions responsible for the separation of NMR derived spectra from the urine of male Hanover-Wistar rats treated with vehicle (control) or CCl_4 at 2.0 mL/kg and sampled at various time points between 6 hours and day 10 post-dosing. Rats were treated dosed by gavage and sampled at the time points shown as described in Section 6.2. Chemical shifts were statistically compared by means of a Students' t-test. Control animals at 6 hours were compared to CCl_4-treated animals at 6 hours; after this, CCl_4-treated animals were compared to CCl_4-treated rats at the previous time point. Values that differ significantly from controls, or CCl_4-treated animals at the previous time point are shown: $^{*}P<0.05$; $^{**}P<0.01$; $^{***}P<0.001$.

Chemical shift (δ), multiplicity	Endogenous metabolite	Control (0-6 hours) vs CCl_4-treated (0 – 6 hours)	6 – 12 hours	12 – 18 hours	18 – 24 hours	48 – 60 hours	60 – 72 hours	86 – 96 hours	Day 10
8.46-8.50 (s)	formate	+***	-	+	+	-	+	-	-
7.70-7.74 (d)	hippurate	+	-	+	+	-	-	-*	+**
7.62-7.66 (t)	hippurate	-***	-***	-	+	+	+	+	-
7.54-7.58 (t)	hippurate	-***	-***	-	+	+	+	+	-
4.06-4.10 (s)	creatinine	+	+	-	+	-	+	+	+
3.98-4.02 (d)	hippurate	-***	-***	-	+*	+	+	+	-
3.94-3.98 (s)	creatine	-	+	+	-	-	-	+	-
3.42-3.46 (t)	taurine	-	+**	+	-	-	-	-	-
3.26-3.30 (t)	taurine	-	+	+	-	-	-	-	-
3.06-3.10 (s)	creatinine	+	+*	-*	+	-*	-	-	-
2.98-3.02 (t)	2-oxoglutarate	-	-	-	+	+	+**	-*	+**
2.70-2.74 (d)	citrate	-	-	-**	-	+***	+	+	-
2.54-2.58 (d)	citrate	-	-	-	-	+**	+	+	-
2.42-2.46 (t)	2-oxoglutarate	+	-*	-*	-	+**	+	+	+*
2.38-2.42 (s)	succinate	+	+	-	+	-	+	-	+

S, singlet; d, doublet; t, triplet.

Table 6.8 OPLS-DA detected 1D ^{1}H NMR chemical shift regions responsible for the separation of NMR derived spectra from the urine of male Hanover-Wistar rats treated with vehicle (control) or CCl_4 at 2.0 mL/kg at 24 hours and at day 10 post-dosing. Rats were dosed by gavage and sampled at the time points shown as described in Section 6.2. Chemical shifts were statistically compared by means of a Students' t-test. CCl_4-treated animals at 24 hours and at day 10 post-dosing were compared to concurrent controls. Values that differ significantly from controls are shown: $^{*}P<0.05$; $^{**}P<0.01$; $^{***}P<0.001$.

Chemical shift (δ), multiplicity	Endogenous metabolite	Control (18-24 hours) vs CCl_4-treated (18-24 hours)	Controls (day 10) vs CCl_4-treated (day 10)
8.46-8.50 (s)	formate	+	-
7.70-7.74 (d)	hippurate	+*	+**
7.62-7.66 (t)	hippurate	-***	-
7.54-7.58 (t)	hippurate	-***	-
4.06-4.10 (s)	creatinine	+	-
3.98-4.02 (d)	hippurate	-**	-
3.94-3.98 (s)	creatine	+	-
3.42-3.46 (t)	taurine	+*	-*
3.26-3.30 (t)	taurine	+*	+
3.06-3.10 (s)	creatinine	+***	-
2.98-3.02 (t)	2-oxoglutarate	-**	-
2.70-2.74 (d)	citrate	-***	+
2.54-2.58 (d)	citrate	-***	+
2.42-2.46 (t)	2-oxoglutarate	-***	-*
2.38-2.42 (s)	succinate	+**	+

S, singlet; d, doublet; t, triplet.

6.4 Discussion

An acute model of CCl_4-induced hepatic injury was developed in Chapter 3 and in this study we investigated the change in urinary metabolites as hepatic injury developed and subsequent regeneration occurred. An ideal marker will be sensitive to early signs of hepatic injury, will remain in the biofluid long enough to be detected and will return to normal levels upon recovery of the injury. Therefore, the purpose of this time course study was to investigate such characteristics in the urinary metabolites that were previously identified in Chapter 3.

The dose level used in the present study was 2.0 mL/kg CCl_4 since this was previously identified in Chapter 3 as below the threshold level for CCl_4-related nephrotoxicity (2.8 mL/kg). The first sample time point was 0-6 hours post-dosing since we thought it would be interesting to determine if injury could be detected in the urinary metabolites as early as 6 hours post-dosing. It is known that CCl_4-induced lipid peroxidation can be detected within 5 minutes of dosing (Recknagel, 1967; Rao and Recknagel, 1968).

Sampling was carried out according to the schedule in Table 6.1. Relative liver weights for CCl_4-treated animals were significantly increased over controls at all terminal time points with the exception of day 10. This suggests injury at 6 hours post-dosing; the maximum fold-increase over controls was observed at 18-24 hours. After 48 hours post-dosing the liver weights began to return to control values.

The trend suggesting hepatic injury as early as 6 hours after a single CCl_4 dose and increasing up to 24-48 hours post-dosing followed by an apparent recovery by day 10 was reflected in the serum ALT, AST, GLDH and ALP measurements (Figure 6.2, Table 6.3, Table 6.4).

At 6 hours post-dosing, the increase in ALT levels, unlike AST and GLDH was not statistically significant due to the large interanimal variability (Figure 6.2). By 96 hours post-dosing it appeared that ALT, AST and GLDH levels had returned to control values. In a previous time course study by Zira and colleagues (2013) male Wistar rats were dosed with 1 mL/kg CCl_4 and autopsied at 12, 24, 36, 48, 60 and 72 hours post-dosing. The authors discovered that ALT and AST levels reached peak plasma concentrations at 36 hours post-treatment. Similar results were described by Giffen and co-workers (2003). Rats were administered with CCl_4 at 0.8 mL/kg and autopsied at 12, 24, 36, 48,

60, 72 hours post-dosing and at 4, 7, 11 and 17 days post-dosing. In this study, levels of serum enzymes ALT, AST and GLDH were also found to have reached peak concentrations at 36 hours post-treatment. By 72 hours after CCl_4 administration, mean enzyme levels had returned to control values (Figure 6.2).

TIMP-1 and A2M levels were also measured in the serum of rats in this study and appeared to follow the same general trend (Table 6.3, Table 6.4). Mean values generally increased with time and reached maximum concentrations at 48 hours post-CCl_4 treatment. TIMP-1 was shown to be a more sensitive serum marker than A2M since mean levels for TIMP-1 were significantly increased 3.26-fold over concurrent controls at the earliest time point (6 hours post-dosing), whereas the first significant difference for A2M was not observed until 12 hours post-dosing (1.41-fold increase; $^{*}P<0.05$). At 48 hours post-dosing there was a 14-fold increase over controls for TIMP-1 compared to a 2-fold increase for A2M. In Chapter 3, TIMP-1 was significantly increased in animals treated with CCl_4 at 1.2 mL/kg whereas for A2M an increase was observed at 2.4 mL/kg and higher. Herbst and colleagues (1997) carried out a time course study investigating the levels of TIMP-1 expression following a single i.p. injection of CCl_4 at 1.25 mL/kg to female Sprague-Dawley rats. This group reported that TIMP-1 expression in the rat liver was increased as early as 1 hour after treatment, and highest serum TIMP-1 levels were present at 72 hours following a single CCl_4 administration (Herbst et al., 1997). TIMP-1 is strongly associated with hepatic inflammation as well as the development of fibrosis therefore the increase in serum levels immediately after a single dose of CCl_4 would be due to the inflammatory response (Roderfeld et al., 2006). A2M has been shown to be involved in the inhibition of collagenase activity and therefore, changes to serum A2M are more often seen during the development of hepatic fibrosis and chronic injury (Barrett and Starkey, 1973; Montfort and Perez-Tamayo, 1978; Truden and Boros, 1988).

In the present study, levels of serum MCP1 were significantly increased over concurrent controls at 6 hours post-dosing and reached maximum concentration at 24 hours before returning to control levels by 72 hours after a single CCl_4 administration (Table 6.3, Table 6.4). MCP1 is a chemotactic factor secreted by HSCs, which are responsible for ECM accumulation during chronic liver injury/disease (Marra et al., 1993). In a study by Czaja et al., (1994), male Sprague-Dawley rats were administered with a single oral dose of CCl_4 at 0.5 mL/100 g of BW and sampled at various times after treatment. The

authors reported increased MCP1 mRNA levels at 2 hours after CCl_4 administration with maximum levels observed between 12 and 48 hours. However, by 60 to 72 hours after CCl_4 treatment MCP mRNA levels had returned to control values (Czaja et al., 1994).

Serum AGP and lipocalin-2 levels were also greatest at 48 hours following a single CCl_4 administration (9.39- and 27.02-fold increase over concurrent controls for AGP and lipocalin-2 serum levels, respectively) (Table 6.3, Table 6.4). Lipocalin-2 was significantly increased over concurrent controls at 12 hours post-dosing whereas AGP did not show evidence of a significant difference until 24 hours post-dosing. Lipocalin-2 is released by the liver in response to inflammation. Previous studies have reported increases in AGP plasma levels following CCl_4-administration which is thought to be in response to the presence of reactive oxygen species following metabolism of CCl_4 (Sugihara et al., 1992).

In this study, histopathological examination confirmed the presence of hepatic injury at 6 hours post-dosing (Figure 6.3). CCl_4-treated livers showed vacuolation of hepatocytes. At 12 and 18 hours post-dosing there was clear evidence of degeneration and necrosis of hepatocytes, and by 24-48 hours pathological changes had progressed. From 72 hours post-dosing regenerative changes were apparent and by 224 hours post-dosing (day 10), the architecture of the liver had returned to near normal. This mirrors what we would have expected from the liver weight and serum enzyme data obtained in this study.

In the study by Giffen and colleagues (2003), histopathological examination of the livers sampled at several time points after administration of CCl_4 at 0.8 mL/kg revealed that the most marked pathological changes occurred at 36 and 48 hours post-dosing, corresponding to the period of maximal injury. By day 4 following CCl_4 treatment there was complete resolution of necrosis and inflammation but hepatocellular vacuolation remained evident in a small proportion of animals until day 17 in the study. A similar pattern of microscopic changes was reported by Zira and co-workers (2013) following the administration of CCl_4 at 1 mL/kg. Maximum injury as determined by the degree of centrilobular inflammation and necrosis occurred between 24 and 36 hours post-dosing. After this time point the livers from CCl_4-treated animals showed evidence of regeneration in the form of an increase in mitotic activity in the hepatocytes. By 72 hours post-dosing livers from treated animals were histopathologically similar to livers from control animals (Zira et al., 2013).

Therefore, the results in our study confirm injury as early as 6 hours post-dosing and reaching a maximum level at 24-48 hours post-dosing. Following this, there is a period of regeneration and return to normal liver by day 10 post-dosing.

Since the purpose of this study was to evaluate potential urinary biomarkers of hepatic injury, the absence of nephrotoxicity was important. In Chapter 4 we evaluated a wide range of biomarkers for nephrotoxicity and our results suggest the most sensitive biomarkers for kidney injury are urinary levels of α-GST, albumin, KIM-1, glucose, clusterin and osteopontin. In the current study these markers were used to determine if CCl_4-induced nephrotoxicity was present (Table 6.5, Table 6.6).

Urinary α-GST was increased over concurrent control levels at 48 hours post-dosing, but this increase was not statistically significant due to the large intragroup variation, 2 animals in this group had very large increases in urinary α-GST compared to the rest of the group. At the other time points in the study α-GST showed some significant decreases and increases compared to concurrent controls, however, the changes were not consistent (Table 6.5, Table 6.6).

Urinary osteopontin was significantly increased in CCl_4-treated animals at 36, 48 and 60 hours post-dosing. It is worth noticing, however, that at these time points, values for control animals were considerably less than at the earlier time points. Urinary lipocalin-2 levels were significantly decreased compared to control animals at 6 hours post-dosing, but at 12 hours after CCl_4 administration a 2.43-fold increase was recorded ($^{***}P<0.001$) and there appeared to be a time-related relationship, with peak urinary concentrations being recorded at 48 hours post-dosing. However, lipocalin-2 is not considered to be a reliable kidney injury biomarker since levels are also known to increase following hepatic damage.

Urinary clusterin levels were also significantly increased above concurrent controls at 36 and 48 hours post-dosing but the highest concentration was recorded at 48 hours following CCl_4-treatment (3.54-fold increase; $^{*}P<0.05$). In the HCBD studies (Chapter 4) clusterin was shown to be a marker of regeneration and peak levels were found at days 4 and 5 after a single nephrotoxicant insult. At these time points in the current study clusterin was significantly decreased compared to controls.

KIM-1 was significantly increased above concurrent controls at 12 and 84 hours post-dosing but did not show evidence of a dose-related effect. Indeed KIM-1 has been previously described as a marker of both kidney injury and regeneration (Chapter 4) (Swain et al., 2012; Maguire et al., 2013). In the present study the increases at 12 hours and 84 hours were 1.72- and 1.50-fold, respectively. In the HCBD-time course study in Chapter 4, KIM-1 urinary levels peaked at day 4 and an 83-fold increased over controls was observed following a single administration of 45 mg/kg HCBD.

Urinary levels of albumin were approximately 28-fold increased over concurrent controls at 48 hours post-dosing ($^{*}P<0.05$) but there was no consistent evidence of an effect at the other time points, and the same was the case for urinary glucose which was significantly decreased at 72 hours and at day 6 post-dosing (Table 6.5, Table 6.6).

It is important to mention however, that at 36 to 60 hours post-dosing there was a great deal of intragroup variation, which is seen in the standard deviations, and potentially reflects the differences in the degree of CCl_4-induced injury, particularly at the time points when the effect was maximal.

These results suggested that perhaps mild kidney injury may have occurred in this study; however, histopathological examination of the kidneys revealed the presence of vacuolation of the proximal tubule which was present to a similar degree in CCl_4-treated animals at all time points. We have seen similar vacuolation of the proximal tubule in control animals in the dose response study in Chapter 3. Therefore, we are confident that renal function was not compromised in the current study.

In the dose response study carried out in Chapter 3 the main urinary metabolite changes following a single dose of CCl_4 were formate, hippurate, creatine, taurine, 2-oxoglutarate and succinate. These metabolites were found to be either increased or decreased 24 hours after CCl_4 administration. In Chapter 3, however, urine samples were collected from 6-24 hours post-dosing; therefore, urinary changes reflect this entire time point.

In the present study we evaluated the change in urinary levels of these metabolites at a series of time points over 10 days following a single dose of CCl_4. At the first time point (0-6 hours) taurine urinary levels decreased in comparison to control samples, but this was followed by increases at the next 2 consecutive time points (6-12 hours and 12-

18 hours). From 18 hours there was a gradual decrease in urinary taurine with time. However, at 24 hours post-dosing taurine levels were still significantly increased over concurrent controls. By day 10, the signals for taurine excretion showed a statistically significant decrease compared to the previous time point, which we suggest is an indication that taurine levels are returning to control levels (Table 6.7, Table 6.8).

In our previous study in Chapter 3, we reported increases in taurine excretion at 24 hours post-CCl_4 administration. Similar results have been described by other groups (Waterfield et al., 1991; Waterfield et al., 1993) and also in a model of acute hydrazine-induced toxicity (Beckwith-Hall et al., 1998; Holmes et al., 2000; Nicholls et al., 2001). In a study by Lin and co-workers (2009), male Wistar rats were given a single administration of CCl_4 at 1 mL/kg and urine samples collected in intervals of 24 hours starting immediately after dosing. Increased taurine levels in the urine, as detected by LC-MS analysis, were observed during the first collection period. The fact that taurine levels in urine increased during the first 18 hours after CCl_4 dosing suggests that it is a reliable marker for the initial pathological changes that occur following a single dose of CCl_4. However, it is interesting that from 18-24 hours when maximum injury is occurring the levels fall compared to at 18 hours but still remain significantly increased over control levels (Table 6.7, Table 6.8).

Formate levels in the urine were significantly increased at 6 hours post-dosing compared to concurrent controls and showed a general trend of increasing with time up to 24 hours post-CCl_4 treatment. In our previous dose-response investigation in Chapter 3, formate levels were also found to be significantly increased over control animals at 24 hours following the administration of 2.0 mL/kg CCl_4. In our current study, urinary formate levels decreased with time after the first 24 hours of treatment, apart from between 60-72 hours post-dosing. By day 10 post-dosing, urinary formate values were decreased compared to control animals (Table 6.7, Table 6.8). Dow and co-workers (2000) carried out a time course study in male Fischer 344 rats following a single oral dose of CCl_4 at 100 mg/kg in corn oil, 5 mL/kg. Urine samples were collected at 24 hour intervals and analysed by ^1H NMR for the detection of formate levels. Excretion of this metabolite was increased at 24 hours post-dosing but levels were greatest on day 2 of the study. The authors also reported evidence of increased formate excretion in the rat urine following administration of chloroform and dichloroacetic acid. These compounds are also known to generate free radicals upon metabolism, similar to CCl_4.

Dow and green (2000) suggested that CCl_4, chloroform and dichloroacetic acid induce vitamin B_{12} deficiency resulting in decreased levels of tetrahydrofolate which is necessary for the metabolism of formate. Decreased levels of tetrahydrofolate will result in increased urinary formate excretion as formate metabolism is impaired (Dow and Green, 2000).

Of the 4 chemicals shifts identified as hippurate, 3 demonstrated a significant decrease with time during the first 6 hours post-dosing, and at 12 and 18 hours, levels further decreased compared to previous time points (Table 6.7). However, at 18 to 24 hours following CCl_4 treatment, levels in the urine were increased compared to the previous time point but still remained less than controls at 24 hours (Table 6.8). In Chapter 3, levels of hippurate were found to be decreased at 24 hours post-dosing. The results from the present study add further proof that urinary hippurate levels decrease during the first 24 hours after dosing with CCl_4. It also suggests that hippurate is a sensitive marker since the decrease compared to control at 6 hours post-dosing is consistent with the decrease seen at 24 hours. Lin and colleagues (2009) described a decrease in the excretion of hippuric acid in the urine of rats immediately after dosing with 1 mL/kg CCl_4. Decreased hippurate levels in the urine occur as a result of ATP depletion which occurs during the process of hepatic necrosis (Gatley and Sherratt, 1977; Kim et al., 2008a). This explains the early decreases in hippurate levels following CCl_4-induced hepatic toxicity. From 48 hours, there appeared to be a trend for hippurate levels to increase with time. However, our results also demonstrate that by day 10 post-dosing, hippurate excretion in the urine was still decreased in CCl_4-treated compared to control animals at the same time point (Table 6.8). This suggests hippurate is a good marker for the early stages of hepatic injury and levels also reflects the liver regeneration phase.

In the current study, levels of TCA cycle intermediates, such as citrate and 2-oxoglutarate were decreased compared to controls during the first 24 hours after CCl_4 treatment and at 24 hours this decrease was statistically significant (Table 6.8), whereas succinate appeared to show a general increasing trend and was increased over controls at 24 hours post-dosing (Table 6.8). In an investigation by Robertson et al., (2000) male albino Wistar rats were given a single i.p. injection of CCl_4 at 10 mL/kg. The authors reported decreased resonances for 2-oxoglutarate, succinate and citrate in the 24 hour period after dosing. In experiments carried out by Holmes et al., (2000), and by Nicholls and colleagues (2001), using a hydrazine-induced hepatotoxicity model in the rat, levels

of TCA cycle intermediates such as citrate, succinate, 2-oxoglutarate and of the metabolite hippurate were reported to be decreased in the urine following hydrazine administration. In both studies, animals were kept in individual metabolism cages with access to food throughout the duration of the study.

In our previous dose response study described in Chapter 3, the level of TCA intermediates in the urine was increased at 24 hours post-dosing following a single dose of CCl_4. However, in Chapter 3, rats were fed for a period of 6 hours immediately after CCl_4-treatment, before being placed in metabolism cages without access to diet for the collection of 18 hour urine samples. In the present time course study, animals were only starved for 6 hour periods during the first 24 hours and for 12 hour periods at all later time points. It is possible that this discrepancy between the studies accounts for the different metabolite levels for TCA intermediates. A study by Connor et al., (2004) investigated the effect of feeding and body weight loss on the ^1H NMR urine spectra of male Hanover-Wistar rats treated with CCl_4 at either 1.58 or 3.16 g/kg. The study used several groups of animals: 2 CCl_4-treated groups, 1 'pair-fed' group for each CCl_4-treatment group where animals were dosed with vehicle and were given the same quantity of food as that actually consumed by animals in the treatment group, and 1 'true control' group that were dosed with vehicle and that had access to food *ad libitum*. In a PCA model of the urine samples, the authors observed the presence of 3 different clusters for each CCl_4 dose level, due mainly to the effect of feeding and weight loss rather than CCl_4 administration. The Connor group reported that citrate and glucose were the metabolites responsible for the separation between control and 'pair-fed' animals, whereas levels of taurine and creatine changed following CCl_4 administration. The authors demonstrated the importance of establishing a correlation between the toxic effect induced by the toxicological compounds used, and possible body weight loss due to a starved state. In our study we assume that the difference observed for some TCA intermediates between the present study and the previous dose-response investigation (Chapter 3) may be related to the different feeding and starved time periods used in these 2 studies. However, this effect of diet and starvation requires further investigation.

In the current study creatine levels in the urine of CCl_4-treated animals appeared to follow the same trend as taurine during the first 24 hours of the toxic insult. Levels were decreased compared to control animals at 6 hours post-dosing, but at the following 2 time points urinary creatine excretion was increased. At 24 hours following CCl_4

administration urinary excretion of creatine was decreased compared to the previous collection period (12-18 hours). However, the levels remained elevated in CCl_4-treated animals compared to vehicle-treated rats at 24 hours post-dosing (Table 6.8). These results reflect the increase in creatine excretion in the urine of male rats dosed at 2.0 mL/kg CCl_4 as reported in Chapter 3. Since creatine is metabolised in the liver, increased urinary excretion is often a result of hepatocyte leakage (Waterfield et al., 1993). In the present study, after 24 hours of CCl_4 administration, there appeared to be a trend for the decrease in creatine excretion in the urine and by day 10 creatine levels were decreased in CCl_4-treated animals compared to concurrent control rats but this was not statistically significant (Table 6.8). We suggest this may be related to the process of hepatic regeneration as reported in the histopathological examination of the livers collected at autopsy, which revealed a decrease in the number of necrotic hepatocytes, which may result in reduced urinary creatine levels.

Throughout the present time course study creatinine levels appeared to increase and decrease intermittently with the 2 chemical shifts for the metabolite showing opposite changes and therefore making interpretation of results difficult. However, the same degree of variability was reported in the urine clinical chemistry data. In the clinical chemistry data in Table 6.6 creatinine was significantly decreased in CCl_4-treated animals compared to controls at 6 hours post-dosing. OPLS-DA analysis of the 1D ^1H NMR data shows the opposite effect at 6 hours. However, other changes with time were generally similar between both methods. At 24 hours post-dosing, urinary creatinine was significantly increased in CCl_4-treated animals compared to control animals at the same time point and by day 10 they appeared to be decreased compared to concurrent controls (Table 6.8).

Similar to the metabolomics study in Chapter 3, this current time course study revealed many other chemical shift changes, however, we were not able to identify these based on previous publications. Future work would attempt to use mass-spectrometry to identify these metabolites.

In the present studies urinary metabolites which were identified in Chapter 3 as being potential markers for CCl_4-induced hepatic injury were further characterised to determine the relationship of injury and metabolite levels with time post dosing. Histopathological examination revealed injury at 6 hours post-dosing; maximal injury at 24-48 hours and a gradual return to almost normal at day 10. Of the metabolites

previously identified taurine, citrate, 2-oxoglutarate and hippurate were the most sensitive to time following a single dose of CCl_4. All showed a similar change in direction in the first 18-24 hours followed by an opposing change in urinary levels during the liver regeneration phase. Citrate appears to be the most sensitive marker showing the progression of injury and then resolution of injury of the injury after 60 hours post-dosing.

These metabolites are sensitive to a single dose of CCl_4 and therefore may have potential to be urinary biomarkers of acute hepatic injury. It will be very interesting to determine if the same urinary metabolites will change in a model of chronic injury. We will therefore, investigate this in Chapter 7 in a CCl_4-induced hepatic fibrosis rat model.

CHAPTER SEVEN

Development of a model of CCl_4-induced liver fibrosis in the male Hanover-Wistar rat and investigation of urine metabolite profile changes using a ^1H NMR-based metabolomics approach

Chapter 7

7.1 Introduction

In Chapters 3, 5 and 6, CCl_4 was used as the hepatotoxicant to induce acute injury to the liver. In Chapter 3, we investigated urinary metabolites associated with the hepatic degeneration and necrosis induced by a single administration of CCl_4. Chapter 6 followed the pattern of change in these metabolites with time from 24 hours to day 10 after a single dose.

In this Chapter we were interested in developing a model of hepatic fibrosis using CCl_4, and in investigating urinary metabolite changes in this model. CCl_4 is known to induce fibrosis of the hepatic tissue which may further progress to cirrhosis if the stimuli persists (Post et al., 1942; Constandinou et al., 2005; Smyth et al., 2007; Smyth et al., 2009a; Fujii et al., 2010). A single dose of CCl_4 initiates lipid peroxidation (Hafeman and Hoekstra, 1977; Lee et al., 1982; Burk et al., 1984; Recknagel et al., 1989) which results in the disruption of cellular and organelle membrane integrity and subsequent leakage of cellular contents into the blood (Recknagel, 1983; Brattin et al., 1985). With continued CCl_4 administration HSCs are activated, become myofibroblast-like cells, and secrete ECM components including collagen as the liver undergoes regenerative processes to repair the damage induced (Friedman et al., 1985; Olaso and Friedman, 1998). Fibrosis develops because of an imbalance between the increased synthesis and the decreased degradation of ECM components, resulting in the formation of bridging fibrosis.

In humans, the gold standard method for the detection of fibrosis has long been liver biopsy (Rossi et al., 2007; Martinez et al., 2011). However, due to the small sample size obtained, liver biopsy may result in erroneous results. Additionally, biopsy cannot be used as a routine clinical tool (Bedossa et al., 2003; Standish et al., 2006; Carey and Carey, 2010) because it is a highly invasive technique causing discomfort to, and even mortality in a patient (Thampanitchawong and Piratvisuth, 1999; Dufour, 2005).

Traditional serum biomarkers of liver injury include enzymes such as ALT, AST and GLDH (Giffen et al., 2002). Increased levels of these enzymes occur following breakdown of the hepatocellular membrane with subsequent leakage of the enzymes

into the blood (Schmidt and Schmidt, 1988; Gores et al., 1990; Van Hoof et al., 1997). However, these serum enzymes lack specificity and sensitivity (Friedman, 1999).

Serum biomarkers for liver fibrosis normally fall into 1 of 2 categories: direct or indirect markers. Direct markers are degradation products of extracellular matrix produced by the HSCs (MMPs, TIMPs, hyaluronic acid (HA), collagens IV and VI). Indirect markers tend to be released into the blood as a result of inflammation (ALT and AST). This category also includes molecules synthesised or excreted by the liver (clotting factors, cholesterol) and markers of processes that can be disrupted as a consequence of impairment of liver function (such as insulin resistance) (Adams, 2011; Castera, 2011).

MMPs are a family of enzymes that are responsible for the degradation of the components of the extracellular matrix (Iredale et al., 1996) and TIMPs act as inhibitors of MMPs (Brew et al., 2000). TIMPs are known to increase in expression as fibrosis progresses and thus this will have an impact on MMP activity, resulting in lower levels of MMPs in serum. Therefore, decreased levels of MMPs in the serum are associated with injury progression, whereas TIMP levels, on the contrary, are increased with the increase in injury severity (Iredale et al., 1996). HA is also classified as a direct marker of liver fibrosis. It is a high molecular weight polymer ($>1x10^6$ Da) (Maharjan et al., 2011) which is synthesised by HSCs (Rostami and Parsian, 2013). Consequently, increased serum levels of HA can be used to measure the progression of liver fibrosis (Rossi et al., 2007; Rostami and Parsian, 2013).

The ideal marker for liver fibrosis should be specific for the liver, able to detect the early stages of liver fibrosis and assess the progression of disease and response to therapy (Marrero and Lok, 2004; Mayeux, 2004).

However, currently, no single serum biomarker can be measured for the reliable detection of liver fibrosis. Many of the biomarkers measured together form a reliable panel of biomarkers for hepatic fibrosis, but are not useful for routine monitoring. Additionally, the measurement of biomarkers in the serum involves the collection of a blood sample, which is an invasive procedure. The use of urinary biomarkers, as the main focus of this thesis, would represent a more ideal situation for the early prediction of fibrosis in the general population. The ability to develop a quick, non-invasive test for early signs of chronic liver injury would have a huge advantage in diagnosis.

In this Chapter we also wish to address the potential for reversibility of a fibrotic injury. Although traditionally liver fibrosis and cirrhosis have been considered to be irreversible, evidence has suggested that this may not be the case, and that fibrosis may reverse to an almost normal histological appearance (Benyon and Iredale, 2000). Our main interest will be focused on the change of urinary metabolites in the male rat during a recovery phase following the induction of fibrosis.

7.2 Animal experimental design

The first experiment was a repeat dose response study to determine the dose level of CCl_4 that upon repeated administration would induce hepatic fibrosis in the rat, without causing injury to other organs or death. The progression of fibrotic injury was monitored during the study by evaluating a panel of serum biomarkers and confirmed by histopathological examination of tissue samples collected during the dosing period.

The CCl_4 dose level determined in the first experiment was then used in a second repeat dose study. In this experiment, serum enzymes, urinary metabolites, biomarkers, gene expression and histopathology were investigated as fibrosis progressed (during the dosing period) and as injury recovered (during a no treatment, recovery period).

7.2.1 Experiment 1: A repeat dose study to determine the dose level of CCl_4 for the development of hepatic fibrosis

Eighty male Hanover-Wistar rats (mean body weight 193.23 ± 4.37 g) were divided into 4 groups (n=20). In each group, n=5 rats were dosed by gavage with CCl_4 at 0 (controls), 0.4, 0.8 and 1.2 mL/kg. Control animals were dosed with equivalent volumes of corn oil by gavage. Animals were dosed 3 times a week on Mondays, Wednesdays and Fridays and volumes were adjusted according to the body weights recorded prior to dosing.

Twenty four hours after the first dose, blood was collected from the tail vein from 5 rats in each CCl_4 dose level group (0, 0.4, 0.8 and 1.2 mL/kg CCl_4). In Chapter 3, serum samples were analysed at 24 hours post-dosing. Therefore, we wished to compare the results from this study with the previously generated data in Chapter 3. In order to avoid having to sacrifice the animals, blood was taken from the tail vein for serum analysis.

Five animals from each group were scheduled to be killed after 3, 6, 9, 12 weeks of dosing. Animals to be dosed for 12 weeks would receive a total of 36 CCl_4 doses. Prior to autopsy animals were placed in metabolism cages for 18 hour urine collection (16:00 hr to 10:00 hr). When not in metabolism cages animals were kept in communal cages with access to water and diet *ad libitum*. All urine samples were collected over ice and stored at -80 ºC until further analysis. However, the health of the animals deteriorated

during the study and CCl_4 dosing had to be stopped at different time points for each dose level before the scheduled autopsies as described in Section 7.3.1.

At each autopsy blood was taken for the preparation of serum and stored at -80 ºC until analysis, except during the autopsies carried out during the recovery period. At these autopsies only organs were removed for histopathological examination. The liver, kidneys, spleen, pancreas, adrenals, thymus, thyroid, testes, heart with lungs inflated and head were removed and placed in the fixative as described in Section 2.8.

7.2.2 Experiment 2: Investigation of protein, gene and metabolite changes during the development of hepatic fibrosis and subsequent recovery

Eighty male Hanover-Wistar rats (mean body weight 185.67 ± 2.56 g) were divided into 8 groups of 10 animals each. The dose level used (0.4 mL/kg) in experiment 2 was chosen based on the data from experiment 1 since this dose level had the lowest mortality rate. Similarly, we decided that the dosing period in experiment 2 should not last for more than 6 weeks since after this time point it was felt that there could have been an increase in mortality.

In each group, 5 animals were dosed by gavage with CCl_4 at 0 (controls) and 5 animals were dosed at 0.4 mL/kg CCl_4. Control animals were dosed with equivalent volumes of corn oil by gavage. Animals were dosed 3 times a week on Mondays, Wednesdays and Fridays and volumes were corrected for changes in body weight as recorded prior to dosing. Ten animals were killed at each of weeks 1, 2, 3, 4, 5 and 6 during the dosing period and weeks 9 and 12 (i.e. weeks 3 and 6 during the recovery period). During the recovery period, blood samples were collected from the tail vein at the weeks when no autopsies were scheduled, that is, at weeks 7, 8, 10 and 11. At week 7, the group of animals to be autopsied at week 9 was bled from the tail vein, whereas at weeks 8, 10 and 11 animals to be autopsied at week 12 were bled from the tail vein.

Each week during the dosing period of the study and at weeks 9 and 12 of the recovery period, 5 control and 5 CCl_4-treated animals were selected for ultrasonographic examination of the abdominal area and images were stored for future analysis. After each session animals were returned to their communal cages.

Throughout the experiment animals were kept in communal cages in groups of 5 with water and diet *ad libitum*. However, before each post-mortem, 5 control rats and 5 CCl_4-treated rats were placed in metabolism cages for the collection of 18 hour urine samples. They were placed in individual metabolism cages at 16:00 hr and removed at 10:00 hr the following day. During this time animals had access to water but not diet. All urine samples were collected over ice and stored at -80 ºC for further analysis. Animals were autopsied at 10:00 hr following removal from the metabolism cages. At each autopsy blood was taken for the preparation of serum and stored at -80 ºC until analysis. The liver, kidneys, spleen, pancreas, adrenals, thymus, thyroid, testes, heart with lungs inflated and head were removed and placed in the fixative as described in Section 2.8. For gene expression analysis a section was cut from the left lobe of the liver, placed in RNALater tubes and stored at 4 ºC until analysis.

7.3 Experiment 1

7.3.1 Observations during the study

Throughout the study animals were observed for signs of ill-health and clinical observations recorded during the post-mortem procedure.

After 3 weeks of dosing at 0, 0.4, 0.8 and 1.2 mL/kg all animals appeared normal. However, at autopsy, livers from CCl_4-treated animals were paler in colour and enlarged compared to control animals, and showed pitting of the surface. Four animals treated with 0.8 mL/kg, and 2 animals treated with 1.2 mL/kg CCl_4 had clear fluid in the abdominal cavity.

Groups were terminated when 3 animals per group were either found dead or killed in extremis. The autopsies schedule is shown in Table 7.1.

At week 4, 2 animals in the 1.2 mL/kg CCl_4-treated group were found dead and it was necessary to kill 1 animal in extremis (K.I.E.). At the beginning of week 5 it was decided that the group should not receive any further doses of CCl_4. At this time point there were 12 animals left in the group that had received a total of 13 CCl_4 administrations. Of these, 9 animals were selected for autopsy and the remaining 3 were left to recover (treatment free) for the rest of the study (8 weeks). However, 1 of the 3 rats in the recovery period had to be killed (K.I.E.) during the second week of the recovery period.

At week 5, 2 animals in the 0.8 mL/kg CCl_4 group were found dead and 1 animal had to be killed. The animals in the group had received a total of 15 CCl_4 doses. Of the remaining 12 animals, 9 were autopsied and 3 rats were left to recover for 4 weeks without CCl_4 treatment.

At week 6, after receiving 18 doses, 2 animals in the 0.4 mL/kg CCl_4 group had to be killed. This was a scheduled autopsy time point, therefore, 5 controls and 5 CCl_4-treated animals were autopsied as planned. However, due to the 2 animals which needed to be killed in extremis, it was decided that this group would not be dosed further. Of the 8 animals remaining 4 were kept for a further 4 weeks without treatment and 4 were were kept for 8 weeks in total without treatment.

At autopsy, livers from treated animals at 0.4, 0.8 and 1.2 mL/kg CCl_4 and collected at the end of the study, were generally paler in colour and showed diffuse pitting of the surface. In some animals, small cysts (1 mm) were reported on the liver surface. These cysts were present in 2 animals treated with 0.4 and 0.8 mL/kg and in 3 animals dosed with 1.2 mL/kg CCl_4. After 3 weeks of treatment the spleens from 2 animals treated at 0.8 and 1.2 mL/kg CCl_4 were enlarged in size but normal in colour. At the group termination autopsies the proportion of animals showing increased size spleens increased to 5 and 6 out of 9 animals in the 0.8 and 1.2 mL/kg CCl_4 respectively, and in the highest dose level group one of these rats showed a reduction in the size of the testes compared to the other animals in the group. There was also the presence of fluid in the abdominal cavity with prominent and enlarged veins in the abdominal wall. After 6 weeks of treatment at 0.4 mL/kg CCl_4 all animals had accumulation of fluid in the abdominal cavity and 3 animals also showed enlarged veins in the abdominal wall. At termination of the 0.8 and 1.2 mL/kg CCl_4 treatment groups all animals showed presence of fluid in the abdominal cavity and 4 and 5 animals also had enlarged veins, respectively.

Animals autopsied during the recovery period showed signs of improved health. In some animals the livers were still slightly paler in colour compared to control rats and showed evidence of diffuse pitting of the surface, but in general, the livers from CCl_4-treated animals had a normal appearance, both in terms of size and colour. Some of the spleens remained enlarged compared to control animals, and both the number of animals with fluid accumulation and the volume of fluid found in the abdominal cavity had significantly reduced compared to the findings during the dosing period.

Table 7.1 Autopsy time points during the dosing period and number of animals autopsied/found dead/killed in extremis during the dosing period, per CCl_4 dose level group and per week.

CCl_4 dose level (mL/kg)	**Day 1**	**Week 3 (9 doses)**	**Week 4/5 (13 doses)**	**Week 5 (15 doses)**	**Week 6 (18 doses)**
	Number of animals dosed	Number of autopsies and unscheduled deaths			
0	20	5	-	-	5
0.4	20	5	-	-	2 [a] + 5
0.8	20	5	-	2 [a] + 1 [b]	-
1.2	20	5	2 [a] + 1 [b]	-	-

[a] number of animals that were found dead; [b] number of animals that were K.I.E (killed in extremis).

7.3.2 Body weight changes

Throughout the study animals were weighed 3 times a week. After day 29 (week 4), some groups had to be terminated which meant that while some animals had begun the recovery phase, others were still in the dosing period. Therefore, time points after day 29 are not shown in Figure 7.1. At day 29 all animals had received 13 doses of CCl_4.

In Figure 7.1 it is clear that animals followed the same pattern in body weight change during the study. Control animals gained weight at a faster rate than CCl_4-treated animals. Rats in the highest dose level group (1.2 mL/kg) remained consistently lighter throughout the study and at the end of the study it appeared that the body weights were dependent on the dose level of CCl_4.

At the last time point (day 29/week 4), control animals had increased in weight by 50 % compared to day 1, whereas the increase recorded for CCl_4-treated animals was smaller (27, 21 and 15 % for 0.4, 0.8 and 1.2 mL/kg treated animals, respectively).

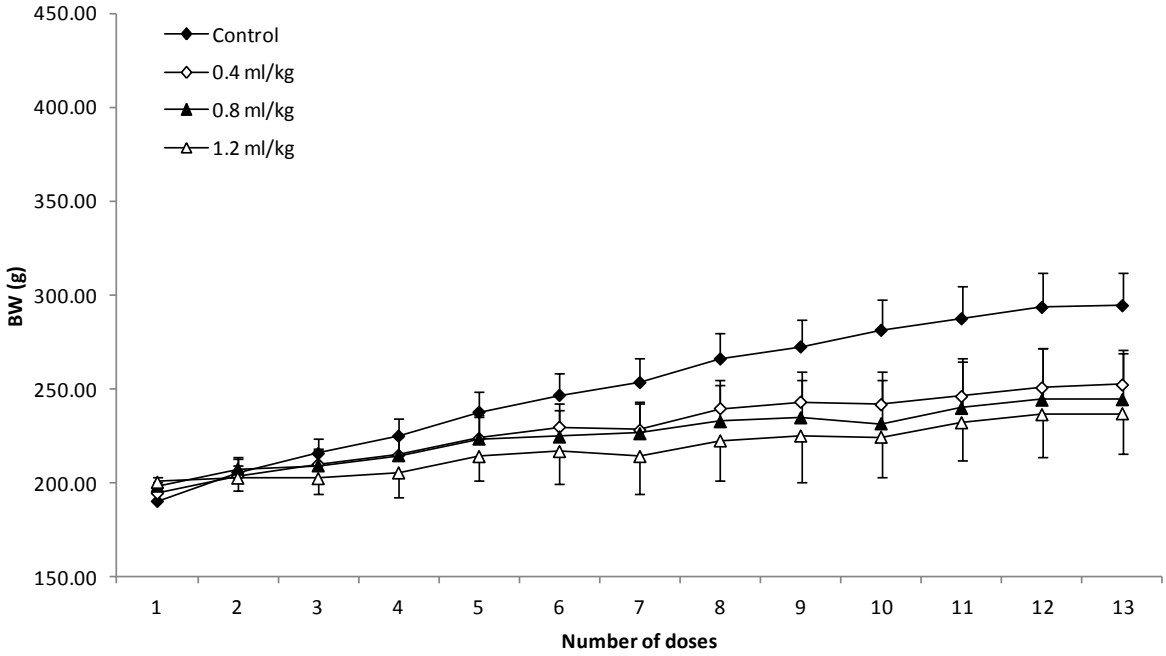

Figure 7.1 Increase in body weight for male Hanover-Wistar rats treated with increasing doses of CCl_4, with increasing number of CCl_4 administrations. Animals were dosed with vehicle (control, 0 mL/kg) or CCl_4 at the doses shown by gavage. Animals were weighed 3 times a week before each administration as described in Section 7.2.1. Results are shown as mean body weight with SD indicated by vertical bars of 20 animals per group (week 1 to week 9) and 15 animals per group (week 10 to 13).

7.3.3 Liver weights

At the week 3 autopsies, livers from CCl_4-treated rats at 0.4, 0.8 and 1.2 mL/kg were significantly heavier than controls ($^{***}P<0.001$). Animals treated with CCl_4 at 0.8 mL/kg had the heavier liver weights which corresponded to a 2.23-fold increase over controls (data not shown).

Relative liver weights for control animals at week 6 were compared to the relative liver weights for CCl_4-treated animals with 0.4, 0.8 and 1.2 mL/kg at the group termination autopsies, that is, at week 6, 5 and 4 respectively. There were no significant differences between control and CCl_4-treated animals. However, at this time point, livers for CCl_4-treated animals were smaller in size compared to livers for treated animals at week 3 (data not shown).

7.3.4 Kidney weights

At week 3, relative kidney weights were significantly increased over controls at 0.8 and 1.2 mL/kg CCl_4 (1.32-fold; $^{**}P<0.01$). The increase in size appeared to be dose-dependent (data not shown).

At the end of the study, relative weights were significantly increased above controls at week 6 at all dose levels ($^{***}P<0.001$), and there appeared to be a dose-related increase in relative kidney weights (data not shown).

7.3.5 Serum clinical chemistry

Clinical chemistry parameters including ALT, AST, GLDH, ALP, albumin, total protein, urea, creatinine and glucose were measured in the serum from control (vehicle-treated animals) and CCl_4-treated rats at day 1 post-dosing, at week 3 and at termination of the study groups (Figure 7.2, Table 7.2). No blood samples were collected from animals that were found dead, killed in extremis or left to recover, and therefore, no serum data is presented for those animals.

At 24 hours after the first dose of CCl_4, levels of serum ALT, AST and GLDH were increased over controls and there appeared to be a dose related trend, reaching maximal levels at 1.2 mL/kg CCl_4 (Figure 7.2 A). At 0.4 mL/kg CCl_4 only serum GLDH was significantly increased over controls ($^{*}P<0.05$). At 0.8 mL/kg CCl_4 both ALT and

GLDH were significantly increased over controls, whereas at the highest dose group (1.2 mL/kg) all enzyme levels were significantly increase over control animals ($^{***}P<0.001$).

Figure 7.2 B and C show the mean levels for ALT, AST and GLDH after 3 weeks of CCl_4 dosing (i.e. 9 doses) and at group termination autopsies, respectively. Levels of these enzymes were significantly increased at all CCl_4 dose levels (0.4, 0.8 and 1.2 mL/kg) over the respective control animals at the same time point. However, mean serum ALT, AST and GLDH were highest in the 0.4 mL/kg CCl_4-treated animals and appeared to decrease with increasing dose level of CCl_4 (Figure 7.2 B and C).

Levels of ALP were slightly increased over controls at 24 hours after a single dose of CCl_4, and at the highest dose level (1.2 mL/kg) this increase was statistically significant ($^{***}P>0.001$) (Table 7.2).

All other parameters that were measured 24 hours after a single CCl_4 dose were similar in CCl_4 treated animals compared to controls.

ALP levels were also significantly increased over controls after 3 weeks (9 doses) of treatment at all CCl_4 dose levels. The mean value was greatest in the 0.8 mL/kg CC_4-treated group (1301.40 compared to 234.00 U/L, for CCl_4-treated and control animals respectively, $^{***}P<0.001$) (Table 7.2). At termination of the groups, mean ALP values were also increased over controls but appeared to decrease with increasing CCl_4 dose level (1465.00, 1290.44 and 1057.67 U/L for animals in the 0.4, 0.8 and 1.2 mL/kg CCl_4-treated groups respectively).

Albumin values were significantly decreased in CCl_4-treated animals at 0.8 mL/kg at week 3 compared to control, and in 0.4, 0.8 and 1.2 mL/kg CCl_4-treated animals at the group termination autopsies (Table 7.2).

At week 3, total protein levels in the serum of 0.8 and 1.2 mL/kg CCl_4-treated rats were significantly decreased compared to controls ($^{***}P<0.001$ and $^{*}P<0.05$, respectively). At termination of the groups, however, mean levels were significantly decreased in all 3 CCl_4-treated groups compared to controls at week 6 (T6) (Table 7.2).

Serum levels of urea were approximately 1.5-fold increased over control in CCl_4-treated animals at 0.4 mL/kg at week 3 (7.56 and 11.08 mmol/L for control and CCl_4-treated animals respectively) ($^{***}P<0.001$) (Table 7.2). However, at the other dose levels there

were no statistical differences between controls and CCl_4-treated animals. At termination, animals in the highest dose level group (1.2 mL/kg) had significantly lower urea levels than control animals at the same time point ($^{*}P<0.05$) but there was no evidence of a dose-related trend.

Creatinine levels in the serum showed no evidence of a CCl_4-treatment related effect, except for animals in the 1.2 mL/kg CCl_4 group at the final autopsy. Animals in this group had significantly lower levels compared to the time-matched control ($^{**}P<0.01$).

Serum glucose levels were slightly decreased in animals treated with CCl_4 at 1.2 mL/kg at the week 3 autopsies but this decrease was not statistically significant. At the final autopsy of the group, serum glucose was significantly decreased in the 0.8 mL/kg when compared to controls ($^{**}P<0.01$) (Table 7.2).

A (Day 2: 1 dose)

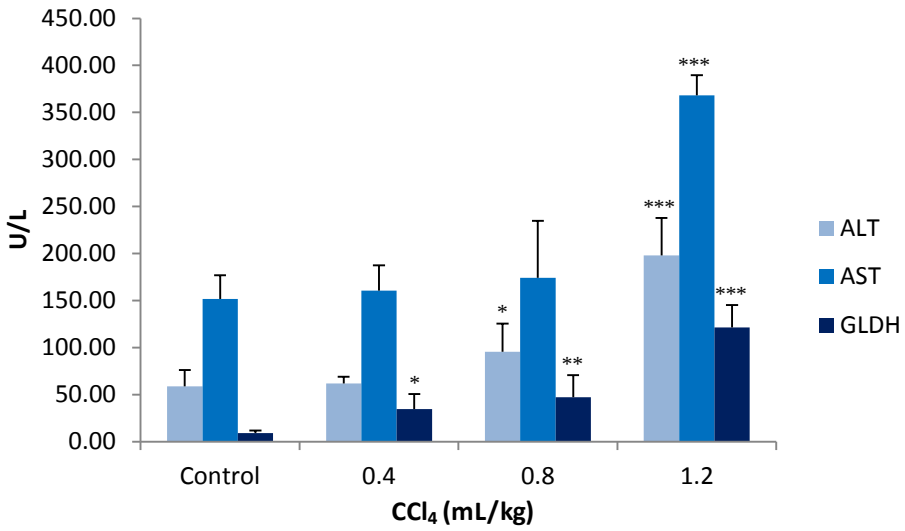

B (Week 3: 9 doses)

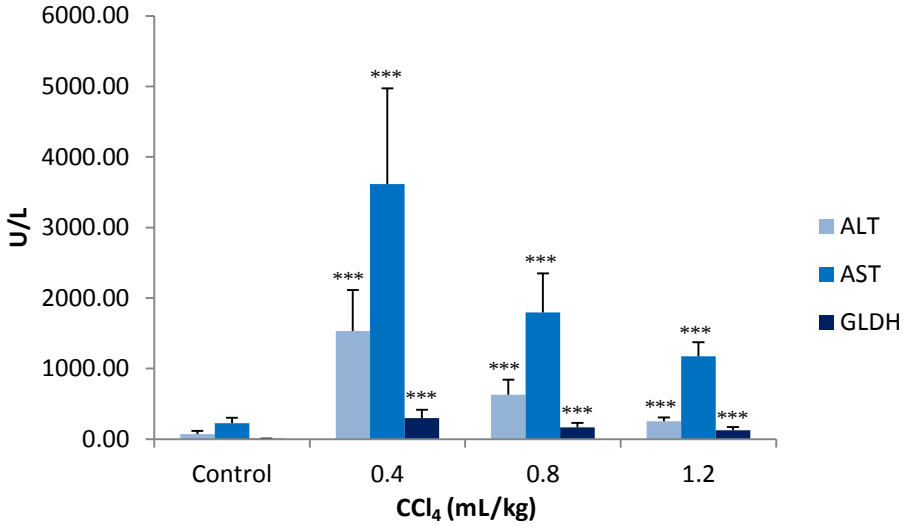

C (Week 4-6: 13-18 doses)

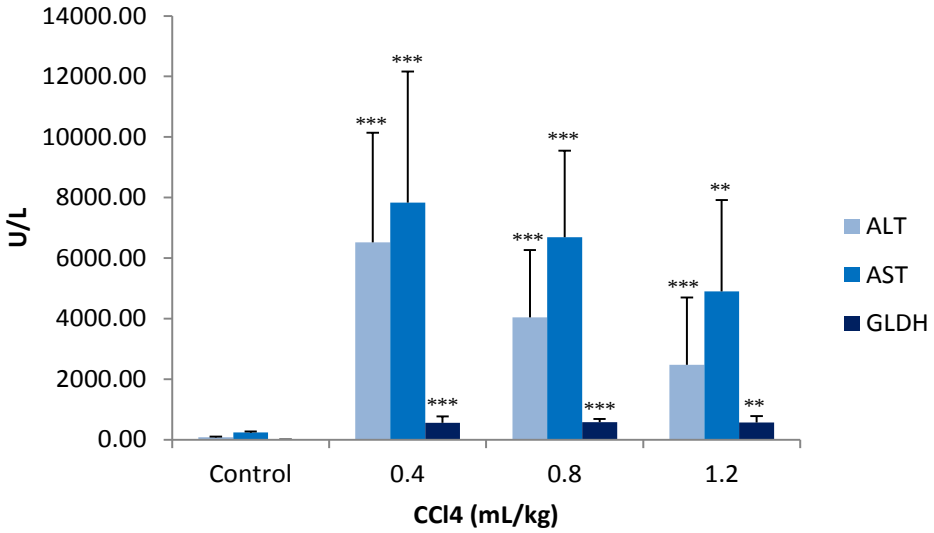

Figure 7.2 Serum ALT, AST and GLDH levels for male Hanover-Wistar rats treated with increasing doses of CCl_4 and sampled at different time points. Animals were dosed with vehicle (control, 0 mL/kg) or CCl_4 by gavage at the doses shown. Blood was collected from the tail at day 2 (24 hours post-dosing) (A), and at autopsy at the following time points (B, C) as described in Section 7.2.1. Enzymes were assayed according to Section 2.7. At day 2 and week 3 values are the means of 5 animals per group. At weeks 4, 5 and 6, values are the means of 5 controls and 5 CCl_4-treated animals at 0.4 mL/kg, and of 9 animals at 0.8 and 1.2 mL/kg CCl_4. SD is represented by vertical bars. Values that differ significantly from controls by one-way ANOVA test are shown: $^{*}P<0.05$; $^{**}P<0.01$; $^{***}P<0.001$.

Table 7.2 Serum clinical chemistry parameters for male Hanover-Wistar rats treated with increasing doses of CCl_4 and sampled at different time points. Animals were dosed with vehicle (control, 0 mL/kg) or CCl_4 by gavage at the doses shown. Blood was collected from the tail at day 2, and at autopsy at the following time points as described in Section 7.2.1. Enzymes were assayed according to Section 2.7. At day 2 and week 3 values are the means and SD of 5 animals per group. At weeks 4, 5 and 6 values are the means of 5 controls and 5 CCl_4-treated animals at 0.4 mL/kg, and of 9 animals at 0.8 and 1.2 mL/kg CCl_4. Values that differ significantly from controls by one-way ANOVA test are shown: $^{*}P<0.05$; $^{**}P<0.01$; $^{***}P<0.001$.

CCl_4 dose level (mL/kg)		**Serum parameters**					
		ALP (U/L)	Albumin (g/L)	Total protein (g/L)	Urea (mmol/L)	Creatinine (µmol/L)	Glucose (mmol/L)
1 dose (day 2)	**0**	569.40 (67.40)	38.02 (1.88)	59.34 (3.19)	7.54 (1.46)	31.67 (11.24)	6.76 (1.07)
	0.4	648.00 (170.00)	37.40 (0.98)	57.77 (1.34)	8.11 (0.70)	24.10 (0.87)	6.63 (1.67)
	0.8	676.60 (122.88)	38.24 (1.27)	58.86 (1.68)	8.98 (1.17)	21.27 (4.27)	5.75 (0.69)
	1.2	754.60*** (35.19)	36.66 (0.85)	56.68 (1.26)	7.38 (1.05)	22.99 (2.33)	6.95 (0.90)
9 doses (week 3)	**0**	234.00 (54.09)	36.80 (1.30)	58.80 (2.86)	7.56 (0.67)	32.80 (5.07)	5.33 (1.95)
	0.4	824.40*** (237.63)	36.00 (1.41)	53.80 (1.79)	11.08*** (1.01)	30.80 (10.21)	4.58 (1.07)
	0.8	1301.40*** (593.88)	31.80* (2.77)	48.80*** (3.27)	8.82 (1.26)	28.00 (4.90)	4.09 (0.53)
	1.2	1076.80*** (392.60)	33.80 (3.35)	52.40* (4.04)	9.18 (1.22)	32.20 (4.09)	3.97 (0.31)
18 (week 6)	**0**	256.80 (90.02)	35.80 (0.84)	59.60 (1.67)	8.22 (0.55)	32.00 (1.41)	5.71 (0.90)
18 (week 6)	**0.4**	1465.00*** (369.28)	28.80** (3.63)	52.20* (4.09)	7.28 (1.39)	26.80 (3.96)	3.78 (1.28)
15 (week 5)	**0.8**	1290.44*** (213.48)	27.11*** (2.09)	47.33*** (2.35)	6.48 (1.30)	32.89 (6.45)	2.95** (0.96)
13 (week 4/5)	**1.2**	1057.67 (244.81)	28.33** (4.00)	47.78*** (4.74)	6.16* (1.42)	24.67** (2.50)	5.77 (1.32)

7.3.6 Urine clinical chemistry

No urine samples were collected from animals that were found dead, killed in extremis or left to recover, and therefore, no urine data is presented for those animals.

Total protein, creatinine and glucose were measured in the urine samples from rats at week 3 and at termination of the groups (Table 7.3).

There appeared to be no CCl_4-treatment-related effect on the levels of total urinary protein except for animals in the highest dose group (1.2 mL/kg) following the administration of 13 doses of CCl_4. These animals had lower levels of urinary protein compared to the time-matched control animals (2.13 mg/c.p. compared to 6.72 mg/c.p.; $^{**}P<0.01$) (Table 7.3).

After 3 weeks of treatment (9 doses) with 1.2 mL/kg CCl_4, the mean urinary creatinine level was 37.00 µmol/c.p., compared to a control value of 51.00 µmol/c.p and this decrease was statistically significant ($^{*}P<0.05$). At the termination autopsies, urinary creatinine was significantly decreased compared to control animals at all CCl_4 dose levels and there appeared to be a dose-related relationship (Table 7.3).

There was no change in urinary glucose levels at week 3 at any of the CCl_4-dose levels. However, at termination (week 4 and 5), glucose levels in the urine were significantly decreased in the 2 highest dose level groups (0.8 and 1.2 mL/kg CCl_4) compared to control rats. Mean values were 4.00, 3.22 and 5.40 µmol/c.p. for 0.8 and 1.2 mL/kg CCl_4-treated rats and control animals, respectively (Table 7.3). There was no effect on the urine volume at any dose level and at any of the time points.

Table 7.3 Urinary biomarkers for male Hanover-Wistar rats treated with increasing doses of CCl_4 and sampled at different time points. Animals were dosed with vehicle (control, 0 mL/kg) or CCl_4 by gavage at the doses shown. Urine was collected for 18 hours before each autopsy as described in Section 7.2.1. Biomarkers were assayed according to Section 2.7. At day 2 and week 3 values are the means and SD of 5 animals per group. At weeks 4, 5 and 6 values are the means of 5 controls and 5 CCl_4-treated animals at 0.4 mL/kg, and of 9 animals at 0.8 and 1.2 mL/kg CCl_4. Values that differ significantly from controls by one-way ANOVA test are shown: $^{*}P<0.05$; $^{***}P<0.001$.

CCl_4 dose level (mL/kg)		**Urinary paramters**			
		Total protein (mg/c.p.)	Creatinine (µmol/c.p.)	Glucose (µmol/c.p.)	Volume (mL)
9 doses (week 3)	**0**	5.20 (2.05)	51.00 (7.31)	4.20 (0.84)	31.40 (5.98)
	0.4	2.68 (0.97)	44.40 (5.03)	4.60 (1.34)	16.00 (7.31)
	0.8	5.14 (5.46)	40.40 (8.17)	5.00 (1.22)	17.20 (4.76)
	1.2	3.54 (1.42)	37.00* (8.22)	4.00 (0.71)	32.40 (22.51)
18 (week 6)	**0**	6.72 (2.03)	77.60 (2.70)	5.40 (1.14)	24.40 (7.27)
18 (week 6)	**0.4**	3.30 (1.76)	47.20*** (3.56)	4.60 (0.89)	22.80 (6.76)
15 (week 5)	**0.8**	6.69 (5.02)	47.44*** (8.56)	4.00* (1.00)	32.78 (8.94)
13 (week 4/5)	**1.2**	2.13** (1.12)	37.33*** (4.87)	3.22** (0.67)	23.78 (11.69)

7.3.7 Histopathology

Animals in this study were autopsied after 3 weeks of dosing and at termination of the study as described in Table 7.1. Animals in the recovery groups were sacrificed as described in Table 7.1.

At autopsy, livers and kidneys were removed and placed in formalin for histopathological examination (Figure 7.3).

After 3 weeks of dosing (9 doses), the histopathological effects in the liver were similar at all dose levels (0.4, 0.8 and 1.2 mL/kg CCl_4). There was hepatocellular vacuolation with some necrosis of individual cells and the presence of mitotic cells. There was also evidence of thickening of the perivascular connective tissue with minimal inflammatory cell infiltrate and fibrotic septae penetrating the liver parenchyma.

At termination of the study (weeks 4, 5 and 6), there was hepatocellular vacuolation in all animals, however, there did not appear be a dose-related trend. Necrotic and mitotic cells were still apparent and the development of fibrotic septae as present at 3 weeks (bridging fibrosis) had progressed.

In the kidneys, at 3 weeks of treatment (i.e. after 9 doses of CCl_4) there were no CCl_4-related findings, apart from vacuolation of the proximal tubules in 2 animals at 1.2 mL/kg CCl_4. At termination of the study groups, vacuolation of the proximal tubules was evident in the majority of the animals receiving the CCl_4 treatment but there were no other renal changes consistent with CCl_4-induced damage.

Histopathological findings in the livers of recovery animals included hepatocellular vacuolation, however, this was much reduced compared to the degree of vacuolation observed during the dosing period. Fibrotic septae were still present but were much narrower during this recovery period and in some cases were reduced to fine collagen strands. In particular individuals there were areas of normal parenchyma indicating almost complete recovery of hepatic injury. The degree of resolution observed, however, did not correlate with the length of time the animal was allowed to recover, therefore, this may reflect the individual variability in the severity of the initial CCl_4-induced injury.

There were no histopathological changes consistent with CCl_4 administration in any of the other organs examined during the dosing period, and there were no abnormalities in the liver or kidneys collected from control animals at any time point.

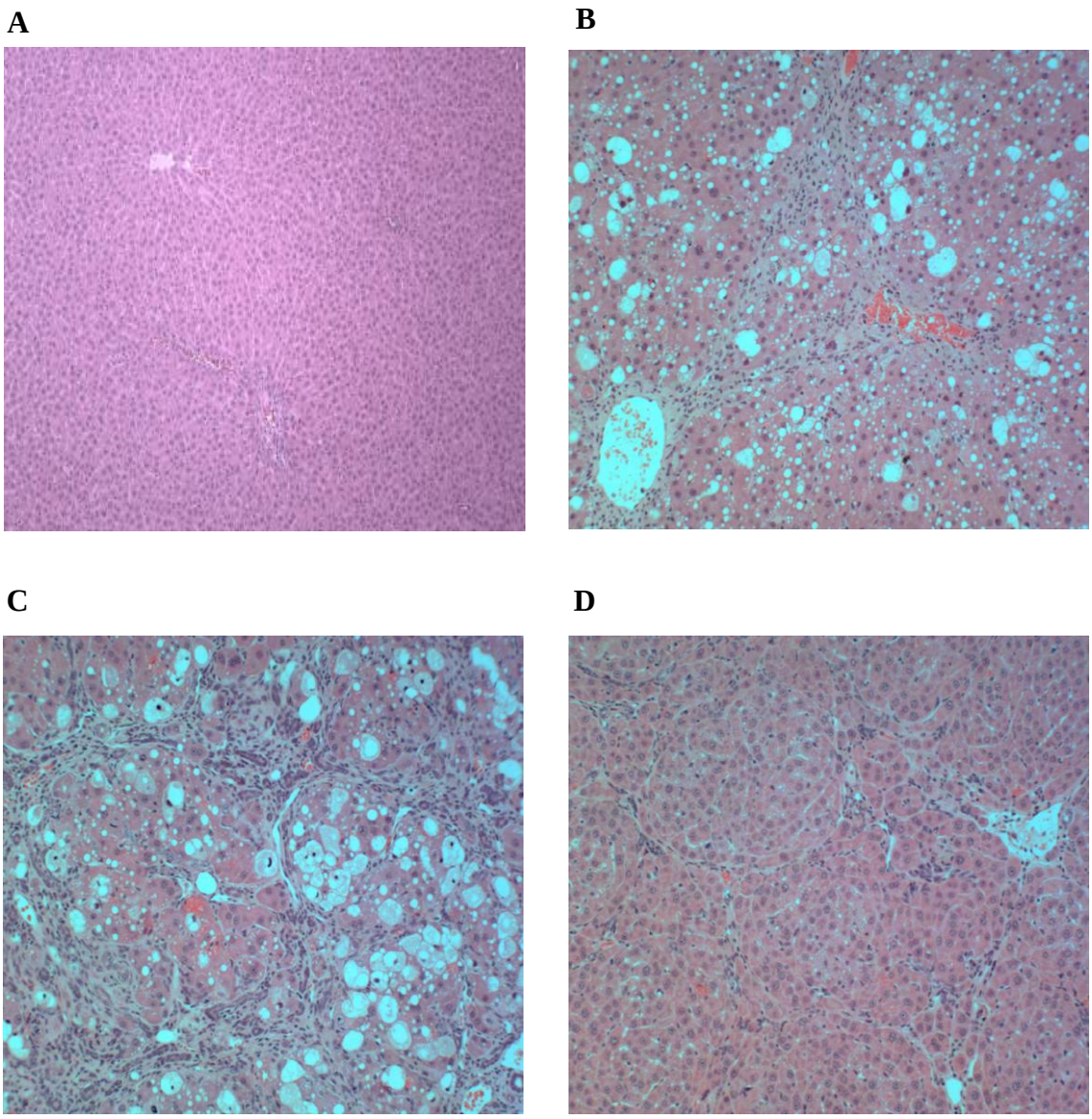

Figure 7.3 Histology of liver sections from male Hanover-Wistar rats treated with increasing doses of CCl_4 and sampled at various time points. Original magnification of all images, x 100; H&E. Rats were treated with vehicle (control, 0 mL/kg) or CCl_4 at 0.4, 0.8 and 1.2 mL/kg as described in Section 7.2.1. At autopsy, liver samples were collected and processed for histopathological examination as described in Section 2.8. (A) Control animal at week 3; (B) 0.4 mL/kg CCl_4-treated rat at week 3 (9 doses): thickening of the perivascular connective tissue around central veins, vacuolated hepatocytes, early development of fibrotic septae; (C) 0.4 mL/kg CCl_4-treated rat at week 6 (18 doses): bridging fibrosis, vacuolated hepatocytes and presence of single cell hepatocyte necrosis; (D) 0.8 mL/kg CCl_4-treated rat for 5 weeks (15 doses) and allowed to recover for 4 weeks without treatment: fibrotic septae are very fine, very few vacuolated hepatocytes.

7.4 Results for experiment 2

7.4.1 Observations during the study

In the present study, animals were administered with CCl_4 at 0.4 mL/kg and dosed 3 times a week for a period of 6 weeks. This dose level was chosen since from the previous experiment it was clear that higher dose levels (0.8 and 1.2 mL/kg) resulted in a greater degree of mortality, and at the same time there was no histopathological difference as to the level of fibrosis induced. Some animals were left to recover for 3 and 6 weeks without treatment (week 9 and 12).

Throughout the study animals were observed for signs of ill-health and clinical observations recorded during the post-mortem procedure.

At week 1, all animals appeared normal. At the week 2 autopsies however, livers from CCl_4-treated animals were paler in colour and enlarged in size compared to control animals. There was also diffuse pitting of the liver surface (further discussed in Section 7.4.9). Veins in the abdominal cavity appeared enlarged and prominent and there was slight accumulation of fluid in the abdominal cavity in some of the CCl_4-treated animals. Similar observations were recorded during autopsies at week 3, 4 and 5 of the dosing-period. Additionally, at weeks 4 and 5, some animals had larger spleens.

After 6 weeks of CCl_4 administration 3 times a week, livers from treated animals were reduced in size compared to CCl_4-treated livers at the previous time point; they were paler in colour compared to control animals, showed diffuse pitting of the surface and a nodular appearance (Section 7.4.9). There was also fluid accumulation in the abdominal cavity, and the abdominal veins and the spleen appeared to be enlarged.

After 3 weeks of recovery (week 9 of the study) the livers of treated animals had a pitted surface and remained slightly paler in colour compared to the control rats. Similar findings were present at the 12 week autopsies (following 6 weeks of recovery).

7.4.2 Liver weights

Figure 7.4 A shows the mean relative liver weights for animals autopsied during this study. Animals were treated 3 times a week with CCl_4 at 0.4 mL/kg and autopsied at weeks 1, 2, 3, 4, 5 and 6 during the dosing period and at weeks 9 and 12 (that is, after 3 and 6 weeks without treatment, respectively).

Relative liver weights for CCl_4-treated rats were compared to control animals at each time point for statistical analysis. During the dosing period relative liver weights were significantly increased over controls between 1 and 5. At week 6, 2 animals had much lower liver weights than the rest of the group. Therefore, the standard deviation of the group is large and may have contributed to the lack of statistical significance.

At week 1 (T1), the relative liver weight for CCl_4-treated animals was 1.52-fold increased over concurrent controls ($^{**}P<0.01$). The heaviest liver weights for CCl_4-treated rats were seen at week 2 (58.51 and 30.86 g/kg BW for CCl_4-treated and control animals respectively). From week 3 of the study, there appeared to be a decrease in relative liver weights in CCl_4-treated animals with time (i.e. number of CCl_4 doses received). By week 9 and 12, (3 and 6 weeks after stopping dosing), liver weights for CCl_4-treated animals were only 1.16- ($^{*}P<0.05$) and 1.21-fold ($^{**}P<0.01$) increased over concurrent controls (Figure 7.4 A).

7.4.3 Kidney weights

Relative kidney weights for CCl_4-treated and control animals are shown in Figure 7.4 B. Kidney weights were significantly increased over controls at week 4, 5 and 6 during the dosing period and at week 12 in the recovery period. At the week 4 autopsies, kidney weights were 3.46 and 4.40 g/kg BW for control and CCl_4-treated animals, respectively; this corresponded to an approximate 1.27-fold increase ($^{**}P<0.01$). It would appear that after 4 weeks of dosing there was a CCl_4-treatment related effect on kidney weight. At week 12 (6 weeks after the end of the dosing period) kidneys were 1.14-fold increased over controls (3.40 and 2.99 g/kg BW for CCl_4-treated and control animals, respectively). However, it is interesting to note that the mean control kidney weights at this time point were lower than at all other time points.

A

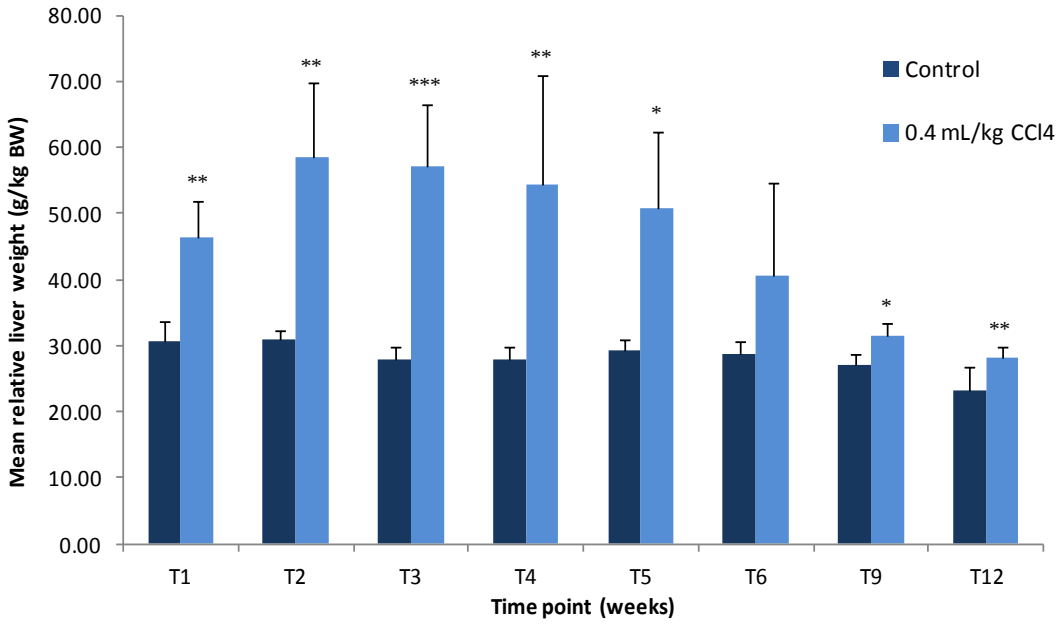

B

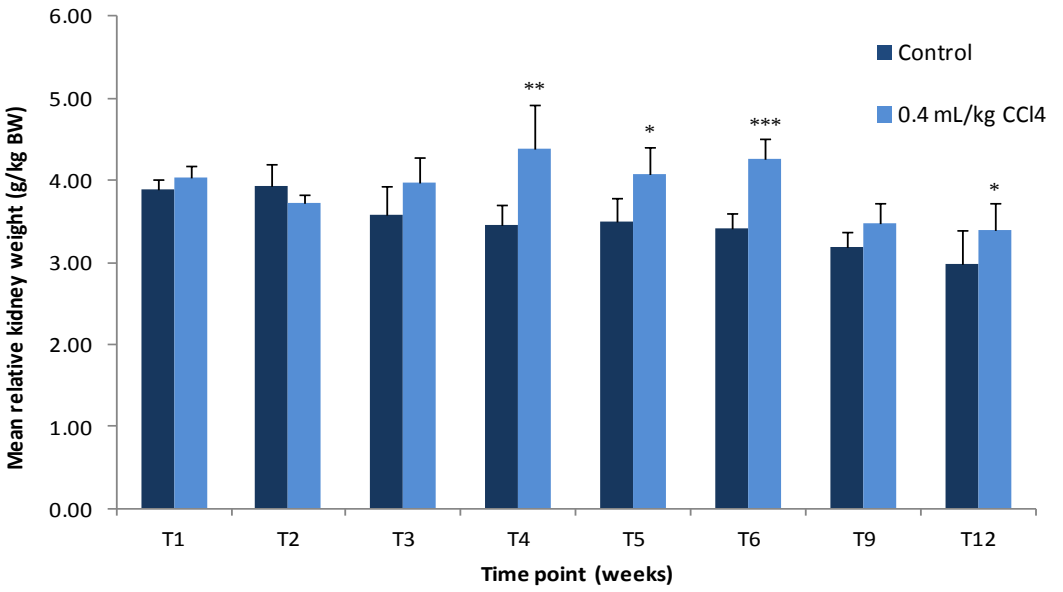

Figure 7.4 Relative liver (A) and kidney (B) weights from male Hanover-Wistar rats treated with vehicle (control) or CCl_4 at 0.4 mL/kg and autopsied at different time points. Animals were dosed by gavage and autopsied at the time points shown as described in Section 7.2.2. At autopsy, animals were killed, livers and kidneys were removed and weighed. The kidney weight was expressed as a mean of the left and right kidneys. Results are shown as mean organ weight per kg body weight with SD indicated by vertical bars of 5 animals per group. Relative organ weights that differ significantly from controls at the same time point by Students' t-test are shown: $^{*}P<0.05$; $^{**}P<0.01$; $^{***}P<0.001$.

7.4.4 Weights of other organs

At post-mortem, the spleen, adrenals, thymus and testes were removed from all animals and the relative organ weights calculated (Table 7.4). Relative weights for each CCl_4-treated group were compared to the concurrent control for statistical significance.

The relative spleen weight was significantly increased above control at week 3 and increased with time up to week 6. At week 6, the spleen weights were 2.03 and 4.52 g/kg BW for control and CCl_4-treated animals respectively (2.23-fold increase; $^{**}P<0.01$). The relative spleen weight was slightly lower than treated animals at week 6 in the recovery animals, but was still significantly increased over concurrent controls at week 9 and 12 (i.e. 3 and 6 weeks of no treatment). The mean relative adrenal weight was significantly increased above concurrent controls at week 4, however, there was no evidence of an effect on relative weights with increasing number of CCl_4 doses. At T4 and T6, the relative thymus weight was significantly decreased compared to concurrent controls ($^{*}P<0.05$) (Table 7.4). There were no statistical differences in the relative testes for CCl_4-treated when compared to control animals at any time point in the study.

Table 7.4 Relative organ weights from male Hanover-Wistar rats treated with vehicle (control) or CCl_4 at 0.4 mL/kg and autopsied at different time points. Animals were dosed by gavage and autopsied at the time points shown as described in Section 7.2.2. At autopsy, animals were killed, organs were removed and weighed. The testes and adrenals weight was expressed as a mean of the left and right organs. Results are shown as mean organ weight per kg body weight (BW) and SD of 5 animals per group. Relative organ weights that differ significantly from controls at the same time point by Students' t-test are shown: $^{*}P<0.05$; $^{**}P<0.01$. C: control; T: CCl_4-treated rat.

Time point (weeks)	Relative organ weight (g/kg BW) (SD)			
	Spleen	Adrenal	Thymus	Mean testes
C1	2.58 (0.20)	0.27 (0.04)	2.50 (0.24)	7.69 (0.81)
T1	2.38 (0.23)	0.32 (0.09)	2.15 (0.29)	7.45 (0.42)
C2	2.39 (0.26)	0.27 (0.03)	2.20 (0.37)	7.10 (0.43)
T2	2.26 (0.30)	0.29 (0.04)	1.80 (0.17)	7.25 (0.26)
C3	2.09 (0.43)	0.27 (0.06)	1.72 (0.24)	6.29 (0.22)
T3	2.68* (0.30)	0.26 (0.02)	1.69 (0.22)	6.38 (1.25)
C4	2.10 (0.18)	0.25 (0.03)	1.88 (0.38)	5.89 (0.74)
T4	3.18* (0.93)	0.32** (0.04)	1.19* (0.45)	6.67 (1.15)
C5	1.99 (0.12)	0.24 (0.04)	1.85 (0.85)	5.72 (0.55)
T5	3.76* (1.25)	0.25 (0.07)	1.15 (0.19)	6.13 (0.54)
C6	2.03 (0.13)	0.24 (0.07)	1.42 (0.18)	5.03 (1.44)
T6	4.52** (1.12)	0.27 (0.08)	1.08* (0.23)	5.70 (1.53)
C9	2.02 (0.20)	0.40 (0.34)	1.30 (0.48)	4.75 (1.19)
T9	3.33** (0.62)	0.20 (0.07)	1.18 (0.20)	4.92 (0.29)
C12	1.77 (0.20)	0.18 (0.34)	1.06 (0.48)	5.43 (1.19)
T12	3.18** (0.67)	0.19 (0.03)	1.31 (0.16)	4.65 (0.76)

7.4.5 Serum clinical chemistry

Figure 7.5 shows the levels of the enzymes ALT, AST and GLDH in serum prepared from blood collected from animals every week during this study (weeks 1 to 12).

Serum ALT and AST levels were significantly increased over concurrent controls at all time points during the dosing period (T1-T6) (Figure 7.5 A and B). Both enzymes increased as the number of CCl_4 doses increased up to week 3. At this time point, the mean values for CCl_4-treated animals and control animals were 8413.00 and 60.80 U/L for ALT, and 7676.00 and 135.00 U/L for AST, respectively. This corresponded to a 139- and a 57-fold increase for ALT and AST. After week 3, the mean level of these enzymes gradually decreased but remained increased above concurrent control levels. At week 6, ALT and AST levels were approximately 41 and 32 times greater than concurrent controls ($^{***}P<0.001$).

During the recovery period, blood samples were collected at T7, T8, T10 and T11 by tail vein bleed, and at autopsy at time points T9 and T12. Mean ALT and AST levels in the serum of CCl_4-treated animals were much lower than levels in CCl_4-treated animals at previous time points (during the dosing period) but were still greater than concurrent controls. At the 12 week autopsies, mean values for CCl_4-treated and control animals were 155.20 and 100.20 U/L, respectively (for ALT); and 238.00 and 180.40 U/L, respectively (for AST) (Figure 7.5 A and B).

Serum GLDH levels were significantly increased over concurrent controls at all time points (dosing and recovery periods) (Figure 7.5 C). The greatest fold increase over controls was seen at week 4 of the study; at this time point GLDH levels were approximately 147-fold greater in CCl_4-treated animals compared to concurrent controls (5.20 and 766.60 U/L for control and CCl_4-treated animals respectively; $^{***}P<0.001$). After week 4, GLDH levels still remained significantly increased over control but the fold increase declined with time. At week 7 (first time point during the recovery period) values for serum GLDH in CCl_4-treated animals had fallen from 367.50 U/L at week 6, to 57.20 U/L at week 7. By week 12, values for CCl_4-treated animals were still 3 times greater than controls ($^{**}P<0.01$).

Serum lipocalin-2 levels were increased over controls at all weeks during the dosing period, but this increase was only statistically significant at weeks 4, 5 and 6 (Table 7.5). Serum levels reached a peak at week 4 (464.40 µg/L and 40.40 µg/L for CCl_4-

treated and control animals, respectively) when they were 11.5-fold increased over control ($^{**}P<0.01$). At all other time points (week 7 to 12, period without treatment), lipocalin-2 levels were similar to controls in CCl_4-treated animals (Table 7.6).

TIMP-1 levels were significantly increased over controls at all time points during the dosing period (Table 7.5). After 4 weeks of treatment, serum TIMP-1 levels were approximately 30-fold increased above control in CCl_4-treated animals ($^{**}P<0.01$). Mean serum levels were still significantly increased over controls at weeks 7, 9, 11 and 12, but at these time points the fold increases were smaller (Table 7.6).

MCP1 levels were significantly increased over control animals at weeks 1 to 4, and were maximal at week 4 (50.00 µg/L and 7.20 µg/L for CCl_4-treated and control animals respectively). At this time point there was a 6.9-fold increase ($^{**}P<0.01$). From this time point onwards there were no other significant differences between control and treated animals (Table 7.5, Table 7.6).

Serum AGP levels were increased over controls at all time points during the dosing period (Table 7.5). At weeks 3 to 6 this increase was statistically significant. At week 6, levels were 1.8-fold increased over controls ($^{**}P<0.01$). Between weeks 7 and 12, AGP levels in CCl_4-treated animals returned to control levels (Table 7.6).

A2M levels in the serum were significantly decreased in CCl_4-treated animals compared to controls at week 1 (45.20 mg/L compared to 30.80 mg/L for control and CCl_4-treated animals respectively; $^{*}P<0.05$) (Table 7.5). After this time point however, serum A2M levels appeared to increase with the number of CCl_4 administrations and reached a peak at week 6 (12.40-fold increase over controls; $^{**}P<0.01$). At weeks 7, 9, 11 and 12 (Table 7.6), A2M levels were still significantly increased over controls in CCl_4-treated animals. However, at the last time point (week 12), the fold increase recorded was only 2.6-fold ($^{**}P<0.01$).

Levels of glucose, albumin, total protein, urea and creatinine were also measured in serum samples from control and CCl_4-treated samples at each time point (Table 7.5, Table 7.6). Serum glucose levels were significantly decreased in CCl_4-treated rats compared to concurrent controls at week 2 and 5 during the dosing period ($^{*}P<0.05$ and $^{**}P<0.01$, respectively). However, at all other time points during the study, glucose levels were similar to controls.

Serum albumin levels were significantly decreased compared to concurrent controls at weeks 5 and 6 of the dosing period (Table 7.5) and at weeks 7 to 10 in the recovery period (Table 7.6). The lowest albumin levels were found at week 6 autopsies (36.40 and 27.40 g/L for control and CCl_4-treated animals respectively; $^{**}P<0.01$) (Table 7.5, Table 7.6). Serum total protein levels were significantly decreased compared to concurrent controls at weeks 5 to 9. At week 6 (the last dosing period time point) the mean level for control animals was 65.40 g/L whereas in CCl_4 treated animals serum total protein was 51.40 g/L ($^{***}P<0.001$).

Urea levels in the serum of CCl_4-treated animals were significantly increased compared to control rats at weeks 1, 2 and 3. At week 2 there was a 1.51-fold increase over control values (9.04 and 13.66 mmol/L for control and treated animals respectively; $^{**}P<0.01$) (Table 7.5). There were no other significant differences during the dosing period. However, at week 8 (recovery period) serum levels for animals receiving CCl_4 were lower than control animals (7.00 and 8.06 mmol/L respectively; $^{*}P<0.05$) (Table 7.6). Serum creatinine was 1.28- and 1.32-fold increased over concurrent controls at weeks 2 and 3 ($^{*}P<0.05$ and $^{**}P<0.01$, respectively) (Table 7.5). However, at T7, T8, T10, T11 and T12 during the recovery period of the study, serum creatinine levels were significantly decreased in CCl_4-treated animals compared to the respective control rats (Table 7.6).

A

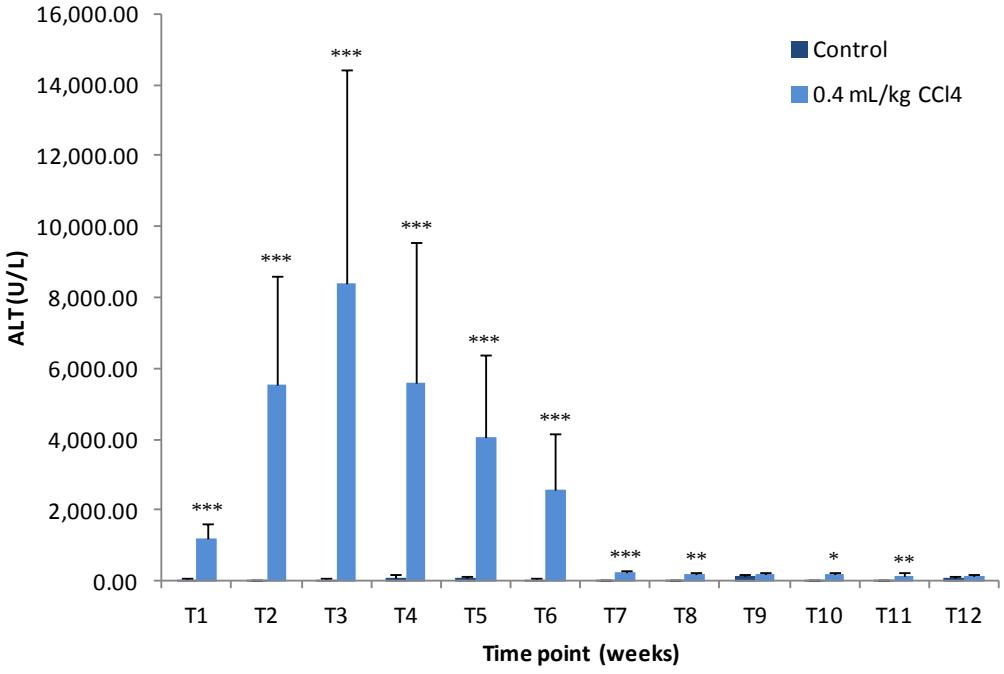

B

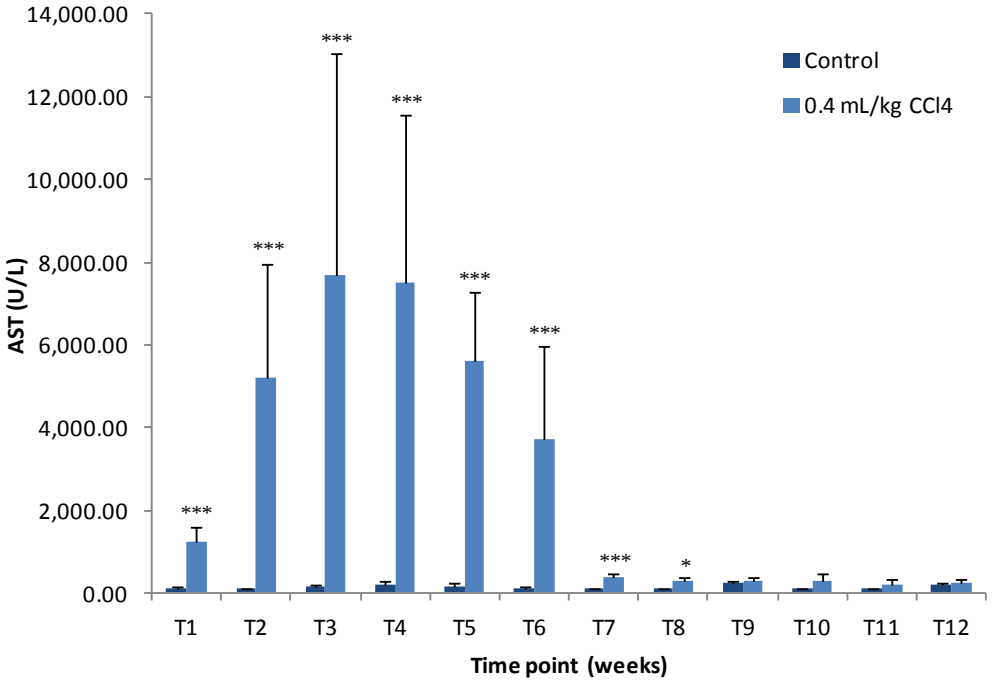

C

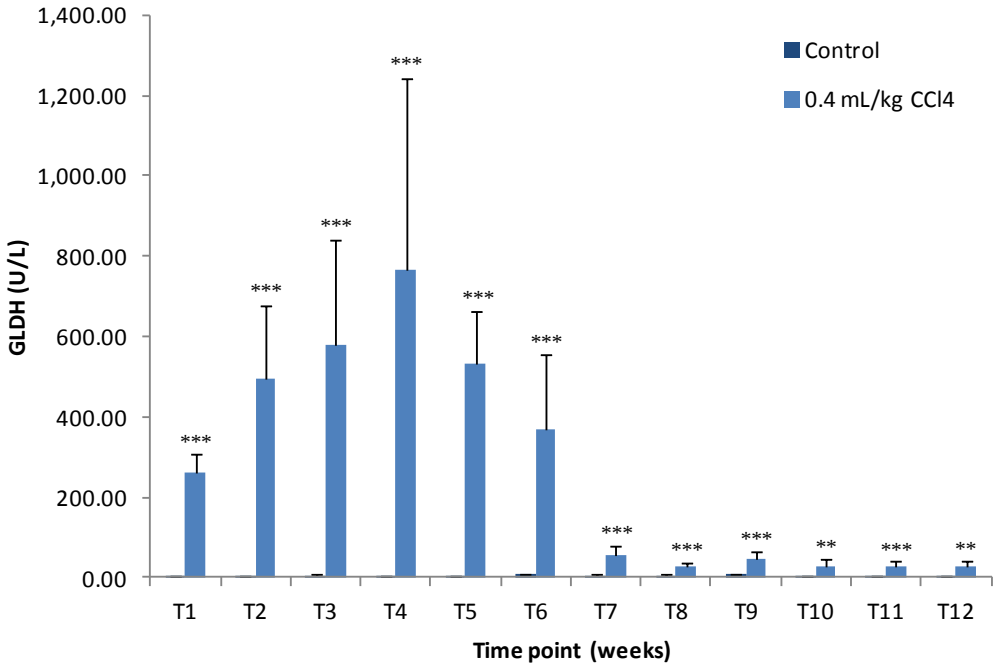

Figure 7.5 Serum ALT, AST and GLDH activities for male Hanover-Wistar rats treated with vehicle (control) or CCl_4 at 0.4 mL/kg and sampled at different time points. Animals were dosed by gavage and sampled at the time points shown. Blood was collected at autopsy at weeks 1-6, 9 and 12; and from the tail vein at weeks 7, 8, 10 and 11, as described in Section 7.2.2. Enzymes were assayed according to Section 2.7. Values are the means with SD indicated by vertical bars of 5 animals per group. Values that differ significantly from controls at the same time point by Students' t-test are shown: $P<0.05$; $^{**}P<0.01$; $^{***}P<0.001$.

Table 7.5 Serum clinical chemistry parameters for male Hanover-Wistar rats treated with vehicle (control) or CCl_4 at 0.4 mL/kg and sampled at different time points during the dosing period. Animals were dosed by gavage and sampled at the time points shown. Blood was collected at autopsy as described in Section 7.2.2. Enzymes were assayed according to Section 2.7. Values are the means and SD of 5 animals per group. Values that differ significantly from controls at the same time point by Students' t-test are shown: $P<0.05$; $^{**}P<0.01$; $^{***}P<0.001$. C: control; T: CCl_4-treated rat.

Time point (weeks)		Serum parameters									
		Lipocalin-2 (µg/L)	TIMP-1 (µg/L)	MCP1 (µg/L)	AGP (mg/L)	A2M (mg/L)	Glucose (mmol/L)	Albumin (g/L)	Total protein (g/L)	Urea (mmol/L)	Creatinine (µmol/L)
1	C	46.40 (15.74)	6.80 (1.64)	8.40 (1.14)	68.80 (11.73)	45.20 (11.32)	6.40 (0.90)	35.00 (1.00)	58.80 (1.10)	7.40 (1.40)	24.00 (1.60)
	T	52.20 (23.69)	23.40*** (6.19)	17.60*** (3.85)	91.40 (24.43)	30.80* (4.76)	6.67 (0.77)	34.40 (0.55)	55.40** (1.82)	10.42* (0.76)	25.40 (3.29)
2	C	41.60 (5.55)	5.40 (0.89)	8.00 (1.00)	57.80 (4.97)	28.20 (5.36)	6.77 (0.73)	34.00 (1.22)	58.00 (1.58)	9.04 (1.00)	27.40 (1.52)
	T	111.20 (60.86)	49.40*** (22.48)	28.60** (10.24)	76.60 (16.92)	29.40 (8.62)	4.13* (1.56)	34.20 (0.84)	55.00* (1.87)	13.66** (1.99)	35.20* (5.22)
3	C	49.80 (8.17)	6.20 (1.30)	8.40 (1.82)	63.20 (5.93)	24.80 (2.77)	3.10 (0.89)	34.40 (1.95)	59.80 (3.70)	7.64 (0.67)	27.40 (2.30)
	T	291.60 (237.42)	69.40** (51.31)	36.40** (29.62)	106.60* (40.15)	61.60** (19.69)	3.85 (1.44)	34.20 (1.30)	57.00 (5.15)	12.30*** (1.73)	36.20** (3.56)
4	C	40.40 (4.83)	5.60 (1.14)	7.20 (0.45)	66.60 (16.91)	16.80 (1.30)	3.89 (1.53)	35.40 (0.55)	61.00 (1.22)	8.00 (1.28)	28.80 (4.21)
	T	464.40** (482.17)	167.40** (186.33)	50.00** (46.15)	102.80* (24.93)	121.60** (66.25)	2.92 (1.38)	26.80 (8.41)	45.80 (13.94)	10.36 (2.70)	31.40 (6.10)
5	C	47.20 (6.53)	5.40 (1.34)	2.40 (0.55)	70.80 (8.79)	16.20 (5.45)	6.50 (0.91)	35.00 (1.41)	60.60 (3.36)	7.60 (0.98)	28.40 (0.89)
	T	179.60*** (57.24)	58.20*** (11.39)	9.00 (8.31)	113.00** (21.12)	161.60*** (80.75)	4.34** (0.75)	30.40* (2.70)	51.20** (3.96)	8.74 (1.34)	29.00 (3.32)
6	C	40.80 (6.91)	5.40 (1.34)	6.00 (2.83)	74.40 (12.18)	15.20 (3.35)	6.56 (2.23)	36.40 (0.89)	65.40 (0.89)	9.54 (1.15)	26.80 (2.39)
	T	253.40** (146.12)	39.00** (32.80)	9.00 (9.90)	133.20** (30.87)	188.60*** (107.09)	4.95 (1.35)	27.40** (4.39)	51.40*** (4.22)	8.00 (0.96)	26.40 (2.97)

TIMP-1: tissue inhibitor of matrix metalloproteinase; MCP 1: monocyte chemoattractant factor 1; AGP: alpha-1 acid glycoprotein; A2M: alpha-2 macroglobulin.

Table 7.6 Serum clinical parameters for male Hanover-Wistar rats treated with vehicle (control) or CCl_4 at 0.4 mL/kg and sampled at different time points during the period without treatment (recovery period). Animals were dosed by gavage and sampled at the time points shown. Blood was collected at autopsy at weeks 9 and 12; and from the tail vein at weeks 7, 8, 10 and 11, as described in Section 7.2.2. Enzymes were assayed according to Section 2.7. Values are the means and SD of 5 animals per group. Values that differ significantly from controls at the same time point by Students' t-test are shown: $P<0.05$; $^{**}P<0.01$; $^{***}P<0.001$. C: control; T: CCl_4-treated rat.

Time point (weeks)		Serum parameters									
		Lipocalin-2 (µg/L)	TIMP-1 (µg/L)	MCP1 (µg/L)	AGP (mg/L)	A2M (mg/L)	Glucose (mmol/L)	Albumin (g/L)	Total protein (g/L)	Urea (mmol/L)	Creatinine (µmol/L)
7	C	41.20 (8.41)	5.00 (1.58)	8.80 (1.30)	83.40 (16.10)	12.80 (1.79)	8.42 (0.41)	35.80 (0.84)	60.60 (2.07)	8.40 (0.97)	27.60 (1.52)
	T	49.80 (17.89)	9.80** (2.39)	8.80 (1.64)	98.20 (22.48)	51.40*** (17.50)	8.61 (1.20)	31.80* (2.39)	53.40** (3.21)	7.54 (1.02)	20.00*** (1.58)
8	C	43.80 (9.86)	9.20 (4.09)	8.80 (1.79)	92.80 (7.60)	53.60 (61.04)	8.50 (0.62)	36.00 (1.22)	59.80 (1.92)	8.06 (0.43)	30.00 (1.87)
	T	43.00 (11.77)	6.60 (2.41)	8.60 (1.34)	90.00 (24.16)	26.40 (22.60)	8.72 (0.51)	30.80** (2.49)	55.00* (2.55)	7.00* (0.57)	22.20*** (2.17)
9	C	33.40 (4.83)	5.00 (1.22)	9.00 (1.22)	82.80 (10.18)	10.00 (0.71)	6.32 (1.46)	34.60 (0.55)	58.20 (1.30)	8.60 (0.72)	33.60 (4.16)
	T	37.80 (5.63)	7.20* (1.30)	8.40 (1.34)	97.60 (14.10)	24.00*** (7.11)	6.98 (1.15)	32.40* (1.34)	55.40* (1.67)	8.52 (0.74)	28.60 (2.88)
10	C	32.20 (4.87)	5.20 (1.10)	8.40 (0.55)	87.40 (18.77)	12.20 (0.84)	7.97 (0.79)	35.80 (0.84)	60.20 (1.64)	7.86 (0.47)	27.80 (1.64)
	T	34.33 (11.02)	7.33 (1.53)	8.33 (2.08)	82.25 (6.70)	44.75 (53.67)	7.59 (1.38)	30.60* (3.97)	54.80 (7.26)	6.94 (0.91)	23.60* (2.07)
11	C	35.75 (8.81)	5.25 (0.96)	8.00 (0.82)	90.50 (27.53)	11.50 (1.29)	7.08 (1.23)	36.20 (0.45)	60.80 (1.30)	9.34 (0.72)	25.40 (0.89)
	T	57.20 (15.80)	9.40* (1.52)	7.60 (1.95)	95.20 (15.17)	31.20* (21.81)	8.32 (0.62)	33.60 (2.70)	58.80 (3.90)	8.88 (0.57)	22.20* (1.79)
12	C	30.20 (11.65)	5.00 (1.41)	6.40 (1.67)	70.40 (22.73)	9.00 (2.55)	6.10 (1.20)	33.40 (1.30)	56.80 (1.60)	8.90 (0.90)	36.00 (2.90)
	T	46.80 (9.12)	9.00** (2.00)	6.60 (0.55)	92.00 (14.92)	23.60** (14.35)	7.03 (0.61)	32.20 (1.48)	55.80 (2.17)	7.84 (1.02)	26.60*** (1.14)

TIMP-1: tissue inhibitor of matrix metalloproteinase; MCP 1: monocyte chemoattractant factor 1; AGP: alpha-1 acid glycoprotein; A2M: alpha-2 macroglobulin.

7.4.6 Urine clinical chemistry

Urinary biomarkers and clinical chemistry parameters were measured in urine samples collected from rats every week during this study (week 1 to 12) to investigate the possibility of CCl_4-induced nephrotoxicity with repeated administration.

Urinary α-GST was decreased in CCl_4-treated animals compared to controls at weeks 1 to 5 during the dosing period, and at weeks 1 and 2 this decrease was statistically significant ($^{*}P<0.05$ and $^{**}P<0.01$, respectively) (Table 7.7). At week 6, urinary α-GST was 1.56-fold increased over control levels in CCl_4-treated animals; however, due to the large standard deviation this increase was not statistically significant. There were no significant differences between CCl_4-treated animals and control animals at any other time point in the study (Table 7.8). GST Yb1 levels in the urine were significantly increased above controls after 6 weeks of CCl_4 treatment. At this time point, mean urinary levels reached a peak and were 196.00 ng/c.p. and 98.00 ng/c.p. for CCl_4-treated animals and control rats, respectively ($^{*}P<0.05$) (Table 7.7). Between weeks 7 and 12 no statistically significant differences were observed (Table 7.8).

Urinary KIM-1 was significantly increased over controls at week 6 (last week during the dosing period), when values were maximal, and a 1.35-fold increase over controls was recorded ($^{*}P<0.05$) (Table 7.7). During the period without treatment, KIM-1 levels in the urine were still significantly increased over controls at all time points (Table 7.8).

Lipocalin-2 levels in the urine were significantly increased over controls at weeks 2 to 6 during the dosing period (Table 7.7). After 6 weeks of CCl_4-treatment there was an approximate 23-fold increase over controls ($^{***}P<0.001$). Between weeks 7 and 10, and at week 12, urinary lipocalin-2 levels were still significantly increased over control; the fold increase was 1.9-fold at week 12 ($^{*}P<0.05$) (Table 7.8).

Osteopontin levels reached a peak in the urine of CCl_4-treated animals at week 4 (102.00 ng/c.p. and 39.00 ng/c.p. for CCl_4-treated and control animals, respectively) ($^{*}P<0.05$). Osteopontin remained significantly increased over controls at week 5 and 6, but by week 7 (first week without treatment) values had returned to control levels and no other significant differences were observed (Table 7.8).

Clusterin values were significantly decreased over controls at week 3 during the dosing period (44.20 ng/c.p. and 14.00 ng/c.p. for CCl_4-treated animals and control rats,

respectively; $^{**}P<0.01$) (Table 7.7); and at weeks 8 and 12 during the period without CCl_4-treatment (Table 7.8).

Mean urinary creatinine was significantly decreased in the urine from CCl_4-treated animals at weeks 5, 6 and 7. However, there was a return to control values after week 7.

Glucose levels in the urine were significantly decreased at week 6, but at all other time points urinary glucose was similar to control (Table 7.7, Table 7.8). Urinary total protein levels were significantly decreased compared to concurrent controls at week 1, 2, 3 and 5 during the dosing period. At T1 the mean value for CCl_4-treated rats was 1.48 mg/c.p., compared to 4.58 mg/c.p. in control animals ($^{***}P<0.001$). This was the lowest total protein value in this study. After week 5, total protein levels appeared to be greater in CCl_4-treated animals than controls. This increase was significant at week 8 (approximately 3-fold greater).

There was no evidence of CCl_4-induced effect in urine volume at any time points (Table 7.7, Table 7.8).

Table 7.7 Urinary biomarkers in male Hanover-Wistar rats treated with vehicle (control) or CCl_4 at 0.4 mL/kg and sampled at different time points during the dosing period. Rats were dosed by gavage and urine collected for 18 hours at the time points shown, as described in Section 7.2.2. Biomarkers were assayed as described in Section 2.7. Values are the means and SD of 5 animals per group and are expressed per c.p. (collection period, 18 hours). Values that differ significantly from controls at the same time point by Students' t-test are shown: $^{*}P<0.05$; $^{**}P<0.01$; $^{***}P<0.001$. C: control; T: CCl_4-treated rat.

Time point (weeks)		Urinary parameters										
		α-GST (ng/c.p.)	GST Yb1 (ng/c.p.)	KIM-1 (ng/c.p.)	Lipocalin-2 (ng/c.p.)	Osteopontin (ng/c.p.)	Clusterin (ng/c.p.)	Albumin (mg/c.p.)	Creatinine (µmol/c.p.)	Glucose (µmol/c.p.)	Total protein (mg/c.p.)	Volume (mL)
1	C	298.00 (238.37)	56.00 (41.59)	9.00 (1.00)	2906.00 (714.97)	20.00 (10.00)	34.80 (17.87)	0.04 (0.05)	38.40 (2.07)	3.60 (0.55)	4.58 (0.66)	24.20 (5.40)
	T	120.00* (41.23)	26.00 (5.48)	10.67 (1.67)	3442.00 (352.66)	66.00** (33.62)	19.80 (6.34)	0.00 (0.00)	35.80 (2.17)	3.80 (0.45)	1.48*** (0.23)	19.80 (6.34)
2	C	392.00 (194.47)	34.00 (8.94)	10.40 (2.30)	2848.00 (699.41)	28.00 (8.37)	25.60 (11.26)	0.06 (0.09)	54.40 (6.62)	5.60 (1.14)	6.40 (1.12)	15.60 (2.70)
	T	126.00** (76.35)	46.00 (18.17)	10.80 (0.84)	6758.00* (3401.02)	98.00*** (26.83)	16.20 (7.29)	0.18 (0.22)	48.20 (4.21)	4.20 (0.84)	2.14*** (0.68)	14.00 (6.75)
3	C	270.00 (85.73)	56.00 (11.40)	10.60 (2.30)	2828.00 (532.89)	34.00 (15.17)	44.20 (23.79)	0.10 (0.10)	65.00 (7.18)	5.00 (1.41)	6.40 (2.65)	23.40 (11.82)
	T	174.00 (164.71)	52.00 (39.62)	10.40 (3.21)	22480.00* (22075.48)	58.00* (20.49)	14.00** (2.92)	0.60 (0.61)	53.80 (8.50)	4.60 (0.89)	3.12* (1.32)	12.40 (3.65)
4	C	452.00 (225.65)	62.00 (32.71)	10.00 (3.24)	2052.00 (592.34)	38.00 (30.33)	68.00 (44.43)	0.04 (0.05)	57.40 (11.04)	4.40 (1.67)	4.48 (1.72)	30.20 (17.24)
	T	412.00 (437.86)	120.00 (88.03)	10.80 (3.42)	53090.00*** (34198.02)	102.00* (37.68)	48.40 (60.40)	1.34 (1.11)	47.00 (14.51)	6.40 (3.21)	4.00 (1.25)	12.40 (2.07)
5	C	400.00 (123.90)	68.00 (31.14)	10.00 (2.24)	2900.00 (614.90)	24.00 (5.48)	62.00 (21.82)	0.08 (0.13)	68.20 (7.33)	5.20 (0.84)	6.50 (1.37)	26.80 (11.88)
	T	286.00 (77.01)	102.00 (60.99)	13.40 (1.82)	29004.00*** (6305.44)	62.00*** (10.95)	50.80 (20.38)	1.16 (0.87)	48.60** (4.83)	4.80 (0.45)	3.48* (1.45)	24.20 (5.02)
6	C	480.00 (226.83)	98.00 (41.47)	11.40 (2.70)	2786.00 (614.68)	32.00 (13.04)	51.00 (10.39)	0.14 (0.17)	80.40 (6.35)	6.80 (0.84)	7.32 (2.01)	19.20 (5.07)
	T	752.00 (473.47)	196.00* (55.05)	15.40* (2.41)	64516.00*** (30151.16)	76.00* (27.02)	51.60 (35.84)	9.60 (6.64)	54.20** (10.01)	4.60* (1.14)	13.90 (8.20)	16.00 (6.67)

α-GST: glutathione S-transferase; GST Yb1: glutathione S-transferase Yb1; KIM-1: kidney injury molecule-1.

Table 7.8 Urinary biomarkers in male Hanover-Wistar rats treated with vehicle (control) or CCl_4 at 0.4 mL/kg and sampled at different time points during the period without treatment (recovery period). Rats were dosed by gavage and urine collected for 18 hours at the time points shown, as described in Section 7.2.2. Biomarkers were assayed as described in Section 2.7. Values are the means and SD of 5 animals per group and are expressed per c.p. (collection period, 18 hours). Values that differ significantly from controls at the same time point by Students' t-test are shown: $^{*}P<0.05$; $^{**}P<0.01$; $^{***}P<0.001$. C: control; T: CCl_4-treated rat.

Time point (weeks)		Urinary parameters										
		α-GST (ng/c.p.)	**GST Yb1 (ng/c.p.)**	**Kim-1 (ng/c.p.)**	**Lipocalin-2 (ng/c.p.)**	**Osteopontin (ng/c.p.)**	**Clusterin (ng/c.p.)**	**Albumin (mg/c.p.)**	**Creatinine (µmol/c.p.)**	**Glucose (µmol/c.p.)**	**Total protein (mg/c.p.)**	**Volume (mL)**
7	C	624.00 (403.03)	70.00 (35.36)	9.40 (0.55)	2098.00 (437.12)	40.00 (12.25)	64.00 (45.19)	0.04 (0.05)	70.40 (4.34)	5.20 (0.45)	6.02 (1.52)	18.20 (9.86)
	T	466.00 (302.37)	44.00 (18.17)	13.60* (2.61)	5466.00** (2936.67)	44.00 (23.02)	55.80 (18.23)	8.20 (6.89)	49.40*** (4.83)	4.60 (0.89)	10.74 (7.06)	19.40 (6.84)
8	C	462.00 (174.56)	62.00 (43.24)	9.20 (1.30)	2544.00 (536.78)	44.00 (11.40)	76.40 (28.47)	0.02 (0.04)	78.00 (8.80)	5.40 (1.14)	5.76 (1.17)	21.80 (6.94)
	T	406.00 (265.25)	76.00 (59.83)	14.20** (1.30)	5828.00* (2788.61)	50.00 (17.32)	39.20* (13.08)	13.18 (11.85)	67.40 (7.48)	5.40 (1.14)	17.80* (8.05)	19.60 (6.54)
9	C	228.00 (125.58)	40.00 (25.50)	8.20 (1.48)	2332.00 (880.89)	48.00 (19.24)	68.20 (55.08)	0.04 (0.09)	64.60 (10.06)	5.00 (1.58)	4.92 (1.75)	18.60 (13.09)
	T	208.00 (98.84)	38.00 (13.04)	14.20* (4.76)	4596.00** (1135.97)	36.00 (15.17)	79.00 (20.40)	1.18 (0.99)	58.96 (22.40)	5.06 (2.07)	6.58 (2.46)	19.15 (4.82)
10	C	328.00 (160.37)	38.00 (30.33)	7.40 (1.14)	2406.00 (436.27)	26.00 (5.48)	61.60 (32.32)	0.00 (0.00)	70.80 (13.85)	4.80 (0.84)	5.00 (1.19)	16.60 (5.08)
	T	626.00 (650.02)	82.00 (50.70)	12.40** (2.30)	5042.00* (3173.96)	28.00 (13.04)	63.20 (62.62)	8.82 (12.86)	67.60 (10.92)	4.80 (1.30)	14.30 (12.11)	18.40 (7.40)
11	C	530.00 (271.29)	80.00 (65.95)	6.00 (1.22)	1928.00 (395.06)	30.00 (12.25)	94.60 (35.49)	0.02 (0.04)	57.40 (13.24)	4.60 (1.14)	4.20 (1.07)	16.00 (3.94)
	T	504.00 (301.71)	76.00 (61.07)	9.60* (3.21)	3376.00 (1513.63)	32.00 (13.04)	62.60 (25.04)	5.50 (7.40)	52.60 (8.32)	4.60 (0.55)	9.26 (7.31)	16.00 (3.24)
12	C	516.00 (224.12)	54.00 (16.73)	7.00 (0.71)	1782.00 (519.63)	34.00 (8.94)	96.20 (36.24)	0.00 (0.00)	75.60 (9.86)	4.40 (0.89)	5.20 (0.69)	16.80 (3.70)
	T	400.00 (285.83)	70.00 (48.99)	11.20*** (1.48)	3384.00* (1178.17)	38.00 (13.04)	53.00* (15.52)	3.50 (4.10)	67.40 (11.84)	5.80 (1.30)	8.18 (3.36)	14.60 (4.34)

α-GST: glutathione S-transferase; GST Yb1: glutathione S-transferase Yb1; KIM-1: kidney injury molecule-1.

7.4.7 Gene expression

Gene expression analysis was performed to follow changes in hepatic gene expression levels during the period of injury progression (week 1 to week 6) and injury recovery and repair (week 9 and 12), and to correlate this information with the metabolism and toxic effects of CCl_4 in the liver (Table 7.9).

Due to the large number of samples generated in the study, liver gene expression data was collected from 6 control animals at week 1, 4, 5, 9 and 12 and from 6 CCl_4-treated animals at all time points. Statistical analysis was performed whereby CCl_4-treated animals at weeks 1 and 2 were compared to control animals at week 1; CCl_4-treated animals at week 3 and 4 were compared to control animals at week 4 and CCl_4-treated animals at week 5 and 6 were compared to control animals at week 6. During the recovery period CCl_4-treated rats were statistically compared against the concurrent controls.

CYP1A2 and CYP2C mRNA expression were downregulated in CCl_4-treated animals compared to the respective controls at all time points. By week 9 (3 weeks without treatment) CYP1A2 and CYP2C levels were increased compared to those at week 6 and by week 12 a return to basal mRNA levels was evident (Table 7.9). NQO1 mRNA expression was increased compared to control animals at week 1, and at all time points during the study (week 1 to 12).

Gene expression of HMOX1 increased from week 1 to week 4 and decreased after this time point; by week 12 it was significantly decreased compared to control animals. LCN2 and TIMP1 mRNA expression was also upregulated at all time points during the study but the fold increases over controls decreased considerably during the recovery period (Table 7.9).

COL1A1 and COL5A2 appeared to follow the same trend; mRNA expression increased consistently during the dosing period and was maximal at week 5 after which it decreased. MMP12, TGF-β and ACTA2 mRNA expression levels were found to be significantly upregulated at week 1, that is, after 3 CCl_4 administrations. There was a general trend for increase in mRNA expression during the dosing period up to week 5, followed by a decrease at weeks 9 and 12 indicating a tendency for return to control levels.

Table 7.9 Liver gene expression in male Hanover-Wistar rats treated with vehicle (control) or CCl_4 at 0.4 mL/kg and sampled at different time points during the study. Rats were dosed by gavage as described in Section 7.2.2. At autopsy, liver expression was measured as described in Section 2.9. Results are represented as copy number [$x10^3$/2 ng cDNA]. Values are the means and SD of 5 animals per group. Values that differ significantly from controls as described in Section 7.4.7, by Students' t-test are shown: $^{*}P<0.05$; $^{**}P<0.01$; $^{***}P<0.001$.

Category/gene name	symbol	Control (week 1)	Time point (weeks) 1	2	3	4	5	6	9	12
Xenobiotic metabolism										
Cytochrome P450 1A2	CYP1A2	2112.90 (409.46)	545.04*** (199.03)	219.93*** (173.61)	208.20*** (168.03)	175.86*** (104.87)	413.01** (91.69)	422.45** (325.99)	2155.56* (910.74)	1856.72 (790.89)
Cytochrome P450 2C	CYP2C	1762.56 (1069.15)	122.63** (122.63)	38.33** (41.07)	127.56*** (203.79)	7.30*** (8.02)	6.08*** (2.89)	9.90*** (7.48)	1038.35 (1061.67)	1166.78 (1539.87)
NAD (P)H dehydrogenase, quinone 1	NQO1	36.22 (21.79)	78.99* (24.36)	42.67 (34.35)	85.40** (35.63)	69.87* (38.04)	87.00* (32.78)	85.51 (56.53)	76.12* (22.94)	65.19 (23.27)
Oxidative stress										
Heme oxygenase (decycling) 1	HMOX1	94.05 (19.53)	335.28* (173.82)	392.10*** (115.23)	473.69** (242.24)	594.9 5 (521.23)	368.29*** (108.43)	207.29* (119.60)	90.33 (25.36)	64.13** (13.95)
Inflammation										
Lipocalin-2	LCN2	8.16 (1.45)	68.70* (50.46)	291.39* (240.76)	655.11* (567.17)	3335.77 (5511.26)	705.07*** (234.01)	1185.50** (754.47)	74.42*** (27.87)	56.67* (45.17)
Tissue inhibitor of metalloproteinase 1	TIMP1	12.69 (3.43)	54.63*** (16.31)	109.40** (46.56)	151.12* (103.51)	314.86* (250.95)	190.00*** (29.10)	116.33* (95.77)	27.50** * (2.90)	26.74* (16.57)
Markers hepatic fibrosis										
Collagen, type 1, alpha 1	COL1A1	20.95 (9.36)	123.21 (121.40)	282.01 (286.61)	564.46** (345.86)	1142.42* (844.33)	1456.83*** (152.73)	822.57** (520.48)	171.39 (40.86)	89.53 (89.55)
Collagen, type 5, alpha 2	COL5A2	12.27 (4.01)	29.70 (18.09)	50.51* (27.90)	75.30** (34.34)	121.84** (56.01)	139.68*** (16.11)	86.41** (42.54)	24.48*** (0.87)	17.18* (8.23)
Matrix metallopeptidase 12	MMP12	0.49 (0.50)	28.18*** (7.19)	125.60** (80.41)	121.37** (70.74)	113.93** (65.44)	136.51*** (29.78)	83.16** (49.54)	23.38*** (3.95)	14.83* (10.37)
Transforming growth factor- β1	TGF-β1	27.36 (4.62)	68.38** (23.49)	69.12** (24.14)	94.91** (31.91)	134.07*** (27.00)	142.94*** (26.74)	123.13** (40.25)	47.85*** (7.89)	45.22* (15.02)
Smooth muscle α-actin	ACTA2	4.19 (1.50)	15.47 (10.96)	57.07 (58.86)	89.04* (78.01)	159.89* (119.47)	101.92** (44.73)	38.35 (45.03)	5.64** (1.18)	6.32* (2.71)

Results for control animals at week 1 are given, results for weeks 2 to 6, and 9 and 12 are not presented.

7.4.8 Ultrasonography

US was performed to carry out a time course evaluation of the liver changes associated with CCl_4 treatment and to develop a potential correlation between the imaging endpoints and the histopathology data. US sessions were scheduled to be conducted every week during the dosing period and at the recovery time points (week 9 and 12) (Figure 7.6).

At each session images of the kidneys were recorded to compare the echographic texture with that of the liver. When examined with ultrasound, body tissues are visualised in various shades of grey. When the sound waves are transmitted into the body they interact with tissues and, consequently, are attenuated, either by absorption, scattering and beam divergence. Some sound waves are reflected (echoes) to the transducer and are converted into an image. Echogenecity refers to the variety of characteristics that define the appearance of tissues.

Due to technical problems it was not possible to carry out an ultrasonographic examination of the animals during the first 2 weeks of the study. At all other time points, a qualitative assessment of the liver was performed by comparing the echogenicity of the liver parenchyma against other organs and between vehicle-treated (controls) and CCl_4-treated animals at each week.

Between weeks 3 and 6 during the dosing period, livers from CCl_4-treated animals appeared to be increased in size in the longitudinal projection, and all treated animals showed increased echogenecity of the liver compared to the kidneys. At week 6, 2 of the CCl_4-treated animals showed the presence of fluid in the abdominal cavity. For the remaining 3 animals in the treated group there were no observable differences from animals at week 5 (Figure 7.6 A, B and C).

After 3 weeks without treatment, which corresponded to week 9 (Figure 7.6 D) in the study, it was observed that livers from CCl_4-treated animals were still hyperechoic (increased echogenicity) and appeared slightly enlarged compared to control animals, but decreased in size compared to the previous US session at week 6. There was no evidence of fluid in the abdominal cavity. After 6 weeks without treatment (week 12), livers showed signs of recovery, although they still remained hyperechoic and slightly enlarged compared to control animals. There was no evidence of the presence of fluid at either of the recovery time points.

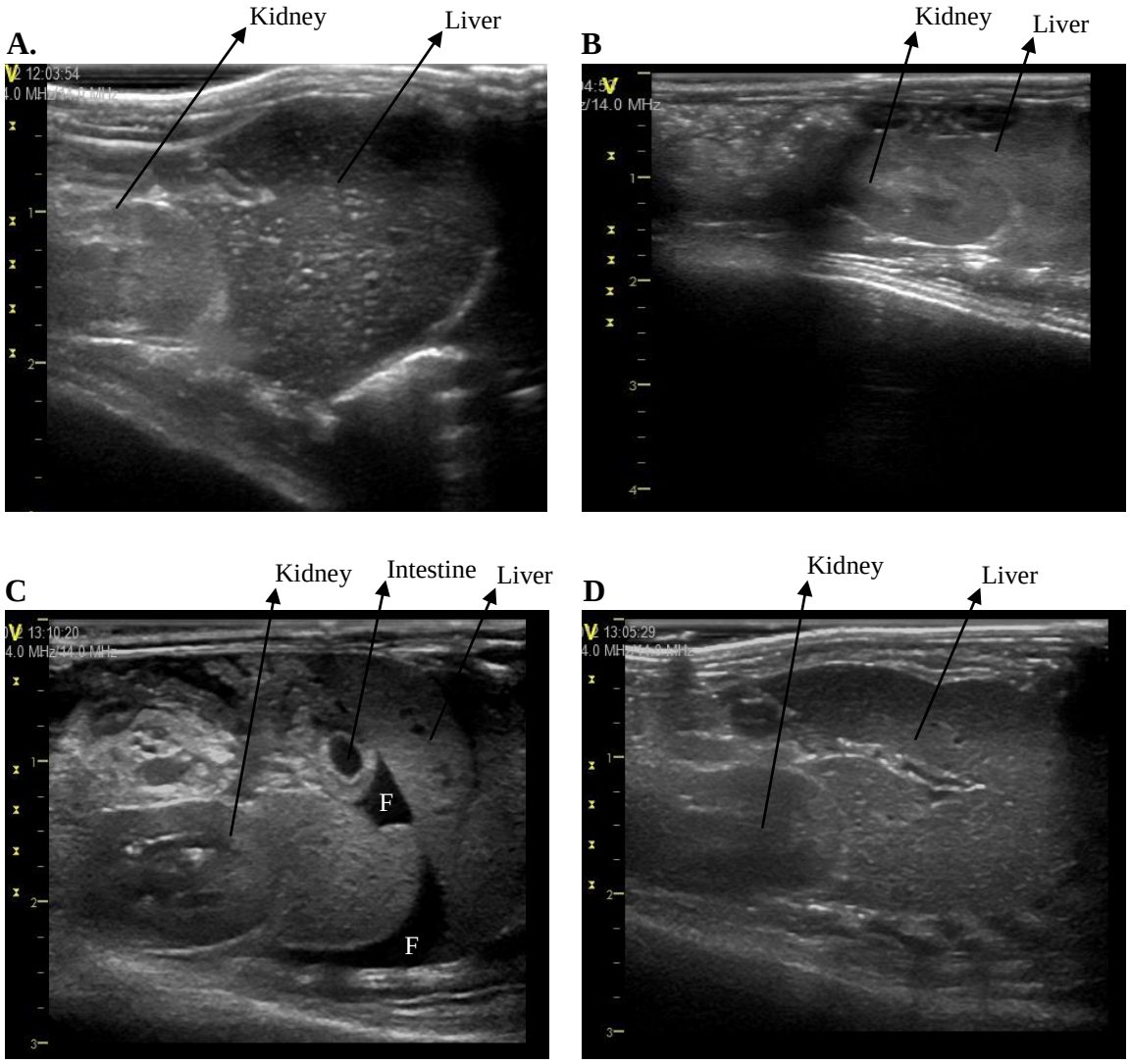

Figure 7.6 Ultrasonography images of male Hanover-Wistar rats treated with vehicle (control) or CCl_4 at 0.4 mL/kg and sampled at various time points. Animals were dosed by gavage and ultrasonography images collected as described in Section 2.5. (A) control animal at week 4: normal echogenecity of the liver with intraparenchymal vasculature texture, and comparison against the kidney; (B) CCl_4-treated animal at week 3: increased echogenecity of the liver compared to the apical pole of the kidney; (C) CCl_4-treated animal at week 6: hyperechoic liver surrounded by fluid in the abdominal cavity (F), transverse sections of the intestine and well defined kidney; (D) CCl_4-treated animal at week 9: slightly hyperechoic liver, intravasculature more evident.

7.4.9 Images collected at autopsy

At each autopsy, photographic images were taken of the macroscopic appearance of the livers from all rats. Figure 7.7 A shows a control liver at week 1, (after 3 administrations of corn oil). The liver surface appeared smooth and shiny and the liver was dark red in colour as would be expected for a control liver. However, after 9 doses of CCl_4 at 0.4 mL/kg (3 weeks), livers appeared paler in colour compared to control

animals (Figure 1.7 B). The surface had diffuse pitting and there was the presence of red blotches in some liver lobes (indicated by arrows).

At the 6 week autopsy (after 18 doses), livers from CCl_4-treated animals were decreased in size and paler in colour compared to control animals at the same time point. There was evidence of more severe pitting of the surface and also the presence of small cysts of approximately 1 mm in diameter (indicated by arrow) (Figure 1.7 C).

Figure 1.7 D shows an image of a liver from an animal that had been treated with CCl_4 for 6 weeks and then allowed to recover for a further 3 weeks without treatment (T9). At this time point livers from CCl_4-treated animals were slightly darker in colour compared to animals at T6, although they remained paler than the controls at the same time point. There was also pitting of the surface but to a lesser extent than at T6. At week 12 livers from animals that had been allowed to recover for 6 weeks (T12) were similar to those at T9.

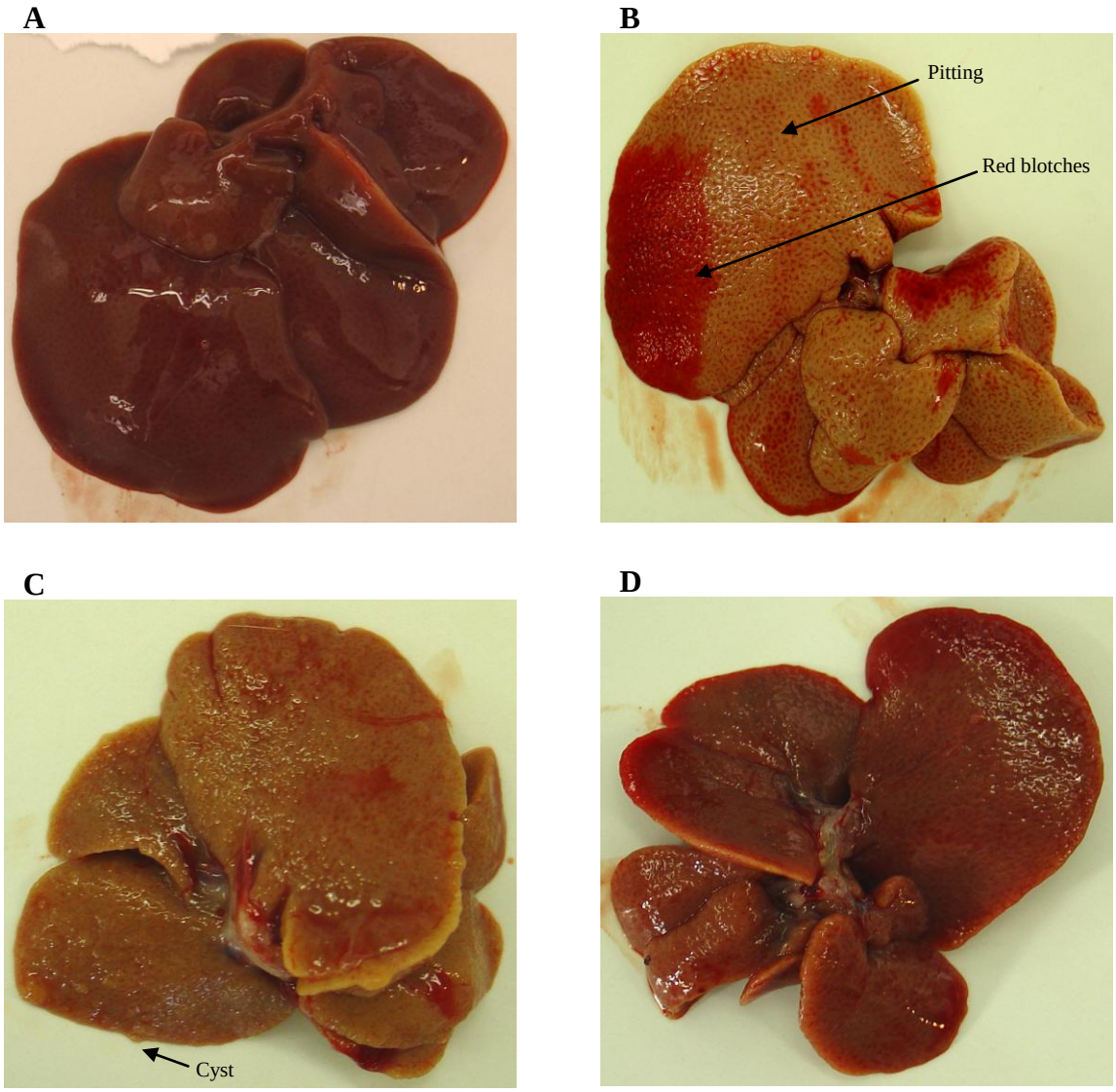

Figure 7.7 Photographic images of livers from male Hanover-Wistar rats treated with vehicle (control) or CCl_4 at 0.4 mL/kg and autopsied at various time points. Rats were dosed by gavage and autopsied as described in Section 7.2.2. (A) control animal autopsied at week 1; (B) 0.4 mL/kg CCl_4-treated animal at week 3: red blotches and pitted surface (indicated by arrows); (C) 0.4 mL/kg CCl_4-treated animal at week 6: cyst in liver surface (indicated by arrow), and (D) 0.4 mL/kg CCl_4-treated animal at week 9 (3 weeks without treatment).

7.4.10 Histopathology

At autopsy, liver and kidneys from control and CCl_4-treated animals were removed for histopathological examination. Additional tissues such as the spleen, pancreas, adrenal glands, lungs and heart, thymus, thyroid, nasal cavity and testes were also removed for histopathological examination. Due to the large number of samples generated during the study, liver and kidneys from only 2 animals from each group (control and CCl_4-

treated) were examined at each time point during the dosing period (T1-T6). This is because we expect fibrosis to develop in this study in the same way that it did in the previous repeat study (experiment 1). During the recovery period, livers from all animals autopsied at week 9 and 12, were examined histopathologically, but only kidneys from 2 control and 2 CCl_4-treated animals at T9 and T12 were examined.

At week 1 (T1), there was evidence of centrilobular necrosis, ballooning and vacuolation mainly in midzonal areas with minimal presence of centrilobular inflammatory cell infiltration. There were also a few cases of periportal hepatocytes in mitosis.

Livers from week 2 animals had centrilobular necrosis, marked ballooning and vacuolation in midzonal areas and there was also mild centrilobular inflammatory cell infiltration with evidence of fibroblasts. The number of periportal hepatocytes in mitosis had also increased compared to T1. At the following time point (week 3) all the injury described above had become more widespread and the centrilobular inflammatory cell infiltrate was associated with thickening of the perivascular structure and there was the presence of small fibrous tissue structures indicating the early formation of septae.

At week 4 (T4), there was minimal hepatocellular necrosis with diffuse ballooning and vacuolation. When compared to animals at week 3 the perivascular thickening had become more pronounced and the fibrous septae were well established. At weeks 5 and 6 the pathological findings described above became more pronounced.

At weeks 9 and 12 (recovery period), livers from treated animals showed no evidence of hepatocellular vacuolation. The fibrous septae as reported during the dosing period remained well established but were narrower than those observed at week 6 of the dosing period.

In the kidneys of animals treated with CCl_4 at all time points there was minimal vacuolation of the proximal tubular epithelium, however, vacuolation was also present in a control animal and therefore, it is less likely that this microscopic finding in the kidney was related to CCl_4 treatment.

With regards to the additional tissues removed at autopsy, there was no histopathological evidence of CCl_4 induced toxicity to the spleen, pancreas, adrenals, lungs and heart, thyroid, thymus, nasal cavity and testes.

A

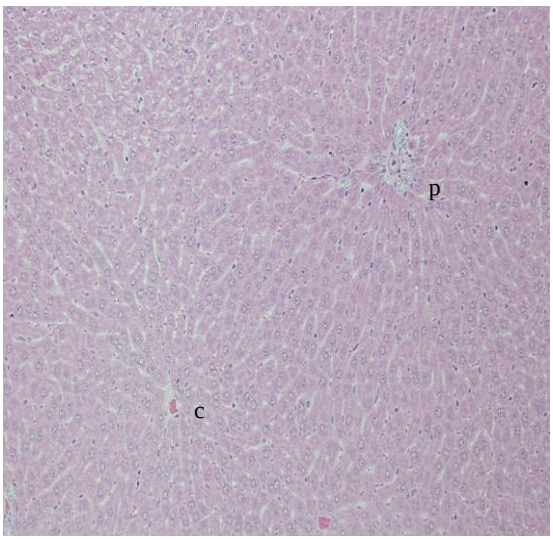

B

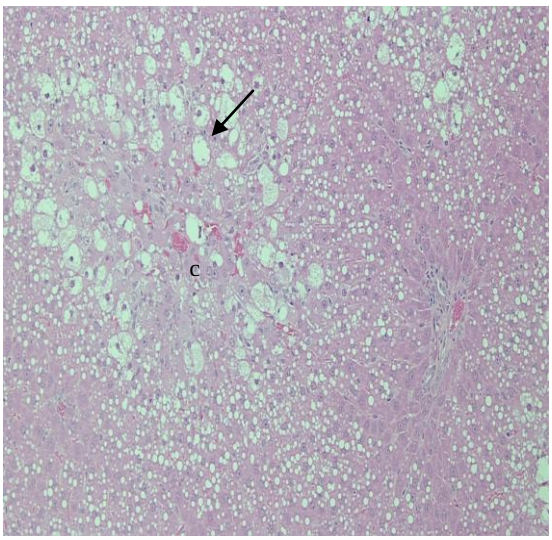

C

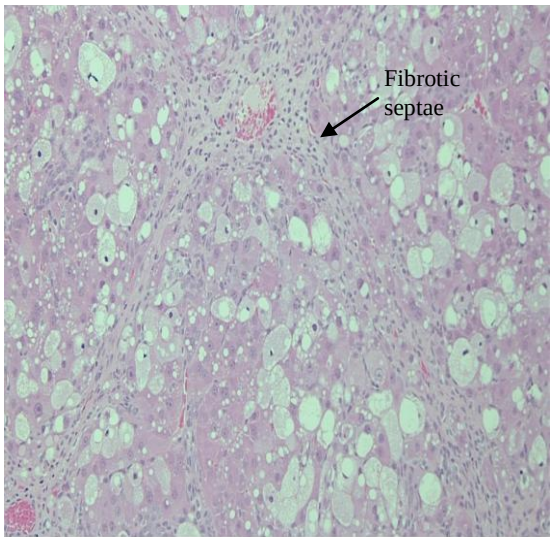

D

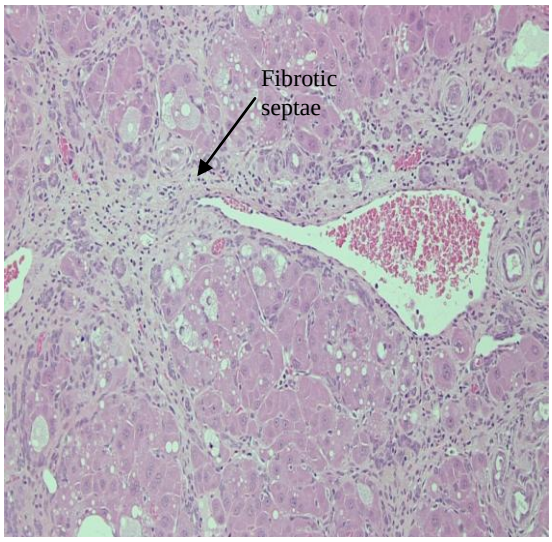

E

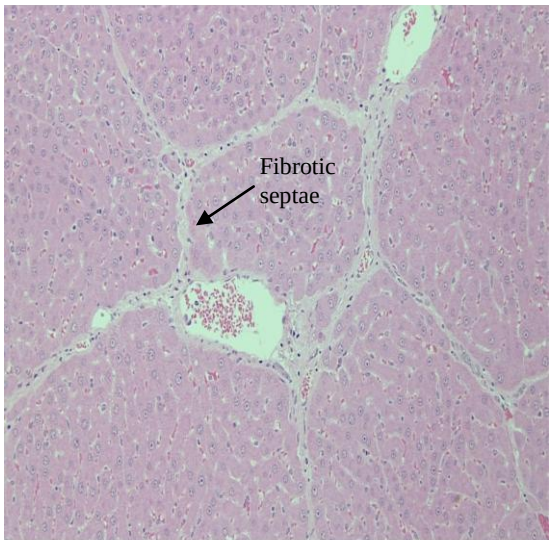

Figure 7.8 Histology of liver sections from male Hanover-Wistar rats treated with vehicle (control) or CCl_4 at 0.4 mL/kg and autopsied at various time points. Original magnification x100; H&E. Rats were dosed by gavage as described in Section 7.2.2. At autopsy, liver samples were collected and processed for histopathological examination as described in Section 2.8. (A) control rat at week 1; (B) CCl_4-treated rat at week 1: centrilobular necrosis and vacuolation (indicated by arrow); (C) CCl_4-treated rat at week 3: early development of fibrous septae; (D) CCl_4-treated rat at week 6: increased fibrous thickening and well establish septae; (E) CCl_4-treated rat for 6 weeks and left to recover for 6 weeks: thinner septae.

7.4.11 1D ^{1}H NMR spectrometry

In this study, we wished to conduct an extensive ^{1}H NMR-based metabolomics investigation into the change in urinary metabolites as CCl_4-induced liver fibrosis developed and with a subsequent recovery period. Urine samples collected from rats weekly during the dosing period (week 1 to 6), and after 3 and 6 weeks of no treatment in the recovery period (T9 and T12) were analysed by 1D ^{1}H NMR.

PCA was used to identify differences and similarities between urine from control and CCl_4-treated animals. Figure 7.9 shows a scores plot from a PCA model derived from the 1D ^{1}H NMR spectral data from urine samples collected at all time points. At first examination of the scores plot it appeared that some points were located outside of the Hotelling's T2 ellipse. To determine whether these samples points should be excluded before further analysis, an investigation was carried out of the individual samples. Serum and urine clinical data, and histopathology data for these animals was analysed to determine if these animals had a greater degree of injury.

Visual analysis of the Hotelling's T2 range plot indicated the presence of significant differences between the 1D ^{1}H NMR spectral data from 2 animals sampled at week 4 (circled in red in the scores plot in Figure 7.9) and the remaining samples in the study. Analysis of the contribution plot of these samples showed integral regions corresponding to the taurine peaks to be increased over the PCA model average, whereas regions matching the creatinine peaks appeared to be decreased compared to the average (Figure 7.10). This was further confirmed by visual inspection of the 1D ^{1}H NMR spectra. Furthermore, analysis of the serum clinical markers such as ALT, AST and GLDH for these individual animals revealed particularly elevated values for these parameters compared to the group average; this could indicate that these animals have a greater degree of CCl_4-induced liver injury. Indeed, histopathological examination of liver tissue collected at autopsy revealed a significant degree of variability in the response of animals within the same group to the CCl_4 treatment. We, therefore, did not consider these samples to be true outliers, and instead it is thought that these samples were from animals with more severe hepatic injury than the group average. The other points, not encircled in the scores plot in Figure 7.9 that appeared outside the Hotelling's T2 ellipse, fell below the 99 % T2 critical value in the Hotelling's T2 range plot, and therefore, were not excluded from analysis.

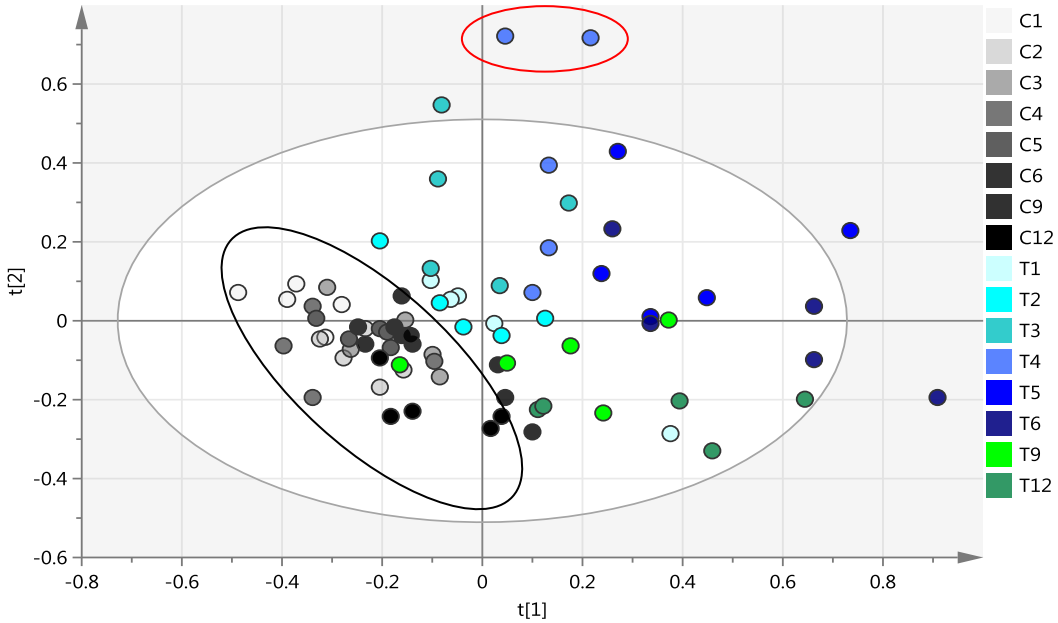

Figure 7.9 PCA scores plot from a PCA model derived from 1D ^{1}H NMR spectral data of urine samples from male Hanover-Wistar rats treated with vehicle (control) or CCl_4 at 0.4 mL/kg and sampled at different time points during the study. Rats were dosed by gavage and urine collected for 18 hours at the time points shown, as described in Section 7.2.2. Each spot in the scores plot represents one urine sample. R^2X (cum) = 0.880, Q^2 (cum) = 0.583. Control samples are circled in black. Samples from animals treated with 0.4 mL/kg CCl_4 for 4 weeks are circled in red.

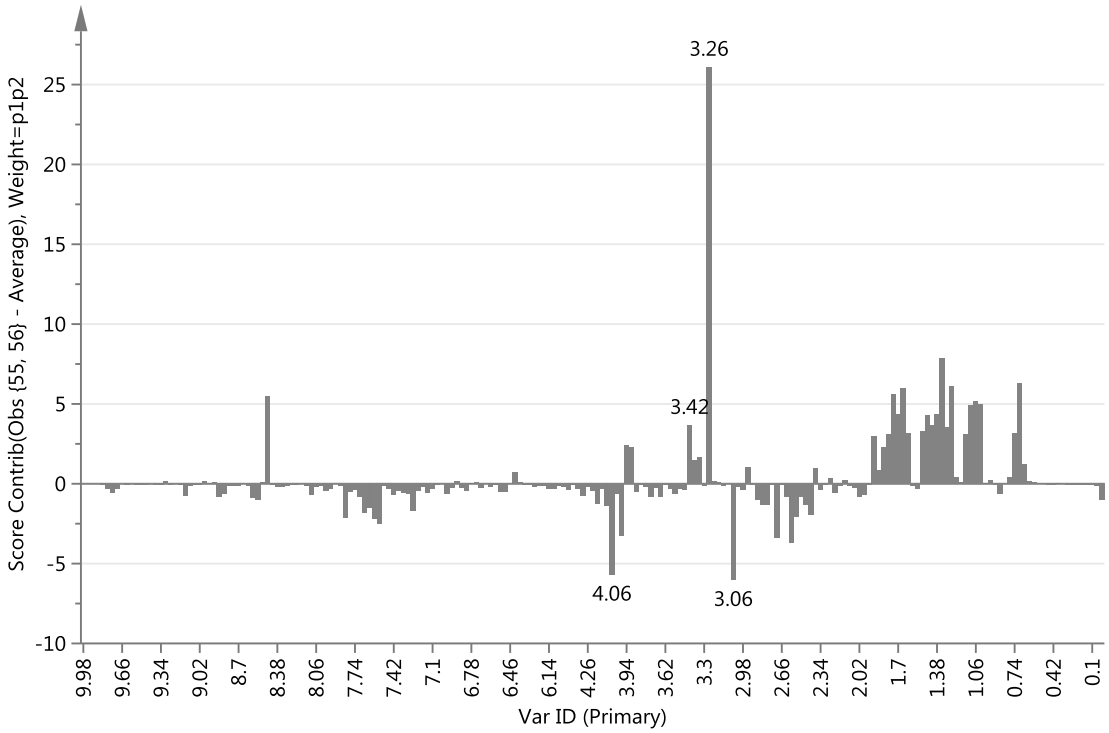

Figure 7.10 Contribution plot of 2 samples treated with CCl_4 for 4 weeks compared to the model average. Rats were treated with vehicle (control, 0 mL/kg) or CCl_4 by gavage and urine collected for 18 hours at various time points as described in Section 7.2.2.

Once the model was verified, it was possible to observe from the PCA scores plot (Figure 7.9) that although there was a considerable degree of overlap between spots, there appeared to be some degree of separation between control samples (grey spots, circled in black), and urine samples collected from CCl_4-treated animals (coloured spots). However, there were too many samples included in this model, coupled with great overlap, to visualise any potential metabolite patterns occurring with the progression of the study from week 1 to 12.

Therefore, a PCA trajectory scores plot was constructed and is shown in Figure 7.11. Each spot in the figure represents the average spectrum for each sample group (control and CCl_4-treated samples). The trajectory from week 1 to week 6, during which animals received 3 weekly administrations of CCl_4, and from week 6 to 12, which represented the recovery period is shown by the arrows. Control samples are circled in black.

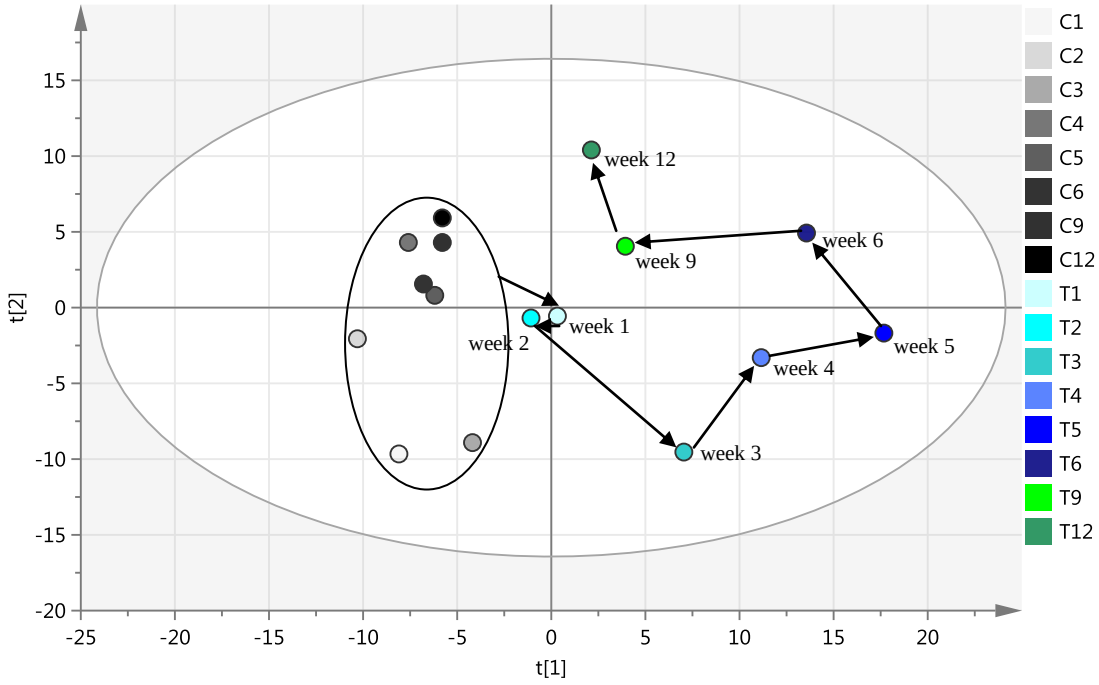

Figure 7.11 PCA trajectory plot from a PCA model derived from 1D ^{1}H NMR spectral data of urine samples from male Hanover-Wistar rats treated with vehicle (control) or CCl_4 at 0.4 ml/kg and sampled at different time points during the study. Rats were dosed by gavage and urine collected for 18 hours at the time points shown, as described in Section 7.2.2. Points in the trajectory plot represent the spectra created from the average of integral regions for each group of samples. R^2X (cum) = 0.878, Q^2 (cum) = 0.494. Arrows represent direction of movement.

This trajectory plot revealed that as fibrosis developed there was a general movement away from control samples (located on the left side of the plot), to the right side of the scores plot. During the recovery period, there was a move back to the left side of the scores plot (T9 and T12). Also, examination of the trajectory plot in Figure 7.11 revealed that, from week 5 to 6, there was a move in CCl_4-treated samples from the lower right quadrant, to the upper right quadrant. This shift was also present in control samples (in grey). Urine samples collected up to week 3 were located in the lower left quadrant, and samples collected at weeks 4, 5, 6, 9 and 12 were located on the upper left quadrant. We suggest that this might be a reflection of an age-related effect.

A PCA model created with ^{1}H NMR spectral data from control samples (data not shown) did not reveal significant differences between the groups of control samples at any time point. Therefore, control samples at week 1 were chosen to be representative of all controls in the study. Figure 7.12 A shows an OPLS scores plot for urine samples from animals treated repeatedly with 0.4 mL/kg CCl_4 and sampled weekly between weeks 1 and 6, and at week 9 and 12, and controls at week 1. By reducing the number

of samples used to construct the model, and by introducing a Y variable corresponding to the number of CCl_4 doses received by the animals it was possible to increase the degree of sample separation for further metabolite profile comparison. However, in this model, samples at 6, 9 and 12 all received the same number of doses, and therefore, the Y variable for these samples was the same.

Figure 7.12 B and C show the corresponding loadings and S-plot for the OPLS model in Figure 7.12 A, and provide information on the chemical shifts most relevant for sample separation. According to both plots, the following chemical shifts were increased in the samples from animals that had received the CCl_4-treatment, compared to controls at week 1: δ 3.42 and δ 3.26 (identified in previous studies as the triplets for taurine), δ 2.70 and δ 2.54 (corresponding to the citrate doublets), δ 2.98 and δ 2.42 (2-oxoglutarate), δ 4.06 and δ 3.06 (creatinine) and δ 3.02 (creatine).

A

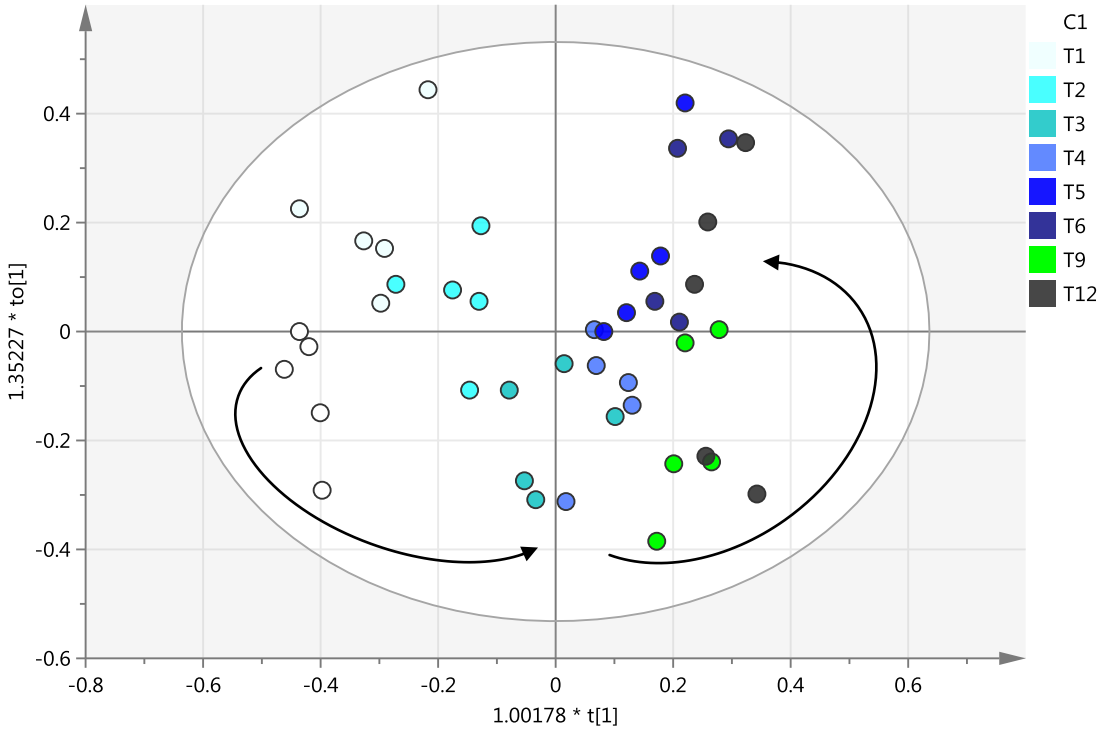

B

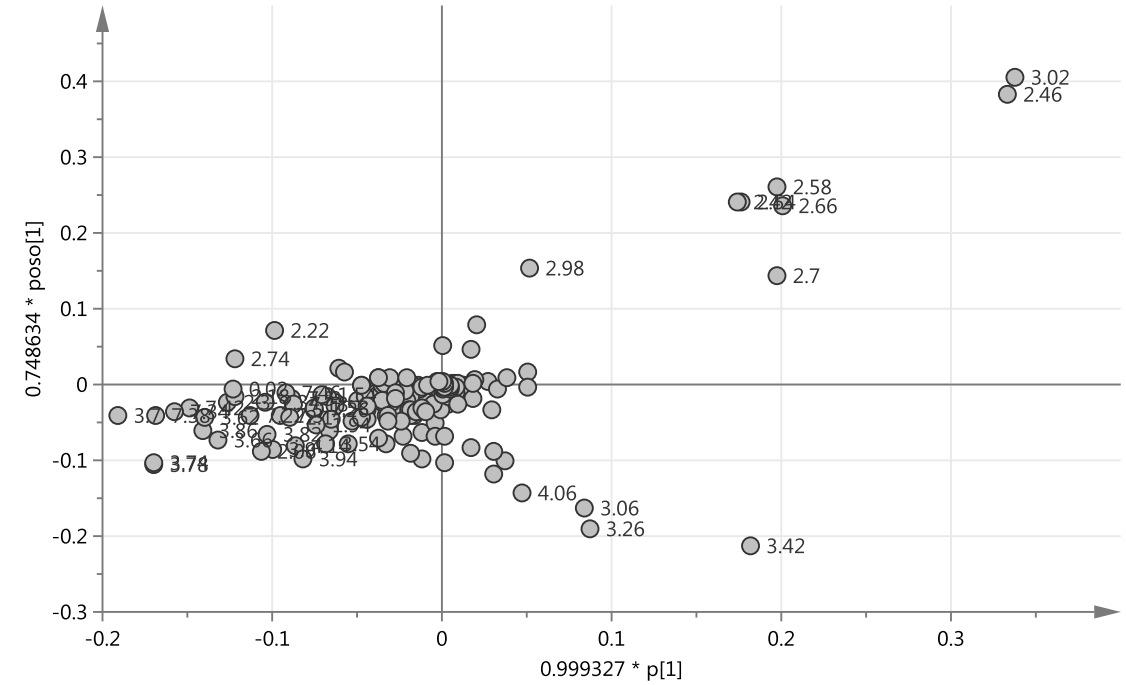

C

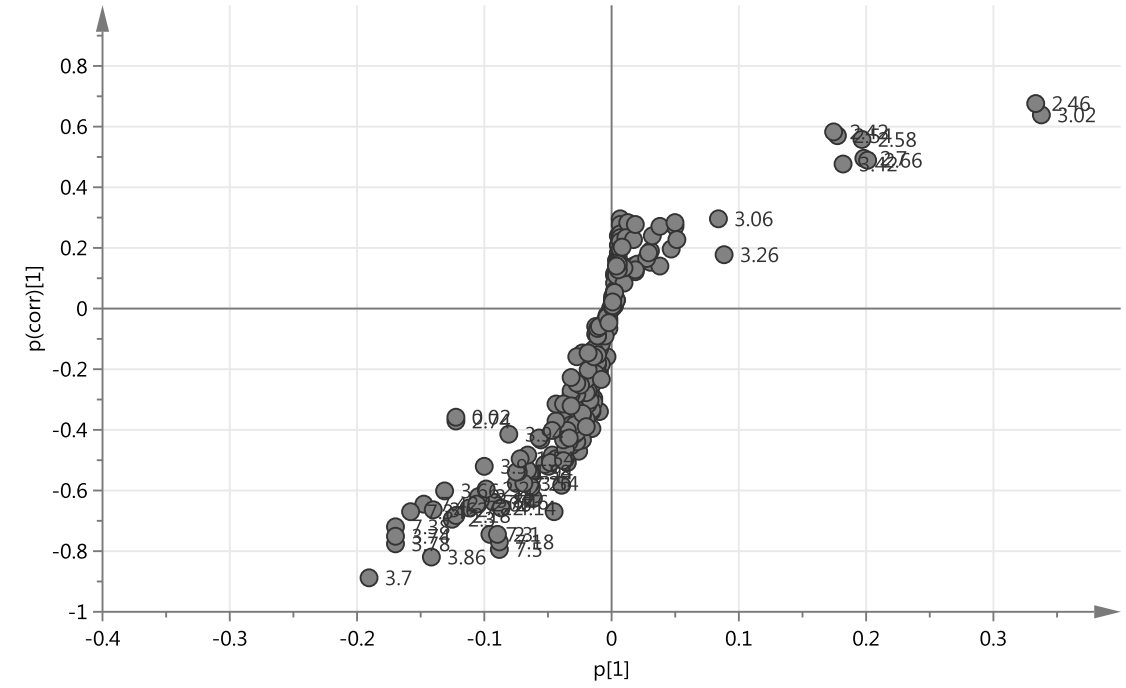

Figure 7.12 OPLS score plot (A), loadings (B) and S-plot (C) from an OPLS model derived from 1D ^{1}H NMR spectral data of urine samples from male Hanover-Wistar rats treated with vehicle (control) or CCl_4 0.4 mL/kg and sampled at different time points during the study. Rats were dosed by gavage and urine collected for 18 hours at the time points shown, as described in Section 7.2.2. Each spot in the scores plot represents one urine sample. Each spot in the loadings and S-plot represents a NMR variable labelled as chemical shift in ppm. R^2X (cum) = 0.626, Q^2 = 0.863. Arrows represent direction of movement.

One limitation of the previously described OPLS model was that samples collected at week 6, 9 and 12 had all received the same number of CCl_4 administrations. Therefore, 2 new OPLS models were created to further confirm the existence of differences at these time points; the first one including urine samples collected during the dosing period (week 1 to 6), which differ in regards to the number of CCl_4 administrations (Figure 7.13 A); and the second with samples collected at week 6 (0 weeks without treatment), 9 and 12 (3 and 6 weeks without treatment respectively) (Figure 7.13 B), and which differ in regards to the number of weeks without treatment. Arrows in Figure 7.13, represent the direction of movement of samples.

A

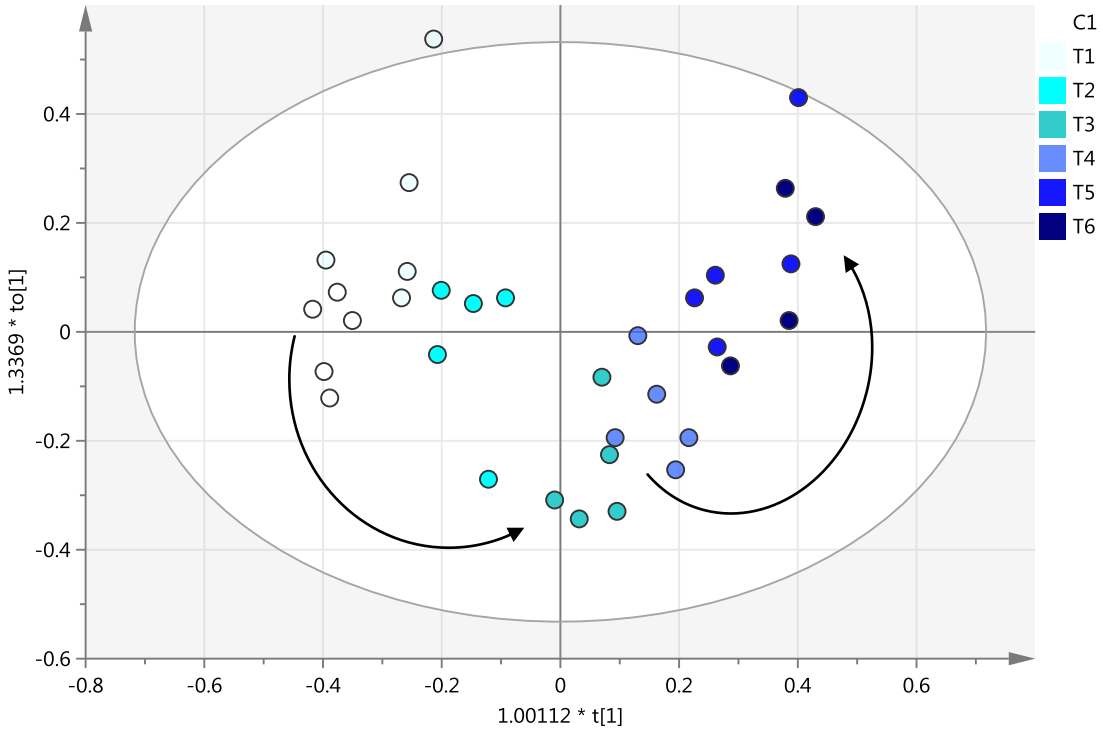

B

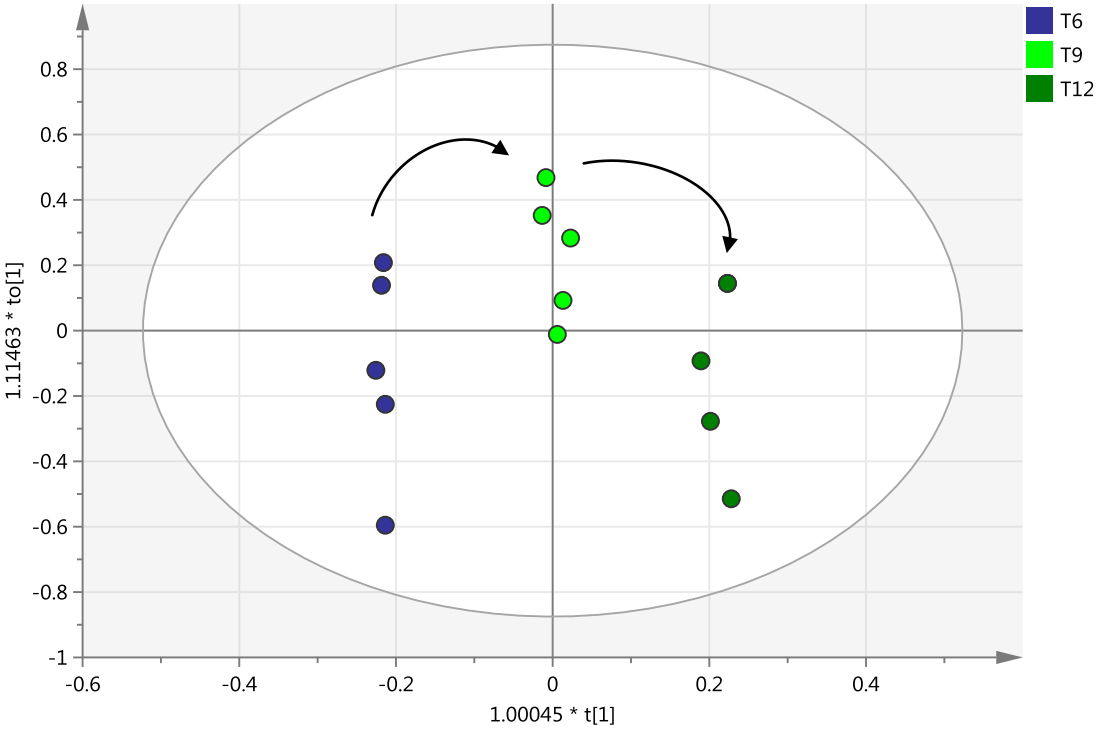

Figure 7.13 OPLS scores plots from OPLS models derived from 1D ^{1}H NMR spectral data of urine samples from male Hanover-Wistar rats treated with vehicle (control) or CCl_4 at 0.4 mL/kg and sampled at different time points during the study. Rats were dosed by gavage and urine collected for 18 hours at the time points shown, as described in Section 7.2.2. (A) samples collected from control animals at week 1 and CCl_4-treated animals at weeks 1 to 6, R^2X (cum) = 0.683, Q^2 = 0.853; (B) samples collected from CCl_4-treated animals at week 6 (dosing period) and at weeks 9 and 12 (recovery period, 3 and 6 weeks without treatment), R^2X (cum) = 0.750, Q^2 = 0.862. Arrows represent direction of movement.

In this experiment 2, a statistical analysis was performed to investigate changes to urinary metabolite levels with increasing number of CCl_4 administrations and thus development of hepatic fibrosis, and also during the recovery/no treatment period. To achieve this, individual OPLS-DA models were constructed using 1D ^{1}H NMR spectral data from the study. The following data paired samples were compared in OPLS-DA models: control and CCl_4-treated samples at week 1; and CCl_4-treated samples at week 1 and 2; 2 and 3; 3 and 4; 4 and 5; 5 and 6; 6 and 9 and 9 and 12 (Figure 7.14).

The scores plot for each OPLS-DA model displayed perfect group separation along the discriminating component 1 (t[1]) whereas the orthogonal component represented the degree of intragroup variability. The S-plot and VIP plot were further analysed for each OLPS-DA model in order to determine the most relevant chemical shifts responsible for the sample separation (data not shown). The statistical significance of chemical shift

differences was determined by performing a Student's t-test comparing consecutive time points, such as chemical shifts from CCl_4-treated animals at week 1 and 2. This data is summarized in Table 1.8.

It appeared that after 1 week of CCl_4-treatment there was an increase in the resonances of formate, taurine, 2-oxoglutarate, citrate and succinate when compared to control animals, and a decrease in the resonances of hippurate, creatinine and creatine. Excretion of hippurate in the urine was further decreased at the next 2 time points (T2 and T3) and formate levels appeared to be increased over control at week 1, but were decreased at week 2 compared to week 1, and at week 3 compared to the previous time point (week 2). Similar findings were reported for 2-oxoglutarate and citrate, both increased in week 1 treated animals but were lower week 2 and again at week 3. However, taurine appeared to increase in concentration as the number of CCl_4 administrations increased up to week 3. Creatinine was also increased at week 2 and 3, but was decreased compared to control animals at week 1. At week 4 most of the metabolites were increased compared to week 3. However, the 2 triplet peaks corresponding to the metabolites taurine, 2-oxoglutarate and hippurate showed opposite signals. At week 5 and 6, taurine was decreased compared to the week 4 and 5 autopsies, respectively, whereas metabolites belonging to the TCA cycle, such as 2-oxoglutarate and citrate, were reported to be increased. At this time point CCl_4-dosing was stopped.

At week 9, 3 weeks after the last CCl_4 administration, urinary excretion of hippurate, creatinine, creatine and taurine were increased compared to controls at week 6. Levels of 2-oxoglutarate, citrate and succinate, however, appeared to have decreased in the recovery period. At the last time point, following 6 weeks of no treatment, taurine, creatinine, creatine and succinate were decreased in the urine, whereas formate, hippurate and citrate were increased compared to the previous time point.

A

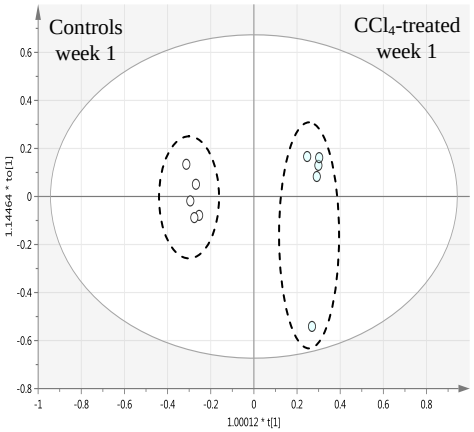
Controls
week 1
CCl4-treated
week 1
1.14464 * to[1]
1.00012 * t[1]

B

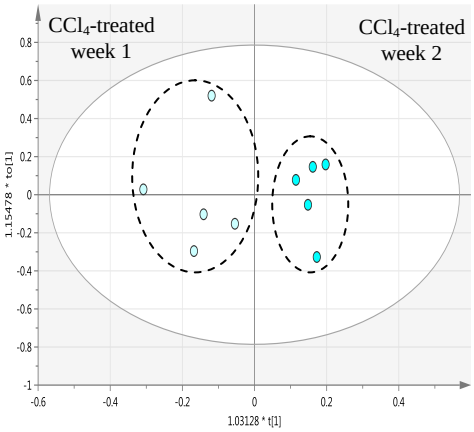
CCl4-treated
week 1
CCl4-treated
week 2
1.15478 * to[1]
1.03128 * t[1]

C

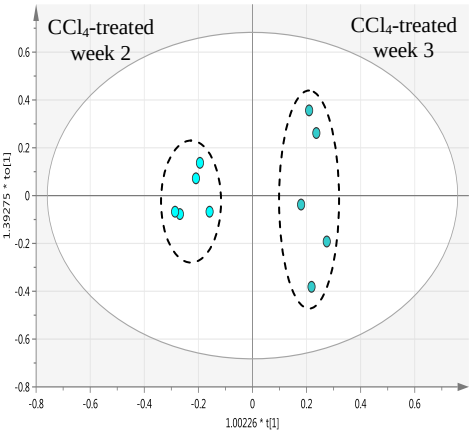
CCl4-treated
week 2
CCl4-treated
week 3
1.39275 * to[1]
1.00226 * t[1]

D

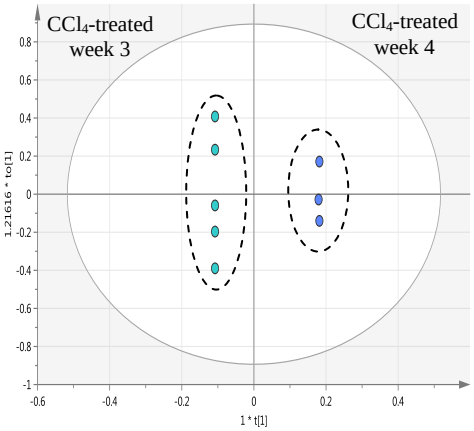
CCl4-treated
week 3
CCl4-treated
week 4
1.21616 * to[1]
1 * t[1]

E

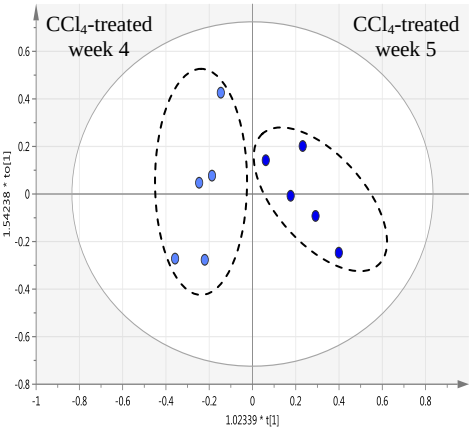
CCl4-treated
week 4
CCl4-treated
week 5
1.54238 * to[1]
1.02339 * t[1]

F

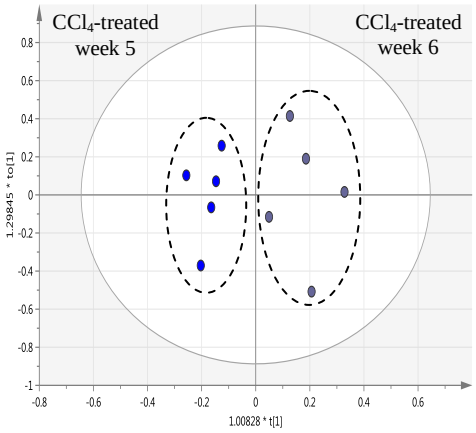
CCl4-treated
week 5
CCl4-treated
week 6
1.29845 * to[1]
1.00828 * t[1]

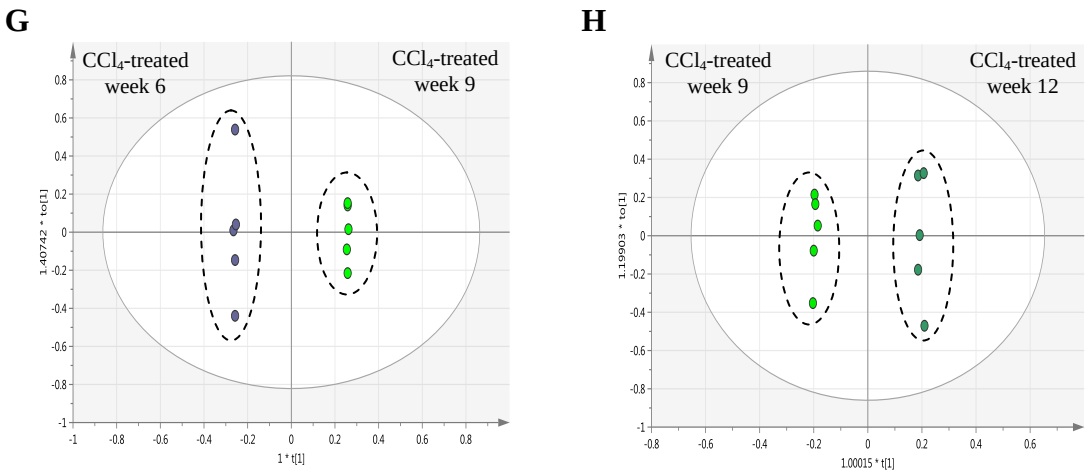

Figure 7.14 Scores plots from OPLS-DA models derived from 1D ^{1}H NMR spectral data of urine samples from male Hanover-Wistar rats treated with vehicle (control) or CCl_4 at 0.4 mL/kg and sampled at different time points during the study. Rats were dosed by gavage and urine collected for 18 hours at the time points shown, as described in Section 7.2.2. (A) control and CCl_4-treated rats at week 1; (B) CCl_4-treated rats at week 1 and 2; (C) CCl_4-treated rats at week 2 and 3; (D) CCl_4-treated rats at week 3 and 4; (E) CCl_4-treated rats at week 4 and 5; (F) CCl_4-treated rats at week 5 and 6; (G) CCl_4-treated rats at week 6 and 9 (0 and 3 weeks recovery without treatment) and (H) CCl_4-treated rats at week 9 and 12 (3 and 6 weeks recovery without treatment).

In addition to investigating the differences between 2 consecutive time points, we were also interested in studying the potential for reversibility. Two OPLS-DA models were created using the ^{1}H NMR spectral data from CCl_4-treated animals at week 1 (3 doses) and week 6 (18 doses) (Figure 7.15), and with the ^{1}H NMR of treated animals at week 6 (last week of dosing period) and week 12 (6 weeks of recovery period without treatment) (Figure 7.15 B).

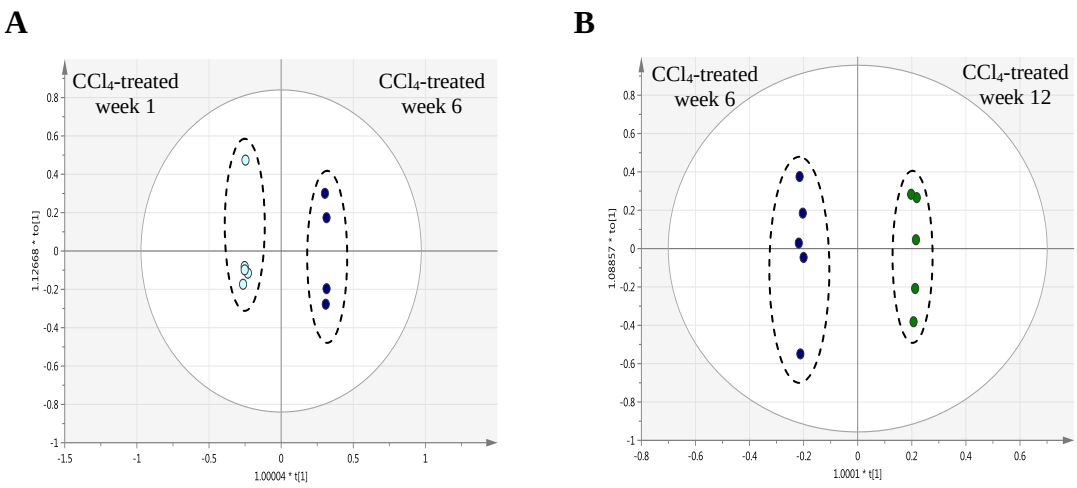

Figure 7.15 Scores plots from OPLS-DA models derived from 1D ^{1}H NMR spectral data of urine samples from male Hanover-Wistar rats treated with CCl_4 at 0.4 mL/kg and sampled at different time points during the study. Rats were dosed by gavage and urine collected for 18 hours at the time points shown, as described in Section 7.2.2. (A) CCl_4-treated rats at week 1 and 6; (B) CCl_4-treated rats at week 6 and 12 (0 and 6 weeks recovery without treatment, respectively).

Figure 7.15 revealed good separation between CCl_4-treated samples collected at different time points during the dosing period (week 1 and 6) and between the dosing and recovery periods (week 6 and 12, respectively).

A statistical analysis of the integral regions corresponding to the chemical shifts identified from the S-plot (data not shown) was performed between treated animals at week 1 and 6, and between week 6 and 12 and is shown in Table 7.11.

It appears from the table that after 6 weeks of CCl_4 treatment, the urinary excretion of formate, hippurate, creatine and succinate was decreased in treated animals compared to animals that had received 3 doses of CCl_4 (week 1), whereas resonances corresponding to the metabolites creatinine, taurine, citrate and 2-oxoglutarate were increased compared to animals at week 1.

At week 12 (6 weeks without treatment) there was a decrease in the urinary levels of formate, taurine, 2-oxoglutarate and succinate compared to animals at the end of the dosing period. On the other hand, hippurate, creatinine, creatine and citrate were increased after 6 weeks of recovery (week 12).

Table 7.10 OPLS-DA detected 1D ^{1}H NMR chemical shift regions responsible for the separation of NMR derived spectra from the urine of male Hanover-Wistar rats treated with vehicle (control) or CCl_4 at 0.4 mL/kg and sampled at different time points. Rats were dosed by gavage and urine collected for 18 hours at the time points shown, as described in Section 7.2.2. Chemical shifts were statistically compared by means of a Students' t-test. Values that differ significantly from controls, or CCl_4-treated animals at the previous time point are shown: $^{*}P<0.05$; $^{**}P<0.01$; $^{***}P<0.001$.

Chemical shift (δ), multiplicity	Endogenous metabolite	C1 vs T1	T1 vs T2	T2 vs T3	T3 vs T4	T4 vs T5	T5 vs T6	T6 vs T9	T9 vs T12
8.46-8.50 (s)	formate	+	-	-	+	+	-	-*	+*
7.70-7.74 (d)	hippurate	-***	-	-	+	-	-	+**	-*
7.62-7.66 (t)	hippurate	-	-	-	+	-	-	+*	+
7.54-7.58 (t)	hippurate	-	-	-	+	+	-	+**	+
4.06-4.10 (s)	creatinine	-**	+*	+	-	-	+	+**	-
3.98-4.02 (d)	hippurate	-	-	-	-	-	-	+**	+
3.94-3.98 (s)	creatine	-	-	+	+	-	-	+*	-
3.42-3.46 (t)	taurine	+*	+	+**	-	-	-	+	-
3.26-3.30 (t)	taurine	+	+	+	+	-	-*	+	-
3.06-3.10 (s)	creatinine	-**	+*	+	-	-	+	+**	-
2.98-3.02 (t)	2-oxoglutarate	+	-*	-	-	+**	-	-	-
2.70-2.74 (d)	citrate	+*	-	-	+	+	+	-	+
2.54-2.58 (d)	citrate	+**	-	-	+	+*	+	-	+
2.42-2.46 (t)	2-oxoglutarate	+	-	-	+	+*	+	-	+
2.38-2.42 (s)	succinate	+*	-	+	-	-	-	-	-*

S, singlet; d, doublet; t, triplet.

Table 7.11 OPLS-DA detected 1D ^{1}H NMR chemical shift regions responsible for the separation of NMR derived spectra from the urine of male Hanover-Wistar rats treated with CCl_4 at 0.4 mL/kg and sampled at different time points. Rats were dosed by gavage and urine collected for 18 hours at the time points shown, as described in Section 7.2.2. Chemical shifts were statistically compared by means of a Students' t-test. Values that differ significantly from CCl_4-treated animals at previous time points are shown: $^{*}P<0.05$; $^{**}P<0.01$; $^{***}P<0.001$.

Chemical shift (δ), multiplicity	Endogenous metabolite	T1 vs T6	T6 vs T12
8.46-8.50 (s)	formate	-*	-*
7.70-7.74 (d)	hippurate	-***	+
7.62-7.66 (t)	hippurate	-**	+**
7.54-7.58 (t)	hippurate	-***	+**
4.06-4.10 (s)	creatinine	+*	+*
3.98-4.02 (d)	hippurate	-***	+**
3.94-3.98 (s)	creatine	-**	+
3.42-3.46 (t)	taurine	+**	-
3.26-3.30 (t)	taurine	+	-
3.06-3.10 (s)	creatinine	+	+*
2.98-3.02 (t)	2-oxoglutarate	-	-
2.70-2.74 (d)	citrate	+**	+
2.54-2.58 (d)	citrate	+**	+
2.42-2.46 (t)	2-oxoglutarate	+**	-
2.38-2.42 (s)	succinate	-	-*

S, singlet; d, doublet; t, triplet.

7.5 Discussion

In Chapter 3, we identified a dose level range of CCl_4 that following a single administration would induce hepatic injury but that would not induce toxicity in other tissues. It was decided in Chapter 3 that dose levels above 2.0 mL/kg are likely to induce nephrotoxicity.

In the current Chapter, we wished to develop a model of chronic liver injury and since this would be a repeat dose study the dose range of CCl_4 chosen was between 0.4 and 1.2 mL/kg, i.e., much lower than 2.0 mL/kg. However, it was still unknown whether lower dose levels administered chronically would induce toxicity in other organs. Therefore, the purpose of experiment 1 in this Chapter was to determine the ideal dose level for our hepatic fibrosis model and investigate the potential for other toxicities.

The dosing regimen used in experiment 1 for the development of fibrosis included 3 weekly administrations of CCl_4 by gavage on alternate days (Monday, Wednesday and Friday). CCl_4 has been shown to be readily absorbed by the GI tract in rats (Kim et al., 1990). In the present studies we wished to induce fibrosis in the rat by administering CCl_4 in the shortest period of time possible and with minimal mortality. One of the aspects that needs to be taken into account when devising a schedule for CCl_4 administration is the fact that free radicals produced as a result of the metabolism of CCl_4 by cytochrome P-450 have the ability to irreversibly inactivate the cytochrome P-450 (Manno et al., 1992). CCl_4, therefore, inhibits its own metabolism; this process is called "suicidal inactivation" and appears to confer some protection against CCl_4-induced toxicity (Ugazio et al., 1972). Therefore, most of the dosing regimens described in the literature consist of 2 or 3 administrations. In the present study, we opted for a model of 3 administrations per week on alternate days using a low dose of CCl_4. This would allow us to increase exposure to CCl_4 at the same time as avoiding a greater degree of cytochrome P-450 inactivation.

In this study, the experimental design involved dosing 80 animals 3 times a week at 0 (controls), 0.4, 0.8 and 1.2 mL/kg CCl_4, and killing 5 animals per group every 3 weeks up to 12 weeks of dosing. However, after week 3, the general bodily condition of some animals in the 0.8 and 1.2 mL/kg CCl_4 began to deteriorate with each CCl_4 administration. Consequently, after 3 unscheduled deaths it was decided that the dosing period would be stopped and the study terminated. However, since we wished to gain as

much information as possible from this preliminary study which would help the development of our fibrosis model, we decided to allow 3 animals in the 0.8 and 1.2 mL/kg CCl_4 groups to recover untreated for a further 6 and 8 weeks respectively. After 2 animals in the 0.4 mL/kg CCl_4 group had to be killed, it was also decided that 4 of the 8 remaining animals would be allowed to recover for 4 weeks, and 4 animals would be allowed to recover for 8 weeks. This would provide us with information regarding the feasibility of recovery from our potential model and the possible period required. Animals that had received the higher dose level (i.e. 1.2 mL/kg) would be allowed to recover for longer.

Clinical observations were recorded at autopsy and it was seen that after 3 weeks of dosing, livers from CCl_4-treated animals with 0.4, 0.8 and 1.2 mL/kg were paler in colour and enlarged compared to control animals, and showed pitting of the surface. Animals in the highest dose level groups (0.8 and 1.2 mL/kg) also showed evidence of fluid in the abdominal cavity. At the end of the study, the livers of CCl_4-treated animals at all CCl_4 dose levels were generally paler in colour. There was also evidence of pitting of the surface and the presence of small cysts (1 mm) on the liver surface which were seen in animals treated with 0.4, 0.8 and 1.2 mL/kg CCl_4. The spleens from some animals were enlarged but normal in colour whereas the testes appeared reduced in size. There was also the presence of fluid in the abdominal cavity with prominent and enlarged veins.

During the study, at all autopsies, livers were removed and weighed and relative weights were calculated. After 3 weeks of CCl_4 dosing, relative liver weights were significantly increased above controls at all CCl_4-dose levels. At later time points, there were no significant differences between relative liver weights from control animals autopsied at week 6, and 0.4, 0.8 and 1.2 mL/kg CCl_4-treated animals at termination. An increase in relative liver weight has been previously documented in Chapter 3 following a single administration of CCl_4 and has also been previously described in chronic dose studies. In a study by Khan and colleagues (2012), male Sprague-Dawley rats were administered with CCl_4 at 3 mL/kg (intraperitoneally) twice a week for a total of 4 weeks and autopsied 24 hours after the last treatment. At post-mortem, relative liver weights were significantly increased compared to control animals. Other studies have reported similar findings following the repeat administration of CCl_4. In one study, male Hanover-Wistar rats were dosed orally, twice a week, with 2 mL/kg CCl_4 for a period of

8 weeks after which a 185 % increase in liver weights over control animals was reported (Fang and Lin, 2008). An increase in liver weight was also reported in female Sprague-Dawley rats following i.p. injections of CCl_4 over an 8 week period (Hauso et al., 2008). Stowell and Lee (1950) attributed this increase in relative weight to a greater fluid accumulation and an increased lipid content of the damaged liver.

Serum biochemistry analysis was performed to further investigate the development of liver toxicity following CCl_4 administration. In the present study, blood samples were collected from the tail vein at 24 hours following the first administration of CCl_4, at week 3 and at group termination autopsies. Blood samples were not collected from animals at the recovery period autopsies.

Serum biochemistry results revealed that after a single dose of CCl_4 (24 hours after the first dose) at 0.4, 0.8 and 1.2 mL/kg, mean serum levels of ALT, AST and GLDH were increased over control to a similar degree as the increases described in Chapter 3 (Figure 7.2 A). This measurement after the first dose was carried out in serum prepared from blood collected via the tail vein whereas in the previous Chapter 3 study the blood was collected from the abdominal aorta at autopsy. During the course of the repeat dose study it was going to be necessary to collect blood from the tail vein at some time points. Therefore, these results confirm the method of blood collection should not affect the serum enzyme levels.

Levels of ALP were slightly increased over controls at 24 hours after a single dose of CCl_4, and at the highest dose level (1.2 mL/kg) this increase was statistically significant ($^{***}P>0.001$) (Table 7.2). No statistically significant changes were recorded for the other parameters measured at 24 hours after a single dose of CCl_4.

After 3 weeks of CCl_4 administration (9 doses in total), mean levels of ALT, AST and GLDH were significantly increased over controls at all CCl_4 dose levels, with a much greater fold increase than at 24 hours after a single dose. However, the fold increase over control for ALT and AST decreased with increasing CCl_4 concentrations, i.e., the levels were greater at 0.4 mL/kg (lowest concentration) (Figure 7.2 B). Levels of ALP were also significantly raised above control at 0.4, 0.8 and 1.2 mL/kg CCl_4, but were maximal at 0.8 mL/kg (5.6-fold increase; $^{***}P<0.001$) (Table 7.2).

At the final autopsies, enzyme levels of ALT, AST, GLDH and ALP followed the same trend as above and the greatest serum enzyme levels were found at the lowest dose level

(0.4 mL/kg) (Figure 7.2 C). However, they were still considerably greater than control values.

It is interesting to note that at the later time points there was a reduction in fold increase over control when compared to the 3 week samples. This trend, and the lower fold increases at the later time point may reflect the severity of the hepatic injury, thus compromising the synthesis of these enzymes. Increased levels of these enzymes are routinely associated with liver injury and have been previously described following repeat CCl_4 administration. In a study by Fu et al. (2008), male Sprague-Dawley rats were injected intraperitoneally at 0.1 mL/100g BW every day for a period of 8 weeks and autopsied at 48 hours after the last administration. Biochemical analysis of serum samples revealed significant increases in ALT, AST and ALP levels in the CCl_4-treated animals compared to control rats. Domitrovic and colleagues (2009) found similar results in a mouse model of CCl_4-induced fibrosis. Mice were injected intraperitoneally with CCl_4 at 0.4 mL/kg, twice a week for 6 weeks. Seventy two hours after the last administration animals were sacrificed and levels of ALT, AST and ALP were significantly elevated above control levels. Smyth et al. (2007) also reported significant increases in ALT, AST and GLDH serum levels after 6 weeks of twice weekly administration of CCl_4 at a range of concentrations varying from 0.06 to 0.36 mL/kg.

Since albumin is synthesised in the liver, decreased serum levels of albumin can often be indicators of chronic liver injury (Carey and Carey, 2010). In this study, after 9 doses (T3), albumin was decreased in the serum of CCl_4-treated animals, but this decrease was only significant at 0.8 mL/kg (Table 7.2). However, at the final time point autopsies, all CCl_4-treated animals showed significantly lower albumin levels compared to control rats. A study by Gou et al. (2013), revealed a significant decrease in serum albumin levels in a model of hepatic fibrosis in rats that had been dosed twice weekly with CCl_4 at 1.0 mL/kg for 9 weeks by i.p. injection.

Levels of total protein in the serum also reflect the synthesis turnover of the liver, and therefore, are often used to assess liver function. In the present experiment 1, serum protein levels were significantly decreased after 9 administrations of CCl_4 at 0.8 and 1.2 mL/kg, and at the final time points in all CCl_4-treated animals (Table 7.2). Similar decreases in serum protein levels have been previously reported in rodent models of CCl_4-induced fibrosis (Castilla-Cortazar et al., 1997; Yang et al., 2010a).

In the present study, serum creatinine levels were significantly decreased in the serum of animals that had received 13 administrations of CCl_4 at 1.2 mL/kg, whereas serum urea levels were significantly increased in animals that received 9 doses of 0.8 mL/kg CCl_4, and at termination urea levels were significantly decreased in animals treated at the highest dose level (1.2 mL/kg CCl_4) (Table 7.2). In fact, decreased urea synthesis (Rudman et al., 1973) and decreased creatinine production (Cocchetto et al., 1983) have been previously reported in cirrhotic patients. One of the mechanisms responsible for decreased creatinine production in cirrhotic patients is the compromise in creatine production as well as decreased muscle mass (Cocchetto et al., 1983). Creatine is synthesised via 2 enzyme-catalysed reactions. The first reaction occurs between arginine and glycine. This process occurs mainly in the kidneys and pancreas and to a lesser extent in the liver. The product of this reaction, guanidinoacetic acid is converted to creatine via a methylation reaction that occurs mainly in the liver and to a lesser extent in other tissues, as the kidneys, pancreas, spleen, brain and testes. The synthesis of creatine does not occur in the muscle tissue, but due to the existence of a specific membrane transport system, creatine accumulates within the skeletal muscle (Cocchetto et al., 1983) where it exists as creatine phosphate (Waters et al., 2005). Therefore, the creatine pool is related primarily to the muscle mass, which is affected by gender and age. Consequently, considerable changes in muscular mass will affect the excretion of urinary creatinine making it a useful and accurate index of body muscle mass.

In advanced stages of liver cirrhosis, the liver function in carbohydrate metabolism is compromised and therefore, both hyperglycaemia and hypoglycaemia may be observed in cirrhotic patients. On the one hand, impaired insulin sensitivity and consequent impaired glucose tolerance, are often seen in states of chronic liver disease such as cirrhosis due to a reduction of liver function (Petrides et al., 1998; Hickman and Macdonald, 2007). Insulin resistance may arise from decreased clearance of insulin by the liver due to reduced hepatic function (Garcia-Compean et al., 2009; Ishikawa et al., 2013). In fact, the liver is the primary site of insulin clearance (Duckworth et al., 1998). Serum glucose levels may thus reflect a change in insulin resistance. On the other hand, hypoglycaemia may be associated with cirrhotic livers due to a reduced rate of glycogenolysis as a result of extensive liver parenchymal destruction (Petersen et al., 1999). In the current study, serum glucose levels were decreased in all CCl_4-treated animals compared to control rats after 9 CCl_4 administrations, and at the final time points of the study the decrease in glucose levels was statistically significant in the 0.8

mL/kg CCl_4-treated group. Similar findings have been previously reported in a study by Cortazar and colleagues (1997) in which cirrhotic rats showed significantly lower levels of serum albumin, total protein and glucose, compared to control animals.

In this study, the presence of fibrotic septae were reported following histopathological examination of the livers after 3 weeks of repeat dosing. By the end of the study this fibrotic process had progressed and bridging fibrosis was apparent. Thus, initial signs of fibrosis were present in experiment 1 after 3 weeks of repeat CCl_4 dosing (Figure 7.3).

Parsons et al. (2004), used a model of CCl_4-induced fibrosis in the male Wistar rat and reported the presence of septal fibrosis and extensive bridging and inflammation at day 24 (week 3.5) into the study. In their study animals were dosed with CCl_4 by gavage at 412 mg CCl_4/kg olive oil. Similar results were reported by Chobert and colleagues (2012) following the administration of CCl_4 at 1.0 mL/kg twice a week, following an initial single dose of CCl_4 at 2.0 mL/kg. After 2 weeks, fibrosis was characterised by the deposition of thin collagen fibres in necrotic areas. Four weeks into the treatment there was evidence of fibrotic septae connecting centrilobular areas and at week 6 there were multiple fibrotic septae interconnected and dividing the hepatic lobules. Smyth et al., (2007) administered CCl_4 at dose levels between 0.4 and 1.0 mL/kg, twice a week for a period of 6 weeks. At 6 weeks there was evidence of fibrosis with bridging between centrilobular, periportal and capsular areas.

In the livers of animals that were allowed to recover, fibrotic septae were still detected by histopathological examination (Figure 7.3). However, the collagen fibres present were considerably narrower than those found in animals during the dosing period. Some individual rats demonstrated almost complete recovery. However, there was no correlation between the degree of resolution and the time allowed for recovery, which reflects the great intragroup variability observed in CCl_4-induced injury. Nevertheless, these preliminary results suggest that our model of hepatic fibrosis has potential to be reversible upon cessation of treatment.

Measurement of urinary levels of total protein, creatinine and glucose in experiment 1 revealed that all 3 were decreased when compared to controls at week 6 in animals treated at the highest dose level (1.2 mL/kg) (Table 7.3). As described earlier, in cirrhosis, due to reduced hepatic synthesis of creatine, serum levels of creatinine are often decreased. Therefore, in conditions of cirrhosis, the level of creatinine does not

provide an accurate reflection of the glomerular filtration rate (Betrosian et al., 2007) and is not reliable for assessing renal function (Mackelaite et al., 2009).

In this experiment it was very important to ensure that repeated CCl_4 administration did not induce nephrotoxicity since we would be using this model to investigate urinary biomarkers. Relative kidney weights were significantly increased over controls at 0.8 and 1.2 mL/kg after 3 weeks, and in all CCl_4-treated animals at the group termination autopsies.

However, the absence of CCl_4-induced nephrotoxicity at all of the dose levels was confirmed by histopathological examination of the kidneys. In addition, no evidence was found of CCl_4-induced changes to any of the other organs examined at any dose level, or any time point. Therefore, we can be confident that the model we chose for the induction of hepatic fibrosis based on the results from this experiment 1 will not induce injury to any other target organs.

From the results obtained in experiment 1 it was clear that our original plan of dosing the animals for 12 weeks was too long and would result in a high mortality rate. Additionally, there was no difference between the CCl_4 dose levels as to the level of fibrosis induced as determined histopathologically. There were no deaths in the 0.4 mL/kg group, until week 6 at which time point 2 animals had to be killed, compared to 3 at each of the higher dose levels that occurred before 6 weeks of treatment. It was therefore decided, that the dose level for our hepatic fibrosis model should be 0.4 mL/kg CCl_4. With regards to the length of time/number of CCl_4 administrations, 6 weeks was chosen as the ideal since it was felt that longer than this could result in morbidity/mortality of the animals. Therefore, our model for hepatic fibrosis was to administer CCl_4 at 0.4 mL/kg by gavage 3 times a week for 6 weeks.

In experiment 2 we used this model to investigate changes to serum enzymes, liver gene expression and urinary metabolites as fibrosis developed. We also included a period of 6 weeks of no treatment at the end of the dosing period to further investigate the potential of reversibility of the lesion.

In general, the organ weight data from experiment 2 compare to the results described in experiment 1. However, relative spleen weights were increased above controls in all CCl_4-treated animals, although in the recovery period the fold increase over control was

less than during the dosing period (Table 7.4). Splenomegaly is frequently observed in humans with cirrhosis-related portal hypertension, known as congestive splenomegaly. In portal hypertension there is an increase in the portal vascular resistance which compromises the blood flow through the splenic vein as it empties into the portal vein (Gusberg et al., 1994).

As with experiment 1, at autopsy, many CCl_4-treated animals had the presence of fluid in the abdominal cavity and showed enlarged veins in the abdominal wall. Accumulation of fluid in the abdominal cavity is known as ascites and is the most common complication of cirrhosis. In cirrhosis there is the development of intrahepatic hypertension and consequently there is retention of sodium and water which eventually move from the capillaries into the peritoneal space (Kashani et al., 2008). Simultaneously, when the pressure in the portal vein increases, there is venous enlargement and development of varices which can bleed (Mahl and Groszmann, 1990).

Relative liver weights were greater in CCl_4-treated animals when compared to controls, and at weeks 1 to 5 this increase was statistically significant (Figure 7.4). However, after week 2, the fold increases declined. At week 6 there was large intragroup variability with regards to liver weight but this is a common finding in CCl_4-induced hepatic injury. By week 9 and 12 (3 and 6 weeks into the recovery period, respectively), relative liver weights were still significantly enlarged compared to concurrent controls but had considerably decreased when compared to livers from treated animals during the dosing period. The results from experiment 2 compare with the results previously described in experiment 1. In advanced stages of cirrhosis it is known that the liver is often decreased in size and nodular due to replacement of healthy tissue by the scar tissue (Carey and Carey, 2010).

As in experiment 1, serum levels of ALT, AST and GLDH were significantly increased over concurrent controls at all time points during the dosing period (Figure 7.5). A similar trend of a reduction in fold increase over control with increasing CCl_4 administrations was also observed. By week 12, the last week of the study, values were still increased over concurrent controls indicating that the liver function was not fully restored following the 6 week recovery period.

In experiment 2, serum lipocalin-2, TIMP-1 and MCP1 levels were increased over concurrent controls at all time points but maximum increases were present at week 4

with 11.5-, 29.9- and 6.9-fold increases over control levels, respectively ($^{**}P<0.01$) (Table 7.5). By week 7 (week 1 of recovery period), mean serum levels of lipocalin-2 and MCP1 had returned to control values, whereas TIMP-1 remained significantly increased over controls, even though the fold increase was significantly smaller (approximately 2-fold increase) ($^{**}P<0.01$). At week 12 (6 weeks without treatment) serum TIMP-1 was still significantly increased over controls (Table 7.6). AGP levels increased as the number of CCl_4 doses increased and were highest after 6 weeks of CCl_4 administration (Table 7.5). During the recovery period AGP levels remained similar to controls. Serum A2M levels also peaked at week 6 (12.4-fold increase over controls; $^{***}P<0.001$) and remained significantly increased over controls during the recovery period apart from weeks 7 and 10 (Table 7.5, Table 7.6). In the acute study carried out in Chapter 3, levels of these biomarkers were also measured in the serum following the single administration of CCl_4. Apart from A2M serum levels, which did not show evidence of a dose-related effect, mean values for all other markers appeared to increase significantly with the CCl_4 dose level.

Increases in serum lipocalin-2 levels have been previously described in models of CCl_4-induced hepatic fibrosis. Kamphorst et al. (2011) used a protocol of twice weekly administrations of CCl_4 at 1.0 mL/kg for a period of 12 weeks to induce fibrosis in the male Sprague-Dawley rat. The authors found increased lipocalin-2 expression in liver tissue and immunohistochemistry revealed strong staining in the hepatocytes. Throughout the experiment, increased serum levels of lipocalin-2 were reported although they did not necessarily correlate with the degree of injury. The authors suggested that damaged hepatocytes were the main source of lipocalin-2 production. In our current study, lipocalin-2 levels were also measured in the urine, as an indicator of CCl_4-induced lesion. Urinary excretion of lipocalin-2 was increased in CCl_4-treated animals at weeks 3 to 6 during the dosing period and levels were maximal at week 6 when there was a 23-fold increase ($^{***}P<0.001$). Levels remained significantly increased over controls at most time points during the recovery period but the fold increases were much smaller. Increases in urinary lipocalin-2 were also reported by Smyth et al., (2009a) following CCl_4-induced fibrosis in a rat model. However, lipocalin-2 is more commonly used to assess kidney injury as discussed in Chapter 3 and 4.

TIMP-1 is produced by activated HSCs and Kupffer cells and has been suggested to be a serum marker of liver fibrosis (Herbst et al., 1997; Roderfeld et al., 2006; Wang et al.,

2011), whereas MCP1 is one of the most important chemotactic factors secreted by HSCs and has also been found to be up-regulated in experimental models of CCl_4-induced hepatotoxicity (Karlmark et al., 2009). In a study by Marsillach et al. (2009) liver fibrosis was induced in male Wistar rats using a model of twice weekly i.p. injections of 0.5 mL CCl_4 diluted 1:1 in olive oil for a period of 12 weeks. Animals were autopsied at 6, 8, 12, 13 and 14 weeks of the study (13 and 14 reflected 1 and 2 weeks of recovery). The authors reported a moderate increase in plasma MCP1 concentrations during the dosing period and a return to normal values during the recovery period.

AGP is an acute phase protein and is mainly secreted by hepatocytes and has been shown to increase following hepatic injury (Fournier et al., 2000). It has been proposed that following necrosis of the hepatic parenchymal cells, pro-inflammatory cytokines, such as IL-6 and TNF-α are released which could trigger the production of acute-phase proteins like AGP (Sugihara et al., 1992). AGP is responsible for regulating the inflammatory response, mainly by inhibiting platelet aggregation so as to reduce tissue damage caused by inflammatory cells (Costello et al., 1979; Janciauskiene, 2001).

A2M has been shown to bind and inactivate proteases from the metalloproteinase class including collagenases; collagenases are responsible for the degradation of collagen (Barrett and Starkey, 1973). Previous studies have shown a decrease in collagenase activity as liver fibrosis progresses (Montfort and Perez-Tamayo, 1978) and A2M is thought to play a major role in mediating this decreased activity and thus allowing the progression of fibrosis (Truden and Boros, 1988). Kawser et al. (1998) studied the role of A2M in fibrosis in male Sprague-Dawley rats dosed by i.p. injection with 0.2 mL/100 g body weight CCl_4 twice a week for 1 week (early fibrosis) and 4 weeks (established fibrosis). The group found an increase in A2M plasma levels in treated animals in both models of fibrosis, providing further evidence that A2M plays a role in the inhibition of collagenases during fibrogenesis (Kawser et al., 1998).

Having been able to characterise changes occurring to serum markers of hepatic fibrosis, we also aimed to investigate the changes in hepatic gene expression with the induction of injury, and with injury recovery. One of the mechanisms for CCl_4-induced toxicity is the generation of reactive oxygen species and free radicals which may cause oxidative stress to the cell. As discussed in Chapter 4, HMOX1, which encodes for heme oxygenase 1, plays a critical role in protecting against oxidative and inflammatory

stress (Gu et al., 2012). Therefore, it is not surprising that a statistically significant increase was seen in the hepatic expression of HMOX1 after 1 week of CCl_4 treatment, as a protective mechanism against CCl_4-induced oxidative stress (Table 7.9). In the present study, hepatic HMOX1 was upregulated compared to control animals at all time points during the dosing period, but by week 9 and 12 a downregulation was seen and at 12 weeks this was statistically significant. In a study by Chung et al., (2005b), Sprague-Dawley rats were injected with 0.5 mL/kg CCl_4, 3 times a week and killed at day 0, 30, 60 and 90. The authors reported an increase in HMOX1 expression compared to controls up to day 60, after which there was a decrease in hepatic expression, which may be a reflection of the severe degree of injury induced to the liver. In the present study, hepatic expression of HMOX1 was maximal at week 4, and decreased after this time point. Similarly, hepatic expression of NQO1 was also significantly upregulated compared to control animals after 3 administrations of CCl_4. The expression of NQO1 is induced by oxidative stress (Nioi and Hayes, 2004) and it encodes an enzyme which prevents the formation of reactive oxygen species (Ross, 2004; Vasiliou et al., 2006). The enzyme NAD(P)H dehydrogenase, quinone 1, has been found to be present in high concentrations in the rat liver (Sharkis and Swenson, 1989) and is considered a detoxification enzyme due to its ability to convert reactive quinones to less reactive hydroquinones which have antioxidant properties. The ability to scavenge $O_2^{-\cdot}$ has also been proposed for NQO1 and may account for the induction of this enzyme following oxidative stress (Siegel et al., 2004). In the study by Chung and co-workers (2005b) NQO1 expression was also upregulated up to day 60 and downregulated at day 90 in a model of rat hepatic fibrosis. Previous studies have also reported increases in NQO1 expression as detected after 8 weeks of CCl_4 subcutaneous injections twice a week at 0.3 mL/100 g of BW to male Sprague-Dawley rats (Wang et al., 2010b). In the present study, the expression of NQO1 mRNA was found to be upregulated to approximately 2.8-fold in CCl_4-treated animals over concurrent controls at week 5 during the dosing period (maximal gene expression) and after this time point NQO1 mRNA levels decreased. These results compare with the liver gene expression data from the dose-response study in Chapter 4, where a 1.7-fold upregulation was recorded for NQO1 in the liver after administration of HCBD at 5 mg/kg.

Hepatic expression of CYP1A2 and CYP2C was also determined at all time points in the study. CYP1A2 and CYP2C mRNA expression was significantly downregulated at week 1 and levels remained significantly downregulated during the dosing period, that

is, up to week 6. However, after this time point, CYP1A2 and CYP2C mRNA levels started to increase and appeared to return to control values. Several studies have focused on the effects of liver function in the levels of cytochromes, particularly of cytochrome P-450. This is because inhibition or induction of these enzymes is often seen in cases of drug interactions. CYP1A2 is predominantly a hepatic enzyme (Floreani et al., 2013). Floreani and colleagues (2013) reported a decrease in CYP1A2 mRNA following the induction of cirrhosis, and this decrease appeared to correlate with the severity of injury. Similar decreases in the levels of CYP1A2 were described by Bastien and co-workers in a rat model of CCl_4-induced cirrhosis. Decreases in the hepatic expression of CYP2C have also been reported in rat models of CCl_4-induced injury (Young et al., 2003). CYP1A2 has a protective role against the production of ROS and therefore, decreased expression of CYP1A2 might be deleterious (Nakai et al., 2008). Levels of CYP1A2 have also been found to be decreased in human samples of cirrhotic livers (Guengerich and Turvy, 1991).

In the category of inflammation, hepatic LCN2 expression was upregulated at all time points. Previous studies have shown that lipocalin-2 is expressed and released by the liver in response to inflammation (Liu and Nilsen-Hamilton, 1995; Flo et al., 2004). Kamphorst et al. (2011) reported increased hepatic expression of lipocalin-2 in the rat liver in a model of CCl_4-induced hepatic fibrosis and suggested the main source of lipocalin-2 production to be the damaged hepatocytes. In the present study, LCN2 mRNA expression was greatest at week 4 which coincided with peak levels of lipocalin-2 observed in the serum.

In the present study, it was observed that TIMP-1 mRNA was increased compared to control at all time points. It appeared to increase up to week 4, after which a decrease in hepatic expression was seen. Increases in TIMP-1 mRNA expression have been previously reported in chronic liver injury studies. Herbst and colleagues (1997) investigated TIMP expression in a chronic model of CCl_4-induced hepatic injury. Herbst injected rats with 1.0 mL/kg every 4 days for 3 weeks and sacrificed at 12, 24 or 48 hours after the last injection. This group found TIMP-1 expression to be upregulated in the fibrotic rat liver. Another study also demonstrated increased levels of TIMP mRNA in a rat model of CCl_4-induced hepatic fibrosis (Iredale et al., 1996). TIMPs are responsible for regulating the activity of MMPs which in turn are responsible for the degradation of extracellular matrix (Iredale et al., 1996). In hepatic fibrosis/cirrhosis

there is an accumulation of extracellular matrix which is caused by decreased MMP activity and increased TIMP activity. In the work carried out by Chung and co-workers (2005b) TIMP-1 was also reported to be upregulated in a rat model of CCl_4-induced fibrosis. The present study has been able to show a good degree of correlation between hepatic expression of TIMP-1 and serum levels. In fact, serum clinical chemistry also reported maximum levels of TIMP-1 after 4 weeks of CCl_4 treatment and similar fold increases were recorded for serum TIMP-1 and TIMP-1 expression at week 1 (3.4-fold and 4.3-fold respectively). The significant decrease seen in TIMP-1 levels at week 9 and 12 is consistent with the process of regeneration and repair of the liver. Significant decreases in TIMP-1 mRNA have been reported as early as 1 week following interruption of CCl_4 administration in models of CCl_4-induced fibrosis (Benyon and Iredale, 2000). The authors reported this decrease in TIMP-1 expression to coincide with a period of rapid collagen degradation and consequent liver regeneration. TIMP-1 appears to be particularly relevant to the inhibition of MMP-13 in the rat (Arthur et al., 1999). In the present study MMP-12 mRNA was significantly increased at all time points but at week 9 and 12 the fold increase was smaller. Similar results to those described in the present study were previously reported by Chung et al (2005b) and by Pellicoro and co-workers (2012a). MMP-12 is expressed by hepatic macrophages in the fibrotic liver and is responsible for the degradation of elastin. Pellicoro et al., (2012a) reported that elastin is expressed from the onset of injury, but unlike collagen I, elastin only accumulates in the late stages of fibrosis. The authors suggested, therefore, that during the initial phases of injury there is degradation of elastin by MMP-12. The authors reported an increase in MMP-12 expression with increasing duration of injury, however, the results also show that there was a concomitant increase in TIMP-1 expression and immunoprecipitation assays showed increased levels of TIMP-1 bound to MMP-12 in severe fibrosis.

COL1A1 and COL5A2 mRNA levels were found to be increased at all time points in the study, however fold increases during the recovery period were much smaller than those recorded during the dosing period. Collagens I and III are 2 of the main components of the extracellular matrix and the major components of these proteins are produced by COL1A1 and COL3A1 (Kanemoto et al., 2011). In a mouse model of CCl_4-induced liver fibrosis, COL1A1 expression was found to be increased after 4 weeks of treatment (Jiang et al., 2004). Another study has suggested that lipid peroxidation stimulates collagen gene transcription; lipid peroxidation is one of the

main features of CCl_4-induced hepatic injury. The authors were able to show the existence of a temporal relationship and co-localisation of lipid peroxidation and increased expression of COL1A1, following a single administration of CCl_4 but not with allyl alcohol. Administration of allyl alcohol induced extensive necrosis but there was no increase in COL1A1 (Bedossa et al., 1994). TGF-β1 hepatic expression levels were also measured throughout the study and were shown be upregulated at all time points, but similarly to COL1A1 and COL5A2, the fold increase decreased considerably during the recovery period. Increased expression of TGF-β1 has been previously reported following the administration of CCl_4 for 4 weeks to mice (Jiang et al., 2004). An investigation into the different cellular sources of TGF-β1 in the liver revealed that, in the normal liver, TGF-β1 was predominantly found in the Kupffer cells (De Bleser et al., 1997). However, in the fibrotic liver, it appears that TGF-β1 mRNA is increased selectively in HSCs, which are the main cells involved in the process of hepatic fibrosis. Indeed, it has been reported that TGF-β1 is particularly important to the response of HSCs to CCl_4. In addition, TGF-β1 has been shown to increase the expression of collagen and fibronectin which are components of the ECM at the same time as enhancing the production of TIMPs (Nakatsukasa et al., 1990). The upregulation of TGF-β1 expression observed during the dosing period in this study is consistent with the development of liver fibrosis as confirmed by histopathology, and appears to follow the same general trend of increased COL1A1, COL5A2 and TIMP-1 mRNA levels between week 1 and 6, with a decrease in expression during the recovery period.

In the present study, ACTA2 mRNA expression was upregulated at all time points, upregulation was maximal at week 5 and by week 9 and 12 there appeared to be a return to control levels. ACTA2 is found mainly in the smooth muscle but has also been reported to be expressed by myofibroblasts (Rockey et al., 2013). Repeated administration of CCl_4 to male Sprague Dawley rats has been shown to cause activation of HSCs into myofibroblast-like cells, with consequent upregulation of ACTA2 mRNA expression and development of fibrosis. Upregulation of ACTA2 in HSCs appears to be involved in the process of cell motility and contractility during the process of cellular activation into myofibroblasts (Rockey et al., 2013). Yang and co-workers also reported increases in ACTA2 mRNA levels in a mice model of CCl_4-induced fibrosis as detected by immunohistochemical analysis. The upregulation in ACTA2 expression reported in the present study constitutes further evidence of the role of ACTA2 in the process of myofibroblast activation associated with the development of hepatic fibrosis/cirrhosis.

Similarly, we suggest that the decrease in mRNA expression at weeks 9 and 12 is associated with the process of liver regeneration.

With this experiment we also wished to assess the potential to use US in a time course evaluation of CCl_4-induced liver changes, and to correlate this information with the data collected from histopathological examination of the livers collected at autopsy. Although histological assessment of the liver remains the gold-standard for the diagnosis of fibrosis, the limitations associated with the procedure compromise its use in clinical practice. US has the ability to detect alterations to the hepatic parenchyma due to moderate to severe liver fibrosis/cirrhosis (Hirata et al., 2001) and it is often the first imaging procedure in cases of suspected liver disease (Tchelepi et al., 2002). US is a non-invasive technique, inexpensive and has been proven to be an important tool in detecting hepatocellular carcinoma (Nishiura et al., 2005). Normally, the hepatic parenchyma is homogeneous with medium level echogenecity and equal or slightly more echogenic than the kidneys and its echogenic texture is interrupted by the portal and hepatic veins. A fibrotic/cirrhotic liver is characterised by heterogeneous patchy or diffuse echogenecity and this is related to the development of fatty liver and scar tissue (Tchelepi et al., 2002). Changes to the liver include changes in the size and shape of the liver, parenchymal nodularity and inhomogeneity, and changes to parenchymal echogenecity which may be increased compared to adjacent organs such as the kidneys (Tchelepi et al., 2002).

In the present study, scanning sessions were performed between weeks 3 and 6 during the dosing period, to assess the progression of injury, and at weeks 9 and 12 to evaluate the potential for recovery. To allow correlation of US images and histopathological data, the same animals were scanned 2 days before their scheduled autopsy.

At weeks 3, 4 and 5, i.e., after receiving 9, 12 and 15 doses of CCl_4, the livers from treated animals were hyperechoic compared to the kidneys and appeared to be enlarged in the longitudinal projection compared to livers from control rats. At week 6 there was evidence of fluid in the abdominal cavity (Figure 7.6 C) which was confirmed during the autopsies. By week 9 and 12 (3 and 6 weeks without treatment) US revealed the presence of some degree of recovery with the absence of fluid in the abdominal cavity, although livers were still hyperechoic and enlarged compared to control livers.

US has been used to evaluate the progression of CCl_4-induced injury in rat models. In a study by Lessa and colleagues (2010), CCl_4-induced cirrhosis was induced in female Wistar rats (0.05 mL/kg CCl_4 by i.p. injection 3 times a week on alternate days for 15 weeks). In this study, animals were examined at the beginning of the experiment and at weeks 4, 8 and 15. The authors reported an increase in liver echogenecity compared to the renal cortex and the presence of ascites in CCl_4-treated animals, there was also development of heterogeneous hepatic parenchyma associated with nodular liver surface which revealed good correlation with the diagnosis of cirrhosis by histopathological examination (Lessa et al., 2010). Dias et al., (2008) used a model of CCl_4-induced cirrhosis to evaluate the potential for reversibility. Female rats were dosed with 0.05 mL/kg CCl_4 3 times a week for a period of 15 weeks. At the end of the dosing period 6 animals were left to recover for 8 weeks. US analysis revealed increased liver echogenecity with heterogeneous hepatic parenchyma at week 15; however, after 8 weeks of recovery the same observations were reported. The presently described study provides further evidence of the potential for liver regeneration and repair in a model of CCl_4-induced injury. Also, we have been able to establish a good degree of correlation between US examination and the morphologic appearance of the livers collected at autopsy.

In this experiment, histopathological examination of the livers confirmed the development of hepatic fibrosis and thus further validated our model. Pathological findings were similar to those described in experiment 1. During the recovery period there was an improvement in the microscopic and gross appearance of the liver, similar to that described in experiment 1. Therefore, while full resolution of the injury did not occur, these results further confirm the reversibility of hepatic fibrosis in this particular model.

In 1991, Fischer and co-workers (1991) described the rat model of CCl_4-induced cirrhosis as irreversible. In the past, fibrosis was also considered to be an irreversible process which resulted from complete destruction of the hepatic parenchyma (Popper and Uenfriend, 1970). More recently, studies have focused on the possibility of reversibility of fibrosis (Benyon and Iredale, 2000; Bataller and Brenner, 2005; Pellicoro et al., 2012b). The discussion of the mechanisms associated with reversibility is ongoing, with some authors suggesting that either removal of HSCs or the reversal or HSCs activation may be necessary for recovery from fibrosis (Benyon and Iredale,

2000). Therefore, the present studies are particularly important to the current debate regarding the development of fibrotic lesion and in the understanding of the potential mechanisms involved in reversibility.

In all of our CCl_4 liver studies we are concerned about the potential for CCl_4 induced nephrotoxicity since the ultimate aim is to identify urinary markers of hepatotoxicity.

In Chapter 4, an investigation was carried out to compare the sensitivity of several urinary markers of kidney injury showed GST Yb1 and α-GST to be the most sensitive markers. These are enzymes which are present in the proximal and distal tubules and are involved in the detoxification process of many compounds (Lock and Reed, 1998; van Lieshout et al., 1998). In the present study, α-GST was significantly decrease compared to control animals at week 1 and 2, but by week 6 it was approximately 1.6-fold increased over controls (Table 7.7, Table 7.8). GST Yb1 was significantly increased over concurrent controls after 6 weeks of CCl_4 treatment (approximately 2-fold increase), and this increase was statistically significant ($^{*}P<0.05$). However, by the end of the first week of recovery (week 7) levels of both enzymes had returned to approximate control values. The fold-increases recorded in the present experiment 2 were, however, much smaller than the ones seen in the time course study in Chapter 4 using a model of HCBD-induced renal toxicity. At 24 hours post-dosing with HCBD, α-GST and GST Yb1 reached peak levels; α-GST was 356.9-fold increased over controls, whereas the fold increase for GST Yb1 was approximately 17-fold. It is important to note that α-GST is located in the hepatocytes and it has also been shown to be released into the blood following marked hepatocellular damage (van Wagensveld et al., 1997; Giffen et al., 2002). Therefore, the increase reported in the current study may be a consequence of the severe degree of injury induced by chronic administration of CCl_4 (Clarke et al., 1997).

Our previous study (Chapter 4) also showed evidence that supported the classification of KIM-1 and osteopontin as markers of both kidney injury and repair. In the currently described fibrotic model the first significant difference in urinary KIM-1 was seen at week 6 at which time point levels reached a peak ($^{*}P<0.05$). During the recovery period mean values slightly decreased compared to that at week 6, but were still increased compared to concurrent controls. Urinary osteopontin was significantly increased in CCl_4-treated animals at all time points during the dosing period and levels were

maximal at week 4. However, by week 7 (first week of recovery period) they were similar to controls.

Urinary levels of clusterin were measured in the urine of rats during the dosing and recovery period. In the present study, clusterin values were significantly decreased over controls at week 3 during the dosing period, and at weeks 8 and 12 during the period without CCl_4-treatment. In 1996 Hogasen and co-workers investigated the relationship between serum clusterin (apolipoprotein J) and decreased hepatic function in cirrhotic patients (Hogasen et al., 1996). The authors reported significantly decreased serum levels in hepatic cirrhosis, suggesting the liver is the main site for clusterin production. We therefore suggest, that the decreased urinary clusterin levels seen in the present study, may be a reflection of decreased clusterin production by the liver.

It should be noted that while some of these kidney biomarkers were increased during the course of this study, the fold difference over control was small and thus confirmation of absence of nephrotoxicity would be made by histopathological examination of the kidneys.

In this study, we found no evidence of an effect in the kidneys that could be attributed to CCl_4 administration. There was minimal vacuolation of the proximal tubular epithelium but this was also recorded in one control animal and therefore no clear association between CCl_4-treatment and the microscopic findings in the kidneys could be established. Therefore, we now had confidence in our hepatic fibrosis model and we could reliably investigate changes to the urinary metabolome during the development of fibrosis and subsequent recovery from the injury induced.

Initial investigation of the PCA scores plot in Figure 7.9 indicated the presence of differences between control animals and animals that received the CCl_4-treatment. However, the degree of cluster separation was compromised by the great number of samples included in the model. A trajectory plot representing the mean ^{1}H NMR urine spectra for control samples and for CCl_4-treated samples at all time points showed a move towards the right side of the plot with CCl_4 treatment with time up to week 5 (Figure 7.11). At week 6 there was a continuation of the trend towards the upper right quadrant, but it is not known why week 6 is located to the left of week 5. This movement to the upper quadrant is similar to what happens in the control samples with time, so it may be a reflection of age-related changes. The greatest change during the

dosing period occurs between week 2 and 3. Between week 6 and 9 there is a distinctive shift back to the left side of the scores plot, this is reflecting changes due to the recovery period. Further investigation of these metabolite changes using OPLS-DA models revealed that after receiving 3 doses of 0.4 mL/kg CCl_4 there was an increase in the resonances of taurine, 2-oxoglutarate, citrate, succinate and formate. Similar findings had been previously reported in the dose response study described in Chapter 3 after a single administration of CCl_4 at 2.0 mL/kg and in other single dose studies (Waterfield et al., 1993; Li et al., 2013; Zira et al., 2013).

Formate levels in the urine were increased at week 1 compared to control animals (Table 7.10). In our previous dose-response investigation (Chapter 3) and time course study (Chapter 6), formate levels were also found to be significantly increased over control animals at 24 hours following the administration of 2.0 mL/kg CCl_4. In the present study formate levels increased at week 4 and 5, but by the time the dosing period finished (week 6), levels were decreased compared to week 1 (Table 7.10). Formate urinary excretion further decreased at week 9 but by week 12 (6 weeks into the recovery period) levels increased again. Decreased urinary levels of formate have been described in the literature as consequence of CCl_4-induced decreased tetrahydrofolate which will result in decreased formate metabolism and subsequent increase in formate urinary excretion (Dow and Green, 2000).

Fatty liver is one of the most commonly seen features of liver cirrhosis. It may develop if there is a decrease in choline, an essential nutrient for phospholipids, which are needed for the elimination of triglycerides from the liver in the form of VLDLs. Choline synthesis requires a carbon from formate that has to be bound to tetrahydrofolate before it can be used (Corbin and Zeisel, 2012). The decrease in formate levels in the present study is further evidence that this may be one of the contributing causes for fatty liver.

Urinary hippurate excretion appeared to decrease with the induction of injury. At week 6, last week of the dosing period, hippurate levels were decreased compared to week 1, but after removal of the toxic agent levels appeared to increase; at week 9 urinary hippurate was increased compared to week 6, and at week 12 (6 weeks without treatment), levels were increased compared to week 9 (3 weeks without treatment) and week 6 (Table 7.10, Table 7.11). Similar results were described for hippurate levels in Chapter 3 and 6 with reported decreases in urinary excretion following a single administration of CCl_4. As described in Chapter 6, decreased hippurate happens as a

consequence of ATP depletion that occurs during the process of hepatic necrosis (Gatley and Sherratt, 1977; Kim et al., 2008a) and which is more severe during the process of liver fibrosis/cirrhosis. During the recovery period, there was an increase in hippurate levels and this suggests the existence of some degree of liver regeneration.

As previously discussed, taurine is synthesised in the liver and increased urinary excretion may result from hepatocyte leakage (Waterfield et al., 1993; Waterfield et al., 1998). Up to week 3, taurine levels appeared to increase consistently but this was followed by a reduction in urinary excretion in weeks 5 and 6 (Table 7.10). The decrease in urinary taurine has been previously described in mice with severe liver damage or cirrhosis (Warskulat et al., 2006). A reduction in the hepatic taurine concentration was also previously reported following the chronic administration of CCl_4 for 5 and 10 weeks in a rat model of fibrosis (Miyazaki et al., 2004; Miyazaki et al., 2005). This is the result of impaired liver function with reduced taurine synthesis in the liver and therefore a decrease in the levels of hepatic taurine, which is reflected by lower levels of urinary excretion.

Our study revealed that even though taurine levels appeared to have been decreasing in the urine of CCl_4-treared rats at weeks 5 and 6, at week 6 they were still increased over week 1 (Table 7.11). At week 9 (3 weeks without treatment), urinary taurine had increased compared to week 6 and this could reflect the initial stage of liver regeneration.

Therefore, this metabolomic study in experiment 2 has added further evidence that the urinary excretion of taurine correlates well with liver injury. Initial increases in urinary taurine levels appear to be a result of hepatocyte necrosis and release of cellular content (Waterfield et al., 1991). However, as the injury progresses less taurine is synthesised and taurine levels in urine appear to decrease as a result of impaired hepatic function. We have also been able to demonstrate, that during the recovery phase, when no further exposure to the toxic stimulus was present, taurine levels increased again. This suggests that hepatic function was returning to normal during the recovery phase but full resolution had not occurred.

Urinary excretion of TCA cycle intermediates such as 2-oxoglutarate, citrate and succinate were increased over controls after 1 week of CCl_4 treatment. Levels of 2-oxoglutarate and citrate were decreased at weeks 2 and 3 when compared to the

previous time point, but at week 4 a rise in urinary excretion was observed compared to at week 3. Urinary succinate on the other hand, was decreased from week 4 onwards. At week 6 levels were decreased compared to week 1 and after 6 weeks of recovery (week 12), urinary succinate excretion remained decreased compared to week 6. In a model of thioacetamide-induced liver fibrosis/cirrhosis in the rat, succinate was found to be increased in the aqueous liver extract as detected using ^{1}H NMR after 1 and 2 months of treatment; at later time points succinate levels decreased (Constantinou et al., 2007).

In a study by Gou et al. (2013) hepatic fibrosis was induced in rats by twice weekly i.p. injection of CCl_4 at 1.0 mL/kg 50% CCl_4 for 9 weeks. This study showed increased urinary levels of citrate. In our study, citrate levels were increased from previous time points from week 4 onwards. At week 9 (3 weeks without treatment) citrate was decreased compared to week 6, but levels appeared to increase with time without treatment, at week 12 (6 weeks recovery), citrate urinary excretion was increased compared to week 9 and week 6 (Table 7.11).

Several enzymes in the TCA cycle, such as α-ketoglutarate dehydrogenase and pyruvate dehydrogenase, have been shown to be inhibited by oxidative stress (Humphries and Szweda, 1998); oxidative stress is one of the major molecular mechanisms involved in CCl_4-induced injury (Humphries and Szweda, 1998). It has also been demonstrated that α-ketoglutarate dehydrogenase is able to produce H_2O_2 and could therefore be a source of ROS in the mitochondria (Tretter and Adam-Vizi, 2004). Inhibition of enzymes is due to modifications of lipoic acid residues bound to one of the subunits of the enzymes, and results in the slowing down of the TCA cycle as a feedback mechanism to reduce the production of free radicals (Humphries and Szweda, 1998). This, in turn, may result in increased levels of TCA cycle intermediates as they are not being used up in the cycle and consequently could be excreted in the urine. Other studies have also reported inhibition of the TCA cycle in a model of D-galactosamine-induced fulminant hepatic failure (Yokoyama et al., 2005). We suggest that this mechanism can be the reason for increased 2-oxoglutarate and citrate levels at week 6 compared to weeks 1 (Table 7.11).

The metabolite creatinine was also identified as a metabolite responsible for sample separation as determined by analysis of the S-plot and VIP plots (data not shown). After 6 weeks of CCl_4 treatment creatinine was increased compared to week 1, and it further increased at week 9. However, at the following time point (week 12; 6 weeks without

treatment), it appeared that creatinine levels decreased slightly but were still increased compared to urinary excretion at the end of the dosing period (week 6) (Table 7.10, Table 7.11). The NMR data for creatinine peaks and the creatinine assay data obtained from the clinical chemistry analysis (Table 7.7, Table 7.8) showed the same pattern of change. This is further evidence of the sensitivity of the NMR spectrometry in our experiments.

As previously discussed, creatinine is produced from creatine which in turn is synthesised in the liver. Therefore, a decreased liver functional capacity as a result of fibrosis/cirrhosis could be reflected by decreased levels of creatine and consequently of creatinine (Cocchetto et al., 1983; Ropero-Miller et al., 2000; Waters et al., 2005). In our study, creatine was found to be decreased in the urine at week 1 and 2 and at weeks 5 and 6, compared to earlier time points, and at week 6, creatine levels in the urine, as measured by ^{1}H NMR were decreased from week 1 (Table 7.10, Table 7.11). Levels of creatine appeared to be increased in the urine after 3 weeks without treatment (week 9 compared to week 6) and were decreased at week 12 compared to week 9 and 6.

Creatine is a by-product of cysteine synthesis in the liver. Cysteine is an amino acid that is necessary for the competitive synthesis of protein and taurine, therefore, changes in the amount of protein synthesis will affect the availability of hepatic cysteine for taurine synthesis. Increased hepatic cysteine availability would result in increased taurine synthesis and consequently, in increased urinary taurine levels, whereas decreased cysteine availability would result in decreased taurine synthesis (Clayton et al., 2003). When protein synthesis is inhibited, as in the case of hepatic impairment, cysteine is diverted and is used in the synthesis of taurine, resulting in hypertaurinuria. However, because there is excess hepatic cysteine there is no need for increased cysteine synthesis and therefore, there is no increased creatine production (Clayton et al., 2003). This may explain the hypertaurinuria without hypercreatinuria that is observed in the first 2 weeks of the study. In fact, both serum and urine clinical chemistry revealed a statistically significant decrease in total protein levels at both week 1 and 2 (Table 7.5, Table 7.7).

With the completion of the 2 experiments described in this study, we have successfully been able to develop an animal model of hepatic fibrosis in the male Hanover-Wistar rat. We have shown that following administration of CCl_4, 3 times a week, for a period of 6 weeks our rat model displays most of the main characteristics of fibrosis seen in humans. After 3 and 6 weeks without treatment, there was evidence of histopathological

regeneration and the histological features of fibrosis showed some degree of recovery even if complete reversibility to a morphologically normal liver was not observed.

There is very limited data regarding changes to urinary metabolites in rat models of CCl_4-induced fibrosis during the period of injury progression and regeneration using ^1H NMR-based metabolomics approach. We suggest that metabolites such as creatinine, citrate and succinate are likely to be better markers of the initial stages of injury, as they significantly changed in the urine at week 1. Citrate and succinate, however, did not show a statistically significant difference at week 9 compared to week 6, further confirming the potential to be early injury markers.

We have shown that after 3 weeks without treatment there was a significant change in the general metabolite profile of urine samples. Hippurate levels showed a decreasing trend during the dosing period, but at week 9, urinary excretion significantly increased and was further increased at week 12, and this appeared to correlate well with both clinical chemistry and histopathology data showing signs of injury recovery. Similarly, we have further established taurine as a marker of liver toxicity and have contributed to the knowledge of the role of urinary taurine in liver fibrosis/cirrhosis. By the end of the dosing period taurine levels were increased over controls, but after CCl_4 administration was stopped, urinary taurine levels decreased. We therefore suggest that urinary levels of hippurate and taurine may also serve as good indicators of regeneration.

Furthermore, this study provides an extensive characterisation of serum and urinary markers, as well as a detailed investigation into the gene expression changes occurring in the liver as a result of repeated CCl_4-administration to the male Hanover-Wistar rat. We were able to assess the progression and regeneration of injury as revealed by biomarkers levels, and to correlate this information with data from US and histopathological examination.

It is relevant to mention that although metabolomic-based investigations are mostly applied to rodent models of liver disease, there are reports in the literature of metabolomics investigations, that appear to parallel the findings described for the rat, in particular the elevation in taurine and 2-oxoglutarate levels seen in models of liver fibrosis/cirrhosis (Gao et al., 2009). Indeed, the metabolites described here are involved in metabolic pathways that are not exclusive to the rat and can also be found in humans. This adds further importance to the results described in the present study in which we

have demonstrated the potential for taurine as a marker of progression of fibrosis and for regeneration from injury.

CHAPTER EIGHT

Conclusion

This project was concerned with the development of models of CCl_4-induced acute injury and hepatic fibrosis in the male Hanover-Wistar rat. CCl_4 was the chosen hepatotoxicant since it has been widely used in rat models for liver injury (Brattin et al., 1984). Extensive 1D ^{1}H NMR-based metabolomics investigations were carried out to determine changes in urinary levels of metabolites with acute and chronic hepatic injury. Urine was chosen as the preferred biofluid since it can be obtained using non-invasive methods.

We began this series of investigations by performing a dose response study examining for possible extra-hepatic sites of CCl_4-induced damage. CCl_4 may cause injury to other organs, particularly the kidneys at high dose levels (Ozturk et al., 2003; Makni et al., 2012). In Chapter 3 we defined the ideal dose level of CCl_4 for the induction of hepatotoxicity to be 2.0 mL/kg. Above this dose level results from serum and urine clinical chemistry as well as histopathological examination of kidney tissue samples revealed evidence of nephrotoxicity consistent with CCl_4 administration. Therefore, in subsequent CCl_4 studies, we kept the dose level administered to the rat below this threshold value.

Since we were interested in urinary biomarkers of hepatic toxicity kidney function was of great concern. Any CCl_4-induced nephrotoxicity could make interpretation of urinary biomarker levels difficult. Therefore, the possibility of renal damage was consistently evaluated in all our CCl_4 liver studies. In Chapter 4 we used a rat model of HCBD-induced nephrotoxicity to evaluate a group of biomarkers recently approved by the FDA for voluntary inclusion in investigational and regulatory studies, which included KIM-1, albumin, clusterin and total protein. These markers were compared for sensitivity in a dose response study and also to determine their response to injury with time from an initial insult in a time course study. It was determined that, of the markers studies, α-GST, KIM-1 and albumin were the most sensitive biomarkers of proximal tubular injury showing significant differences compared to control animals at the lowest dose levels and with greater fold changes. Therefore, we decided that these sensitive markers would be useful to measure in our CCl_4 liver studies alongside histopathological evaluation of kidney tissue samples to rule out CCl_4-induced nephrotoxicity.

One of our concerns for the chronic hepatic fibrosis study was that as the animals age and reach sexual maturity this may have an effect on the degree of CCl_4-induced injury as well as on the levels of urinary metabolites. For this reason, a series of animal

experiments were devised in Chapter 5, in which samples were collected between 3 and 13 weeks of age. The results from these experiments revealed a dramatic increase in urinary testosterone levels between 54 and 68 days of age. This time point corresponded to the histological findings that suggested animals were both sexually mature and fully fertile at 63 days old. Interestingly, our experiment also revealed that urinary levels of α-GST, GST Yb1 and total protein followed the same pattern as testosterone. Age-related differences in urinary protein levels in the rat have been extensively studied in the literature (Sellers et al., 1950; Neuhaus and Flory, 1978; Owen and Heywood, 1986; Williams et al., 2005) and there is undergoing investigation regarding the relationship between the urinary protein profile and the levels of testosterone in the urine of the male rat (Vettorazzi et al., 2013). The results from our investigations add further evidence to the proposed existence of a relationship between testosterone levels and proteinuria and greatly contribute to the ongoing debate. However, the mechanism behind sexual maturity and increased urinary protein is yet to be fully explained.

1D ^{1}H NMR combined with PCA/OPLS analysis of the urine samples collected at different ages, also revealed significant differences to the concentration of urinary metabolites. There was a general trend of a dramatic increase in urinary levels of many metabolites at 84 days followed by a decrease at 91 days. Metabolites which followed this pattern included creatinine, creatine, taurine, 2-oxoglutarate, citrate and succinate. This proved that the urinary metabolites were affected by the male sexual maturation process.

Our comparative study of CCl_4-induced toxicity in pre- and post-sexually mature animals (7 and 13 weeks old respectively) revealed no significant differences in the severity of liver damage as confirmed by histopathological examination. However, it appeared from ^{1}H NMR analysis of urine samples that older animals excreted greater levels of creatinine, hippurate, creatine and taurine in the urine, and lower quantities of 2-oxoglutarate, citrate and succinate compared to 7 week old rats. We hypothesise that the change observed in urinary testosterone may be related to the changes in urinary metabolites; however, confirmation of this observation requires further investigation. Since the peak in testosterone levels appears to decline after the animals reach sexual maturity it is thought that any changes to the metabolites may be temporary.

In Chapter 6 we investigated the time course at which injury and subsequent recovery occurs following a single dose of CCl_4. As early as 6 hours post-dosing there were

significant increases in serum markers including AST, GLDH, TIMP-1 and MCP1. In general, there was an increasing trend in serum levels with time reflecting the progression of injury and reaching maximum levels at 24 to 48 hours post-dosing. By 96 hours (i.e. day 4 post-dosing) it appeared that serum levels had returned to baseline values. The pattern observed in the serum chemistry analysis was confirmed by histopathological examination revealing maximal severity at 24-48 hours, and a return to normal by day 10.

^{1}H NMR analysis of urine samples in this study contributed further to our knowledge of the metabolite changes seen at 24 hours post-dosing as described in Chapter 3. Taurine, citrate, 2-oxoglutarate and hippurate were considered the most sensitive urinary markers and all showed a general change in the first 18-24 hours followed by an opposing change in urinary levels during the liver regeneration phase.

Using the information collected from our acute liver injury model generated in Chapter 3 we developed a model of CCl_4-induced fibrosis in the rat in Chapter 7. Our model involved the administration of 0.4 ml/kg CCl_4, 3 times a week for 6 weeks. We included a 6 week period without treatment at the end of the dosing period to evaluate the potential of reversibility of the lesion.

The pathological changes observed in this model reflect many of the most frequently seen complications of fibrosis and cirrhosis in humans, such as ascites and splenomegaly (Gusberg et al., 1994; Kashani et al., 2008).

Using this hepatic fibrosis model we conducted a detailed investigation into serum markers and gene expression changes during both the dosing period and subsequent recovery. Serum ALT, AST and GLDH showed a similar profile, with increasing levels up to week 3-4 followed by a decrease and a tendency to return to control levels by week 12 (i.e. after 6 weeks without treatment). The same pattern was evident in the serum concentrations of other markers including lipocalin-2, TIMP-1 and MCP1. Histopathological examination showed progression of injury from week 1 to week 6 with the presence of fibrous tissue structures reflecting the formation of septae. During the recovery period, it was observed that the fibrous septae were narrower than at week 6, thus possibly indicating some degree of reversibility.

Urinary metabolites were analysed in the urine samples collected at relevant time points during the study by ^{1}H NMR. Taurine levels were increased following chronic injury therefore suggesting this metabolite could be a useful marker of both acute and chronic liver damage. Interestingly, the urinary excretion of taurine appeared to correlate with histopathological evidence of regeneration at weeks 9 and 12, with an increase in urinary levels compared to previous time points. However, urinary metabolites including creatinine, citrate and succinate appeared to be more sensitive to the initial stages of injury. The urinary excretion of these metabolites changed in comparison to control animals as early as 1 week of CCl_4 treatment but a reverse change occurred at week 6 of the dosing period. On the other hand, hippurate levels showed a decreasing trend during the dosing period, which was followed by an increase during the reversibility period, therefore appearing to correlate with the process of hepatic regeneration. This also suggests hippurate could be a sensitive marker for injury and subsequent recovery.

In these studies, we developed and characterised models of both acute and chronic CCl_4-induced hepatotoxicity in the male Hanover-Wistar rat. We were able to determine changes to urinary metabolite levels at 24 hours following a single dose of CCl_4, and to investigate the profile of urinary metabolites in a time course study up to day 10 post-dosing. Similar metabolites were changed in the hepatic fibrosis model and thus we were able to correlate changes to the urinary concentration during induction of fibrosis and subsequent recovery.

During our 1D ^{1}H NMR investigations many chemical shifts were revealed to be relevant for cluster separation, however, it was not possible to identify or quantify all of the metabolites in the time frame of this project. We suggest that future work may involve the use of two-dimensional (2D) NMR methods such as 2D ^{1}H NMR *J*-resolved (JRES) NMR spectroscopy which has the ability to increase peak dispersion compared to a 1D NMR spectrum, and therefore facilitates spectral assignments and quantification. Alternatively, we propose the use of LC-MS for urinary metabolite identification. Some of these metabolites may prove to be very sensitive and specific markers for hepatic injury.

CHAPTER NINE

References

AARDEMA, M. J. & MACGREGOR, J. T. (2002) Toxicology and genetic toxicology in the new era of "toxicogenomics": impact of "-omics" technologies. *Mutat Res,* 499**,** 13-25.

ABRAHAM, P., WILFRED, G. & CATHRINE (1999) Oxidative damage to the lipids and proteins pf the lungs, testis and kidney of rats during carbon tetrachloride intoxication. *Clin Chim Acta,* 289**,** 177-9.

ADAMS, L. A. (2011) Biomarkers of liver fibrosis. *J Gastroenterol Hepatol,* 26**,** 802-9.

ADIELS, M., OLOFSSON, S. O., TASKINEN, M. R. & BOREN, J. (2008) Overproduction of very low-density lipoproteins is the hallmark of the dyslipidemia in the metabolic syndrome. *Arterioscler Thromb Vasc Biol,* 28**,** 1225-36.

ALREFAI, W. A. & GILL, R. K. (2007) Bile acid transporters: structure, function, regulation and pathophysiological implications. *Pharm Res,* 24**,** 1803-23.

ALVARO, D., BENEDETTI, A., MARUCCI, L., DELLE MONACHE, M., MONTERUBBIANESI, R., DI COSIMO, E., PEREGO, L., MACARRI, G., GLASER, S., LE SAGE, G. & ALPINI, G. (2000) The function of alkaline phosphatase in the liver: regulation of intrahepatic biliary epithelium secretory activities in the rat. *Hepatology,* 32**,** 174-84.

AMARAPURKAR, P. D. & AMARAPURKAR, D. N. (2011) Management of coagulopathy in patients with decompensated liver cirrhosis. *Int J Hepatol,* 2011**,** 695470.

ARCHER, I. V. J. (1997) Epoxide hydrolases as asymmetric catalysts. *Tetrahedron,* 53**,** 15617-15662.

ARGUTUS (2010) Argutus AKI Test (rat) Assay kit. MSD toxicology assays.

ARIOSTO, F., RIGGIO, O., CANTAFORA, A., COLUCCI, S., GAUDIO, E., MECHELLI, C., MERLI, M., SERI, S. & CAPOCACCIA, L. (1989) Carbon tetrachloride-induced experimental cirrhosis in the rat: a reappraisal of the model. *Eur Surg Res,* 21**,** 280-6.

ARMSTRONG, R. N. (1997) Structure, catalytic mechanism, and evolution of the glutathione transferases. *Chem Res Toxicol,* 10**,** 2-18.

ARREDONDO, J., CHERNYAVSKY, A. I., KARAOUNI, A. & GRANDO, S. A. (2005) Novel mechanisms of target cell death and survival and of therapeutic action of IVIg in Pemphigus. *Am J Pathol,* 167**,** 1531-44.

ARTHUR, M. J., IREDALE, J. P. & MANN, D. A. (1999) Tissue inhibitors of metalloproteinases: role in liver fibrosis and alcoholic liver disease. *Alcohol Clin Exp Res,* 23**,** 940-3.

ASHALATHA, P. & DEEPA, G. (2011) *Textbook of anatomy and physiology for nurses,* Third edition, Jaypee Brothers Medical Publishers.978-93-5025-423-3

ASPLIN, J. R., ARSENAULT, D., PARKS, J. H., COE, F. L. & HOYER, J. R. (1998) Contribution of human uropontin to inhibition of calcium oxalate crystallization. *Kidney Int,* 53**,** 194-9.

ASTOR, B. C., KOTTGEN, A., HWANG, S. J., BHAVSAR, N., FOX, C. S. & CORESH, J. (2011) Trefoil factor 3 predicts incident chronic kidney disease: a case-control study nested within the Atherosclerosis Risk in Communities (ARIC) study. *Am J Nephrol,* 34**,** 291-7.

ATKINSON, J. C., W. DEGRUTTOLA, V. DEMETS, D. DOWNING, G. HOTH, D. OATES, J. PECK, C. SCHOOLEY, R. SPILKER, B. WOODCOCK, J. & ZEGER, S. (2001) Biomarkers and surrogate endpoints: preferred definitions and conceptual framework. *Clin Pharmacol Ther,* 69**,** 89-95.

BAGCHI, D., BAGCHI, M., HASSOUN, E. & STOHS, S. J. (1993) Carbon-tetrachloride-induced urinary excretion of formaldehyde, malondialdehyde, acetaldehyde and acetone in rats. *Pharmacology,* 47**,** 209-16.

BALCI, M. (2005) *Basic 1H- and 13C-NMR spectroscopy,* First edition, Elsevier.0-444-51811-8

BANOUB, J. & LIMBACH, P. (2010) *Mass spectrometry of nucleosides and nucleic acids,* First edition, Taylr & Francis Group.978-1-4200-4402-7

BARANOVA, A., LAL, P., BIRERDINC, A. & YOUNOSSI, Z. M. (2011) Non-invasive markers for hepatic fibrosis. *BMC Gastroenterol,* 11**,** 91.

BARRETT, A. J. & STARKEY, P. M. (1973) The interaction of alpha 2-macroglobulin with proteinases. Characteristics and specificity of the reaction, and a hypothesis concerning its molecular mechanism. *Biochem J,* 133**,** 709-24.

BASSIL, N., ALKAADE, S. & MORLEY, J. E. (2009) The benefits and risks of testosterone replacement therapy: a review. *Ther Clin Risk Manag,* 5**,** 427-48.

BATALLER, R. & BRENNER, D. A. (2005) Liver fibrosis. *J Clin Invest,* 115**,** 209-18.

BECKONERT, O., KEUN, H. C., EBBELS, T. M., BUNDY, J., HOLMES, E., LINDON, J. C. & NICHOLSON, J. K. (2007) Metabolic profiling, metabolomic and metabonomic procedures for NMR spectroscopy of urine, plasma, serum and tissue extracts. *Nat Protoc,* 2**,** 2692-703.

BECKWITH-HALL, B. M., NICHOLSON, J. K., NICHOLLS, A. W., FOXALL, P. J., LINDON, J. C., CONNOR, S. C., ABDI, M., CONNELLY, J. & HOLMES, E. (1998) Nuclear magnetic resonance spectroscopic and principal components analysis investigations into biochemical effects of three model hepatotoxins. *Chem Res Toxicol,* 11**,** 260-72.

BEDOSSA, P. & CARRAT, F. (2009) Liver biopsy: the best, not the gold standard. *J Hepatol,* 50**,** 1-3.

BEDOSSA, P., DARGERE, D. & PARADIS, V. (2003) Sampling variability of liver fibrosis in chronic hepatitis C. *Hepatology,* 38**,** 1449-57.

BEDOSSA, P., HOUGLUM, K., TRAUTWEIN, C., HOLSTEGE, A. & CHOJKIER, M. (1994) Stimulation of collagen alpha 1(I) gene expression is associated with lipid peroxidation in hepatocellular injury: a link to tissue fibrosis? *Hepatology,* 19**,** 1262-71.

BEGER, R. D., SUN, J. & SCHNACKENBERG, L. K. (2010) Metabolomics approaches for discovering biomarkers of drug-induced hepatotoxicity and nephrotoxicity. *Toxicol Appl Pharmacol,* 243**,** 154-66.

BELINSKY, S. A., POPP, J. A., KAUFFMAN, F. C. & THURMAN, R. G. (1984) Trypan blue uptake as a new method to investigate hepatotoxicity in periportal and pericentral regions of the liver lobule: studies with allyl alcohol in the perfused liver. *J Pharmacol Exp Ther,* 230**,** 755-60.

BELL, J. D., SADLER, P. J., MORRIS, V. C. & LEVANDER, O. A. (1991) Effect of aging and diet on proton NMR spectra of rat urine. *Magn Reson Med,* 17**,** 414-22.

BENYON, R. C. & ARTHUR, M. J. (2001) Extracellular matrix degradation and the role of hepatic stellate cells. *Semin Liver Dis,* 21**,** 373-84.

BENYON, R. C. & IREDALE, J. P. (2000) Is liver fibrosis reversible? *Gut,* 46**,** 443-6.

BERGMEYER, H. U., HORDER, M. & REJ, R. (1986a) International Federation of Clinical Chemistry (IFCC) Scientific Committee, Analytical Section: approved recommendation (1985) on IFCC methods for the measurement of catalytic concentration of enzymes. Part 3. IFCC method for alanine aminotransferase (L-alanine: 2-oxoglutarate aminotransferase, EC 2.6.1.2). *J Clin Chem Clin Biochem,* 24**,** 481-95.

BERGMEYER, H. U., HORDER, M. & REJ, R. (1986b). International Federation of Clinical Chemistry (IFCC) Scientific Committee, Analytical Section: approved recommendation (1985) on IFCC methods for the measurement of catalytic concentration of enzymes. Part 2. IFCC method for aspartate aminotransferase (L-aspartate: 2-oxoglutarate aminotransferase, EC 2.6.1.1). *J Clin Chem Clin Biochem,* 24**,** 497-510.

BERNDT, W. O. & MEHENDALE, H. M. (1979) Effects of hexachlorobutadiene (HCBD) on renal function and renal organic ion transport in the rat. *Toxicology,* 14**,** 55-65.

BETROSIAN, A. P., AGARWAL, B. & DOUZINAS, E. E. (2007) Acute renal dysfunction in liver diseases. *World J Gastroenterol,* 13**,** 5552-9.

BHUNCHET, E. & WAKE, K. (1998) The portal lobule in rat liver fibrosis: a re-evaluation of the liver unit. *Hepatology,* 27**,** 481-7.

BIRNBAUM, L. S. (1991) Pharmacokinetic basis of age-related changes in sensitivity to toxicants. *Annu Rev Pharmacol Toxicol,* 31**,** 101-28.

BIRNER, G., WERNER, M., OTT, M. M. & DEKANT, W. (1995) Sex differences in hexachlorobutadiene biotransformation and nephrotoxicity. *Toxicol Appl Pharmacol,* 132**,** 203-12.

BIRNER, G., WERNER, M., ROSNER, E., MEHLER, C. & DEKANT, W. (1998) Biotransformation, excretion, and nephrotoxicity of the hexachlorobutadiene metabolite

(E)-N-acetyl-S-(1,2,3,4, 4-pentachlorobutadienyl)-L-cysteine sulfoxide. *Chem Res Toxicol,* 11**,** 750-7.

BISHOP, J. H., GREEN, R. & THOMAS, S. (1978) Effects of glucose on water and sodium reabsorption in the proximal convoluted tubule of rat kidney. *J Physiol,* 275**,** 481-93.

BLOUIN, A., BOLENDER, R. P. & WEIBEL, E. R. (1977) Distribution of organelles and membranes between hepatocytes and nonhepatocytes in the rat liver parenchyma. A stereological study. *J Cell Biol,* 72**,** 441-55.

BODE, D. C., PAGANI, E. D., CUMISKEY, W. R., VON ROEMELING, R., HAMEL, L. & SILVER, P. J. (2000) Comparison of urinary desmosine excretion in patients with chronic obstructive pulmonary disease or cystic fibrosis. *Pulm Pharmacol Ther,* 13**,** 175-80.

BOEKELHEIDE, K. & SCHUPPE-KOISTINEN, I. (2012) SOT/EUROTOX debate: biomarkers from blood and urine will replace traditional histopathological evaluation to determine adverse responses. *Toxicol Sci,* 129**,** 249-55.

BOLATI, D., SHIMIZU, H., YISIREYILI, M., NISHIJIMA, F. & NIWA, T. (2013) Indoxyl sulfate, a uremic toxin, downregulates renal expression of Nrf2 through activation of NF-kappaB. *BMC Nephrol,* 14**,** 56.

BOLIGNANO, D., LACQUANITI, A., COPPOLINO, G., DONATO, V., CAMPO, S., FAZIO, M. R., NICOCIA, G. & BUEMI, M. (2009) Neutrophil gelatinase-associated lipocalin (NGAL) and progression of chronic kidney disease. *Clin J Am Soc Nephrol,* 4**,** 337-44.

BOLISETTY, S. & AGARWAL, A. (2011) Urine albumin as a biomarker in acute kidney injury. *Am J Physiol Renal Physiol,* 300**,** F626-7.

BOLL, M., WEBER, L. W., BECKER, E. & STAMPFL, A. (2001) Hepatocyte damage induced by carbon tetrachloride: inhibited lipoprotein secretion and changed lipoprotein composition. *Z Naturforsch C,* 56**,** 283-90.

BOLLARD, M. E., STANLEY, E. G., LINDON, J. C., NICHOLSON, J. K. & HOLMES, E. (2005) NMR-based metabonomic approaches for evaluating physiological influences on biofluid composition. *NMR Biomed,* 18**,** 143-62.

BONVENTRE, J. V., VAIDYA, V. S., SCHMOUDER, R., FEIG, P. & DIETERLE, F. (2010) Next-generation biomarkers for detecting kidney toxicity. *Nat Biotechnol,* 28**,** 436-40.

BORKHAM-KAMPHORST, E., DREWS, F. & WEISKIRCHEN, R. (2011) Induction of lipocalin-2 expression in acute and chronic experimental liver injury moderated by pro-inflammatory cytokines interleukin-1beta through nuclear factor-kappaB activation. *Liver Int,* 31**,** 656-65.

BORKHAM-KAMPHORST, E., VAN DE LEUR, E., ZIMMERMANN, H. W., KARLMARK, K. R., TIHAA, L., HAAS, U., TACKE, F., BERGER, T., MAK, T. W. & WEISKIRCHEN, R. (2013) Protective effects of lipocalin-2 (LCN2) in acute liver

injury suggest a novel function in liver homeostasis. *Biochim Biophys Acta,* 1832**,** 660-73.

BOUTHILLIER, L., GRESELIN, E., BRODEUR, J., VIAU, C. & CHARBONNEAU, M. (1991) Male rat specific nephrotoxicity resulting from subchronic administration of hexachlorobenzene. *Toxicology and Applied Pharmacology,* 110**,** 315-326.

BOYD, M. R., STATHAM, C. N. & LONGO, N. S. (1980) The pulmonary clara cell as a target for toxic chemicals requiring metabolic activation; studies with carbon tetrachloride. *J Pharmacol Exp Ther,* 212**,** 109-14.

BRANTON, M. H. & KOPP, J. B. (1999) TGF-beta and fibrosis. *Microbes Infect,* 1**,** 1349-65.

BRATTIN, W. J., GLENDE, E. A., JR. & RECKNAGEL, R. O. (1985) Pathological mechanisms in carbon tetrachloride hepatotoxicity. *J Free Radic Biol Med,* 1**,** 27-38.

BRATTIN, W. J., PENCIL, S. D., WALLER, R. L., GLENDE, E. A., JR. & RECKNAGEL, R. O. (1984) Assessment of the role of calcium ion in halocarbon hepatotoxicity. *Environ Health Perspect,* 57**,** 321-3.

BREW, K., DINAKARPANDIAN, D. & NAGASE, H. (2000) Tissue inhibitors of metalloproteinases: evolution, structure and function. *Biochim Biophys Acta,* 1477**,** 267-83.

BRIDGES, J. W., BENFORD, D. J. & HUBBARD, S. A. (1983) Mechanisms of toxic injury. *Ann N Y Acad Sci,* 407**,** 42-63.

BROWN, W., FOOTE, C., IVERSON, B. & ANSLYN, E. (2012) *Organic Chemistry,* Sixth edition, Brookes / Cole.13-978-0-8400-5498-2

BRUCKNER, J. V., MACKENZIE, W. F., MURALIDHARA, S., LUTHRA, R., KYLE, G. M. & ACOSTA, D. (1986) Oral toxicity of carbon tetrachloride: acute, subacute, and subchronic studies in rats. *Fundam Appl Toxicol,* 6**,** 16-34.

BRUNING, T., SUNDBERG, A. G., BIRNER, G., LAMMERT, M., BOLT, H. M., APPELKVIST, E. L., NILSSON, R. & DALLNER, G. (1999) Glutathione transferase alpha as a marker for tubular damage after trichloroethylene exposure. *Arch Toxicol,* 73**,** 246-54.

BULACIO, R. P. & TORRES, A. M. (2013) Organic anion transporter 5 (Oat5) renal expression and urinary excretion in rats treated with cisplatin: a potential biomarker of cisplatin-induced nephrotoxicity. *Arch Toxicol,* 87**,** 1953-62.

BURK, R. F., LANE, J. M. & PATEL, K. (1984) Relationship of oxygen and glutathione in protection against carbon tetrachloride-induced hepatic microsomal lipid peroxidation and covalent binding in the rat. Rationale for the use of hyperbaric oxygen to treat carbon tetrachloride ingestion. *J Clin Invest,* 74**,** 1996-2001.

BURKE, T. J., ARNOLD, P. E., GORDON, J. A., BULGER, R. E., DOBYAN, D. C. & SCHRIER, R. W. (1984) Protective effect of intrarenal calcium membrane blockers before or after renal ischemia. Functional, morphological, and mitochondrial studies. *J Clin Invest,* 74**,** 1830-41.

CABALLERO, M. E., BERLANGA, J., RAMIREZ, D., LOPEZ-SAURA, P., GOZALEZ, R., FLOYD, D. N., MARCHBANK, T. & PLAYFORD, R. J. (2001) Epidermal growth factor reduces multiorgan failure induced by thioacetamide. *Gut,* 48**,** 34-40.

CAMPION, S. N., CARVALLO, F. R., CHAPIN, R. E., NOWLAND, W. S., BEAUCHAMP, D., JAMON, R., KOITZ, R., WINTON, T. R., CAPPON, G. D. & HURTT, M. E. (2013) Comparative assessment of the timing of sexual maturation in male Wistar Han and Sprague-Dawley rats. *Reprod Toxicol,* 38**,** 16-24.

CAMPO, G. M., SQUADRITO, F., CECCARELLI, S., CALO, M., AVENOSO, A., CAMPO, S., SQUADRITO, G. & ALTAVILLA, D. (2001) Reduction of carbon tetrachloride-induced rat liver injury by IRFI 042, a novel dual vitamin E-like antioxidant. *Free Radic Res,* 34**,** 379-93.

CANNAS, A., CALVO, L., CHIACCHIO, T., CUZZI, G., VANINI, V., LAURIA, F. N., PUCCI, L., GIRARDI, E. & GOLETTI, D. (2010) IP-10 detection in urine is associated with lung diseases. *BMC Infect Dis,* 10**,** 333.

CARAKOSTAS, M. C., GOSSETT, K. A., CHURCH, G. E. & CLEGHORN, B. L. (1986) Evaluating toxin-induced hepatic injury in rats by laboratory results and discriminant analysis. *Vet Pathol,* 23**,** 264-9.

CAREY, E. & CAREY, W. D. (2010) Non-invasive tests for liver disease, fibrosis, and cirrhosis: Is liver biopsy obsolete? *Cleve Clin J Med,* 77**,** 519-27.

CAROTTI, S., MORINI, S., CORRADINI, S. G., BURZA, M. A., MOLINARO, A., CARPINO, G., MERLI, M., DE SANTIS, A., MUDA, A. O., ROSSI, M., ATTILI, A. F. & GAUDIO, E. (2008) Glial fibrillary acidic protein as an early marker of hepatic stellate cell activation in chronic and posttransplant recurrent hepatitis C. *Liver Transpl,* 14**,** 806-14.

CARPINO, G., MORINI, S., GINANNI CORRADINI, S., FRANCHITTO, A., MERLI, M., SICILIANO, M., GENTILI, F., ONETTI MUDA, A., BERLOCO, P., ROSSI, M., ATTILI, A. F. & GAUDIO, E. (2005) Alpha-SMA expression in hepatic stellate cells and quantitative analysis of hepatic fibrosis in cirrhosis and in recurrent chronic hepatitis after liver transplantation. *Dig Liver Dis,* 37**,** 349-56.

CASTERA, L. (2011) Non-invasive assessment of liver fibrosis in chronic hepatitis C. *Hepatol Int,* 5**,** 625-34.

CASTILLA-CORTAZAR, I., GARCIA, M., MUGUERZA, B., QUIROGA, J., PEREZ, R., SANTIDRIAN, S. & PRIETO, J. (1997) Hepatoprotective effects of insulin-like growth factor I in rats with carbon tetrachloride-induced cirrhosis. *Gastroenterology,* 113**,** 1682-91.

CHEN, H., HARDY, M. P., HUHTANIEMI, I. & ZIRKIN, B. R. (1994) Age-related decreased Leydig cell testosterone production in the brown Norway rat. *J Androl,* 15**,** 551-7.

CHEN, Q., YU, K. & STEVENS, J. L. (1992) Regulation of the cellular stress response by reactive electrophiles. The role of covalent binding and cellular thiols in

transcriptional activation of the 70-kilodalton heat shock protein gene by nephrotoxic cysteine conjugates. *J Biol Chem,* 267**,** 24322-7.

CHEN, W. J., CHI, E. Y. & SMUCKLER, E. A. (1977) Carbon tetrachloride-induced changes in mixed function oxidases and microsomal cytochromes in the rat lung. *Lab Invest,* 36**,** 388-94.

CHESNEY, R. W. (1985) Taurine: its biological role and clinical implications. *Adv Pediatr,* 32**,** 1-42.

CHIDA, K. & TAGUCHI, M. (2011) Localization of alkaline phosphatase and cathepsin D during cell restoration after colchicine treatment in primary cultures of fetal rat hepatocytes. *Acta Histochem Cytochem,* 44**,** 155-8.

CHIUSOLO, A., DEFAZIO, R., ZANETTI, E., MONGILLO, M., MORI, N., CRISTOFORI, P. & TREVISAN, A. (2010) Kidney injury molecule-1 expression in rat proximal tubule after treatment with segment-specific nephrotoxicants: a tool for early screening of potential kidney toxicity. *Toxicol Pathol,* 38**,** 338-45.

CHOBERT, M. N., COUCHIE, D., FOURCOT, A., ZAFRANI, E. S., LAPERCHE, Y., MAVIER, P. & BROUILLET, A. (2012) Liver precursor cells increase hepatic fibrosis induced by chronic carbon tetrachloride intoxication in rats. *Lab Invest,* 92**,** 135-50.

CHUNG, H., HONG, D. P., JUNG, J. Y., KIM, H. J., JANG, K. S., SHEEN, Y. Y., AHN, J. I., LEE, Y. S. & KONG, G. (2005a) Comprehensive analysis of differential gene expression profiles on carbon tetrachloride-induced rat liver injury and regeneration. *Toxicol Appl Pharmacol,* 206**,** 27-42.

CHUNG, H., HONG, D. P., KIM, H. J., JANG, K. S., SHIN, D. M., AHN, J. I., LEE, Y. S. & KONG, G. (2005b) Differential gene expression profiles in the steatosis/fibrosis model of rat liver by chronic administration of carbon tetrachloride. *Toxicol Appl Pharmacol,* 208**,** 242-54.

CICCARESE, M., TONOLO, G., BRIZZI, P., SECCHI, G., GARRUCCIU, G., SPANEDDA, M., SALIS, S., CALVIA, P., ASARA, A., WONG, F. K., MAIOLI, M. & REALDI, G. (1998) Serum apolipoprotein(a) concentrations and Apo(a) phenotypes in patients with liver cirrhosis. *Am J Gastroenterol,* 93**,** 1505-9.

CLARKE, C. J. & HASELDEN, J. N. (2008) Metabolic profiling as a tool for understanding mechanisms of toxicity. *Toxicol Pathol,* 36**,** 140-7.

CLARKE, H., EGAN, D. A., HEFFERNAN, M., DOYLE, S., BYRNE, C., KILTY, C. & RYAN, M. P. (1997) Alpha-glutathione s-transferase (alpha-GST) release, an early indicator of carbon tetrachloride hepatotoxicity in the rat. *Hum Exp Toxicol,* 16**,** 154-7.

CLAYTON, T. A., LINDON, J. C., EVERETT, J. R., CHARUEL, C., HANTON, G., LE NET, J. L., PROVOST, J. P. & NICHOLSON, J. K. (2003) An hypothesis for a mechanism underlying hepatotoxin-induced hypercreatinuria. *Arch Toxicol,* 77**,** 208-17.

CLAYTON, T. A., LINDON, J. C., EVERETT, J. R., CHARUEL, C., HANTON, G., LE NET, J. L., PROVOST, J. P. & NICHOLSON, J. K. (2004) Hepatotoxin-induced hypercreatinaemia and hypercreatinuria: their relationship to one another, to liver damage and to weakened nutritional status. *Arch Toxicol,* 78**,** 86-96.

CLOUTHIER, D. E., COMERFORD, S. A. & HAMMER, R. E. (1997) Hepatic fibrosis, glomerulosclerosis, and a lipodystrophy-like syndrome in PEPCK-TGF-beta1 transgenic mice. *J Clin Invest,* 100**,** 2697-713.

COCCHETTO, D. M., TSCHANZ, C. & BJORNSSON, T. D. (1983) Decreased rate of creatinine production in patients with hepatic disease: implications for estimation of creatinine clearance. *Ther Drug Monit,* 5**,** 161-8.

COCKERELL, G. L., MCKIM, J. M. & VONDERFECHT, S. L. (2002) Strategic importance of research support through pathology. *Toxicol Pathol,* 30**,** 4-7.

CONNOR, S. C., WU, W., SWEATMAN, B. C., MANINI, J., HASELDEN, J. N., CROWTHER, D. J. & WATERFIELD, C. J. (2004) Effects of feeding and body weight loss on the 1H-NMR-based urine metabolic profiles of male Wistar Han rats: implications for biomarker discovery. *Biomarkers,* 9**,** 156-79.

CONSTANDINOU, C., HENDERSON, N. & IREDALE, J. P. (2005) Modeling liver fibrosis in rodents. *Methods Mol Med,* 117**,** 237-50.

CONSTANTINOU, M. A., THEOCHARIS, S. E. & MIKROS, E. (2007) Application of metabonomics on an experimental model of fibrosis and cirrhosis induced by thioacetamide in rats. *Toxicol Appl Pharmacol,* 218**,** 11-9.

CONTI, M., MOUTEREAU, S., ZATER, M., LALLALI, K., DURRBACH, A., MANIVET, P., ESCHWEGE, P. & LORIC, S. (2006) Urinary cystatin C as a specific marker of tubular dysfunction. *Clin Chem Lab Med,* 44**,** 288-91.

CORBIN, K. D. & ZEISEL, S. H. (2012) Choline metabolism provides novel insights into nonalcoholic fatty liver disease and its progression. *Curr Opin Gastroenterol,* 28**,** 159-65.

COSTELLO, M., FIEDEL, B. A. & GEWURZ, H. (1979) Inhibition of platelet aggregation by native and desialised alpha-1 acid glycoprotein. *Nature,* 281**,** 677-8.

CRAIG, A., CLOAREC, O., HOLMES, E., NICHOLSON, J. K. & LINDON, J. C. (2006) Scaling and normalisation effects in NMR spectroscopic metabonomic data sets. *Anal Chem,* 78**,** 2262-7.

CRISTOFORI, P., DEFAZIO, R., CHIUSOLO, A., MONGILLO, M., BARTOLUCCI, G. B., CHIARA, F. & TREVISAN, A. (2013) Hyaline droplet accumulation in kidney of rats treated with hexachloro-1:3-butadiene: influence of age, dose and time-course. *J Appl Toxicol,* 33**,** 183-9.

CRISTOFORI, P., ZANETTI, E., FREGONA, D., PIAIA, A. & TREVISAN, A. (2007) Renal proximal tubule segment-specific nephrotoxicity: an overview on biomarkers and histopathology. *Toxicol Pathol,* 35**,** 270-5.

CRYER, D. R., MATSUSHIMA, T., MARSH, J. B., YUDKOFF, M., COATES, P. M. & CORTNER, J. A. (1986) Direct measurement of apolipoprotein B synthesis in human very low density lipoprotein using stable isotopes and mass spectrometry. *J Lipid Res,* 27**,** 508-16.

CUBERO, F. J. & NIETO, N. (2012) Arachidonic acid stimulates TNFalpha production in Kupffer cells via a reactive oxygen species-pERK1/2-Egr1-dependent mechanism. *Am J Physiol Gastrointest Liver Physiol,* 303**,** G228-39.

CUMMINGS, B. S., ZANGAR, R. C., NOVAK, R. F. & LASH, L. H. (1999) Cellular distribution of cytochromes P-450 in the rat kidney. *Drug Metab Dispos,* 27**,** 542-8.

CURRAN, S. & MURRAY, G. I. (2000) Matrix metalloproteinases: molecular aspects of their roles in tumour invasion and metastasis. *Eur J Cancer,* 36**,** 1621-30.

CZAJA, A. J. (2014) Review article: the prevention and reversal of hepatic fibrosis in autoimmune hepatitis. *Aliment Pharmacol Ther,* 39**,** 385-406.

CZAJA, M. J., GEERTS, A., XU, J., SCHMIEDEBERG, P. & JU, Y. (1994) Monocyte chemoattractant protein 1 (MCP-1) expression occurs in toxic rat liver injury and human liver disease. *J Leukoc Biol,* 55**,** 120-6.

DA SILVA, J. L., ZAND, B. A., YANG, L. M., SABAAWY, H. E., LIANOS, E. & ABRAHAM, N. G. (2001) Heme oxygenase isoform-specific expression and distribution in the rat kidney. *Kidney Int,* 59**,** 1448-57.

DARZYNKIEWICZ, Z., JUAN, G., LI, X., GORCZYCA, W., MURAKAMI, T. & TRAGANOS, F. (1997) Cytometry in cell necrobiology: analysis of apoptosis and accidental cell death (necrosis). *Cytometry,* 27**,** 1-20.

DAVIDSON, M. H. (2000) Does differing metabolism by cytochrome p450 have clinical importance? *Curr Atheroscler Rep,* 2**,** 14-9.

DAVIS, M. E., BERNDT, W. O. & MEHENDALE, H. M. (1980) Disposition and nephrotoxicity of hexachloro-1,3-butadiene. *Toxicology,* 16**,** 179-91.

DAWISKIBA, T., DEJA, S., MULAK, A., ZABEK, A., JAWIEN, E., PAWELKA, D., BANASIK, M., MASTALERZ-MIGAS, A., BALCERZAK, W., KALISZEWSKI, K., SKORA, J., BARC, P., KORTA, K., PORMANCZUK, K., SZYBER, P., LITARSKI, A. & MLYNARZ, P. (2014) Serum and urine metabolomic fingerprinting in diagnostics of inflammatory bowel diseases. *World J Gastroenterol,* 20**,** 163-74.

DE BLESER, P. J., NIKI, T., ROGIERS, V. & GEERTS, A. (1997) Transforming growth factor-beta gene expression in normal and fibrotic rat liver. *J Hepatol,* 26**,** 886-93.

DE ZEEUW, D., PARVING, H. H. & HENNING, R. H. (2006) Microalbuminuria as an early marker for cardiovascular disease. *J Am Soc Nephrol,* 17**,** 2100-5.

DE ZWART, L. L., HERMANNS, R. C., MEERMAN, J. H., COMMANDEUR, J. N., SALEMINK, P. J. & VERMEULEN, N. P. (1998) Evaluation of urinary biomarkers for radical-induced liver damage in rats treated with carbon tetrachloride. *Toxicol Appl Pharmacol,* 148**,** 71-82.

DEACIUC, I. V., BAGBY, G. J., LANG, C. H. & SPITZER, J. J. (1993) Hyaluronic acid uptake by the isolated, perfused rat liver: an index of hepatic sinusoidal endothelial cell function. *Hepatology,* 17**,** 266-72.

DEB, C. & CHAKRAVARTY, B. (1962) Histochemistry of the rat's kidney after carbon tetrachloride intoxication. *Acta Anat (Basel),* 50**,** 158-62.

DEKANT, W., BERTHOLD, K., VAMVAKAS, S. & HENSCHLER, D. (1988) Thioacylating agents as ultimate intermediates in the beta-lyase catalysed metabolism of S-(pentachloro-butadienyl)-L-cysteine. *Chem Biol Interact,* 67**,** 139-48.

DEKANT, W., VAMVAKAS, S., BERTHOLD, K., SCHMIDT, S., WILD, D. & HENSCHLER, D. (1986) Bacterial beta-lyase mediated cleavage and mutagenicity of cysteine conjugates derived from the nephrocarcinogenic alkenes trichloroethylene, tetrachloroethylene and hexachlorobutadiene. *Chem Biol Interact,* 60**,** 31-45.

DEVARAJAN, P. (2007) Proteomics for biomarker discovery in acute kidney injury. *Semin Nephrol,* 27**,** 637-51.

DHARNIDHARKA, V. R., KWON, C. & STEVENS, G. (2002) Serum cystatin C is superior to serum creatinine as a marker of kidney function: a meta-analysis. *Am J Kidney Dis,* 40**,** 221-6.

DI VINICIUS, I., BAPTISTA, A. P., BARBOSA, A. A. & ANDRADE, Z. A. (2005) Morphological signs of cirrhosis regression. Experimental observations on carbon tetrachloride-induced liver cirrhosis of rats. *Pathol Res Pract,* 201**,** 449-56.

DIAS, J. V., PAREDES, B. D., MESQUITA, L. F., CARVALHO, A. B., KOZLOWSKI, E. O., LESSA, A. S., TAKIYA, C. M., RESENDE, C. M., COELHO, H. S., CAMPOS-DE-CARVALHO, A. C., REZENDE, G. F. & GOLDENBERG, R. C. (2008) An ultrasound and histomorphological analysis of experimental liver cirrhosis in rats. *Braz J Med Biol Res,* 41**,** 992-9.

DIAZ-GIL, J. J., SANCHEZ, G., SANTAMARIA, L., TRILLA, C., ESTEBAN, P., ESCARTIN, P. & GEA, T. (1987) A liver DNA synthesis promoter induced in rat plasma by injection of dimethylnitrosamine (DMNA) or thioacetamide. *Br J Cancer,* 55**,** 599-604.

DIETERLE, F., PERENTES, E., CORDIER, A., ROTH, D. R., VERDES, P., GRENET, O., PANTANO, S., MOULIN, P., WAHL, D., MAHL, A., END, P., STAEDTLER, F., LEGAY, F., CARL, K., LAURIE, D., CHIBOUT, S. D., VONDERSCHER, J. & MAURER, G. (2010) Urinary clusterin, cystatin C, beta2-microglobulin and total protein as markers to detect drug-induced kidney injury. *Nat Biotechnol,* 28**,** 463-9.

DOI, K., YUEN, P. S., EISNER, C., HU, X., LEELAHAVANICHKUL, A., SCHNERMANN, J. & STAR, R. A. (2009) Reduced production of creatinine limits its use as marker of kidney injury in sepsis. *J Am Soc Nephrol,* 20**,** 1217-21.

DOMITROVIC, R., JAKOVAC, H., TOMAC, J. & SAIN, I. (2009) Liver fibrosis in mice induced by carbon tetrachloride and its reversion by luteolin. *Toxicol Appl Pharmacol,* 241**,** 311-21.

DOUMAS, B. T., WATSON, W. A. & BIGGS, H. G. (1971) Albumin standards and the measurement of serum albumin with bromcresol green. *Clin Chim Acta,* 31**,** 87-96.

DOW, J. L. & GREEN, T. (2000) Trichloroethylene induced vitamin B12 and folate deficiency leads to increased formic acid excretion in the rat. *Toxicology,* 146**,** 123-136.

DUCE, A. M., ORTIZ, P., CABRERO, C. & MATO, J. M. (1988) S-adenosyl-L-methionine synthetase and phospholipid methyltransferase are inhibited in human cirrhosis. *Hepatology,* 8**,** 65-8.

DUCKWORTH, W. C., BENNETT, R. G. & HAMEL, F. G. (1998) Insulin degradation: progress and potential. *Endocr Rev,* 19**,** 608-24.

DUFOUR, D. R. (2005) Assessment of liver fibrosis: Can serum become the sample of choice? *Clin Chem,* 51**,** 1763-4.

EATON, D. L. & BAMMLER, T. K. (1999) Concise review of the glutathione S-transferases and their significance to toxicology. *Toxicol Sci,* 49**,** 156-64.

EIPEL, C., ABSHAGEN, K. & VOLLMAR, B. (2010) Regulation of hepatic blood flow: the hepatic arterial buffer response revisited. *World J Gastroenterol,* 16**,** 6046-57.

EL-SERAG, H. B. & RUDOLPH, K. L. (2007) Hepatocellular carcinoma: epidemiology and molecular carcinogenesis. *Gastroenterology,* 132**,** 2557-76.

ELIAS, N., PATTERSON, B. W. & SCHONFELD, G. (1999) Decreased production rates of VLDL triglycerides and ApoB-100 in subjects heterozygous for familial hypobetalipoproteinemia. *Arterioscler Thromb Vasc Biol,* 19**,** 2714-21.

ELMORE, S. (2007) Apoptosis: a review of programmed cell death. *Toxicol Pathol,* 35**,** 495-516.

ERIKSSON, L., JOHANSSON, E., WOLD, N., TRYGG, J., WIKSTROM, J. & WOLD, S. (2006) *Multi- and megavariate data analysis part I,* Second edition, Umetrics.91-973730-2-8

EVERITT, B. & HOTHORN, T. (2011) *An introduction to applied multivariate analysis with R,* First edition, Springer.978-1-4419-9649-7

FALLOWFIELD, J. A. (2011) Therapeutic targets in liver fibrosis. *Am J Physiol Gastrointest Liver Physiol,* 300**,** G709-15.

FANELLI, S. L. & CASTRO, J. A. (1993) Carbon tetrachloride promoted malondialdehyde formation in liver microsomal and nuclear preparations from Sprague Dawley or Osborne Mendel male rats. *Res Commun Chem Pathol Pharmacol,* 82**,** 233-6.

FANG, H.-L. & LIN, W.-C. (2008) Corn oil enhancing hepatic lipid peroxidation induced by CCl4 does not aggravate liver fibrosis in rats. *Food and Chemical Toxicology,* 46**,** 2267-2273.

FDA http://www.fda.gov/NewsEvents/Newsroom/PressAnnouncements/2008/ucm116911.htm 16.02.2014

FISCHER-NIELSEN, A., POULSEN, H. E., HANSEN, B. A., HAGE, E. & KEIDING, S. (1991) CCl4 cirrhosis in rats: irreversible histological changes and differentiated functional impairment. *J Hepatol,* 12**,** 110-7.

FLO, T. H., SMITH, K. D., SATO, S., RODRIGUEZ, D. J., HOLMES, M. A., STRONG, R. K., AKIRA, S. & ADEREM, A. (2004) Lipocalin 2 mediates an innate immune response to bacterial infection by sequestrating iron. *Nature,* 432**,** 917-21.

FLOREANI, M., DE MARTIN, S., GABBIA, D., BARBIERATO, M., NASSI, A., MESCOLI, C., ORLANDO, R., BOVA, S., ANGELI, P., GOLA, E., STICCA, A. & PALATINI, P. (2013) Severe liver cirrhosis markedly reduces AhR-mediated induction of cytochrome P450 in rats by decreasing the transcription of target genes. *PLoS One,* 8**,** e61983.

FORNER, A., LLOVET, J. M. & BRUIX, J. (2012) Hepatocellular carcinoma. *Lancet,* 379**,** 1245-55.

FOURNIER, T., MEDJOUBI, N. N. & PORQUET, D. (2000) Alpha-1-acid glycoprotein. *Biochim Biophys Acta,* 1482**,** 157-71.

FOX, M. & WHITESELL, J. (2004) *Organic chemistry,* Third edition, Jones and Bartlett.0-7637-2197-2

FRIEDMAN, S. L. (1993) Seminars in medicine of the Beth Israel Hospital, Boston. The cellular basis of hepatic fibrosis. Mechanisms and treatment strategies. *N Engl J Med,* 328**,** 1828-35.

FRIEDMAN, S. L. (1999) Evaluation of fibrosis and hepatitis C. *Am J Med,* 107**,** 27S-30S.

FRIEDMAN, S. L. (2003) Liver fibrosis -- from bench to bedside. *J Hepatol,* 38 Suppl 1**,** S38-53.

FRIEDMAN, S. L. (2008) Mechanisms of hepatic fibrogenesis. *Gastroenterology,* 134**,** 1655-69.

FRIEDMAN, S. L., ROLL, F. J., BOYLES, J. & BISSELL, D. M. (1985) Hepatic lipocytes: the principal collagen-producing cells of normal rat liver. *Proc Natl Acad Sci U S A,* 82**,** 8681-5.

FRIEDRICH-RUST, M., ROSENBERG, W., PARKES, J., HERRMANN, E., ZEUZEM, S. & SARRAZIN, C. (2010) Comparison of ELF, FibroTest and FibroScan for the non-invasive assessment of liver fibrosis. *BMC Gastroenterol,* 10**,** 103.

FU, Y., ZHENG, S., LIN, J., RYERSE, J. & CHEN, A. (2008) Curcumin protects the rat liver from CCl4-caused injury and fibrogenesis by attenuating oxidative stress and suppressing inflammation. *Mol Pharmacol,* 73**,** 399-409.

FUJII, T., FUCHS, B. C., YAMADA, S., LAUWERS, G. Y., KULU, Y., GOODWIN, J. M., LANUTI, M. & TANABE, K. K. (2010) Mouse model of carbon tetrachloride induced liver fibrosis: Histopathological changes and expression of CD133 and epidermal growth factor. *BMC Gastroenterol,* 10**,** 79.

FUJITA, S., CHIBA, M., OHTA, M., KITANI, K. & SUZUKI, T. (1990) Alteration of plasma sex hormone levels associated with old age and its effect on hepatic drug metabolism in rats. *J Pharmacol Exp Ther,* 253**,** 369-74.

GALAN, A., HERNANDEZ, J. & JIMENEZ, O. (2001) Measurement of blood acetoacetate and beta-hydroxybutyrate in an automatic analyser. *J Autom Methods Manag Chem,* 23**,** 69-76.

GAO, H., LU, Q., LIU, X., CONG, H., ZHAO, L., WANG, H. & LIN, D. (2009) Application of 1H NMR-based metabonomics in the study of metabolic profiling of human hepatocellular carcinoma and liver cirrhosis. *Cancer Sci,* 100**,** 782-5.

GARCIA-COMPEAN, D., JAQUEZ-QUINTANA, J. O., GONZALEZ-GONZALEZ, J. A. & MALDONADO-GARZA, H. (2009) Liver cirrhosis and diabetes: risk factors, pathophysiology, clinical implications and management. *World J Gastroenterol,* 15**,** 280-8.

GARCIA-MARTINEZ, J. D., TVARIJONAVICIUTE, A., CERON, J. J., CALDIN, M. & MARTINEZ-SUBIELA, S. (2012) Urinary clusterin as a renal marker in dogs. *J Vet Diagn Invest,* 24**,** 301-6.

GARTLAND, K. P., BONNER, F. W. & NICHOLSON, J. K. (1989) Investigations into the biochemical effects of region-specific nephrotoxins. *Mol Pharmacol,* 35**,** 242-50.

GATLEY, S. J. & SHERRATT, H. S. (1977) The synthesis of hippurate from benzoate and glycine by rat liver mitochondria. Submitochondrial localization and kinetics. *Biochem J,* 166**,** 39-47.

GAUTIER, J. C., RIEFKE, B., WALTER, J., KURTH, P., MYLECRAINE, L., GUILPIN, V., BARLOW, N., GURY, T., HOFFMAN, D., ENNULAT, D., SCHUSTER, K., HARPUR, E. & PETTIT, S. (2010) Evaluation of novel biomarkers of nephrotoxicity in two strains of rat treated with Cisplatin. *Toxicol Pathol,* 38**,** 943-56.

GEORGE, J., TSUTSUMI, M. & TAKASE, S. (2004) Expression of hyaluronic acid in N-nitrosodimethylamine induced hepatic fibrosis in rats. *Int J Biochem Cell Biol,* 36**,** 307-19.

GHANADIAN, R., LEWIS, J. G. & CHISHOLM, G. D. (1975) Serum testosterone and dihydrotestosterone changes with age in rat. *Steroids,* 25**,** 753-62.

GIFFEN, P. S., PICK, C. R., PRICE, M. A., WILLIAMS, A. & YORK, M. J. (2002) Alpha-glutathione S-transferase in the assessment of hepatotoxicity--its diagnostic utility in comparison with other recognized markers in the Wistar Han rat. *Toxicol Pathol,* 30**,** 365-72.

GIFFEN, P. S., TURTON, J., ANDREWS, C. M., BARRETT, P., CLARKE, C. J., FUNG, K. W., MUNDAY, M. R., ROMAN, I. F., SMYTH, R., WALSHE, K. & YORK, M. J. (2003) Markers of experimental acute inflammation in the Wistar Han rat with particular reference to haptoglobin and C-reactive protein. *Arch Toxicol,* 77**,** 392-402.

GINÈS, P., GUEVARA, M., ARROYO, V. & RODÉS, J. (2003) Hepatorenal syndrome. *The Lancet,* 362**,** 1819-1827.

GOLDBERG, M., FOUAD, F. M. & RUHENSTROTH-BAUER, G. (1983) Changes in plasma protein profiles in serum and in liver DNA synthesis of rats following administration of alpha-amanitin, phalloidin and/or carbon tetrachloride. *J Clin Chem Clin Biochem,* 21**,** 125-8.

GOLDSMITH, P., FENTON, H., MORRIS-STIFF, G., AHMAD, N., FISHER, J. & PRASAD, K. R. (2010) Metabonomics: a useful tool for the future surgeon. *J Surg Res,* 160**,** 122-32.

GORES, G. J., HERMAN, B. & LEMASTERS, J. J. (1990) Plasma membrane bleb formation and rupture: a common feature of hepatocellular injury. *Hepatology,* 11**,** 690-8.

GOU, X., TAO, Q., FENG, Q., PENG, J., ZHAO, Y., DAI, J., WANG, W., ZHANG, Y., HU, Y. & LIU, P. (2013) Urine metabolic profile changes of CCl4-liver fibrosis in rats and intervention effects of Yi Guan Jian Decoction using metabonomic approach. *BMC Complement Altern Med,* 13**,** 123.

GRANDALIANO, G., GESUALDO, L., RANIERI, E., MONNO, R., MONTINARO, V., MARRA, F. & SCHENA, F. P. (1996) Monocyte chemotactic peptide-1 expression in acute and chronic human nephritides: a pathogenetic role in interstitial monocytes recruitment. *J Am Soc Nephrol,* 7**,** 906-13.

GRIGORESCU, M., RUSU, M., NECULOIU, D., RADU, C., SERBAN, A., CATANAS, M. & GRIGORESCU, M. D. (2007) The FibroTest value in discriminating between insignificant and significant fibrosis in chronic hepatitis C patients. The Romanian experience. *J Gastrointestin Liver Dis,* 16**,** 31-7.

GU, Q., WU, Q., JIN, M., XIAO, Y., XU, J., MAO, C., ZHAO, F. & ZHANG, Y. (2012) Heme oxygenase-1 alleviates mouse hepatic failure through suppression of adaptive immune responses. *J Pharmacol Exp Ther,* 340**,** 2-10.

GUENGERICH, F. P. & TURVY, C. G. (1991) Comparison of levels of several human microsomal cytochrome P-450 enzymes and epoxide hydrolase in normal and disease states using immunochemical analysis of surgical liver samples. *J Pharmacol Exp Ther,* 256**,** 1189-94.

GUSBERG, R. J., PETEREC, S. M., SUMPIO, B. E. & MEIER, G. H. (1994) Splenomegaly and variceal bleeding--hemodynamic basis and treatment implications. *Hepatogastroenterology,* 41**,** 573-7.

HAFEMAN, D. G. & HOEKSTRA, W. G. (1977) Protection against carbon tetrachloride-induced lipid peroxidation in the rat by dietary vitamin E, selenium, and methionine as measured by ethane evolution. *J Nutr,* 107**,** 656-65.

HAHN, E., WICK, G., PENCEV, D. & TIMPL, R. (1980) Distribution of basement membrane proteins in normal and fibrotic human liver: collagen type IV, laminin, and fibronectin. *Gut,* 21**,** 63-71.

HALL, M. C., YOUNG, D. A., WATERS, J. G., ROWAN, A. D., CHANTRY, A., EDWARDS, D. R. & CLARK, I. M. (2003) The comparative role of activator protein 1 and Smad factors in the regulation of Timp-1 and MMP-1 gene expression by transforming growth factor-beta 1. *J Biol Chem,* 278**,** 10304-13.

HAN, W. K., BAILLY, V., ABICHANDANI, R., THADHANI, R. & BONVENTRE, J. V. (2002) Kidney Injury Molecule-1 (KIM-1): a novel biomarker for human renal proximal tubule injury. *Kidney Int,* 62**,** 237-44.

HAN, Y. P. (2006) Matrix metalloproteinases, the pros and cons, in liver fibrosis. *J Gastroenterol Hepatol,* 21 Suppl 3**,** S88-91.

HANNA, M. H., SEGAR, J. L., TEESCH, L. M., KASPER, D. C., SCHAEFER, F. S. & BROPHY, P. D. (2013) Urinary metabolomic markers of aminoglycoside nephrotoxicity in newborn rats. *Pediatr Res,* 73**,** 585-91.

HARD, G. C. (2008) Some aids to histological recognition of hyaline droplet nephropathy in ninety-day toxicity studies. *Toxicol Pathol,* 36**,** 1014-7.

HARMOINEN, A., VUORINEN, P. & JOKELA, H. (1987) Turbidimetric measurement of microalbuminuria. *Clin Chim Acta,* 166**,** 85-9.

HARRISON, D. J., KHARBANDA, R., CUNNINGHAM, D. S., MCLELLAN, L. I. & HAYES, J. D. (1989) Distribution of glutathione S-transferase isoenzymes in human kidney: basis for possible markers of renal injury. *J Clin Pathol,* 42**,** 624-8.

HASCHEK, W., WALLIG, M. & ROUSSEAUX, C. (2010) *Fundamentals of toxicologic pathology,* Second edition, Elsevier.978-0-12-370469-6

HAUSO, O., GUSTAFSSON, B. I., NORDRUM, I. S. & WALDUM, H. L. (2008) The effect of terguride in carbon tetrachloride-induced liver fibrosis in rat. *Exp Biol Med (Maywood),* 233**,** 1385-8.

HAUTEKEETE, M. L. & GEERTS, A. (1997) The hepatic stellate (Ito) cell: its role in human liver disease. *Virchows Arch,* 430**,** 195-207.

HAYES, A. (2007) *Principles and methods of toxicology*, CRC Press.978-084933778X

HERBST, H., WEGE, T., MILANI, S., PELLEGRINI, G., ORZECHOWSKI, H. D., BECHSTEIN, W. O., NEUHAUS, P., GRESSNER, A. M. & SCHUPPAN, D. (1997) Tissue inhibitor of metalloproteinase-1 and -2 RNA expression in rat and human liver fibrosis. *Am J Pathol,* 150**,** 1647-59.

HERGET-ROSENTHAL, S., VAN WIJK, J. A., BROCKER-PREUSS, M. & BOKENKAMP, A. (2007) Increased urinary cystatin C reflects structural and functional renal tubular impairment independent of glomerular filtration rate. *Clin Biochem,* 40**,** 946-51.

HEWITT, S. M., DEAR, J. & STAR, R. A. (2004) Discovery of protein biomarkers for renal diseases. *J Am Soc Nephrol,* 15**,** 1677-89.

HICKMAN, I. J. & MACDONALD, G. A. (2007) Impact of diabetes on the severity of liver disease. *Am J Med,* 120**,** 829-34.

HIDAKA, S., KRANZLIN, B., GRETZ, N. & WITZGALL, R. (2002) Urinary clusterin levels in the rat correlate with the severity of tubular damage and may help to differentiate between glomerular and tubular injuries. *Cell Tissue Res,* 310**,** 289-96.

HIRATA, M., AKBAR, S. M., HORIIKE, N. & ONJI, M. (2001) Non-invasive diagnosis of the degree of hepatic fibrosis using ultrasonography in patients with chronic liver disease due to hepatitis C virus. *Eur J Clin Invest,* 31**,** 528-35.

HIYOSHI, M., KONISHI, H., UEMURA, H., MATSUZAKI, H., TSUKAMOTO, H., SUGIMOTO, R., TAKEDA, H., DAKESHITA, S., KITAYAMA, A., TAKAMI, H., SAWACHIKA, F., KIDO, H. & ARISAWA, K. (2009) D-Dopachrome tautomerase is a candidate for key proteins to protect the rat liver damaged by carbon tetrachloride. *Toxicology,* 255**,** 6-14.

HOGASEN, K., HOMANN, C., MOLLNES, T. E., GRAUDAL, N., HOGASEN, A. K., HASSELQVIST, P., THOMSEN, A. C. & GARRED, P. (1996) Serum clusterin and vitronectin in alcoholic cirrhosis. *Liver,* 16**,** 140-6.

HOHMANN, B., FROHNERT, P. P., KINNE, R. & BAUMANN, K. (1974) Proximal tubular lactate transport in rat kidney: a micropuncture study. *Kidney Int,* 5**,** 261-70.

HOLMES, E., LOO, R. L., CLOAREC, O., COEN, M., TANG, H., MAIBAUM, E., BRUCE, S., CHAN, Q., ELLIOTT, P., STAMLER, J., WILSON, I. D., LINDON, J. C. & NICHOLSON, J. K. (2007) Detection of urinary drug metabolite (xenometabolome) signatures in molecular epidemiology studies via statistical total correlation (NMR) spectroscopy. *Anal Chem,* 79**,** 2629-40.

HOLMES, E., NICHOLLS, A. W., LINDON, J. C., CONNOR, S. C., CONNELLY, J. C., HASELDEN, J. N., DAMMENT, S. J., SPRAUL, M., NEIDIG, P. & NICHOLSON, J. K. (2000) Chemometric models for toxicity classification based on NMR spectra of biofluids. *Chem Res Toxicol,* 13**,** 471-8.

HOLMES, E., NICHOLSON, J. K. & TRANTER, G. (2001) Metabonomic characterization of genetic variations in toxicological and metabolic responses using probabilistic neural networks. *Chem Res Toxicol,* 14**,** 182-91.

HOOK, J. B., ISHMAEL, J. & LOCK, E. A. (1983) Nephrotoxicity of Hexachloro-1:3-butadiene in the rat: the effect of age, sex, and strain. *Toxicol Appl Pharmacol,* 67**,** 122-31.

HORN, M. M., RAMOS, A. R., WINKELMANN, L., MATTE, U. S., GOLDANI, H. A. & SILVEIRA, T. R. (2006) Seminiferous epithelium of rats with food restriction and carbon tetrachloride-induced cirrhosis. *Int Braz J Urol,* 32**,** 94-9; discussion 99.

HUMPHRIES, K. M. & SZWEDA, L. I. (1998) Selective inactivation of alpha-ketoglutarate dehydrogenase and pyruvate dehydrogenase: reaction of lipoic acid with 4-hydroxy-2-nonenal. *Biochemistry,* 37**,** 15835-41.

HUNT, C. M., STRATER, S. & STAVE, G. M. (1990) Effect of normal aging on the activity of human hepatic cytochrome P450IIE1. *Biochem Pharmacol,* 40**,** 1666-9.

ICHI, I., NAKAHARA, K., FUJII, K., IIDA, C., MIYASHITA, Y. & KOJO, S. (2007) Increase of ceramide in the liver and plasma after carbon tetrachloride intoxication in the rat. *J Nutr Sci Vitaminol (Tokyo),* 53**,** 53-6.

ICHIMURA, T., ASSELDONK, E. J., HUMPHREYS, B. D., GUNARATNAM, L., DUFFIELD, J. S. & BONVENTRE, J. V. (2008) Kidney injury molecule-1 is a

phosphatidylserine receptor that confers a phagocytic phenotype on epithelial cells. *J Clin Invest,* 118**,** 1657-68.

ICHIMURA, T., BROOKS, C. R. & BONVENTRE, J. V. (2012) Kim-1/Tim-1 and immune cells: shifting sands. *Kidney Int,* 81**,** 809-11.

ICHIMURA, T., HUNG, C. C., YANG, S. A., STEVENS, J. L. & BONVENTRE, J. V. (2004) Kidney injury molecule-1: a tissue and urinary biomarker for nephrotoxicant-induced renal injury. *Am J Physiol Renal Physiol,* 286**,** F552-63.

IREDALE, J. P., BENYON, R. C., ARTHUR, M. J., FERRIS, W. F., ALCOLADO, R., WINWOOD, P. J., CLARK, N. & MURPHY, G. (1996) Tissue inhibitor of metalloproteinase-1 messenger RNA expression is enhanced relative to interstitial collagenase messenger RNA in experimental liver injury and fibrosis. *Hepatology,* 24**,** 176-84.

IREDALE, J. P., BENYON, R. C., PICKERING, J., MCCULLEN, M., NORTHROP, M., PAWLEY, S., HOVELL, C. & ARTHUR, M. J. (1998) Mechanisms of spontaneous resolution of rat liver fibrosis. Hepatic stellate cell apoptosis and reduced hepatic expression of metalloproteinase inhibitors. *J Clin Invest,* 102**,** 538-49.

ISHIKAWA, T., SHIRATSUKI, S., MATSUDA, T., IWAMOTO, T., TAKAMI, T., UCHIDA, K., TERAI, S., YAMASAKI, T. & SAKAIDA, I. (2013) Occlusion of portosystemic shunts improves hyperinsulinemia due to insulin resistance in cirrhotic patients with portal hypertension. *J Gastroenterol*.

ISHMAEL, J. & LOCK, E. A. (1986) Nephrotoxicity of hexachlorobutadiene and its glutathione-derived conjugates. *Toxicol Pathol,* 14**,** 258-62.

ISHMAEL, J., PRATT, I. & LOCK, E. A. (1982) Necrosis of the pars recta (S3 segment) of the rat kidney produced by hexachloro 1:3 butadiene. *J Pathol,* 138**,** 99-113.

ITOH, T., ORBA, Y., TAKEI, H., ISHIDA, Y., SAITOH, M., NAKAMURA, H., MEGURO, T., HORITA, S., FUJITA, M. & NAGASHIMA, K. (2002) Immunohistochemical detection of hepatocellular carcinoma in the setting of ongoing necrosis after radiofrequency ablation. *Mod Pathol,* 15**,** 110-5.

JACKSON, J. (1991) *A user's guide to principal components* First edition, Wiley.0-471-62267-2

JACOBS, S. C., RAMEY, J. R., SKLAR, G. N. & BARTLETT, S. T. (2004) Laparoscopic kidney donation from patients older than 60 years. *J Am Coll Surg,* 198**,** 892-7.

JACOBSEN, J. G. & SMITH, L. H. (1968) Biochemistry and physiology of taurine and taurine derivatives. *Physiol Rev,* 48**,** 424-511.

JAMES, L. P., MAYEUX, P. R. & HINSON, J. A. (2003) Acetaminophen-induced hepatotoxicity. *Drug Metab Dispos,* 31**,** 1499-506.

JANAKAT, S. & AL-MERIE, H. (2002) Optimization of the dose and route of injection, and characterisation of the time course of carbon tetrachloride-induced

hepatotoxicity in the rat. *Journal of Pharmacological and Toxicological Methods,* 48**,** 41-44.

JANCIAUSKIENE, S. (2001) Conformational properties of serine proteinase inhibitors (serpins) confer multiple pathophysiological roles. *Biochim Biophys Acta,* 1535**,** 221-35.

JARAMILLO-JUAREZ, F., RODRIGUEZ-VAZQUEZ, M. L., RINCON-SANCHEZ, A. R., CONSOLACION MARTINEZ, M., ORTIZ, G. G., LLAMAS, J., ANIBAL POSADAS, F. & REYES, J. L. (2008) Acute renal failure induced by carbon tetrachloride in rats with hepatic cirrhosis. *Ann Hepatol,* 7**,** 331-8.

JIANG, Y., LIU, J., WAALKES, M. & KANG, Y. J. (2004) Changes in the gene expression associated with carbon tetrachloride-induced liver fibrosis persist after cessation of dosing in mice. *Toxicol Sci,* 79**,** 404-10.

JIAO, J., FRIEDMAN, S. L. & ALOMAN, C. (2009) Hepatic fibrosis. *Curr Opin Gastroenterol,* 25**,** 223-9.

JORRES, A., KORDONOURI, O., SCHIESSLER, A., HESS, S., FARKE, S., GAHL, G. M., MULLER, C. & DJURUP, R. (1994) Urinary excretion of thromboxane and markers for renal injury in patients undergoing cardiopulmonary bypass. *Artif Organs,* 18**,** 565-9.

KAMATAKI, T., MAEDA, K., SHIMADA, M., KITANI, K., NAGAI, T. & KATO, R. (1985) Age-related alteration in the activities of drug-metabolizing enzymes and contents of sex-specific forms of cytochrome P-450 in liver microsomes from male and female rats. *J Pharmacol Exp Ther,* 233**,** 222-8.

KAMATAKI, T., MAEDA, K., YAMAZOE, Y., NAGAI, T. & KATO, R. (1983) Sex difference of cytochrome P-450 in the rat: purification, characterization, and quantitation of constitutive forms of cytochrome P-450 from liver microsomes of male and female rats. *Arch Biochem Biophys,* 225**,** 758-70.

KAMATH, P. S., CARPENTER, H. A., LLOYD, R. V., MCKUSICK, M. A., STEERS, J. L., NAGORNEY, D. M. & MILLER, V. M. (2000) Hepatic localization of endothelin-1 in patients with idiopathic portal hypertension and cirrhosis of the liver. *Liver Transpl,* 6**,** 596-602.

KAMIIKE, W., FUJIKAWA, M., KOSEKI, M., SUMIMURA, J., MIYATA, M., KAWASHIMA, Y., WADA, H. & TAGAWA, K. (1989) Different patterns of leakage of cytosolic and mitochondrial enzymes. *Clin Chim Acta,* 185**,** 265-70.

KAMIJO, A., KIMURA, K., SUGAYA, T., YAMANOUCHI, M., HIKAWA, A., HIRANO, N., HIRATA, Y., GOTO, A. & OMATA, M. (2004) Urinary fatty acid-binding protein as a new clinical marker of the progression of chronic renal disease. *J Lab Clin Med,* 143**,** 23-30.

KANEMOTO, H., OHNO, K., SAKAI, M., NAKASHIMA, K., TAKAHASHI, M., FUJINO, Y. & TSUJIMOTO, H. (2011) Expression of fibrosis-related genes in canine chronic hepatitis. *Vet Pathol,* 48**,** 839-45.

KAPLAN, M. M. & RIGHETTI, A. (1970) Induction of rat liver alkaline phosphatase: the mechanism of the serum elevation in bile duct obstruction. *J Clin Invest,* 49**,** 508-16.

KARLMARK, K. R., WEISKIRCHEN, R., ZIMMERMANN, H. W., GASSLER, N., GINHOUX, F., WEBER, C., MERAD, M., LUEDDE, T., TRAUTWEIN, C. & TACKE, F. (2009) Hepatic recruitment of the inflammatory Gr1+ monocyte subset upon liver injury promotes hepatic fibrosis. *Hepatology,* 50**,** 261-74.

KASHANI, A., LANDAVERDE, C., MEDICI, V. & ROSSARO, L. (2008) Fluid retention in cirrhosis: pathophysiology and management. *QJM,* 101**,** 71-85.

KAWSER, C. A., IREDALE, J. P., WINWOOD, P. J. & ARTHUR, M. J. (1998) Rat hepatic stellate cell expression of alpha2-macroglobulin is a feature of cellular activation: implications for matrix remodelling in hepatic fibrosis. *Clin Sci (Lond),* 95**,** 179-86.

KELISHADI, R., FARAJIAN, S. & MIRLOHI, M. (2013) Probiotics as a novel treatment for non-alcoholic Fatty liver disease; a systematic review on the current evidences. *Hepat Mon,* 13**,** e7233.

KHAN, R. A., KHAN, M. R. & SAHREEN, S. (2012) CCl4-induced hepatotoxicity: protective effect of rutin on p53, CYP2E1 and the antioxidative status in rat. *BMC Complement Altern Med,* 12**,** 178.

KHARASCH, E. D., THORNING, D., GARTON, K., HANKINS, D. C. & KILTY, C. G. (1997) Role of renal cysteine conjugate beta-lyase in the mechanism of compound A nephrotoxicity in rats. *Anesthesiology,* 86**,** 160-71.

KHURANA, I. (2009) *Textbook of medical physiology,* First edition, Elsevier.978-81-8147-850-4

KIM, H. J., BRUCKNER, J. V., DALLAS, C. E. & GALLO, J. M. (1990) Effect of dosing vehicles on the pharmacokinetics of orally administered carbon tetrachloride in rats. *Toxicol Appl Pharmacol,* 102**,** 50-60.

KIM, J. W., RYU, S. H., KIM, S., LEE, H. W., LIM, M. S., SEONG, S. J., YOON, Y. R. & KIM, K. B. (2013) Pattern recognition analysis for hepatotoxicity induced by acetaminophen using plasma and urinary 1H NMR-based metabolomics in humans. *Anal Chem,* 85**,** 11326-34.

KIM, K.-B., CHUNG, M., UM, S., OH, J., KIM, S., NA, M., OH, H., CHO, W.-S. & CHOI, K. (2008a) Metabolomics and biomarker discovery: NMR spectral data of urine and hepatotoxicity by carbon tetrachloride, acetaminophen, and d-galactosamine in rats. *Metabolomics,* 4**,** 377-392.

KIM, K.-B., CHUNG, M. W., UM, S. Y., OH, J. S., KIM, S. H., NA, M. A., OH, H. Y., CHO, W.-S. & CHOI, H. H. (2008b) Metabolomics and biomarkers discovery: NMR spectral data of urine and hepatotoxicity by carbon tetrachloride, acetaminophen and D-galactosamine in rats. *Metabolomics***,** 377-392.

KIMBALL, S. R. & JEFFERSON, L. S. (1992) Regulation of protein synthesis by modulation of intracellular calcium in rat liver. *Am J Physiol,* 263**,** E958-64.

KJELDSEN, L., BAINTON, D. F., SENGELOV, H. & BORREGAARD, N. (1994) Identification of neutrophil gelatinase-associated lipocalin as a novel matrix protein of specific granules in human neutrophils. *Blood,* 83**,** 799-807.

KLAASSEN, C. D. (1972) Immaturity of the newborn rat's hepatic excretory function for ouabain. *J Pharmacol Exp Ther,* 183**,** 520-6.

KLAASSEN, C. D. (1973) Hepatic excretory function in the newborn rat. *J Pharmacol Exp Ther,* 184**,** 721-8.

KLEINMAN, J. G., BESHENSKY, A., WORCESTER, E. M. & BROWN, D. (1995) Expression of osteopontin, a urinary inhibitor of stone mineral crystal growth, in rat kidney. *Kidney Int,* 47**,** 1585-96.

KNITTEL, T., MEHDE, M., GRUNDMANN, A., SAILE, B., SCHARF, J. G. & RAMADORI, G. (2000) Expression of matrix metalloproteinases and their inhibitors during hepatic tissue repair in the rat. *Histochem Cell Biol,* 113**,** 443-53.

KOGURE, K., ISHIZAKI, M., NEMOTO, M., KUWANO, H. & MAKUUCHI, M. (1999) A comparative study of the anatomy of rat and human livers. *J Hepatobiliary Pancreat Surg,* 6**,** 171-5.

KORENCHEVSKY, V. & ROSS, M. A. (1940) Kidneys and Sex Hormones. *Br Med J,* 1**,** 645-8.

KRINKLE, G. (2000) *The laboratory rat,* First edition, Academic Press.0-12-426400-X

KRISHNAMURTHY, S., KORENBLAT, K. M. & SCOTT, M. G. (2009) Persistent increase in aspartate aminotransferase in an asymptomatic patient. *Clin Chem,* 55**,** 1573-5.

KRIZHANOVSKY, V., YON, M., DICKINS, R. A., HEARN, S., SIMON, J., MIETHING, C., YEE, H., ZENDER, L. & LOWE, S. W. (2008) Senescence of activated stellate cells limits liver fibrosis. *Cell,* 134**,** 657-67.

KROEMER, G., GALLUZZI, L., VANDENABEELE, P., ABRAMS, J., ALNEMRI, E. S., BAEHRECKE, E. H., BLAGOSKLONNY, M. V., EL-DEIRY, W. S., GOLSTEIN, P., GREEN, D. R., HENGARTNER, M., KNIGHT, R. A., KUMAR, S., LIPTON, S. A., MALORNI, W., NUNEZ, G., PETER, M. E., TSCHOPP, J., YUAN, J., PIACENTINI, M., ZHIVOTOVSKY, B. & MELINO, G. (2009) Classification of cell death: recommendations of the Nomenclature Committee on Cell Death 2009. *Cell Death Differ,* 16**,** 3-11.

KUJOVICH, J. L. (2005) Hemostatic defects in end stage liver disease. *Crit Care Clin,* 21**,** 563-87.

KUO, C.-H. & HOOK, J. B. (1983) Effects of age and sex on hexachloro-1,3-butadiene toxicity in the fischer 344 rat. *Life Sciences,* 33**,** 517-523.

LARSSON, S. C. (2013) Urinary magnesium excretion as a marker of heart disease risk. *Am J Clin Nutr,* 97**,** 1159-60.

LAURIDSEN, M., HANSEN, S. H., JAROSZEWSKI, J. W. & CORNETT, C. (2007) Human urine as test material in 1H NMR-based metabonomics: recommendations for sample preparation and storage. *Anal Chem,* 79**,** 1181-6.

LAZZARA, M. J. & DEEN, W. M. (2007) Model of albumin reabsorption in the proximal tubule. *Am J Physiol Renal Physiol,* 292**,** F430-9.

LEE, E., VAUGHAN, D. E., PARIKH, S. H., GRODZINSKY, A. J., LIBBY, P., LARK, M. W. & LEE, R. T. (1996) Regulation of matrix metalloproteinases and plasminogen activator inhibitor-1 synthesis by plasminogen in cultured human vascular smooth muscle cells. *Circ Res,* 78**,** 44-9.

LEE, G. P., JEONG, W. I., JEONG, D. H., DO, S. H., KIM, T. H. & JEONG, K. S. (2005) Diagnostic evaluation of carbon tetrachloride-induced rat hepatic cirrhosis model. *Anticancer Res,* 25**,** 1029-38.

LEE, J. W. (2009) Renal dysfunction in patients with chronic liver disease. *Electrolyte Blood Press,* 7**,** 42-50.

LEE, P. Y., MCCAY, P. B. & HORNBROOK, K. R. (1982) Evidence for carbon tetrachloride-induced lipid peroxidation in mouse liver. *Biochem Pharmacol,* 31**,** 405-9.

LEE, V. W., DE KRETSER, D. M., HUDSON, B. & WANG, C. (1975) Variations in serum FSH, LH and testosterone levels in male rats from birth to sexual maturity. *J Reprod Fertil,* 42**,** 121-6.

LEHMAN-MCKEEMAN, L. D., RIVERA-TORRES, M. I. & CAUDILL, D. (1990) Lysosomal degradation of alpha 2u-globulin and alpha 2u-globulin-xenobiotic conjugates. *Toxicol Appl Pharmacol,* 103**,** 539-48.

LESSA, A. S., PAREDES, B. D., DIAS, J. V., CARVALHO, A. B., QUINTANILHA, L. F., TAKIYA, C. M., TURA, B. R., REZENDE, G. F., CAMPOS DE CARVALHO, A. C., RESENDE, C. M. & GOLDENBERG, R. C. (2010) Ultrasound imaging in an experimental model of fatty liver disease and cirrhosis in rats. *BMC Vet Res,* 6**,** 6.

LEWIN, D. A. & WEINER, M. P. (2004) Molecular biomarkers in drug development. *Drug Discov Today,* 9**,** 976-83.

LEWIS, R. E., KUNZ, A. L. & BELL, R. E. (1966) Error of intraperitoneal injections in rats. *Lab Anim Care,* 16**,** 505-9.

LEYLAND, H., GENTRY, J., ARTHUR, M. J. & BENYON, R. C. (1996) The plasminogen-activating system in hepatic stellate cells. *Hepatology,* 24**,** 1172-8.

LI, D. & FRIEDMAN, S. L. (1999) Liver fibrogenesis and the role of hepatic stellate cells: new insights and prospects for therapy. *J Gastroenterol Hepatol,* 14**,** 618-33.

LI, X., ZHANG, F., WANG, D., LI, Z., QIN, X. & DU, G. (2013) NMR-based metabonomic and quantitative real-time PCR in the profiling of metabolic changes in carbon tetrachloride-induced rat liver injury. *J Pharm Biomed Anal,* 89C**,** 42-49.

LIEBER, C. S. (2002) S-adenosyl-L-methionine: its role in the treatment of liver disorders. *Am J Clin Nutr,* 76**,** 1183S-7S.

LIN, X. Z., HORNG, M. H., SUN, Y. N., SHIESH, S. C., CHOW, N. H. & GUO, X. Z. (1998) Computer morphometry for quantitative measurement of liver fibrosis:

comparison with Knodell's score, colorimetry and conventional description reports. *J Gastroenterol Hepatol,* 13**,** 75-80.

LIN, Y., SI, D., ZHANG, Z. & LIU, C. (2009) An integrated metabonomic method for profiling of metabolic changes in carbon tetrachloride induced rat urine. *Toxicology,* 256**,** 191-200.

LINDON, J. C., KEUN, H. C., EBBELS, T. M., PEARCE, J. M., HOLMES, E. & NICHOLSON, J. K. (2005) The Consortium for Metabonomic Toxicology (COMET): aims, activities and achievements. *Pharmacogenomics,* 6**,** 691-9.

LINDON, J. C., NICHOLSON, J. K., HOLMES, E., ANTTI, H., BOLLARD, M. E., KEUN, H., BECKONERT, O., EBBELS, T. M., REILY, M. D., ROBERTSON, D., STEVENS, G. J., LUKE, P., BREAU, A. P., CANTOR, G. H., BIBLE, R. H., NIEDERHAUSER, U., SENN, H., SCHLOTTERBECK, G., SIDELMANN, U. G., LAURSEN, S. M., TYMIAK, A., CAR, B. D., LEHMAN-MCKEEMAN, L., COLET, J. M., LOUKACI, A. & THOMAS, C. (2003) Contemporary issues in toxicology the role of metabonomics in toxicology and its evaluation by the COMET project. *Toxicol Appl Pharmacol,* 187**,** 137-46.

LINDROS, K. O. (1997) Zonation of cytochrome P450 expression, drug metabolism and toxicity in liver. *Gen Pharmacol,* 28**,** 191-6.

LINDROS, K. O., CAI, Y. A. & PENTTILA, K. E. (1990) Role of ethanol-inducible cytochrome P-450 IIE1 in carbon tetrachloride-induced damage to centrilobular hepatocytes from ethanol-treated rats. *Hepatology,* 12**,** 1092-7.

LIU, Q. & NILSEN-HAMILTON, M. (1995) Identification of a new acute phase protein. *J Biol Chem,* 270**,** 22565-70.

LIU, X., XU, J., BRENNER, D. A. & KISSELEVA, T. (2013) Reversibility of Liver Fibrosis and Inactivation of Fibrogenic Myofibroblasts. *Curr Pathobiol Rep,* 1**,** 209-214.

LOCK, E. A. & ISHMAEL, J. (1979) The acute toxic effects of hexachloro-1 : 3-butadiene on the rat kidney. *Arch Toxicol,* 43**,** 47-57.

LOCK, E. A. & ISHMAEL, J. (1981) Hepatic and renal nonprotein sulfhydryl concentration following toxic doses of hexachloro-1,3-butadiene in the rat: the effect of Aroclor 1254, phenobarbitone, or SKF 525A treatment. *Toxicol Appl Pharmacol,* 57**,** 79-87.

LOCK, E. A., ISHMAEL, J. & PRATT, I. (1982) Hydropic change in rat liver induced by hexachloro-1:3-butadiene. *J Appl Toxicol,* 2**,** 315-20.

LOCK, E. A., PRATT, I. S. & ISHMAEL, J. (1985) Hexachloro-1,3-butadiene-induced hydropic change in mouse liver. *J Appl Toxicol,* 5**,** 74-9.

LOCK, E. A. & REED, C. J. (1998) Xenobiotic metabolizing enzymes of the kidney. *Toxicol Pathol,* 26**,** 18-25.

LOMBARDI, B. & UGAZIO, G. (1965) Serum lipoproteins in rats with carbon tetrachloride-induced fatty liver. *J Lipid Res,* 6**,** 498-505.

LOTE, C. (2012) *Principles of renal physiology,* Firth edition, Springer.978-1-4614-3784-0

LU, C., WANG, Y., SHENG, Z., LIU, G., FU, Z., ZHAO, J., YAN, X., ZHU, B. & PENG, S. (2010) NMR-based metabonomic analysis of the hepatotoxicity induced by combined exposure to PCBs and TCDD in rats. *Toxicol Appl Pharmacol,* 248**,** 178-84.

LUBRAN, M. M. (1978) The measurement of total serum proteins by the Biuret method. *Ann Clin Lab Sci,* 8**,** 106-10.

LUND, S. A., GIACHELLI, C. M. & SCATENA, M. (2009) The role of osteopontin in inflammatory processes. *J Cell Commun Signal,* 3**,** 311-22.

LUNDH, H. A. (1964) Sequence Comparison between Kidney and Liver Lesions in the Rat Following Carbon Tetrachloride Poisoning. *J Occup Med,* 6**,** 123-8.

MACHADO, M. V. & DIEHL, A. M. (2014) Liver renewal: detecting misrepair and optimizing regeneration. *Mayo Clin Proc,* 89**,** 120-30.

MACKELAITE, L., ALSAUSKAS, Z. C. & RANGANNA, K. (2009) Renal failure in patients with cirrhosis. *Med Clin North Am,* 93**,** 855-69, viii.

MACKIE, J. T., ATSHAVES, B. P., PAYNE, H. R., MCINTOSH, A. L., SCHROEDER, F. & KIER, A. B. (2009) Phytol-induced hepatotoxicity in mice. *Toxicol Pathol,* 37**,** 201-8.

MADRAHIMOV, N., DIRSCH, O., BROELSCH, C. & DAHMEN, U. (2006) Marginal hepatectomy in the rat: from anatomy to surgery. *Ann Surg,* 244**,** 89-98.

MAGUIRE, D. P., TURTON, J. A., SCUDAMORE, C. L., SWAIN, A. J., MCCLURE, F. J., SMYTH, R., PEREIRA, I. B., MUNDAY, M. R. & YORK, M. J. (2013) Correlation of histopathology, urinary biomarkers, and gene expression responses following hexachloro-1:3-butadiene-induced acute nephrotoxicity in male Hanover Wistar rats: a 28-day time course study. *Toxicol Pathol,* 41**,** 779-94.

MAHARJAN, A. S., PILLING, D. & GOMER, R. H. (2011) High and low molecular weight hyaluronic acid differentially regulate human fibrocyte differentiation. *PLoS One,* 6**,** e26078.

MAHER, J. J. & MCGUIRE, R. F. (1990) Extracellular matrix gene expression increases preferentially in rat lipocytes and sinusoidal endothelial cells during hepatic fibrosis *in vivo*. *J Clin Invest,* 86**,** 1641-8.

MAHL, T. C. & GROSZMANN, R. J. 1990. Pathophysiology of portal hypertension and variceal bleeding. *Surg Clin North Am,* 70**,** 251-66.

MAJNO, G. & JORIS, I. (1995) Apoptosis, oncosis, and necrosis. An overview of cell death. *Am J Pathol,* 146**,** 3-15.

MAKNI, M., CHTOUROU, Y., GAROUI, E. M., BOUDAWARA, T. & FETOUI, H. (2012) Carbon tetrachloride-induced nephrotoxicity and DNA damage in rats: protective role of vanillin. *Hum Exp Toxicol,* 31**,** 844-52.

MALLAT, A., FOUASSIER, L., PREAUX, A. M., GAL, C. S., RAUFASTE, D., ROSENBAUM, J., DHUMEAUX, D., JOUNEAUX, C., MAVIER, P. & LOTERSZTAJN, S. (1995) Growth inhibitory properties of endothelin-1 in human hepatic myofibroblastic Ito cells. An endothelin B receptor-mediated pathway. *J Clin Invest,* 96**,** 42-9.

MAMMEN, E. F. (1992) Coagulation abnormalities in liver disease. *Hematol Oncol Clin North Am,* 6**,** 1247-57.

MANDL, J., GARZO, T. & ANTONI, F. (1982) Epinephrine inhibits protein synthesis in isolated mouse hepatocytes through alpha adrenergic receptors in a calcium dependent way. *Biochem Pharmacol,* 31**,** 1656-8.

MANJREKAR, A. P., JISHA, V., BAG, P. P., ADHIKARY, B., PAI, M. M., HEGDE, A. & NANDINI, M. (2008) Effect of Phyllanthus niruri Linn. treatment on liver, kidney and testes in CCl4 induced hepatotoxic rats. *Indian J Exp Biol,* 46**,** 514-20.

MANNERVIK, B., ALIN, P., GUTHENBERG, C., JENSSON, H., TAHIR, M. K., WARHOLM, M. & JORNVALL, H. (1985) Identification of three classes of cytosolic glutathione transferase common to several mammalian species: correlation between structural data and enzymatic properties. *Proc Natl Acad Sci U S A,* 82**,** 7202-6.

MANNO, M., FERRARA, R., CAZZARO, S., RIGOTTI, P. & ANCONA, E. (1992) Suicidal inactivation of human cytochrome P-450 by carbon tetrachloride and halothane *in vitro*. *Pharmacol Toxicol,* 70**,** 13-8.

MARK, M. P., PRINCE, C. W., GAY, S., AUSTIN, R. L. & BUTLER, W. T. (1988) 44-kDal bone phosphoprotein (osteopontin) antigenicity at ectopic sites in newborn rats: kidney and nervous tissues. *Cell Tissue Res,* 251**,** 23-30.

MARONPOT, R. R., YOSHIZAWA, K., NYSKA, A., HARADA, T., FLAKE, G., MUELLER, G., SINGH, B. & WARD, J. M. (2010) Hepatic enzyme induction: histopathology. *Toxicol Pathol,* 38**,** 776-95.

MARRA, F., DEFRANCO, R., GRAPPONE, C., MILANI, S., PASTACALDI, S., PINZANI, M., ROMANELLI, R. G., LAFFI, G. & GENTILINI, P. (1998) Increased expression of monocyte chemotactic protein-1 during active hepatic fibrogenesis: correlation with monocyte infiltration. *Am J Pathol,* 152**,** 423-30.

MARRA, F., VALENTE, A. J., PINZANI, M. & ABBOUD, H. E. (1993) Cultured human liver fat-storing cells produce monocyte chemotactic protein-1. Regulation by proinflammatory cytokines. *J Clin Invest,* 92**,** 1674-80.

MARRERO, J. A. & LOK, A. S. (2004) Newer markers for hepatocellular carcinoma. *Gastroenterology,* 127**,** S113-9.

MARSHALL, W. J. & MCLEAN, A. E. (1969) The effect of nutrition and hormonal status on cytochrome P-450 and its induction. *Biochem J,* 115**,** 27P-28P.

MARSILLACH, J., CAMPS, J., FERRE, N., BELTRAN, R., RULL, A., MACKNESS, B., MACKNESS, M. & JOVEN, J. (2009) Paraoxonase-1 is related to inflammation, fibrosis and PPAR delta in experimental liver disease. *BMC Gastroenterol,* 9**,** 3.

MARTINEZ, S. M., CRESPO, G., NAVASA, M. & FORNS, X. (2011) Non-invasive assessment of liver fibrosis. *Hepatology,* 53**,** 325-35.

MATSUBARA, T., MORI, S., TOUCHI, A., MASUDA, Y. & TAKEUCHI, Y. (1983) Carbon tetrachloride-induced hepatotoxicity in rats: evidence for different susceptibilities of rat liver lobes. *Jpn J Pharmacol,* 33**,** 435-45.

MAUGEAIS, C., TIETGE, U. J., TSUKAMOTO, K., GLICK, J. M. & RADER, D. J. (2000) Hepatic apolipoprotein E expression promotes very low density lipoprotein-apolipoprotein B production *in vivo* in mice. *J Lipid Res,* 41**,** 1673-9.

MAYEUX, R. (2004) Biomarkers: potential uses and limitations. *NeuroRx,* 1**,** 182-8.

MCANULTY, R. J., CAMPA, J. S., CAMBREY, A. D. & LAURENT, G. J. (1991) The effect of transforming growth factor beta on rates of procollagen synthesis and degradation *in vitro*. *Biochim Biophys Acta,* 1091**,** 231-5.

MCQUEEN, C. (2010) *Comprehensive toxicology,* Second edition, Elsevier.978-0-08-046868-6

MENDY, M. & WALTON, R. (2009) Molecular pathogenesis and early detection of hepatocellular carcinoma--perspectives from West Africa. *Cancer Lett,* 286**,** 44-51.

MICHAEL, B., YANO, B., SELLERS, R. S., PERRY, R., MORTON, D., ROOME, N., JOHNSON, J. K., SCHAFER, K. & PITSCH, S. (2007) Evaluation of organ weights for rodent and non-rodent toxicity studies: a review of regulatory guidelines and a survey of current practices. *Toxicol Pathol,* 35**,** 742-50.

MICHALOPOULOS, G. K. (2007) Liver regeneration. *J Cell Physiol,* 213**,** 286-300.

MICHALOPOULOS, G. K. (2011) Liver regeneration: alternative epithelial pathways. *Int J Biochem Cell Biol,* 43**,** 173-9.

MINEHIRA, K., YOUNG, S. G., VILLANUEVA, C. J., YETUKURI, L., ORESIC, M., HELLERSTEIN, M. K., FARESE, R. V., JR., HORTON, J. D., PREITNER, F., THORENS, B. & TAPPY, L. (2008) Blocking VLDL secretion causes hepatic steatosis but does not affect peripheral lipid stores or insulin sensitivity in mice. *J Lipid Res,* 49**,** 2038-44.

MIRPURI, E., GARCíA-TREVIJANO, E. R., CASTILLA-CORTAZAR, I., BERASAIN, C., QUIROGA, J., RODRIGUEZ-ORTIGOSA, C., MATO, J. M., PRIETO, J. & AVILA, M. A. A. (2002) Altered liver gene expression in CCl4-cirrhotic rats is partially normalised by insulin-like growth factor-I. *The International Journal of Biochemistry & Cell Biology,* 34**,** 242-252.

MISHRA, J., MORI, K., MA, Q., KELLY, C., BARASCH, J. & DEVARAJAN, P. (2004) Neutrophil gelatinase-associated lipocalin: a novel early urinary biomarker for cisplatin nephrotoxicity. *Am J Nephrol,* 24**,** 307-15.

MITCH, W. E. & WALSER, M. (1978) A proposed mechanism for reduced creatinine excretion in severe chronic renal failure. *Nephron,* 21**,** 248-54.

MIURA, K., GOLDSTEIN, R. S., MORGAN, D. G., PASINO, D. A., HEWITT, W. R. & HOOK, J. B. (1987) Age-related differences in susceptibility to renal ischemia in rats. *Toxicol Appl Pharmacol,* 87**,** 284-96.

MIYATA, T., JADOUL, M., KUROKAWA, K. & VAN YPERSELE DE STRIHOU, C. (1998) Beta-2 microglobulin in renal disease. *J Am Soc Nephrol,* 9**,** 1723-35.

MIYAZAKI, T., KARUBE, M., MATSUZAKI, Y., IKEGAMI, T., DOY, M., TANAKA, N. & BOUSCAREL, B. (2005) Taurine inhibits oxidative damage and prevents fibrosis in carbon tetrachloride-induced hepatic fibrosis. *J Hepatol,* 43**,** 117-25.

MIYAZAKI, T., MATSUZAKI, Y., IKEGAMI, T., MIYAKAWA, S., DOY, M., TANAKA, N. & BOUSCAREL, B. (2004) The harmful effect of exercise on reducing taurine concentration in the tissues of rats treated with CCl4 administration. *J Gastroenterol,* 39**,** 557-62.

MOCHIDA, S., OGATA, I., OHTA, Y., YAMADA, S. & FUJIWARA, K. (1989) *In situ* evaluation of the stimulatory state of hepatic macrophages based on their ability to produce superoxide anions in rats. *J Pathol,* 158**,** 67-71.

MONTEIRO, M. S., CARVALHO, M., BASTOS, M. L. & GUEDES DE PINHO, P. (2013) Metabolomics analysis for biomarker discovery: advances and challenges. *Curr Med Chem,* 20**,** 257-71.

MONTFORT, I. & PEREZ-TAMAYO, R. (1978) Collagenase in experimental carbon tetrachloride cirrhosis of the liver. *Am J Pathol,* 92**,** 411-20.

MOSS, G. A., BONDAR, R. J. & BUZZELLI, D. M. (1975) Kinetic enzymatic method for determining serum creatinine. *Clin Chem,* 21**,** 1422-6.

MOTTA, P. M. (1984) The three-dimensional microanatomy of the liver. *Arch Histol Jpn,* 47**,** 1-30.

MURPHY, G., DOCHERTY, A. J., HEMBRY, R. M. & REYNOLDS, J. J. (1991) Metalloproteinases and tissue damage. *Br J Rheumatol,* 30 Suppl 1**,** 25-31.

NAGASE, H., VISSE, R. & MURPHY, G. (2006) Structure and function of matrix metalloproteinases and TIMPs. *Cardiovasc Res,* 69**,** 562-73.

NAITO, M., HASEGAWA, G., EBE, Y. & YAMAMOTO, T. (2004) Differentiation and function of Kupffer cells. *Med Electron Microsc,* 37**,** 16-28.

NAKAI, K., TANAKA, H., HANADA, K., OGATA, H., SUZUKI, F., KUMADA, H., MIYAJIMA, A., ISHIDA, S., SUNOUCHI, M., HABANO, W., KAMIKAWA, Y., KUBOTA, K., KITA, J., OZAWA, S. & OHNO, Y. (2008) Decreased expression of cytochromes P450 1A2, 2E1, and 3A4 and drug transporters Na+-taurocholate-cotransporting polypeptide, organic cation transporter 1, and organic anion-transporting peptide-C correlates with the progression of liver fibrosis in chronic hepatitis C patients. *Drug Metab Dispos,* 36**,** 1786-93.

NAKATSUKASA, H., NAGY, P., EVARTS, R. P., HSIA, C. C., MARSDEN, E. & THORGEIRSSON, S. S. (1990) Cellular distribution of transforming growth factor-beta

1 and procollagen types I, III, and IV transcripts in carbon tetrachloride-induced rat liver fibrosis. *J Clin Invest,* 85**,** 1833-43.

NASH, J. A., KING, L. J., LOCK, E. A. & GREEN, T. (1984) The metabolism and disposition of hexachloro-1:3-butadiene in the rat and its relevance to nephrotoxicity. *Toxicol Appl Pharmacol,* 73**,** 124-37.

NATH, K. A. (2006) Heme oxygenase-1: a provenance for cytoprotective pathways in the kidney and other tissues. *Kidney Int,* 70**,** 432-43.

NEUHAUS, O. W. & FLORY, W. (1978) Age-dependent changes in the excretion of urinary proteins by the rat. *Nephron,* 22**,** 570-6.

NICHOLLS, A. W., HOLMES, E., LINDON, J. C., SHOCKCOR, J. P., FARRANT, R. D., HASELDEN, J. N., DAMMENT, S. J., WATERFIELD, C. J. & NICHOLSON, J. K. (2001) Metabonomic investigations into hydrazine toxicity in the rat. *Chem Res Toxicol,* 14**,** 975-87.

NICHOLSON, J., KEUN, H. & EBBELS, T. (2007) COMET and the challenge of drug safety screening. *J Proteome Res,* 6**,** 4098-9.

NICHOLSON, J. K., TIMBRELL, J. A. & SADLER, P. J. (1985) Proton NMR spectra of urine as indicators of renal damage. Mercury-induced nephrotoxicity in rats. *Mol Pharmacol,* 27**,** 644-51.

NIKI, T., DE BLESER, P. J., XU, G., VAN DEN BERG, K., WISSE, E. & GEERTS, A. (1996) Comparison of glial fibrillary acidic protein and desmin staining in normal and CCl4-induced fibrotic rat livers. *Hepatology,* 23**,** 1538-45.

NIOI, P. & HAYES, J. D. (2004) Contribution of NAD(P)H:quinone oxidoreductase 1 to protection against carcinogenesis, and regulation of its gene by the Nrf2 basic-region leucine zipper and the arylhydrocarbon receptor basic helix-loop-helix transcription factors. *Mutat Res,* 555**,** 149-71.

NISHIURA, T., WATANABE, H., ITO, M., MATSUOKA, Y., YANO, K., DAIKOKU, M., YATSUHASHI, H., DOHMEN, K. & ISHIBASHI, H. (2005) Ultrasound evaluation of the fibrosis stage in chronic liver disease by the simultaneous use of low and high frequency probes. *Br J Radiol,* 78**,** 189-97.

NIU, Y., JIANG, Y., XU, C., WANG, X., LIU, Y., ZHAO, H., HAN, B. & JIANG, L. (2012) Preliminary results of metabolite in serum and urine of lung cancer patients detected by metabolomics. *Zhongguo Fei Ai Za Zhi,* 15**,** 195-201.

NORDLIE, R. C., FOSTER, J. D. & LANGE, A. J. (1999) Regulation of glucose production by the liver. *Annu Rev Nutr,* 19**,** 379-406.

NOTO, A., OGAWA, Y., MORI, S., YOSHIOKA, M., KITAKAZE, T., HORI, T., NAKAMURA, M. & MIYAKE, T. (1983) Simple, rapid spectrophotometry of urinary N-acetyl-beta-D-glucosaminidase, with use of a new chromogenic substrate. *Clin Chem,* 29**,** 1713-6.

O'BRIEN, P. J., SLAUGHTER, M. R., POLLEY, S. R. & KRAMER, K. (2002) Advantages of glutamate dehydrogenase as a blood biomarker of acute hepatic injury in rats. *Lab Anim,* 36**,** 313-21.

OGETURK, M., KUS, I., KAVAKLI, A., ONER, J., KUKNER, A. & SARSILMAZ, M. (2005) Reduction of carbon tetrachloride-induced nephropathy by melatonin administration. *Cell Biochem Funct,* 23**,** 85-92.

OLASO, E. & FRIEDMAN, S. L. (1998) Molecular regulation of hepatic fibrogenesis. *J Hepatol,* 29**,** 836-47.

OLIVER, S. G., WINSON, M. K., KELL, D. B. & BAGANZ, F. (1998) Systematic functional analysis of the yeast genome. *Trends in Biotechnology,* 16**,** 373-378.

OLSON, M. J., JOHNSON, J. T. & REIDY, C. A. (1990) A comparison of male rat and human urinary proteins: implications for human resistance to hyaline droplet nephropathy. *Toxicol Appl Pharmacol,* 102**,** 524-36.

OTIENO, M. A., BAGGS, R. B., HAYES, J. D. & ANDERS, M. W. (1997) Immunolocalization of microsomal glutathione S-transferase in rat tissues. *Drug Metab Dispos,* 25**,** 12-20.

OUTWATER, E. K. (2010) Imaging of the liver for hepatocellular cancer. *Cancer Control,* 17**,** 72-82.

OWEN, R. A. & HEYWOOD, R. (1986) Age-related variations in renal structure and function in Sprague-Dawley rats. *Toxicol Pathol,* 14**,** 158-67.

OZTURK, F., UCAR, M., OZTURK, I. C., VARDI, N. & BATCIOGLU, K. (2003) Carbon tetrachloride-induced nephrotoxicity and protective effect of betaine in Sprague-Dawley rats. *Urology,* 62**,** 353-6.

PAAKKO, P., ANTTILA, S., SORMUNEN, R., ALA-KOKKO, L., PEURA, R., FERRANS, V. J. & RYHANEN, L. (1996) Biochemical and morphological characterization of carbon tetrachloride-induced lung fibrosis in rats. *Arch Toxicol,* 70**,** 540-52.

PAGE-MCCAW, A., EWALD, A. J. & WERB, Z. (2007) Matrix metalloproteinases and the regulation of tissue remodelling. *Nat Rev Mol Cell Biol,* 8**,** 221-33.

PAHLER, A., BIRNER, G., OTT, M. M. & DEKANT, W. (1997) Binding of hexachlorobutadiene to alpha 2u-globulin and its role in nephrotoxicity in rats. *Toxicol Appl Pharmacol,* 147**,** 372-80.

PAN, Z. & RAFTERY, D. (2007) Comparing and combining NMR spectroscopy and mass spectrometry in metabolomics. *Anal Bioanal Chem,* 387**,** 525-7.

PARAGAS, N., QIU, A., ZHANG, Q., SAMSTEIN, B., DENG, S. X., SCHMIDT-OTT, K. M., VILTARD, M., YU, W., FORSTER, C. S., GONG, G., LIU, Y., KULKARNI, R., MORI, K., KALANDADZE, A., RATNER, A. J., DEVARAJAN, P., LANDRY, D. W., D'AGATI, V., LIN, C. S. & BARASCH, J. (2011) The Ngal reporter mouse detects the response of the kidney to injury in real time. *Nat Med,* 17**,** 216-22.

PARKIN, D. M., BRAY, F., FERLAY, J. & PISANI, P. (2005) Global cancer statistics, 2002. *CA Cancer J Clin,* 55**,** 74-108.

PARSONS, C. J., BRADFORD, B. U., PAN, C. Q., CHEUNG, E., SCHAUER, M., KNORR, A., KREBS, B., KRAFT, S., ZAHN, S., BROCKS, B., FEIRT, N., MEI, B., CHO, M. S., RAMAMOORTHI, R., ROLDAN, G., NG, P., LUM, P., HIRTH-DIETRICH, C., TOMKINSON, A. & BRENNER, D. A. (2004) Antifibrotic effects of a tissue inhibitor of metalloproteinase-1 antibody on established liver fibrosis in rats. *Hepatology,* 40**,** 1106-15.

PELLICORO, A., AUCOTT, R. L., RAMACHANDRAN, P., ROBSON, A. J., FALLOWFIELD, J. A., SNOWDON, V. K., HARTLAND, S. N., VERNON, M., DUFFIELD, J. S., BENYON, R. C., FORBES, S. J. & IREDALE, J. P. (2012a) Elastin accumulation is regulated at the level of degradation by macrophage metalloelastase (MMP-12) during experimental liver fibrosis. *Hepatology,* 55**,** 1965-75.

PELLICORO, A., RAMACHANDRAN, P. & IREDALE, J. P. (2012b) Reversibility of liver fibrosis. *Fibrogenesis Tissue Repair,* 5 Suppl 1**,** S26.

PENCIL, S. D., BRATTIN, W. J., JR., GLENDE, E. A., JR. & RECKNAGEL, R. O. (1984) Evidence against involvement of calcium in carbon tetrachloride-dependent inhibition of lipid secretion by isolated hepatocytes. *Biochem Pharmacol,* 33**,** 2425-9.

PENNEMANS, V., DE WINTER, L. M., MUNTERS, E., NAWROT, T. S., VAN KERKHOVE, E., RIGO, J. M., REYNDERS, C., DEWITTE, H., CARLEER, R., PENDERS, J. & SWENNEN, Q. (2011) The association between urinary kidney injury molecule 1 and urinary cadmium in elderly during long-term, low-dose cadmium exposure: a pilot study. *Environ Health,* 10**,** 77.

PERAZELLA, M. A. (2009) Renal vulnerability to drug toxicity. *Clin J Am Soc Nephrol,* 4**,** 1275-83.

PERSY, V. P., VERSTREPEN, W. A., YSEBAERT, D. K., DE GREEF, K. E. & DE BROE, M. E. (1999) Differences in osteopontin up-regulation between proximal and distal tubules after renal ischemia/reperfusion. *Kidney Int,* 56**,** 601-11.

PETERS, J. M. & BOYD, E. M. (1966) Organ weights and water levels of the rat following reduced food intake. *J Nutr,* 90**,** 354-60.

PETERSEN, K. F., KRSSAK, M., NAVARRO, V., CHANDRAMOULI, V., HUNDAL, R., SCHUMANN, W. C., LANDAU, B. R. & SHULMAN, G. I. (1999) Contributions of net hepatic glycogenolysis and gluconeogenesis to glucose production in cirrhosis. *Am J Physiol,* 276**,** E529-35.

PETRIDES, A. S., STANLEY, T., MATTHEWS, D. E., VOGT, C., BUSH, A. J. & LAMBETH, H. (1998) Insulin resistance in cirrhosis: prolonged reduction of hyperinsulinemia normalizes insulin sensitivity. *Hepatology,* 28**,** 141-9.

PFALLER, W. & GSTRAUNTHALER, G. (1998) Nephrotoxicity testing *in vitro*--what we know and what we need to know. *Environ Health Perspect,* 106 Suppl 2**,** 559-69.

PINCHES, M., BETTS, C., BICKERTON, S., BURDETT, L., THOMAS, H., DERBYSHIRE, N., JONES, H. B. & MOORES, M. (2012) Evaluation of novel renal

biomarkers with a cisplatin model of kidney injury: gender and dosage differences. *Toxicol Pathol,* 40**,** 522-33.

PINZANI, M., ROSSELLI, M. & ZUCKERMANN, M. (2011) Liver cirrhosis. *Best Pract Res Clin Gastroenterol,* 25**,** 281-90.

POPOVTZER, M. M., PINGGERA, W. F., HOLMES, J. H., HALGRIMSON, C. G. & STARZL, T. E. (1971) Hypernatremia. Complication of renal homotransplantation. *Archives of internal medicine,* 127**,** 1129-1132.

POPPER, H. & UENFRIEND, S. (1970) Hepatic fibrosis. Correlation of biochemical and morphologic investigations. *Am J Med,* 49**,** 707-21.

POST, J., EARLE, D. P., PATEK, A. J. & VICTOR, J. (1942) Effects of Yeast and Food Intake on Experimental carbon Tetrachloride Cirrhosis of the Liver in the Rat. *Am J Pathol,* 18**,** 661-73.

PROCTOR, E. & CHATAMRA, K. (1983) Controlled induction of cirrhosis in the rat. *Br J Exp Pathol,* 64**,** 320-30.

RAMACHANDRAN, P. & IREDALE, J. P. (2012) Liver fibrosis: a bidirectional model of fibrogenesis and resolution. *QJM,* 105**,** 813-7.

RAMADORI, G., MORICONI, F., MALIK, I. & DUDAS, J. (2008) Physiology and pathophysiology of liver inflammation, damage and repair. *J Physiol Pharmacol,* 59 Suppl 1**,** 107-17.

RAMAIAH, S. K. (2007) A toxicologist guide to the diagnostic interpretation of hepatic biochemical parameters. *Food Chem Toxicol,* 45**,** 1551-7.

RAO, K. S. & RECKNAGEL, R. O. (1968) Early onset of lipoperoxidation in rat liver after carbon tetrachloride administration. *Exp Mol Pathol,* 9**,** 271-8.

RAO, K. S. & RECKNAGEL, R. O. (1969) Early incorporation of carbon-labeled carbon tetrachloride into rat liver particulate lipids and proteins. *Exp Mol Pathol,* 10**,** 219-28.

RAO, M. S. & REDDY, J. K. (2001) Peroxisomal beta-oxidation and steatohepatitis. *Semin Liver Dis,* 21**,** 43-55.

RAO, P. S., DALU, A., KULKARNI, S. G. & MEHENDALE, H. M. (1996) Stimulated tissue repair prevents lethality in isopropanol-induced potentiation of carbon tetrachloride hepatotoxicity. *Toxicol Appl Pharmacol,* 140**,** 235-44.

RAO, P. S., MANGIPUDY, R. S. & MEHENDALE, H. M. (1997) Tissue injury and repair as parallel and opposing responses to CCl4 hepatotoxicity: a novel dose-response. *Toxicology,* 118**,** 181-93.

RAPPAPORT, A. M. (1958) The structural and functional unit in the human liver (liver acinus). *Anat Rec,* 130**,** 673-89.

Rec Gscc (DGKC) (1972) Optimised standard colorimetric methods. *J Clin Chem Clin Biochem* 10:182.

RECKNAGEL, R. O. (1967) Carbon tetrachloride hepatotoxicity. *Pharmacol Rev,* 19**,** 145-208.

RECKNAGEL, R. O. (1983) A new direction in the study of carbon tetrachloride hepatotoxicity. *Life Sci,* 33**,** 401-8.

RECKNAGEL, R. O. & GHOSHAL, A. K. (1966) Lipoperoxidation of rat liver microsomal lipids induced by carbon tetrachloride. *Nature,* 210**,** 1162-3.

RECKNAGEL, R. O., GLENDE, E. A., JR., DOLAK, J. A. & WALLER, R. L. (1989) Mechanisms of carbon tetrachloride toxicity. *Pharmacol Ther,* 43**,** 139-54.

REDDY, J. K. & RAO, M. S. (2006) Lipid metabolism and liver inflammation. II. Fatty liver disease and fatty acid oxidation. *Am J Physiol Gastrointest Liver Physiol,* 290**,** G852-8.

REES, K. R., SINHA, K. P. & SPECTOR, W. G. (1961) The pathogenesis of liver injury in carbon tetrachloride and thioacetamide poisoning. *J Pathol Bacteriol,* 81**,** 107-18.

RENAUD, H. J., CUI, J. Y., KHAN, M. & KLAASSEN, C. D. (2011) Tissue distribution and gender-divergent expression of 78 cytochrome P450 mRNAs in mice. *Toxicol Sci,* 124**,** 261-77.

REZZI, S., RAMADAN, Z., FAY, L. B. & KOCHHAR, S. (2007) Nutritional metabonomics: applications and perspectives. *J Proteome Res,* 6**,** 513-25.

RIKANS, L. E. (1989) Hepatic drug metabolism in female Fischer rats as a function of age. *Drug Metab Dispos,* 17**,** 114-6.

RIKANS, L. E., DECICCO, L. A., HORNBROOK, K. R. & YAMANO, T. (1999) Effect of age and carbon tetrachloride on cytokine concentrations in rat liver. *Mech Ageing Dev,* 108**,** 173-82.

RIKANS, L. E. & NOTLEY, B. A. (1982) Age-related changes in hepatic microsomal drug metabolism are substrate selective. *J Pharmacol Exp Ther,* 220**,** 574-8.

RINNERT, M., HINZ, M., BUHTZ, P., REIHER, F., LESSEL, W. & HOFFMANN, W. (2010) Synthesis and localization of trefoil factor family (TFF) peptides in the human urinary tract and TFF2 excretion into the urine. *Cell Tissue Res,* 339**,** 639-47.

ROBB, G. W., AMANN, R. P. & KILLIAN, G. J. (1978) Daily sperm production and epididymal sperm reserves of pubertal and adult rats. *J Reprod Fertil,* 54**,** 103-7.

ROBERTSON, D. G. (2005) Metabonomics in toxicology: a review. *Toxicol Sci,* 85**,** 809-22.

ROBERTSON, D. G., REILY, M. D., SIGLER, R. E., WELLS, D. F., PATERSON, D. A. & BRADEN, T. K. (2000) Metabonomics: evaluation of nuclear magnetic resonance (NMR) and pattern recognition technology for rapid *in vivo* screening of liver and kidney toxicants. *Toxicol Sci,* 57**,** 326-37.

ROCKEY, D. C. (1997) New concepts in the pathogenesis of portal hypertension: hepatic wounding and stellate cell contractility. *Clin Liver Dis,* 1**,** 13-29.

ROCKEY, D. C., WEYMOUTH, N. & SHI, Z. (2013) Smooth Muscle alpha Actin (Acta2) and Myofibroblast Function during Hepatic Wound Healing. *PLoS One,* 8**,** e77166.

RODERFELD, M., GEIER, A., DIETRICH, C. G., SIEWERT, E., JANSEN, B., GARTUNG, C. & ROEB, E. (2006) Cytokine blockade inhibits hepatic tissue inhibitor of metalloproteinase-1 expression and up-regulates matrix metalloproteinase-9 in toxic liver injury. *Liver Int,* 26**,** 579-86.

ROKUSHIMA, M., FUJISAWA, K., FURUKAWA, N., ITOH, F., YANAGIMOTO, T., FUKUSHIMA, R., ARAKI, A., OKADA, M., TORII, M., KATO, I., ISHIZAKI, J. & OMI, K. (2008) Transcriptomic analysis of nephrotoxicity induced by cephaloridine, a representative cephalosporin antibiotic. *Chem Res Toxicol,* 21**,** 1186-96.

ROPERO-MILLER, J. D., PAGET-WILKES, H., DOERING, P. L. & GOLDBERGER, B. A. (2000) Effect of oral creatine supplementation on random urine creatinine, pH, and specific gravity measurements. *Clin Chem,* 46**,** 295-7.

ROSENBERG, M. E. & SILKENSEN, J. (1995) Clusterin and the kidney. *Exp Nephrol,* 3**,** 9-14.

ROSENBLOOM, J., MENDOZA, F. A. & JIMENEZ, S. A. (2013) Strategies for anti-fibrotic therapies. *Biochim Biophys Acta,* 1832**,** 1088-103.

ROSS, D. (2004) Quinone reductases multitasking in the metabolic world. *Drug Metab Rev,* 36**,** 639-54.

ROSSI, E., ADAMS, L., PRINS, A., BULSARA, M., DE BOER, B., GARAS, G., MACQUILLAN, G., SPEERS, D. & JEFFREY, G. (2003) Validation of the FibroTest biochemical markers score in assessing liver fibrosis in hepatitis C patients. *Clin Chem,* 49**,** 450-4.

ROSSI, E., ADAMS, L. A., BULSARA, M. & JEFFREY, G. P. (2007) Assessing liver fibrosis with serum marker models. *Clin Biochem Rev,* 28**,** 3-10.

ROSTAMI, S. & PARSIAN, H. (2013) Hyaluronic acid: from biochemical characteristics to its clinical translation in assessment of liver fibrosis. *Hepat Mon,* 13**,** e13787.

ROUSSEAU, R., GOVAERTS, B., VERLEYSEN, M. & BOULANGER, B. (2008) Comparison of some chemometric tools for metabonomics biomarker identification. *Chemometrics and Intelligent Laboratory Systems,* 91**,** 54-66.

ROY, A. K., NEUHAUS, O. W. & HARMISON, C. R. (1966) Preparation and characterization of a sex-dependent rat urinary protein. *Biochim Biophys Acta,* 127**,** 72-81.

ROZELL, B., HANSSON, H. A., GUTHENBERG, C., TAHIR, M. K. & MANNERVIK, B. (1993) Glutathione transferases of classes alpha, mu and pi show selective expression in different regions of rat kidney. *Xenobiotica,* 23**,** 835-49.

RUDMAN, D., DIFULCO, T. J., GALAMBOS, J. T., SMITH, R. B., 3RD, SALAM, A. A. & WARREN, W. D. (1973) Maximal rates of excretion and synthesis of urea in normal and cirrhotic subjects. *J Clin Invest,* 52**,** 2241-9.

SADEGHNIA, H. R., YOUSEFSANI, B. S., RASHIDFAR, M., BOROUSHAKI, M. T., ASADPOUR, E. & GHORBANI, A. (2013) Protective effect of rutin on hexachlorobutadiene-induced nephrotoxicity. *Ren Fail,* 35**,** 1151-5.

SAEGUSA, S., ISAJI, S. & KAWARADA, Y. (2002) Changes in serum hyaluronic acid levels and expression of CD44 and CD44 mRNA in hepatic sinusoidal endothelial cells after major hepatectomy in cirrhotic rats. *World J Surg,* 26**,** 694-9.

SANCHEZ-CARBAYO, M., URRUTIA, M., GONZALEZ DE BUITRAGO, J. M. & NAVAJO, J. A. (2000) Evaluation of two new urinary tumor markers: bladder tumor fibronectin and cytokeratin 18 for the diagnosis of bladder cancer. *Clin Cancer Res,* 6**,** 3585-94.

SANDS, J. M. & LAYTON, H. E. (2009) The physiology of urinary concentration: an update. *Semin Nephrol,* 29**,** 178-95.

SASAKI, Y. (2006) Does oxidative stress participate in the development of hepatocellular carcinoma? *J Gastroenterol,* 41**,** 1135-48.

SAXENA, R., THEISE, N. D. & CRAWFORD, J. M. (1999) Microanatomy of the human liver-exploring the hidden interfaces. *Hepatology,* 30**,** 1339-46.

SCATENA, R., BOTTONI, P., BOTTA, G., MARTORANA, G. E. & GIARDINA, B. (2007) The role of mitochondria in pharmacotoxicology: a reevaluation of an old, newly emerging topic. *Am J Physiol Cell Physiol,* 293**,** C12-21.

SCHEUER, P. J. (1970) Liver biopsy in the diagnosis of cirrhosis. *Gut,* 11**,** 275-8.

SCHMIDT, E. S. & SCHMIDT, F. W. (1988) Glutamate dehydrogenase: biochemical and clinical aspects of an interesting enzyme. *Clin Chim Acta,* 173**,** 43-55.

SCHMUCKER, D. L. & WANG, R. K. (1981) Effects of aging and phenobarbital on the rat liver microsomal drug-metabolizing system. *Mech Ageing Dev,* 15**,** 189-202.

SCHREIER, C., KREMER, W., HUBER, F., NEUMANN, S., PAGEL, P., LIENEMANN, K. & PESTEL, S. (2013) Reproducibility of NMR Analysis of Urine Samples: Impact of Sample Preparation, Storage Conditions, and Animal Health Status. *BioMed Research International,* 2013**,** 19.

SCHRENK, D. & DEKANT, W. (1989) Covalent binding of hexachlorobutadiene metabolites to renal and hepatic mitochondrial DNA. *Carcinogenesis,* 10**,** 1139-41.

SCHRIER, R. W. (2008) Blood urea nitrogen and serum creatinine: not married in heart failure. *Circ Heart Fail,* 1**,** 2-5.

SCHUPPAN, D. & AFDHAL, N. H. (2008) Liver cirrhosis. *Lancet,* 371**,** 838-51.

SCHWEDHELM, E., BARTLING, A., LENZEN, H., TSIKAS, D., MAAS, R., BRUMMER, J., GUTZKI, F. M., BERGER, J., FROLICH, J. C. & BOGER, R. H.

(2004) Urinary 8-iso-prostaglandin F2alpha as a risk marker in patients with coronary heart disease: a matched case-control study. *Circulation,* 109**,** 843-8.

SELLERS, A. L., GOODMAN, H. C., MARMORSTON, J. & SMITH, M. (1950) Sex difference in proteinuria in the rat. *Am J Physiol,* 163**,** 662-7.

SELMI, C., BOWLUS, C. L., GERSHWIN, M. E. & COPPEL, R. L. (2011) Primary biliary cirrhosis. *Lancet,* 377**,** 1600-9.

SERPAGGI, J., CARNOT, F., NALPAS, B., CANIONI, D., GUECHOT, J., LEBRAY, P., VALLET-PICHARD, A., FONTAINE, H., BEDOSSA, P. & POL, S. (2006) Direct and indirect evidence for the reversibility of cirrhosis. *Hum Pathol,* 37**,** 1519-26.

SHARKIS, D. H. & SWENSON, R. P. (1989) Purification by cibacron blue F3GA dye affinity chromatography and comparison of NAD(P)H:quinone reductase (E.C.1.6.99.2) from rat liver cytosol and microsomes. *Biochem Biophys Res Commun,* 161**,** 434-41.

SHERWOOD, L. (2013) *Human physiology: from cells to systems,* Eighth Edition, Yolanda Cossio.19-978-1-111-57743-8

SHIHABI, Z. K., KONEN, J. C. & O'CONNOR, M. L. (1991) Albuminuria vs urinary total protein for detecting chronic renal disorders. *Clin Chem,* 37**,** 621-4.

SHMAEFSKY, B. (2006) *Biotechnology 101,* First edition, Greenwood Press.0-313-33528-1

SIEBUHR, A. S., WANG, J., KARSDAL, M., BAY-JENSEN, A. C., Y, J. & Q, Z. (2012) Matrix metalloproteinase-dependent turnover of cartilage, synovial membrane, and connective tissue is elevated in rats with collagen induced arthritis. *J Transl Med,* 10**,** 195.

SIEGEL, D., GUSTAFSON, D. L., DEHN, D. L., HAN, J. Y., BOONCHOONG, P., BERLINER, L. J. & ROSS, D. (2004) NAD(P)H:quinone oxidoreductase 1: role as a superoxide scavenger. *Mol Pharmacol,* 65**,** 1238-47.

SIEGMUND, S. V., DOOLEY, S. & BRENNER, D. A. (2005) Molecular mechanisms of alcohol-induced hepatic fibrosis. *Dig Dis,* 23**,** 264-74.

SKALLI, O., ROPRAZ, P., TRZECIAK, A., BENZONANA, G., GILLESSEN, D. & GABBIANI, G. (1986) A monoclonal antibody against alpha-smooth muscle actin: a new probe for smooth muscle differentiation. *J Cell Biol,* 103**,** 2787-96.

SLATER, T. F. (1966) Necrogenic action of carbon tetrachloride in the rat: a speculative mechanism based on activation. *Nature,* 209**,** 36-40.

SLATER, T. F. (1978) Mechanisms of protection against the damage produced in biological systems by oxygen-derived radicals. *Ciba Found Symp***,** 143-76.

SLATER, T. F., CHEESEMAN, K. H. & INGOLD, K. U. (1985) Carbon tetrachloride toxicity as a model for studying free-radical mediated liver injury. *Philos Trans R Soc Lond B Biol Sci,* 311**,** 633-45.

SLEYSTER, E. C. & KNOOK, D. L. (1982) Relation between localization and function of rat liver Kupffer cells. *Lab Invest,* 47**,** 484-90.

SLUPSKY, C. M., STEED, H., WELLS, T. H., DABBS, K., SCHEPANSKY, A., CAPSTICK, V., FAUGHT, W. & SAWYER, M. B. (2010) Urine metabolite analysis offers potential early diagnosis of ovarian and breast cancers. *Clin Cancer Res,* 16**,** 5835-41.

SMYTH, R., LANE, C. S., ASHIQ, R., TURTON, J. A., CLARKE, C. J., DARE, T. O., YORK, M. J., GRIFFITHS, W. & MUNDAY, M. R. (2009a) Proteomic investigation of urinary markers of carbon-tetrachloride-induced hepatic fibrosis in the Hanover Wistar rat. *Cell Biol Toxicol,* 25**,** 499-512.

SMYTH, R., MUNDAY, M. R., YORK, M. J., CLARKE, C. J., DARE, T. & TURTON, J. A. (2007) Comprehensive characterization of serum clinical chemistry parameters and the identification of urinary superoxide dismutase in a carbon tetrachloride-induced model of hepatic fibrosis in the female Hanover Wistar rat. *Int J Exp Pathol,* 88**,** 361-76.

SMYTH, R., MUNDAY, M. R., YORK, M. J., CLARKE, C. J., DARE, T. & TURTON, J. A. (2009b) Dose response and time course studies on superoxide dismutase as a urinary biomarker of carbon tetrachloride-induced hepatic injury in the Hanover Wistar rat. *Int J Exp Pathol,* 90**,** 500-11.

SMYTH, R., TURTON, J. A., CLARKE, C. J., YORK, M. J., DARE, T. O., LANE, C. S. & MUNDAY, M. R. (2008) Identification of superoxide dismutase as a potential urinary marker of carbon tetrachloride-induced hepatic toxicity. *Food Chem Toxicol,* 46**,** 2972-83.

SOHRABPOUR, A. A., MOHAMADNEJAD, M. & MALEKZADEH, R. (2012) Review article: the reversibility of cirrhosis. *Aliment Pharmacol Ther,* 36**,** 824-32.

SOLTER, P. F. (2005) Clinical pathology approaches to hepatic injury. *Toxicol Pathol,* 33**,** 9-16.

STANDISH, R. A., CHOLONGITAS, E., DHILLON, A., BURROUGHS, A. K. & DHILLON, A. P. (2006) An appraisal of the histopathological assessment of liver fibrosis. *Gut,* 55**,** 569-78.

STEVENS, J. L. (1985a) Cysteine conjugate beta-lyase activities in rat kidney cortex: subcellular localization and relationship to the hepatic enzyme. *Biochem Biophys Res Commun,* 129**,** 499-504.

STEVENS, J. L. (1985b) Isolation and characterization of a rat liver enzyme with both cysteine conjugate beta-lyase and kynureninase activity. *J Biol Chem,* 260**,** 7945-50.

STOICA, B. A. & FADEN, A. I. (2010) Cell death mechanisms and modulation in traumatic brain injury. *Neurotherapeutics,* 7**,** 3-12.

STOWELL, R. E. & LEE, C. S. (1950) Histochemical studies of mouse liver after single feeding of carbon tetrachloride. *AMA Arch Pathol,* 50**,** 519-37.

STRIKER, G. E., SMUCKLER, E. A., KOHNEN, P. W. & NAGLE, R. B. (1968) Structural and functional changes in rat kidney during CCl4 intoxication. *Am J Pathol,* 53**,** 769-89.

STURGILL, M. G. & LAMBERT, G. H. (1997) Xenobiotic-induced hepatotoxicity: mechanisms of liver injury and methods of monitoring hepatic function. *Clin Chem,* 43**,** 1512-26.

SUGIHARA, N., FURUNO, K., KITA, N., MURAKAMI, T. & YATA, N. (1992) Plasma alpha 1-acid glycoprotein concentration in rats with chemical liver injury. *Chem Pharm Bull (Tokyo),* 40**,** 2516-9.

SUZUKI, Y., IMAI, K., TAKAI, K., HANAI, T., HAYASHI, H., NAIKI, T., NISHIGAKI, Y., TOMITA, E., SHIMIZU, M. & MORIWAKI, H. (2013) Hepatocellular carcinoma patients with increased oxidative stress levels are prone to recurrence after curative treatment: a prospective case series study using the d-ROM test. *J Cancer Res Clin Oncol,* 139**,** 845-52.

SWAIN, A., TURTON, J., SCUDAMORE, C., MAGUIRE, D., PEREIRA, I., FREITAS, S., SMYTH, R., MUNDAY, M., STAMP, C., GANDHI, M., SONDH, S., ASHALL, H., FRANCIS, I., WOODFINE, J., BOWLES, J. & YORK, M. (2012) Nephrotoxicity of hexachloro-1:3-butadiene in the male Hanover Wistar rat; correlation of minimal histopathological changes with biomarkers of renal injury. *J Appl Toxicol,* 32**,** 417-28.

SWAIN, A., TURTON, J., SCUDAMORE, C. L., PEREIRA, I., VISWANATHAN, N., SMYTH, R., MUNDAY, M., MCCLURE, F., GANDHI, M., SONDH, S. & YORK, M. (2011) Urinary biomarkers in hexachloro-1:3-butadiene-induced acute kidney injury in the female Hanover Wistar rat; correlation of alpha-glutathione S-transferase, albumin and kidney injury molecule-1 with histopathology and gene expression. *J Appl Toxicol.*

SWAIN, M. G., VERGALLA, J. & JONES, E. A. (1993) Plasma endopeptidase 24.11 (enkephalinase) activity is markedly increased in cholestatic liver disease. *Hepatology,* 18**,** 556-8.

SWEENEY, G. D. (1981) Functional heterogeneity among liver cells: implications for drug toxicity and metabolism. *Trends in Pharmacological Sciences,* 2**,** 141-144.

SWENBERG, J. A. (1993) Alpha 2u-globulin nephropathy: review of the cellular and molecular mechanisms involved and their implications for human risk assessment. *Environ Health Perspect,* 101 Suppl 6**,** 39-44.

TAKAHASHI, T., MORITA, K., AKAGI, R. & SASSA, S. (2004) Heme oxygenase-1: a novel therapeutic target in oxidative tissue injuries. *Curr Med Chem,* 11**,** 1545-61.

TALAGERI, V. R., SAMARTH, K. D., BAXI, A. J. & VENKATARAMAN, P. R. (1951) Alkaline phosphatase levels in plasma and liver following carbon tetrachloride administration. *Br J Exp Pathol,* 32**,** 118-23.

TALKE, H. & SCHUBERT, G. E. (1965) Enzymatic Urea Determination in the Blood and Serum in the Warburg Optical Test. *Klin Wochenschr,* 43**,** 174-5.

TATEISHI, M., SUZUKI, S. & SHIMIZU, H. (1978) Cysteine conjugate beta-lyase in rat liver. A novel enzyme catalyzing formation of thiol-containing metabolites of drugs. *J Biol Chem,* 253**,** 8854-9.

TCHELEPI, H., RALLS, P. W., RADIN, R. & GRANT, E. (2002) Sonography of diffuse liver disease. *J Ultrasound Med,* 21**,** 1023-32; quiz 1033-4.

TESCHKE, R., VIERKE, W. & GELLERT, J. (1984) Effect of ethanol on carbon tetrachloride levels and hepatotoxicity after acute carbon tetrachloride poisoning. *Arch Toxicol,* 56**,** 78-82.

TESCHKE, R., VIERKE, W. & GOLDERMANN, L. (1983) Carbon tetrachloride (CCl4) levels and serum activities of liver enzymes following acute CCl4 intoxication. *Toxicol Lett,* 17**,** 175-80.

THAMPANITCHAWONG, P. & PIRATVISUTH, T. (1999) Liver biopsy:complications and risk factors. *World J Gastroenterol,* 5**,** 301-304.

THOMAS, P. E., BANDIERA, S., MAINES, S. L., RYAN, D. E. & LEVIN, W. (1987) Regulation of cytochrome P-450j, a high-affinity N-nitrosodimethylamine demethylase, in rat hepatic microsomes. *Biochemistry,* 26**,** 2280-9.

TIGGELMAN, A. M., LINTHORST, C., BOERS, W., BRAND, H. S. & CHAMULEAU, R. A. (1997) Transforming growth factor-beta-induced collagen synthesis by human liver myofibroblasts is inhibited by alpha2-macroglobulin. *J Hepatol,* 26**,** 1220-8.

TIMBRELL, J. A., WATERFIELD, C. J. & DRAPER, R. P. (1995) Use of urinary taurine and creatine as biomarkers of organ dysfunction and metabolic perturbations. *Comparative Haematology International,* 5**,** 112-119.

TJALVE, H. & LOFBERG, B. (1983) Extrahepatic sites of metabolism of carbon tetrachloride in rats. *Chem Biol Interact,* 46**,** 299-316.

TOWNSEND, D. M., DENG, M., ZHANG, L., LAPUS, M. G. & HANIGAN, M. H. (2003) Metabolism of Cisplatin to a nephrotoxin in proximal tubule cells. *J Am Soc Nephrol,* 14**,** 1-10.

TRETTER, L. & ADAM-VIZI, V. (2004) Generation of reactive oxygen species in the reaction catalyzed by alpha-ketoglutarate dehydrogenase. *J Neurosci,* 24**,** 7771-8.

TRUDELL, J. R., BOSTERLING, B. & TREVOR, A. J. (1982) Reductive metabolism of carbon tetrachloride by human cytochromes P-450 reconstituted in phospholipid vesicles: mass spectral identification of trichloromethyl radical bound to dioleoyl phosphatidylcholine. *Proc Natl Acad Sci U S A,* 79**,** 2678-82.

TRUDEN, J. L. & BOROS, D. L. (1988) Detection of alpha 2-macroglobulin, alpha 1-protease inhibitor, and neutral protease-antiprotease complexes within liver granulomas of *Schistosoma mansoni*-infected mice. *Am J Pathol,* 130**,** 281-8.

TURTON, J. & HOOSON, J. (2005) *Target organ pathology,* First edition, Taylor & Francis.0-203-48192-5

UGAZIO, G., KOCH, R. R. & RECKNAGEL, R. O. (1972) Mechanism of protection against carbon tetrachloride by prior carbon tetrachloride administration. *Exp Mol Pathol,* 16**,** 281-5.

UNANUE, E. R. (2007) Ito cells, stellate cells, and myofibroblasts: new actors in antigen presentation. *Immunity,* 26**,** 9-10.

VAIDYA, V. S., FERGUSON, M. A. & BONVENTRE, J. V. (2008) Biomarkers of acute kidney injury. *Annu Rev Pharmacol Toxicol,* 48**,** 463-93.

VAIDYA, V. S., OZER, J. S., DIETERLE, F., COLLINGS, F. B., RAMIREZ, V., TROTH, S., MUNIAPPA, N., THUDIUM, D., GERHOLD, D., HOLDER, D. J., BOBADILLA, N. A., MARRER, E., PERENTES, E., CORDIER, A., VONDERSCHER, J., MAURER, G., GOERING, P. L., SISTARE, F. D. & BONVENTRE, J. V. (2010) Kidney injury molecule-1 outperforms traditional biomarkers of kidney injury in preclinical biomarker qualification studies. *Nat Biotechnol,* 28**,** 478-85.

VAIDYA, V. S., RAMIREZ, V., ICHIMURA, T., BOBADILLA, N. A. & BONVENTRE, J. V. (2006) Urinary kidney injury molecule-1: a sensitive quantitative biomarker for early detection of kidney tubular injury. *Am J Physiol Renal Physiol,* 290**,** F517-29.

VAN HOOF, V. O., DENG, J. T. & DE BROE, M. E. (1997) How do plasma membranes reach the circulation? *Clin Chim Acta,* 266**,** 23-31.

VAN LIESHOUT, E. M., KNAPEN, M. F., LANGE, W. P., STEEGERS, E. A. & PETERS, W. H. (1998) Localization of glutathione S-transferases alpha and pi in human embryonic tissues at 8 weeks gestational age. *Hum Reprod,* 13**,** 1380-6.

VAN WAGENSVELD, B. A., SCHEEPERS, J. J., VAN GULIK, T. M., FREDERIKS, W. M., BLEEKER, W. K., OBERTOP, H. & GOUMA, D. J. (1997) Alpha glutathione S-transferase as novel parameter for hepatocellular damage in the isolated perfused rat liver. *Transplant Proc,* 29**,** 3449-51.

VASILIOU, V., ROSS, D. & NEBERT, D. W. (2006) Update of the NAD(P)H:quinone oxidoreductase (NQO) gene family. *Hum Genomics,* 2**,** 329-35.

VERHULST, A., PERSY, V. P., VAN ROMPAY, A. R., VERSTREPEN, W. A., HELBERT, M. F. & DE BROE, M. E. (2002) Osteopontin synthesis and localization along the human nephron. *J Am Soc Nephrol,* 13**,** 1210-8.

VERSTREPEN, W. A., PERSY, V. P., VERHULST, A., DAUWE, S. & DE BROE, M. E. (2001) Renal osteopontin protein and mRNA upregulation during acute nephrotoxicity in the rat. *Nephrol Dial Transplant,* 16**,** 712-24.

VETTORAZZI, A., WAIT, R., NAGY, J., MONREAL, J. I. & MANTLE, P. (2013) Changes in male rat urinary protein profile during puberty: a pilot study. *BMC Res Notes,* 6**,** 232.

VISSE, R. & NAGASE, H. (2003) Matrix metalloproteinases and tissue inhibitors of metalloproteinases: structure, function, and biochemistry. *Circ Res,* 92**,** 827-39.

VOLLHARDT, K. & SCHORE, N. (2003) *Organic chemistry,* Fourth edition, W. H. Freeman.0716743744

VOLLMAR, B., WOLF, B., SIEGMUND, S., KATSEN, A. D. & MENGER, M. D. (1997) Lymph vessel expansion and function in the development of hepatic fibrosis and cirrhosis. *Am J Pathol,* 151**,** 169-75.

WALKER, G. S., RYDER, T. F., SHARMA, R., SMITH, E. B. & FREUND, A. (2011) Validation of isolated metabolites from drug metabolism studies as analytical standards by quantitative NMR. *Drug Metab Dispos,* 39**,** 433-40.

WALLACE, D. C. (1999) Mitochondrial diseases in man and mouse. *Science,* 283**,** 1482-8.

WALLER, R. L. & RECKNAGEL, R. O. (1982) Evaluation of a role for phosgene production in the hepatotoxic mechanism of action of carbon tetrachloride and bromotrichloromethane. *Toxicol Appl Pharmacol,* 66**,** 172-81.

WALLIN, A., JONES, T. W., VERCESI, A. E., COTGREAVE, I., ORMSTAD, K. & ORRENIUS, S. (1987) Toxicity of S-pentachlorobutadienyl-L-cysteine studied with isolated rat renal cortical mitochondria. *Arch Biochem Biophys,* 258**,** 365-72.

WANG, E. J., SNYDER, R. D., FIELDEN, M. R., SMITH, R. J. & GU, Y. Z. (2008) Validation of putative genomic biomarkers of nephrotoxicity in rats. *Toxicology,* 246**,** 91-100.

WANG, H., LAFDIL, F., WANG, L., YIN, S., FENG, D. & GAO, B. (2011) Tissue inhibitor of metalloproteinase 1 (TIMP-1) deficiency exacerbates carbon tetrachloride-induced liver injury and fibrosis in mice: involvement of hepatocyte STAT3 in TIMP-1 production. *Cell Biosci,* 1**,** 14.

WANG, J. H., BYUN, J. & PENNATHUR, S. (2010a) Analytical approaches to metabolomics and applications to systems biology. *Semin Nephrol,* 30**,** 500-11.

WANG, L., TANG, Y., LIU, S., MAO, S., LING, Y., LIU, D., HE, X. & WANG, X. (2013) Metabonomic profiling of serum and urine by (1)H NMR-based spectroscopy discriminates patients with chronic obstructive pulmonary disease and healthy individuals. *PLoS One,* 8**,** e65675.

WANG, Y. P., CHENG, M. L., ZHANG, B. F., MU, M. & WU, J. (2010b) Effects of blueberry on hepatic fibrosis and transcription factor Nrf2 in rats. *World J Gastroenterol,* 16**,** 2657-63.

WARSKULAT, U., BORSCH, E., REINEHR, R., HELLER-STILB, B., MONNIGHOFF, I., BUCHCZYK, D., DONNER, M., FLOGEL, U., KAPPERT, G., SOBOLL, S., BEER, S., PFEFFER, K., MARSCHALL, H. U., GABRIELSEN, M., AMIRY-MOGHADDAM, M., OTTERSEN, O. P., DIENES, H. P. & HAUSSINGER, D. (2006) Chronic liver disease is triggered by taurine transporter knockout in the mouse. *FASEB J,* 20**,** 574-6.

WATANABE, N., KAMEI, S., OHKUBO, A., YAMANAKA, M., OHSAWA, S., MAKINO, K. & TOKUDA, K. (1986) Urinary protein as measured with a pyrogallol

red-molybdate complex, manually and in a Hitachi 726 automated analyzer. *Clin Chem,* 32**,** 1551-4.

WATERFIELD, C. J., ASKER, D. S., PATEL, S. & TIMBRELL, J. A. (1998) Is there a correlation between taurine levels and xenobiotic-induced perturbations in protein synthesis?: a study with tetracycline in rats. *Amino Acids,* 15**,** 161-77.

WATERFIELD, C. J., TURTON, J. A., SCALES, M. D. & TIMBRELL, J. A. (1991) Taurine, a possible urinary marker of liver damage: a study of taurine excretion in carbon tetrachloride-treated rats. *Arch Toxicol,* 65**,** 548-55.

WATERFIELD, C. J., TURTON, J. A., SCALES, M. D. & TIMBRELL, J. A. (1993) Investigations into the effects of various hepatotoxic compounds on urinary and liver taurine levels in rats. *Arch Toxicol,* 67**,** 244-54.

WATERS, E., WANG, J. H., REDMOND, H. P., WU, Q. D., KAY, E. & BOUCHIER-HAYES, D. (2001) Role of taurine in preventing acetaminophen-induced hepatic injury in the rat. *Am J Physiol Gastrointest Liver Physiol,* 280**,** G1274-9.

WATERS, N. J., WATERFIELD, C. J., FARRANT, R. D., HOLMES, E. & NICHOLSON, J. K. (2005) Metabonomic deconvolution of embedded toxicity: application to thioacetamide hepato- and nephrotoxicity. *Chem Res Toxicol,* 18**,** 639-54.

WAUTHIER, V., VERBEECK, R. K. & BUC CALDERON, P. (2004) Age-related changes in the protein and mRNA levels of CYP2E1 and CYP3A isoforms as well as in their hepatic activities in Wistar rats. What role for oxidative stress? *Arch Toxicol,* 78**,** 131-8.

WAXMAN, D. J., DANNAN, G. A. & GUENGERICH, F. P. (1985) Regulation of rat hepatic cytochrome P-450: age-dependent expression, hormonal imprinting, and xenobiotic inducibility of sex-specific isoenzymes. *Biochemistry,* 24**,** 4409-17.

WEBER, L. W., BOLL, M. & STAMPFL, A. (2003) Hepatotoxicity and mechanism of action of haloalkanes: carbon tetrachloride as a toxicological model. *Crit Rev Toxicol,* 33**,** 105-36.

WEI, L., LIAO, P., WU, H., LI, X., PEI, F., LI, W. & WU, Y. (2008) Toxicological effects of cinnabar in rats by NMR-based metabolic profiling of urine and serum. *Toxicol Appl Pharmacol,* 227**,** 417-29.

WELLS, R. G. (2008) Cellular sources of extracellular matrix in hepatic fibrosis. *Clin Liver Dis,* 12**,** 759-68, viii.

WERNER, M., COSTA, M. J., MITCHELL, L. G. & NAYAR, R. (1995) Nephrotoxicity of xenobiotics. *Clin Chim Acta,* 237**,** 107-54.

WIGHT, T. N. & POTTER-PERIGO, S. (2011) The extracellular matrix: an active or passive player in fibrosis? *Am J Physiol Gastrointest Liver Physiol,* 301**,** G950-5.

WIKLUND, S. (2008) *Multivariate data analysis for omics,* First edition, Umetrics

WILLIAMS, A. L. & HOOFNAGLE, J. H. (1988) Ratio of serum aspartate to alanine aminotransferase in chronic hepatitis. Relationship to cirrhosis. *Gastroenterology,* 95**,** 734-9.

WILLIAMS, H. R., COX, I. J., WALKER, D. G., COBBOLD, J. F., TAYLOR-ROBINSON, S. D., MARSHALL, S. E. & ORCHARD, T. R. (2010) Differences in gut microbial metabolism are responsible for reduced hippurate synthesis in Crohn's disease. *BMC Gastroenterol,* 10**,** 108.

WILLIAMS, J. C., JR. & SCHAFER, J. A. (1987) A model of osmotic and hydrostatic pressure effects on volume absorption in the proximal tubule. *Am J Physiol,* 253**,** F563-75.

WILLIAMS, R. E., LENZ, E. M., LOWDEN, J. S., RANTALAINEN, M. & WILSON, I. D. (2005) The metabonomics of aging and development in the rat: an investigation into the effect of age on the profile of endogenous metabolites in the urine of male rats using 1H NMR and HPLC-TOF MS. *Mol Biosyst,* 1**,** 166-75.

WINAU, F., HEGASY, G., WEISKIRCHEN, R., WEBER, S., CASSAN, C., SIELING, P. A., MODLIN, R. L., LIBLAU, R. S., GRESSNER, A. M. & KAUFMANN, S. H. (2007) Ito cells are liver-resident antigen-presenting cells for activating T cell responses. *Immunity,* 26**,** 117-29.

WISSE, E. (1974) Observations on the fine structure and peroxidase cytochemistry of normal rat liver Kupffer cells. *J Ultrastruct Res,* 46**,** 393-426.

WITZGALL, R., BROWN, D., SCHWARZ, C. & BONVENTRE, J. V. (1994) Localization of proliferating cell nuclear antigen, vimentin, c-Fos, and clusterin in the postischemic kidney. Evidence for a heterogenous genetic response among nephron segments, and a large pool of mitotically active and dedifferentiated cells. *J Clin Invest,* 93**,** 2175-88.

WOLD, S. (1995) Chemometrics; what do we mean with it, and what do we want from it? *Chemometrics and Intelligent Laboratory Systems,* 30**,** 109-115.

WOLF, S., RAVE, K., HEINEMANN, L. & ROGGEN, K. (2009) Renal glucose excretion and tubular reabsorption rate related to blood glucose in subjects with type 2 diabetes with a critical reappraisal of the "renal glucose threshold" model. *Horm Metab Res,* 41**,** 600-4.

WRIGHT, W. R., RAINWATER, J. C. & TOLLE, L. D. 1971. Glucose assay systems: evaluation of a colorimetric hexokinase procedure. *Clin Chem,* 17**,** 1010-5.

WROBLEWSKI, F. (1959) The clinical significance of transaminase activities of serum. *Am J Med,* 27**,** 911-23.

WU, C. L., ZHAO, S. P. & YU, B. L. (2013) Microarray analysis provides new insights into the function of apolipoprotein O in HepG2 cell line. *Lipids Health Dis,* 12**,** 186.

WU, D. J., ZHU, B. J. & WANG, X. D. (2011) Metabonomics-based omics study and atherosclerosis. *J Clin Bioinforma,* 1**,** 30.

WU, H., ZHANG, X., LI, X., LI, Z., WU, Y. & PEI, F. (2005) Comparison of metabolic profiles from serum from hepatotoxin-treated rats by nuclear-magnetic-resonance-spectroscopy-based metabonomic analysis. *Anal Biochem,* 340**,** 99-105.

WU, J., CHEN, Y. D. & GU, W. (2010) Urinary proteomics as a novel tool for biomarker discovery in kidney diseases. *J Zhejiang Univ Sci B,* 11**,** 227-37.

XIE, Y., NISHI, S., IGUCHI, S., IMAI, N., SAKATSUME, M., SAITO, A., IKEGAME, M., IINO, N., SHIMADA, H., UENO, M., KAWASHIMA, H., ARAKAWA, M. & GEJYO, F. (2001a) Expression of osteopontin in gentamicin-induced acute tubular necrosis and its recovery process. *Kidney Int,* 59**,** 959-74.

XIE, Y., SAKATSUME, M., NISHI, S., NARITA, I., ARAKAWA, M. & GEJYO, F. (2001b) Expression, roles, receptors, and regulation of osteopontin in the kidney. *Kidney Int,* 60**,** 1645-57.

XU, E. Y., PERLINA, A., VU, H., TROTH, S. P., BRENNAN, R. J., ASLAMKHAN, A. G. & XU, Q. (2008) Integrated pathway analysis of rat urine metabolic profiles and kidney transcriptomic profiles to elucidate the systems toxicology of model nephrotoxicants. *Chem Res Toxicol,* 21**,** 1548-61.

YAMAGUCHI, K., NAKAMURA, M., SHIRAHANE, K., KONOMI, H., TORATA, N., HAMASAKI, N., KAWAKITA, M. & TANAKA, M. (2005) Urine diacetylspermine as a novel tumour maker for pancreatobiliary carcinomas. *Dig Liver Dis,* 37**,** 190-4.

YANG, F. R., FANG, B. W. & LOU, J. S. (2010a) Effects of Haobie Yangyin Ruanjian decoction on hepatic fibrosis induced by carbon tetrachloride in rats. *World J Gastroenterol,* 16**,** 1458-64.

YANG, J., WU, G., FENG, Y., LV, Q., LIN, S. & HU, J. (2010b) Effects of taurine on male reproduction in rats of different ages. *J Biomed Sci,* 17 Suppl 1**,** S9.

YANG, J., WU, G., FENG, Y., SUN, C., LIN, S. & HU, J. (2010c) CSD mRNA expression in rat testis and the effect of taurine on testosterone secretion. *Amino Acids,* 39**,** 155-60.

YOKOYAMA, T., BANTA, S., BERTHIAUME, F., NAGRATH, D., TOMPKINS, R. G. & YARMUSH, M. L. (2005) Evolution of intrahepatic carbon, nitrogen, and energy metabolism in a D-galactosamine-induced rat liver failure model. *Metab Eng,* 7**,** 88-103.

YOUNG, M. B., DISILVESTRO, M. R., SENDERA, T. J., FREUND, J., KRIETE, A. & MAGNUSON, S. R. (2003) Analysis of gene expression in carbon tetrachloride-treated rat livers using a novel bioarray technology. *Pharmacogenomics J,* 3**,** 41-52.

YU, J. S., SHIM, J. H., CHUNG, J. J., KIM, J. H. & KIM, K. W. (2010a) Double contrast-enhanced MRI of viral hepatitis-induced cirrhosis: correlation of gross morphological signs with hepatic fibrosis. *Br J Radiol,* 83**,** 212-7.

YU, X., ANTONIADES, H. N. & GRAVES, D. T. (1993) Expression of monocyte chemoattractant protein 1 in human inflamed gingival tissues. *Infect Immun,* 61**,** 4622-8.

YU, Y., JIN, H., HOLDER, D., OZER, J. S., VILLARREAL, S., SHUGHRUE, P., SHI, S., FIGUEROA, D. J., CLOUSE, H., SU, M., MUNIAPPA, N., TROTH, S. P., BAILEY, W., SENG, J., ASLAMKHAN, A. G., THUDIUM, D., SISTARE, F. D. & GERHOLD, D. L. (2010b) Urinary biomarkers trefoil factor 3 and albumin enable early detection of kidney tubular injury. *Nat Biotechnol,* 28**,** 470-7.

YUSA, N., WATANABE, K., YOSHIDA, S., SHIRAFUJI, N., SHIMOMURA, S., TANI, K., ASANO, S. & SATO, N. (2000) Transcription factor Sp3 activates the liver/bone/kidney-type alkaline phosphatase promoter in hematopoietic cells. *J Leukoc Biol,* 68**,** 772-7.

ZAMBON, A., BERTOCCO, S., VITTURI, N., POLENTARUTTI, V., VIANELLO, D. & CREPALDI, G. (2003) Relevance of hepatic lipase to the metabolism of triacylglycerol-rich lipoproteins. *Biochem Soc Trans,* 31**,** 1070-4.

ZHANG, S. (1999) *An atlas of histology,* First edition.0-387-94954-2

ZHOU, Y., VAIDYA, V. S., BROWN, R. P., ZHANG, J., ROSENZWEIG, B. A., THOMPSON, K. L., MILLER, T. J., BONVENTRE, J. V. & GOERING, P. L. (2008) Comparison of kidney injury molecule-1 and other nephrotoxicity biomarkers in urine and kidney following acute exposure to gentamicin, mercury, and chromium. *Toxicol Sci,* 101**,** 159-70.

ZHU, H., ZHANG, L., AMIN, A. R. & LI, Y. (2008) Coordinated upregulation of a series of endogenous antioxidants and phase 2 enzymes as a novel strategy for protecting renal tubular cells from oxidative and electrophilic stress. *Exp Biol Med (Maywood),* 233**,** 753-65.

ZIRA, A., KOSTIDIS, S., THEOCHARIS, S., SIGALA, F., ENGELSEN, S. B., ANDREADOU, I. & MIKROS, E. (2013) 1H NMR-based metabonomics approach in a rat model of acute liver injury and regeneration induced by CCl4 administration. *Toxicology,* 303**,** 115-124.

ZORDOKY, B. N., ANWAR-MOHAMED, A., ABOUTABL, M. E. & EL-KADI, A. O. (2011) Acute doxorubicin toxicity differentially alters cytochrome P450 expression and arachidonic acid metabolism in rat kidney and liver. *Drug Metab Dispos,* 39**,** 1440-50.